2 mid

NASA TECHNICAL MEMORANDUM

NASA TM X-64757

21

TERRESTRIAL ENVIRONMENT (CLIMATIC) CRITERIA GUIDELINES FOR USE IN AEROSPACE VEHICLE DEVELOPMENT, 1973 REVISION

Glenn E. Daniels, Editor
Aero-Astrodynamics Laboratory

July 5, 1973

NASA-TM-X-64757) TERRESTRIAL ENVIRONMENT
CLIMATIC) CRITERIA GUIDELINES FOR USE IN
EROSPACE VEHICLE DEVELOPMENT, 1973
EVISION (NASA) ~~472~~ 469 p HC CSCL 04B G3/20

N74-16292
THRU
N74-16311
Unclas
27362

NASA

George C. Marshall Space Flight Center
Marshall Space Flight Center, Alabama

TECHNICAL REPORT STANDARD TITLE PAGE

1. REPORT NO. TM X-64757	2. GOVERNMENT ACCESSION NO.	3. RECIPIENT'S CATALOG NO.
4. TITLE AND SUBTITLE Terrestrial Environment (climatic) Criteria Guidelines for Use in Aerospace Vehicle Development, 1973 Revision		5. REPORT DATE July 5, 1973
		6. PERFORMING ORGANIZATION CODE
7. AUTHOR(S) Glenn E. Daniels, Editor		8. PERFORMING ORGANIZATION REPORT #
9. PERFORMING ORGANIZATION NAME AND ADDRESS George C. Marshall Space Flight Center Marshall Space Flight Center, Alabama 35812		10. WORK UNIT NO.
		11. CONTRACT OR GRANT NO.
		13. TYPE OF REPORT & PERIOD COVERED
12. SPONSORING AGENCY NAME AND ADDRESS National Aeronautics and Space Administration Washington, D.C. 20546		
		14. SPONSORING AGENCY CODE

15. SUPPLEMENTARY NOTES This document was prepared based on the engineering problems which developed or are anticipated for future programs by design and operational personnel of the NASA field centers. Various staff members of the Aerospace Environment Division, Aero-Astrodynamics Laboratory, MSFC, contributed to the contents of this document.

16. ABSTRACT

This document provides guidelines on probable climatic extremes and probabilities-of-occurrence of terrestrial environment data specifically applicable for NASA space vehicles and associated equipment development. The geographic areas encompassed are The Eastern Test Range (Cape Kennedy, Florida); Huntsville, Alabama; New Orleans, Louisiana; The Space and Missile Test Center (Vandenberg AFB California); Sacramento, California; Wallops Test Range (Wallops Island, Virginia); White Sands Missile Range, New Mexico; and intermediate transportation areas. In addition, sections have been included to provide information on the general distribution of natural environment extremes in the United States (excluding Alaska and Hawaii), cloud cover, and some worldwide climatic extremes. Although all these areas are covered, the major emphasis is given to the Kennedy Space Center launch area and Vandenburg Air Force Base due to importance in NASA's future large space vehicle programs.

This document presents the latest available information on probable climatic extremes, and supersedes information presented in TM X-64589. The information in this document is recommended for employment in the development of space vehicles and associated equipment design and operational criteria, unless otherwise stated in contract work specifications.

17. KEY WORDS environment criteria, terrestrial environment, surface extremes, wind, temperature, solar radiation, humidity, precipitation, density, pressure, atmospheric electricity, cloud cover	18. DISTRIBUTION STATEMENT Unclassified-Unlimited E. D. GEISSLER Director, Aero-Astrodynamics Laboratory

19. SECURITY CLASSIF. (of this report) Unclassified	20. SECURITY CLASSIF. (of this page) Unclassified	21. NO. OF PAGES 463	22. PRICE NTIS

MSFC - Form 3292 (Rev December 1972)

For sale by National Technical Information Service, Springfield, Virginia 22151

ACKNOWLEDGMENT

The editor wishes to acknowledge the suggestions, comments and encouragement of Mr. William W. Vaughan and the technical contributions of the authors listed in each chapter who are employed in the Aerospace Environment Division, Aero-Astrodynamics Laboratory, MSFC, in the formulation and revision of this document. The constructive comments of numerous users of the previous editions of this document and of other publications prepared by this division are sincerely appreciated. It is through these comments that we have been able to add to and improve the engineering utility of these data presentations. Acknowledgment is also made to the many people who have prepared technical reports which are referenced in this document. Credit is given to these people because it would have been impossible to prepare this document without the source material that was available.

In addition, acknowledgment is made to Prof. C. B. Moore, Dr. Marx Brook, Dr. H. Kasimir, Dr. E. Pierce, Dr. M. Uman, Dr. E. Lewis, and many others working in the atmospheric electricity area whose contributions, both directly and indirectly, have provided the information needed to revise Section IX on Atmospheric Electricity.

Much of the data revised or added to this edition resulted from the more extensive requirements of the Space Shuttle developement efforts by NASA and the associated contractors. The close working relationships and exchange of information between all concerned with the environment interface areas has contributed to the increased value of this edition for Space Shuttle applications.

Various programs of NASA's Office of Manned Space Flight, Office of Aeronautics and Space Technology, Office of Applications, and Office of Space Science provided resources required for the preparation of this document.

TABLE OF CONTENTS

TABLE OF CONTENTS (Continued)

TABLE OF CONTENTS (Continued)

TABLE OF CONTENTS (Continued)

TABLE OF CONTENTS (Continued)

TABLE OF CONTENTS (Continued)

TABLE OF CONTENTS (Continued)

TABLE OF CONTENTS (Continued)

TABLE OF CONTENTS (Continued)

TABLE OF CONTENTS (Continued)

TABLE OF CONTENTS (Continued)

N74-16293

TECHNICAL MEMORANDUM X- 64757

TERRESTRIAL ENVIRONMENT (CLIMATIC) CRITERIA GUIDELINES FOR USE IN AEROSPACE VEHICLE DEVELOPMENT, 1973 REVISION

Glenn E. Daniels, Editor

SUMMARY

This document provides guidelines on probable climatic extremes of terrestrial environment data specifically applicable for NASA space vehicles and associated equipment development. The geographic areas encompassed are the Eastern Test Range (Kennedy Space Center) ; Huntsville, Alabama; New Orleans, Louisiana; The Space and Missile Test Center (Vandenberg AFB, California); Sacramento, California; Wallops Test Range (Wallops Island, Virginia); White Sands Missile Range, New Mexico; and intermediate transportation areas. In addition, a section has been included to provide information on the general distribution of natural environmental extremes in the continental United States that may be needed to specify design criteria in the transportation of space vehicle components. Although not considered as a specific space vehicle design criterion, a section on atmospheric attenuation has been added, since certain earth orbital experiment missions are influenced by the earth's atmosphere. A new section on environmental hazards from aerospace vehicles has also been added. A summary of climatic extremes for worldwide operational conditions is included. This document is a revision of the 1971 edition(Ref. 1.1).

Design guideline values are established for the following environmental parameters: (1) thermal (temperature and solar radiation), (2) humidity, (3) precipitation, (4) winds, (5) pressure, (6) density, (7) electricity (atmospheric), (8) corrosion (atmospheric), (9) sand and dust, (10) fungi and bacteria, (11) atmospheric oxidants, (12) composition of the atmosphere, and (13) inflight thermodynamic properties. Data are presented and discussions

of these data are given relative to interpretation as design guidelines. Additional information on the different parameters may be located in the numerous references cited in the text following each section.

FOREWORD

For climatic extremes, there is no known physical upper or lower bound, except for certain conditions; that is, for wind speed, there does exist a strict physical lower bound of zero. Therefore, for any observed extreme condition, there is a finite probability of its being exceeded. Consequently, climatic extremes for design must be accepted with the knowledge there is some risk of the values being exceeded. Also, the accuracy of measurement of many environmental parameters is not as precise as desired. In some cases, theoretical estimates of extreme values are believed to be more representative than those indicated by empirical distributions from short periods of record. Therefore, theoretical values are given considerable weight in selecting extreme values for some parameters, i. e. , the peak surface winds.

With regard to surface and inflight winds, shears, turbulence and electrical activity, space vehicles are not designed for launch and flight in severe weather conditions; that is, hurricanes, thunderstorms, and squalls. Wind conditions are presented for various percentiles based on available data samples. Caution should be exercised in the interpretation of these percentiles in vehicle studies to ensure consistency with physical reality and the specific design and operational problems of concern.

Environment data in this document are limited to information below 90 kilometers. Reference 1.2 provides information above 90 kilometers. Specific space vehicle natural environmental design criteria are normally specified in the appropriate organizational space vehicle design ground rules and design criteria data documentation. The information in this document is recommended for use in the development of space vehicles and associated equipment, unless otherwise stated in contract work specifications.

Considerably more information is available, but not in final form, on some of the topics in this document, viz. , solar radiation, surface and inflight winds, and thermodynamic properties. Users of this document who have questions or require further information on the data provided may direct their requests to the Aerospace Environment Division (S&E-AERO-Y) , Aero-Astrodynamics Laboratory, Marshall Space Flight Center.

The data in all sections are based on conditions which have actually occurred, or are statistically probable in nature, over a longer reference period than the available data. When possible, cycles (diurnal or other) are given to provide information for environmental testing in the laboratory. In many cases, the natural test cycles do not agree with standard laboratory tests, frequently being less severe; although occasionally the natural cycle as given is more severe than the laboratory test. Such cycles need careful consideration to determine whether the laboratory tests need adjustment.

Assesment of the natural environment in early stages of a space vehicle development program will be advantageous in developing a space vehicle with a minimum operational sensitivity to the environment. For those areas of the environment that need to be monitored prior to and during tests and operations, this early planning will permit development of the required measuring and communication systems for accurate and timely monitoring of the environment. Reference 1.3 is an example of this type of study.

The environment criteria data presented in this document were formulated based on discussions and requests from engineers involved in space vehicle development and operations; therefore, they represent responses to actual engineering problems and are not just a general compilation of environmental data. This report is used extensively by the Marshall Space Flight Center (MSFC), the Johnson Space Center (JSC), and the Kennedy Space Center (KSC) in design and operational studies. Inquiries may be directed through appropriate organizational channels for subsequent communications to the Aerospace Environment Division at NASA, Marshall Space Flight Center.

N74-16294

SECTION I. INTRODUCTION

By

Glenn E. Daniels and William W. Vaughan

1.1 General

A knowledge of the earth's atmospheric environmental parameters is necessary for the establishment of design requirements for space vehicles and associated equipment. Such data are required to define the design condition for fabrication, storage, transportation, test, pre-flight, and in-flight design conditions and should be considered for both the whole system and the components which make up the system. The purpose of this document is to provide guideline data on natural environmental conditions for the various major geographic locations which are applicable to the design of space vehicles and associated equipment for the National Aeronautics and Space Administration.

Good engineering judgment must be exercised in the application of the earth's atmospheric data to space vehicle design analysis. Consideration must be given to the overall vehicle mission and performance requirements. Knowledge still is lacking on the relationships between some of the atmopheric variates which are required as inputs to the design of space vehicles. Also, interrelationships between space vehicle parameters and atmospheric variables cannot always be clearly defined. Therefore, a close working relationship and team philosophy should exist between the design/operational engineer and the respective organization's aerospace meteorologists. Although a space vehicle design should accommodate all expected operational atmospheric conditions, it is neither economically nor technically feasible to design space vehicles to withstand all atmospheric extremes. For this reason, consideration should be given to protection of space vehicles from some extremes by use of support equipment, and by using specialized forecast personnel to advise of the expected occurrence of critical environmental conditions. The services of specialized forecast personnel may be very economical in comparison with more expensive designing which would be necessary to cope with all environmental possibilities.

This document does not specify how the designer should use the data in regard to a specific space vehicle design. Such specifications may be established only through analysis and study of a particular design problem. Although of operational significance, descriptions of some atmospheric conditions have been omitted since they are not of direct concern for structural and control system design. Induced environments (vehicle caused) may be more critical than natural environments for certain vehicle operational situations, and in some cases the combination of natural and induced environments will be more severe than either environment alone. Induced environments are considered in other space vehicle criteria documents which should be consulted for such data.

1.2 Geographical Areas Covered (Fig. 1.1)

a. Huntsville, Alabama.

b. River transportation: Between Huntsville, Alabama (via Tennessee, Ohio, and Mississippi Rivers) and New Orleans, Louisiana.

c. New Orleans, Louisiana; Mississippi Test Operations, Mississippi; Houston, Texas; and transportation zones between these locations.

d. Gulf transportation: Between New Orleans, Louisiana (via Gulf of Mexico and up east coast of Florida) and Cape Kennedy, Florida.

e. Panama Canal transportation: Between Los Angeles or SAMTEC, California (via West Coast of California and Mexico, through the Panama Canal, and Gulf of Mexico) and New Orleans, Louisiana.

f. Eastern Test Range (ETR), Kennedy Space Center, Florida.

g. Space and Missile Test Center (SAMTEC), Vandenberg AFB, California.

h. Sacramento, California.

i. Wallops Test Range, Wallops Island, Virginia.

j. West coast transportation: Between Los Angeles, California, and Sacramento, California.

k. White Sands Missile Range, New Mexico.

l. Edwards Air Force Base, California.

FIGURE 1. MAIN GEOGRAPHICAL AREAS COVERED IN DOCUMENT

1.3 Units of Conversion

Numerical values in this document are given in the International System of Units (Ref. 1.4, 1.5). The values in parentheses are equivalent U.S. Customary Units.* The metric and U. S. Customary Units employed in this report are those normally used for measuring and reporting atmospheric data.

By definition, the following fundamental conversion factors are exact (Ref. 1.4, 1.5, 1.6).

Type	U. S. Customary Units	Metric
Length	1 U. S. yard (yd)	0.9144 meter (m)
Mass	1 avoirdupois pound (lb)	453.59237 gram (g)
Time	1 second (s)	1 second (s)
Temperature	1 degree Rankine(°R)	5/9 degrees Kelvin (°K)
Electric current	1 ampere (A)	1 ampere (A)
Light intensity	1 candela (cd)	1 candela (cd)

To aid in conversion of units given in this document, conversion factors based on the above fundamental conversion factors are given in Table 1.1. Geometric altitude as employed herein is with reference to mean sea level (MSL) unless otherwise stated.

1.4 Definition of Percentiles

The values of the data corresponding to the cumulative percentage frequencies are called percentiles. The relationship between percentiles and probability is as follows: Given that the 90th percentile of the wind speed is, say, 60 m/s means that there is a probability of 0.90 that this value of the wind speed will not be exceeded, and there is probability of 0.10 that it will be exceeded for the sample of data from which the percentile was computed. Stated in another way: There is a 90 percent chance that the given wind speed of 60 m/s will not be exceeded or there is a 10 percent chance that it will be exceeded. If one considers the 10th and 90th percentiles for the wind speeds, it is clear that 80 percent of the wind speeds occur within the 10-90 percentiles range.

---

*English Units adopted for use by the United States of America.

TABLE 1.1 CONVERSION OF UNITS

TYPE OF DATA		METRIC		U.S. CUSTOMARY		CONVERSION		
		UNIT	ABBREVIATION	UNIT	ABBREVIATION	MULTIPLY	BY	TO GET
SOLAR RADIATION	Solar Intensity	langley (per minute)	ly (min^{-1})	watt per square foot	watt ft^{-2}	ly (min^{-1})	0.69733	kJ m^{-2}(s^{-1})
				British Thermal Unit per square foot (per minute)	B.T.U. ft^{-2} (min^{-1})	kJ m^{-2} (s^{-1})	1.4340	ly (min^{-1})
		gram-calorie per square centimeter (per minute)	g-cal cm^{-2}(min^{-1})			ly (min^{-1})	1.000*	g-cal cm^{-2}(min^{-1})
						g-cal cm^{-2}(min^{-1})	1.000*	ly (min^{-1})
		watt per square meter	watt m^{-2}			watt m^{-2}	0.09290304*	watt ft^{-2}
		kilojoule per square meter (per second)	kJ m^{-2}(s^{-1})			watt ft^{-2}	10.7639	watt m^{-2}
						g-cal cm^{-2}(min^{-1})	64.784	watt ft^{-2}
						g-cal cm^{-2}(min^{-1})	697.33	watt m^{-2}
						watt ft^{-2}	0.015436	g-cal cm^{-2}(min^{-1})
						watt m^{-2}	0.0014340	g-cal cm^{-2}(min^{-1})
						g-cal cm^{-2}(min^{-1})	3.6867	B.T.U. ft^{-2} (min^{-1})
						B.T.U.ft^{-2}(min^{-1})	0.27125	g-cal cm^{-2}(min^{-1})
	Solar Insolation	gram-calorie per square centimeter per minute	g-cal cm^{-2} min^{-1}	British Thermal Unit per square foot per hour	B.T.U. ft^{-2} hr^{-1}	g-cal cm^{-2} min^{-1}	221.20	B.T.U. ft^{-2} hr^{-1}
						B.T.U. ft^{-2} hr^{-1}	0.0045208	g-cal cm^{-2} min^{-1}
TEMPERATURE	Ambient Temperature	degree Celsius	^{o}C	degree Fahrenheit	^{o}F	^{o}F - 32	0.5556	^{o}C
		degree Kelvin	^{o}K	degree Rankine	^{o}R	^{o}C	1.8*	^{o}F - 32
						^{o}R	1.00*	^{o}F + 459.67
						^{o}R - 459.67	1.00*	^{o}F
						^{o}K	1.00*	^{o}C + 273.15
						^{o}K - 273.15	1.00*	^{o}C
	Temperature Change	degree Celsius	^{o}C	degree Fahrenheit	^{o}F	^{o}C or ^{o}K	1.8*	temp. change ^{o}F or ^{o}R
		degree Kelvin	^{o}K	degree Rankine	^{o}R	^{o}F or ^{o}R	0.5556	temp. change ^{o}C or ^{o}K

* Defined exact conversion factor

TABLE 1.1 CONVERSION OF UNITS (Contiuned)

TYPE OF DATA		METRIC		U.S. CUSTOMARY		CONVERSION		
		UNIT	ABBREVIATION	UNIT	ABBREVIATION	MULTIPLY	BY	TO GET
DENSITY	Water Vapor Vapor Concentration (Absolute Humidity)	gram per cubic meter gram per cubic centimeter	$g\ m^{-3}$ $g\ cm^{-3}$	grain per cubic foot	$gr\ ft^{-3}$	$g\ m^{-3}$	0.43700	$gr\ ft^{-3}$
						$gr\ ft^{-3}$	2.2883	$g\ m^{-3}$
						$g\ m^{-3}$	10^{-6}*	$g\ cm^{-3}$
						$g\ cm^{-3}$	4.370×10^{5}	$gr\ ft^{-3}$
						$gr\ ft^{-3}$	2.288×10^{-6}	$g\ cm^{-3}$
	Air, Dust, and Hail	gram per cubic centimeter	$g\ cm^{-3}$	pound per cubic foot	$lb\ ft^{-3}$	$g\ cm^{-3}$	62.43	$lb\ ft^{-3}$
						$lb\ ft^{-3}$	1.6018×10^{-2}	$g\ cm^{-3}$
PRECIPITATION	Snow Unit Depth Mass	kilogram per square meter per centimeter (of depth)	$kg\ m^{-2}\ cm^{-1}$	pound per square foot per inch (of depth)	$lb\ ft^{-2}\ in.^{-1}$	$kg\ m^{-2}\ cm^{-1}$	0.5202	$lb\ ft^{-2}\ in.^{-1}$
						$lb\ ft^{-2}\ in.^{-1}$	1.922	$kg\ m^{-2}\ cm^{-1}$
	Snow Storm Total Mass	kilogram per square meter	$kg\ m^{-2}$	pound per square foot	$lb\ ft^{-2}$	$kg\ m^{-2}$	0.2048	$lb\ ft^{-2}$
						$lb\ ft^{-2}$	4.882	$kg\ m^{-2}$
	Depth	centimeter	cm	inch	in.	cm	0.3937	in.
						in.	2.54*	cm
WIND	Wind Speed	meter per second	$m\ s^{-1}$	mile per hour	mph	$m\ s^{-1}$	2.2369	mph
				knots	knots	mph	0.44704*	$m\ s^{-1}$
				feet per second	$ft\ s^{-1}$	$m\ s^{-1}$	1.9438	knots
						knots	0.51444	$m\ s^{-1}$
						mph	0.868976	knots
						knots	1.15078	mph
						$m\ s^{-1}$	3.2808	$ft\ s^{-1}$
						$ft\ s^{-1}$	0.3048*	$m\ s^{-1}$

*Defined exact conversion factor

TABLE 1.1 CONVERSION OF UNITS (Continued)

TYPE OF DATA		METRIC		U.S. CUSTOMARY		CONVERSION		
		UNIT	ABBREVIATION	UNIT	ABBREVIATION	MULTIPLY	BY	TO GET
PRESSURE	Atmospheric	newton per square meter	newton m^{-2}	pound force per square inch	lb $in.^{-2}$	mb	10^{-3}*	bar
						bar	10^{3}*	mb
		millimeter of Mercury	mmHg	inch of Mercury	in.Hg	newton m^{-2}	10^{-2}*	mb
						newton m^{-2}	$1.4504X10^{-4}$	lb $in.^{-2}$
						lb $in.^{-2}$	$6.8948X10^{3}$	newton m^{-2}
		bar	bar			mb	$1.4504X10^{-2}$	lb $in.^{-2}$
		millibar	mb			lb $in.^{-2}$	68.948	mb
		dyne per square centimeter (microbar)	dyne cm^{-2}			mb	10^{3}*	dyne cm^{-2}
						dyne cm^{-2}	10^{-3}*	mb
		kilogram force per square meter	kg m^{-2}			lb $in.^{-2}$	$6.8948X10^{4}$	dyne cm^{-2}
						dyne cm^{-2}	$1.4504X10^{-5}$	lb. $in.^{-2}$
						mb	10.1972	kg m^{-2}
						kg m^{-2}	0.0980665	mb
						lb $in.^{-2}$	703.0696	kg m^{-2}
						kg m^{-2}	0.0014223	lb $in.^{-2}$
						mb	$2.9530X10^{-2}$	in.Hg (32^{o} F)
						mb	0.75006	mmHg (0^{o} C)
						in.Hg(32^{o} F)	25.40*	mmHg (0^{o} C)
						mmHg(0^{o} C)	1.33322	mb
						in.Hg(32^{o} F)	33.8639	mb

* Defined exact conversion factor

TABLE 1.1 CONVERSION OF UNITS (Concluded)

TYPE OF DATA		METRIC		U.S. CUSTOMARY		CONVERSION		
		UNIT	ABBREVIATION	UNIT	ABBREVIATION	MULTIPLY	BY	TO GET
DISTANCE	Length	meter	m	feet	ft	m	3.2808	ft
		micron	μ	inch	in.	ft	0.3048*	m
		Ångstrom unit	Å			in.	2.54X10^{+4}*	μ
						in.	2.54X10^{+8}*	Å
						m	10^{+6}*	μ
						m	10^{+10}*	Å
						μ	10^{-6}*	m
						μ	3.937X10^{-5}	in.
						Å	10^{-10}*	m
						Å	3.937X10^{-9}	in.
MASS	Weight	gram	g	grain	gr	lb	0.45359237*	kg
		kilogram	kg	pound	lb	lb	453.59237*	g
						kg	2.20462	lb
						g	15.4324	gr
						gr	0.06480	g

* Defined exact conversion factor

REFERENCES

1.1 Daniels, Glenn E.: "Terrestrial Environment (Climatic) Criteria Guidelines for Use in Space Vehicle Development, 1971 Revision." May 10, 1971, NASA TM X-64589. NASA-Marshall Space Flight Center, Alabama.

1.2 "Space and Planetary Environment Criteria Guidelines for Use in Space Vehicle Development (1971 Revision)." TM X-64627, November 15, 1971. NASA-Marshall Space Flight Center, Huntsville, Alabama.

1.3 Carter, E. A.: "Natural Environment Support for Space Shuttle Tests and Operations," NASA CR-61346, Marshall Space Flight Center, Alabama, 1971.

1.4 "International System of Units, Resolution No. 12." NASA-TT-F-8365, NASA, Washington, D. C., 1963.

1.5 Mechtly, E. A.: "The Internation System of Units, Physical Constants and Conversion Factors." NASA SP-7012, National Aeronautics and Space Administration, Washington, D. C., 1964.

1.6 "Units of Weight and Measure (United States Customary and Metric) Definitions and Tables of Equivalents." United States Department of Commerce, National Bureau of Standards, Miscellaneous Publication 233, 1960.

SECTION II. THERMAL

By

Glenn E. Daniels

2. 0 Introduction

One of the more important environmental influences on a vehicle is the thermal environment. Combinations of air temperature, solar radiation, and sky radiation can cause various structural problems. Some examples of potential problems are: (1) Heating of one side of the vehicle by the sun while the other side is cooled by a clear sky causes stresses since the vehicle sides will be of different length; (2) the temperature of the fuel influences the volume/mass relationship; and (3) too high a temperature may destroy the usefulness of a lubricant. The heating or cooling of a surface by air temperature and radiation is a function of the heat transfers taking place; therefore, methods of determining these relationships are presented in this section.

2. 1 Definitions

The following terms and meanings are used in this section.

Absorption bands are those portions of the solar (or other continuous) spectrum which have lesser intensity because of absorption by gaseous elements or molecules. In general, elements give sharp lines, but molecules such as water vapor or carbon dioxide in the infrared give broad diffuse bands.

Air mass is the amount of atmosphere that the solar radiation passes through, whereas one air mass is referenced to when the sun is at its zenith.

Air temperature (surface) is the free or ambient air temperature measured under standard conditions of height, ventilation, and radiation shielding. The air temperature is normally measured with liquid-in-glass thermometers in a louvered wooden shelter, painted white inside and outside, with the base of the shelter normally 1. 22 meter (4 ft) above a close-cropped grass surface (Ref. 2. 1, page 59). Unless an exception is stated, surface air temperatures given in this report are temperatures measured under these standard conditions.

2. 2

Astronomical unit is a unit of length defined as equal to the mean distance between the earth and sun. The current accepted value is 1. 495978930 x 10^8 kilometers.

Atmospheric transmittance is the ratio between the intensity of the extraterrestrial solar radiation and intensity of the solar radiation after passing through the atmosphere.

Black body is an ideal emitter which radiates energy at the maximum possible rate per unit area at each wavelength for any given temperature and which absorbs all incident radiation at all wavelengths.

Diffuse sky radiation is the solar radiation reaching the earth's surface after having been scattered from the direct solar beam by molecules or suspensoids in the atmosphere. It is measured on a surface after the direct solar radiation is subtracted from the total horizontal radiation.

Direct solar radiation is the solar radiation received on a surface directly from the sun, and does not include diffuse sky radiation.

Emittance is the ratio of the energy emitted by a body to the energy which would be emitted by a black body at the same temperature. All real bodies will emit energy in different amounts from a black body at various wavelengths; i.e., colored bodies are colored because of higher emittance at specific wavelengths. In this document, the assumption is made that the absorptivity of an object is numerically equal to the emittance of the object at the same wavelengths. Therefore, the value of the emittance can be used to determine the portion of the energy received by the object which heats (or energy lost which cools) the object.

Extraterrestrial solar radiation is that solar radiation received outside the earth's atmosphere at one astronomical unit from the sun. The term "solar spectral irradiance" is used when the extraterrestrial solar radiation at small wavelength intervals is considered.

Fraunhofer lines are the dark absorption bands in the solar spectrum caused by gases in the outer portions of the sun and earth's atmosphere.

Horizontal solar radiation is the solar radiation measured on a horizontal surface. This is frequently referred to as "global radiation" or "total horizontal radiation" when solar and diffuse sky radiation are included.

Irradiation is often used to mean solar radiation received by a surface.

Normal incident solar radiation is the radiation received on a surface, normal to the direction of the sun, direct from the sun, and does not include diffuse sky radiation.

Radiation temperature is the absolute temperature of a radiating black body determined by Wien's displacement law, expressed as

$$T_R = \frac{w}{\lambda\, max} \quad , \tag{2.1}$$

where

T_R = absolute temperature of the radiating body

w = Wien's displacement constant (0. 2880 cm •K)

$\lambda\, max$ = the wavelength of the maximum radiation intensity for the black body.

Sky radiation temperature is the average radiation temperature of the sky when it is assumed to be a black body. Sky radiation is the radiation to and through the atmosphere from outer space. While this radiation is normally termed nocturnal radiation, it takes place under clear skies even during daylight hours.

Solar radiation in this document will be defined as the radiant energy from the sun between 0. 22 and 20. 0 microns (subsection 2. 2. 2).

Surface temperature is the temperature which a given surface will have when exposed to air temperature and radiation within the approximate wavelength interval of 0. 22 to 20. 0 microns.

2. 2 Special Distribution of Radiation

2. 2. 1 Introduction

All objects radiate energy in the electromagnetic spectrum. The amount and frequency of the radiation distribution is a function of temperature. The higher the temperature, the greater the amount of total energy emitted and the higher the frequency (shorter the wavelength) of the peak energy emission.

2.2.2 Solar Radiation

The sun emits energy in the electromagnetic spectrum from 10^{-7} to greater than 10^5 microns. This radiation ranges from cosmic rays through the very long wave radio waves. The total amount of radiation from the sun is nearly constant in intensity with time.

Of the total electromagnetic spectrum of the sun, only the radiant energy from that portion of the spectrum between 0.22 and 20.0 microns (the light spectrum) will be considered in this document since it contains 99.8 percent of the total electromagnetic energy. The spectral distribution of this region closely resembles the emission of a gray body radiating at 6000°K. This is the spectral region which causes nearly all of the heating or cooling of an object.

Solar radiation outside the earth's atmosphere is distributed in a continuous spectrum with many narrow absorption bands caused by the elements and molecules in the colder solar atmosphere. These absorption bands are the Fraunhofer lines, whose widths are usually very small ($< 10^{-4}\mu$ in most cases).

The earth's atmosphere also absorbs a part of the solar radiation such that the major portion of the solar radiation reaching the earth's surface is between about 0.35 and 4.00 microns. The distribution of the solar energy outside the earth's atmosphere* (extraterrestrial) is as follows:

Region (μ)	Distribution (%)	Solar Intensity* g-cal cm^{-2} (min^{-1})
Ultraviolet below 0.38	7.003	0.136
0.38 to 0.75	44.688	0.867
Infrared above 0.75	48.309	0.937

The first detailed information published for use by engineers on the distribution of solar radiation energy (solar irradiation) wavelength was that by Parry Moon in 1940 (Ref. 2.2). These data were generally based on theoretical curves, but are still used as the basic solar radiation in design by many engineers.

---

* At one Astronomical Unit on a surface normal to the sun.

2. 2. 3 Intensity Distribution

Table 2. 1 presents data on the distribution with wavelength of solar radiation outside the earth's atmosphere and at the earth's surface after 1. 0 atmosphere absorption. The solar radiation distribution data outside the earth's atmosphere (solar spectral irradiance) are based on recent extraterrestrial data obtained by high-flying aircraft and published by Thekarkara (Ref. 2. 3). The values of solar radiation for 1. 0 atmosphere absorption are representative of a very clear atmosphere which provides a minimum of atmospheric absorption. This gives a total normal solar radiation value (area under the spectral curve) equal to the highest values measured at the earth's surface in mid-latitudes. These data are for use in solar radiation design studies when extreme solar radiation effects are desired at the earth's surface. The same data is shown in graphical form in Figure 2.1.

2. 2. 4 Atmospheric Transmittance of Solar Radiation

The atmosphere of the earth is composed of a mixture of gases, aerosols, and dust which absorb radiation in different amounts at various wavelengths. If the ratio is taken of the solar spectral irradiance I_o to that of the solar radiation after absorption through one air mass $I_{1.00}$, an atmospheric transmittance factor M can be found [equation (2. 2)]:

$$M = \frac{I_o}{I_{1.00}} \tag{2. 2}$$

The atmospheric transmittance constant can be used in the following equation for computations of intensities for any other number of air masses:

$$I_N = I_o (M^N) \quad , \tag{2. 3}$$

where

I_N = intensity of solar radiation for N air mass thickness

N = number of air masses.

Equation (2. 3) can also be used to obtain solar radiation intensities versus wavelengths for other total normal incident solar radiation intensities

TABLE 2.1 SOLAR SPECTRAL IRRADIANCE (outside atmosphere) AND SOLAR RADIATION AFTER ABSORPTION BY CLEAR ATMOSPHERE

Wavelength (microns) λ	Solar Spectral Irradiance (watts cm^{-2} μ^{-1})	Area Under Solar Spectral Irradiance Curve (watts cm^{-2})	Solar Radiation After One Atmosphere Absorption (watts cm^{-2} μ^{-1})	Area Under One Atmosphere Solar Radiation Curve (watts cm^{-2})	Percentage of Solar Radiation After One Atmosphere Absorption for Wavelengths Shorter than λ (%)
0.120	0.000010	0.00000060	0.000000	0.000000	0.00
0.140	0.000003	0.00000073	0.000000	0.000000	0.00
0.150	0.000007	0.00000078	0.000000	0.000000	0.00
0.160	0.000023	0.00000093	0.000000	0.000000	0.00
0.170	0.000063	0.00000136	0.000000	0.000000	0.00
0.180	0.000125	0.00000230	0.000000	0.000000	0.00
0.190	0.000271	0.00000428	0.000000	0.000000	0.00
0.200	0.00107	0.000010	0.000001	0.000000	0.00
0.210	0.00229	0.000027	0.000003	0.000000	0.00
0.220	0.00575	0.000067	0.000007	0.000000	0.00
0.225	0.00649	0.000098	0.000007	0.000000	0.00
0.230	0.00667	0.000131	0.000008	0.000000	0.00
0.235	0.00593	0.000162	0.000007	0.000000	0.00
0.240	0.00630	0.000193	0.000007	0.000000	0.00
0.245	0.00723	0.000227	0.000008	0.000000	0.00
0.250	0.00704	0.000263	0.000008	0.000000	0.00
0.255	0.0104	0.000306	0.000012	0.000000	0.00
0.260	0.0130	0.000365	0.000015	0.000000	0.00
0.265	0.0185	0.000443	0.000021	0.000000	0.00
0.270	0.0232	0.000548	0.000026	0.000000	0.00
0.275	0.0204	0.000657	0.000023	0.000000	0.00
0.280	0.0222	0.000763	0.000025	0.000000	0.00
0.285	0.0315	0.000897	0.000036	0.000001	0.00
0.290	0.0482	0.001097	0.000055	0.000001	0.00
0.295	0.0584	0.001363	0.000066	0.000001	0.00
0.300	0.0514	0.001638	0.006677	0.000035	0.03
0.305	0.0603	0.001917	0.019830	0.000134	0.12
0.310	0.0689	0.002240	0.029084	0.000279	0.25
0.315	0.0764	0.002603	0.038941	0.000474	0.42
0.320	0.0830	0.003002	0.047684	0.000712	0.64
0.325	0.0975	0.003453	0.062018	0.001022	0.92
0.330	0.1059	0.003961	0.073829	0.001392	1.25
0.335	0.1081	0.004496	0.080896	0.001796	1.61
0.340	0.1074	0.005035	0.084636	0.002219	1.99
0.345	0.1069	0.005571	0.087080	0.002655	2.39
0.350	0.1093	0.006111	0.091327	0.003111	2.80
0.355	0.1083	0.006655	0.092186	0.003572	3.40
0.360	0.1068	0.007193	0.092857	0.004036	3.63
0.365	0.1132	0.007743	0.099873	0.004536	4.08
0.370	0.1181	0.008321	0.105507	0.005063	4.55
0.375	0.1157	0.008906	0.104596	0.005586	5.03
0.380	0.1120	0.009475	0.102971	0.006101	5.49
0.385	0.1098	0.010030	0.102273	0.006613	5.95
0.390	0.1098	0.010579	0.103977	0.007132	6.42
0.395	0.1189	0.011150	0.114309	0.007704	6.93
0.400	0.1429	0.011805	0.137403	0.008391	7.55
0.405	0.1644	0.012573	0.158076	0.009181	8.26
0.410	0.1751	0.013422	0.168365	0.010023	9.02
0.415	0.1774	0.014303	0.170576	0.010876	9.79
0.420	0.1747	0.015183	0.167980	0.011716	10.54
0.425	0.1693	0.016043	0.162788	0.012530	11.28
0.430	0.1639	0.016876	0.157596	0.013318	11.99
0.435	0.1663	0.017702	0.159903	0.014117	12.71
0.440	0.1810	0.018570	0.174038	0.014988	13.40
0.445	0.1922	0.019503	0.184807	0.015912	14.30
0.450	0.2006	0.020485	0.192884	0.016876	15.19
0.455	0.2057	0.021501	0.195904	0.017656	16.07
0.460	0.2066	0.022532	0.196761	0.018839	16.96
0.465	0.2048	0.023560	0.196923	0.019824	17.84
0.470	0.2033	0.024580	0.195480	0.020801	18.72

TABLE 2.1 SOLAR SPECTRAL IRRADIANCE (outside atmosphere) AND SOLAR RADIATION AFTER ABSORPTION BY CLEAR ATMOSPHERE (Continued)

Wavelength (microns) λ	Solar Spectral Irradiance (watts $cm^{-2} \mu^{-1}$)	Area Under Solar Spectral Irradiance Curve (watts cm^{-2})	Solar Radiation After One Atmosphere Absorption (watts $cm^{-2} \mu^{-1}$)	Area Under One Atmosphere Solar Radiation Curve (watts cm^{-2})	Percentage of Solar Radiation After One Atmosphere Absorption for Wavelengths Shorter than λ (%)
0.475	0.2044	0.025600	0.196538	0.021784	19.61
0.480	0.2074	0.026629	0.197523	0.022772	20.50
0.485	0.1976	0.027642	0.186415	0.023704	21.34
0.490	0.1950	0.028623	0.183962	0.024624	22.17
0.495	0.1960	0.029601	0.183177	0.025539	22.99
0.500	0.1942	0.030576	0.179814	0.026439	23.80
0.505	0.1920	0.031542	0.176146	0.027319	24.60
0.510	0.1882	0.032492	0.172660	0.028183	25.37
0.515	0.1833	0.033421	0.168165	0.029023	26.13
0.520	0.1833	0.034337	0.168165	0.029864	26.88
0.525	0.1852	0.035259	0.169908	0.030714	27.65
0.530	0.1842	0.036182	0.168990	0.031559	28.41
0.535	0.1818	0.037097	0.166788	0.032393	29.16
0.540	0.1783	0.037997	0.163977	0.033211	29.90
0.545	0.1754	0.038882	0.160917	0.034015	30.62
0.550	0.1725	0.039751	0.158256	0.034806	31.33
0.555	0.1720	0.040613	0.157798	0.035595	32.05
0.560	0.1695	0.041466	0.155504	0.036373	32.75
0.565	0.1705	0.042316	0.156422	0.037155	33.45
0.570	0.1712	0.043171	0.157064	0.037940	34.16
0.575	0.1719	0.044028	0.157726	0.038729	34.87
0.580	0.1715	0.044887	0.157339	0.039516	35.57
0.585	0.1712	0.045744	0.157064	0.040301	36.28
0.590	0.1700	0.046597	0.155963	0.041081	36.98
0.595	0.1682	0.047442	0.154311	0.041852	37.68
0.600	0.1666	0.048279	0.152844	0.042616	38.37
0.605	0.1647	0.049107	0.151100	0.043372	39.05
0.610	0.1635	0.049928	0.150000	0.044122	39.72
0.620	0.1602	0.051546	0.146972	0.045592	41.05
0.630	0.1570	0.053132	0.145370	0.047045	42.30
0.640	0.1544	0.054689	0.144299	0.048488	43.66
0.650	0.1511	0.056217	0.142547	0.049914	44.94
0.660	0.1486	0.057715	0.141523	0.051329	46.22
0.670	0.1456	0.059186	0.140000	0.052729	47.48
0.680	0.1427	0.060628	0.137211	0.054101	48.71
0.690	0.1402	0.062042	0.134807	0.055449	49.93
0.700	0.1369	0.063428	0.131634	0.056766	51.11
0.710	0.1344	0.064784	0.129230	0.058058	52.27
0.720	0.1314	0.066113	0.126346	0.059321	53.41
0.730	0.1290	0.067415	0.124038	0.060562	54.53
0.740	0.1260	0.068690	0.121153	0.061773	55.62
0.750	0.1235	0.069938	0.118750	0.062961	56.69
0.800	0.1107	0.075793	0.106442	0.068283	61.48
0.850	0.0988	0.081030	0.095000	0.073033	65.76
0.900	0.0889	0.085723	0.080090	0.077037	69.36
0.950	0.0835	0.090033	0.077314	0.080903	72.84
1.000	0.0746	0.093985	0.071730	0.084490	76.07
1.100	0.0592	0.100675	0.056923	0.090182	81.20
1.200	0.0484	0.106055	0.046538	0.094836	85.39
1.300	0.0396	0.110455	0.036000	0.098436	88.63
1.400	0.0336	0.114115	0.002240	0.098660	88.83
1.500	0.0287	0.117230	0.027333	0.101393	91.29
1.600	0.0244	0.119885	0.023461	0.103739	93.40
1.700	0.0202	0.122115	0.019423	0.105681	95.15
1.800	0.0159	0.123920	0.013826	0.107064	96.40
1.900	0.0126	0.125345	0.000126	0.107077	96.41
2.000	0.0103	0.126490	0.009809	0.108057	97.29
2.100	0.0090	0.127455	0.008653	0.108923	98.07
2.200	0.0079	0.128300	0.007596	0.109682	98.76
2.300	0.0068	0.129035	0.006538	0.110336	99.34

TABLE 2.1 SOLAR SPECTRAL IRRADIANCE (outside atmosphere) AND SOLAR RADIATION AFTER ABSORPTION BY CLEAR ATMOSPHERE (Concluded)

Wavelength (microns) λ	Solar Spectral Irradiance (watts cm^{-2} μ^{-1})	Area Under Solar Spectral Irradiance Curve (watts cm^{-2})	Solar Radiation After One Atmosphere Absorption (watts cm^{-2} μ^{-1})	Area Under One Atmosphere Solar Radiation Curve (watts cm^{-2})	Percentage of Solar Radiation After One Atmosphere Absorption for Wavelengths Shorter than λ (%)
2.4	0.0064	0.129695	0.006153	0.110951	99.90
2.5	0.0054	0.130285	0.001080	0.111059	100.00
2.6	0.0048	0.130795	0.000005	0.111060	100.00
2.7	0.0043	0.131250	0.000004	0.111060	100.00
2.8	0.00390	0.131660	0.000004	0.111061	100.00
2.9	0.00350	0.132030	0.000004	0.111061	100.00
3.0	0.00310	0.132360	0.000003	0.111061	100.00
3.1	0.00260	0.132645	0.000002	0.111062	100.00
3.2	0.00226	0.132888	0.000002	0.111062	100.00
3.3	0.00192	0.133097	0.000002	0.111062	100.00
3.4	0.00166	0.133276	0.000001	0.111062	100.00
3.5	0.00146	0.133432	0.000001	0.111062	100.00
3.6	0.00135	0.133573	0.000001	0.111062	100.00
3.7	0.00123	0.133702	0.000001	0.111062	100.00
3.8	0.00111	0.133819	0.000001	0.111063	100.00
3.9	0.00103	0.133926	0.000001	0.111063	100.00
4.0	0.00095	0.134025	0.000001	0.111063	100.00
4.1	0.00087	0.134116	0.000001	0.111063	100.00
4.2	0.00078	0.134198	0.000000	0.111063	100.00
4.3	0.00071	0.134273	0.000000	0.111063	100.00
4.4	0.00065	0.134341	0.000000	0.111063	100.00
4.5	0.00059	0.134403	0.000000	0.111063	100.00
4.6	0.00053	0.134459	0.000000	0.111063	100.00
4.7	0.00048	0.134509	0.000000	0.111063	100.00
4.8	0.00045	0.134556	0.000000	0.111063	100.00
4.9	0.00041	0.134599	0.000000	0.111063	100.00
5.0	0.0003830	0.13463906	0.000000	0.111063	100.00
6.0	0.0001750	0.13491806	0.000000	0.111063	100.00
7.0	0.0000990	0.13505506	0.000000	0.111063	100.00
8.0	0.0000600	0.13513456	0.000000	0.111063	100.00
9.0	0.0000380	0.13518356	0.000000	0.111063	100.00
10.0	0.0000250	0.13521506	0.000000	0.111063	100.00
11.0	0.0000170	0.13523606	0.000000	0.111063	100.00
12.0	0.0000120	0.13525056	0.000000	0.111063	100.00
13.0	0.0000087	0.13526091	0.000000	0.111063	100.00
14.0	0.0000055	0.13526801	0.000000	0.111063	100.00
15.0	0.0000049	0.13527321	0.000000	0.111063	100.00
16.0	0.0000038	0.13527756	0.000000	0.111063	100.00
17.0	0.0000031	0.13528101	0.000000	0.111063	100.00
18.0	0.0000024	0.13528376	0.000000	0.111063	100.00
19.0	0.0000020	0.13528596	0.000000	0.111063	100.00
20.0	0.0000016	0.13528776	0.000000	0.111063	100.00
25.0	0.000000610	0.13529328	0.000000	0.111063	100.00
30.0	0.000000300	0.13529556	0.000000	0.111063	100.00
35.0	0.000000160	0.13529671	0.000000	0.111063	100.00
40.0	0.000000094	0.13529734	0.000000	0.111063	100.00
50.0	0.000000038	0.13529800	0.000000	0.111063	100.00
60.0	0.000000019	0.13529829	0.000000	0.111063	100.00
80.0	0.000000007	0.13529855	0.000000	0.111063	100.00
100.0	0.000000003	0.13529865	0.000000	0.111063	100.00
1000.0	0.000000000	0.13530000	0.000000	0.111063	100.00

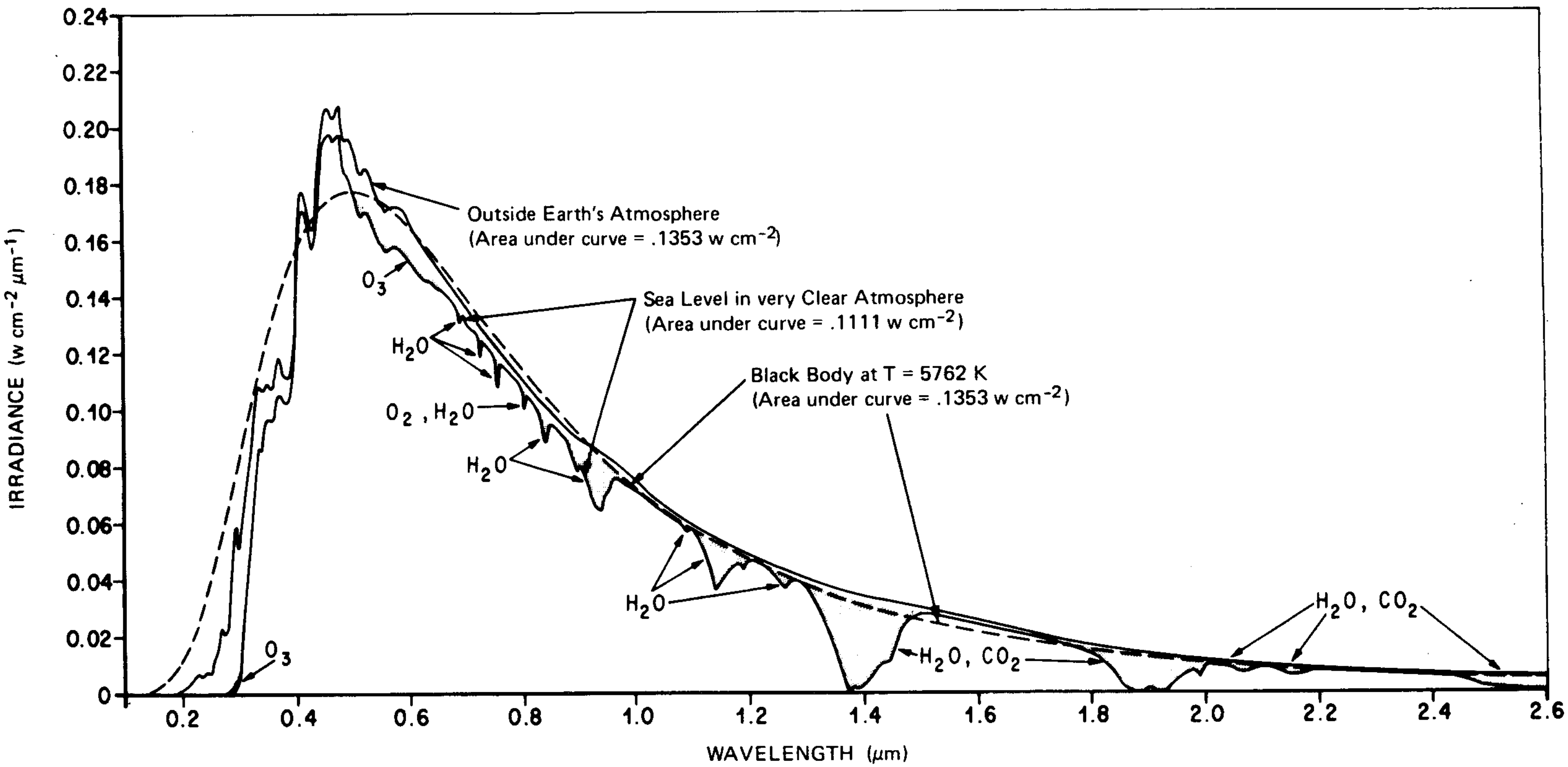

FIGURE 2.1. NORMALLY INCIDENT SOLAR RADIATION AT SEA LEVEL ON VERY CLEAR DAYS (SEC. 2.1.2.2), SOLAR SPECTRAL IRRADIANCE OUTSIDE THE EARTH'S ATMOSPHERE AT 1 AU (REF. 2.3), AND BLACK BODY SPECTRAL IRRADIANCE CURVE AT T= 5762°K (NORMALIZED TO 1 AU)

(area under curve) by computation of new values of atmospheric transmittance as follows:

$$M_N = M \frac{I_{TN}}{0.1111} \quad , \qquad (2.4)$$

where

I_{TN} = new value of total normal incident solar radiation intensity in $W\,cm^{-2}$

M = value for atmospheric transmittance given in Table 2.1

M_N = new value of atmospheric transmittance.

Equations (2.3) and (2.4) are valid only for locations relatively near the earth's surface (below 5 km altitude). For higher altitudes, corrections would be needed for the change of the amount of ozone and water vapor in the atmosphere. Also, equation (2.4) should be used only for values of I_{TN} greater than 0.0767 $W\,cm^{-2}$ (1.10 g-cal cm^{-2} min^{-1}) since values lower than this would indicate a considerably higher ratio of water vapor to ozone in the atmosphere and require that the curve be adjusted to give more absorption in the infrared water vapor bands at long wavelengths (infrared) and a smaller increase for the ozone at shorter wavelengths.

2.2.5 Sky (Diffuse) Radiation

When solar radiation, which is a nearly parallel beam of light, enters the atmosphere of the earth, molecules of air, dust particles, and aerosols such as water vapor droplets either diffuse or absorb a part of the radiation. The diffuse radiation then reaches the earth as nonparallel light from all directions.

2.2.5.1 Scattered Radiation

The scattered radiation gives the sky its brightness and color. The color is a result of selective scattering at certain wavelengths as a function of the size of the molecules and particles.

On a clear day the amount of scattering is very low because there are few particles and water droplets. The clear sky can be as little as 10^{-6} as bright as the surface of the sun. This sky radiation is called "diffuse radiation" in this document. The total energy contribution from the diffuse radiation from the entire sky hemisphere to a horizontal surface is only between 0.0007 and 0.014 W cm^{-2} (0.01 and 0.20 g-cal cm^{-2}).

As a black body radiator, the clear sky is consided equivalent to a cold source (See Table 2.6). The temperature of the clear sky is the same during the daytime as at nightime. Values of sky radiation for several localities are given in Table 2.5. It is the clear sky at night acting as a cold sink, without the solar radiation heating the surface of the earth, that causes air temperatures to be lower than the daytime values.

With clouds the amount of diffuse radiation is greater. The total hemisphere during an overcast day may contribute as much as 0.069 W cm^{-2} (1.0 g-cal cm^{-2}) of radiation to a horizontal surface.

The greater scattering by clouds makes the effective temperature of the clouds warmer than the clear air. At night the clouds act as a barrier to the outgoing radiation. Since they are warmer than the clear sky, the air near the ground will not cool to as low a temperature.

2.2.5.2 Absorbed Radiation

The various gases in the atmosphere selectively absorb some of the incoming radiation. Absorption changes some of the radiation into heat or radiation at wavelengths different from that received. Absorption by gases is observed in the solar spectrum as bands of various widths. The major gases in the earth's atmosphere, which show as absorption bands in the solar spectrum, are water vapor, carbon dioxide, ozone, and molecular oxygen.

2.3 Average Emittance of Colored Objects

In thermal engineering studies, the color of a painted surface is not important when one considers low-temperature radiation, i.e., from 10° to 68°C, since most painted surfaces have the same absorptivity at these low temperatures. Colored surfaces may differ in absorptivity. In Reference 2.4, a table on page 38 lists values of emissivity and absorptivity for various surfaces and different colors of paint exposed to solar radiation. Similar data are given in other publications but give either a range of values or mean values for the type of surface. The change of temperature (above or below the air temperature), which is the amount of heating or cooling, is proportional to the emissivity or absorptivity; therefore, the accuracy of determining the temperature of a surface is related to the accuracy of the emissivity and absorptivity. Spectral distribution curves of emittance are available for many surfaces.

The average emittance of any surface can be computed by the following method:

a. Divide the spectral emittance curve (i. e. , Figure 2. 1) into small intervals that have little or no change of emittance within the interval.

b. Using the same intervals from the spectral distribution of radiation (i. e. from Table 2. 1), multiply each value of emittance over the selected interval by the percentage of radiation over the interval.

c. Sum the resultant products to give the average emittance.

Table 2. 2 is an example of such computations. Data from Figure 2. 1 and Table 2. 1 are used. Similar computations can be accomplished for other sources of radiation such as the night sky or from cloudy skies.

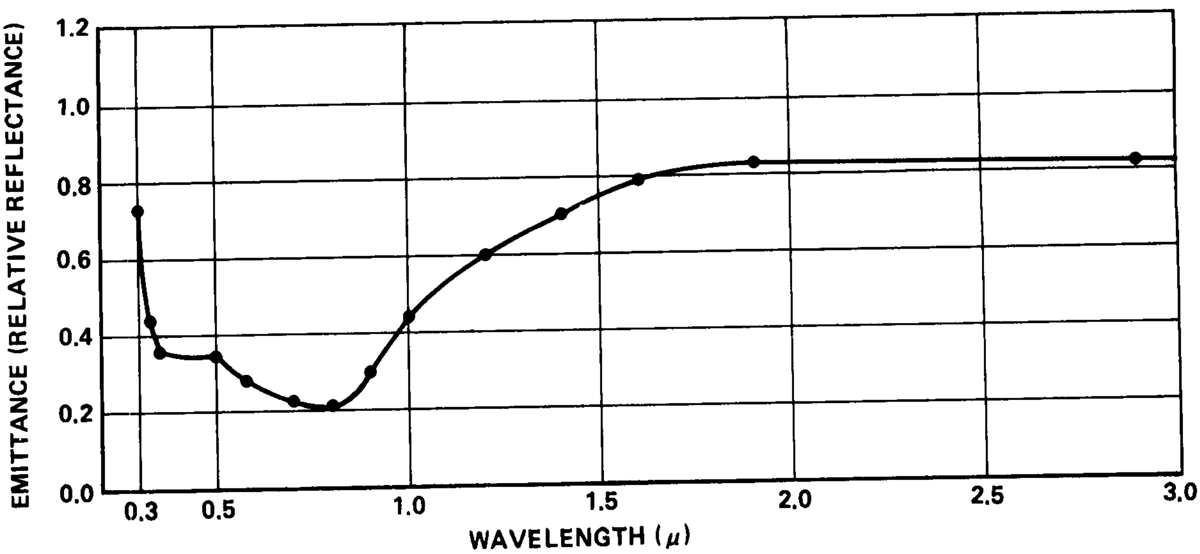

FIGURE 2. 2 EMITTANCE OF BARIUM SULPHATE AND MAGNESIUM OXIDE VERSUS WAVELENGTH

2. 4 Computation of Surface Temperature for Several Simultaneous Radiation Sources

The extreme value of temperature which a surface may reach when exposed to daytime (solar) or nighttime (night sky) radiation with no wind (calm), assuming it has no mass or heat transfer within the object, is

$$T_S = T_A + E(\Delta T_{BS}) \quad , \tag{2.5}$$

TABLE 2.2 COMPUTATION OF EMITTANCE OF WHITE PAINT EXPOSED TO DIRECT SOLAR RADIATION AT THE EARTH'S SURFACE

Wavelength (μ)	Emittance	Average Emittance	Solar Radiation, 1 Atmosphere (%)	Solar Radiation over Interval (%)	Product of Average Emittance and Percent Solar Radiation over Interval Divided by 100
0.300	0.73	0.590	0.03	1.22	0.0072
0.330	0.45	0.410	1.25	1.55	0.0063
0.350	0.37	0.365	2.80	21.00	0.0766
0.500	0.36	0.325	23.80	11.77	0.0382
0.580	0.29	0.260	35.57	15.54	0.4040
0.700	0.23	0.225	51.11	10.37	0.0233
0.800	0.22	0.260	61.48	7.88	0.0205
0.900	0.30	0.370	69.36	6.71	0.0248
1.000	0.44	0.520	76.07	9.32	0.0485
1.200	0.60	0.650	85.39	3.44	0.0224
1.400	0.70	0.745	88.83	4.57	0.0340
1.600	0.79	0.810	93.40	3.01	0.0244
1.900	0.83	0.830	96.41	3.59	0.0298
50.000	0.83		100.00		
			Sum = average emittance = 0.396		

where

T_S = surface temperature (°K)

T_A = air temperature (°K)

E = emittance of surface

ΔT_{BS} = increase in black body temperature (°K) from daytime solar radiation (plus) or decrease in black body temperature (°K) from nighttime sky radiation (minus), calculated from

$$\Delta T_{BS} = \left(\frac{I_{TS}}{\sigma} \right)^{\frac{1}{4}} - T_A \quad . \tag{2.6}$$

Extreme values of ΔT_{BS} can be obtained from Figure 2.4A or Table 2.8, where

I_{TS} = total radiation (solar by day) (sky for night) received at surface. These values can be extremes from Tables 2.3, 2.4, or 2.6 from this report.

σ = Stefan-Boltzmann constant

= 8.1296×10^{-11} g-cal cm^{-2} K^{-4}

= 5.6692×10^{-12} W cm^{-2} K^{-4}

The term $\left(\frac{I_{TS}}{\sigma} \right)^{\frac{1}{4}}$ is equal to the extreme black body surface temperature.

If a correction for wind speed is desired, equation (2.5) can be used as follows:

$$T_S = T_A + E(\Delta T_{BS}) \frac{Wc}{100} \quad , \tag{2.5A}$$

where Wc is the correction for wind speed in percent from Figure 2.4B. Equations (2.5), (2.6), and (2.5A) are only for computing the effect of one source of radiation on a surface. When more than one radiation source is received by an object, then a more complex method must be used, as given in the following discussion.

If we have a black body with several radiation sources and no convection, then

$$\sigma T^4 = \sum_1^n I_i \qquad i = 1, 2, 3 \ldots n \quad . \tag{2.7}$$

Then

$$T - T_A = \Delta T = \frac{\sum_{1}^{n} I_i}{\sigma}^{\frac{1}{4}} - T_A \quad , \qquad (2.8)$$

where T_A is the air temperature.

For any object exposed to radiation in the earth's atmosphere

$$\Delta T = f_w \left(\frac{\sum_{1}^{n} E_i \, I_i}{\sigma} \right)^{\frac{1}{4}} - T_A \quad , \qquad (2.9)$$

where

E_i = emittance of object for corresponding radiation source I_i

$\Delta T = T - T_A$ (2.10)

f_w = wind effect (convection)

$$f_w = \frac{0.325}{\sqrt{w}} \qquad (2.11)$$

w = wind speed (m/sec) .

2.5 Total Solar Radiation

2.5.1 Introduction

The standard solar radiation sensors measure the intensity of direct solar radiation from the sun falling on a horizontal surface plus the diffuse (sky) radiation from the total sky hemisphere. Diffuse radiation is lowest with dry clear air; it increases with increasing dust and moisture in the air. With extremely dense clouds or fog, the measured horizontal solar radiation will be nearly all diffuse radiation. The higher (≥ 95 percentile) values of measured horizontal solar radiation occur under clear skies or under conditions of scattered fair weather cumulus clouds which reflect additional solar radiation onto the measuring sensor.

In this document all solar radiation values given are intensitites. Solar radiation intensities are measured in gram calories per square centimeter (same as langleys per square centimeter) by stations of the National Oceanic and Atmospheric Administration, National Weather Service; therefore, these units are used in this section. Intensities of solar radiation are numerically equal to solar insolation per minute; i.e., gram calories per square centimeter per minute.

2.5.2 Use of Solar Radiation in Design

When radiation data are used in design studies, the direct solar radiation should be applied from one direction as parallel rays, and at the same time, the diffuse radiation should be applied as rays from all directions of a hemisphere (Figure 2.2).

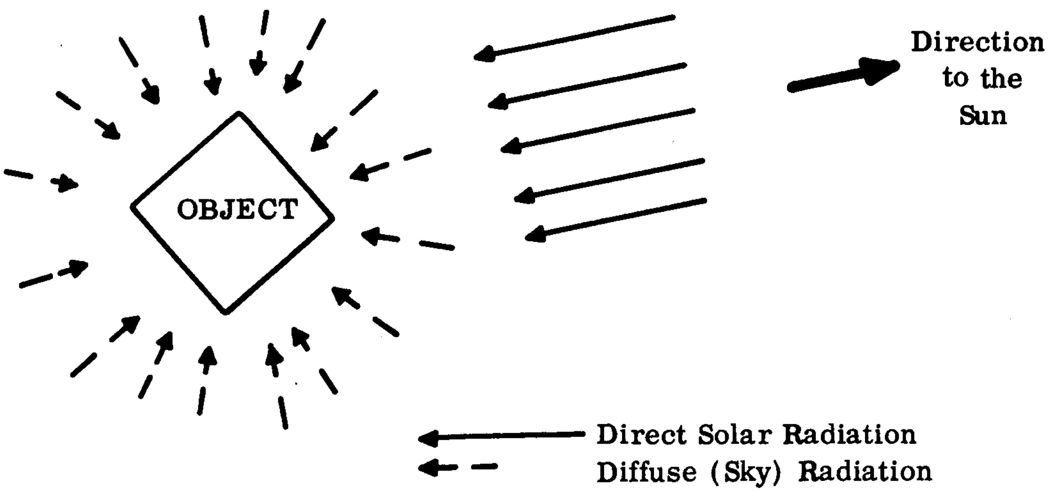

FIGURE 2.3 METHOD OF APPLYING RADIATION FOR DESIGN

Because the sun provides heat (from radiation) from a specific direction, differential heating of an object occurs; i.e., one part is heated more than another, resulting in stress and deformation. As an example, the sun heats the side of the Apollo/Saturn V vehicle facing the sun, while the sky cools the opposite side. This differential heating causes the vehicle to bend away from the sun sufficiently at the top to require consideration in design of platforms surrounding the vehicle. These platforms are used to ready the vehicle on the launch pad and must be designed so as to prevent damage to the vehicle skin as the vehicle bends away from the sun.

2.5.3 Total Solar Radiation Extremes

Ten years of total horizontal solar and sky radiation data at two stations were selected for analysis to determine the frequency distribution of solar radiation for use in design. The data analysis was made by The National Oceanic and Atmospheric Administration, National Climatic Center, under contract to NASA-Marshall Space Flight Center.

2.5.3.1 Basic Data Computations

The basic data used were hourly totals of horizontal solar and sky radiation (I_{TH}) for each hour of the day for 10-year periods at each of two stations: Apalachicola, Florida, and Santa Maria, California. The hourly totals were divided by 60 to obtain the average solar radiation values per minute for each hour. The average values per minute are numerically equal to intensity, and these values were used in the computations of frequency distributions. The diffuse sky radiation intensities I_{DH} were empirically estimated for each value based on the amount of total horizontal solar and sky radiation and solar altitude, similar to the method used in Reference 2.5. After the diffuse sky radiation is subtracted from the total horizontal solar and sky radiation, the resultant horizontal solar radiation I can be used to compute the direct normal incident solar radiation I_{DN} by using the following equation (Refs. 2.6 and 2.7):

$$I_{DN} = \frac{I}{\sin b} \quad , \qquad (2.12)$$

where

I_{DN} = direct normal incident solar radiation

I = horizontal solar radiation = $I_{TH} - I_{dH}$

b = sun's altitude[1] (Ref. 2.8).

The total normal incident solar radiation I_{TN} values were found by adding the direct normal incident solar radiation I_{DN} and the diffuse sky radiation I_{dH} previously estimated. This method of finding the total normal

1. Horizon system of coordinates such as those used by surveyors and astronomers.

incident solar radiation may result in a slight overestimate of the value for low solar altitudes because the sky hemisphere is intercepted by the ground surface. This error is insignificant, however, when extreme values are used and would be small for values equal to or greater than the mean plus one standard deviation.

Total solar radiation intensities on a south-facing surface, with the normal to the surface at 45 degrees to the horizontal, are calculated as follows:

$$I_{D45} = I\,(\sin 45 \text{ deg} + \cot b \cos a \cos 45 \text{ deg}) \quad , \qquad (2.13)$$

where

I_{D45} = intensity of direct solar radiation on a south-facing surface, with normal 45 degrees to the horizontal

I = horizontal solar radiation = $I_{TH} - I_{dH}$

a = sun's azimuth measured from south direction

b = sun's altitude.

2.5.3.2 Solar Radiation Extreme and 95 Percentile

To present the solar radiation data in a simplified form, the month of June was selected to represent the summer and the longest period of daylight and December for the winter and shortest period of daylight. The June data for normal incident solar radiation from Santa Maria, California, were increased for the period from 1100 to 1900 hours to reflect the higher values which occur early in July (first week) during the afternoon. Tables 2.3 and 2.4 give the frequency distributions for the extreme[2] values and the 95 percentile values of solar radiation for hours of the day. The values given for diffuse radiation are the values which occurred associated with the other extreme and 95 percentile values of the other solar radiations given. Since the diffuse radiation decreases with increasing horizontal radiation, the values given in Tables 2.3 and 2.4 are considerably lower than the highest values of diffuse radiation occurring during the period of record. Solar radiation data recommended for use in design are given in Table 2.4A and Figure 2.4, valid for all areas.

---

2. Extreme as used in this section is the highest measured value of record.

TABLE 2.3 EXTREME VALUES OF SOLAR RADIATION FOR THE SPACE AND MISSILE TEST CENTER, WEST COAST TRANSPORTATION, SACRAMENTO, WHITE SANDS MISSILE RANGE, AND EDWARDS AFB

TIME OF DAY (Local Standard Time)	Total Horizontal Solar Radiation g-cal cm^{-2}		Diffuse Radiation Associated with Total Horizontal Solar Radiation Extremes g-cal cm^{-2}		Total Normal Incident Solar Radiation g-cal cm^{-2}		Total 45° Surface Solar Radiation g-cal cm^{-2}	
	JUNE							
	EXTREME	95 Percentile	EXTREME	95 Percentile	EXTREME	95 Percentile	EXTREME	95 Percentile
0500	0	0	0	0	0	0	0	0
0600	0.16	0.11	.02	.04	1.14	0.78	0.04	0
0700	0.46	0.40	.05	.08	1.34	1.08	0.19	0.16
0800	0.82	0.76	.06	.09	1.54	1.38	0.34	0.31
0900	1.16	1.11	.04	.08	1.74	1.62	0.84	0.77
1000	1.45	1.42	0	.03	1.79	1.71	1.19	1.12
1100	1.64	1.56	0	.10	1.79	1.69	1.39	1.31
1200	1.69	1.63	0	.08	1.74	1.68	1.49	1.38
1300	1.69	1.64	0	.07	1.74	1.68	1.49	1.40
1400	1.59	1.54	.06	.12	1.74	1.68	1.34	1.29
1500	1.45	1.39	0	.06	1.79	1.70	1.14	1.09
1600	1.21	1.19	0	.02	1.79	1.71	0.89	0.78
1700	0.87	0.83	.03	.05	1.69	1.60	0.34	0.18
1800	0.46	0.42	.05	.08	1.39	1.23	0.19	0.13
1900	0.14	0.12	.02	.04	1.19	0.93	0.04	0
2000	0	0	0	0	0	0	0	0
	DECEMBER							
	EXTREME	95 Percentile	EXTREME	95 Percentile	EXTREME	95 Percentile	EXTREME	95 Percentile
0800	0	0	0	0	0	0	0	0
0900	0.35	0.32	0.04	0.05	1.59	1.39	0.99	0.85
1000	0.65	0.60	0.03	0.05	1.64	1.53	1.29	1.21
1100	0.86	0.80	0	0.04	1.84	1.64	1.64	1.49
1200	0.96	0.89	0.02	0.06	1.79	1.69	1.74	1.63
1300	0.99	0.89	0	0.06	1.84	1.70	1.79	1.64
1400	0.85	0.80	0.01	0.04	1.79	1.64	1.59	1.49
1500	0.66	0.60	0.02	0.05	1.69	1.54	1.34	1.21
1600	0.38	0.31	0.02	0.05	1.64	1.38	1.04	0.87
1700	0	0	0	0	0	0	0	0

TABLE 2.4 EXTREME VALUES OF SOLAR RADIATION FOR EASTERN TEST RANGE, NEW ORLEANS, GULF TRANSPORTATION, AND HUNTSVILLE

TIME OF DAY (Local Standard Time)	Total Horizontal Solar Radiation g-cal cm^{-2}		Diffuse Radiation Associated with Total Horizontal Solar Radiation Extremes g-cal cm^{-2}		Total Normal Incident Solar Radiation g-cal cm^{-2}		Total 45° Surface Solar Radiation g-cal cm^{-2}	
	JUNE							
	EXTREME	95 Percentile	EXTREME	95 Percentile	EXTREME	95 Percentile	EXTREME	95 Percentile
0500	0	0	0	0	0	0	0	0
0600	0.12	0.07	0	0	1.09	1.00	0	0
0700	0.42	0.36	0.05	0.07	1.29	1.04	0.19	0.16
0800	0.82	0.71	0.04	0.10	1.59	1.30	0.34	0.27
0900	1.23	1.02	0	0.10	1.59	1.48	0.49	0.41
1000	1.35	1.30	0.02	0.06	1.59	1.54	0.99	0.95
1100	1.52	1.45	0.03	0.09	1.59	1.54	1.19	1.14
1200	1.58	1.53	0.10	0.16	1.64	1.55	1.29	1.24
1300	1.58	1.50	0.10	0.20	1.64	1.53	1.29	1.24
1400	1.50	1.44	0.05	0.12	1.59	1.52	1.19	1.09
1500	1.35	1.30	0.02	0.06	1.59	1.52	1.04	0.95
1600	1.10	1.01	0.05	0.12	1.54	1.44	0.54	0.44
1700	0.77	0.72	0.05	0.09	1.49	1.33	0.34	0.30
1800	0.48	0.40	0.03	0.06	1.44	1.14	0.19	0.18
1900	0.11	0.08	0	0	1.14	1.00	0.14	0.03
2000	0	0	0	0	0	0	0	0
	DECEMBER							
	EXTREME	95 Percentile	EXTREME	95 Percentile	EXTREME	95 Percentile	EXTREME	95 Percentile
0700	0	0	0	0	0	0	0	0
0800	0.16	0.10	0	0	1.34	1.12	0.64	0.50
0900	0.46	0.42	0.04	0.06	1.44	1.36	0.94	0.89
1000	0.79	0.71	0.01	0.07	1.69	1.60	1.39	1.29
1100	0.95	0.92	0.02	0.04	1.79	1.68	1.64	1.56
1200	1.09	1.02	0	0.03	1.79	1.70	1.74	1.66
1300	1.05	1.02	0	0.03	1.79	1.78	1.74	1.66
1400	0.94	0.89	0.02	0.05	1.74	1.67	1.59	1.63
1500	0.79	0.70	0	0.03	1.74	1.57	1.39	1.27
1600	0.46	0.41	0.04	0.06	1.54	1.40	0.99	0.91
1700	0.16	0.10	0	0	1.34	1.12	0.64	0.50
1800	0	0	0	0	0	0	0	0

TABLE 2.4A RECOMMENDED DESIGN SOLAR RADIATION DATA

Time of Day	Design High Solar Radiation		Design Low Solar Radiation	
Hour	BTU/ft^2/hr	gm-cal/cm^2/min	BTU/ft^2/hr	gm-cal/cm^2/min
0500	0	0.00	0	0.00
1100	363	1.64	70	0.32
1300			80	0.36
1400	363	1.64		
2000	0	0.00	0	0.00

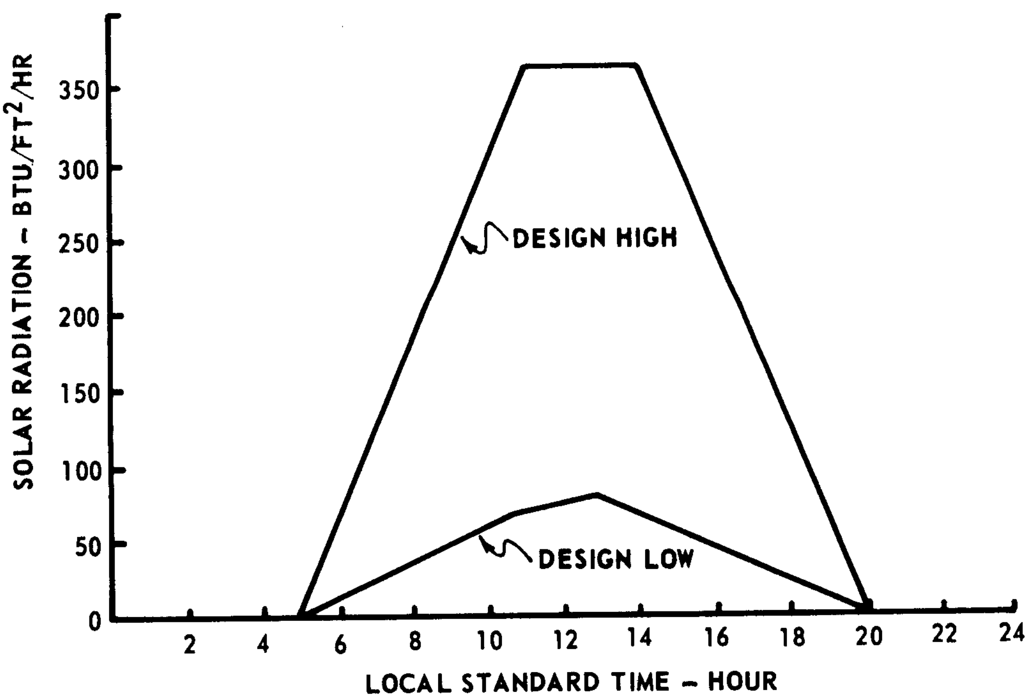

FIGURE 2.4 RECOMMENDED DESIGN SOLAR RADIATION DATA

2. 5. 3. 3 Variation with Altitude

Solar radiation intensity on a surface will increase with altitude above the earth's surface, with clear skies, according to the following equation:

$$I_H = I_{DN} + (1.94 - I_{DN}) \left(1 - \frac{\rho_H}{\rho_S}\right) \quad , \qquad (2.14)$$

where

I_H = intensity of solar radiation normal to surface at required height

I_{DN} = intensity of solar radiation normal to surface at the earth's surface assuming clear skies ($I_{DN} = I_{TN} - I_{dH}$)

ρ_H = atmospheric density at required height (from U. S. Standard, U. S. Supplemental Atmospheres, or this document) (kg m^{-3})

ρ_S = atmospheric density at sea level (from U. S. Standard, U. S. Supplemental Atmospheres, or this document) (kg m^{-3})

1. 94 = solar constant (g-cal cm^{-2}).

The diffuse radiation I_{dH} decreases with altitude above the earth's surface, with clear skies. A good estimate of the value can be obtained from the following equation[3]:

$$I_{dH} = 0.7500 - 0.4076\, I_H \quad , \qquad (2.15)$$

where

I_{dH} = intensity of diffuse radiation

I_H = intensity of solar radiation normal to surface.

Equation (2. 15) is valid for values of I_H from equation (2. 14) up to 1. 84 g-cal cm^{-2}. For values of I_H greater than 1. 84 g-cal cm^{-2}, $I_{dH} = 0$.

---

3. Equation (2. 15) is based on a cloudless and dust free atmosphere.

2. 5. 3. 4 Solar Radiation during Extreme Conditions

When ground winds occur exceeding the 95, 99, or 99. 9 percentile design winds given in this document in Section V, the associated weather normally is such that clouds, rain, or dust are generally present; therefore, the intensity of the incoming solar radiation will be less than the maximum values given in Tables 2. 3 and 2. 4. Maximum values of solar radiation intensity to use with corresponding wind speeds are given in Table 2. 5.

TABLE 2. 5 SOLAR RADIATION MAXIMUM VALUES ASSOCIATED WITH EXTREME WIND VALUES

	Maximum Solar Radiation (Normal Incident)					
Steady-State Ground Wind Speed at 18 m Height	Huntsville, New Orleans River Transportation, Gulf Transportation, Eastern Test Range, Western Test Range, Sacramento, West Coast Transportation and Wallops Test Range			White Sands Missile Range		
($m\ sec^{-1}$)	($kJm^{-2}\ sec^{-1}$)	($g\text{-}cal\ cm^{-2}\ min^{-1}$)	($BTU\ ft^{-2}\ hr^{-1}$)	($kJm^{-2}\ sec^{-1}$)	($g\text{-}cal\ cm^{-2}\ min^{-1}$)	($BTU\ ft^{-2}\ hr^{-1}$)
10	0. 84	1. 20	265	1. 05	1. 50	332
15	0. 56	0. 80	177	0. 70	1. 00	221
≥20	0. 35	0. 50	111	0. 56	0. 80	177

2. 6 Temperature

Several types of temperatures at the earth's boundary layer may be considered in design. These are as follows:

a. Air temperature normally measured at 1. 22 meters (4 ft) above a grass surface.

b. Changes of air temperature (Usually the rapid changes which occur in less than 24 hours are considered.)

c. Surface or skin temperature measured of a surface exposed to radiation.

d. Temperatures within a closed compartment.

All of the above will be discussed in the following subsections.

2.6.1 Air Temperature Near the Surface

Surface air temperature extremes (maximum, minimum, and the 95 percentile values) and the extreme minimum sky radiation (equal to the outgoing radiation) are given in Table 2.6 for various geographical areas. Maximum and minimum temperature values should be expected to last only a few hours during a daily period. Generally, the maximum temperature is reached after 12 noon and before 5 p.m., while the minimum temperature is reached just before sunrise. Table 2.7A shows the maximum and minimum air temperatures which have occurred on each hour at Kennedy Space Center, but not necessarily on the same day, although these curves represent a cold and hot extreme day. The method of sampling the day (frequency of occurrence of observations) will result in the same extreme values if the same period of time for the data is used, but the 95 percentile values will be different for hourly, daily, and monthly data reference periods. Selection of the reference period depends on engineering application. Table 2.7B gives month mean temperatures, standard deviations and 2.5 and 97.5 percentiles of values of temperature for Kennedy Space Center, Florida and Vandenberg AFB, California.

2.6.2 Extreme Air Temperature Change

a. For all areas the design values of extreme air temperature changes (thermal shock) are:

(1) An increase of air temperature of 10°C (18°F) with a simultaneous increase of solar radiation (measured on a normal surface) from 0.50 g-cal cm^{-2} min^{-1} (110 BTU ft^{-2} hr^{-1}) to 1.85 g-cal cm^{-2} min^{-1} (410 BTU ft^{-2} hr^{-1}) may occur in a 1-hour period. Likewise, the reverse change of the same magnitude may occur for decreasing air temperature and solar radiation.

(2) A 24-hour change may occur with an increase of 27.7° C (50°F) in air temperature in a 5-hour period, followed by 4 hours of constant air temperature, then a decrease of 27.7°C (50°F) in a 5-hour period, followed by 10 hours of constant air temperature.

b. For Eastern Test Range (Kennedy Space Center), the 99.9 percentile air temperature changes are as follows:

(1) An increase of air temperature of 5.6°C (11°F) with a simultaneous increase of solar radiation (measured on a normal surface) from 0.50 g-cal cm^{-2} min^{-1} (110 BTU ft^{-2} hr^{-1}) to 1.60 g-cal cm^{-2} min^{-1} (354 BTU ft^{-2} hr^{-1}), or a decrease of air temperature of 9.4°C (17°F) with a simultaneous decrease of solar radiation from 1.60 g-cal cm^{-2} min^{-1} (354 BTU ft^{-2} hr^{-1}) to 0.50 g-cal cm^{-2} min^{-1} (110 BTU ft^{-2} hr^{-1}) may occur in a 1-hour period.

TABLE 2. 6 SURFACE AIR AND SKY RADIATION TEMPERATURE EXTREMES

Area		Surface Air Temperature Extremes[a]				Sky Radiation	
		Maximum		Minimum		Equivalent Temperature Minimum Extreme	Equivalent Radiation (g-cal cm^{-2} min^{-1})
		Extreme	95%	Extreme	95%		
Huntsville	°C	43. 9	41. 7[b]	-23. 3	-21. 7[b]	-30. 0	0. 28
	°F	111	107[b]	-10	-7[b]	-22	
River Transporatation	°C	43. 9	NA	-30. 6	NA	-37. 2	0. 25
	°F	111	NA	-23	NA	-35	
New Orleans	°C	37. 8	31. 7[c]	-12. 8	7. 8[c]	-17. 8	0. 35
	°F	100	89[c]	9	46[c]	0	
Gulf Transportation	°C	40. 6	NA	-12. 8	NA	-17. 8	0. 35
	°F	105	NA	9	NA	0	
Kennedy Space Center	°C	37. 2	30. 0[c]	-3. 9	12. 2[c]	-15. 0	0. 36
	°F	99	86[c]	25	54[c]	5	
	°C	37. 2	31. 7[d]	-3. 9	6. 7[d]		
	°F	99	89[d]	25	44[d]		
Panama Canal Transportation	°C	41. 7	NA	-12. 8	NA	15. 0	0. 36
	°F	107	NA	9	NA	5	
Space and Missile Test Center	°C	37.2	23. 8[b]	-1.1	0. 0[b]	-15. 0	0. 36
	°F	99	83[b]	30	32[b]	5	
West Coast Transportation	°C	46. 1	NA	-6. 1	NA	-17. 8	0. 35
	°F	115	NA	21	NA	0	
Sacramento	°C	46. 1	36. 7[c]	-6. 1	1.1[c]	-17. 8	0. 35
	°F	115	98[c]	21	34[c]	0	
White Sands Missile Range	°C	41. 1	37.2[c]	-21. 1	-5. 6[c]	-30. 0	0. 28
	°F	106	99[c]	-6	22[c]	-22	
Wallops Test Range	°C	39. 4	33. 3[c]	-15. 0	-3.3[c]	-17. 8	0. 35
	°F	103	92[c]	5	26[c]	0	
Edwards AFB	°C	43. 3	39. 4[d]	-15. 0	- 3. 9	-30. 0	0. 28
	°F	110	103[d]	5	25[d]	-22	

a. The extreme maximum and minimum temperatures will be encountered during periods of wind speeds less than about 1 meter per second.

b. Based on worst month extreme

c. Based on hourly observations

d. Based on daily extreme (maximum or minimum) observations.

TABLE 2.7 MAXIMUM AND MINIMUM SURFACE AIR TEMPERATURES AT EACH HOUR FOR EASTERN TEST RANGE[4]

Time	Annual Maximum		Annual Minimum	
	°C	°F	°C	°F
1 a.m.	28.9	84	1.1	34
2	28.9	84	0.6	33
3	29.4	85	-1.1	30
4	28.3	83	-0.6	29
5	28.3	83	-1.1	28
6	29.4	85	-1.1	27
7	30.6	87	-1.7	26
8	30.6	87	-2.2	25
9	31.7	89	-0.6	28
10	33.9	93	1.1	30
11	35.0	95	2.2	35
12 noon	35.6	96	5.0	41
1 p.m.	37.2	99	5.6	42
2	35.6	97	5.0	41
3	35.6	97	5.6	42
4	35.6	97	5.6	42
5	35.6	97	5.6	42
6	35.0	95	3.9	39
7	33.3	92	2.2	36
8	31.7	89	2.2	36
9	30.0	86	1.7	35
10	30.0	86	1.7	35
11	30.0	86	1.1	34
12 mid	30.0	86	1.1	34

4. Based on 10 years of record for Patrick Air Force Base and Kennedy Space Center.

TABLE 2.7B MONTHLY MEAN, STANDARD DEVIATIONS (STD), AND 2.5 and 97.5 PERCENTILE VALUES OF TEMPERATURE FOR KENNEDY SPACE CENTER AND VANDENBERG AFB, CALIFORNIA

	Kennedy Space Center				Vandenberg AFB			
			Percentiles				Percentiles	
Month	Monthly Mean or 50% (°F)	STD 30-day avg.	30-Day 2.5%[5] (°F)	Average 97.5%[5] (°F)	Monthly Mean or 50% (°F)	STD 30-day avg.	30-Day 2.5%[5] (°F)	Average 97.5%[5] (°F)
Jan.	60.3	2.9	54.6	66.0	52.2	2.0	48.3	56.1
Feb.	61.7	4.0	53.9	69.4	52.6	1.9	48.9	56.3
Mar.	65.3	3.3	58.8	71.8	52.3	1.8	48.8	55.8
Apr.	70.0	2.6	64.9	75.1	54.2	1.7	50.9	57.5
May	74.8	2.2	70.5	79.1	53.9	1.5	51.0	56.8
June	79.2	1.6	76.1	82.3	56.8	1.5	53.9	59.7
July	80.7	0.5	79.7	81.7	58.4	1.4	55.7	61.1
Aug.	80.9	0.8	79.3	82.5	59.8	1.5	56.9	62.7
Sept.	80.0	1.2	77.7	82.4	60.2	1.8	56.7	63.7
Oct.	75.2	2.3	70.7	79.7	60.1	1.9	56.4	63.8
Nov.	68.0	3.5	61.1	74.9	55.8	2.0	51.9	59.7
Dec.	61.7	4.0	53.9	69.5	53.1	2.5	48.2	58.0

5. Recommended for use in Solid Rocket Motor Propellant bulk temperature preditions for design analyses.

NOTE: See Office memorandum S & E-AERO-YT-15-73, subject " Ambient Temperature for Space Shuttle SRB Propellant Temperature Predictions", Aerospace Environment Division, Marshall Space Flight Center, Alabama, for additonal information.

(2) A 24-hour temperature change may occur as follows: An increase of 16.1°C (29°F) in air temperature (wind speed under 5 m/sec) in an 8-hour period, followed by 2 hours of constant air temperature (wind speed under 5 m/sec), then a decrease of 21.7°C (39°F) in air temperature (wind speed between 7 and 10 m/sec) in a 14-hour period.

2.6.3 Surface (Skin) Temperature

The temperature of the surface of an object exposed to solar, day sky, or night sky radiation is usually different from the air temperature (Refs. 2.9 and 2.10). The amount of the extreme difference in temperature between the object and the surrounding air temperature is given in Table 2.8 and Figure 2.5, Part A, for exposure to a clear night (or day)[5] sky or to the sun on a clear day. Since the flow of air across an object changes the balance between the heat transfers from radiation and convection-conduction between the air and the object, the difference in the temperature between the air and the object will decrease with increasing wind speed (Ref. 2.9). Part B of Figure 2.5 provides information for making the corrections for wind speed Values are tabulated in Table 2.8 for various wind speeds.

2.6.4 Compartment Temperature

2.6.4.1 Introduction

A cover of thin material enclosing an air space will conduct heat to (or remove heat from) the inside air when the cover is heated by solar radiation (or cooled by the night sky). This results in the compartment air space being frequently considerably hotter or cooler than the surrounding air. The temperature reached in a compartment is dependent on the location of the air space with respect to the heated surface, the type and thickness of the surface material, the type of construction, and the insulation; i. e., an addition of a layer of insulation on the inside surface of the compartment will greatly reduce the heating or cooling of the air in the compartment space (Refs. 2.11 and 2.12).

2.6.4.2 Compartment Extreme High Temperature

A compartment probable extreme average high temperature of 87.8° C (190° F) for a period of 1 hour and an average high temperature of 65.6° C (150° F) for a period of 6 hours must be considered at all geographic locations while aircraft or other transportaion equipment are stationary on the ground without air conditioning in the compartment. These extremes will be found at the top and center of the compartment.

5. Without the sun's rays striking, the daytime sky is about as cold as the nighttime sky.

TABLE 2.8 EXTREME SURFACE (skin) TEMPERATURE ABOVE OR BELOW AIR TEMPERATURE OF AN OBJECT NEAR THE EARTH'S SURFACE

Air Temperature	Surface Temperature (°C)									
	Clear Night					Clear Day				
	Wind Speed (m sec^{-1})					Wind Speed (m sec^{-1})				
	0	2	4	10	20	0	2	4	10	20
(°C)	Correction Factor					Correction Factor				
	1.00	0.25	0.17	0.11	0.08	1.00	0.25	0.17	0.11	0.08
-25	-5.0	-1.2	-0.8	-0.6	-0.4	16.9	4.2	2.9	1.9	1.4
-20	-6.5	-1.6	-1.1	-0.7	-0.5	19.2	4.8	3.3	2.1	1.5
-15	-8.2	-2.0	-1.4	-0.9	-0.6	22.0	5.5	3.7	2.4	1.8
-10	-10.2	-2.6	-1.7	-1.1	-0.8	25.1	6.3	4.3	2.8	2.0
- 5	-12.2	-3.0	-2.1	-1.3	-1.0	28.5	7.1	4.8	3.1	2.3
0	-14.5	-3.6	-2.5	-1.6	-1.2	32.0	8.0	5.4	3.5	2.6
5	-16.9	-4.2	-2.9	-1.9	-1.4	36.0	9.0	6.1	4.0	2.9
10	-19.4	-4.8	-3.3	-2.1	-1.6	40.0	10.0	6.8	4.4	3.2
15	-21.9	-5.5	-3.7	-2.4	-1.8	44.0	11.0	7.5	4.8	3.5
20	-24.6	-6.2	-4.2	-2.7	-2.0	48.0	12.0	8.2	5.3	3.8
25	-27.4	-6.8	-4.6	-3.0	-2.2	52.0	13.0	8.8	5.7	4.2
30	-30.5	-7.6	-5.2	-3.4	-2.4	56.0	14.0	9.5	6.2	4.5
35	-34.0	-8.5	-5.8	-3.7	-2.7	60.0	15.0	10.2	6.6	4.8
40	-37.7	-9.4	-6.4	-4.1	-3.0	64.0	16.0	10.9	7.0	5.1
45	-41.7	-10.4	-7.1	-4.6	-3.3	68.0	17.0	11.6	7.5	5.4

NOTE: Values are given for an emittance value of 1.0 Temperature differences for other emittance can be determined by multiplying tabular value by the appropriate emittance.

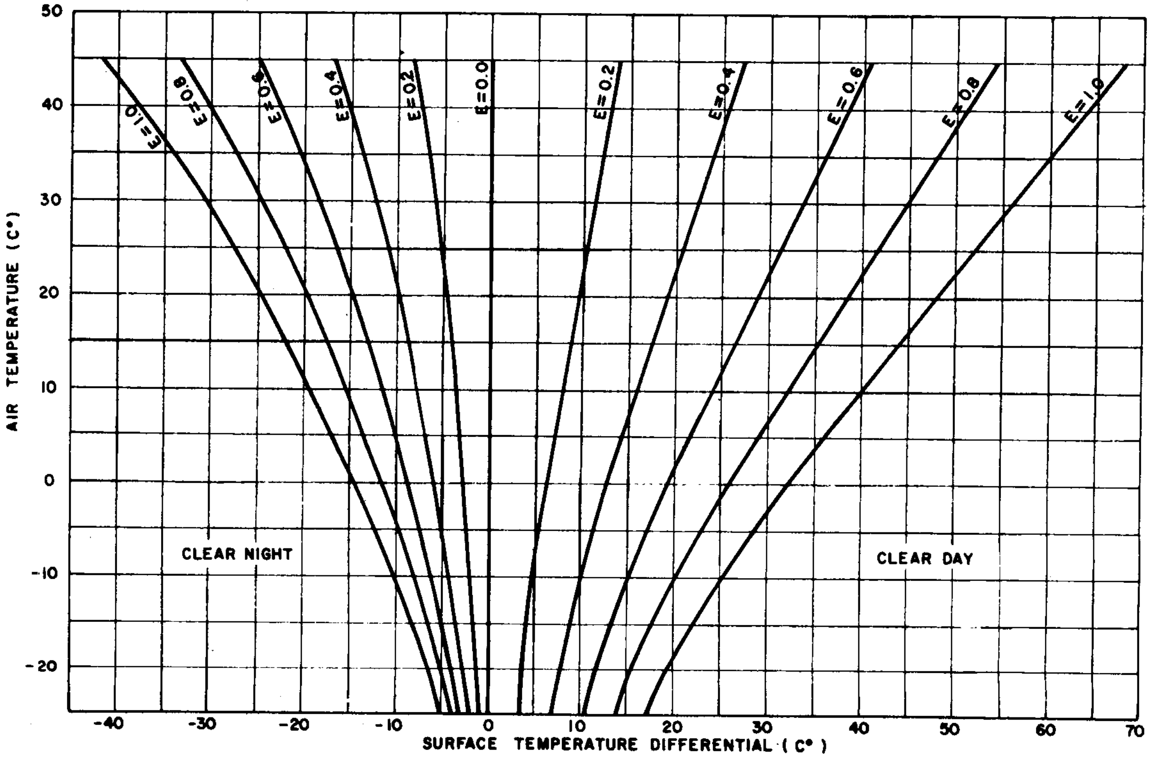

A. Surface temperature differentials with respect to air temperature for surface of emittance from 0.0 to 1.0 for calm wind conditions. Temperature difference after correction for wind is to be added or subtracted to the air temperature to give surface (skin) temperature.

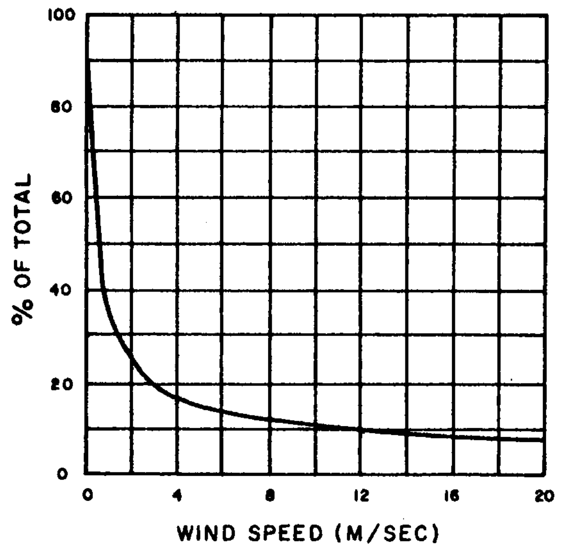

B. Correction for wind speed obtained from Graph A. Valid only for a pressure of one atmosphere.

FIGURE 2.5 EXTREME SURFACE (skin) TEMPERATURE OF AN OBJECT NEAR THE EARTH'S SURFACE (0 to 300 m) FOR CLEAR SKY

2. 7 Data on Air Temperature Distribution with Altitude

Data on air temperature distribution with altitude are given in Section XIV

REFERENCES

2.1 Middleton, W. E. K.; and Spilhaus, A. F.: "Meteorological Instruments." University of Toronto Press, 3rd Edition, revised 1960.

2.2 Moon, Parry: "Proposed Standard Solar Radiation Curves for Engineering Use." Journal of the Franklin Institute, vol. 230, Nov. 1940, pp. 583-617.

2.3 Thekarkara, Mathew P., Editor, "The Solar Constant and the Solar Spectrum Measured from a Research Aircraft." NASA TR R-351, National Aeronautics and Space Administration, Washington, D. C., Oct. 1970.

2.4 ASHRAE Handbook of Fundamentals (New York; American Society of Heating, Refrigerating and Air Conditioning Engineers, 1967).

2.5 Parmalee, G. V.: "Irradiation of Vertical and Horizontal Surfaces by Diffuse Solar Radiation from Cloudless Skies." Heating, Piping and Air Conditioning, vol. 26, Aug. 1954, pp. 129-136.

2.6 Becker, C. F.; and Boyd, J. S.: "Solar Radiation Availability on Surfaces in the United States as Affected by Season, Orientation, Latitude, Altitude, and Cloudiness." Journal of Solar Engineering, Science and Engineering, vol. 1, Jan. 1957, pp. 13-21.

2.7 Ornstein, M. P.: "Solar Radiation." Journal of Environmental Sciences, vol. 5, Apr. 1962, pp. 24-27.

2.8 "Tables of Computed Altitude and Azimuth," Publication H. O. No. 214, United States Hydrographic Office, United States Government Printing Office, 1940.

2.9 Fishenden, Margaret; and Saunders, Owen A.: "The Calculation of Heat Transmission." His Majesty's Stationary Office, London, 1932.

2.10 Daniels, Glenn E.: "Measurement of Gas Temperature and the Radiation Compensating Thermocouple." Journal of Applied Meteorology, vol. 7, 1968, pp. 1026-1035.

REFERENCES (Concluded)

2.11 Porter, William L.: "Occurrence of High Temperatures in Standing Boxcars." Technical Report EP-27, Headquarters Quartermaster Research and Development Center, United States Army, Natick, Massachusetts, Feb. 1956.

2.12 Cavell, W. W.; and Box, R. H.: "Temperature Data on Standard and Experimental Cartridges in Pilot Ejection Devices in a B47E Aircraft Stationed at Yuma, Arizona." Memo Report No. M60-16-1, Frankford Arsenal, Pitman-Dunn Laboratories Group, Philadelphia, Pennsylvania, 1960.

2.13 "Solar Electromagnetic Radiation," NASA SP-8005, Rev April 1971, National Aeronautics and Space Administration, Washington, D. C.

SECTION III. HUMIDITY

By

Glenn E. Daniels

3.1 Definitions. (Ref. 3.1)

Dew point is the temperature to which a given parcel of air must be cooled at constant pressure and constant water vapor content in order for saturation to occur. Further cooling below the dew point normally produces condensation or sublimation.

Relative humidity is the ratio of the actual amount of water vapor in a given volume of air to the amount of water vapor that the same volume of air at the same temperature holds if saturated. Values given are in percent.

Vapor concentration [previously called absolute humidity (Ref. 3.2)] is the ratio of the mass of water vapor present to the volume occupied by the mixture, i.e., the density of the water vapor content. This is expressed in grams of water vapor per cubic meter of air.

Water vapor is water in gaseous state.

3.2 Vapor Concentration.

Water in vapor form in the atmosphere is invisible; however, the amount of liquid water available from a volume of warm air near saturation is considerable and must be considered in design of space vehicles because:

a. Small solid particles (dust) which settle on surfaces cause condensation (frequently when the atmosphere is not at the saturation level) and will dissolve. The resultant solution may be corrosive. Galvanic corrosion resulting from contact of dissimilar metals also takes place at a rapid rate in the presence of moisture. The rate of corrosion of the surface increases with higher humidity (Ref. 3.3). See Section X of this document for further details.

b. Humidity conditions can impair the performance of electrical equipment. This may be by an alteration of the electrical constants of tuned circuits, deterioration of parts (resistors, capacitors, etc.), electrical breakdown of air gaps in high-voltage areas, or shorting of sections by conductive solutions formed from solid particles dissolving in the liquid formed.

c. To grow well, bacteria and fungi usually require high humidities associated with high temperatures.

d. A decrease in the temperature of the air to the dew point will result in condensation of water from the atmosphere in liquid or frozen form. Considerable difficulty may result from ice forming on space vehicles when moist air is cooled by the low temperature of the fuel, especially if pieces of this ice should drop into equipment areas of the vehicle or supporting ground equipment before or during takeoff. Optical surfaces (such as lenses of television cameras) may become coated with water droplets or ice crystals.

Test specifications still use an accelerated humidity test of temperature of 71.1°C (160°F) at a relative humidity of 95 percent ±5 percent for 10 cycles of 6 hours each spread over a total period of 240 hours. This represents a dew point of 68.9°C (156°F), values that are much higher than any natural extreme in the world. Dew points above 32.2°C (90°F) are extremely unlikely in nature (Ref. 3.4), since the dew point temperature is limited by the source of the water vapor; i.e., the surface temperature of the water body from which the water evaporates (Ref. 3.5). These tests with high temperatures can be advantageously used only as an aggravated test if high temperatures are not significant in the test after correlation of deterioration with that encountered in natural extremes. Also, if the mass of the test object is large, moisture may not condense on the test object because of thermal lag in the test object. Therefore, referenced specifications for tests which require high temperature must be carefully evaluated and should be used as guidelines along with this document.

3.2.1 High Vapor Concentration at Surface.

a. Huntsville, River Transportation, New Orleans, Gulf Transportation, Eastern Test Range, and Wallops Test Range:

(1) The following extreme humidity cycle of 24 hours with a wind of less than 5 m sec^{-1} (9.7 knots) should be considered in design: Three hours of 37.2°C (99°F) air temperature at 50 percent relative humidity and a vapor concentration of 22.2 g m^{-3} (9.7 gr ft^{-3}); six hours of decreasing air temperature to 24.4°C (76°F) with relative humidity increasing to 100 percent (saturation); eight hours of decreasing air temperature to 21.1°C (70°F), with a release of 3.8 grams of water as liquid per cubic meter of air (1.7 gr

of water per cubic foot of air),* humidity remaining at 100 percent; and seven hours of increasing air temperature to 37.2°C (99°F) and a decrease to 50 percent relative humidity (Fig. 3.1).

(2) An extreme relative humidity between 75 and 100 percent and air temperature between 22.8°C (73°F) and 27.8°C (82°F), which would result in corrosion and bacterial and fungal growths, can be expected for a period of 15 days. A humidity of 100 percent occurs one-fourth of the time at the lower temperature in cycles not exceeding 24 hours. Any loss of water vapor from the air by condensation is replaced from outside sources to maintain at least 75 percent relative humidity at the higher temperature.

b. Panama Canal Transportation:

(1) The following extreme humidity cycle of 24 hours with a wind of less than 5 m sec^{-1} (9.7 knots) should be considered in design: Three hours of 32.2°C (90°F) air temperature at 75 percent relative humidity, and a vapor concentration of 25.4 g m^{-3} (11.1 gr ft^{-3}); six hours of decreasing air temperature to 26.7°C (80°F) with relative humidity increasing to 100 percent; eight hours of decreasing air temperature to 21.7°C (71°F) with a release of 6.3 grams of water as liquid per cubic meter of air (2.8 gr of water per cubic foot of air),* humidity remaining at 100 percent; four hours of increasing air temperature to 26.7°C (80°F) and a decrease to 75 percent relative humidity; and three hours of increasing air temperature to 32.2°C (90°F) with the relative humidity remaining at 75 percent (moisture added to air by evaporation, mixing, or replacement with air of higher vapor concentration). See Figure 3.2.

(2) An extreme relative humidity between 85 and 100 percent and air temperature between 23.9°C (75°F) and 26.1°C (79°F), which would result in corrosion and bacterial and fungal growth, can be expected for a period of 30 days. The humidity should be 100 percent during one-fourth of the time at the lower temperature in cycles not exceeding 24 hours. Any loss of water vapor from the air by condensation is replaced from outside sources to maintain at least 85 percent relative humidity at the higher temperature.

---

* The release of water as a liquid on the test object may be delayed for several hours after the start of this part of the test because of thermal lag in a large test object. If the lag is too large, the test should be extended in time for each cycle to allow condensation.

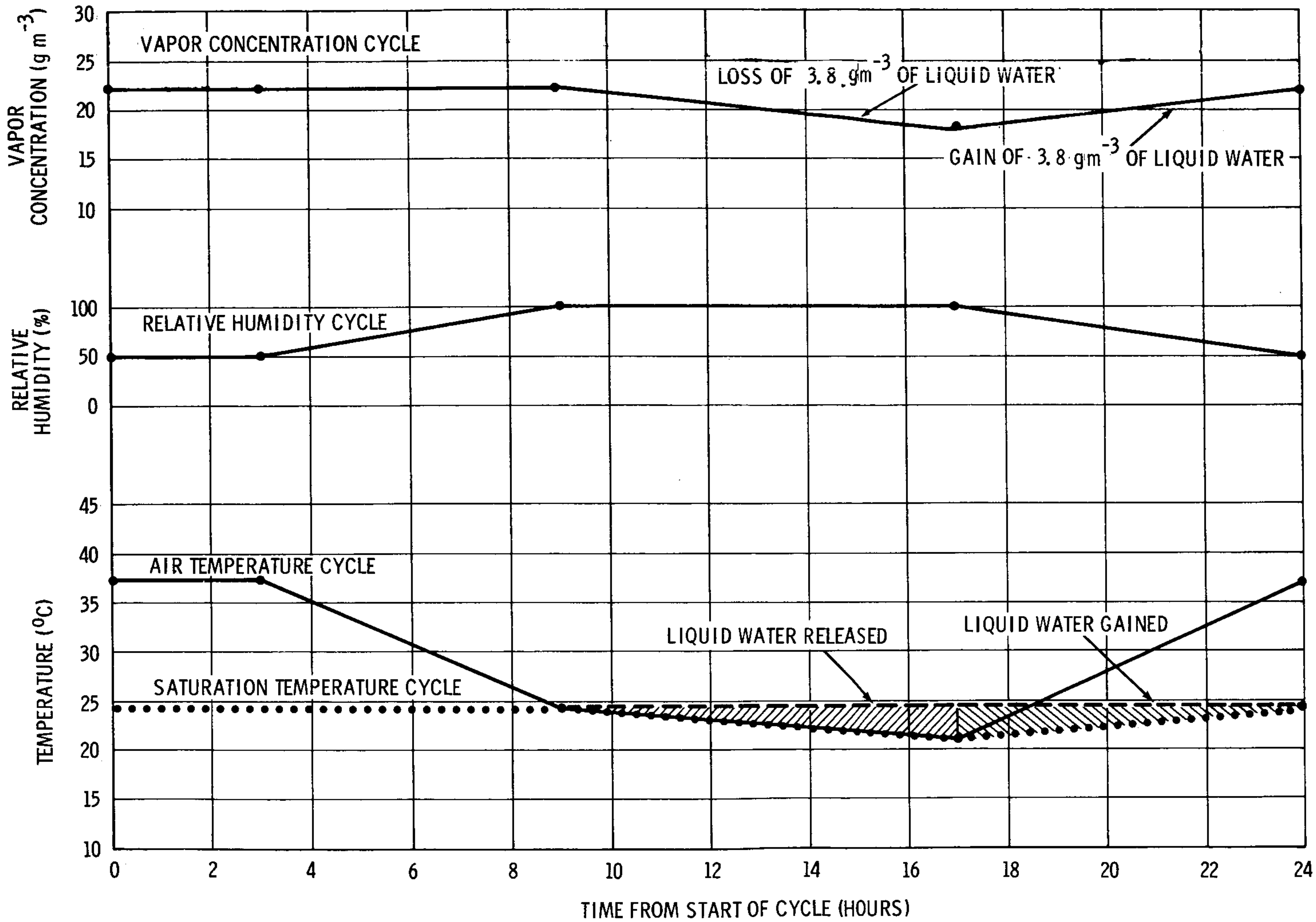

FIGURE 3.1 EXTREME HIGH VAPOR CONCENTRATION CYCLE FOR HUNTSVILLE, RIVER TRANSPORTATION, NEW ORLEANS, GULF TRANSPORTATION, EASTERN TEST RANGE, AND WALLOPS TEST RANGE

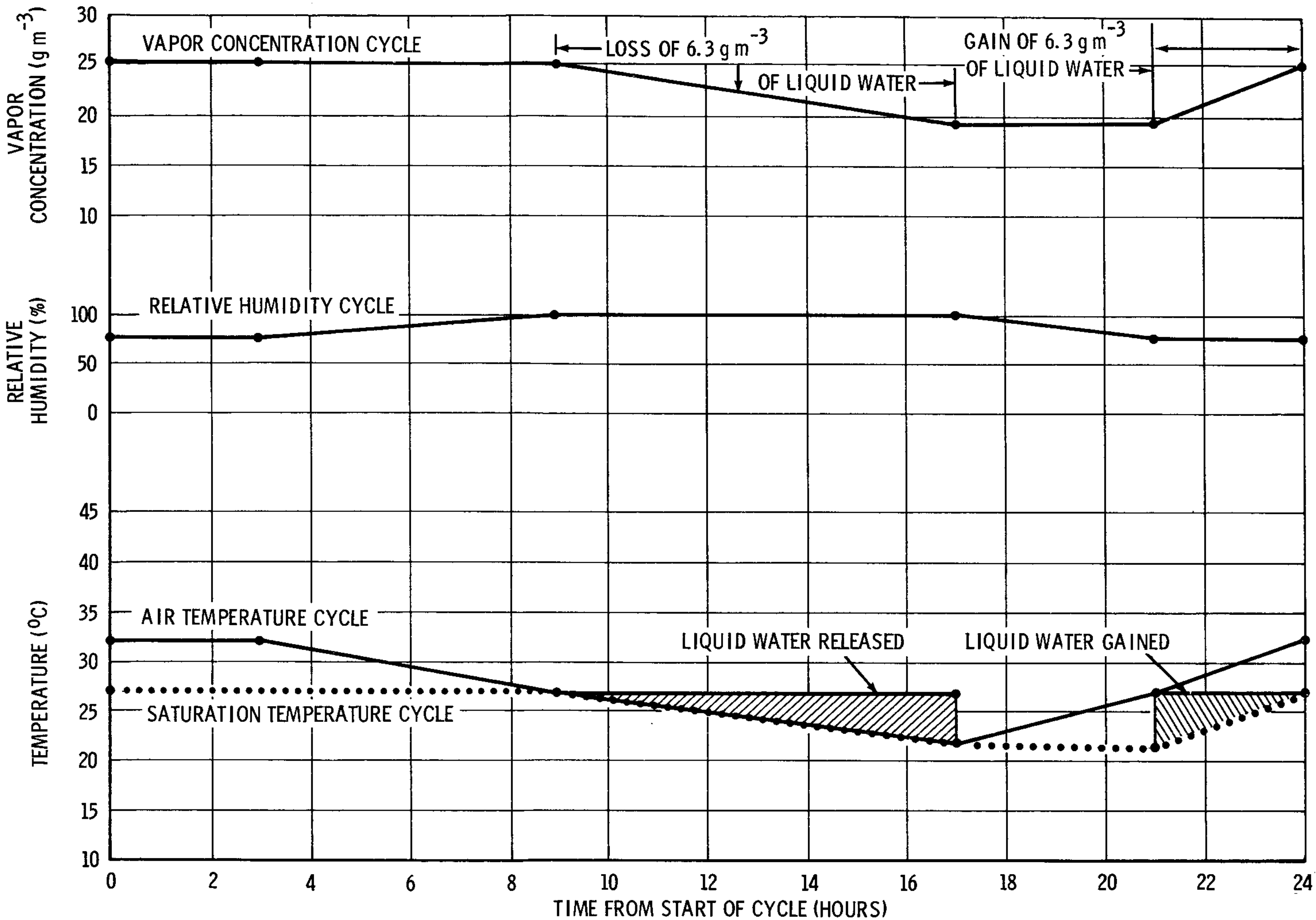

FIGURE 3.2 EXTREME HIGH VAPOR CONCENTRATION CYCLE
FOR PANAMA CANAL TRANSPORTATION

(3) Equipment shipped from the West Coast, through the Panama Canal by ship may accumulate moisture (condensation) while in the ship's hold because of the increasing moisture content of the air while traveling south to the Panama Canal, and the slower increase of temperature of the equipment being transported. This condensation may result in corrosion, rusting, or other deterioration of the equipment (Ref. 3.6). Extreme values of condensation are:

(a) Maximum condensation conditions occur during the period between December and March, but condensation conditions may occur during all months.

(b) The maximum dew point expected is 30.0° C (86° F), with dew points over 21.1° C (70° F) for ship travel of 6 days prior to arrival at the Panama Canal from the west coast, and for the remainder of the trip to Cape Kennedy.

c. The Space and Missile Test Center, West Coast Transportation, and Sacramento:

(1) The following extreme humidity cycle of 24 hours with a wind of less than 5 m sec^{-1} (9.7 knots) should be considered in design: Three hours of 23.9° C (75° F) air temperature at 75 percent relative humidity and a vapor concentration of 16.2 g m^{-3} (7.9 gr ft^{-3}); six hours of decreasing air temperature to 18.9° C (66° F) with relative humidity increasing to 100 percent; eight hours of decreasing air temperature to 12.8° C (55° F) with a release of 5.0 grams of water as liquid per cubic meter of air (2.2 gr of water per cubic foot of air),* humidity at 100 percent; and seven hours of increasing air temperature to 23.9° C (75° F) and the relative humidity decreasing to 75 percent (Fig. 3.3).

(2) Bacterial and fungal growth should present no problem because of the lower temperatures in this area. For corrosion, an extreme humidity of between 75 and 100 percent relative humidity and air temperature between 18.3° C (65° F) and 23.3° C (74° F) can be expected for a period of 15 days. The humidity should be 100 percent during one-fourth of the time at the lower temperature in cycles not exceeding 24 hours. Any loss of water vapor from the air condensation is replaced from outside sources to maintain at least 75 percent relative humidity at the higher temperature.

---

* See footnote, page 3.3

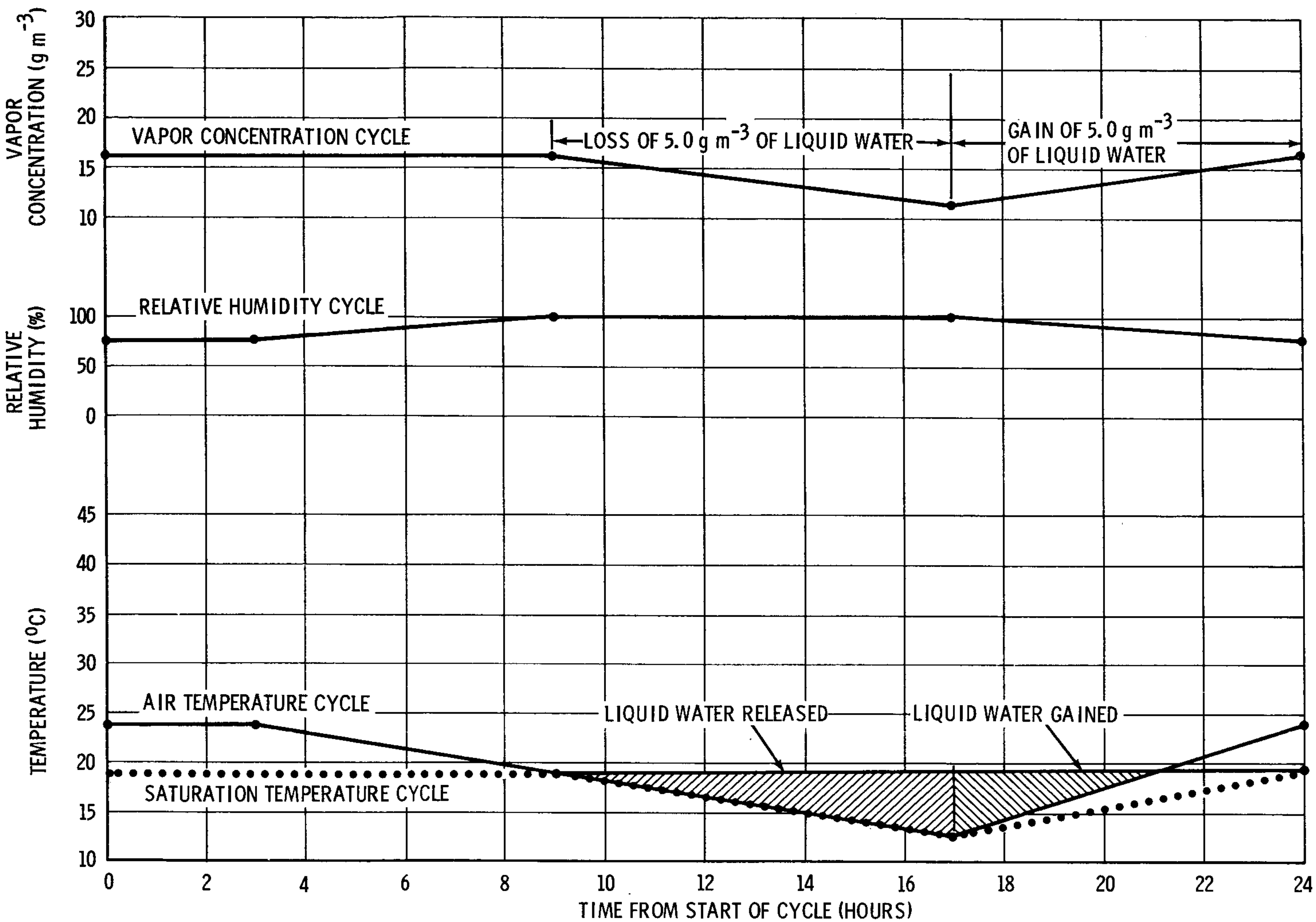

FIGURE 3.3 EXTREME HIGH VAPOR CONCENTRATION CYCLE FOR SAMTEC, WEST COAST TRANSPORTATION AND SACRAMENTO

d. White Sands Missile Range: This area is located at 1216 meters (4000 ft) above sea level, and is on the eastern side of higher mountains. The mean annual rainfall of 250 cm (10 inches) is rapidly absorbed in the sandy soil. Fog rarely occurs. Therefore, at this location, a high-vapor concentration over periods longer than a few hours, need not be considered.

3.2.2 Low Vapor Concentration at Surface.

3.2.2.1 Introduction. Low water-vapor concentration can occur at very low or at high temperatures when the air is very dry. In both cases, the dew points are very low. However, in the case of low dew points and high temperatures, the relative humidity is low. When any storage area or compartment of a vehicle is heated to temperatures well above the ambient air temperature (such as the high temperatures of the storage area in an aircraft standing on the ground in the sun), the relative humidity will be even lower than the relative humidity of the ambient air. These two types of low water-vapor concentrations have entirely different environment effects. In the case of low air temperatures, ice or condensation may form on equipment while in the high temperature-low humidity condition; organic materials may dry and split or otherwise deteriorate. When a storage area (or aircraft) is considerably warmer than the ambient air (even when the air is cold), the drying increases even more. Low relative humidities may also result in another problem — that of static electricity. Static electrical charges on equipment may ignite fuel or result in shocks to personnel when discharged. Because of this danger two types of low water-vapor concentrations (dry extremes) are given for the surface.

3.2.2.2 Surface Extremes of Low Vapor Concentration.

a. Huntsville, River Transportation, Wallops Test Range, and White Sands Missile Range:

(1) A vapor concentration of 2.1 g m^{-3} (0.9 gr ft^{-3}), with an air temperature of -11.7°C (+11°F) and a relative humidity between 98 and 100 percent for a duration of 24 hours, must be considered.

(2) A vapor concentration of 4.5 g m^{-3} (2.0 gr ft^{-3}), corresponding to a dew point of -1.1°C (30°F) at an air temperature of 28.9°C (84°F) and a relative humidity of 15 percent occurring for 6 hours each 24 hours, and a maximum relative humidity of 34 percent at an air temperature of 15.6°C (60°F) for the remaining 18 hours of each 24 hours for a 10-day period, must be considered.

b. New Orleans, Gulf Transportation, Panama Canal Transportation, and Eastern Test Range:

(1) A vapor concentration of 4.2 g m^{-3} (1.8 gr ft^{-3}), with an air temperature of -2.2° C (28° F) and a relative humidity of 98 to 100 percent for a duration of 24 hours, must be considered.

(2) A vapor concentration of 5.6 g m^{-3} (2.4 gr ft^{-3}) corresponding to a dew point of 2.2° C (36° F) at an air temperature of 22.2° C (72° F) and a relative humidity of 29 percent occurring for 8 hours, and a maximum relative humidity of 42 percent at an air temperature of 15.6° C (60° F) for the remaining 16 hours of each 24 hours for 10 days, must be considered.

c. Space and Missile Test Center:

(1) A vapor concentration of 4.2 g m^{-3} (1.8 gr ft^{-3}), with an air temperature of -2.2° C (28° F) and a relative humidity of 98 to 100 percent for a duration of 24 hours, must be considered.

(2) A vapor concentration of 4.8 g m^{-3} (2.1 gr ft^{-3}), corresponding to a dew point of 0.0° C (32° F) at an air temperature of 37.8° C (100° F) and a maximum relative humidity of 26 percent at an air temperature of 21.1° C (70° F) for the remaining 20 hours of each 24 hours for 10 days, must be considered.

d. West Coast Transportation and Sacramento:

(1) A vapor concentration of 3.1 g m^{-3} (1.4 gr ft^{-3}), with an air temperature of -6.1° C (21° F) and a relative humidity of 98 to 100 percent for a duration of 24 hours, must be considered.

(2) A vapor concentration of 10.1 g m^{-3} (4.4 gr ft^{-3}), corresponding to a dew point of 11.1° C (52 °F) at an air temperature of 37.8° C (100° F) and a relative humidity of 22 percent occurring for 4 hours each 24 hours, and a maximum relative humidity of 55 percent at an air temperature of 21.1° C (70° F) for the remaining 20 hours of each 24 hours for 10 days, must be considered.

3.2.3 Compartment Vapor Concentration at Surface.

A low water-vapor concentration extreme of 10.1 g m^{-3} (44. gr ft^{-3}), corresponding to a dew point of 11.1° C (52 °F) at a temperature of 87.8 °C (190° F) and a relative humidity of two percent occurring for one hour, a linear change over a four-hour period to an air temperature of 37.8° C (100°F) and a relative humidity of 22 percent occurring for 15 hours, then a linear change over a four-hour period to the initial conditions, must be considered at all locations.

3.3 Vapor Concentration at Altitude.

In general, the vapor concentration decreases with altitude in the troposphere because of the decrease of temperature with altitude. The data given in this section on vapor concentration are appropriate for design purposes.

3.3.1 High Vapor Concentration at Altitude.

The following table present the relationship between maximum vapor concentration and the associated temperature normally expected as a function of altitude (Ref. 3.7).

a. Maximum Vapor Concentrations for Eastern Test Range, Table 3.1.

b. Maximum Vapor Concentrations for Wallops Test Range, Table 3.2.

c. Maximum vapor concentrations for White Sands Missile Range, Table 3.3.

TABLE 3.1. MAXIMUM VAPOR CONCENTRATION FOR EASTERN TEST RANGE

Geometric Altitude		Vapor Concentration		Temperature Associated with Maximum Vapor Concentration	
(km)	(ft)	(g m^{-3})	(gr ft^{-3})	(°C)	(°F)
SRF (0.005 MSL)	(16)	27.0	11.8	30.5	87
1	3,300	19.0	8.3	24.5	76
2	6,600	13.3	5.8	18.0	64
3	9,800	9.3	4.1	12.0	54
4	13,100	6.3	2.8	5.5	42
5	16,400	4.5	2.0	-0.5	31
6	19,700	2.9	1.3	-6.8	20
7	23,000	2.0	0.9	-13.0	9
8	26,200	1.2	0.5	-20.0	-4
9	29,500	0.6	0.3	-27.0	-17
10	32,800	0.3	0.1	-34.5	-30
16.2	53,100	0.025	0.01	-57.8	-72
20	65,600	0.08	0.03	-47.8	-54

TABLE 3.2. MAXIMUM VAPOR CONCENTRATION FOR WALLOPS TEST RANGE

Geometric Altitude		Vapor Concentration		Temperature Associated with Maximum Vapor Concentration	
(km)	(ft)	(g m^{-3})	(gr ft^{-3})	(°C)	(°F)
SRF (0.002 MSL)	(8)	22.5	9.8	27.5	81
1	3,300	20.0	8.7	26.1	79
2	6,600	13.9	6.1	17.2	63
3	9,800	10.3	4.5	12.8	55
4	13,100	7.4	3.2	7.8	46
5	16,400	6.0	2.6	2.8	37
6	19,700	3.9	1.7	-1.1	30
7	23,000	2.6	1.1	-5.0	23
8	26,200	1.7	0.7	-11.1	12
9	29,500	0.9	0.4	-17.8	0
10	32,800	0.4	0.2	-27.8	-18
16.5	54,100	0.08	0.03	-47.2	-44
20	65,600	0.09	0.04	-46.2	-43

TABLE 3.3. MAXIMUM VAPOR CONCENTRATION FOR WHITE SANDS MISSILE RANGE

Geometric Altitude		Vapor Concentration		Temperature Associated with Maximum Vapor Concentration	
(km)	(ft)	(g m^{-3})	(gr ft^{-3})	(° C)	(°F)
SRF (1.2 MSL)	(3,989)	16.0	7.0	21.5	70
2	6,600	13.2	5.8	18.9	66
3	9,800	9.0	3.9	12.8	55
4	13,100	6.8	3.0	7.8	46
5	16,400	4.9	2.1	2.2	36
6	19,700	3.4	1.5	-2.2	28
7	23,000	2.2	1.0	-10.0	14
8	26,200	1.3	0.6	-16.1	3
9	29,500	0.6	0.3	-22.8	-9
10	32,800	0.2	0.1	-30.0	-22
16.5	54,100	0.08	0.03	-47.8	-44
20	65,600	0.05	0.02	-52.2	-47

3.3.2 Low Vapor Concentration at Altitude

The values presented as low extreme vapor concentrations in the following tables are based on data measured by standard radiosonde equipment.

a. Minimum Vapor Concentrations for Eastern Test Range, Table 3.4.

b. Minimum Vapor Concentrations for Wallops Test Range, Table 3.5.

c. Minimum Vapor Concentrations for White Sands Missile Range, Table 3.6.

TABLE 3.4. MINIMUM VAPOR CONCENTRATIONS FOR EASTERN TEST RANGE

Geometric Altitude		Vapor Concentration		Temperature Associated with Minimum Vapor Concentration	
(km)	(ft)	(g m^{-3})	(gr ft^{-3})	(°C)	(°F)
SRF (0.005 MSL)	(16)	4.0	1.7	29	84.2
1	3,300	0.5	0.2	6	42.8
2	6,600	0.2	0.1	0	32.0
3	9,800	0.1	0.04	-11	12.2
4	13,100	0.1	0.04	-14	6.8

TABLE 3.5. MINIMUM VAPOR CONCENTRATION FOR WALLOPS TEST RANGE

Geometric Altitude		Vapor Concentration		Temperature Associated with Minimum Vapor Concentration	
(km)	(ft)	(g m^{-3})	(gr ft^{-3})	(°C)	(°F)
SRF (0.002 MSL)	(8)	0.5	0.2	-4	24.8
1	3,300	0.3	0.1	-11	12.2
2	6,600	0.2	0.1	-17	1.4
3	9,800	0.2	0.1	-23	-9.4
4	13,100	0.2	0.1	-31	-23.8
5	16,400	0.1	0.04	-39	-38.2
7.5	24,600	0.08	0.03	-47	-43.9
10	32,800	0.017	0.007	-61	-51.7

TABLE 3.6. MINIMUM VAPOR CONCENTRATION FOR WHITE SANDS MISSILE RANGE

Geometric Altitude		Vapor Concentration		Temperature Associated with Minimum Vapor Concentration	
(km)	(ft)	(g m^{-3})	(gr ft^{-3})	(°C)	(°F)
SRF (1.2 MSL)	(3,989)	1.2	0.5	-1	30.2
2	6,600	0.9	0.4	-5	23.0
3	9,800	0.6	0.3	-12	10.4
4	13,100	0.4	0.2	-20	-4.0
5	16,400	0.2	0.1	-26	-14.8
6	19,700	0.1	0.04	-36	-37.8
7	23,000	0.09	0.03	-42	-41.1
8	26,200	0.07	0.03	-49	-45.0
9	29,500	0.03	0.01	-55	-48.3
10	32,800	0.02	0.01	-60	-51.1

REFERENCES

3.1 American Meteorological Society: "Glossary of Meteorology." Boston, Massachusetts, 1959.

3.2 Sheppard, P. A.: "The Physical Properties of Air With Reference to Meteorological Practice and the Air-Conditioning Engineer." ASME, vol. 71, 1949, pp. 915-919.

3.3 "Climatic and Environmental Criteria for Aircraft Design." ANC-22, Munitions Board Aircraft Committee, 1952.

3.4 Sissenwine, Norman; and Court, Arnold: "Climatic Extremes for Military Equipment." Report No. 146, Environmental Protection Branch, Research and Development Division, Office of the Quartermaster General, Washington D. C., 1951.

3.5 Sverdrup, H. V.: "Oceanography for Meteorologists." Prentice-Hall, Inc., New York, 1942.

3.6 Cohen, Raymond K. and Nelson, Michael: "Evaluation and Control of Sweat Damage." Stanford Research Institute, Menlo Park, California, Final Report SR 1 Project No. S-2179, July 1, 1959.

3.7 Sissenwine, Norman; Grantham, D. D.; and Salmela, H. A.: "Mid-Latitude Humidity to 32 km." Journal of the Atmospheric Sciences, Vol. 25, 1968, pp. 1129-1140.

N74-16296

SECTION IV. PRECIPITATION

4.1 Introduction

Of all the atmospheric parameters quantitatively measured routinely, precipitation is the only one occurring in discrete events. In some desert areas of the world, precipitation does not occur for several years. Even in areas of moderate to heavy rainfall, there are many periods of time without rain. Because precipitation does occur in discrete events, statistical presentations may be misleading unless accompanied with appropriate explanations. Precipitation occurs in a variety of forms, with most of the differences of form as a result of the temperature. Definitions used in this report are given in following paragraphs.

Precipitation is usually defined as all forms of hydrometeors, liquid or solid, which are free in the atmosphere and which reach the ground. In this report the definition is extended to those hydrometeors which do not reach the ground, but impinge on a flying surface, such as space vehicles. Accumulation is reported in depth over a horizontal surface; i.e., millimeters or inches for the liquid phase and in depth or equivalent depth of water equivalent for the frozen phase.

Snow is defined as all forms of frozen precipitation except large hail. It encompasses snow pellets, snow grains, ice crystals, ice pellets, and small hail.

Hail is precipitation in the form of balls or irregular lumps of ice and is always produced by convective clouds. Through established convention the diameter of the ice must be 5 mm or more, and the specific gravity between 0.60 and 0.92 to be classified as hail.

Freezing rain is rain that falls in liquid form but freezes upon impact to form a coating of glaze upon the ground or exposed objects.

Small hail is precipitation in the form of semitransparent, round, or conical grains or frozen water under 5 mm in diameter. Each grain consists of a nucleus of soft hail (ball of snow) surrounded by a very thin ice layer. They are not crisp and do not usually rebound when striking a hard surface.

The previously described precipitation forms are sufficiently different that each needs to be considered separately in design problems.

4.2 Rainfall

There are four major rainfall-producing atmospheric conditions. (1) the monsoon which produces the heaviest precipitation over long periods (most world records of rainfall rates for periods greater than 12 hr are a result of monsoons), (2) thunderstorms which generate high rates of precipitation for short periods, (3) cold and warm frontal systems, frequently accompanied by bands of steady light rain which fall at any one station for periods up to a maximum of approximately three days (thunderstorms may occur with frontal systems to give heavier rain), and (4) hurricanes which produce heavy rain associated with winds. These four rainfall types are defined in the following paragraphs.

Monsoon: The monsoon is a seasonal wind which blows for long periods of time, usually several months from one direction. When these winds blow from the water to land with increasing elevation from the water, the orographic lifting of the moisture-laden air releases precipitation in heavy amounts. In Cherrapunji, India 9144 mm (360 in.) of rain has fallen in a one-month period from monsoon rains. The amount of rain from monsoons at low elevations is considerably less than at higher elevations.

Thunderstorm: In general a thunderstorm (local storm) is produced either by lifting of unstable moist air, heating of the land mass, lifting by frontal systems or a combination of these conditions. Cumulonimbus clouds, which are produced by these storms, are always accompanied by lightning and thunder. The thunderstorm is a consequence of atmospheric instability and is defined loosely as an overturning of air layers in order to achieve a stable condition. Strong wind gusts, heavy rain, severe electrical disharges, and sometimes hail occurs with the thunderstorm with the most frequent and severe occurrences in the late afternoons and evenings.

Cold and Warm Front Precipitation: When two masses of air-one more dense than the other-meet, the lighter air mass (warm) will slide up over the more dense air mass (cold). If sufficient moisture is in the air mass being lifted, then the moisture will be condensed out and fall as precipitation, either rain or snow, depending on the temperatures of air masses.

Hurricanes: A hurricane is a severe "tropical cyclone" which forms over the various oceans and seas almost always in tropical latitudes. At maturity the tropical cyclone is one of the most intense and feared storms in the world; winds exceeding 90 m sec^{-1} (175 knots) have been measured, and its rainfall can be torrential. The wind speed must exceed 33 m sec^{-1} (64 knots) to be a hurricane.

4.2.1 Record Rainfall

In design analysis, the maximum amounts of rainfall for various periods need to be considered. These extreme values vary considerably in different areas of the world, but in areas of similar climatic conditions the extreme values are similar.

4.2.1.1 World Record Rainfall

To best study the maximum amounts of rainfall that have occurred worldwide for different periods, log-log graph paper is used. Figure 4.1 shows these worldwide values and the envelope of these values as a straight line with the equation

$$R = 36.3\sqrt{D} \qquad (1)$$

where

R = Depth of Rainfall in mm for period D.
D = Duration of Rainfall in hours.

4.2.1.2 Design Rainfall Rates

For design and testing, the rate of rainfall per unit time is more useful than the total depth of rainfall. The normal rates used are shown in millimeters per hour or inches per hour. Figure 4.2 shows the envelope of world record values plotted as the rate per hour (inches and millimeters) versus duration. The Eastern Test Range (Kennedy Space Center) and Vandenberg AFB (SAMTEC) design rainfall rate curves are also shown in Figure 4.2 with the 5-yr and 100-yr return period data for a few selected stations. The 5-yr and 100-yr return period data were taken from Rainfall-Intensity-Duration-Frequency curves published by the U.S. Department of Commerce, Weather Bureau [4.1]. This data was analyzed by the Extreme Value Method of Gumble [4.2].

The term " return period " is frequently used in statistics relating to precipitation. Return periods can be expressed as probabilities as shown in Table 4.1.

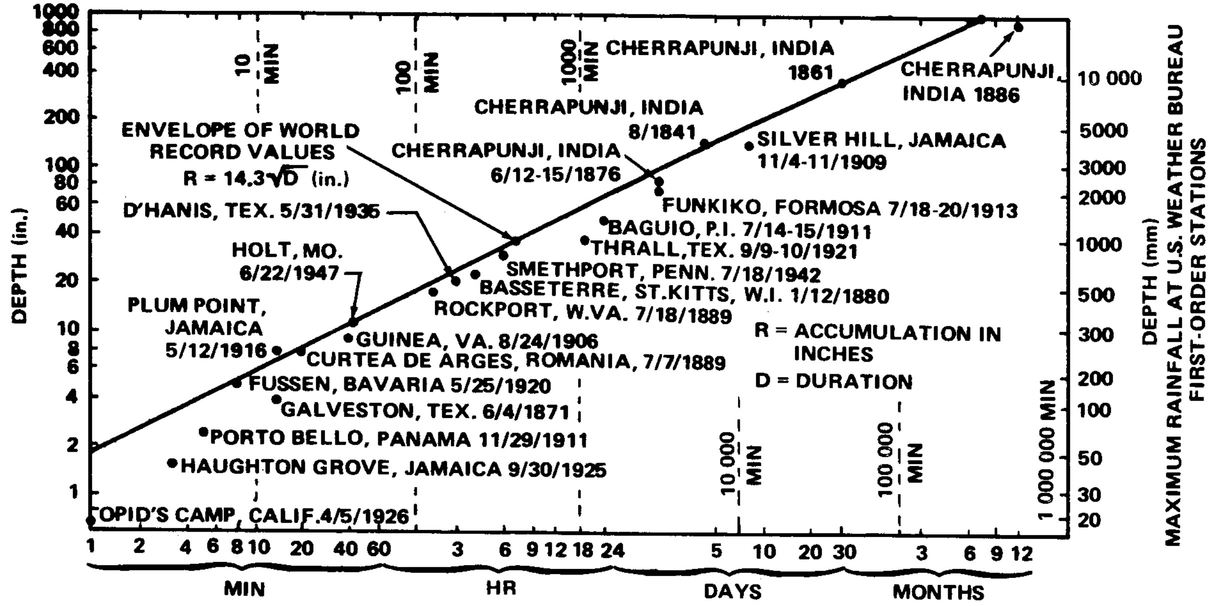

Figure 4.1 World record rainfalls and an envelope of world record values. (After R. D. Fletchter and D. Sartos, Air Weather Service Tech. Rept. No. 105-81, 1951.)

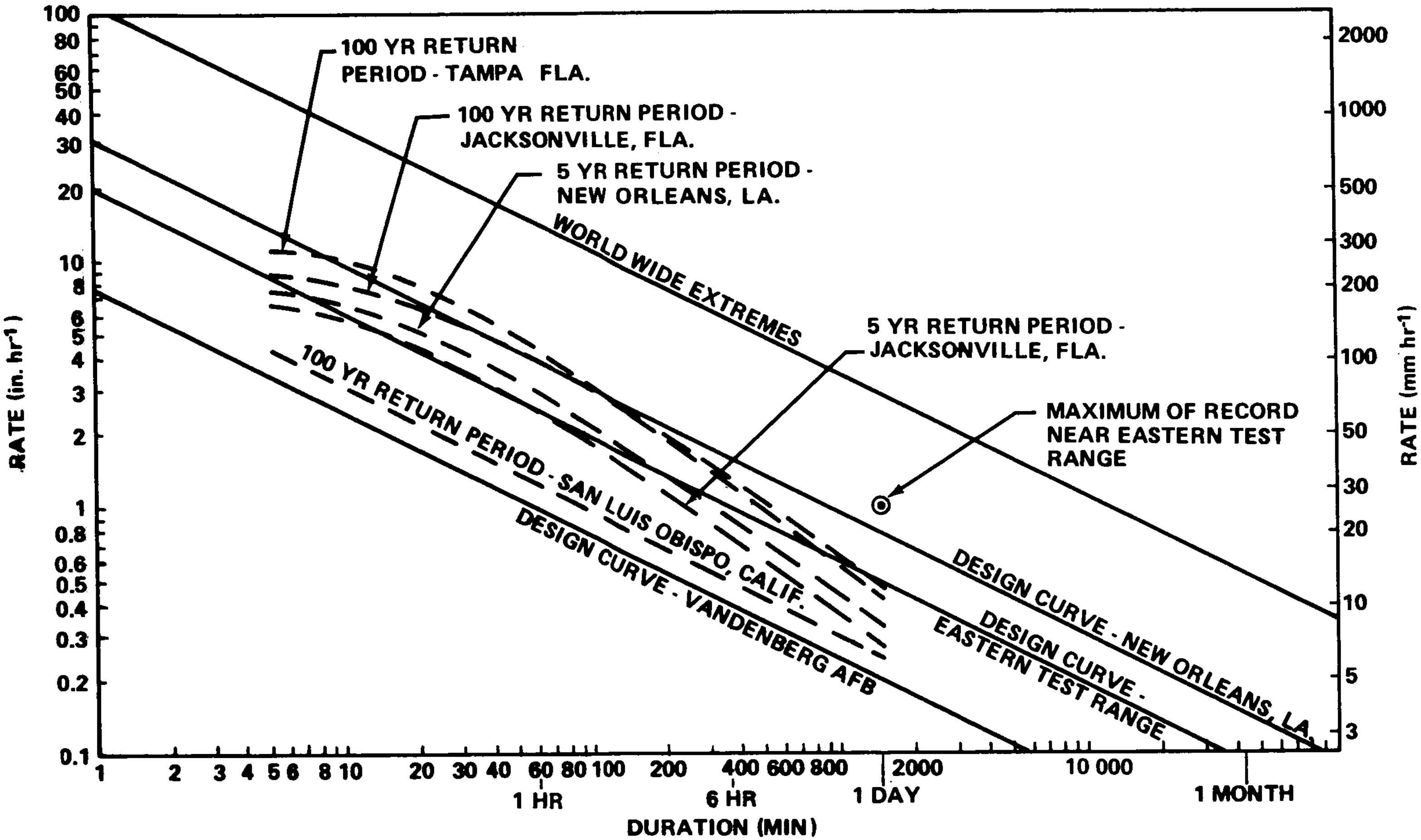

Figure 4.2 Design rainfall rates.

TABLE 4.1 RELATIONSHIP OF RETURN PERIODS TO PROBABILITIES

Return Period (yr)	Percentile (%)	Return Period (yr)	Percentile (%)
2	50	50	98
5	80	100	99
10	90	1000	99.9

Values of design rainfall for various locations and world-wide extremes of rainfall are given in Tables 4.2, 4.3, 4.4, and 4.5 with values of the corresponding drop size. For design purposes, use values of wind speed and temperature given in Table 4.18. The world-wide extremes would not normally be used for design of space vehicles, but may be needed for facility design, tracking stations, etc. The values of rainfall rates are represented with the following equation:

$$r = \frac{C\sqrt{D}}{D} = \frac{C}{\sqrt{D}} \qquad (2)$$

where

r = rate per hour
D = Time in minutes
C = Constant for location as given in Table 4.6

4.2.2 Raindrop Size

A knowledge of raindrop sizes is required to: (1) simulate rainfall tests in the laboratory, (2) know the rate of fall of the raindrops and impact energy, and (3) use in erosion tests of materials.

At the surface, the size of the raindrops vary with the rate of rainfall per unit time, the heavier the rainfall, the larger the drops. Any one rainstorm will contain a variety of sizes of raindrops ranging in size from less than 0.5 mm (the lower limit of size measurement) to greater than 4.0 mm. The more intense the storm (higher the rate of fall) the larger some of the drops will be. Reference 4.3 shows data on probability of occurence of various raindrop sizes with relation to types of rain-producing storms; (1) thunder storms, (2) rain showers, and (3) continuous rain. Thunderstorms have the greatest occurrence of the larger drops (over 2 mm). Rain showers have

TABLE 4.2 DESIGN RAINFALL, KENNEDY SPACE CENTER, FLA.; HUNTSVILLE, ALA.; AND WALLOPS TEST RANGE, VA.; BASED ON YEARLY LARGEST RATE FOR STATED DURATIONS

Time Period	Rainfall Rate		Rainfall Total Accumulation		Raindrop Size Average	Raindrop Size Largest	Average Rate of Fall
	mm hr^{-1}	in. hr^{-1}	mm	in.	mm	mm	m sec^{-1}
1 min	492	19.4	8	0.3	2.0	6.0	6.5
5 min	220	8.7	18	0.7	2.0	5.8	6.5
15 min	127	5.0	32	1.25	2.0	5.7	6.5
1 hr	64	2.5	64	2.5	2.0	5.0	6.5
6 hr	26	1.0	156	6.1	1.8	5.0	6.5
12 hr	18	0.7	220	8.7	1.6	4.5	6.5
24 hr	13	0.5	311	12.2	1.5	4.5	6.5

TABLE 4.3 DESIGN RAINFALL, NEW ORLEANS, LA.; BASED ON YEARLY LARGEST RATE FOR STATED DURATIONS

Time Period	Rainfall Rate		Rainfall Total Accumulation		Raindrop Size		Average Rate of Fall
					Average	Largest	
	mm hr⁻¹	in. hr⁻¹	mm	in.	mm	mm	m sec⁻¹
1 min	787	31.0	13	0.5	2.1	6.0	6.5
5 min	352	13.9	29	1.2	2.0	6.0	6.5
15 min	203	8.0	51	2.0	2.0	5.7	6.5
1 hr	102	4.0	102	4.0	2.0	5.5	6.5
6 hr	41	1.6	249	9.8	1.9	5.0	6.5
12 hr	29	1.2	352	13.9	1.8	5.0	6.5
24 hr	21	0.8	498	19.6	1.6	5.0	6.5

TABLE 4.4 DESIGN RAINFALL, VANDENBERG AFB (SAMTEC), CALIF.; EDWARDS AFB, CALIF.; AND WHITE SANDS MISSILE RANGE, N.M.; BASED ON YEARLY LARGEST RATE FOR STATED DURATIONS

Time Period	Rainfall Rate		Rainfall Total Accumulation		Raindrop Size		Average Rate of Fall
					Average	Largest	
	mm hr^{-1}	in. hr^{-1}	mm	in.	mm	mm	m sec^{-1}
1 min	197	7.7	3	0.1	2.0	5.6	6 5
5 min	88	3.5	7	0.3	2.0	5.3	6.5
15 min	51	2.0	13	0.5	2.0	5.0	6.5
1 hr	25	1.0	25	1.0	1.8	5.0	6.5
6 hr	10	0.4	62	2.4	1.5	4.6	6.0
12 hr	7	0.3	88	3.5	1.3	4.3	5.8
24 hr	5	0.2	124	4.9	1.3	4.0	5.5

TABLE 4.5 DESIGN RAINFALL, WORLDWIDE EXTREMES, BASED ON YEARLY LARGEST RATE FOR STATED DURATIONS

Time Period	Rainfall Rate		Rainfall Total Accumulation		Raindrop Size		Average Rate of Fall
					Average	Largest	
	mm hr^{-1}	in. hr^{-1}	mm	in.	mm	mm	m sec^{-1}
1 min	2813	110.8	47	1.8	2.5	6.0	6.5
5 min	1258	49.5	105	4.1	2.2	6.0	6.5
15 min	726	28.6	182	7.1	2.1	6.0	6.5
1 hr	363	14.3	363	14.3	2.0	6.0	6.5
6 hr	148	5.8	890	35.3	2.0	5.8	6.5
12 hr	105	4.1	1258	49.5	2.0	5.5	6.5
24 hr	74	2.9	1779	70.1	2.0	5.2	6.5

the next greatest occurrence, while the continuous rain produces the lowest occurrence of the larger drops. Raindrop sizes below 2-mm diam. occur with near equal probability from all types of storms. In comparing drop sizes with various rainfall rates, the larger drops occurred with the highest probability from the highest rainfall rates. Raindrops over 6 mm in diameter are not expected to occur frequently because the rate of fall breaks these large drops into smaller ones.

TABLE 4.6 CONSTANTS TO USE WITH EQUATION (2)
FOR RAINFALL RATES

	Eastern Test Range Huntsville, Wallops Test Range	New Orleans	Vandenberg AFB (SAMTEC) Edwards AFB, White Sands Missile Range	World-wide Extremes
in. hr^{-1} mm hr^{-1}	19.365 491.87	30.984 786.99	7.746 196.75	110.767 2813.48
Values given in Table No.	2	3	4	5

4.2.3 Statistics of Rainfall Occurrences

One set of statistical data on precipitation will not be satisfactory for all needs in design; therefore, several sets of statistical data are presented in this section as follows:

4.2.3.1 Design Rainfall Rates

The design rainfall rates in Figure 4.2 and Tables 4.2, 4.3, 4.4, and 4.5 are based on precipitation occurrences; i.e., if precipitation is occurring what is the probability of exceeding a rate? These data are based on occurrences over a year and would be used in design of items continuously exposed, such as launch facilities.

4.2.3.2 Probability that Precipitation Will Not Exceed a Specific Amount in Any One Day

Values for each month with the probability that precipitation will not exceed a specified amount in any one day are given for several selected sites of Aerospace vehicle design interest-Cape Kennedy, Fla.; Edwards Air Force Base and Vandenberg Air Force Base, Calif.; New Orleans, La.; and Wallops Test Range, Va. in Tables 4.7, 4.8, 4.9, 4.10, and 4.11 respectively. The

TABLE 4.7 PROBABILITY THAT PRECIPITATION WILL NOT EXCEED A SPECIFIC AMOUNT IN ANY ONE DAY, CAPE KENNEDY, FLA.

Amount (in.)	Amount (mm)	Jan %	Feb %	March %	Apr %	May %	June %
0.00	0.00	68.1	60.8	62.2	70.6	64.2	54.7
Trace	Trace	77.1	71.4	71.3	80.0	76.2	65.7
0.01	0.25	79.0	74.3	72.5	82.7	79.4	68.4
0.05	1.27	84.8	79.4	77.5	86.6	84.7	74.1
0.10	2.54	87.1	82.3	81.6	89.3	89.4	75.8
0.25	6.35	90.0	85.8	87.8	93.5	92.9	82.8
0.50	12.70	93.9	91.6	91.6	95.9	96.4	90.8
1.00	25.40	97.1	96.1	96.3	98.0	99.3	97.1
2.50	63.50	99.4	100.0	99.5	99.5	100.0	99.8
5.00	127.00	100.0	100.0	99.8	99.8	100.0	100.0

Amount (in.)	Amount (mm)	July %	Aug %	Sept %	Oct %	Nov %	Dec %
0.00	0.00	56.8	52.6	40.0	47.4	62.1	64.2
Trace	Trace	65.8	63.9	53.9	61.6	74.2	78.1
0.01	0.25	68.4	66.2	57.5	63.9	77.2	81.0
0.05	1.27	73.2	69.4	62.7	72.0	83.9	86.8
0.10	2.54	75.8	74.9	67.9	76.8	86.9	89.4
0.25	6.35	83.5	80.7	75.8	85.5	90.8	93.3
0.50	12.70	88.3	88.4	83.7	91.3	92.6	96.5
1.00	25.40	93.8	93.6	92.2	95.5	96.2	99.1
2.50	63.50	99.6	99.7	97.4	99.4	99.2	100.0
5.00	127.00	99.6	100.0	99.8	99.7	99.5	100.0

The 100% values in the table indicate no chance of exceeding certain amounts of precipitation during most of the months, however, it should be realized that the length of available data records is not long and that there is always a chance of any meteorological extreme of record being exceeded.

TABLE 4.8 PROBABILITY THAT PRECIPITATION WILL NOT EXCEED A SPECIFIC AMOUNT IN ANY ONE DAY, EDWARDS AFB, CALIF.

Amount		Jan	Feb	March	Apr	May	June
(in.)	(mm)	%	%	%	%	%	%
0.00	0.00	81.7	81.8	82.6	86.7	95.1	98.8
Trace	Trace	88.0	88.9	89.6	93.8	98.6	99.5
0.01	0.25	88.9	89.5	91.3	94.8	99.0	99.5
0.05	1.27	91.7	92.1	93.8	96.4	99.1	99.5
0.10	2.54	93.5	93.5	95.5	97.6	99.4	99.5
0.25	6.35	96.9	95.6	98.0	99.0	100.0	99.9
0.50	12.70	98.8	98.3	99.1	99.6	100.0	100.0
1.00	25.40	99.8	99.6	99.8	100.0	100.0	100.0
2.50	63.50	100.0	100.0	99.9	100.0	100.0	100.0
5.00	127.00	100.0	100.0	100.0	100.0	100.0	100.0

Amount		July	Aug	Sept	Oct	Nov	Dec
(in.)	(mm)	%	%	%	%	%	%
0.00	0.00	94.7	95.2	94.6	93.0	89.8	85.2
Trace	Trace	99.0	98.1	97.8	95.8	94.2	90.8
0.01	0.25	99.3	98.1	98.2	96.1	94.4	91.4
0.05	1.27	99.7	98.9	98.9	97.2	96.4	93.7
0.10	2.54	99.7	99.3	98.9	98.2	97.0	94.9
0.25	6.35	100.0	99.6	99.2	99.2	98.4	96.7
0.50	12.70	100.0	99.9	99.8	99.6	99.3	99.0
1.00	25.40	100.0	100.0	99.9	99.7	100.0	99.9
2.50	63.50	100.0	100.0	100.0	100.0	100.0	100.0
5.00	127.00	100.0	100.0	100.0	100.0	100.0	100.0

The 100% values in the table indicate no chance of exceeding certain amounts of precipitation during most of the months, however, it should be realized that the length of available data records is not long and that there is always a chance of any meteorological extreme of record being exceeded.

TABLE 4.9 PROBABILITY THAT PRECIPITATION WILL NOT EXCEED A SPECIFIC AMOUNT IN ANY ONE DAY, VANDENBERG AFB, CALIF.

Amount		Jan	Feb	March	Apr	May	June
(in.)	(mm)	%	%	%	%	%	%
0.00	0.00	69.4	70.4	61.7	70.4	71.8	70.0
Trace	Trace	79.1	75.9	72.2	80.4	94.0	94.8
0.01	0.25	81.1	76.9	74.6	82.5	96.8	97.7
0.05	1.27	83.5	81.4	83.9	87.9	98.0	100.0
0.10	2.54	88.3	84.4	85.9	90.8	98.8	100.0
0.25	6.35	91.5	90.4	91.5	95.4	99.6	100.0
0.50	12.70	95.1	94.4	96.3	97.5	100.0	100.0
1.00	25.40	98.3	96.9	98.7	99.2	100.0	100.0
2.50	63.50	99.9	99.9	99.5	100.0	100.0	100.0
5.00	127.00	100.0	100.0	99.9	100.0	100.0	100.0
Amount		July	Aug	Sept	Oct	Nov	Dec
(in.)	(mm)	%	%	%	%	%	%
0.00	0.00	62.4	63.4	77.9	79.4	73.3	73.8
Trace	Trace	98.2	94.9	95.4	95.1	82.6	80.6
0.01	0.25	98.9	98.1	95.8	95.5	83.3	83.1
0.05	1.27	100.0	98.8	97.5	95.9	85.9	87.4
0.10	2.54	100.0	99.5	97.9	96.7	87.4	89.2
0.25	6.35	100.0	99.9	98.7	97.5	90.0	93.5
0.50	12.70	100.0	100.0	99.9	98.7	94.4	97.1
1.00	25.40	100.0	100.0	100.0	99.5	98.8	99.6
2.50	63.50	100.0	100.0	100.0	99.9	99.9	100.0
5.00	127.00	100.0	100.0	100.0	100.0	100.0	100.0

The 100% values in the table incicate no chance of exceeding certain amounts of precipitation during most of the months, however, it should be realized that the length of available data records is not long and that there is always a chance of any meteorological extreme of record being exceeded.

TABLE 4.10 PROBABILITY THAT PRECIPITATION WILL NOT EXCEED A SPECIFIC AMOUNT IN ANY ONE DAY, NEW ORLEANS, LA.

Amount (in.)	Amount (mm)	Jan %	Feb %	March %	Apr %	May %	June %
0.00	0.00	77.1	70.2	73.6	79.7	75.9	72.2
0.01	0.25	77.7	71.1	74.1	79.9	76.4	72.6
0.05	1.27	80.9	74.5	78.1	81.9	78.0	77.7
0.10	2.54	85.7	76.4	81.0	83.6	82.9	82.3
0.20	5.08	89.1	80.4	82.8	87.0	86.5	85.3
0.50	12.70	94.0	88.8	88.6	91.2	92.2	90.3
1.00	25.40	97.4	93.8	92.9	95.3	95.6	93.8
2.00	50.8	98.9	97.8	97.9	97.8	99.0	98.8
5.00	127.00	99.7	99.7	99.7	100.0	100.0	100.0
10.00	254.00	100.0	100.0	100.0	100.0	100.0	100.0
Amount (in.)	**Amount (mm)**	**July %**	**Aug %**	**Sept %**	**Oct %**	**Nov %**	**Dec %**
0.00	0.00	54.5	70.1	69.2	84.4	83.4	77.6
0.01	0.25	55.8	71.3	71.1	85.6	84.7	78.2
0.05	1.27	61.4	74.4	76.3	88.2	85.7	80.7
0.10	2.54	67.4	79.3	79.2	90.5	87.4	83.2
0.20	5.08	73.3	83.5	84.4	93.4	89.4	85.2
0.50	12.70	81.5	92.4	90.3	96.0	94.0	91.9
1.00	25.40	91.5	95.7	94.5	98.0	97.3	95.2
2.00	50.80	96.7	98.2	98.0	99.7	98.3	99.4
5.00	127.00	100.0	100.0	99.0	100.0	99.7	99.7
10.00	254.00	100.0	100.0	100.0	100.0	100.0	100.0

The 100% values in the table indicate no chance of exceeding certain amounts of precipitation during most of the months, however, it should be realized that the length of available data records is not long and that there is always a chance of any meteorological extreme of record being exceeded.

TABLE 4.11 PROBABILITY THAT PRECIPITATION WILL NOT EXCEED A SPECIFIC AMOUNT IN ANY ONE DAY, WALLOPS TEST RANGE, VA. (BASED ON LANGLEY AFB DATA)

Amount		Jan	Feb	March	Apr	May	June
(in.)	(mm)	%	%	%	%	%	%
0.00	0.00	54.2	51.4	50.0	51.7	54.2	54.0
Trace	Trace	68.8	66.8	65.5	70.1	69.3	70.0
0.01	0.25	71.2	69.0	68.7	72.4	71.4	71.2
0.05	1.27	75.9	74.3	74.2	78.8	76.1	76.0
0.10	2.54	80.5	78.0	78.9	82.4	79.4	79.5
0.25	6.35	87.7	84.3	86.3	89.2	86.6	87.2
0.50	12.70	93.3	90.2	92.5	94.5	92.8	92.9
1.00	25.40	98.0	97.7	97.7	97.7	97.5	97.4
2.50	63.50	99.0	100.0	99.8	100.0	99.5	99.5
5.00	127.00	100.0	100.0	100.0	100.0	100.0	99.8
10.00	254.00	100.0	100.0	100.0	100.0	100.0	99.9

Amount		July	Aug	Sept	Oct	Nov	Dec
(in.)	(mm)	%	%	%	%	%	%
0.00	0.00	52.6	55.2	62.8	64.0	58.1	59.4
Trace	Trace	68.0	69.0	75.4	76.5	71.0	72.6
0.01	0.25	70.1	72.5	77.8	78.0	73.2	74.5
0.05	1.27	74.2	77.7	81.5	81.8	78.7	79.1
0.10	2.54	78.2	79.8	84.7	85.6	82.8	83.2
0.25	6.35	84.0	85.3	88.0	90.2	88.3	88.2
0.50	12.70	90.6	90.5	91.6	93.4	93.2	93.1
1.00	25.40	94.9	94.8	96.3	96.9	97.6	98.6
2.50	63.50	99.2	98.8	99.2	99.6	99.8	99.9
5.00	127.00	100.0	99.9	99.8	99.8	100.0	100.0

The 100% values in the table indicate no chance of exceeding certain amounts of precipitation during most of the months, however, it should be realized that the length of available data records is not long and that there is always a chance of any meteorological extreme of record being exceeded.

values in the tables should not be interpreted to mean that the amount of precipitation occurs uniformly over the 24-hr period, since it is more likely that most or all of the amounts occurred in a short period of the day.

4.2.3.3 Rainfall Rates Versus Duration for 50th, 95th, and 99th Percentile, Given a Day with Rain for the Highest Rain Month, Kennedy Space Center, Fla.

Rainfall rates for various durations for the 50th, 95th, and 99th percentiles, given a day with rain in the highest rain month are given in Table 4.12 for Kennedy Space Center, Fla. The values for precipitation amounts over the duration given should not be interpreted to mean that the amount of precipitation occurred uniformly over the period, since it is possible to have had the total amount of the rain (at rates as high as those given in Table 4.2) in a shorter period of time within the duration to obtain the total rate for the period. The 99th percentile total of 49 mm (1.93 in.) (Table 4.12) could have occurred as 7.6 mm (0.3 in.) in 1 min, 17.8 mm (0.7 in.) in 5 min, and 23.6 mm (0.93 in.) in 11 min [at 15-min rate of 132 mm (5.0 in. hr^{-1})] at rates as high as those in Table 4.12.

4.2.4 Distribution of Rainfall Rates with Altitude

Rainfall rates normally decrease with altitude when rain is striking the ground. The rainfall rates at various altitudes in percent of the surface rates are given in Table 4.13 for all areas [4.4].

Precipitation above the ground is generally colder than at the ground and frequently occurs as supercooled drops which may cause icing on objects moving through the drops. Such icing can be expected to occur when the air temperature is -2.2° C (28° F). The amount of icing (i.e., rate of formation) is related to the speed and shape of the object. For the geographic areas considered in this report, these conditions usually occur between 30- and 10-km altitude.

4.2.5 Types of Ice Formation

The type of ice which will form on the outside exposed surfaces of cryogenic tanks is related to the temperature of the tank surface, precipitation rate, drop size, and the wind velocity (or tank velocity). In general, the larger the drop size and the higher the temperature, precipitation rate, and wind speed, the denser the ice will form until a condition is reached where surface temperatures are too high for ice to form. If the precipitation is at too high a temperature at relatively high precipitation rates and wind speed, it may warm the tank sufficient to melt ice which previously formed.

Table 4.14 summarizes ice types for various tank wall temperatures with moderate precipitation (over 10 mm hr^{-1}).

TABLE 4.12 HIGHEST RAINFALL RATE VERSUS DURATION FOR VARIOUS PROBABILITIES, GIVEN A DAY WITH RAIN FOR THE HIGHEST RAIN MONTH KENNEDY SPACE CENTER, FLA.

Duration	PERCENTILE											
	50				95				99			
	(in.)	(mm)	in. hr^{-1}	mm hr^{-1}	(in.)	(mm)	in. hr^{-1}	mm hr^{-1}	(in.)	(mm)	in. hr^{-1}	mm hr^{-1}
5 min	0.22	5.6	2.6	66.0	0.72	18.0	8.7	221.0	1.00	25.0	12.0	305.0
15 min	0.23	5.8	0.93	24.0	0.88	22.0	3.5	89.0	1.30	33.0	5.2	132.0
1 hr	0.25	6.4	0.25	6.4	1.17	30.0	1.17	30.0	1.93	49.0	1.93	49.0
6 hr	0.28	7.1	0.05	1.3	1.55	39.0	0.26	6.6	3.18	81.0	0.53	13.0
24 hr	0.43	10.9	0.02	0.5	2.62	67.0	0.11	2.8	5.00	127.0	0.21	5.3

TABLE 4.13. DISTRIBUTION OF RAINFALL RATES WITH HEIGHT FOR ALL LOCATIONS

Height (Geometric) Above Surface (km)	% Surface Rate
SRF	100
1	90
2	75
3	57
4	34
5	15
6	7
7	2
8	1
9	0.1
10 and over	< 0.1

TABLE 4.14. ICE TYPES AS A FUNCTION OF TANK WALL TEMPERATURES

Temperature of Tank Wall			Density Range		
°F	°C	Type of Ice	lb ft^{-3}	g cm^{-3}	Remarks
23 to 32	-5 to 0	Clear ice	60	0.69	hard dense ice
0 to 23	-18 to -5	milky ice or clear ice with air bubbles	43-53	0.69-0.85	
below 15	below -9	Rime ice	18-25	0.29-0.40	crumbly

4.2.6 Hydrometeor Characteristics with Altitude

Raindrops falling on the surface may originate at higher altitude as some other form of hydrometeor, such as ice or snow. The liquid water content of these hydrometeors per unit volume would have a distribution similar to that given in Table 4.9 for rainfall.

A summary of the hydrometeor characteristics from Reference 4.6 is given in Table 4.15.

TABLE 4.15. SUMMARY OF HYDROMETEOR CHARACTERISTICS

Type of Hydrometeor	Altitude (km)	Drop Diameter (μm)		Concentration per Unit Volume (cm^3)		Liquid Water Content Per Unit Volume ($g\ m^{-3}$)		Ambient Temperature (°C)
	Range	Range	Rep.	Range	Rep.	Range	Rep.	Range ≈
Layer Clouds	sfc-1.5	<1-40	11	<10-10 000	500	<0.1-1	0.2	+30 to -15
Layer Clouds	2.5-7.5	<1-50	12	<20-1000	100	<0.1-1	0.2	+20 to -25
Layer Clouds (ice crystals)	7.5-15.0	<10-10 000	100	<0.1-10	0.2	<0.01-0.1	0.02	-10 to -55
Convective Clouds Fair Weather Cumulus	0.5-8.0	<1-75	12	<10-10 000	300	<0.1-1	0.5	+20 to -30
Cumulus Congestus	0.5-13.0	<1-200	25	<10-10 000	150	<1-10	4.0	+20 to -55
Continuous Type Rain	sfc-6.0	<500-3000	1000	<50-3000*	500*	<0.05-0.7	0.1	+30 to -15
Shower Type Rain	sfc-13.0	<500-7000	2000	<10-3000*	500*	<0.1-30	1.0	+30 to -55
Coalescence (Warm) Rain	sfc-5.0	<100-1000	500	<500-50 000*	3000*	<0.05-0.1	0.1	+30 to 0
Hail	sfc-13.0	<0.01-13cm	0.8cm	<0.5-1000*	50*	<0.1-0.9**	0.8**	+15 to -55
Ice and Snow Crystals	sfc-13.0	<100-20 000	5000	<1-1000*	100*	<0.001-0.7***	0.07***	+5 to -55

1. Rep.: Representative value or value most frequently encountered
* Per m^3
** Density of particles ($g\ cm^{-3}$)
*** Mass of crystals (mg)

4.3 Snow

The accumulation of snow on a surface produces stress. For a flat horizontal surface, the stress is proportional to the weight of the snow directly above the surface. For long narrow objects, such as pipes or wires lying horizontally above a flat surface (which can accumulate the snow), the stress can be figured as approximately equal to the weight of the wedge of snow with the sharp edge along the object and extending above the object in both directions at about 45 deg to the vertical. (In such cases, the snow load would be computed for the weight of the snow wedge above the object and not the total snow depth on the ground). The weight of new fallen snow on a surface varies between 0.5 kg m^{-2} per cm of depth (0.25 lb $ft^{-2}in.^{-1}$) and 2.0 kg m^{-2} per cm of depth (1.04 lb $ft^{-2}in.^{-1}$), depending on the atmospheric conditions at the time of snowfall.

4.3.1 Snow Loads at Surface

Maximum snow loads for the following areas are:

a. Huntsville, Wallops Test Range, and Edwards Air Force Base. For horizontal surfaces a snow load of 25 kg m^{-2} (5.1 lb ft^{-2}) per 24-hr period (equivalent to a 10-in. snowfall) to a maximum of 50 kg m^{-2} (10.2 lb ft^{-2}) in a 72-hr period, provided none of the snow is removed from the surface during that time, should be considered for design purposes.

b. Vandenberg Air Force Base, White Sands Missile Range, and Sacramento areas. For horizontal surfaces, a maximum snow load of 10 kg m^{-2} (2.0 lb ft^{-2}) per one 24-hr period should be considered for design purposes.

c. Kennedy Space Center and New Orleans area snow loads need not be considered.

4.3.2 Snow Particle Size

Snow particles may penetrate openings (often openings of minute size) in equipment and cause malfunction of mechanical or electrical components, either before or after melting. Particle size, associated wind speed, and air temperature to be considered are as follows:

a. Huntsville, Wallops Test Range, and Edwards Air Force Base. Snow particles 0.1-mm (0.0039-in.) to 5-mm (0.20-in.) diam.; wind speed 10 m sec^{-1} (19 knots); air temperature -17.8°C (0° F).

4.22

b. Vandenberg Air Force Base, White Sands Missile Range, and Sacramento areas. Snow particles 0.5-mm (0.020-in.) to 5-mm (0.20-in.) diam.; wind speed 10 m sec^{-1} (19 knots); air temperature -5.0° C (23° F).

4.4 Hail

Hail is one of the most destructive weather forces in nature, being exceeded only by hurricanes and tornadoes. Hail normally forms in extremely well-developed thunderstorms during warm weather and rarely occurs in winter months or when the air temperature is below 0° C (32° F). Although the average diameter of hailstones is 8 mm (0.31 in.) [4.4], hailstones larger than 12.7 mm (0.5 in.) in diameter frequently fall, while stones 50 mm (2.0 in.) in diameter can be expected annually somewhere in the United States. The largest measured hailstone in the Unites States was 137 mm (5.4 in.) in diameter and had a weight of 0.68 kg (1.5 lb) [4.6 and 4.7]. Three environmental effects on equipment must be considered.

The accumulation of hail, as with snow, stresses the object by its weight. Although hail has a higher density than snow, 2.4 kg m^{-2} cm^{-1} (1.25 lb $ft^{-2}in.^{-1}$), the extreme load from hail will not exceed the extreme snow load at any area of interest; therefore, the snow load design will adequately cover any hail loads expected.

Large hailstones, because of weight and velocity of fall, are responsible for structural damage to property [4.7]. To actually designate locations where hailstones, with specific sizes of hail, will fall is not possible. However, the following information can be used as a guide for design and scheduling (these values are most applicable to the design of ground support equipment and protective covering for the space vehicles during the transporting of vehicles).

4.4.1 Hail at Surface

a. Huntsville, Edwards Air Force Base, Gulf Transportation, New Orleans, Wallops Test Range, and White Sands Missile Range.

1. A maximum hailstone size of 50 mm (2 in.) in diameter with an occurrence probability of one time in 15 yr.

2. Damaging hailstorms occur most frequently between 3 p.m. and 9 p.m. during May through September. April is the month of highest frequency-of-occurrence of hailstorms for Huntsville and Gulf Transportation. March is the month of highest frequency-of-occurrence of hailstorms for White Sands Missile Range and Edwards Air Force Base; and May is the month of highest frequency-of-occurrence of hailstorms for Wallops Test Range.

3. The period of large hail (over 25 mm in diameter) will not be expected to last more than 15 min and should have a maximum total accumulation of 50 mm (2 in.) for depth of hailstones on horizontal surfaces.

4. Velocity of fall equals 30.5 m sec^{-1} (100 ft sec^{-1}) for each stone.

5. Wind speed equals 10 m sec^{-1} (33 ft sec^{-1}).

6. Density of hailstones equals 0.80 g cm^{-3} (50 lb ft^{-3}).

b. Eastern Test Range

1. A maximum hailstone size of 25.4 mm (1 in.) in diameter with an occurrence probability of one time in 30 yr may be expected.

2. Damaging hailstones occur most frequently between 3 p.m. and 9 p.m. during April through June. May is the month of highest frequency of occurrence for hailstorms.

3. The period of large hail will not be expected to last more than 15 min and should have a maximum total accumulation of 12.5 mm (0.5 in.) for depth of hailstones on horizontal surfaces.

4. Velocity of fall equals 20 m sec^{-1} (66 ft sec^{-1}) for each stone.

5. Wind speed equals 10 m sec^{-1} (33 ft sec^{-1}).

6. Density of hailstones equals 0.80 g cm^{-3} (50 lb ft^{-3}).

c. Vandenberg Air Force Base will not need consideration for hail.

4.4.2 Distribution of Hail with Altitude.

Although it is not the current practice to design space vehicles for flight in thunderstorms, data on distribution with altitude are presented as an item of importance. The probability of hail increases with altitude from the surface to 5 km and then decreases rapidly with increasing height. Data on Florida thunderstorms, giving the number of times hail was encountered at various altitudes during aircraft flights [4.8], are given in Table 4.16 for areas specified in Paragraph 4.4.1.

TABLE 4.16. DISTRIBUTION OF HAIL WITH HEIGHT FOR ALL LOCATIONS [4.9]

Height (Geometric) Above Surface (km)	Occurrence of Hail % of Flights Through Thunderstorms
2	0
3	3.5
5	10
6	4
8	3

4.5 Laboratory Test Simulation

In the laboratory, simulated rain droplets are usually produced by use of a single orifice, mounted above the equipment being tested. Such a test will not necessarily duplicate the natural occurrence of precipitation and may or may not reflect the true effect of natural precipitation on the equipment since. a single orifice produces drops all nearly the same size.

Each test should be evaluated to determine if the following three factors which occur in natural precipitation are important in the test.

4.5.1 Rate of Fall of Raindroplets

Natural raindroplets will have usually fallen a sufficient distance to reach their terminal velocity (maximum rates of fall). Simulation of such rates of fall in the laboratory requires the droplets to fall a suitable distance. Large droplets (4-mm diam. and greater) will require about 12 m (39 ft) to reach terminal velocity.

The higher velocities of fall will modify the effect of the droplets on equipment. Values of terminal velocities of water droplets were measured by Gunn and Kinzer [4.9]. Their results gave the values in Table 4.17. Reference 4.9 should be obtained for more detailed information.

Gunn and Kinzer [Ref 4.9] found that water droplets greater than 5.8 mm would usually break up before the terminal velocity was reached.

4.5.2 Raindrop Size and Distribution

Normal rainfall has a variety of drop sizes with a distribution as shown in Figure 4.3. Figure 4.3 illustrates the wider distribution of droplet sizes in

TABLE 4.17. VALUES OF TERMINAL VELOCITIES OF WATER DROPLETS [4.9]

Drop Diameter (m)	Terminal Velocity ($m\ sec^{-1}$)
1	4.0
2	6.5
3	8.1
4	8.8
5	9.1
5.8	9.2

the heavier rain which has the larger droplets. The maximum drop diameter distribution could be adequately simulated by a number of orifices, all at the same water pressure, to produce droplets of about 1-, 2-, 3-, and 4- and 5-mm diam. For the median drop diameter, the use of a single orifice to produce 1-mm droplets would be suitable.

4.5.3 Wind Speed

In most cases of natural rain there will be wind blowing near horizontal. This wind will modify the droplet paths from a vertical path to a path at some angle to the vertical; thus causing the rain droplets to strike at an angle. In addition, unless the equipment is streamlined in the direction of the wind, small vortices may develop at the surface of the equipment. These vortices may cause a considerable amount of the precipitation to flow in a variety of directions, including upward against the bottom of the equipment.

Studies of thunderstorms with rainfall rates from 12.7 to 7 mm hr^{-1} (0.5 to 3.0 in. hr^{-1}) with relationship to wind speeds occurring at the same time have shown an average mean wind speed of 5 m sec^{-1} for all storms combined. Peak winds were as high as 16 m sec^{-1}. All storms, except one with rates exceeding 25 mm hr^{-1}, had peak winds at least 5 m sec^{-1} greater than the mean wind for the same storm.

4.5.4 Temperatures

The air temperature at the ground usually decreases several degrees at the start of rainfall with rates in excess of 12.7 mm hr^{-1} (0.5 in. hr^{-1}). The amount of the temperature decrease is greatest in the summer when the temperature is high [greater than 32° C (90° F)] with the final temperature approximately 24° C (75° F). In the winter the temperature decrease is usually about 28° C (5° F). At the end of the rainfall the summer temperature will

C7

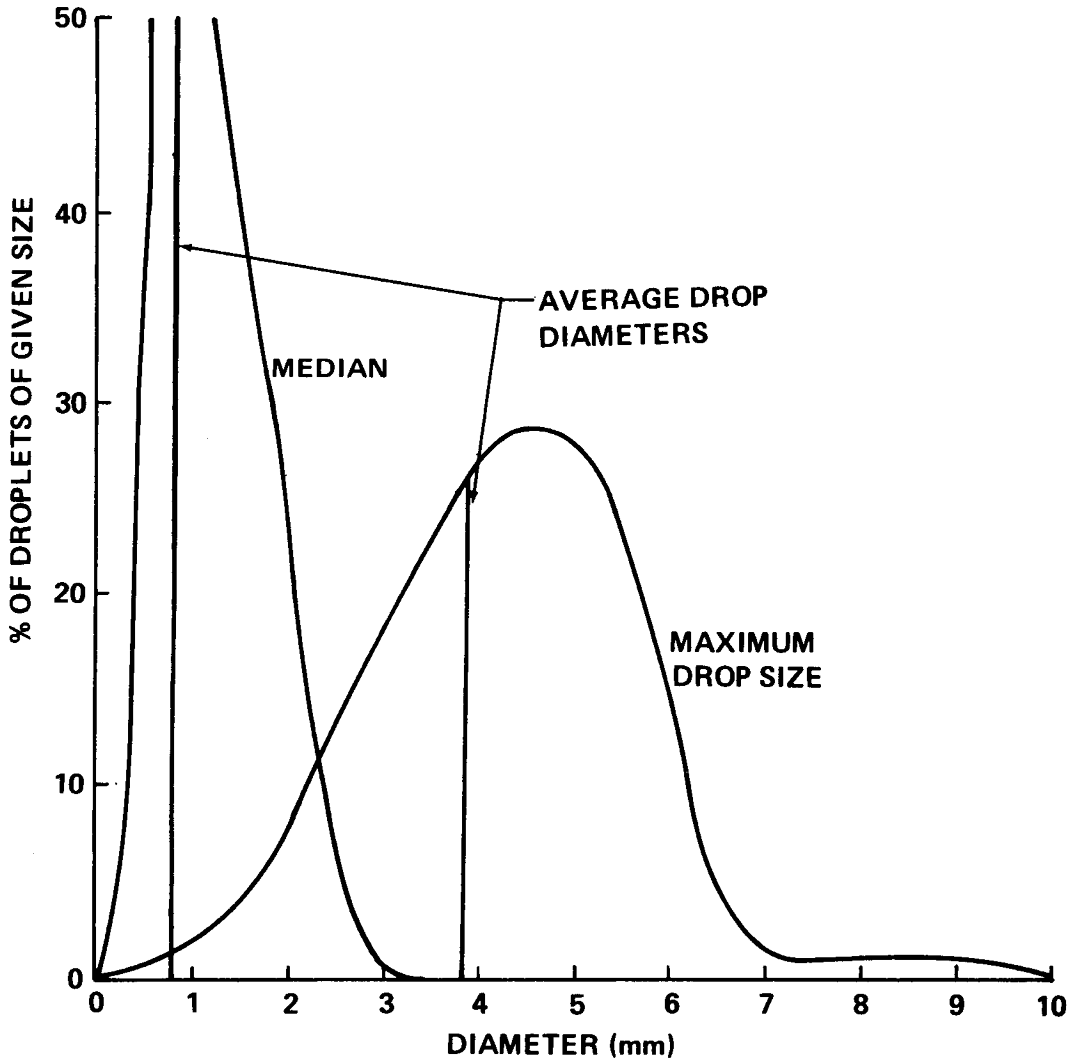

Figure 4.3 Distribution of drop sizes of rain.

increase again to nearly the same values as before the storm, but in the winter there is no general pattern of warming. This decrease in temperature is caused by the water droplets being colder than the surface air temperature.

4.5.5 Recommended Items to Include in Laboratory Rainfall Tests

The following items need to be considered in rainfall tests in the laboratory:

a. Raindrop size distribution.
Rates less than 25 mm hr^{-1} — drop size of 1 mm.
Rates greater than 25 mm hr^{-1} — drop size from 1 to 5 mm.

b. Rate of fall of drops. Drops should fall at least 12 m to obtain terminal velocity.

c. Wind Speed. A mean wind of 5 m sec^{-1} with gusts of 15 m sec^{-1} of 30-sec duration at least once in each 15-min period.

d. Temperature. The temperature in the chamber should decrease from 32° C (90° F) to 24° C (75° F) at the start of rainfall for representative summer tests and should be maintained at 10° C (50° F) for winter tests. The decrease in air temperature may be obtained by using water at, or slightly below 24° C for the summer tests.

4.5.5.1 Idealized Rain Cycle, Kennedy Space Center, Fla.

For design studies and laboratory tests, the idealized rain cycle shown in Figure 4.4 and Table 4.18 should be used. The rainfall in the cycle is representative of the 95th percentile Cape Kennedy rainfall on any day with rain during the worst rain month and the associated wind speeds, temperatures, and drop sizes expected with the rain.

4.6 Rain Erosion

4.6.1 Introduction

With the advent of high-speed aircraft a new phenomenon was encountered in the erosion of paint coatings, structural plastic components, and even metallic parts by the impingement of raindrops on surfaces. This was first observed soon after World War II on fighter aircraft capable of speeds over 178 m sec^{-1} (400 mph) [4.10]. This initiated rain erosion research at the Air Force Materials Laboratory, Wright-Patterson Air Force Base and at the Royal Aircraft Establishment, Farmborough, England. Tests conducted by the British Ministry of Aviation at the Royal Aircraft Establishment [4.11] have

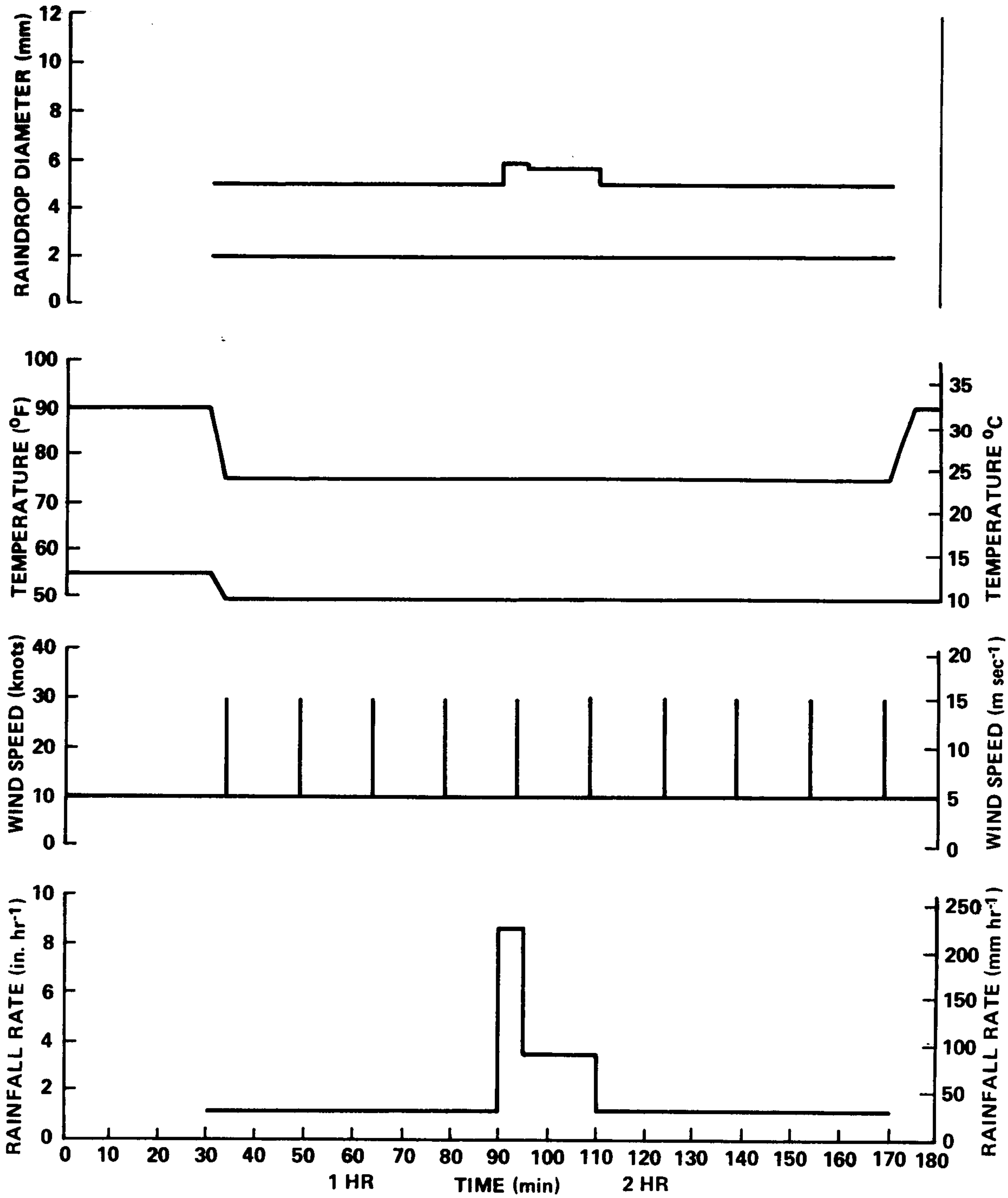

Figure 4.4 Idealized Rain Cycle, Kennedy Space Center, Fla.; based on highest rain month.

TABLE 4.18. IDEALIZED RAIN CYCLE, KENNEDY SPACE CENTER, FLA.; BASED ON HIGHEST RAIN MONTH

Cycle	Rainfall Rate		Wind Speed		Raindrop Size		Temperature			
					largest	average	Summer		Winter	
min	mm hr^{-1}	in. hr^{-1}	m sec^{-1}	knots	mm	mm	°F	°C	°F	°C
0	0	0	5.1	10	0	0	90	32	55	13
30	3.0	1.17	5.1	10	5.0	2	90	32	55	13
32	3.0	1.17	5.1	10	5.0	2	75	24	50	10
33.5	3.0	1.17	15.4	30	5.0	2	75	24	50	10
34	3.0	1.17	5.1	10	5.0	2	75	24	50	10
48.5	3.0	1.17	15.4	30	5.0	2	75	24	50	10
49	3.0	1.17	5.1	10	5.0	2	75	24	50	10
63.5	3.0	1.17	15.4	30	5.0	2	75	24	50	10
64	3.0	1.17	5.1	10	5.0	2	75	24	50	10
78.5	3.0	1.17	15.4	30	5.0	2	75	24	50	10
79	3.0	1.17	5.1	10	5.0	2	75	24	50	10
90	22.0	8.7	5.1	10	5.9	2	75	24	50	10
93.5	22.0	8.7	15.4	30	5.9	2	75	24	50	10
94	22.0	8.7	5.1	10	5.9	2	75	24	50	10
95	8.9	3.5	5.1	10	5.8	2	75	24	50	10
108.5	8.9	3.5	15.4	30	5.8	2	75	24	50	10
109	8.9	3.5	5.1	10	5.8	2	75	24	50	10
110	3.0	1.17	5.1	10	5.0	2	75	24	50	10
123.5	3.0	1.17	15.4	30	5.0	2	75	24	50	10
124	3.0	1.17	5.1	10	5.0	2	75	24	50	10
138.5	3.0	1.17	15.4	30	5.0	2	75	24	50	10
139	3.0	1.17	5.1	10	5.0	2	75	24	50	10
153.5	3.0	1.17	15.4	30	5.0	2	75	24	50	10
154	3.0	1.17	5.1	10	5.0	2	75	24	50	10
168.5	3.0	1.17	15.4	30	5.0	2	75	24	50	10
169	3.0	1.17	5.1	10	5.0	2	75	24	50	10
170	0	0	5.1	10	0	0	75	24	50	10
180	0	0	5.1	10	0	0	90	32	50	10

resulted in a table of rates of erosion for various materials and coatings. These materials and coatings were tested at speeds of 220 m sec^{-1} (428 knots). At the Air Force Materials Laboratory, a number of rotating (whirling) arm apparatuses have been used. The current rotating arm apparatus will permit testing of samples of materials at speeds up to 403 m sec^{-1} (900 mph) (Mach 1.2) with simulated rainfall variable through a wide variety of rates. Normally the tests are made at 224 m sec^{-1} (500 mph) and at 25.4 mm hr^{-1} (1 in. hr^{-1}) or 50.8 mm hr^{-1} (2 in. hr^{-1}) of rainfall [4.12]. A number of flight tests using F-80 aircraft in rain were made and compared with the rotating arm tests. The ranking of the test materials for rain erosion was similar for the variety of materials tested, but the time to erode materials varied because of differences in the intensities of the various environments. The natural erosion conditions included hail, ice crystal, and liquid water impingement [4.13].

4.6.2 Rain Erosion Criteria

Rain erosion may be severe enough to affect the performance of a space vehicle. Sufficient data are not available to present specific extreme values of exposure for various materials used in design. Experience and results of the various tests indicate that materials should be carefully considered. Any materials in which failure in rain erosion would have an effect on the mission should be subjected to tests for rain erosion. Criteria for rain-eriosion tests should be based on Table 4.19.

Tests by A.A. Fyall at the Royal Aircraft Establishment [4.14] on single rain droplets have shown that the rain erosion rate may increase considerably with lower air pressure (higher altitude) because of the lower cushioning effect of the air on the droplets at impact.

TABLE 4.19. RAIN EROSION CRITERIA

Rainfall Rate		Duration of Test	Velocity** of Test	Raindrop Size	Angle of Attack
(mm hr^{-1})	(in. hr^{-1})	(min)		(mm)	(deg)
2.5	0.10	60	selected by the maximum velocity of the space vehicle in areas of rainfall	2	selected by use of material, i.e. 10° 20°, 40°, etc. (wind and tail leading edges) 70°, 80°, 90° nose cap
12.5	0.50	10		2	
25.4	1.00	10		2	
50.8	2.00*	10		2	

* A rate of 50.8 mm hr^{-1} (2.00 in. hr^{-1}) would only be used for the most critical materials.
** The velocities selected could modify the duration of test since any areas in clouds of rainfall rates in excess of 12.8 mm hr^{-1} (0.5 in. hr^{-1}) would be limited in size ~ 97 km (~ 60 mi) and the length of time for the space vehicle to travel a distance of 97 km would decrease with increased speed.

REFERENCES

4.1 Rainfall Intensity Duration-Frequency Curves for Selected Stations in the United States, Alaska, Hawaiian Islands, and Puerto Rico. Technical Paper No. 25, U. S. Department of Commerce, Washington, D.C., Dec. 1955.

4.2 Gumble, E. J.: Statistics of Extremes. Columbia University Press, 1958.

4.3 Billions, Novella S.: A Study of Raindrop Size Distributions and Probability of Occurrence. Report No. RR-TR-65-1, U. S. Army Missile Command, Redstone Arsenal, Ala., 1965.

4.4 Handbook of Geophysics, Revised Edition, The MacMillan Company, N.Y., 1960.

4.5 Vaughan, William W.: Distribution of Hydrometeors with Altitude for Missile Design and Performance Studies. ABMA DA-TM-138-59, Army Missile Command, Huntsville, Ala., 1959.

4.6 1941 Yearbook of Agriculture, Climate and Man. United States Department of Agriculture, United States Government Printing Office, Washington, D. C., 1941.

4.7 National Summary, Annual 1960, Climatological Data. United States Department of Commerce Weather Bureau, 1960.

4.8 Byers, Horace R.; and Braham, Roscoe R., Jr.: The Thunderstorm. United States Government Printing Office, Washington 25, D. C., 1949.

4.9 Gunn, Ross; and Kinzer, Gilbert D.: The Terminal Velocity of Fall for Water Droplets in Stagnant Air. Journal of Meteorology. Vol. 6, Aug. 1949, pp. 243-248.

4.10 Wahl, Norman E.: Investigation of the Phenomena of Rain Erosion at Subsonic and Supersonic Speeds. Technical Report AFML-TR-65-330, Air Force Materials Laboratory, Research and Technology Division, Air Force Systems Command, Wright-Patterson Air Force Base, Ohio, Oct. 1965.

4.11 Fyall, A. A.; King, R. B.; and Strain, R. N. C.: Rain Erosion Aspects of Aircraft and Guided Missiles. Journal of the Royal Aeronautical Society, Vol. 66, July 1962, pp. 447-453.

REFERENCES (Concluded)

4.12 Hurley, Charles J.; and Schmitt, George F. Jr.: Development and Calibration of a Mach 1.2 Rain Erosion Test Apparatus. AFML-TR-70-240, Air Force Material Laboratory, Air Force Systems Command, Wright-Patterson Air Force Base, Ohio, Oct. 1970.

4.13 Schmitt, George F., Jr.: Flight Test-Whirling Army Correlation of Rain Erosion Resistance of Materials. AFML-TR-67-420, Air Force Materials Laboratory, Air Force Systems Command, Wright-Patterson Air Force Base, Ohio, Sept. 1968.

4.14 Fyall, A. A.: Single Impact Studies of Rain Erosion. Tech Air. Vol. 26, Oct. 1970, pp. 4-11.

N74-16297

SECTION V. WIND

By

Margaret B. Alexander, S. Clark Brown, Dennis W. Camp,
Glenn E. Daniels, Lee W. Falls, George H. Fichtl, Kelly Hill
John Kaufman, Orvel E. Smith, and William W. Vaughan

5. 0 Introduction

A space vehicle's response to atmospheric disturbances cannot be reduced to the evaluation of one set of response criteria, such as vehicle loads, but it must include many response parameters, the choice of criteria (parameters) depending upon the vehicle configuration and the specific mission. It is also impractical to use only one response calculation method for all phases of vehicle design. Therefore, the studies must be separated into their various phases and parts, using different approaches and methods of evaluation, as the particular phase demands. Although not independent, these phases include (1) preliminary design, (2) final structural design, (3) guidance and control system design and optimization (preliminary and final), and (4) establishment of limits and procedures for launch and flight operations. Thus, the proper selection, representation, and use of wind information require the skillfully coordinated efforts of aerospace meteorologists and engineers.

Winds are characterized by three-dimensional motions of the air, accompanied by large temporal and spatial variations. The characteristics of these variations are a function of synoptic conditions, atmospheric stability, and season, as well as the geographic location of the launch site. It is necessary, therefore, to use good technical judgment and to consider the engineering application of the wind data in preparing criteria that are descriptive and yet concise. The wind environment affects the various vehicle design and operational problem areas in a different manner and requires a unique interpretation and application of the data for each analysis.

During the initial and intermediate phases of the development cycle, the synthetic ground and inflight wind criteria concept has its major value and contribution to the design. Although a certain overall vehicle performance capability in terms of probability may be mentioned as a guideline, it is not realistic to expect a design to be developed that will precisely meet this specified performance capability because of the many unknowns in the vehicle characteristics and design criteria. With the status of current space vehicle technology it is not possible to make, as a result of design procedures or tests, a candid statement about the specific calculated overall design risk or operational capability of a space vehicle. Therefore, it makes good engineering sense to establish a set of idealized or synthetic ground and inflight wind models, which characterize such features as wind magnitude versus height, gust factors, turbulence spectra, wind shears, and directional features of the wind magnitude. They may then be referenced and used in a consistent manner to establish the preliminary and intermediate designs necessary to ensure accomplishment of the expected range of missions for the vehicle development. Furthermore, they assist in isolating those aspects of the wind structure critical to a vehicle design area.

It is currently the accepted practice to use the synthetic wind criteria approach described herein for NASA space vehicle developments during the preliminary and intermediate design phases. These criteria should be carefully formulated to ensure that the appropriate data are employed for vehicle studies in order to be consistent with the degree of resolution available from other vehicle input criteria and the structural/control system simulation models. The synthetic wind profile features may readily be employed to isolate specific design problem areas without resorting to elaborate computations, which are not justified with respect to the other unknown system parameters. In addition, by use of this approach, the designer may, for example, closely approximate the steady-state wind limits for a design or operational configuration. The other features of the wind forcing function may be accommodated with a specified risk level. Using these steady-state wind limits, a multitude of mission and performance analysis studies can rapidly be accomplished relative to launch windows, etc., using the entire available historical record from the steady-state inflight wind (rawinsonde) or ground wind measurement systems. Such records, described in this section, are available for all major launch areas. These statistical records and the synthetic profile concept are also adequate for bias of pitch and yaw programs, range safety studies, preliminary abort analysis, water entry of space vehicles (Space Shuttle solid rocket motor water entry, for example), and related space vehicle operational problems.

When adequately documented and referenced, the synthetic wind criteria concept provides a powerful tool for ensuring consistent design inputs for all users, and it essentially avoids the problem of any oversight errors, which may be very costly to correct in later development phases. Furthermore, they enable various design teams to simultaneously conduct studies and to compare their results on a common basis.

During the latter stages of a vehicle development program, when adequate vehicle response data are available, it is considered highly desirable, if not mandatory, to simulate the vehicle ascent flight and response to actual wind velocity profiles. However, these wind profiles should contain an adequate frequency content in order to encompass the significant periods of response of the vehicle (control mode frequency, first bending mode frequency, etc.). Anything short of this suggested approach would correspond to the use of only another preliminary design approximation of the natural environment. The current acceptable practice is to use a selection of detailed inflight wind profiles (resolution to at least one cycle per 100 meters) obtained by the FPS-16 Radar/Jimsphere technique for the major launch range(s) of concern. These data and their availability are discussed elsewhere in this document. The number of flight performance simulations and detailed wind profiles selected will depend upon the particular vehicle and the design problem involved and how well the vehicle characteristics were established during the preliminary and intermediate design work. The vehicle simulation to detailed inflight wind profiles should constitute, essentially, a verification of the design. It should provide the design organization with added confidence in the capability of the vehicle design and enable it to isolate any critical areas requiring further indepth study to refine the control and structural systems. The profiles used should constitute a selection from the available detailed wind profile records. This selection should be based upon the mission objectives and should be established through discussions between the affected design group and the cognizant organization concerned with wind criteria.

For the prelaunch simulation and flight evaluation of a space vehicle relative to the inflight wind environment, it is recommended that established ground wind reference height anemometers and detailed inflight wind profiles measured by the FPS-16 Radar/Jimsphere system be used to provide adequate resolution, accurate data, and timely measurements. A rapid reduction scheme to ensure a prompt input into prelaunch flight simulation programs is required. It is during the prelaunch phase that accurate and near real-time wind data are mandatory, especially if an almost critical launch wind condition exists. The consequences are obvious. Furthermore, adequate flight evaluations cannot be made without timely and accurate launch wind data.

The above remarks are intended to reflect some currently accepted engineering practices for use of available wind data in the design, development, mission analysis, prelaunch, and flight evaluation phases of a space vehicle program. It is apparent that the wind input employed in terms of resolution, accuracy, representativeness, etc., will depend upon the status of the space vehicle design and the use of reliable data that are consistent with the design requirements at the particular stage of development. An understanding of the use and limitations of wind data in making engineering decisions is required for the design of a space vehicle for a given mission objective(s). This can only be accomplished through a team relationship between the design engineer and meteorologist concerned with wind criteria.

5.4

The information given in this section constitutes guidelines for data that are applicable to various design problems. The selected risk levels employed to determine those characteristics of the ground and inflight winds used in the design are a matter of organizational design philosophy and management decision. To maximize performance flexibility, it is considered best to utilize those data associated with the minimum acceptable risk levels. In addition, such critical mission related parameters as exposure time of a vehicle to natural environment during the various operational plans, launch windows, and launch turnaround period should be carefully considered. Initial design work using unbiased (wind) trajectories on the basis of nondirectional ground or inflight winds is recommended unless the vehicle and its mission are well known and the exact launch azimuth and time(s) are established and rigidly adhered to throughout the project. In designs that use wind-biased trajectories and directional wind criteria, rather severe wind constraints can result if the vehicle is used for another mission, different flight azimuths, or in another configuration. Therefore, caution must be exercised in the employment of wind data to ensure consistency with the physical interpretation relative to the specific design problem. References 5.1 through 5.6 are a few of the many available references which discuss the problems related to the development and specification of wind environments for space vehicle programs.

5.1 Definitions

The following terms are used in this section with the meanings specified here.

5.1.1 Ground Winds

Ground Winds are winds which affect space vehicles during ground operations and immediately on launch and for purposes of this document, can be considered to be winds below a height of about 150 meters above the natural grade.

Average wind speed — See steady-state wind speed.

Gust is a sudden increase in the ground wind speed. It is frequently stated with respect to a mean wind speed. A sudden decrease in the wind speed is sometimes also referred to as a gust (negative).

Free-standing winds are the ground winds that are applied when the vehicle is standing on the launch pad (with or without fuel), after any service structure, support, or shelter has been removed.

Gust factor is the ratio of peak ground wind speed to the average or mean ground wind speed over a finite time period.

Launch design winds are the peak ground winds for which the vehicle can be launched, normally involving a stated design wind at a reference height plus the associated peak wind profile (~99.9%) shape.

On-pad winds are the ground winds that are applied when the vehicle is on the launch pad with protective measures in place, i.e., service structures, support, or shelter.

Peak wind speed is the maximum (essentially, instantaneous) wind speed measured during a specified reference period, such as hour, day, or month.

Steady-state or average wind speed is the mean over a period of about 10 minutes or longer, of the wind speed measured at a fixed height. It is usually assumed constant as, for example, in spectral calculations. Thus, the steady-state or average wind should be the mean which filters out, over a sufficient duration, the effects that would very definitely contribute to the random responses of aerospace vehicles and structures. The average wind speed is sometimes referred to as quasi-steady-state winds.

Reference height (ground winds) is the height above the ground surface (natural grade) to which wind speeds are referred for the establishment of climatological conditions, reference for construction of design wind profiles, and statements of an operational wind constraint. Normally during the design and development phase, a reference height near the base of the vehicle (usually given as the 10- or 18.3-m level) is used. After completion of vehicle development, the operational constraints are stated with respect to a reference height near the top of the vehicle, the height of which is now established at the 152.4-meter level for LC 39 at Kennedy Space Center.

Causes of high ground winds are summarized as follows:

a. Tornadoes: Upper limit unknown; estimated about 103 m/sec (200 knots).

b. Hurricanes: By definition, a tropical storm with winds greater than 33 m/sec (64 knots), upper limit unknown; estimated about 82 m/sec (160 knots).

c. Tropical Storms: By definition, a storm with winds less than 33 m/sec (64 knots) and greater than 17 m/sec (34 knots).

d. Thunderstorms: Upper limit not defined; typical values about 23 m/sec (45 knots); severe thunderstorm by definition greater than 26 m/sec (50 knots).

e. Frontal Passages: Without thunderstorms; winds less than 18 m/sec (35 knots), with squalls same as for thunderstorms.

f. Pressure Gradients: Long duration gusty winds; winds less than 31 m/sec (60 knots).

5.1.2 Inflight Winds

Inflight winds are those winds above a height of about 150 meters.

Design verification data tapes are a selection of detail wind profile data compiled from FPS-16 Radar/Jimsphere data records for use in vehicle final design verification analysis. They consist of a representative monthly selection of wind profiles from which the integrated response of a vehicle to the combined effect of speed, direction, shear, and turbulence (gusts) may be derived. It has application to computation of absolute values of launch probability for a given vehicle.

Design wind speed profile envelopes are envelopes of scalar or component wind speeds representing the extreme steady-state inflight wind value for any selected altitude that will not be exceeded by the probability selected for a given reference period.

Detail wind profile is a wind profile measured by the FPS-16 Radar/Jimsphere or equivalent technique and having a resolution to at least one cycle per 100 meters. Application intended for final design verification purposes and launch delay risk calculations.

Steady-state inflight wind, in this document, refers to the mean wind speed as measured with the rawinsonde system and averaged over approximately 1000 meters in the vertical direction. The assigned height of this wind measurement will be the middle of the 1000 meter layer.

Reference height (inflight winds) is that referred to in constructing a synthetic wind profile.

Scale-of-distance is the vertical distance (thickness of layer) between two wind measurements used in computing wind shears.

Serial complete data represent the completion of a sample of rawinsonde data (selected period) by filling in (inserting) missing data by interpolation, by extrapolation, or by use of data from nearby stations. This operation is performed by professional meteorological personnel familiar with the data.

Shear build-up envelope is the curve determined by combining the reference height wind speed from the wind speed profile envelope with the shears (wind speed change) below the selected altitude (reference height). The shear build-up envelope curve usually starts at zero altitude difference (scale-of-distance) and zero wind speed and ends at the design wind speed value at the referenced altitude for inflight wind response studies.

Synthetic wind speed profile is a design wind profile representing the combination of a reference height design wind with associated envelope shears (wind speed change) and gusts for engineering design and mission analysis purposes.

Wind speed change envelopes (wind shear) represent the values of the change in wind speed over various increments of altitude (100 to 5000 m), computed for a given probability level and associated reference height or related wind speed value at the reference height. These values are combined, and an envelope of the wind speed change is found useful in constructing synthetic wind profiles. Usually the 99 percentile probability level is used for design purposes.

5.1.3 General

Calm winds are those winds with a speed less than 0.5 m/sec (1 knot).

Component wind speed is the equivalent wind speed that any selected wind vector would have if resolved to a specific direction, that is, a wind from the northeast (45-deg azimuth) of 60 m/sec would have a component from the east (90-deg azimuth) of 42.4 m/sec. This northeast wind would be equivalent to a 42.4 m/sec head wind on the vehicle, if the vehicle is launched on an east (90-deg) azimuth.

Percentile — The P percentile is that value of a variable at or below which lies the lowest P percent of a set of data. Section I, page 1.8 of this document should also be consulted for more details on percentiles and probabilities (P). The following relationships exist between probabilities (P) and percentiles in a NORMAL or GAUSSIAN DISTRIBUTION function:

Percentiles	Probability P(%) for normal distribution
Minimum	0.000
Mean - 3σ (standard deviation)	0.135
Mean - 2σ (standard deviation)	2.275
Mean - 1σ (standard deviation)	15.866
Mean ± 0σ (standard deviation)	50.000
Mean + 1σ (standard deviation)	84.134
Mean + 2σ (standard deviation)	97.725
Mean + 3σ (standard deviation)	99.865
Maximum	100.000

Scalar wind speed is the magnitude of the wind vector without regard to direction.

Wind direction is the direction from which the wind is blowing, measured clockwise from true North.

Windiest monthly reference period is the month that has the highest wind speeds at a given probability level.

Wind shear is equal to the difference between wind speeds measured at two specific positions.

5.2 Ground Winds (1-150m)

5.2.1 Introduction

Ground winds for space vehicle applications are defined in this document to be those winds in the lowest 150 meters of the atmosphere. A vehicle positioned vertically on-pad may penetrate this entire region. The winds in this layer of the atmosphere are characterized by very complicated three-dimensional flow patterns with rapid variations in magnitude and direction in space and time. An engineering requirement exists for models which define the structure of wind in this layer because of the complicated and possible critical manner in which a vehicle might respond to certain aspects of the flow in this layer, both while the vehicle is stationary on the launch pad and while in the first few seconds of launch. Some examples of wind effects on space vehicles are von Karman vortex shedding forces resulting in lateral displacements of the vehicle while on pad, and steady-state and time dependent aerodynamic drag forces resulting in base bending moments (steady and time-dependent) in the case of vehicles on pad and vehicle drift and pitch and yaw-plane angular accelerations during vehicle lift-off. Other equally important examples can be cited. The basic treatment of the ground wind problem relative to vertically erect vehicles on-pad and during lift-off has been to statistically define the steady-state and time-dependent aspects of the wind profile along the vertical in such a manner that a particular aspect of the wind environment crucial to space vehicle operations can be specified upon specifying the risk of encountering that particular aspect of the wind environment. It should be noted that in addition to the engineering requirements for on-pad and launch winds for vertically ascending vehicles, a requirement for ground wind models also exists for horizontally flying vehicles for take-off and landing. In a space vehicle context this is especially true for the return flight of the Space Shuttle orbiter vehicle. In this case, there exists in addition to the vertical definition of winds a requirement for models to define the horizontal structure or rather the structure of wind along the landing flight path of the vehicle. This aspect of the natural wind environment will be discussed in Section 5.3.14.

Until recently, several years of average wind speed data measured at the 10-meter level above ground were the only available records with which to develop design and launch ground wind profile criteria. With the evolution of larger and more sophisticated space vehicles, the requirements for more adequate wind profile information have increased. For example, to fulfill the need to provide improved ground wind data, a 150-meter ground wind tower facility was constructed on Merritt Island, Kennedy Space Center, Florida, in close proximity to the Apollo/Saturn launch complex 39. Wind and temperature profile data from this facility have been used in many new studies that have contributed to a significant portion of the information in this chapter on wind profile shaping, gusts, and turbulence spectra. Similar towers are in operation at the various national ranges.

Since ground wind data are applied by space vehicle engineers in various ways and degrees, dependent upon the specific problem, various view-points and kinds of analytical techniques were utilized to obtain the environmental models presented herein. Program planning, for instance, requires considerable climatological insight to determine the frequency and persistence distributions for wind speeds and wind directions. However, for design purposes the space vehicle must withstand certain unique predetermined structural loads that are generated from exposure to known peak ground wind conditions. Ground wind profiles and the ground wind turbulence spectra contribute to the development of the design ground wind models. Surface roughness, thermal environment, and various transient local and large-scale meteorological systems influence the ground wind environment for each launch site.

5.2.2. Considerations in Ground Wind Design Criteria

To establish the ground wind design criteria for aerospace vehicles, several important factors must be considered.

a. Where is the vehicle to operate?

b. What is the launch location?

c. What are the proposed vehicle missions?

d. How many hours, days, or months will the vehicle be exposed to ground winds?

e. What are the consequences of operational constraints that may be imposed upon the vehicle because of wind constraints?

f. What are the consequences if the vehicle is destroyed or damaged by ground winds?

g. What are the cost and engineering practicalities for designing a functional vehicle to meet the desired mission requirements?

h. What is the risk that the vehicle will be destroyed or damaged by excessive wind loading?

In view of this list of questions or any similar list that a design group may enumerate, it becomes obvious that in establishing the ground wind environment design cirteria for a space vehicle an interdisciplinary approach between the several engineering and scientific disciplines is required.

Furthermore, the process is an iterative one. To begin the iterative process, specific information on ground winds is required.

5.2.3 Introduction to Exposure Period Analysis

Valid, quantitative answers to such questions as the following are of primary concern in the design, mission planning, and operations of space vehicles.

a. How probable is it that the peak surface wind at some specified reference height will exceed (or not exceed) a given magnitude in some specified time period?

b. Given a design wind profile in terms of peak wind speed versus height from 10 to 150 meters, how probable is it that the design wind profile will be exceeded in some specified time period?

Given a statistical sample of peak wind measurements for a specific location, the first question can be answered in as much detail as a statistical analyst finds necessary and sufficient. This first question has been thoroughly analyzed for Cape Kennedy and partially for Vandenberg AFB, and to a lesser degree for other locations of interest.

The analysis becomes considerably more complex in answering the second question. A wind profile model is required, and, to develop the model, measurements of the wind profiles by properly instrumented ground wind towers are required as well as a program for scheduling the measurements and data reduction. Every instantaneous wind profile is unique; similarity is a matter of degree. Given the peak wind speed at one height, there is a whole family of possible profiles extending from the specified wind at that height. Thus for each specified wind speed at a given height, there is a statistical distribution of wind profiles. Recommended profile shapes for Cape Kennedy and other locations are given in this report. The analysis needed to answer the second question is not complete, but we can assume that, given a period of time, the design wind profile shape will occur for a specified wind speed at a given height. In the event that a thunderstorm passes over the vehicle, it is logical to assume that the design wind profile shape (~99.9 shape) will occur and that the chance of the design wind profile being exceeded is the same as the probability that the peak wind during the passage of the thunderstorm will strike the vehicle or point of interest.

5.2.4 Development of Extreme Value Concept

It has been estimated from wind tunnel tests that only a few seconds are required for the wind to produce near steady-state drag loads on a vehicle such as the Saturn V in an exposed condition on the launch pad. For this and other reasons (subsection 5.2.5), we have adopted the peak wind speed as our fundamental measurement of wind. Equally important, when the engineering applications of winds can be made in terms of peak wind speeds, it is possible to obtain an appropriate statistical sample that conforms to the fundamental principles of extreme value theory. One hour is a convenient and physically meaningful minimum time interval from which to select the peak wind. The reader is referenced to Section 5.2.5.5.1 for details concerning averaging times in the context of structural response. An hourly peak wind speed sample has been established for Cape Kennedy from wind information on continuous recording charts. Peak wind samples for Vandenberg AFB have been derived from hourly steady-state wind measurements using statistical and physical principles.

5. 2. 4. 1 Envelope of Distributions

In the development of the statistics for peak winds, it was recognized that the probability of hourly, daily, and monthly peak winds exceeding (or not exceeding) specified values varied with time of day and from month to month. In other words, the distributions of like variables were different for the various reference periods. Even so, the Gumbel distribution was an excellent fit to the samples of all hourly, daily, monthly, bimonthly (in two combinations), and trimonthly (in three combinations) periods taken over the complete period of record, justifying the use of these distributions. However, in establishing vehicle wind design criteria for the peak winds versus exposure time, it is desired to present a simple set of wind statistics is such a manner that every reference period and exposure time would not have to be examined to determine the probability that the largest peak wind during the exposure time would exceed some specified magnitude. To accomplish this objective, envelopes of the distributions of the largest peak winds for various time increments from which the extremes were taken for the various reference periods were constructed. For example to obtain the envelope distribution of hourly peak winds for the month of March, the largest peak wind was selected at each percentage point from the twenty-four peak wind distributions (one for each hour). The annual envelope distribution is the envelope of the twelve hourly envelopes (one for each month).

Selected envelopes of distributions are given in subsection 5.2.5. It is recommended that these envelopes of distributions be used for vehicle wind design considerations. This recommendation is made under the assumption that it is not known what time of day or season of year critical vehicle operations are to be conducted; furthermore, it is not desirable to design a vehicle to operate only during selected hours or months. Should all other design alternatives fail to lead to a functionally engineered vehicle with an acceptable risk of not being compromised by wind loads, then distributions for peak winds by time of day for monthly reference periods may be considered for limited missions. For vehicle operations, detailed statistics of peak winds for specific missions are meaningful for management decisions, in planning missions, and in establishing mission rules and alternatives to the operational procedures. To present the wind statistics for these purposes is beyond the scope of this document. Each space mission has many facets that make it difficult to generalize and to present the statistics in brief form. Specific data for these applications are available upon request.

5.2.5 Design Wind Profiles (Vehicles)

Specific information about the wind profile is required to calculate ground wind loads on space vehicles. The earth's surface is a rigid boundary that exerts a frictional force on the lower layers of the atmosphere, causing the wind to vanish at the ground. In addition, the characteristic length and velocity scales of the mean (steady-state) flow in the first 150 meters (boundary layer) of the atmosphere combine to yield extremely high Reynolds numbers with values that range between approximately 10^6 and 10^8, so that for most conditions (wind speeds > 1 m/sec) the flow is fully turbulent. The lower boundary condition, the thermal and dynamic stability properties of the boundary layer, the distributions of the large scale pressure, the Coriolis forces, and the structure of the turbulence combine to yeild an infinity of wind profiles.

Data on basic wind speed profiles given in this section are to be used for vehicle design. With respect to design practices, the application of peak winds and the associated turbulence spectra and discrete gusts should be considered. The maximum response obtained for the selected risk levels for each physically realistic combination of conditions should be employed in the design. Care should be exercised so that wind inputs are not taken into account more than once. For example, the discrete gust and spectrum of turbulence are representations of the same thing, namely atmospheric turbulence. Thus, one should not calculate the responses of a vehicle due to the discrete gust and spectrum and then combine the results by addition, root-sum-square or any other procedure since these inputs represent the same thing. Rather the responses should be calculated with each input and then enveloped.

5.2.5.1 Philosophy

An example of a peak wind speed is given in Figure 5.2.1. Peak wind statistics have three advantages over mean wind statistics. First, peak wind statistics do not depend upon an averaging operation as do mean wind statistics. Second, to construct a mean wind sample, a chart reader or weather observer must perform an "eyeball" average of the wind data, causing the averaging process to vary from day to day according to the mood of the observer, and from observer to observer. Hourly peak wind speed readings avoid this subjective averaging process. Third, to monitor winds during the countdown phase of a space vehicle launch, it is easier to monitor the peak wind speed than the mean wind speed.

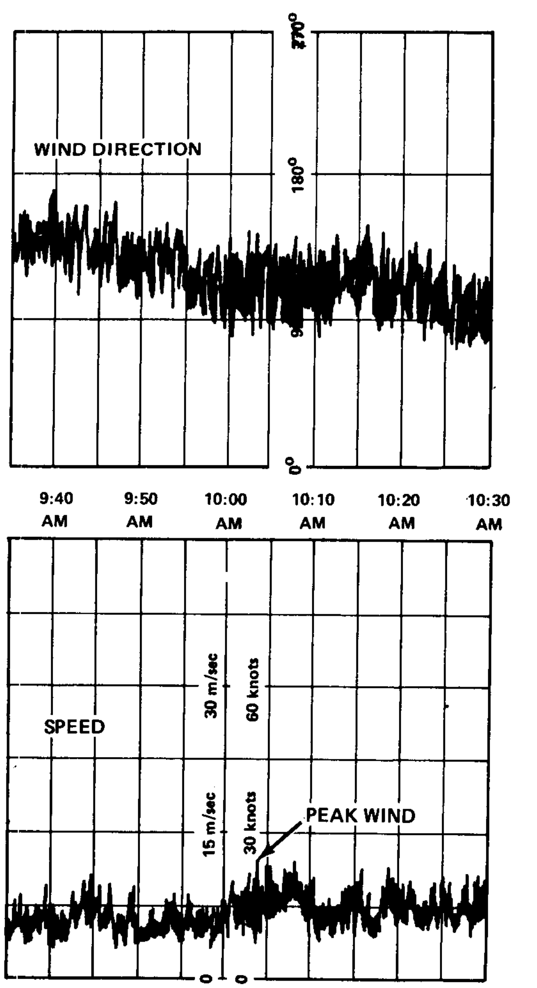

FIGURE 5.2.1 EXAMPLE OF PEAK WIND SPEED RECORDS

Smith et al. (Ref. 5.7) have performed extensive statistical analyses with peak wind speed samples measured at the 10-meter level. In the course of the work, he and his collaborators introduced the concept of exposure period probabilities into the design and operation of space vehicles. By determining the distribution functions of peak wind speeds for various periods of exposure (hour, day, month, year, etc.), it is possible to determine the probability of occurrence of a certain peak wind speed magnitude occurring during a prescribed period of exposure of a space vehicle to the natural environment. Thus, if an operation requires, for example, 1 hour to complete, and if the critical wind loads on the space vehicle can be defined in terms of the peak wind speed, then it is the probability of occurrence of the peak wind speed during a 1-hour period that gives a measure of the risk of the occurrence of structural failure. Similarly, if an operation requires 1 day to complete, then it is the probability of occurrence of the peak wind speed during a 1-day period that gives a measure of the risk of structural failure.

All probability statements concerning the capabilities of the space vehicles that are launched at NASA's Kennedy Space Center are prescribed in terms of Smith's peak wind speed exposure statistics. These peak wind statistics are usually transformed to the 18.3-meter (60-foot) reference level for design purposes (or higher levels for operational applications). However, to perform loading and response calculations resulting from steady-state and random turbulence drag loads and von Karman vortex shedding loads, the engineer requires information about the vertical variation of the mean wind and the structure of turbulence in the atmospheric boundary layer. The philosophy is to extrapolate the peak wind statistics up into the atmosphere via a peak wind profile, and the associated steady-state or mean wind profile is obtained by applying a gust factor that is a function of wind speed and height.

5.2.5.2 Peak Wind Profile Shapes

To develope a peak wind profile model, approximately 6000 hourly peak wind speed profiles measured at NASA's ground wind tower facility at Kennedy Space Center have been analyzed. The sample, comprised of profiles of hourly peak wind speeds measured at the 18-, 30-, 60-, 90-, 120-, and 150-meter levels, showed that the variation of the peak wind speed in the vertical, below 150 meters, for engineering purposes, could be described with a power law relationship given by

$$u(z) = u_{18.3} \left(\frac{z}{18.3} \right)^k \quad , \tag{5.1}$$

where $u(z)$ is the peak wind speed at height z in meters above natural grade and $u_{18.3}$ is a known peak wind speed at $z = 18.3$ meters. The peak wind is referenced to the 18.3-meter level because this level has been selected as the standard reference for the Kennedy Space Center launch area. A reference level should always be stated when discussing ground winds to avoid confusion in interpretation of risk statements and structural load calculations.

A statistical analysis of the peak wind speed profile data revealed that, for engineering purposes, k is distributed normally for any particular value of the peak wind speed at the 18.3-meter level. Thus, for a given percentile level of occurrence, k is approximately equal to a constant for $u_{18.3} > 2$ m/sec. For $u_{18.3} > 2$ m/sec,

$$k = c\,(u_{18.3})^{-3/4}, \tag{5.2}$$

where $u_{18.3}$ has the units of meter per second. The parameter, c, for engineering purposes, is distributed normally with mean value 0.52 and standard deviation 0.36 and have units of $m^{3/4} sec^{-3/4}$. The distribution of k as a function $u_{18.3}$ is depicted in Figure 5.2.2. The $\overline{k} + 3\sigma$ values are used in design studies.

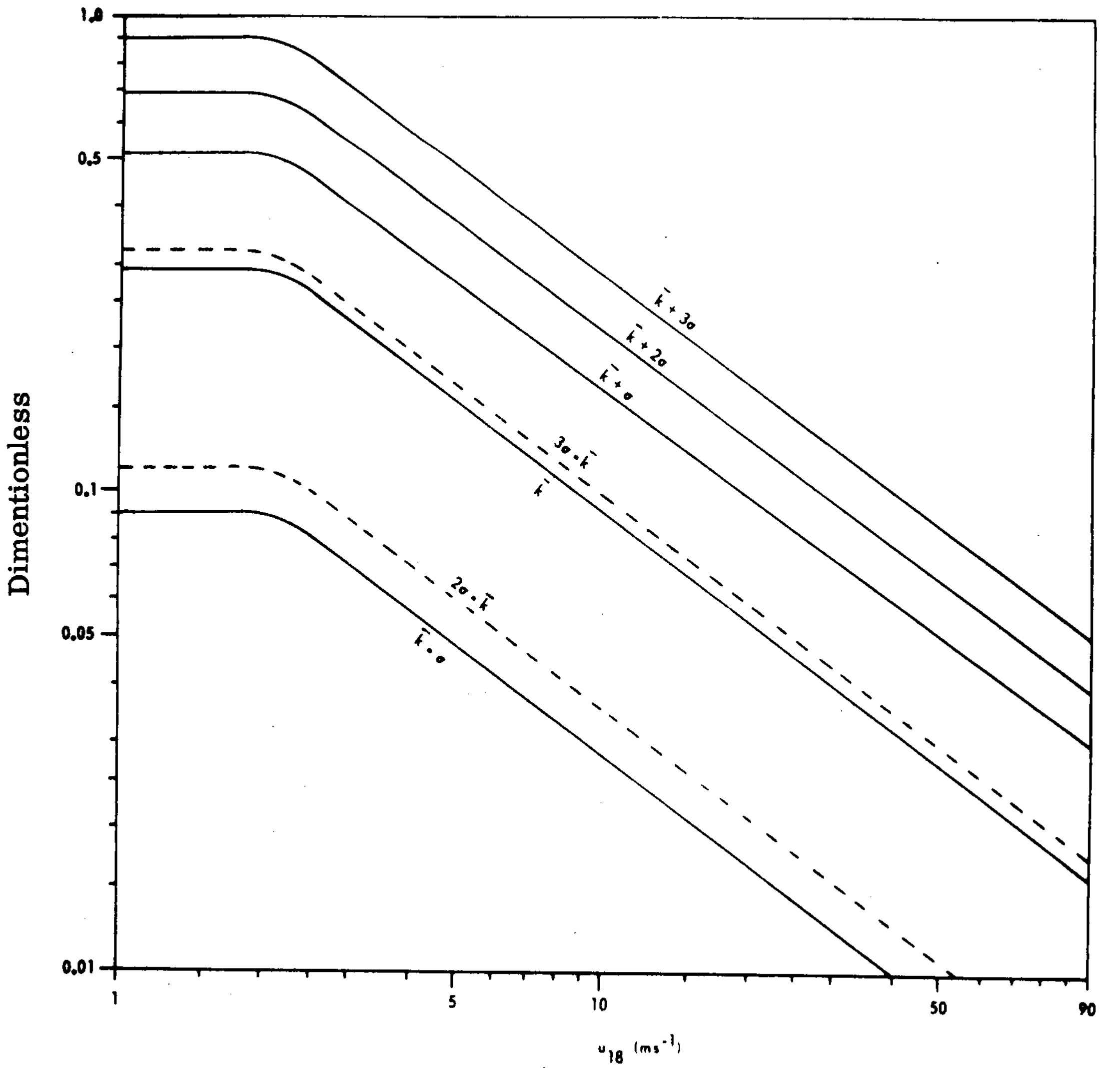

FIGURE 5.2.2 DISTRIBUTION OF THE PEAK WIND PROFILE PARAMETER k FOR VARIOUS WIND SPEEDS AT THE 18.3-m LEVEL FOR THE EASTERN TEST RANGE

5.2.5.3 Instantaneous Extreme Wind Profiles

The probability that the hourly peak wind speeds at all levels occur simultaneously is small. Accordingly, the practice of using peak wind profiles introduces some conservatism into the design criteria; however, the probability is relatively large that when the hourly peak wind occurs at the 18.3-meter level, the winds at the other levels almost take on the hourly peak values.

To gain some insight into this question, approximately 35 hours of digitized magnetic tape data were analyzed. The data were digitized at 0.1-second intervals in real time and partitioned into 0.5-, 2-, 5-, and 10-minute samples. The vertical average peak wind speed $\bar{u}_P$ and the 18-meter mean wind $\bar{u}_{18}$ were calculated for each sample. In addition, the instantaneous vertical average wind speed time history at 0.1-second intervals was calculated for each sample, and the peak instantaneous vertical average wind speed $\bar{u}_I$ was selected from each sample. The quantity $\bar{u}_I/\bar{u}_P$ was then interpreted to be a measure of how well the peak wind profile approximates the instantaneous extreme wind profile. Figure 5.2.3 is a plot of $\bar{u}_I/\bar{u}_P$ as a function of $\bar{u}_{18}$. The data points tend to scatter about a mean value of $\bar{u}_I/\bar{u}_P \simeq 0.93$,; however, some of the data points have values equal to 0.98. These results justify the use of peak wind profiles for engineering purposes.

5.2.5.4 Peak Wind Profile Shapes for Other Test Ranges and Sites

Detailed analyses of wind profile statistics are not available for other test ranges and sites. The exponent k in equation (5.1) is a function of wind speed, surface roughness, etc. For moderate surface roughness conditions, the extreme value of k is usually equal to 0.2 or less during high winds ($\gtrsim$ 15 m/sec). For design and planning purposes for test ranges and sites other than the Eastern Test Range, it is recommended that the values of k given in Table 5.2.1 be used. These values of k are the only values used in this report for sites other than the Eastern Test Range and represent estimates for 99.87 percentile-mean + 3σ (0.13 percent risk) values for the peak wind speed profile shape.

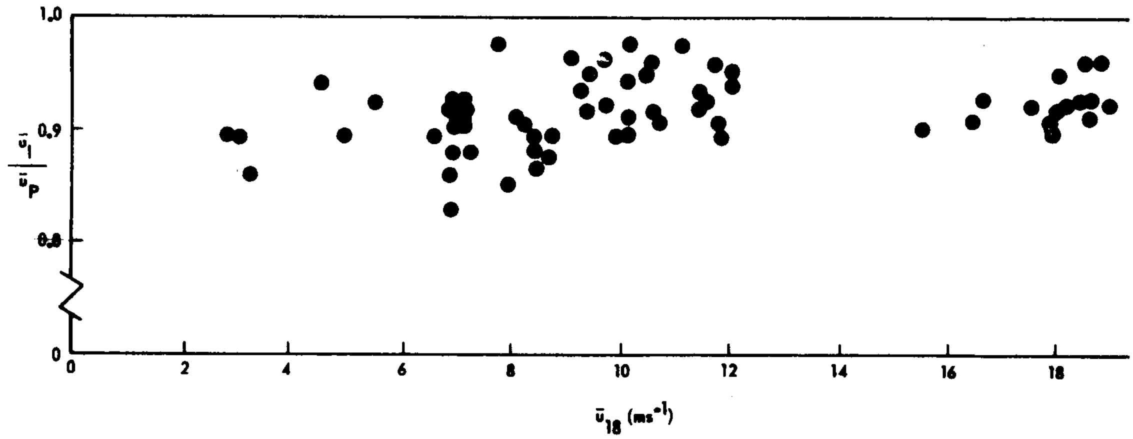

FIGURE 5. 2. 3 THE RATIO $\bar{u}_I/\bar{u}_P$ AS A FUNCTION OF THE 18. 3-m MEAN WIND SPEED ($\bar{u}_{18}$) FOR A 10-min SAMPLING PERIOD

TABLE 5. 2. 1 VALUES OF k TO USE FOR TEST RANGES OTHER THAN THE EASTERN TEST RANGE

k Value	18. 3-Meter Level Peak Wind Speed (ms^{-1})
k = 0. 2	$7 \leq u_{18.3} < 22$
k = 0. 14	$22 \leq u_{18.3}$

5. 2. 5. 5 Aerospace Vehicle Design Wind Profiles

The data presented in this section provide basic peak wind speed profile (envelope) information for use in studies to determine load factors for test, free-standing, launch, and lift-off conditions to ensure satisfactory performance of the space vehicle. To establish vehicle response requirements, the peak design surface winds are assumed to act normal to the longitudinal axis of the vehicle on the launch pad and to be from the most critical direction.

5. 2. 5. 5. 1 Design Wind Profiles for the Eastern Test Range

Peak wind profiles are characterized by two parameters, the peak wind speed at the 18. 3-meter level and the shape parameter k. Once these two quantities are defined, the peak wind speed profile envelope is completely specified. Accordingly, to construct a peak wind profile envelope for the Eastern Test Range, in the context of launch vehicle loading and response calculations, two pieces of information are required. First, the risk of exceeding the design wind peak speed at the reference level for a given period must be specified. Once this quantity is given, the design peak wind speed at the reference level is automatically specified (Figure 5.2.4). Second, the risk associated with compromising the structural integrity of the vehicle, once the reference level design wind occurs, must be specified. This second quantity and the reference level peak wind speed will determine the value of k that is to be used in equation (5. 1).

It is recommended that the $\bar{k} + 3\sigma$ value of k be used for the design of space vehicles. Thus, if a space vehicle designed to withstand a particular value of peak wind speed at the 18.3-meter reference level is exposed to that peak wind speed, the vehicle has at least a 99.865-percent chance of withstanding possible peak wind profile conditions.

Operational ground wind contraints for established vehicles should be determined for a reference level (above natural grade) near the top of the vehicle while on the launch pad. The profile may be calculated using equations (5. 1) and (5. 2) with a value of $k = \bar{k} - 3\sigma$. This will produce a peak wind profile envelope associated with an upper reference level ground wind constraint. Tables for these calculations and those associated with the design reference level are available for various wind speeds and k values applicable to Kennedy Space Center upon request to the Aerospace Environment Division, NASA, Marshall Space Flight Center, Alabama.

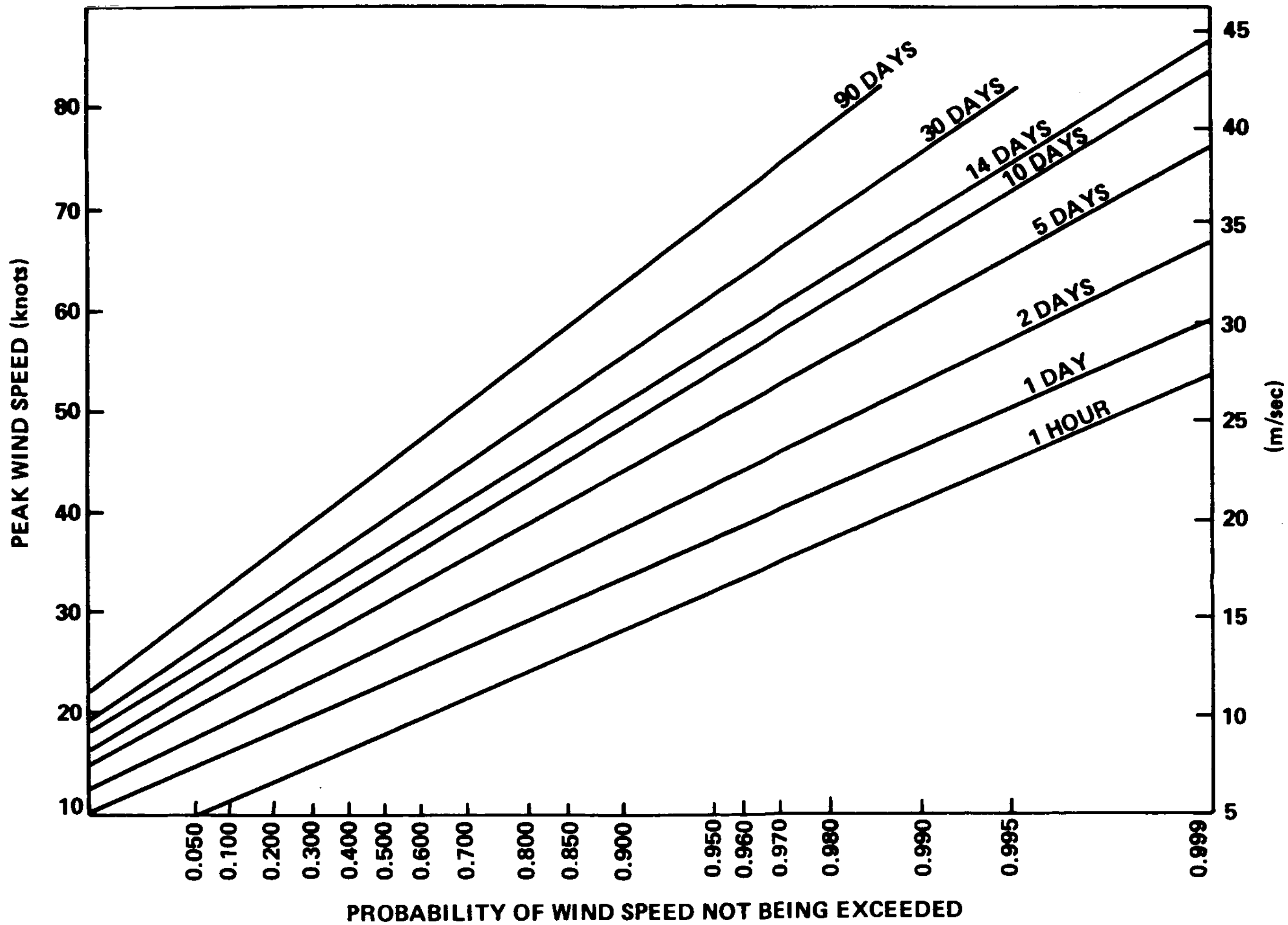

FIGURE 5.2.4. 18.3-m REFERENCE LEVEL; CAPE KENNEDY PEAK WIND SPEED FOR WINDIEST REFERENCE PERIOD VERSUS PROBABILITY FOR SEVERAL EXPOSURE PERIODS APPLICABLE TO VEHICLE DESIGN CRITERIA DEVELOPMENT

Table 5.2.2 contains peak wind speed profiles for various envelope values of peak wind speed at the 10-meter level for fixed values of risk for the worst monthly-hourly reference periods of the year for a 1-hour exposure. To construct these profiles, the 1-hour exposure period statistics for each hour in each month were constructed. This exercise yielded 288 distribution functions (12 months times 24 hours), which were enveloped to yield the largest or "worst" 10-meter level peak wind speed associated with a given level of risk for all monthly-hourly reference periods. Thus, for example, according to Table 5.2.2 there is at most a 10-percent risk that the peak wind speed will exceed 13.9 m/sec (27.0 knots) during any particular hour in any particular month at the 10-meter level, and if a peak wind speed equal to 13.9 m/sec (27.0 knots) should occur at the 10-meter level, then there is only a 0.135-percent chance that the peak wind speed will exceed 24.1 m/sec (46.8 knots) at the 152.4-meter level or the corresponding values given at the other heights.

Tables 5.2.3 through 5.2.5 contain peak wind profile envelopes for various values of peak wind speed at the 10-meter level and fixed values of risk for various exposure periods. The 1-day exposure values of peak wind speed were obtained by constructing the daily peak wind statistics for each month and then enveloping these distributions to yield the worst 1-day exposure, 10-meter level peak wind speed for a specified value of risk (daily-monthly reference period). The 30-day exposure envelope peak wind speeds were obtained by constructing the monthly peak wind statistics for each month and then constructing the envelope of the distributions (monthly-annual reference period). The 10-day exposure statistics were obtained by interpolating between the 1- and 30-day exposure period results. The envelopes of the 90-day exposure period statistics are the 90-day exposure statistics associated with the 12 trimonthly periods (January-February-March, February-March-April, March-April-May, and so forth) (90-day-annual reference period). Finally, the 365-day exposure period statistics were calculated with the annual peak wind sample (17 data points) to yield one distribution. Tables 5.2.3 through 5.2.5 contain the largest or "worst" 10-meter level peak wind speed associated with a given level of risk for the stated exposure periods.

It is recommended that the data in Tables 5.2.2 through 5.2.5 be used as the basis for space vehicle design for Cape Kennedy/Kennedy Space Center Operations. Wind profile statistics for the design of permanent ground support equipment are discussed in subsection 5.2.10.

TABLE 5.2.2 PEAK WIND SPEED PROFILE ENVELOPES FOR VARIOUS VALUES OF RISK OF EXCEEDING THE 10-m LEVEL PEAK WIND SPEED FOR 1-hr EXPOSURE (hourly-monthly reference period) FOR CAPE KENNEDY[2]

Height		Risk (%)									
		20		10		5		1		0.1	
(m)	(ft)	knots	ms^{-1}	knots	ms^{-1}	knots	ms^{-1}	knots	ms^{-1}	knots	ms^{-1}
10.0	33	22.9	11.8	27.0	13.9	30.8	15.8	39.5	20.3	51.9	26.7
18.3	60	26.3	13.5	30.5	15.7	34.4	17.7	43.4	22.3	56.0	28.8
30.5	100	29.5	15.2	33.8	17.4	37.9	19.5	47.0	24.2	59.8	30.8
61.0	200	34.5	17.8	38.9	20.0	43.0	22.1	52.3	26.9	65.4	33.6
91.4	300	37.8	19.5	42.2	21.7	46.4	23.9	55.7	28.7	68.9	35.4
121.9	400	40.4	20.8	44.7	23.0	48.9	25.2	58.3	30.0	71.5	36.8
152.4	500	42.5	21.9	46.8	24.1	51.0	26.2	60.3	31.0	73.6	37.8

TABLE 5.2.3 PEAK WIND SPEED PROFILE ENVELOPES FOR A 10-PERCENT RISK VALUE OF EXCEEDING THE 10-m LEVEL PEAK WIND SPEED FOR VARIOUS REFERENCE PERIODS OF EXPOSURE, FOR CAPE KENNEDY[2]

Height		Exposure (days)									
		1		10		30		90		365	
(m)	(ft)	knots	ms^{-1}	knots	ms^{-1}	knots	ms^{-1}	knots	ms^{-1}	knots	ms^{-1}
10.0	33	32.1	16.5	46.9	24.1	53.9	27.7	61.0	31.4	70.0	36.0
18.3	60	35.8	18.4	51.0	26.2	58.2	29.9	65.3	33.6	74.5	38.3
30.5	100	39.2	20.2	54.7	28.1	62.0	31.9	69.3	35.7	78.5	40.4
61.0	200	44.4	22.8	60.2	31.0	67.6	34.8	75.0	38.6	84.4	43.4
91.4	300	47.8	24.6	63.6	32.7	71.1	36.6	78.5	40.4	88.0	45.3
121.9	400	50.3	25.9	66.2	34.1	73.7	37.9	81.1	41.7	90.6	46.6
152.4	500	52.4	27.0	68.3	35.1	75.8	39.0	83.2	42.8	92.8	47.7

2. Recommended for design criteria development.

TABLE 5.2.4 PEAK WIND SPEED PROFILE ENVELOPES FOR A 5-PERCENT RISK VALUE OF EXCEEDING THE 10-m LEVEL PEAK WIND SPEED FOR VARIOUS REFERENCE PERIODS OF EXPOSURE FOR CAPE KENNEDY[3]

Height		Exposure (days)									
		1		10		30		90		365	
(m)	(ft)	knots	ms^{-1}	knots	ms^{-1}	knots	ms^{-1}	knots	ms^{-1}	knots	ms^{-1}
10.0	33	36.1	18.5	52.3	26.9	60.1	30.9	67.8	34.9	77.7	40.0
18.3	60	39.8	20.5	56.5	29.1	64.4	33.1	72.3	37.2	82.4	42.4
30.5	100	43.3	22.3	60.3	31.0	68.3	35.1	76.3	39.3	86.5	44.5
61.0	200	48.6	25.0	65.9	33.9	74.0	38.1	82.1	42.2	92.5	47.6
91.4	300	52.0	26.8	69.4	35.7	77.6	40.0	85.7	44.1	96.1	49.4
121.9	400	54.5	28.0	72.0	37.0	80.2	41.3	88.4	45.5	98.8	50.8
152.4	500	56.6	29.1	74.1	38.1	82.3	42.3	91.0	46.8	101.0	52.0

TABLE 5.2.5 PEAK WIND SPEED PROFILE ENVELOPES FOR A 1-PERCENT RISK VALUE OF EXCEEDING THE 10-m LEVEL PEAK WIND SPEED FOR VARIOUS REFERENCE PERIODS OF EXPOSURE FOR CAPE KENNEDY[3]

Height		Exposure (days)									
		1		10		30		90		365	
(m)	(ft)	knots	ms^{-1}	knots	ms^{-1}	knots	ms^{-1}	knots	ms^{-1}	knots	ms^{-1}
10.0	33	45.0	23.1	65.4	33.6	74.0	38.1	83.4	42.9	95.4	49.1
18.3	60	49.0	25.2	69.9	36.0	78.6	40.4	88.2	45.4	100.3	51.6
30.5	100	52.6	27.1	73.9	38.0	82.8	42.6	92.4	47.5	104.7	53.9
61.0	200	58.1	30.0	79.7	41.0	88.6	45.6	98.4	50.6	110.9	57.1
91.4	300	61.5	31.6	83.2	42.8	92.3	47.5	102.1	52.5	114.6	59.0
121.9	400	64.1	33.0	85.9	44.2	95.0	48.9	104.8	53.9	117.4	60.4
152.4	500	66.1	34.0	88.0	45.3	97.1	50.0	107.0	55.0	119.6	61.5

3. Recommended for design criteria development.

Mean wind profiles or steady-state wind profiles can be obtained from the peak wind profiles by dividing the peak wind by the appropriate gust factor (subsection 5.2.7). It is recommended that the 10-minute gust factors be used for structural design purposes. Application of the 10-minute gust factors to the peak wind profile corresponds to averaging the wind speed over a 10-minute period. This averaging period appears to result in a stable mean value of the wind speed. Within the range of variation of the data, the 1-hour and 10-minute gust factors are approximately equal for sufficiently high wind speed. This occurs because the spectrum of the horizontal wind speed near the ground is characterized by a broad energy gap centered at a frequency approximately equal to 0.000278 hertz (1 cycle/hr) and typically extends over the frequency domain 0.000139 hertz (0.5 cycles/hr) $< \omega <$ 0.0014 hertz (5 cycles/hr) (Ref. 5.50). The Fourier spectral components associated with frequencies less than 0.000278 hertz (1 cycle/hr) correspond to the meso- and synoptic-scale motions, while the remaining high-frequency spectral components correspond to mechanically and thermally produced turbulence. Thus, a statistically stable estimate of the mean or steady-state wind speed can be obtained by averaging over a period in the range from 10 minutes to an hour. Davenport (Ref. 5.5) points out that this period for averaging is also suitable for structural analysis. Since this period is far longer than any natural period of structural vibration, it assures that effects caused by the mean wind properly represent steady-state, nontransient effects. The steady-state wind profiles, calculated with the 10-minute gust factors, that correspond to those in Tables 5.2.2 through 5.2.5 are given in Tables 5.2.6 through 5.2.9.

5.2.5.5.2 Design Ground Wind Profiles for Other Locations

Tables 5.2.10 through 5.2.21 contain recommended design ground wind profiles for several different risks of exceeding the 10-meter level peak wind speed and 10-minute mean wind speed for a 1-hour exposure period. These tables are based on the same philosophy as Table 5.2.2 and Table 5.2.6 for the Eastern Test Range. The locations for which data are provided include Wallops Island, Virginia; White Sands Missile Range, New Mexico; Air Force Flight Center, Edwards AFB, California; Space and Missile Test Center, Vandenberg AFB, California; Huntsville, Alabama; and the New Orleans, Louisiana-Mississippi Test Facility area.

TABLE 5.2.6 10-min MEAN WIND SPEED PROFILE ENVELOPES FOR VARIOUS VALUES OF RISK OF EXCEEDING THE 10-m LEVEL MEAN WIND SPEED FOR A 1-hr EXPOSURE (hourly-monthly reference period) FOR CAPE KENNEDY

Height		Risk (%)									
		20		10		5		1		0.1	
(m)	(ft)	knots	ms^{-1}	knots	ms^{-1}	knots	ms^{-1}	knots	ms^{-1}	knots	ms^{-1}
10.0	33	14.1	7.2	16.6	8.6	19.1	9.8	24.6	12.7	32.4	16.7
18.3	60	17.1	8.8	19.9	10.3	22.6	11.7	28.7	14.8	37.2	19.1
30.5	100	20.0	10.3	23.1	11.9	26.0	13.4	32.6	16.8	41.6	21.4
61.0	200	24.7	12.7	28.1	14.5	31.3	16.1	38.3	19.7	48.1	24.7
91.4	300	27.8	14.3	31.3	16.1	34.7	17.9	42.0	21.6	52.1	26.8
121.9	400	30.3	15.6	33.9	17.4	37.3	19.2	44.8	23.0	55.1	28.3
152.4	500	32.3	16.6	35.9	18.5	39.4	20.3	47.0	24.2	57.5	29.6

TABLE 5.2.7 10-min MEAN WIND SPEED PROFILE ENVELOPES FOR A 10-PERCENT RISK VALUE OF EXCEEDING THE 10-m LEVEL MEAN WIND SPEED FOR VARIOUS REFERENCE PERIODS OF EXPOSURE FOR CAPE KENNEDY

Height		Exposure (days)									
		1		10		30		90		365	
(m)	(ft)	knots	ms^{-1}	knots	ms^{-1}	knots	ms^{-1}	knots	ms^{-1}	knots	ms^{-1}
10.0	33	20.0	10.3	29.3	15.1	33.7	17.3	38.1	19.6	43.8	22.5
18.3	60	23.6	12.1	33.8	17.4	38.7	19.9	43.3	22.3	49.5	25.5
30.5	100	27.1	13.9	38.0	19.5	43.1	22.2	48.2	24.8	54.6	28.1
61.0	200	32.4	16.7	44.2	22.7	49.6	25.5	55.1	28.3	62.1	31.9
91.4	300	35.8	18.4	48.1	24.7	53.8	27.7	59.4	30.6	66.6	34.3
121.9	400	38.5	19.8	51.0	26.2	56.8	29.2	62.6	32.2	69.9	36.0
152.4	500	40.6	20.9	53.3	27.4	59.2	30.5	65.1	33.5	72.6	37.3

TABLE 5.2.8 10-min MEAN WIND SPEED PROFILE ENVELOPES FOR A 5-PERCENT RISK VALUE OF EXCEEDING THE 10-m LEVEL MEAN WIND SPEED FOR VARIOUS REFERENCE PERIODS OF EXPOSURE FOR CAPE KENNEDY

Height		Exposure (days)									
		1		10		30		90		365	
(m)	(ft)	knots	ms^{-1}	knots	ms^{-1}	knots	ms^{-1}	knots	ms^{-1}	knots	ms^{-1}
10.0	33	22.5	11.6	32.7	16.8	37.6	19.3	42.5	21.9	48.6	25.0
18.3	60	26.3	13.5	37.5	19.3	42.8	22.0	48.1	24.7	54.8	28.2
30.5	100	30.0	15.4	41.9	21.6	47.5	24.4	53.2	27.4	60.2	31.0
61.0	200	35.5	18.3	48.4	24.9	54.5	28.0	60.4	31.1	68.1	35.0
91.4	300	39.2	20.2	52.5	27.0	58.7	30.2	64.9	33.4	72.9	37.5
121.9	400	41.9	21.6	55.5	28.6	61.9	31.8	68.2	35.1	76.3	39.3
152.4	500	44.0	22.6	57.9	29.8	64.4	33.1	70.9	36.4	79.1	40.7

TABLE 5.2.9 10-min MEAN WIND SPEED PROFILE ENVELOPES FOR A 1-PERCENT RISK VALUE OF EXCEEDING THE 10-m LEVEL MEAN WIND SPEED FOR VARIOUS REFERENCE PERIODS OF EXPOSURE FOR CAPE KENNEDY

Height		Exposure (days)									
		1		10		30		90		365	
(m)	(ft)	knots	ms^{-1}	knots	ms^{-1}	knots	ms^{-1}	knots	ms^{-1}	knots	ms^{-1}
10.0	33	28.1	14.5	40.9	21.0	46.3	23.8	52.2	26.9	59.7	30.7
18.3	60	32.5	16.7	46.5	23.9	52.2	26.9	58.6	30.1	66.7	34.3
30.5	100	36.6	18.8	51.4	26.4	57.6	29.6	64.3	33.1	72.9	37.5
61.0	200	42.6	21.9	58.6	30.1	65.2	33.5	72.5	37.3	81.6	42.0
91.4	300	47.2	24.3	63.0	32.4	69.9	36.0	77.4	39.8	86.9	44.7
121.9	400	49.4	25.4	66.3	34.1	73.4	37.8	81.0	41.7	90.7	46.7
152.4	500	51.7	26.6	68.9	35.4	76.1	39.1	83.8	43.1	93.7	48.2

TABLE 5. 2. 10 PEAK WIND SPEED PROFILE ENVELOPES FOR VARIOUS VALUES OF RISK OF EXCEEDING THE 10-m LEVEL PEAK WIND SPEED FOR 1-hr EXPOSURE (hourly-monthly reference period) FOR HUNTSVILLE, ALABAMA

Height		Risk (%)									
		20		10		5		1		0.1	
(m)	(ft)	knots	ms^{-1}	knots	ms^{-1}	knots	ms^{-1}	knots	ms^{-1}	knots	ms^{-1}
10.0	33	19.1	9.8	21.6	11.1	24.0	12.4	31.5	16.2	47.5	24.5
18.3	60	21.5	11.1	24.4	12.5	27.1	14.0	35.6	18.3	51.7	26.7
30.5	100	23.9	12.3	27.0	13.9	30.0	15.5	39.4	20.3	55.5	28.6
61.0	200	27.4	14.1	31.0	15.9	34.5	17.8	45.2	23.3	61.0	31.5
91.4	300	29.7	15.3	33.6	17.3	37.4	19.3	49.1	25.2	64.7	33.4
121.9	400	31.5	16.2	35.6	18.3	39.6	20.5	52.0	26.7	67.4	34.7
152.4	500	33.0	16.9	37.3	19.2	41.5	21.4	54.4	28.0	69.5	35.8

TABLE 5. 2. 11 10-min MEAN WIND SPEED PROFILE ENVELOPES FOR VARIOUS VALUES OF RISK OF EXCEEDING THE 10-m LEVEL MEAN SPEED FOR 1-hr EXPOSURE (hourly-monthly reference period) FOR HUNTSVILLE, ALABAMA

Height		Risk (%)									
		20		10		5		1		0.1	
(m)	(ft)	knots	ms^{-1}	knots	ms^{-1}	knots	ms^{-1}	knots	ms^{-1}	knots	ms^{-1}
10.0	33	13.6	7.0	15.4	7.9	17.1	8.8	22.5	11.6	33.9	17.5
18.3	60	15.4	7.9	17.4	9.0	19.4	10.0	25.4	13.1	36.9	19.0
30.5	100	17.1	8.8	19.3	9.9	21.4	11.1	28.1	14.5	39.6	20.4
61.0	200	19.6	10.1	22.2	11.4	24.6	12.7	32.3	16.6	43.6	22.5
91.4	300	21.3	10.9	24.0	12.4	26.7	13.8	35.0	18.0	46.2	23.8
121.9	400	22.5	11.6	25.5	13.1	28.3	14.6	37.1	19.1	48.1	24.8
152.4	500	23.6	12.1	26.7	13.7	29.6	15.3	38.9	20.0	49.6	25.6

TABLE 5.2.12 SURFACE PEAK WIND SPEED PROFILE ENVELOPES FOR VARIOUS VALUES OF RISK OF EXCEEDING THE 10-m LEVEL PEAK WIND SPEED FOR 1-hr EXPOSURE (hourly-monthly reference period) FOR NEW ORLEANS AND MISSISSIPPI TEST FACILITY AREA

Height		Risk (%)									
		20		10		5		1		0.1	
(m)	(ft)	knots	ms^{-1}	knots	ms^{-1}	knots	ms^{-1}	knots	ms^{-1}	knots	ms^{-1}
10.0	33	19.8	10.2	23.9	12.3	27.6	14.2	37.2	19.1	53.0	27.3
18.3	60	22.4	11.5	27.0	13.9	31.2	16.0	42.0	21.5	57.7	29.7
30.5	100	24.8	12.8	29.9	15.4	34.5	17.8	46.5	23.9	61.9	31.8
61.0	200	28.4	14.6	34.3	17.7	39.6	20.4	53.4	27.4	68.1	35.1
91.4	300	30.8	15.9	37.2	19.2	43.0	22.1	57.9	29.8	72.2	37.2
121.9	400	32.7	16.8	39.4	20.3	45.5	23.4	61.4	31.5	75.2	38.7
152.4	500	34.2	17.6	41.3	21.3	47.7	24.5	64.3	33.0	77.5	39.9

TABLE 5.2.13 SURFACE MEAN WIND SPEED PROFILE ENVELOPES FOR VARIOUS VALUES OF RISK OF EXCEEDING THE 10-m LEVEL 10-min MEAN WIND SPEED FOR 1-hr EXPOSURE (hourly-monthly reference period) FOR NEW ORLEANS AND MISSISSIPPI TEST FACILITY AREA

Height		Risk (%)									
		20		10		5		1		0.1	
(m)	(ft)	knots	ms^{-1}	knots	ms^{-1}	knots	ms^{-1}	knots	ms^{-1}	knots	ms^{-1}
10.0	33	14.1	7.3	17.1	8.8	19.7	10.1	26.6	13.7	37.9	19.5
18.3	60	16.0	8.2	19.3	9.9	22.3	11.4	30.0	15.4	41.2	21.2
30.5	100	17.7	9.1	21.4	11.0	24.7	12.7	33.2	17.1	44.2	22.8
61.0	200	20.3	10.5	24.5	12.6	28.3	14.6	38.2	19.6	48.6	25.0
91.4	300	22.0	11.3	26.6	13.7	30.7	15.8	41.4	21.3	51.6	26.6
121.9	400	23.3	12.0	28.2	14.5	32.5	16.7	43.8	22.5	53.7	27.7
152.4	500	24.4	12.6	29.5	15.2	34.1	17.5	45.9	23.6	55.4	28.5

TABLE 5.2.14 SURFACE PEAK WIND SPEED PROFILE ENVELOPES FOR VARIOUS VALUES OF RISK OF EXCEEDING THE 10-m LEVEL PEAK WIND SPEED FOR 1-hr EXPOSURE (hourly-monthly reference period) FOR THE SPACE AND MISSILE TEST CENTER,[4] VANDENBERG AFB, CALIFORNIA

Height		Risk (%)									
		20		10		5		1		0.1	
(m)	(ft)	knots	ms^{-1}	knots	ms^{-1}	knots	ms^{-1}	knots	ms^{-1}	knots	ms^{-1}
10.0	33	18.3	9.4	23.1	11.9	27.6	14.2	36.5	18.8	45.0	23.2
18.3	60	20.7	10.6	26.1	13.4	31.2	16.0	41.2	21.2	49.0	25.2
30.5	100	22.9	11.8	28.9	14.9	34.5	17.8	45.7	23.5	52.6	27.1
61.0	200	26.3	13.5	33.2	17.1	39.6	20.4	52.4	27.0	57.8	29.8
91.4	300	28.5	14.6	36.0	18.5	43.0	22.1	56.9	29.3	61.3	31.6
121.9	400	30.2	15.5	38.1	19.6	45.5	23.4	60.2	31.0	63.8	32.9
152.4	500	31.6	16.2	39.9	20.6	47.7	24.5	63.1	32.5	65.8	33.9

TABLE 5.2.15 SURFACE MEAN WIND SPEED PROFILE ENVELOPES FOR VARIOUS VALUES OF RISK OF EXCEEDING THE 10-m LEVEL 10-min MEAN WIND SPEED FOR 1-hr EXPOSURE (hourly-monthly reference period) FOR THE SPACE AND MISSILE TEST CENTER, VANDENBERG AFB, CALIFORNIA [4]

Height		Risk (%)									
		20		10		5		1		0.1	
(m)	(ft)	knots	ms^{-1}	knots	ms^{-1}	knots	ms^{-1}	knots	ms^{-1}	knots	ms^{-1}
10.0	33	13.1	6.7	16.5	8.5	19.7	10.1	26.1	13.4	32.1	16.5
18.3	60	14.8	7.6	18.6	9.6	22.3	11.4	29.4	15.2	35.0	18.0
30.5	100	16.4	8.4	20.6	10.6	24.7	12.7	32.6	16.8	37.5	19.4
61.0	200	18.8	9.6	23.7	12.2	28.3	14.6	37.4	19.3	41.3	21.3
91.4	300	20.4	10.5	25.7	13.2	30.7	15.8	40.6	20.9	43.8	22.6
121.9	400	21.6	11.1	27.2	14.0	32.5	16.7	43.0	22.2	45.6	23.5
152.4	500	22.6	11.6	28.5	14.7	34.1	17.5	45.1	23.2	47.0	24.2

4. Formerly Western Test Range.

TABLE 5.2.16 SURFACE PEAK WIND SPEED PROFILE ENVELOPES FOR VARIOUS VALUES OF RISK OF EXCEEDING THE 10-m LEVEL PEAK WIND SPEED FOR 1-hr EXPOSURE (hourly-monthly reference period) FOR WALLOPS TEST RANGE

Height		Risk (%)									
		20		10		5		1		0.1	
(m)	(ft)	knots	ms^{-1}	knots	ms^{-1}	knots	ms^{-1}	knots	ms^{-1}	knots	ms^{-1}
10.0	33	22.9	11.8	27.1	13.9	31.2	16.1	38.6	19.9	55.0	28.3
18.3	60	25.9	13.3	30.6	15.7	35.2	18.2	43.6	22.5	59.8	30.8
30.5	100	28.6	14.8	33.9	17.4	39.0	20.1	48.3	24.9	64.3	33.1
61.0	200	32.9	16.9	38.9	20.0	44.8	23.1	55.4	28.6	70.6	36.3
91.4	300	35.7	18.4	42.2	21.7	48.6	25.1	60.1	31.0	74.9	38.6
121.9	400	37.8	19.5	44.7	22.9	51.5	26.6	63.7	32.8	78.0	40.1
152.4	500	39.6	20.4	46.8	24.0	53.9	27.8	66.7	34.4	80.5	41.4

TABLE 5.2.17 SURFACE MEAN WIND SPEED PROFILE ENVELOPES FOR VARIOUS VALUES OF RISK OF EXCEEDING THE 10-m LEVEL 10-min MEAN WIND SPEED FOR 1-hr EXPOSURE (hourly-monthly reference period) FOR WALLOPS TEST RANGE

Height		Risk (%)									
		20		10		5		1		0.1	
(m)	(ft)	knots	ms^{-1}	knots	ms^{-1}	knots	ms^{-1}	knots	ms^{-1}	knots	ms^{-1}
10.0	33	16.4	8.4	19.3	9.9	22.3	11.5	27.6	14.2	39.3	20.2
18.3	60	18.5	9.5	21.9	11.2	25.2	13.0	31.1	16.1	42.7	22.0
30.5	100	20.5	10.5	24.2	12.4	27.9	14.4	34.5	17.8	45.9	23.6
61.0	200	23.5	12.1	27.8	14.3	32.0	16.5	39.6	20.4	50.4	26.0
91.4	300	25.5	13.1	30.2	15.5	34.7	17.9	42.9	22.1	53.5	27.5
121.9	400	27.0	13.9	31.9	16.4	36.8	19.0	45.5	23.5	55.7	28.7
152.4	500	28.3	14.6	33.5	17.2	38.5	19.9	47.7	24.6	57.5	29.6

TABLE 5.2.18 SURFACE PEAK WIND SPEED PROFILE ENVELOPES FOR VARIOUS VALUES OF RISK OF EXCEEDING THE 10-m LEVEL PEAK WIND SPEED FOR 1-hr EXPOSURE (hourly-monthly reference period) FOR WHITE SANDS MISSILE RANGE

Height		Risk (%)									
		20		10		5		1		0.1	
(m)	(ft)	knots	ms^{-1}	knots	ms^{-1}	knots	ms^{-1}	knots	ms^{-1}	knots	ms^{-1}
10.0	33	15.3	7.9	20.9	10.7	24.7	12.7	34.3	17.7	52.1	26.8
18.3	60	17.3	8.9	23.6	12.1	27.9	14.3	38.7	20.0	56.7	29.2
30.5	100	19.1	9.9	26.1	13.4	30.9	15.9	42.9	22.1	60.9	31.3
61.0	200	22.0	11.3	30.0	15.4	35.5	18.2	49.3	25.4	66.9	34.4
91.4	300	23.8	12.3	32.6	16.7	38.5	19.8	53.4	27.6	71.0	36.5
121.9	400	25.2	13.0	34.5	17.7	40.8	21.0	56.6	29.2	73.9	38.0
152.4	500	26.4	13.7	36.1	18.5	42.7	22.0	59.3	30.6	76.2	39.2

TABLE 5.2.19 SURFACE MEAN WIND SPEED PROFILE ENVELOPES FOR VARIOUS VALUES OF RISK OF EXCEEDING THE 10-m LEVEL 10-min MEAN WIND SPEED FOR 1-hr EXPOSURE (hourly-monthly reference period) FOR WHITE SANDS MISSILE RANGE

Height		Risk (%)									
		20		10		5		1		0.1	
(m)	(ft)	knots	ms^{-1}	knots	ms^{-1}	knots	ms^{-1}	knots	ms^{-1}	knots	ms^{-1}
10.0	33	10.9	5.6	14.9	7.7	17.6	9.1	24.5	12.6	37.2	19.2
18.3	60	12.3	6.4	16.9	8.6	19.9	10.2	27.7	14.3	40.5	20.8
30.5	100	13.7	7.1	18.7	9.6	22.1	11.3	30.7	15.8	43.4	22.4
61.0	200	15.7	8.1	21.4	11.0	25.3	13.0	35.2	18.2	47.8	24.6
91.4	300	17.0	8.8	23.3	11.9	27.5	14.1	38.2	19.7	50.7	26.1
121.9	400	18.0	9.3	24.6	12.6	29.1	15.0	40.4	20.9	52.8	27.1
152.4	500	18.9	9.8	25.8	13.2	30.5	15.7	42.3	21.9	54.4	28.0

TABLE 5.2.20 SURFACE PEAK WIND SPEED PROFILE ENVELOPES FOR VARIOUS VALUES OF RISK OF EXCEEDING THE 10-m LEVEL PEAK WIND SPEED FOR 1-hr EXPOSURE (hourly-monthly reference period) FOR EDWARDS AIR FORCE BASE

Height		Risk (%)									
		20		10		5		1		0.1	
(m)	(ft)	knots	ms^{-1}	knots	ms^{-1}	knots	ms^{-1}	knots	ms^{-1}	knots	ms^{-1}
10.0	33	24.4	12.6	28.3	14.6	31.5	16.2	38.4	19.8	47.0	24.2
18.3	60	27.6	14.2	32.0	16.5	35.6	18.3	43.4	22.4	51.1	26.3
30.5	100	30.5	15.8	35.4	18.3	39.4	20.3	48.0	24.8	54.9	28.3
61.0	200	35.0	18.1	40.6	21.0	45.2	23.3	55.1	28.4	60.3	31.1
91.4	300	38.0	19.6	44.1	22.7	49.1	25.2	59.8	30.8	64.0	33.0
121.9	400	40.3	20.8	46.7	24.1	52.0	26.7	63.4	32.7	66.6	34.3
152.4	500	42.2	21.8	48.9	25.2	54.4	28.0	66.4	34.2	68.8	35.4

TABLE 5.2.21 SURFACE MEAN WIND SPEED PROFILE ENVELOPES FOR VARIOUS VALUES OF RISK OF EXCEEDING THE 10-m LEVEL 10-min MEAN WIND SPEED FOR 1-hr EXPOSURE (hourly-monthly reference period) FOR EDWARDS AIR FORCE BASE

Height		Risk (%)									
		20		10		5		1		0.1	
(m)	(ft)	knots	ms^{-1}	knots	ms^{-1}	knots	ms^{-1}	knots	ms^{-1}	knots	ms^{-1}
10.0	33	17.4	9.0	20.2	10.4	22.5	11.6	27.4	14.1	33.6	17.3
18.3	60	19.7	10.2	22.8	11.8	25.4	13.1	31.0	16.0	36.5	18.8
30.5	100	21.8	11.3	25.3	13.0	28.1	14.5	34.4	17.7	39.2	20.2
61.0	200	25.0	12.9	29.0	15.0	32.3	16.6	39.4	20.3	43.1	22.2
91.4	300	27.1	14.0	31.5	16.2	35.0	18.0	42.7	22.0	45.7	23.5
121.9	400	28.8	14.9	33.4	17.2	37.1	19.1	45.3	23.3	47.6	24.5
152.4	500	30.1	15.6	34.9	18.0	38.9	20.0	47.4	24.4	49.1	25.3

The peak/mean wind profiles were constructed with a 1.4 gust factor and mean $+3\sigma$ value of k, as given in subsection 5.2.5.4. Some additional general ground wind data are given in References 5.46 and 5.47 for several other locations. See Section 18.5 for a discussion of low level profiles over water for Space Shuttle Solid Rocket Booster (SRB) water entry studies.

5.2.5.5.3 Frequency of Calm Winds

Generally, design criteria wind problems are concerned with high wind speeds, but a condition of calm or very low speeds may also be important. For example, with no wind to disperse venting vapors such as LOX, a poor visibility situation could develop around the vehicle. Calm wind conditions can also have significant inplications relative to the atmospheric diffusion of vehicle exhaust clouds. In addition calm wind in conjunction with high solar heating, can result in significantly high vehicle compartment temperatures. Table 5.2.22 shows the frequency of calm winds at the 10-meter for Cape Kennedy as a function of time of day and month. The maximum percentage of calms appear in the summer and during the early morning hours, with the minimum percentage appearing throughout the year during the afternoon. Similar tables for other location are available upon request.

5.2.6 Spectral Ground Wind Turbulence Model

Under most conditions ground winds are fully developed turbulent flows. This is particularly true when the wind speed is greater than a few meters per second, the atmosphere is unstable, or when both conditions exist. During nighttime conditions when the wind speed is typically low and the stratification is stable, the intensity of turbulence is small if not nil. Spectral methods are a particularly useful way of representing the turbulent portion of the ground wind environment for launch vehicle design purposes, as well as for use in diffusion calculations of toxic fuels and atmospheric pollutants.

5.2.6.1 Introduction

At a fixed point in the atmospheric boundary layer, the instantaneous wind vector fluctuates in time about the horizontal steady-state wind vector. The vector departure of the horizontal component of the instantaneous wind vector from the quasi-steady wind vector is the horizontal vector component of turbulence. This vector departure can be represented by two components, the longitudinal and the lateral components of turbulence which are parallel and perpendicular to the steady-state wind vector in the horizontal plane (Figure 5.2.5). The model contained herein is a spectral representation

TABLE 5.2.22 FREQUENCY (%) OF CALM WIND AT THE 10-m LEVEL, CAPE KENNEDY

Hour EST	Month												Annual
	Jan	Feb	Mar	Apr	May	June	July	Aug	Sept	Oct	Nov	Dec	
00	4.8	4.0	3.6	1.3	7.3	9.2	11.7	13.7	6.3	6.9	6.3	6.0	6.8
01	2.8	1.3	2.4	1.7	8.9	8.3	10.9	14.1	7.1	4.8	6.3	6.5	6.3
02	4.8	2.2	3.6	2.9	7.7	10.0	11.7	13.7	10.4	7.3	5.4	4.0	7.0
03	5.2	3.1	2.0	3.8	8.5	12.1	11.3	17.3	12.1	5.2	2.9	3.2	7.3
04	2.8	4.4	2.4	3.8	5.2	13.8	14.5	13.7	10.8	5.2	4.6	2.8	7.0
05	4.4	4.0	3.2	2.9	9.7	16.3	15.3	18.5	13.3	3.6	4.6	4.4	8.4
06	4.4	4.0	4.4	2.9	8.9	16.3	19.8	19.0	13.3	3.2	5.0	5.2	8.9
07	3.6	4.4	4.8	6.3	10.5	16.7	18.1	19.4	15.8	4.4	5.4	5.6	9.6
08	3.6	6.6	6.5	2.9	2.4	5.4	6.0	6.9	4.6	4.0	8.8	4.4	5.2
09	3.6	1.8	2.0	2.1	2.8	3.8	4.8	1.6	4.2	0.8	4.6	5.6	3.1
10	0.4	1.8	1.6	1.7	0.4	3.8	4.0	2.8	2.1	a	1.3	2.4	1.8
11	0.4	1.3	1.2	1.7	0.8	1.3	2.4	0.8	2.9	0.8	1.7	0.8	1.3
12	1.6	0.4	a	a	a	0.8	0.8	0.4	1.3	0.4	2.1	1.2	0.8
13	2.0	0.4	a	a	0.4	1.3	0.4	1.6	0.8	0.4	1.7	0.4	0.8
14	0.8	4.0	0.8	0.4	0.4	0.8	1.2	1.6	1.3	0.8	a	0.4	0.7
15	0.4	1.3	a	a	a	0.8	0.4	1.6	2.5	0.4	0.4	0.4	0.7
16	0.4	0.4	0.4	a	0.8	0.4	0.8	0.4	1.3	0.8	a	0.8	0.5
17	1.6	0.4	a	0.4	0.4	2.1	0.8	3.2	2.1	1.6	1.7	2.0	1.4
18	4.0	1.8	0.8	0.4	1.6	2.5	3.2	4.0	2.9	1.2	5.0	7.7	2.9
19	2.8	3.5	2.0	a	1.6	5.0	2.8	5.2	4.6	1.2	7.1	6.5	3.5
20	4.4	3.5	2.8	1.7	3.2	6.7	5.6	8.5	7.5	1.6	6.3	6.0	4.8
21	5.2	4.0	3.2	1.3	4.8	7.5	10.5	8.9	8.3	4.4	5.0	6.0	5.8
22	3.6	2.2	2.4	1.7	6.0	7.5	7.7	12.9	7.9	4.8	6.3	5.2	5.7
23	5.6	3.5	4.8	0.8	6.5	8.3	10.5	15.3	10.0	5.6	4.6	5.2	6.8
All Hours	3.1	2.5	2.3	1.7	4.1	6.7	7.3	8.6	6.4	2.9	4.0	3.9	4.5

a. values < 0.4 percent

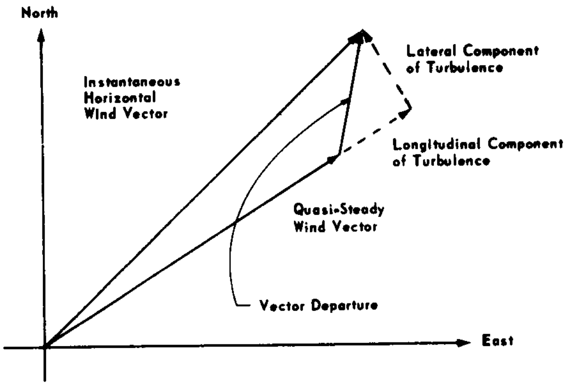

FIGURE 5.2.5 THE RELATIONSHIP BETWEEN THE QUASI-STEADY AND THE HORIZONTAL INSTANTANEOUS WIND VECTORS AND THE LONGITUDINAL AND LATERAL COMPONENTS OF TURBULENCE

of the characteristics of the longitudinal and lateral components of turbulence. The model analytically defines the spectra of these components of turbulence for the first 200 meters of the boundary layer. In addition, it defines the longitudinal and lateral cospectra, quadrature spectra, and the corresponding coherence functions associated with any pair of levels in the boundary layer. Details concerning the model herein can be found in References 5.8, 5.9, and 5.10.

5.2.6.2 Turbulence Spectra

The longitudinal and lateral spectra of turbulence at frequency ω and height z can be represented by a dimensionless function of the form

$$\frac{\omega\, S(\omega)}{\beta u_*^{\,2}} = \frac{c_1\, f/f_m}{\left[1 + 1.5\,(f/f_m)^{c_2}\right]^{5/3\, c_2}} , \qquad (5.3)$$

where

$$f = \frac{\omega z}{u(z)} \qquad (5.4)$$

$$f_m = c_3 \left(\frac{z}{z_r}\right)^{c_4} \qquad (5.5)$$

$$\beta = \left(\frac{z}{z_r}\right)^{c_5} \qquad (5.6)$$

$$u_* = c_6\, u(z_r) \qquad (5.7)$$

In these equations z_r is a reference height equal to 18.3 meters (60 ft); $\bar{u}(z)$ is the quasi-steady wind speed at height z; and the quantities c_i $(i = 1, 2, 3, 4, 5)$ are dimensionless constants that depend upon the site and

TABLE 5.2.23 DIMENSIONLESS CONSTANTS FOR THE LONGITUDINAL SPECTRUM OF TURBULENCE FOR THE EASTERN TEST RANGE

Condition	c_1	c_2	c_3	c_4	c_5
Light Wind Daytime Conditions	2.905	1.235	0.04	0.87	-0.14
Strong Winds	6.198	0.845	0.03	1.00	-0.63

TABLE 5.2.24 DIMENSIONLESS CONSTANTS FOR THE LATERAL SPECTRUM OF TURBULENCE FOR THE EASTERN TEST RANGE

Condition	c_1	c_2	c_3	c_4	c_5
Light Wind Daytime Conditions	4.599	1.144	0.033	0.72	-0.04
Strong Winds	3.954	0.781	0.1	0.58	-0.35

the stability. The frequency ω is defined with respect to a structure or vehicle at rest relative to the earth. The reader is refered to Sections 5.3.13 and 5.3.14 for the definition of turbulence spectral inputs for application to the take-off and landing of conventional aeronautical systems and the landing of the Shuttle Orbiter Vehicle. The spectrum $S(\omega)$ is defined so that integration over the domain $0 \leq \omega \leq \infty$ yields the variance of the turbulence. Engineering values of c_i are given in Table 5.2.23 for the longitudinal spectrum and Table 5.2.24 for the lateral spectrum. The constant c_6 can be estimated with the equation

$$c_6 = \frac{0.4}{\ln\left(\frac{z_r}{z_0}\right) - \Psi} , \qquad (5.8)$$

where z_0 is the surface roughness length of the site and Ψ is a parameter that depends upon the stability. If z_0 is not available for a particular site, then an estimate of z_0 can be obtained by taking 10 percent of the typical height of the surface obstructions (grass, shrubs, trees, rocks, etc.) over

TABLE 5.2.25 TYPICAL VALUES OF SURFACE ROUGHNESS LENGTH (z_0) FOR VARIOUS TYPES OF SURFACES

Type of Surface	z_0 (m)	z_0 (ft)
Mud flats, ice	10^{-5} - $3\cdot 10^{-5}$	$3\cdot 10^{-5}$ - 10^{-4}
Smooth sea	$2\cdot 10^{-4}$ - $3\cdot 10^{-4}$	$7\cdot 10^{4}$ - 10^{-3}
Sand	10^{-4} - 10^{-3}	$3\cdot 10^{-4}$ - $3\cdot 10^{-3}$
Snow surface	10^{-3} - $6\cdot 10^{-3}$	$3\cdot 10^{-4}$ - $2\cdot 10^{-2}$
Mown grass (~ 0.01 m)	10^{-3} - 10^{-2}	$3\cdot 10^{-3}$ - $3\cdot 10^{-2}$
Low grass, steppe	10^{-2} - $4\cdot 10^{-2}$	$3\cdot 10^{-2}$ - 10^{-1}
Fallow field	$2\cdot 10^{-2}$ - $3\cdot 10^{-2}$	$6\cdot 10^{-2}$ - 10^{-1}
High grass	$4\cdot 10^{-2}$ - 10^{-1}	10^{-1} - $3\cdot 10^{-1}$
Palmetto	10^{-1} - $3\cdot 10^{-1}$	$3\cdot 10^{-1}$ - 1
Suburbia	1 - 2	3 - 6
City	1 - 4	3 - 13

a fetch from the site with length equal to approximately 1500 meters. The parameter Ψ vanishes for strong wind conditions and is of order unity for light wind unstable daytime conditions at the Kennedy Space Center. Typical values of z_0 for various surfaces are given in Table 5.2.25.

The function given by equation (5.3) is depicted in Figures 5.2.6 and 5.2.7. Upon prescribing the steady-state wind profile $u(z)$ and the site (z_0), the longitudinal and lateral spectra are completely specified functions of height z and frequency ω. A discussion of the units of the various parameters mentioned above is given in subsection 5.2.6.4.

5.2.6.3 The Cospectrum and Quadrature Spectrum

The cospectrum and the quadrature spectrum associated with either the longitudinal or lateral components of turbulence at levels z_1 and z_2 can be represented by the following:

$$C(\omega, z_1, z_2) = \sqrt{S_1 S_2}\ \exp\left(-0.3465 \frac{\Delta f}{\Delta f_{0.5}}\right) \cos(2\pi\gamma\Delta f) \qquad (5.9)$$

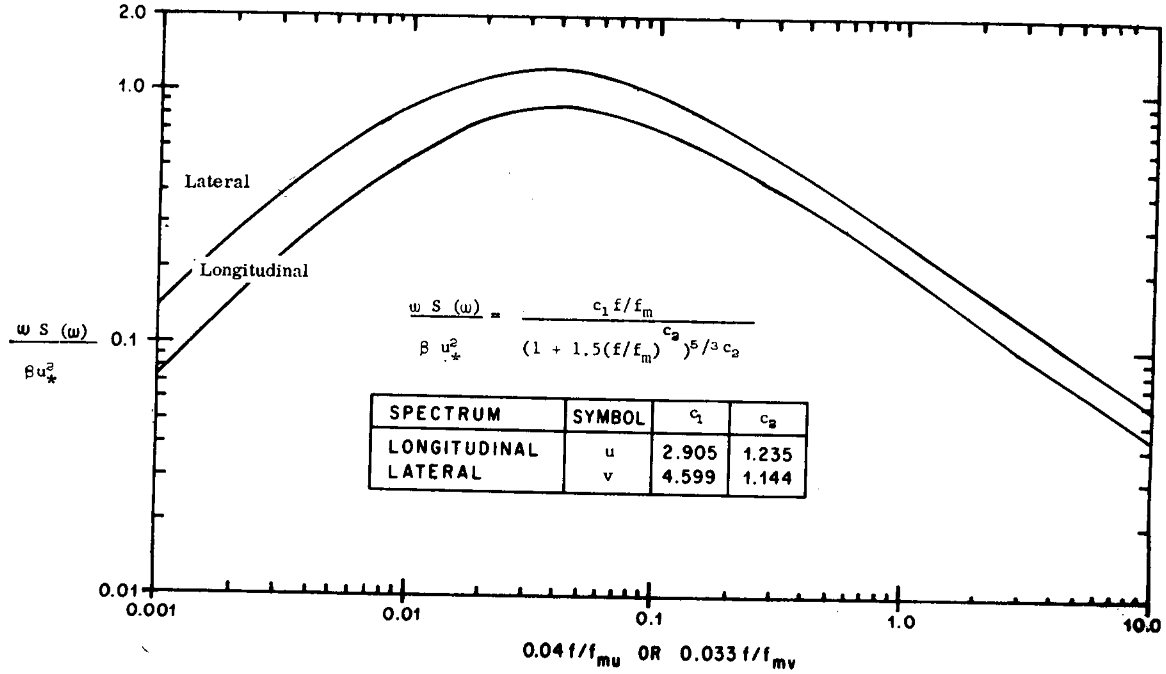

$$\frac{\omega S(\omega)}{\beta u_*^2} = \frac{c_1 f/f_m}{(1 + 1.5(f/f_m)^{c_2})^{5/3 c_2}}$$

SPECTRUM	SYMBOL	c_1	c_2
LONGITUDINAL	u	2.905	1.235
LATERAL	v	4.599	1.144

FIGURE 5.2.6 $\frac{\omega S(\omega)}{\beta u_*^2}$ VERSUS $\frac{0.04f}{f_m}$ (longitudinal) AND $\frac{0.033f}{f_m}$ (lateral) FOR LIGHT WIND DAYTIME CONDITIONS.

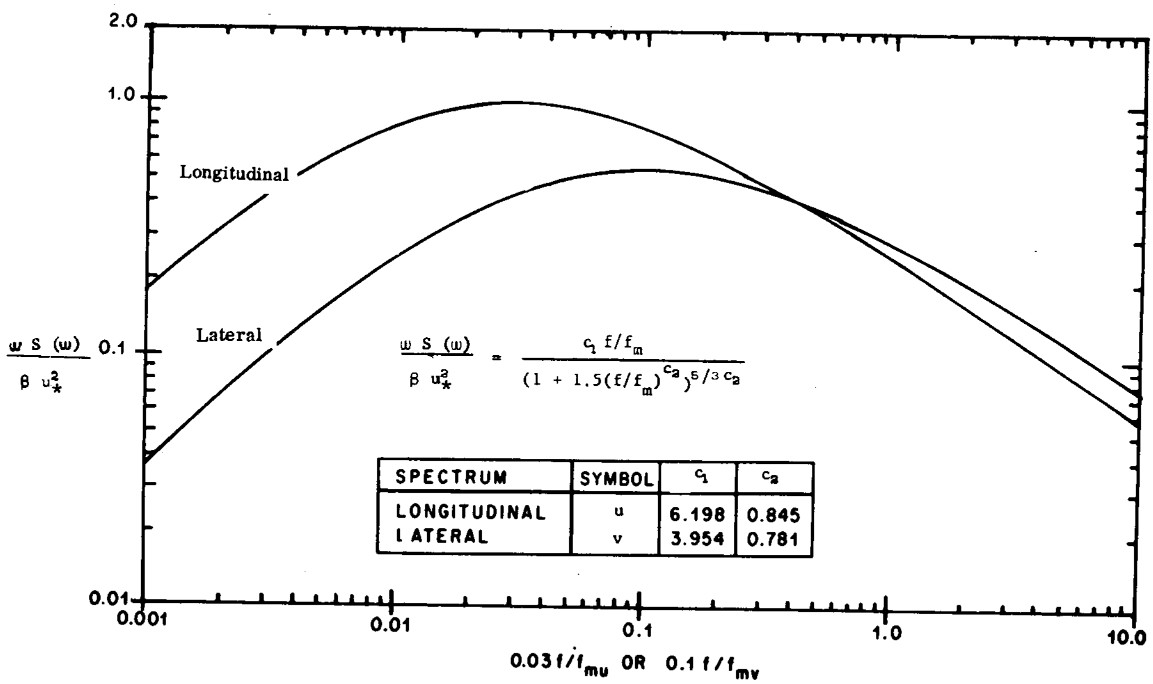

$$\frac{\omega S(\omega)}{\beta u_*^2} = \frac{c_1 f/f_m}{(1 + 1.5(f/f_m)^{c_2})^{5/3 c_2}}$$

SPECTRUM	SYMBOL	c_1	c_2
LONGITUDINAL	u	6.198	0.845
LATERAL	v	3.954	0.781

FIGURE 5.2.7 $\frac{\omega S(\omega)}{\beta u_*^2}$ VERSUS $\frac{0.03f}{f_m}$ (longitudinal) AND $\frac{0.1f}{f_m}$ (lateral) FOR STRONG WIND CONDITIONS

$$Q(\omega, z_1, z_2) = \sqrt{S_1 S_2}\ \exp\left(-0.3465\ \frac{\Delta f}{\Delta f_{0.5}}\right)\ \sin(2\pi\gamma\Delta f)\quad , \tag{5.10}$$

where

$$\Delta f = \frac{\omega z_2}{\bar{u}(z_2)} - \frac{\omega z_1}{\bar{u}(z_1)}\quad . \tag{5.11}$$

TABLE 5.2.26 VALUES OF $\Delta f_{0.5}$ FOR THE EASTERN TEST RANGE

Turbulence Component	Light Wind Daytime Conditions	Strong Winds
Longitudinal	0.04	0.036
Lateral	0.06	0.045

TABLE 5.2.27 VALUES OF γ FOR THE EASTERN TEST RANGE

Turbulence Component	$(z_1 + z_2)/2 \leq 100$m	$(z_1 + z_2)/2 > 100$m
Longitudinal	0.7	0.3
Lateral	1.4	0.5

The quantities S_1 and S_2 are the longitudinal or lateral spectra at levels z_1 and z_2, respectively, and $\bar{u}(z_1)$ and $\bar{u}(z_2)$ are the steady-state wind speeds at levels z_1 and z_2. The quantity $\Delta f_{0.5}$ is a nondimensional function of stability, and values of this parameter for the Eastern Test Range are given in Table 5.2.26. The nondimensional quantity γ should depend upon height and stability. However, it has only been possible to detect a dependence on height at the Eastern Test Range. Based upon analysis of turbulence data measured at the NASA 150 ground wind facility at the Kennedy Space Center, the values of γ in Table 5.2.27 are suggested for the Eastern Test Range. The quantity $\Delta f_{0.5}$ can be interpreted by constructing the coherence function, which is defined to be

$$\mathrm{coh}(\omega, z_1, z_2) = \frac{C^2 + Q^2}{S_1 S_2}\quad . \tag{5.12}$$

Substituting equations (5.9) and (5.10) into equation (5.12) yields

$$\mathrm{coh}(\omega, z_1, z_2) = \exp\left(-0.693\ \frac{\Delta f}{\Delta f_{0.5}}\right)\quad . \tag{5.13}$$

It is clear from this relationship that $\Delta f_{0.5}$ is that value of Δf for which the coherence (coh) is equal to 0.5.

5.2.6.4 Units

The spectral model of turbulence presented in subsections 5.2.6.2 and 5.2.6.3 is a dimensionless model. Accordingly, the user is free to select the system of units he desires, except that ω must have the units of cycles per unit time. Table 5.2.28 gives the appropriate metric and U. S. customary units for the various quantities in the model.

TABLE 5.2.28 METRIC AND U. S. CUSTOMARY UNITS OF VARIOUS QUANTITIES IN THE TURBULENCE MODEL

Quantity	Metric Units	U. S. Customary Units
ω	Hz	Hz
$S(\omega)$, $Q(\omega)$, $C(\omega)$	$m^2 s^{-2}/Hz$	$ft^2 s^{-2}/Hz$
f, f_m, Δf, $\Delta f_{0.5}$	Dimensionless	Dimensionless
z, z_r, z_0	m	ft
u, u_*	ms^{-1}	$ft\ s^{-1}$
β	Dimensionless	Dimensionless
Coh	Dimensionless	Dimensionless
γ	Dimensionless	Dimensionless
Ψ	Dimensionless	Dimensionless

5.2.7 Ground Wind Gust Factors

The gust factor G is defined to be

$$G = \frac{u}{\bar{u}} \tag{5.14}$$

where

u = maximum wind speed at height z within an averaging period of length τ in time

$\bar{u}$ = mean wind speed associated with the averaging period τ, given by

$$\bar{u} = \frac{1}{\tau} \int_0^\tau u_i(t)\, dt \tag{5.15}$$

$u_i(t)$ = instantaneous wind speed at time t

t = time reckoned from the beginning of the averaging period.

If $\tau = 0$, then $\bar{u} = u$ according to equation (5.15), and it follows from equation (5.14) that G = 1.0. As τ increases, $\bar{u}$ departs from u, and $\bar{u} \leq u$ and G > 1.0. Also, as τ increases, the probability of finding a maximum wind of a given magnitude increases. In other words, the maximum wind speed increases as τ increases. In the case of $\bar{u} \to 0$ and $u \geq 0$ ($\bar{u} = 0$ might correspond to windless free convection), $G \to \infty$. As $\bar{u}$ or u increases, G tends to decrease for fixed $\tau > 0$; while for very high wind speeds, G tends to approach a constant value for given values of z and τ. Finally, as z increases, G decreases. Thus, the gust factor is a function of the averaging time τ over which the mean wind speed is calculated, the height z, and the wind speed (mean or maximum).

5.2.7.1 Gust Factor as a Function of Peak Wind Speed ($u_{18.3}$) at Reference Height for Cape Kennedy

Investigations (Ref. 5.48) of gust factor data have revealed that the vertical variation of the gust factor can be described with the following relationship:

$$G = 1 + \frac{1}{g_0} \left(\frac{18.3}{z} \right)^p , \tag{5.16}$$

where z is the height in meters above natural grade. The parameter p, a function of the 18.3-meter peak wind speed in meters per second, is given by

$$p = 0.283 - 0.435\, e^{-0.2\, u_{18.3}} . \tag{5.17}$$

The parameter g_0, depends on the averaging time and the 18.3-meter peak wind speed and is given by

$$g_0 = 0.085 \left(\ln \frac{\tau}{10}\right)^2 - 0.329 \left(\ln \frac{\tau}{10}\right) + 1.98 - 1.887 e^{-0.2 u_{18.3}} , \qquad (5.18)$$

where τ is given in minutes and, $u_{18.3}$ in meters per second.

These relationships are valid for $u_{18.3} \geq 4$ m/sec and $\tau \leq 10$ min. In the interval 10 min $\leq \tau \leq$ 60 min, G is a slowly increasing monotonic function of τ, and for all engineering purposes the 10-minute gust factor (τ = 10 min) can be used as estimates of the gust factors associated with averaging times greater than 10 minutes and less than 60 minutes (10 min $\leq \tau \leq$ 60 min).

The dependence of the gust factor upon the averaging time and the peak wind speed is shown in Figure 5.2.8. Figure 5.2.9 illustrates the dependence of the 10-minute gust factors upon the peak wind speed and height.

The calculated mean gust factors for 10 minutes for values of $u_{18.3}$ in the interval 4.63 m/sec $\leq u_{18.3} \leq \infty$ are presented in Table 5.2.29 in both the U. S. Customary and Metric units for $u_{18.3}$ and z. As an example, the gust factor profile for τ = 10 minutes and $u_{18.3}$ = 9.27 m/sec (18 knots) is given by Table 5.2.30.

Since the basic wind statistics are given in terms of hourly peak winds, use the τ = 10 minute gust factors to convert the peak winds to mean winds by dividing by G. All gust factors in these sections are expected values for any particular set of values for u, τ, and z.

5.2.7.2 Gust Factors for Other Locations

For design purposes, the gust factor value of 1.4 will be used over all altitudes of the ground wind profile at other test ranges. This gust factor should correspond to approximately a 10-minute averaging period.

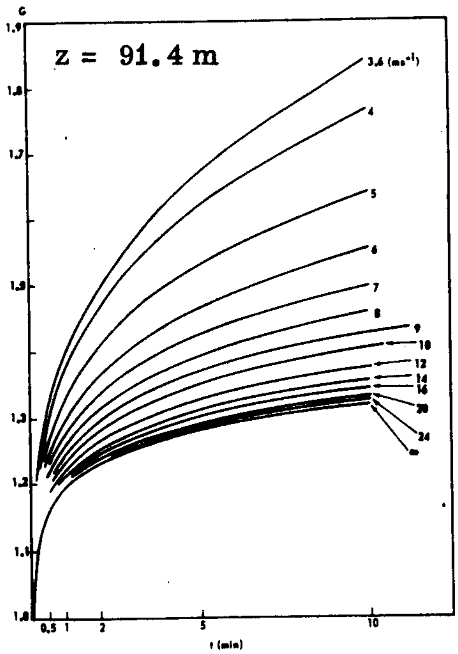

FIGURE 5.2.8 GUST FACTOR AS A FUNCTION OF TIME FOR VARIOUS VALUES OF $u_{18.3}$ IN THE INTERVAL

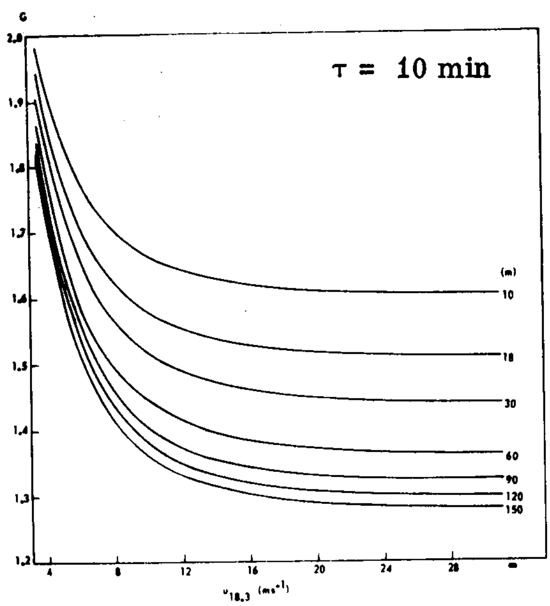

FIGURE 5.2.9 GUST FACTOR AS A FUNCTION OF PEAK WIND (u) FOR VARIOUS HEIGHTS

5.2.8 Ground Wind Shear

Wind shear near the surface, for design purposes, is a shear that acts upon a space vehicle, free-standing on the pad, or at time of lift-off. For overturning moment calculations the wind shear shall be computed by first subtracting the ten-minute mean wind speed at the height corresponding to the base of the vehicle from the peak wind speed at the height corresponding to the top of the vehicle (See Section 5.2.5.5 for mean and peak wind profiles) and then dividing the difference by the distance between the two profiles. The reader should consult references 5.63, 5.65. 5.66, and 5.67 for a detailed discussion of the statistical properties of wind shear near the ground for engineering applications.

TABLE 5.2.29 10-min GUST FACTORS FOR CAPE KENNEDY

60-ft (18.3-m) peak wind kts (ms^{-1})	Height Above Natural Grade in Feet (meters)						
	33 (10.0)	60 (18.3)	100 (30.5)	200 (61.0)	300 (91.4)	400 (121.9)	500 (152.4)
9.0 (4.63)	1.868	1.812	1.767	1.710	1.679	1.658	1.642
10.0 (5.15)	1.828	1.766	1.718	1.657	1.624	1.602	1.585
11.0 (5.66)	1.795	1.729	1.678	1.614	1.580	1.556	1.539
12.0 (6.18)	1.768	1.699	1.645	1.579	1.544	1.520	1.502
13.0 (6.69)	1.746	1.674	1.618	1.550	1.514	1.489	1.471
14.0 (7.21)	1.727	1.652	1.595	1.525	1.488	1.464	1.446
15.0 (7.72)	1.712	1.634	1.576	1.505	1.467	1.442	1.424
16.0 (8.24)	1.698	1.619	1.559	1.487	1.449	1.424	1.406
17.0 (8.75)	1.686	1.606	1.545	1.472	1.434	1.409	1.390
18.0 (9.27)	1.676	1.594	1.532	1.459	1.421	1.395	1.377
19.0 (9.78)	1.668	1.584	1.522	1.447	1.409	1.384	1.365
20.0 (10.30)	1.660	1.575	1.512	1.437	1.399	1.374	1.355
25.0 (12.87)	1.634	1.545	1.480	1.403	1.365	1.339	1.321
30.0 (15.44)	1.619	1.528	1.462	1.385	1.346	1.321	1.302
∞ (∞)	1.599	1.505	1.437	1.359	1.320	1.295	1.277

TABLE 5.2.30 GUST FACTOR PROFILE FOR τ = 10 min AND $u_{18.3}$ = 9.27 m/sec (18 knots)

Height		Gust Factor (G)
(ft)	(m)	
33	10.0	1.676
60	18.3	1.594
100	30.5	1.532
200	61.0	1.459
300	91.4	1.421
400	121.9	1.395
500	152.4	1.377

5.2.9 Ground Wind Direction Characteristics

Figure 5.2.1 (Subsection 5.2.5) shows a time trace of wind direction (section of a wind direction recording chart). This wind direction trace may be visualized as being composed of a mean wind direction plus fluctuations about the mean. An accurate measure of wind direction near the ground is difficult to obtain sometimes because of the interference of the structure that supports the instrumentation and other obstacles in the vicinity of the measurement location (Ref. 5.11). This is particularly true for launch pads, so that care must be exercised in locating wind sensors in order to obtain representative measurements of wind direction.

General information such as that which follows is available and may be used to specify conditions for particular studies. For instance, in Reference 5. 12 is discussed the variation of lateral wind-direction for various stability regimes. A graph is shown in Reference 5. 12 that gives values of the standard deviation of the lateral wind direction σ_θ as a function of height for a sampling time of about 10 minutes. It states that σ_θ for sampling periods greater than 1 minute with some given stability condition will always be larger when the wind is light than when it is strong. In general, the more stable the air, the smaller the σ_θ, except for the case of meandering wind directions for very low wind speeds and very stable conditions.

5.2.10 Design Winds for Facilities and Ground Support Equipment

5.2.10.1 Introduction

In this section, the important relationships between desired lifetime N, calculated risk U, design return period T_D, and design wind W_D will be described for use in facilities design for several locations.

a. The desired lifetime N is expressed in years, and preliminary estimates must be made as to how many years the proposed facility is to be used.

b. The calculated risk U is a probability expressed either as a percentage or as a decimal fraction. Calculated risk, sometimes referred to as design risk, is a probability measure of the risk the designer is willing to accept that the facility will be destroyed by wind loading in less time than the desired lifetime.

c. The design return period T_D is expressed in years and is a function of desired lifetime and calculated risk.

d. The design wind W_D is a function of the desired lifetime and calculated risk and is derived from the design return period and a probability distribution function of yearly peak winds.

5.2.10.2 Development of Relationships

From the theory of repeated trial probability we can derive the following expression:

$$N = \frac{\ln (1 - U)}{\ln \left(1 - \frac{1}{T_D}\right)} \qquad (5.19)$$

Equation (5.19) gives the important relationships for the three variables, calculated risk U, design return period T_D, and desired lifetime N. If estimates for any two variables are available, the third can be determined from this equation.

Design return period T_D, calculated with equation (5.19), for various values of desired lifetime N and design risk are given in Table 5.2.31. In Table 5.2.31, the exact and adopted values for design return period versus desired lifetime for various design risk are presented. The adopted values for T_D are in some cases greatly oversized to facilitate a convenient use of the tabulated probabilities for the distributions of yearly peak winds.

TABLE 5.2.31 EXACT AND ADOPTED VALUES FOR DESIGN RETURN PERIOD (T_D, years) VERSUS DESIRED LIFETIME (N, years) FOR VARIOUS DESIGN RISKS (U)

N (years)	Design Return Period (years)									
	U = 0.50%		U = 0.20%		U = 10%		U = 5%		U = 1%	
	Exact	Adopted	Exact	Adopted	Exact	Adopted	Exact	Adopted	Exact	Adopted
1	2	2	15	5	10	10	20	20	100	100
10	15	15	45	50	95	100	196	200	996	1000
20	29	30	90	100	190	200	390	400	1991	2000
25	37	40	113	125	238	250	488	500		
30	44	50	135	150	285	300	585	600		
50	73	100	225	250	475	500	975	1000		
100	145	150	449	500	950	1000	1950	2000		

5.2.10.3 Design Winds for Facilities at Cape Kennedy

To obtain the design wind, it is required that the wind speed corresponding to the design return period be determined. Since the design return period is a function of risk, either of two procedures can be used to determine the design wind: One is through a graphical or numerical interpolation procedure; the second is based on an analytical function. A knowledge of the distribution of yearly peak winds is required for both procedures. For the greatest statistical efficiency in arriving at a knowledge of the probability that peak winds will be less than or equal to some specified value of yearly peak winds, the choice of an appropriate probability distribution function is made, and the parameters for the function are estimated from the sample of yearly peak winds. From an investigation leading to the distribution of hourly, daily, monthly, and yearly peaks it was learned that the Gumbel distribution was an excellent fit for the 17 years of yearly peak ground winds at the 10-meter level for Cape Kennedy. The distribution of yearly peak wind (10-meter level), as obtained by the Gumbel distribution, is tabulated for various percentiles along with the corresponding return periods in Table 5.2.32. The values for the parameters α and μ for this distribution are also given in this table.

The design wind can now be determined by making a choice for desired lifetime and design risk and by taking the design return period from Table 5.2.31 and looking up the wind speed corresponding to the return period given in Table 5.2.32. For combinations not tabulated in Tables 5.2.31 and 5.2.32, the design return period can be interpolated.

5.2.10.4 Procedure to Determine Design Winds for Facilities

The design wind, W_D as a function of desired lifetime, N and calculated risk, U for the Gumbel distribution of peak winds at the 10-meter reference level, can be derived as

$$W_D = \frac{1}{\alpha}\{-\ell n[-\ell n(1 - U)] + \ell n\ N\} + \mu \quad , \qquad (5.20)$$

where α and μ are estimated from the sample of yearly peak winds.

TABLE 5. 2. 32 GUMBEL DISTRIBUTION FOR YEARLY PEAK WIND SPEED, 10-m REFERENCE LEVEL, INCLUDING HURRICANE WINDS, CAPE KENNEDY

Return Period (years)	Probability	y	m/sec	Knots
2	0. 50	0. 36651	25. 45	49. 47
5	0. 80	1. 49994	31. 79	61. 79
10	0. 90	2. 25037	35. 98	69. 95
15	0. 933	2. 66859	38. 33	74. 50
20	0. 95	2. 97020	40. 01	77. 77
30	0. 967	3. 39452	42. 38	82. 39
45	0. 978	3. 80561	44. 68	86. 86
50	0. 98	3. 90191	45. 22	87. 90
90	0. 9889	4. 49523	48. 54	94. 35
100	0. 99	4. 60015	49. 12	95. 49
150	0. 9933	5. 00229	51. 37	99. 86
200	0. 995	5. 29581	53. 01	103. 05
250	0. 996	5. 51946	54. 26	105. 48
300	0. 9967	5. 71218	55. 34	107. 58
400	0. 9975	5. 99021	56. 90	110. 60
500	0. 9980	6. 21361	58. 14	113. 02
600	0. 9983	6. 37628	58. 75	114. 20
1 000	0. 9990	6. 90726	62. 02	120. 56
10 000	0. 9999	9. 21029	74. 90	145. 60

α^{-1} = 5.5917 m/sec (10. 8695 knots) | μ = 23. 4 m/sec (45. 49 knots)

$$\Phi = e^{-e^{-y}}, \text{ where } y = \alpha[x-\mu]$$

Taking the values for α^{-1} = 5.5917 m/sec (10.8695 knots) and for μ = 23. 4 m/sec (45. 49 knots) from Table 5. 2. 32 and evaluating equation (5. 21) for selected values of N and U, yields the data in Table 5. 2. 33.

TABLE 5.2.33 FACILITY DESIGN WIND $\left(W_{D_{10}}\right)$ WITH RESPECT TO THE 10-m REFERENCE LEVEL PEAK WIND SPEED FOR VARIOUS LIFETIMES (N), CAPE KENNEDY

U	1 - U	ln [ln (1 - U)]	Design Wind $\left(W_{D_{10}}\right)$ for Various Lifetimes (N)[a] N = 1 (m/sec)	N = 1 (knots)	N = 10 (m/sec)	N = 10 (knots)	N = 30 (m/sec)	N = 30 (knots)	N = 100 (m/sec)	N = 100 (knots)
0.63212	0.36788	0	23.40	45.49	36.28	70.52	42.42	82.46	49.15	95.55
0.50	0.50	0.36651	25.45	49.47	38.33	74.50	44.47	86.44	51.20	99.53
0.4296	0.5704	0.57722	26.62	51.76	39.50	76.79	45.65	88.73	52.38	101.82
0.40	0.60	0.67173	27.16	52.79	40.03	77.82	46.18	89.76	52.92	102.85
0.30	0.70	1.03093	29.17	56.70	42.04	81.72	48.19	93.67	54.92	106.75
0.20	0.80	1.49994	31.79	61.79	44.66	86.82	50.81	98.76	57.54	111.85
0.10	0.90	2.25037	35.99	69.95	48.86	94.98	55.00	106.92	61.74	120.01
0.05	0.95	2.97020	40.01	77.77	52.88	102.80	59.03	114.74	65.76	127.83
0.01	0.99	4.60016	49.12	95.49	62.00	120.52	68.14	132.46	74.88	145.55

a. Values of N are given in years.

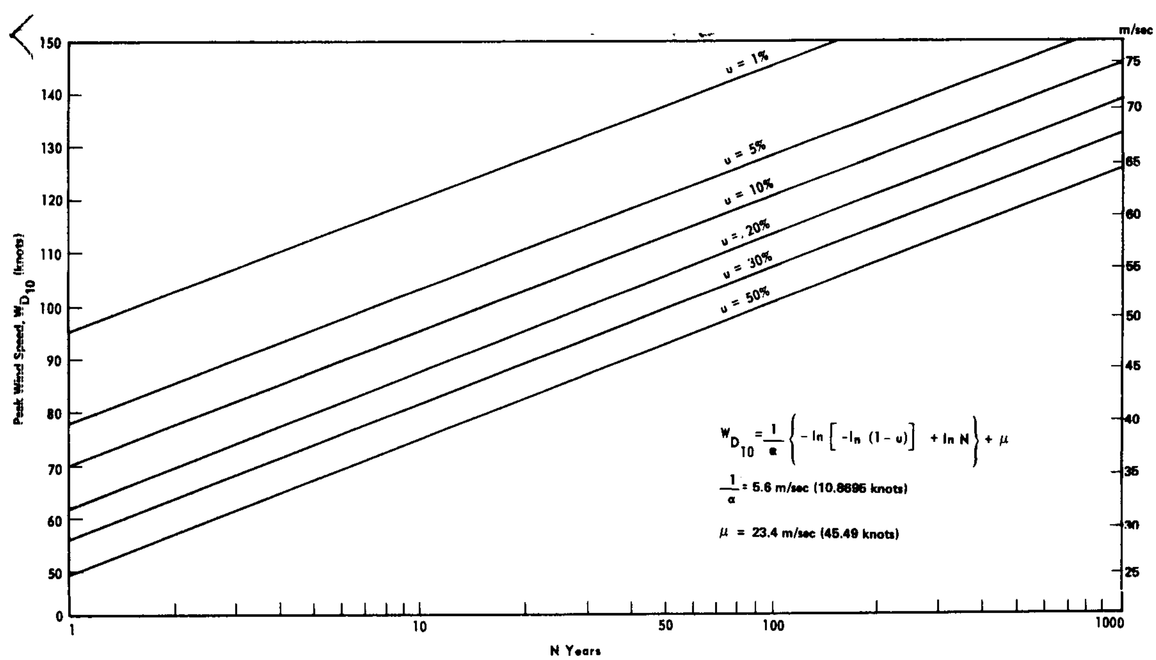

FIGURE 5.2.10 FACILITY DESIGN WIND $\left(W_{D_{10}}\right)$ WITH RESPECT TO THE 10-m REFERENCE LEVEL PEAK WIND SPEED FOR VARIOUS LIFETIMES (N), CAPE KENNEDY

A convenient plot for design wind versus desired lifetime is illustrated in Figure 5.2.10. The slopes of the lines in Figure 5.2.10 are equal.

5.2.10.5 Requirements for Wind Load Calculations

The design wind for a structure cannot be determined solely by wind statistics at a particular height. The design engineer is most interested in designing a structure which satisfies the user's requirements for utility, which will have a small risk of failure within the desired lifetime of the structure, and which can carry a sufficiently large wind load and be constructed at a sufficiently low cost. The total wind loading on a structure is composed of two interrelated components, steady-state drag wind loads and dynamic wind loads (time dependent drag loads, vortex shedding, forces, etc.). The time required for a structure to respond to the drag wind loads dictates the averaging time for the wind profile. In general, the structure response time depends upon the shape and size of the structure. The natural frequency of the structure and the size and shape of the structure and its components are important in estimating the dynamic wind load. It is conceivable that a structure could be designed to withstand very high wind speeds without structural failure and still oscillate in moderate wind speeds. If such a structure, for example, is to be used to support a precision tracking radar, then there may be little danger of overloading the structure by high winds; but the structure might be useless for its intended purpose if it were to oscillate in a moderate wind. Also, a building may have panels or small members that could respond to dynamic loading in such a way that long-term vibrations could cause failure, without any structural failure of the main supporting members. Since dynamic wind loading requires an intricate knowledge of the particular facility and its components, no attempt is made here to state generalized design criteria for dynamic wind loading. The emphasis in this section is upon winds for estimating drag wind loads in establishing design wind criteria for structures. Reference is made to subsection 5.2.5 for information appropriate to dynamic wind loads.

5. 2. 10. 6 Wind Profile Construction

Given the peak wind at the 10-meter level, the peak wind profile can be constructed with the peak wind profile law from subsection 5. 2. 5. Steady-state wind profiles can be obtained by using appropriate gust factors which are discussed in subsection 5.2.7.

To illustrate the procedures and operations in deriving the wind profile and the application of the gust factor, three examples are worked out for Cape Kennedy. The peak wind speed at the 10-meter level of 36, 49, and 62 m/sec (70, 95, and 120 knots) have been selected for these examples. These three wind speeds were selected because they correspond to a return period of 10, 100, and 1000 years for a peak wind at the 10-meter level at Cape Kennedy (see Table 5.2.32). Table 5.2.34 contains the risks of exceeding these peak winds for various values of desired lifetime.

FIGURE 5. 2. 34 CALCULATED RISK (U) VERSUS DESIRED LIFETIME (N, years) FOR ASSIGNED DESIGN WINDS RELATED TO PEAK WINDS AT THE 10-m REFERENCE LEVEL, CAPE KENNEDY

N (years)	$W_{D_{10}}$ = 36 m/sec (70 knots) T_D = 10 years U%	$W_{D_{10}}$ = 49 m/sec (95 knots) T_D = 100 years U%	$W_{D_{10}}$ = 62 m/sec (120 knots) T_D = 1000 years U%
1	10	1. 0	0. 1
10	65	10	1
20	88	18	2
25	93	22	2. 5
30	95. 8	26	3
50	99. 5	39. 5	5
100	99. 997	63. 397	10
T_D = Design return period			

Table 5.2.35 gives the peak design wind profiles corresponding to the desired lifetimes and calculated risks presented in Table 5.2.34. These profiles were calculated with equation (5.1).

5.2.10.7 Use of Gust Factors Versus Height

In estimating the drag load on a particular structure, it may be determined that wind force of a given magnitude must act on the structure for some period (for example, 1 min) to produce a critical drag load. To obtain the wind profile corresponding to a time averaged wind, the peak wind profile values are divided by the required gust factors. The gust factors for winds greater than 15 m/sec (29 knots) versus height given in Table 5.2.36 are taken from subsection 5.2.7. This operation may seem strange to someone who is accustomed to multiplying the given wind by a gust factor in establishing the design wind. This is because most literature on this subject gives the reference wind as averaged over some time increment (for example, 1, 2, or 5 min) or in terms of the "fastest mile" of wind that has a variable averaging time depending upon the wind speed. The design wind profiles for the three examples, that is, in terms of the peak winds of 36, 49, and 62 m/sec (70, 95, and 120 knots) at the 10-meter level, for various averaging times τ, given in minutes, are illustrated in Tables 5.2.37, 5.2.38, and 5.2.39. Following the procedures presented by this example, the design engineer can objectively derive several important design parameters that can be used in meeting the objective of designing a facility that will (1) meet the requirements for utility and desired lifetime, (2) withstand a sufficiently large wind loading with a known calculated risk of failure, caused by wind loads, and (3) allow him to proceed with trade-off studies between the design parameters and to estimate the cost of building a structure to best meet these design objectives.

5.2.10.8 Recommended Design Risk Versus Desired Lifetime

Unfortunately, there is not a clear-cut precedent from building codes to follow in recommending design risk for a given desired lifetime of a structure. This could be because the consequences of total loss of a structure due to wind forces differ according to the purpose of the structure. Conceivably, a value analysis in terms of original investment cost, replacement cost, safety of property and human life, loss of national prestige, and many other factors could be made to give a measure of the consequences for the loss of a particular structure in arriving at a decision as to what risk management is willing to accept for the loss within the desired lifetime of the structure. If the structure

TABLE 5.2.35 DESIGN[6] PEAK WIND PROFILES FOR DESIGN WIND RELATIVE TO THE 10-m REFERENCE LEVEL, CAPE KENNEDY

Height		$W_{D_{10}}$ = 36 m/sec (70 knots)		$W_{D_{10}}$ = 49 m/sec (95 knots)		$W_{D_{10}}$ = 62 m/sec (120 knots)	
(ft)	(m)	(knots)	(ms^{-1})	(knots)	(ms^{-1})	(knots)	(ms^{-1})
33	10	70.0	36.0	95.0	48.9	120.0	61.8
60	18.3	74.5	38.4	99.9	51.4	125.2	64.5
100	30.5	78.6	40.4	104.2	53.7	129.8	66.8
200	61.0	84.4	43.4	110.4	56.8	136.2	70.1
300	91.4	88.0	45.3	114.2	58.8	140.2	72.2
400	121.9	90.7	46.7	117.0	60.2	143.0	73.62
500	152.4	92.8	47.8	119.1	61.3	145.3	74.8

TABLE 5.2.36 GUST FACTORS FOR VARIOUS AVERAGING TIMES (τ) FOR PEAK WINDS > 15 m/sec (30 knots) AT THE 10-m REFERENCE LEVEL VERSUS HEIGHT, CAPE KENNEDY

Height		Various Averaging Times (τ, min)				
(ft)	(m)	τ=0.5	τ=1	τ=2	τ=5	τ=10
33	10	1.318	1.372	1.435	1.528	1.599
60	18.3	1.268	1.314	1.366	1.445	1.505
100	30.5	1.232	1.271	1.317	1.385	1.437
200	61.0	1.191	1.223	1.261	1.316	1.359
300	91.4	1.170	1.199	1.232	1.282	1.320
400	121.9	1.157	1.183	1.214	1.260	1.295
500	152.4	1.147	1.172	1.201	1.244	1.277

6. See Table 5.2.34 for calculated risk values versus desired lifetime for these design winds.

TABLE 5. 2. 37 DESIGN[7] WIND PROFILES FOR VARIOUS AVERAGING TIMES (τ) FOR PEAK DESIGN WIND OF 36. 0 m/sec (70 knots) RELATIVE TO THE 10-m REFERENCE LEVEL, CAPE KENNEDY

Height		Design Wind Profiles for Various Averaging Times (τ) in minutes											
(ft)	(m)	τ=0		τ=0. 5		τ=1		τ=2		τ=5		τ=10	
		(m/sec)	(knots)	(m/sec)	(knots)	(m/sec)	(knots)	(m/sec)	(knots)	(m/sec)	(knots)	(m/sec)	(knots)
33	10	36. 0	70. 0	27. 3	53. 1	26. 2	51. 0	25. 1	48. 8	23. 6	45. 8	22. 5	43. 8
60	18. 3	38. 3	74. 5	30. 2	58. 8	29. 2	56. 7	28. 0	54. 5	26. 5	51. 6	25. 5	49. 5
100	30. 5	40. 4	78. 6	32. 8	63. 8	31. 8	61. 8	30. 7	59. 7	29. 2	56. 8	28. 1	54. 7
200	61. 0	43. 4	84. 4	36. 5	70. 9	35. 5	69. 0	34. 4	66. 9	33. 0	64. 1	31. 9	62. 1
300	91. 4	45. 3	88. 0	38. 7	75. 2	37. 8	73. 4	36. 7	71. 4	35. 3	68. 6	34. 3	66. 7
400	121. 9	46. 7	90. 7	40. 3	78. 4	39. 5	76. 7	38. 4	74. 7	37. 0	72. 0	36. 0	70. 0
500	152. 4	47. 7	92. 8	41. 6	80. 9	40. 7	79. 2	39. 8	77. 3	38. 4	74. 6	37. 4	72. 7

TABLE 5. 2. 38 DESIGN[7] WIND PROFILES FOR VARIOUS AVERAGING TIMES (τ) FOR PEAK DESIGN WIND OF 49. 0 m/sec (95 knots) RELATIVE TO THE 10-m REFERENCE LEVEL, CAPE KENNEDY

Height		Design Wind Profiles for Various Averaging Times (τ) in minutes											
(ft)	(m)	τ=0		τ=0. 5		τ=1		τ=2		τ=5		τ=10	
		(m/sec)	(knots)	(m/sec)	(knots)	(m/sec)	(knots)	(m/sec)	(knots)	(m/sec)	(knots)	(m/sec)	(knots)
33	10	48. 9	95. 0	37. 1	72. 1	35. 6	69. 2	34. 1	66. 2	32. 0	62. 2	30. 6	59. 4
60	18. 3	51. 4	99. 9	40. 5	78. 8	39. 1	76. 0	37. 6	73. 1	35. 5	69. 1	34. 2	66. 4
100	30. 5	53. 6	104. 2	43. 5	84. 6	42. 2	82. 0	40. 7	79. 1	38. 7	75. 2	37. 3	72. 5
200	61. 0	56. 8	110. 4	47. 7	92. 7	46. 5	90. 3	45. 0	87. 5	43. 2	83. 9	41. 8	81. 2
300	91. 4	58. 7	114. 2	50. 2	97. 6	49. 0	95. 2	47. 7	92. 7	45. 8	89. 1	44. 5	86. 5
400	121. 9	60. 2	117. 0	52. 0	101. 1	50. 9	98. 9	49. 6	96. 4	47. 8	92. 9	46. 5	90. 3
500	152. 4	61. 3	119. 1	53. 4	103. 8	52. 3	101. 6	51. 0	99. 2	49. 2	95. 7	48. 0	93. 3

7. See Table 5. 2. 34 for calculated risk values versus desired lifetime for these design winds.

TABLE 5.2.39 DESIGN WIND[8] PROFILES FOR VARIOUS AVERAGING TIMES (τ) FOR PEAK DESIGN WIND OF 62.0 m/sec (120 knots) RELATIVE TO THE 10-m REFERENCE LEVEL, CAPE KENNEDY

Height		Design Wind Profiles for Various Averaging Times (τ) in minutes											
(ft)	(m)	τ=0		τ=0.5		τ=1		τ=2		τ=5		τ=10	
		(m/sec)	(knots)	(m/sec)	(knots)	(m/sec)	(knots)	(m/sec)	(knots)	(m/sec)	(knots)	(m/sec)	(knots)
33	10	61.7	120.0	46.8	91.0	45.0	87.5	43.0	83.6	40.4	78.5	38.6	75.0
60	18.3	64.4	125.2	50.8	98.7	49.0	95.3	47.2	91.7	44.6	86.6	42.8	83.2
100	30.5	66.8	129.8	54.2	105.4	52.5	102.1	50.7	98.6	48.2	93.7	46.5	90.3
200	61.0	70.1	136.2	58.9	114.4	57.3	111.4	55.6	108.0	53.2	103.5	51.5	100.2
300	91.4	72.1	140.2	61.6	119.8	60.1	116.9	58.5	113.8	56.3	109.4	54.6	106.2
400	121.9	73.6	143.0	63.6	123.6	62.2	120.9	60.6	117.8	58.4	113.5	56.8	110.4
500	152.4	74.7	145.3	65.2	126.7	63.8	124.0	62.2	121.0	60.1	116.8	58.5	113.8

is an isolated shed then obviously its loss is not as great as a structure that would house many people or a structure that is critical to the mission of a large organization; nor is it as potentially unsafe as the loss of a nuclear power plant or storage facility for explosives or highly radioactive materials. To give a starting point for design studies aimed at meeting the design objectives, it is recommended that a design risk of 10 percent for the desired lifetime be used in determining the wind loading on structures that have a high replacement cost. Should the loss of the structure be extremely hazardous to life or property, or critical to the mission of a large organization, then a design risk of five percent or less for the desired lifetime is recommended. These are subjective recommendations involving arbitrary assumptions about the design objectives. Note that the larger the desired lifetime, the greater the design risk is for a given wind speed (or wind loading). Therefore, realistic appraisals should be made for desired lifetimes.

5.2.10.9 Design Winds for Facilities at The Space and Missile Test Center, (Vandenberg AFB), Wallops Island, White Sands Missile Range, Edwards Air Force Base, New Orleans,[9] and Huntsville

5.2.10.9.1 The Wind Statistics

The basic wind statistics for these five locations are taken from Reference 5.13, which presents isotach maps for the United States for the

8. See Table 5.2.34 for calculated risk values versus desired lifetime for these design winds.

9. Includes Mississippi Test Facility Area.

50, 98, and 99 percentile values for the yearly maximum "fastest mile" of wind the 30-foot (~ 10-m) reference height above natural grade. By definition, the fastest mile is the fastest wind speed in miles per hour of any mile of wind during a specified period (usually taken as the 24-hour observational day), and the largest of these in a year for the period of record constitutes the statistical sample of yearly fastest mile. From this definition, it is noted that the fastest mile as a measure of wind speed has a variable averaging time; for example, if the wind speed is 60 miles per hour, the averaging time for the fastest mile of wind is 1 minute. For a wind speed of 120 miles per hour, the averaging time for the fastest mile of wind is 0.5 minute. Thom reports that the Fréchet probability distribution function fits his samples of fastest mile very well. The Fréchet distribution function is given as

$$F(x) = e^{-\left(\frac{x}{\beta}\right)^{-\gamma}} \tag{5.21}$$

where the two parameters β and γ are estimated from the sample by the maximum likelihood method. From Thom's maps of the 50, 98, and 99 percentiles of fastest mile of wind for yearly extremals, we have estimated (interpolated) for these percentiles for the five locations and calculated the values for the parameters β and γ for the Fréchet distribution function and computed several additional percentiles, as shown in Table 5. 2. 40. To have units consistent with the other sections of this document, the percentiles and the parameters β and γ have been converted from miles per hour to knots and m/sec. Thus, Table 5. 2. 40 gives the Fréchet distribution for the fastest mile of winds at the 30-foot (~10-m) level for the five locations with the units in knots and m/sec.

The discussion in subsection 5. 2. 10. 2. 4, devoted to desired lifetime, calculated risk, and design winds with respect to the wind statistics at a particular height (10-m level) is applicable here, except that the reference statistics are with respect to the fastest mile converted to knots and m/sec.

5. 2. 10. 9. 2 Conversion of Fastest Mile to Peak Winds

It was mentioned in subsection 5. 2. 10. 3 that the Fréchet distribution for the 17-year sample of yearly peak winds for Cape Kennedy was an acceptable fit to this sample. The Fréchet distributions for the fastest mile were obtained from Thom's analysis for Cape Kennedy. From these two distributions (the Fréchet for the peak winds as well as for the fastest mile), the ratio of the percentiles of the fastest mile to the peak winds were taken. This ratio varied from 1.12 to 1.09, over the range of probabilities from 30 to 99 percent. Thus we adopted 1.10 as a factor to multiply the statistics of the

TABLE 5.2.40 FRECHET DISTRIBUTION OF FASTEST MILE WIND AT THE 10-m HEIGHT OF YEARLY EXTREMES FOR THE INDICATED STATIONS

P Probability	T_D Return Period (years)	Fastest Mile Wind									
		Huntsville		New Orleans		Space and Missile Test Center [a]		Wallops Island		Edwards AFB	
		(m/sec)	(knots)	(m/sec)	(knots)	(m/sec)	(knots)	(m/sec)	(knots)	(m/sec)	(knots)
0.50	2	20.1	39.0	22.1	42.9	18.0	34.9	24.6	47.9	11.3	22.0
0.80	5	23.9	46.4	26.6	51.8	21.6	42.0	29.6	57.6	15.0	29.1
0.90	10	26.8	52.0	30.1	58.6	24.4	47.4	33.4	65.0	18.1	35.2
0.95	20	29.8	58.0	33.9	65.9	27.4	53.3	37.6	73.0	21.6	42.0
0.98	50	34.5	67.0	39.6	76.9	31.8	61.9	43.7	84.9	27.3	53.0
0.99	100	38.3	74.4	44.4	86.4	35.7	69.4	48.9	95.0	32.4	63.1
0.9933	150	40.7	79.2	47.4	92.2	38.0	73.9	52.2	101.4	35.1	68.3
0.995	200	42.3	82.2	49.7	96.7	39.9	77.6	54.7	106.3	38.6	75.0
0.996	250	44.1	85.7	51.6	100.4	41.4	80.4	56.7	110.2	40.8	79.3
0.99667	300	45.4	88.2	53.2	103.5	42.6	82.9	58.4	113.6	42.7	83.1
0.9975	400	47.4	92.1	55.8	108.4	44.6	86.7	61.2	118.9	45.8	89.1
0.998	500	49.0	95.3	57.9	112.5	46.2	89.9	63.4	123.2	48.5	94.2
0.99833	600	50.2	97.6	59.4	115.5	47.5	92.3	65.1	126.6	50.5	98.1
0.99875	800	52.7	102.4	62.6	121.6	50.3	97.7	68.4	133.0	54.0	105.0
0.999	1000	54.5	106.0	64.9	126.1	51.8	100.6	70.9	137.8	57.6	111.9
γ	Unitless	6.54686		6.08075		6.19591		6.19949		4.02093	
$1/\gamma$	Unitless	0.15274		0.16445		0.16140		0.16130		0.24870	
$\ln \beta$	Unitless	3.60758		3.70093		3.49620		3.81208		2.99989	
β	m/sec (knots)	18.979 (36.892)		20.829 (40.488)		16.968 (32.983)		23.274 (45.241)		10.322 (20.065)	

fastest mile of wind to obtain peak (instantaneous) wind statistics. This procedure is based on the evidence of only one station. A gust factor of 1.10 is often applied to the fastest mile statistics in facility design work to account for gust loads.

5.2.10.9.3 The Peak Wind Profile

The peak wind profile law adopted for the five locations for peak winds at the 10-meter level greater than 22.6 m/sec (44 knots) is

$$u = u_{10}\left(\frac{z}{10}\right)^{1/7} \tag{5.22}$$

where u_{10} is the peak wind at the 10-meter height and u is the peak wind at height z in meters.

5.2.10.9.4 The Mean Wind Profile

To obtain the mean wind profile for various averaging times, the gust factors given in subsection 5.2.7, are applied to the peak wind profile as determined by equation (5.22).

5.2.10.9.5 Design Wind Profiles for Six Station Locations

The design peak wind profiles for the peak winds in Table 5.2.41 are obtained from the adopted peak wind power law given by equation (5.22), and the mean wind profile for various averaging times are obtained by dividing by the gust factors for the various averaging times. (The gust factors versus height and averaging times are presented in Table 5.2.36.) The resulting selected design wind profiles for design return periods of 10, 100, and 1000 years for the five stations are given in Tables 5.2.42 through 5.2.56, in which values of τ are given in minutes. The design risk versus desired lifetime for the design return periods of 10, 100, and 1000 years is presented in Table 5.2.34.

5.2.11 Runway Orientation Optimization

Runway orientation is influenced by a number of factors; for example winds, terrain features, population interference, etc. In some cases the frequency of occurrence of crosswind components of some significant speed have received insufficient consideration. Aligning the runway with the prevailing wind will not insure that crosswinds will be minimized. In fact, two common synoptic situations (one producing light easterly winds, and the other causing strong northerly winds)

TABLE 5.2.41 PEAK WINDS (fastest mile values times 1.10) FOR THE 10-m REFERENCE LEVEL FOR 10-, 100-, AND 1000-YEAR RETURN PERIODS

T_D (years)	Peak Winds									
	Huntsville		New Orleans		SAMTEC[a] and White Sands		Wallops Island		Edwards AFB	
	(m/sec)	(knots)	(m/sec)	(knots)	(m/sec)	(knots)	(m/sec)	(knots)	(m/sec)	(knots)
10	29. 4	57. 2	33. 2	64. 5	26. 8	52. 1	36. 8	71. 5	19. 9	38. 7
100	42. 1	81. 8	48. 9	95. 0	39. 3	76. 3	53. 8	104. 5	35. 7	69. 4
1000	60. 0	116. 6	71. 4	138. 7	56. 9	110. 7	78. 0	151. 6	63. 4	123. 2

a. Vandenberg AFB, California.

TABLE 5. 2. 42 FACILITIES DESIGN WIND AS A FUNCTION OF AVERAGING TIME (τ) FOR A PEAK WIND OF 29. 4 m/sec (57. 2 knots) (10-year return period) FOR HUNTSVILLE, ALABAMA

Height		Facilities Design Wind as a Function of Averaging Time (τ) in minutes											
(ft)	(m)	τ=0 (peak)		τ=0. 5		τ=1		τ=2		τ=5		τ=10	
		(m/sec)	(knots)	(m/sec)	(knots)	(m/sec)	(knots)	(m/sec)	(knots)	(m/sec)	(knots)	(m/sec)	(knots)
33	10	29. 4	57. 2	22. 3	43. 4	21. 5	41. 7	20. 5	39. 9	19. 2	37. 4	18. 4	35. 8
60	18. 3	32. 1	62. 4	25. 3	49. 2	24. 4	47. 5	23. 5	45. 7	22. 2	43. 2	21. 3	41. 5
100	30. 5	34. 5	67. 1	28. 0	54. 5	27. 2	52. 8	26. 2	50. 9	24. 9	48. 4	24. 0	46. 7
200	61. 0	38. 1	74. 1	32. 0	62. 2	31. 2	60. 6	30. 2	58. 8	29. 0	56. 3	28. 0	54. 5
300	91. 4	40. 4	78. 5	34. 5	67. 1	33. 7	65. 5	32. 8	63. 7	31. 5	61. 2	30. 6	59. 5
400	121. 9	42. 1	81. 8	36. 4	70. 7	31. 2	60. 7	34. 7	67. 4	33. 4	64. 9	32. 5	63. 2
500	152. 4	43. 0	83. 6	37. 5	72. 9	36. 7	71. 3	35. 8	69. 6	34. 6	67. 2	33. 7	65. 5

TABLE 5.2.43 FACILITIES DESIGN WIND AS A FUNCTION OF AVERAGING TIME (τ) FOR A PEAK WIND OF 42.1 m/sec (81.8 knots) (100-year return period) FOR HUNTSVILLE, ALABAMA

Height		Facilities Design Wind as a Function of Averaging Time (τ) in minutes											
(ft)	(m)	τ=0 (peak)		τ=0.5		τ=1		τ=2		τ=5		τ=10	
		(m/sec)	(knots)	(m/sec)	(knots)	(m/sec)	(knots)	(m/sec)	(knots)	(m/sec)	(knots)	(m/sec)	(knots)
33	10	42.1	81.8	31.9	62.1	30.7	59.6	29.3	57.0	27.5	53.5	26.3	51.2
60	18.3	45.9	89.2	36.2	70.3	34.9	67.9	33.6	65.3	31.7	61.7	30.5	59.3
100	30.5	49.3	95.9	40.0	77.8	38.8	75.5	37.5	72.8	35.6	69.2	34.3	66.7
200	61.0	54.5	105.9	45.7	88.9	44.6	86.6	43.2	84.0	41.4	80.5	40.1	77.9
300	91.4	57.7	112.2	49.3	95.9	48.2	93.6	46.9	91.1	45.0	87.5	43.7	85.0
400	121.9	59.9	116.5	51.8	100.7	50.7	98.5	49.4	96.0	47.6	92.5	46.3	90.0
500	152.4	61.5	119.5	53.6	104.2	52.5	102.0	51.2	99.5	49.4	96.1	48.2	93.6

TABLE 5.2.44 FACILITIES DESIGN WIND AS A FUNCTION OF AVERAGING TIME (τ) FOR A PEAK WIND OF 60.0 m/sec (116.6 knots) (1000-year return period) FOR HUNTSVILLE, ALABAMA

Height		Facilities Design Wind as a Function of Averaging Time (τ) in minutes											
(ft)	(m)	τ=0 (peak)		τ=0.5		τ=1		τ=2		τ=5		τ=10	
		(m/sec)	(knots)	(m/sec)	(knots)	(m/sec)	(knots)	(m/sec)	(knots)	(m/sec)	(knots)	(m/sec)	(knots)
33	10	60.0	116.6	45.5	88.5	43.7	85.0	41.8	81.3	39.2	76.3	37.5	72.9
60	18.3	65.3	127.0	51.5	100.2	49.7	96.7	47.8	93.0	45.2	87.9	43.4	84.4
100	30.5	70.3	136.6	57.1	110.9	55.3	107.5	53.3	103.7	50.7	98.6	48.9	95.1
200	61.0	77.6	150.8	65.1	126.6	63.4	123.3	61.5	119.6	59.0	114.6	57.1	111.0
300	91.4	82.2	159.8	70.3	136.6	68.6	133.3	66.7	129.7	64.1	124.6	62.3	121.1
400	121.9	85.7	166.5	74.0	143.9	72.4	140.7	70.5	137.1	68.0	132.1	66.2	128.6
500	152.4	88.4	171.9	77.1	149.9	75.5	146.7	73.6	143.1	71.1	138.2	69.2	134.6

TABLE 5. 2. 45 FACILITIES DESIGN WIND AS A FUNCTION OF AVERAGING TIME (τ) FOR A PEAK WIND OF 33. 2 m/sec (64. 5 knots) (10-year return period) FOR NEW ORLEANS

Height		Facilities Design Wind as a Function of Averaging Time (τ) in minutes											
(ft)	(m)	τ=0 (peak)		τ=0. 5		τ=1		τ=2		τ=5		τ=10	
		(m/sec)	(knots)	(m/sec)	(knots)	(m/sec)	(knots)	(m/sec)	(knots)	(m/sec)	(knots)	(m/sec)	(knots)
33	10	33. 2	64. 5	25. 2	48. 9	24. 2	47. 0	23. 1	44. 9	21. 7	42. 2	20. 7	40. 3
60	18. 3	36. 2	70. 3	28. 5	55. 4	27. 5	53. 5	26. 5	51. 5	25. 1	48. 7	24. 0	46. 7
100	30. 5	38. 9	75. 6	31. 6	61. 4	30. 6	59. 5	29. 5	57. 4	28. 1	54. 6	27. 1	52. 6
200	61. 0	43. 0	83. 5	36. 1	70. 1	35. 1	68. 3	34. 1	66. 2	32. 6	63. 4	31. 6	61. 4
300	91. 4	45. 5	88. 5	38. 9	75. 6	38. 0	73. 8	36. 9	71. 8	35. 5	69. 0	34. 5	67. 0
400	121. 9	47. 4	92. 2	41. 0	79. 7	40. 1	77. 9	39. 0	75. 9	37. 7	73. 2	36. 6	71. 2
500	152. 4	48. 5	94. 3	42. 3	82. 2	41. 4	80. 5	40. 4	78. 5	39. 0	75. 8	38. 0	73. 8

TABLE 5. 2. 46 FACILITIES DESIGN WIND AS A FUNCTION OF AVERAGING TIME (τ) FOR A PEAK WIND OF 48. 9 m/sec (95. 0 knots) (100-year return period) FOR NEW ORLEANS

Height		Facilities Design Wind as a Function of Averaging Time (τ) in minutes											
(ft)	(m)	τ=0 (peak)		τ=0. 5		τ=1		τ=2		τ=5		τ=10	
		(m/sec)	(knots)	(m/sec)	(knots)	(m/sec)	(knots)	(m/sec)	(knots)	(m/sec)	(knots)	(m/sec)	(knots)
33	10	48. 9	95. 0	37. 1	72. 1	35. 6	69. 2	34. 1	66. 2	32. 0	62. 2	30. 6	59. 4
60	18. 3	53. 3	103. 6	42. 0	81. 7	40. 5	78. 8	39. 0	75. 8	36. 9	71. 7	35. 4	68. 8
100	30. 5	57. 3	111. 4	46. 5	90. 4	45. 1	87. 6	43. 5	84. 6	41. 4	80. 4	40. 8	79. 3
200	61. 0	63. 3	123. 0	53. 1	103. 3	51. 8	100. 6	50. 2	97. 5	48. 1	93. 5	46. 6	90. 5
300	91. 4	67. 0	130. 3	57. 3	111. 4	55. 9	108. 7	54. 4	105. 8	52. 3	101. 6	50. 8	98. 7
400	121. 9	69. 9	135. 8	60. 4	117. 4	59. 1	114. 8	57. 6	111. 9	55. 5	107. 8	54. 0	104. 9
500	152. 4	71. 4	138. 8	62. 2	121. 0	60. 9	118. 4	59. 5	115. 6	57. 4	111. 6	55. 9	108. 7

TABLE 5. 2. 47 FACILITIES DESIGN WIND AS A FUNCTION OF AVERAGING TIME (τ) FOR A PEAK WIND OF 71. 4 m/sec (138. 7 knots) (1000-year return period) FOR NEW ORLEANS

Height		Facilities Design Wind as a Function of Averaging Time (τ) in minutes											
(ft)	(m)	τ=0 (peak)		τ=0. 5		τ=1		τ=2		τ=5		τ=10	
		(m/sec)	(knots)	(m/sec)	(knots)	(m/sec)	(knots)	(m/sec)	(knots)	(m/sec)	(knots)	(m/sec)	(knots)
33	10	71. 4	138. 7	54. 1	105. 2	52. 0	101. 1	49. 7	96. 7	46. 7	90. 8	44. 6	86. 7
60	18. 3	77. 8	151. 2	61. 3	119. 2	59. 2	115. 1	56. 9	110. 7	53. 8	104. 6	51. 7	100. 5
100	30. 5	83. 7	162. 7	68. 0	132. 1	65. 8	128. 0	63. 5	123. 5	60. 4	117. 5	58. 2	113. 2
200	61. 0	92. 4	179. 6	77. 6	150. 8	75. 6	146. 9	73. 3	142. 4	70. 2	136. 5	68. 0	132. 2
300	91. 4	97. 9	190. 3	83. 6	162. 6	81. 6	158. 7	79. 5	154. 5	76. 3	148. 4	74. 2	144. 2
400	121. 9	102. 0	198. 2	88. 1	171. 3	86. 2	167. 5	84. 0	163. 3	80. 9	157. 3	78. 8	153. 1
500	152. 4	104. 3	202. 7	90. 9	176. 7	89. 0	173. 0	86. 8	168. 8	83. 8	162. 9	81. 6	158. 7

TABLE 5. 2. 48 FACILITIES DESIGN WIND AS A FUNCTION OF AVERAGING TIME (τ) FOR A PEAK WIND OF 26. 8 m/sec (52. 1 knots) (10-year return period) FOR THE SPACE AND MISSILE TEST CENTER AND WHITE SANDS MISSILE RANGE

Height		Facilities Design Wind as a Function of Averaging Time (τ) in minutes											
(ft)	(m)	τ=0 (peak)		τ=0. 5		τ=1		τ=2		τ=5		τ=10	
		(m/sec)	(knots)	(m/sec)	(knots)	(m/sec)	(knots)	(m/sec)	(knots)	(m/sec)	(knots)	(m/sec)	(knots)
33	10	26. 8	52. 1	20. 3	39. 5	19. 5	38. 0	18. 7	36. 3	17. 5	34. 1	16. 8	32. 6
60	18. 3	29. 2	56. 8	23. 0	44. 8	22. 2	43. 2	21. 4	41. 6	20. 2	39. 3	19. 4	37. 7
100	30. 5	31. 4	61. 1	25. 5	49. 6	24. 7	48. 1	23. 9	46. 4	22. 7	44. 1	21. 9	42. 5
200	61. 0	34. 7	67. 5	29. 2	56. 7	28. 4	55. 2	27. 5	53. 5	26. 4	51. 3	25. 6	49. 7
300	91. 4	36. 8	71. 5	31. 4	61. 1	30. 7	59. 6	29. 8	58. 0	28. 7	55. 8	27. 9	54. 2
400	121. 9	38. 3	74. 5	33. 1	64. 4	32. 4	63. 0	31. 6	61. 4	30. 4	59. 1	29. 6	57. 5
500	152. 4	39. 1	76. 1	34. 1	66. 3	33. 4	64. 9	32. 6	63. 3	31. 5	61. 2	30. 7	59. 6

TABLE 5. 2. 49 FACILITIES DESIGN WIND AS A FUNCTION OF AVERAGING TIME (τ) FOR A PEAK WIND OF 39. 3 m/sec (76. 3 knots) (100-year return period) FOR THE SPACE AND MISSILE TEST CENTER AND WHITE SANDS MISSILE RANGE

Height		Facilities Design Wind as a Function of Averaging Time (τ) in minutes											
(ft)	(m)	τ=0 (peak)		τ=0. 5		τ=1		τ=2		τ=5		τ=10	
		(m/sec)	(knots)	(m/sec)	(knots)	(m/sec)	(knots)	(m/sec)	(knots)	(m/sec)	(knots)	(m/sec)	(knots)
33	10	39. 3	76. 3	29. 8	57. 9	28. 6	55. 6	27. 4	53. 2	25. 7	49. 9	24. 5	47. 7
60	18. 3	42. 8	83. 2	33. 7	65. 6	32. 6	63. 3	31. 3	60. 9	29. 6	57. 6	28. 4	55. 3
100	30. 5	46. 0	89. 5	37. 3	72. 6	36. 2	70. 4	35. 0	68. 0	33. 2	64. 6	32. 0	62. 3
200	61. 0	50. 8	98. 8	42. 7	83. 0	41. 6	80. 8	40. 3	78. 4	38. 6	75. 1	37. 4	72. 7
300	91. 4	53. 9	104. 7	46. 0	89. 5	44. 9	87. 3	43. 7	85. 0	42. 0	81. 7	40. 8	79. 3
400	121. 9	56. 1	109. 1	48. 5	94. 3	47. 4	92. 2	46. 2	89. 9	44. 6	86. 6	43. 3	84. 2
500	152. 4	57. 4	111. 5	50. 0	97. 2	48. 9	95. 1	47. 7	92. 8	46. 1	89. 6	44. 9	87. 3

TABLE 5. 2. 50 FACILITIES DESIGN WIND AS A FUNCTION OF AVERAGING TIME (τ) FOR A PEAK WIND OF 56. 9 m/sec (110. 7 knots) (1000-year return period) FOR THE SPACE AND MISSILE TEST CENTER AND WHITE SANDS MISSILE RANGE

Height		Facilities Design Wind as a Function of Averaging Time (τ) in minutes											
(ft)	(m)	τ=0 (peak)		τ=0. 5		τ=1		τ=2		τ=5		τ=10	
		(m/sec)	(knots)	(m/sec)	(knots)	(m/sec)	(knots)	(m/sec)	(knots)	(m/sec)	(knots)	(m/sec)	(knots)
33	10	56. 9	110. 7	43. 2	84. 0	41. 5	80. 7	39. 7	77. 1	37. 2	72. 4	35. 6	69. 2
60	18. 3	62. 1	120. 7	49. 0	95. 2	47. 3	91. 9	45. 5	88. 4	43. 0	83. 5	41. 3	80. 2
100	30. 5	66. 8	129. 8	54. 2	105. 4	52. 5	102. 1	50. 7	98. 6	48. 2	93. 7	46. 5	90. 3
200	61. 0	73. 7	143. 3	61. 9	120. 3	60. 3	117. 2	58. 4	113. 6	56. 0	108. 9	54. 2	105. 4
300	91. 4	78. 1	151. 9	66. 8	129. 8	65. 2	126. 7	63. 4	123. 3	61. 0	118. 5	59. 2	115. 1
400	121. 9	81. 4	158. 2	70. 3	136. 7	68. 8	133. 7	67. 0	130. 3	64. 6	125. 6	62. 9	122. 2
500	152. 4	83. 2	161. 8	72. 6	141. 1	71. 0	138. 1	69. 3	134. 7	66. 9	130. 1	65. 2	126. 7

TABLE 5. 2. 51 FACILITIES DESIGN WIND AS A FUNCTION OF AVERAGING TIME (τ) FOR A PEAK WIND OF 36. 8 m/sec (71. 5 knots) (10-year return period) FOR WALLOPS TEST RANGE

Height		Facilities Design Wind as a Function of Averaging Time (τ) in minutes											
(ft)	(m)	τ=0 (peak)		τ=0. 5		τ=1		τ=2		τ=5		τ=10	
		(m/sec)	(knots)	(m/sec)	(knots)	(m/sec)	(knots)	(m/sec)	(knots)	(m/sec)	(knots)	(m/sec)	(knots)
33	10	36. 8	71. 5	27. 9	54. 2	26. 8	52. 1	25. 6	49. 8	24. 1	46. 8	23. 0	44. 7
60	18. 3	40. 1	77. 9	31. 6	61. 4	30. 5	59. 3	29. 3	57. 0	27. 7	53. 9	26. 6	51. 8
100	30. 5	43. 1	83. 8	35. 0	68. 0	33. 9	65. 9	32. 7	63. 6	31. 1	60. 5	30. 0	58. 3
200	61. 0	47. 6	92. 6	40. 0	77. 7	38. 9	75. 7	37. 8	73. 4	36. 2	70. 4	35. 0	68. 1
300	91. 4	50. 5	98. 1	43. 1	83. 8	42. 1	81. 8	40. 9	79. 6	39. 4	76. 5	38. 2	74. 3
400	121. 9	52. 6	102. 2	45. 4	88. 3	44. 4	86. 4	43. 3	84. 2	41. 7	81. 1	40. 6	78. 9
500	152. 4	53. 8	104. 5	46. 9	91. 1	45. 9	89. 2	44. 8	87. 0	43. 2	84. 0	42. 1	81. 8

TABLE 5. 2. 52 FACILITIES DESIGN WIND AS A FUNCTION OF AVERAGING TIME (τ) FOR A PEAK WIND OF 53. 8 m/sec (104. 5 knots) (100-year return period) FOR WALLOPS TEST RANGE

Height		Facilities Design Wind as a Function of Averaging Time (τ) in minutes											
(ft)	(m)	τ=0 (peak)		τ=0. 5		τ=1		τ=2		τ=5		τ=10	
		(m/sec)	(knots)	(m/sec)	(knots)	(m/sec)	(knots)	(m/sec)	(knots)	(m/sec)	(knots)	(m/sec)	(knots)
33	10	53. 8	104. 5	40. 8	79. 3	39. 2	76. 2	37. 5	72. 8	35. 2	68. 4	33. 6	65. 4
60	18. 3	58. 6	113. 9	46. 2	89. 8	44. 6	86. 7	42. 9	83. 4	40. 5	78. 8	38. 9	75. 7
100	30. 5	63. 0	122. 5	51. 1	99. 4	49. 6	96. 4	47. 8	93. 0	45. 5	88. 4	43. 8	85. 2
200	61. 0	69. 6	135. 3	58. 4	113. 6	56. 9	110. 6	55. 2	107. 3	52. 9	102. 8	51. 2	99. 6
300	91. 4	73. 8	143. 4	63. 1	122. 6	61. 5	119. 6	59. 9	116. 4	57. 6	111. 9	55. 9	108. 6
400	121. 9	76. 9	149. 4	66. 4	129. 1	65. 0	126. 3	63. 3	123. 1	61. 0	118. 6	59. 4	115. 4
500	152. 4	78. 6	152. 7	68. 5	133. 1	67. 0	130. 3	65. 4	127. 1	63. 1	122. 7	61. 5	119. 6

TABLE 5. 2. 53 FACILITIES DESIGN WIND AS A FUNCTION OF AVERAGING TIME (τ) FOR A PEAK WIND OF 78. 0 m/sec (151. 6 knots) (1000-year return period) FOR WALLOPS TEST RANGE

Height		Facilities Design Wind as a Function of Averaging Time (τ) in minutes											
(ft)	(m)	τ=0 (peak)		τ=0. 5		τ=1		τ=2		τ=5		τ=10	
		(m/sec)	(knots)	(m/sec)	(knots)	(m/sec)	(knots)	(m/sec)	(knots)	(m/sec)	(knots)	(m/sec)	(knots)
33	10	78. 0	151. 6	59. 2	115. 0	56. 8	110. 5	54. 3	105. 6	51. 0	99. 2	48. 8	94. 8
60	18. 3	85. 0	165. 3	67. 1	130. 4	64. 7	125. 8	62. 2	121. 0	58. 9	114. 4	56. 5	109. 8
100	30. 5	91. 5	177. 8	74. 2	144. 3	72. 0	139. 9	69. 4	135. 0	66. 1	128. 4	63. 6	123. 7
200	61. 0	101. 0	196. 3	84. 8	164. 8	82. 6	160. 5	80. 1	155. 7	76. 8	149. 2	74. 3	144. 4
300	91. 4	107. 0	208. 0	91. 5	177. 8	89. 3	173. 5	86. 9	168. 9	83. 4	162. 2	81. 1	157. 6
400	121. 9	111. 5	216. 7	96. 4	187. 3	94. 2	183. 2	91. 8	178. 5	88. 5	172. 0	86. 1	167. 3
500	152. 4	113. 9	221. 5	99. 3	193. 1	97. 2	189. 0	94. 9	184. 4	91. 6	178. 1	89. 3	173. 5

TABLE 5. 2. 54 FACILITIES DESIGN WIND AS A FUNCTION OF AVERAGING TIME (τ) FOR A PEAK WIND OF 19. 9 m/sec (38. 7 knots) (10-year return period) FOR EDWARDS AFB

Height		Facilities Design Wind as a Function of Averaging Time (τ) in minutes											
(ft)	(m)	τ=0 (peak)		τ=0. 5		τ=1		τ=2		τ=5		τ=10	
		(knots)	(m/sec)	(knots)	(m/sec)	(knots)	(m/sec)	(knots)	(m/sec)	(knots)	(m/sec)	(knots)	(m/sec)
33	10	38. 7	19. 9	29. 4	15. 1	28. 2	14. 5	27. 0	13. 9	25. 3	13. 0	24. 2	12. 4
60	18. 3	42. 1	21. 7	33. 2	17. 1	32. 0	16. 5	30. 8	15. 8	29. 1	15. 0	28. 0	14. 4
100	30. 5	45. 1	23. 2	36. 6	18. 8	35. 5	18. 3	34. 2	17. 6	32. 6	16. 8	31. 4	16. 2
200	61. 0	50. 1	25. 8	42. 1	21. 7	41. 0	21. 1	39. 7	20. 4	38. 1	19. 6	36. 9	19. 0
300	91. 4	53. 1	27. 3	45. 4	23. 4	44. 3	22. 8	43. 1	22. 2	41. 4	21. 3	40. 2	20. 7
400	121. 9	55. 3	28. 4	47. 8	24. 6	46. 7	24. 0	45. 6	23. 5	43. 9	22. 6	42. 7	22. 0
500	152. 4	57. 1	29. 4	49. 8	25. 6	48. 7	25. 1	47. 5	24. 4	45. 9	23. 6	44. 7	23. 0

TABLE 5. 2. 55 FACILITIES DESIGN WIND AS A FUNCTION OF AVERAGING TIME (τ) FOR A PEAK WIND OF 35. 7 m/sec (69. 4 knots) (100-year return period) FOR EDWARDS AFB

Height		Facilities Design Wind as a Function of Averaging Time (τ) in minutes											
(ft)	(m)	τ=0 (peak)		τ=0. 5		τ=1		τ=2		τ=5		τ=10	
		(knots)	(m/sec)	(knots)	(m/sec)	(knots)	(m/sec)	(knots)	(m/sec)	(knots)	(m/sec)	(knots)	(m/sec)
33	10	69. 4	35. 7	52. 7	27. 1	50. 6	26. 0	48. 4	24. 9	45. 4	23. 4	43. 4	22. 3
60	18. 3	75. 5	38. 8	59. 5	30. 6	57. 5	29. 6	55. 3	28. 4	52. 2	26. 9	50. 2	25. 8
100	30. 5	80. 9	41. 6	65. 7	33. 8	63. 7	32. 8	61. 4	31. 6	58. 4	30. 0	56. 3	29. 0
200	61. 0	89. 9	46. 2	75. 5	38. 8	73. 5	37. 8	71. 3	36. 7	68. 3	35. 1	66. 2	34. 1
300	91. 4	95. 2	49. 0	81. 4	41. 9	79. 4	40. 8	77. 3	39. 8	74. 3	38. 2	72. 1	37. 1
400	121. 9	99. 2	51. 0	85. 7	44. 1	83. 9	43. 2	81. 7	42. 0	78. 7	40. 5	76. 6	39. 4
500	152. 4	102. 4	52. 7	89. 3	45. 9	87. 4	45. 0	85. 3	43. 9	82. 3	42. 3	80. 2	41. 3

TABLE 5. 2. 56 FACILITIES DESIGN WIND AS A FUNCTION OF AVERAGING TIME (τ) FOR A PEAK WIND OF 63. 3 m/sec (123. 0 knots) (1000-year return period) FOR EDWARDS AFB

Height		Facilities Design Wind as a Function of Averaging Time (τ) in minutes											
(ft)	(m)	τ=0 (peak)		τ=0. 5		τ=1		τ=2		τ=5		τ=10	
		(knots)	(m/sec)	(knots)	(m/sec)	(knots)	(m/sec)	(knots)	(m/sec)	(knots)	(m/sec)	(knots)	(m/sec)
33	10	123. 0	63. 3	93. 3	48. 0	89. 7	46. 1	85. 7	44. 1	80. 5	41. 4	76. 9	39. 6
60	18. 3	133. 8	68. 8	105. 5	54. 3	101. 8	52. 4	98. 0	50. 4	92. 6	47. 6	88. 9	45. 7
100	30. 5	143. 2	73. 7	116. 2	59. 8	112. 7	58. 0	108. 7	55. 9	103. 4	53. 2	99. 7	51. 3
200	61. 0	159. 3	82. 0	133. 8	68. 8	130. 3	67. 0	126. 3	65. 0	121. 0	62. 2	117. 2	60. 3
300	91. 4	168. 7	86. 8	144. 2	74. 2	140. 7	72. 4	136. 9	70. 4	131. 6	67. 7	127. 8	65. 7
400	121. 9	175. 8	90. 4	151. 9	78. 1	148. 6	76. 4	144. 8	74. 5	139. 5	71. 8	135. 8	69. 9
500	152. 4	181. 5	93. 4	158. 2	81. 4	154. 9	79. 7	151. 1	77. 7	145. 9	75. 1	142. 1	73. 1

might exist in such a relationship that a runway oriented with the prevailing wind might be the least useful to an aircraft constrained by crosswind components. Two methods, one empirical, the other theoretical, of determining the optimum runway orientation to minimize critical crosswind component speeds are available (Ref. 5.51).

In the empirical method the runway crosswind components are computed for all azimuth and wind speed categories in the wind rose (Ref. 5.51). From these values the optimum runway orientation can be selected that will minimize the risk of occurrence of any specified crosswind speed.

The theoretical method requires that the wind components are bivariate normally distributed; i.e., a vector wind data sample is resolved into wind components in a rectangular coordinate system and the bivariate normal elliptical distribution is applied to the data sample of component winds. For example, let x_1 and x_2 be normally distributed variables with parameters (ξ_1, σ_1) and (ξ_2, σ_2). ξ_1 and ξ_2 are the respective means, while σ_1 and σ_2 are the respective standard deviations. Let ρ be the dependence between x_1 and x_2. Now, the bivariate normal density function is

$$p(x_1, x_2) = \left[2\pi\sigma_1\sigma_2(1-\rho^2)^{1/2}\right]^{-1} \exp\left\{-[2(1-\rho^2)]^{-1}\left[\left(\frac{x_1-\xi_1}{\sigma_1}\right)^2 - 2\rho\left(\frac{x_1-\xi_1}{\sigma_1}\right)\left(\frac{x_2-\xi_2}{\sigma_2}\right) + \left(\frac{x_2-\xi_2}{\sigma_2}\right)^2\right]\right\} \quad . \qquad (5.23)$$

Let α be any arbitrary angle in the rectangular coordinate system. From the statistics in the (x_1, x_2) space, the statistics for any rotation of the axes of the bivariate normal distribution through any arbitrary angle α may be computed (Ref. 5.52). Let $\Delta\alpha$ denote the desired increments for which runway orientation accuracy is required; e.g., one may wish to minimize the probability of crosswinds with a runway orientation accuracy down to $\Delta\alpha = 10$ deg. This means we must rotate the bivariate normal axes through every 10 degrees. It is only necessary to rotate the bivariate normal surface through 180 degrees since the distribution is symmetric in the other two quadrants. Let (y_1, y_2) denote the bivariate normal space after rotation. This rotation process will result in 18 sets of statistics in the (y_1, y_2) space. The quantity y_1 is the head wind component while y_2 is the crosswind component. Since we are concerned with minimizing the probability of cross winds (y_2) only, we now examine the marginal distributions $p(y_2)$ for the 18 orientations (α). Since $p(y_1, y_2)$ is bivariate normal, the 18 marginal distributions $p(y_2)$ must be univariate normal:

$$p(y_2) = \left[\sigma_2 \, (2\pi)^{1/2}\right]^{-1} \exp \left\{-\tfrac{1}{2} \left[(y_2 - \xi_2)/\sigma_2\right]^2\right\} \quad . \qquad (5.24)$$

ξ_2 and σ_2 are replaced by their sample estimates $\bar{Y}_2$ and S_{y_2}. Now, let

$$z = \frac{Y_2 - \bar{Y}_2}{S_{y_2}} \quad , \qquad (5.25)$$

where y_2 is the critical crosswind of interest. The quantity z is a standard normal variable and the probability of its exceedance is easily calculated from the tables of the standard normal integral. Since a right or left crosswind (y_2) is a constraint to an aircraft, the critical region (exceedance region) for the normal distribution is two-tailed; i.e., we are interested in twice the probability of exceeding $[y_2]$. Let this probability of exceedance of risk equal R. Now, the orientation for which R is a minimum is the desired optimum runway orientation. The procedure described may be used for any station. Only parameters estimated from the data are required as input. Consequently, many runways and locations may be examined rapidly.

Either the empirical or theoretical method may be used to determine an aircraft runway orientation that minimizes the probability of critical crosswinds. Again, it is emphasized that the wind components must be bivariate normally distributed to use the theoretical method. In practical applications, the following steps are suggested:

1. Test the component wind samples for bivariate normally if these samples are available. See Reference 5.53 for bivariate normal goodness-of-fit tests.

2. If the component winds are available and cannot be rejected as bivariate normal using the bivariate normal goodness-of-fit test, use the theoretical method since it is more expedient and easily programmed.

3. If the component wind data samples are not available and there is doubt concerning the assumption of bivariate normality of the wind components, use the empirical method.

5.3 Inflight Winds

5.3.1 Introduction

Inflight wind speed profiles are used in vehicle design studies primarily to establish structural and control system capabilities and compute performance requirements. The inflight wind speeds selected for vehicle design may not represent the same percentile value as the design surface wind speed. The selected wind speeds (inflight and surface) are determined by the desired vehicle launch capability and can differ in the percentile level since the inflight and surface wind speeds differ in degree of persistance for a given reference time period and can be treated as being statistically independent for engineering purposes.

Wind information for inflight design studies is presented in two basic forms: discrete or synthetic profies and measured profile samples. A detailed discussion of these two types of presentations and their uses may be found in Reference 5.14. There are certain limitations to each of these wind input forms, and their utility in design studies depends upon a number of considerations such as, (1) accuracy of basic measurements, (2) complexity of input to vehicle design, (3) economy and practicality for design use, (4) ability to represent significant features of the wind profile, (5) statistical assumption versus physical representation of the wind profile, (6) ability of input to ensure control system and structural integrity of the vehicle, and (7) flexibility of use in design trade-off studies.

An accurate and adequate number of measured wind profiles are necessary for developing a valid statistical description of the wind profile. Fortunately, current records of data from some locations (Cape Kennedy in particular) fulfill these requirements, although a continuing program of data acquisition is vital to further enhance the confidence of the statistical information generated. Various methods and sensors for obtaining inflight profiles include the rawinsonde, the FPS-16 Radar/Jimsphere, and the rocketsonde. The statistical analyses performed on the inflight wind profiles provide detailed descriptions of the upper winds and an understanding of the profile characteristics such as temporal and height variations, as well as indications of the frequency and the persistence of transient meteorological systems.

The synthetic type of wind profile is the oldest method used to present inflight design wind data. The synthetic wind profile data are presented in this document since this method of presentation provides a reasonable approach for most design studies when properly used, especially during the early design periods. Also, the concept of synthetic wind profiles is generally understood and employed in most aerospace organizations for design computations. It should be understood that the synthetic wind profile includes the wind speed, wind speed change, maximum wind layer thickness, and gusts that are required to establish vehicle design values.

Generally, launch vehicles for use at various launch sites and in comprehensive space research mission and payload configurations are designed by use of synthetic wind profiles based upon scalar wind speeds without regard to specific wind directions. However, if a vehicle is restricted to a given launch site, rather narrow flight azimuths, and a specific configuration and mission, winds based upon components (head, tail, left cross or right cross) are used. For a given percentile, the magnitudes of component winds are equal to or less than those of the scalar winds. Component or directional dependent winds should not be employed in initiated design studies unless specifically authorized by the cognizant design organization.

Selection of a set of detailed wind profiles for final design verification and launch delay risk calculations requires the matching of vehicle simultaion resolution and technique to frequency or information content of the profile. A detailed wind profile data set is available for KSC. Data acquisition programs are currently underway to acquire data to develop corresponding sets for other test ranges. (See Section 5.3.11).

The synthetic wind profile provides a conditionalized wind shear/gust state with respect to the given design wind speed. Therefore, in concept, the synthetic wind profile should produce a vehicle desihich lich has a launch delay risk not greater than a specified value which is generally the value associated with the design wind speed. This statement, although generally correct, depends on the control system response characteristics, the vehicle structural integrity, etc. In using the design verification selection of detailed wind profiles a joint condition of wind shear, gust, and speeds is given. Therefore, the resulting launch delay risk for a given vehicle design is the specified value of risk computed from the vehicle responses associated with the various profiles. For the synthetic profile a vehicle inflight wind speed capability and maximum launch delay risk may be stated which is conditional upon the wind/gust design values. However, for the selection of detailed wind profiles only a vehicle launch risk value may be given, since the wind characteristics are treated as a joint condition. These two differences in philosophy should be understood to avoid misinterpretation of vehicle response calculation comparisons. In both cases allowance for dispersions in vehicle characteristics should be made prior to flight simulation through the wind profiles and establishment of vehicle design response or operational launch delay risk values. The objective is to insure that a space vehicle will accommodate the desired percentage of wind profiles or conditions in its non-nominal flight mode.

5.3.2 Wind Aloft Climatology

The development of design wind speed profiles and associated shears and gusts requires use of the measured wind speed and wind direction data collected at the area of interest for some reasonably long period of time, i.e., five years or longer. The subject of wind climatology for an area, if treated in detail, would make up a voluminous document. The intent here is to give a brief treatment of selected topics that are frequently considered in space vehicle development and operations problems and provide references to more extensive information.

Considerable data summaries (monthly and seasonal) exist on wind aloft statistics for the world. However, it is necessary to interpret these data in terms of the engineering design problem and design philosophy. For example, wind requirements for performance calculations relative to aircraft fuel consumption requirements must be derived for the specific routes and design reference period. Such data are available on request.

5. 3. 3 Wind Component Statistics

Wind component statistics are used in mission planning to provide information on the probability of exceeding a given wind speed in the pitch or yaw planes and to bias the tilt program at a selected launch time.

Computations of the wind component statistics is made for various launch azimuths (15-degree intervals were selected at MSFC) for each month for the pitch plane (range) and yaw plane (cross range) at the Eastern Test Range and the Space and Missile Test Center (Vandenberg AFB, California).

References 5.15, 5.16, 5.17, 5.18, 5.54, and 5.55 contain information on the statistical distributions of wind speeds and component wind speeds for the test ranges at Cape Kennedy, Florida; El Paso, Texas; Santa Monica, California; and Wallops Island, Virginia. The Range Reference Atmosphere Documents (Ref. 5.18) provide similar information for other test ranges.

5. 3. 3. 1 Idealized Annual Wind Component Envelopes — Windiest Monthly Reference Period Concept

To provide information on the wind distribution for an entire year, envelopes for the Space and Missile Test Center (Ref. 5. 19) are most useful because the data are based upon monthly wind distributions. Thus, the data can be used to determine the worst condition expected for a selected launch azimuth during any month of the entire year. Similar data are available for the Eastern Test Range (Ref. 5.20) (Also see subsection 5.3.5.2).

5.3.3.2 Upper Wind Correlations

Coefficients of correlations of wind components between altitude levels with means and standard deviations at altitude levels may be used in a statistical model to derive representative wind profiles. A method of preparing synthetic wind profiles by use of correlation coefficients between wind components is described in Reference 5.21. In addition, these correlation data are applicable to certain statistical studies of vehicle responses (Ref. 5.22).

Data on correlations of wind between altitude levels for various geographical locations are presented in References 5.23, 5.24, and 5.25. The reports give values of the interlevel and intralevel coefficients of linear correlations between wind components. Because of the occurrence of the regular increase of winds with altitude below and the decrease of winds above the 10- to 14-kilometer level, the correlation coefficients decrease with greater altitude separation of the levels being correlated. Likewise, the highest correlation coefficients between components occur in the 10- to 14-kilometer level.

Correlations between wind components separated by a horizontal distance are now becoming available. The reader is referenced to the work of Buell (Refs. 5.56 and 5.57) for a detailed discussion of the subject.

5.3.3.3 Thickness of Strong Wind Layers

Wind speeds in the middle latitudes generally increase with altitude to a maximum between 10- and 14-kilometers. Above 14 kilometers, the wind speeds decrease with altitude, then increase at higher altitude, depending upon season and location. Frequently, these winds exceed 50 m/sec in the jet stream, a core of maximum winds over the midlatitudes in the 10- to 14-kilometer altitudes. The vertical extent of the core of maximum winds, or the sharpness of the extent of peak winds on the wind profile is important in some vehicle design studies. For information concerning the thickness of strong wind layers the reader is referred to Reference 5.26.

Table 5.3.1 shows design values of vertical thickness (based on maximum thickness) of the wind layers for wind speeds for the Eastern Test Range. Similar data for the Space and Missile Test Center are given in Table 5.3.2. At both ranges, the thickness of the layer decreases with increase of wind speed; that is, the sharpness of the wind profile in the vicinity of the jet core becomes more pronounced as wind speed increases.

TABLE 5.3.1 DESIGN THICKNESS FOR STRONG WIND LAYERS AT THE EASTERN TEST RANGE

Quasi-Steady-State Wind Speed ($\pm 5\ ms^{-1}$)	Maximum Thickness (km)	Altitude Range (km)
50	4	8.5 to 16.5
75	2	10.5 to 15.5
92	1	10.0 to 14.0

TABLE 5.3.2 DESIGN THICKNESS FOR STRONG WIND LAYERS AT THE SPACE AND MISSILE TEST CENTER (Vandenberg AFB, California)

Quasi-Steady-State Wind Speed ($\pm 5\ ms^{-1}$)	Maximum Thickness (km)	Altitude Range (km)
50	4	8.0 to 16
75	2	9.5 to 14

5.3.3.4 Exceedance Probabilities

The probability of inflight winds exceeding or not exceeding some critical wind speed for a specified time duration may be of considerable importance in mission planning, and in many cases, more information than just the occurrence of critical winds is desired. If a dual launch, with the second vehicle being launched 1 to 3 days after the first, is planned, and if the launch opportunity extends over a 10-day period, what is the probability that winds below (or above) critical levels will last for the entire 10 days? What is the probability of 2 or 3 consecutive days of favorable winds in the 10-day period? Suppose the winds are favorable on the scheduled launch day, but the mission is delayed for other reasons. Now, what is the probability that the winds will remain favorable for 3 or 4 more days? Answers to these questions could also be used for certain design considerations involving specific vehicles prepared for a given mission and launch window. A body of statistics is available from the Aerospace Environment Division, which can be used to answer these and possibly other related questions. An example of the kind of wind persistence statistics that are available is given in Fig. 5.3.1.

This figure gives the probability of the maximum wind speed in the 10 to 15 km region being less than, equal to, or greater than 50 and 75 m/sec^{-1} as the case may be for various multiples of 12 hours for the month of January. Thus, for example, there is approximately an 18% chance that the wind speed will be greater than or equal to 50 m/sec for ten consecutive 12-hour periods in January.

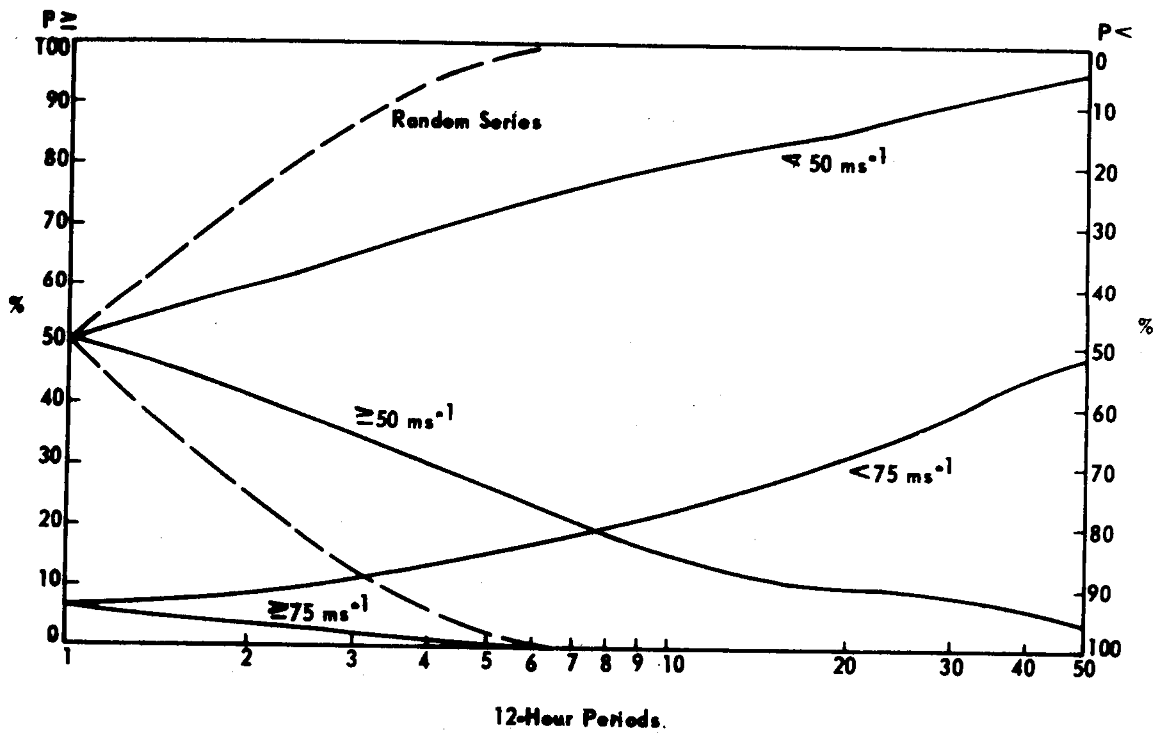

FIGURE 5.3.1 PROBABILITY OF THE MAXIMUM WIND SPEED IN THE 10- TO 15-km LAYER BEING LESS THAN, EQUAL TO, OR GREATER THAN SPECIFIED VALUES FOR k-CONSECUTIVE 12-hr PERIODS DURING JANUARY AT CAPE KENNEDY

5.3.3.5 Design Scalar Wind Speeds (10-15 km Altitude Layer)

The distributions of design scalar wind speed in the 10- to 15-kilometer altitude layer over the United States are shown in Figure 5.3.2 for the 95 percentile and Figure 5.3.3 for the 99 percentile values. The line of local maximum in the isopleths (maximum wind speeds) is shown by heavy lines with arrows. These winds occur at approximately the level of maximum dynamic pressure for most space vehicles.

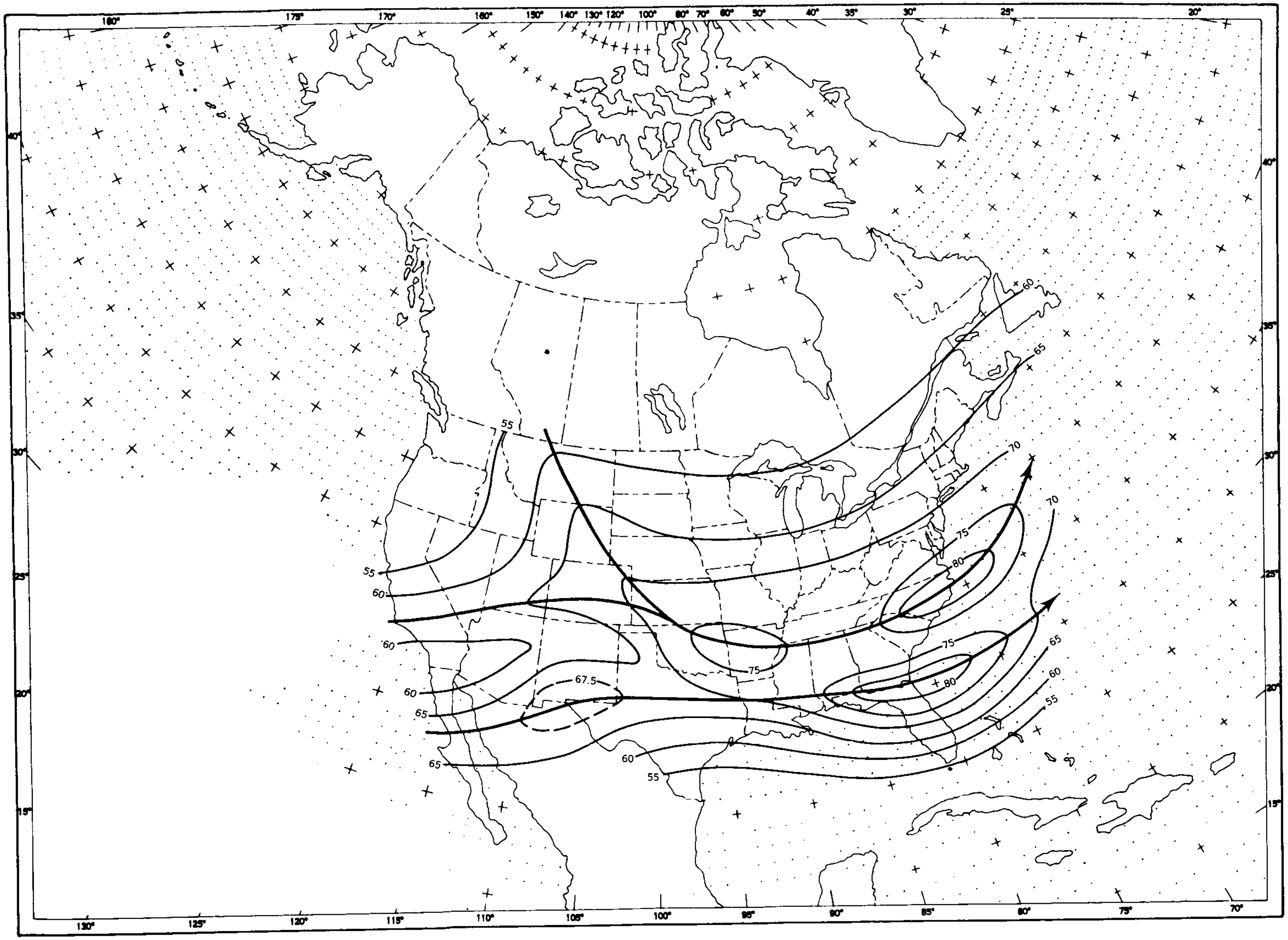

FIGURE 5. 3. 2 DESIGN SCALAR WIND SPEEDS (m/sec) 95 PERCENTILE ENVELOPE ANALYSIS PREPARED FROM WINDIEST MONTH AND MAXIMUM WINDS IN THE 10- TO 15-km LAYER

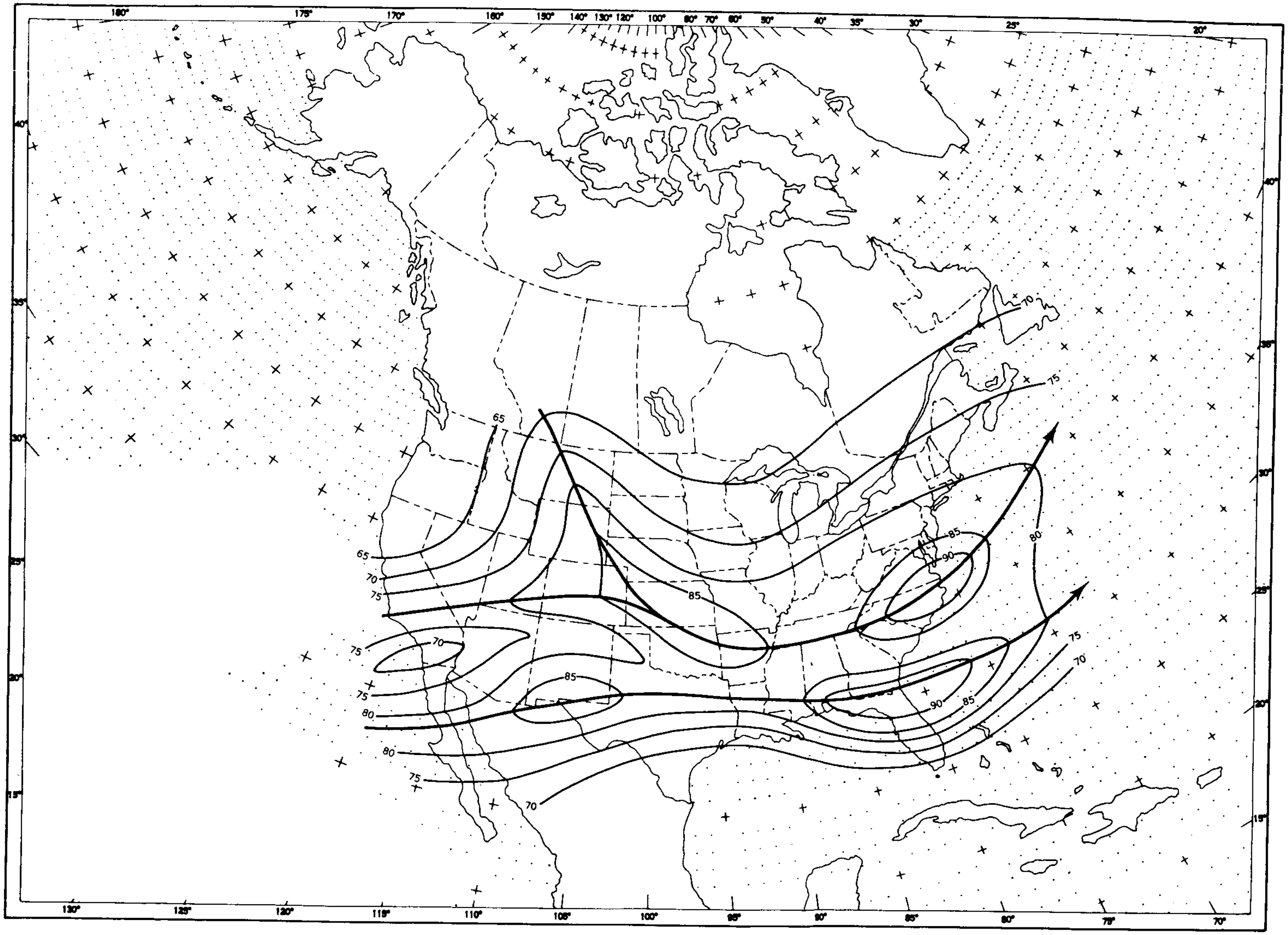

FIGURE 5. 3. 3 DESIGN SCALAR WIND SPEEDS (m/sec) 99 PERCENTILE ENVELOPE ANALYSIS PREPARED FROM WINDIEST MONTH AND MAXIMUM WINDS IN THE 10- TO 15-km LAYER

5.3.3.6 Temporal Wind Changes

Atmosphere flows at a point change in time. Wind direction and speed change can occur over time scales as short as a few minutes. There is no upper bound limit on the time scale over which the wind field can change. In order to develop wind biasing programs for space vehicle control purposes, which involve the use of wind profiles observed a number of hours prior to launch, it is necessary that consideration be given to the changes in wind speed and direction that can occur during the time elapsed from entering the biasing profile into the vehicle control system logic to the time of launch. Thus, for example, if the observed wind profile eight hours prior to launch is to be used as a wind biasing profile, then consideration should be given to the dispersions in wind direction and speed that could occur over this period of time. Wind speed and direction change data are also useful for mission operation purposes. At the present time studies are being conducted by the Aerospace Environment Division to define these dispersions in a statistical context. Some preliminary results are now available and are presented herein in part.

In order to account for the differences between the dynamics of the flow in the atmospheric boundary layer and the free atmosphere, the atmosphere is usually partitioned at the 2-kilometer level in studies of the temporal changes of the wind field. Below the 2-kilometer level the flow is significantly influenced by the surface of the earth and the flow is predominantly a turbulent one. In the free atmosphere above the 2-kilometer level the flow is for all practical purposes free of the effects of the surface of the earth.

Figures 5.3.4 and 5.3.5 contain idealized 99% wind direction and speed changes as a function of elapsed time and observed or referemce wind speed for altitudes between 3 m and 2 km for ETR. The wind speed may increase or decrease from the reference profile value; thus, envelopes of each category are presented in Figure 5.3.5. Figures 5.3.6 and 5.3.7 are the idealized 99% wind direction and speed changes as a function of elapsed time and observed or reference wind speed for altitudes between 2 to 16 km.

A few cautionary statements regarding the data given above are in order. They are applicable only to the Eastern Test Range, Cape Kennedy launch area because differences are known to exist in the data with the geographical sites. Conclusions should not be drawn relative to frequency content and phase relationships of the wind profile since the data given herein provides only envelope conditions for ranges of speed and direction changes. Direction correlations have not been developed between the changes of wind direction and wind speed.

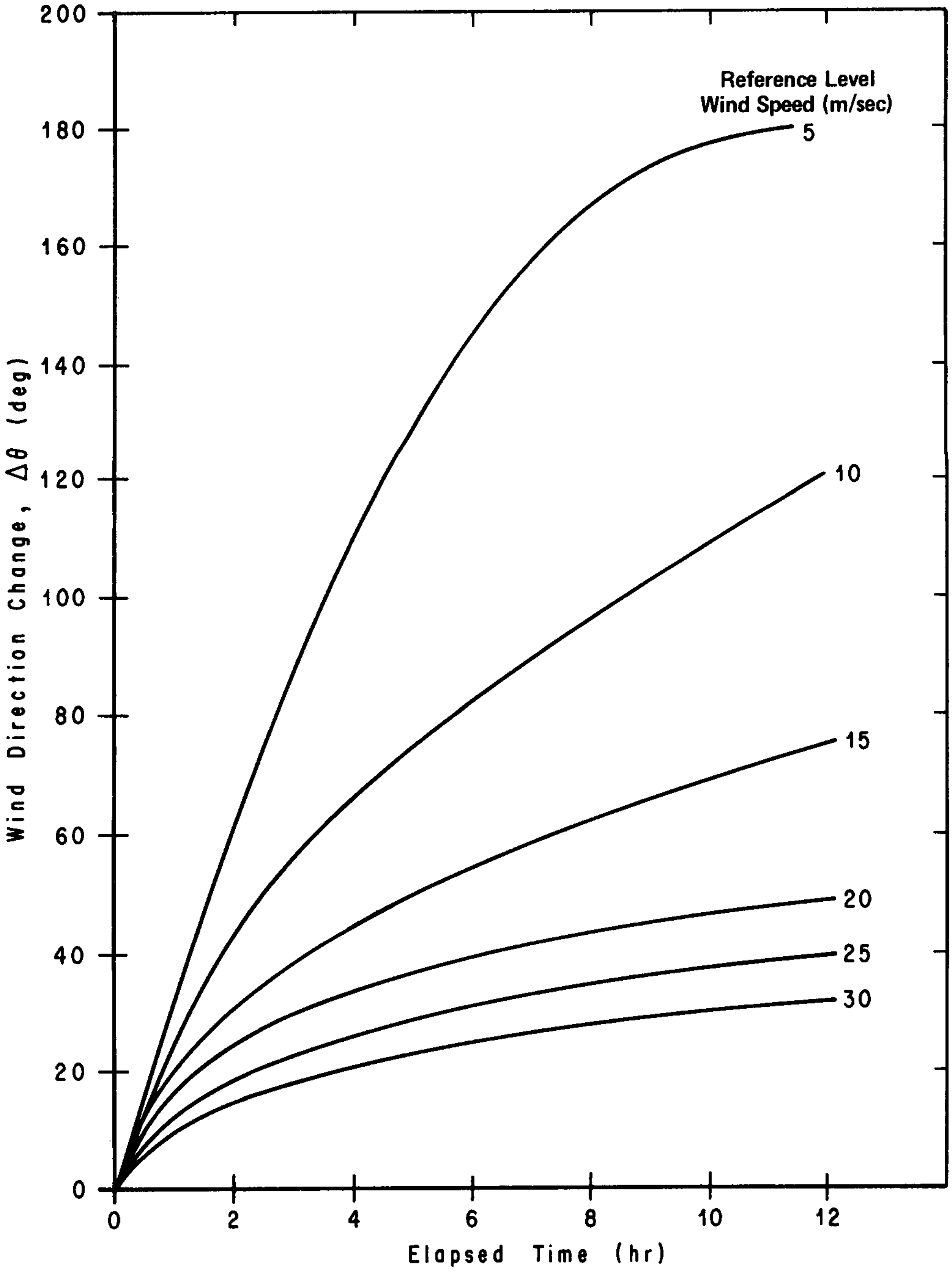

Figure 5.3.4 IDEALIZED 99% WIND DIRECTION CHANGE AS A FUNCTION OF TIME AND WIND SPEED IN THE 3M TO 2KM ALTITUDE REGION OF THE EASTERN TEST RANGE

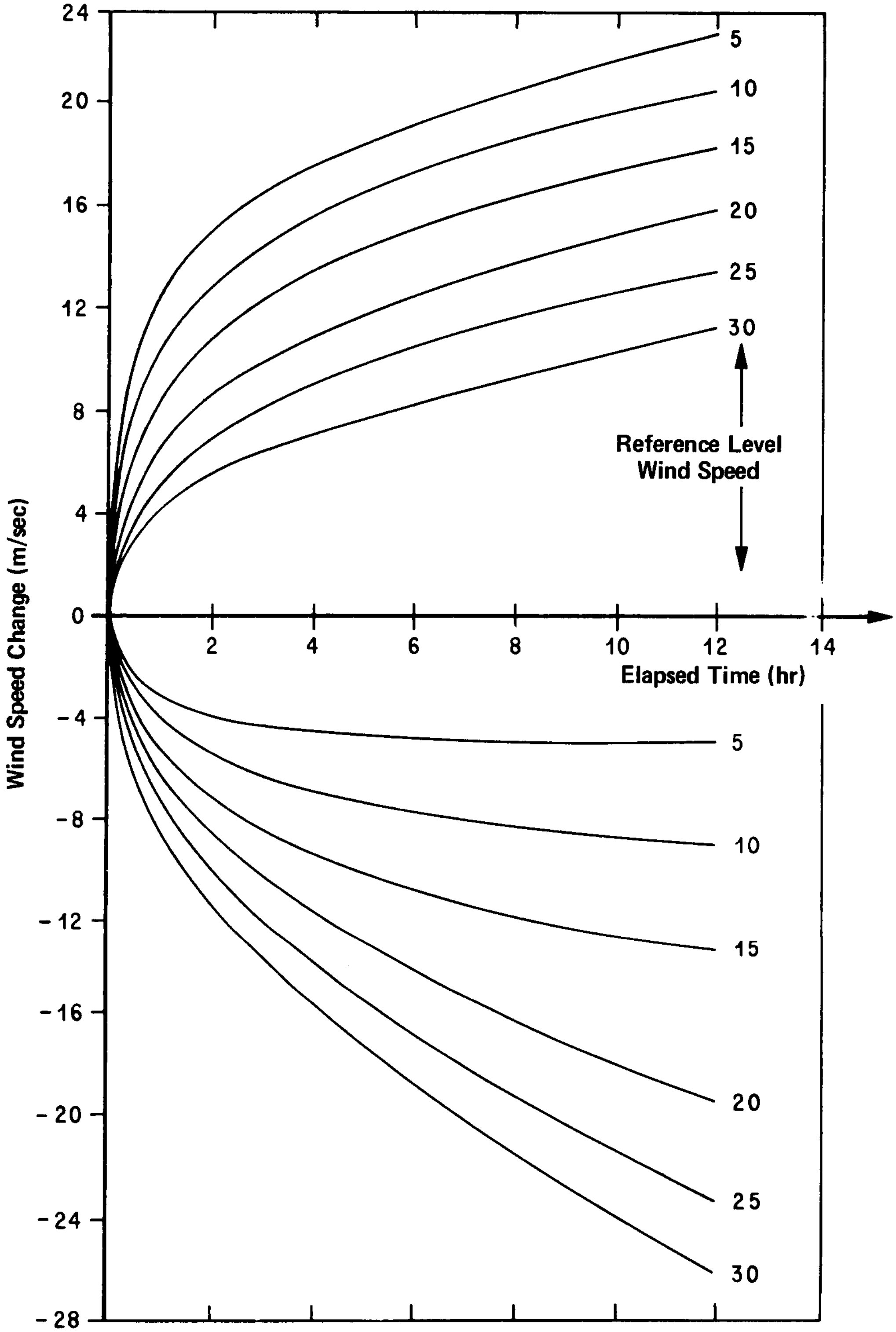

Figure 5.3.5 IDEALIZED 99% WIND SPEED CHANGE AS A FUNCTION OF TIME AND WIND SPEED IN THE 3M TO 2KM ALTITUDE REGION OF THE EASTERN TEST RANGE.

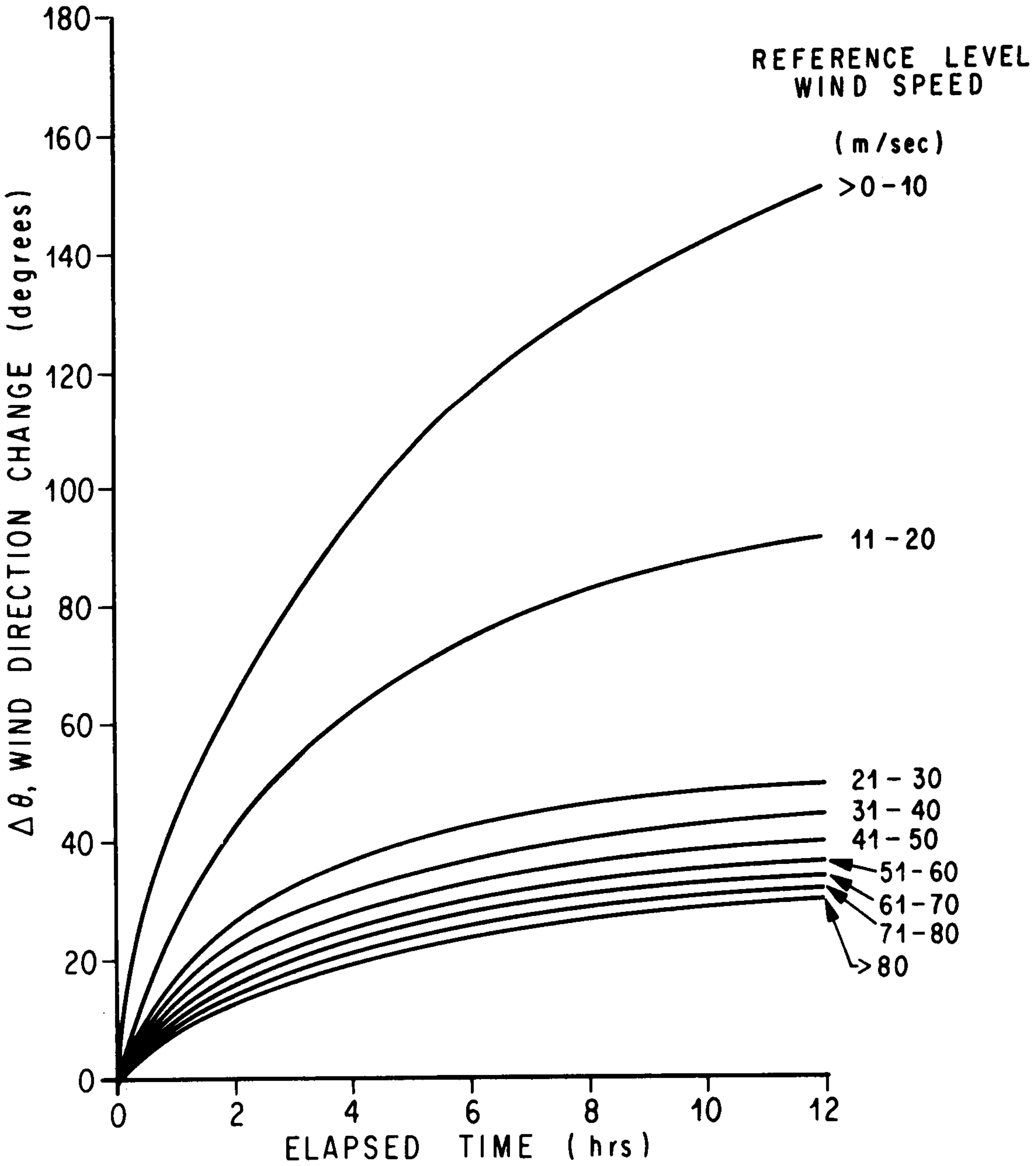

Figure 5.3.6 IDEALIZED 99% WIND DIRECTION CHANGE AS A FUNCTION OF TIME AND WIND SPEED IN THE 2 - 16KM REGION OF THE EASTERN TEST RANGE.

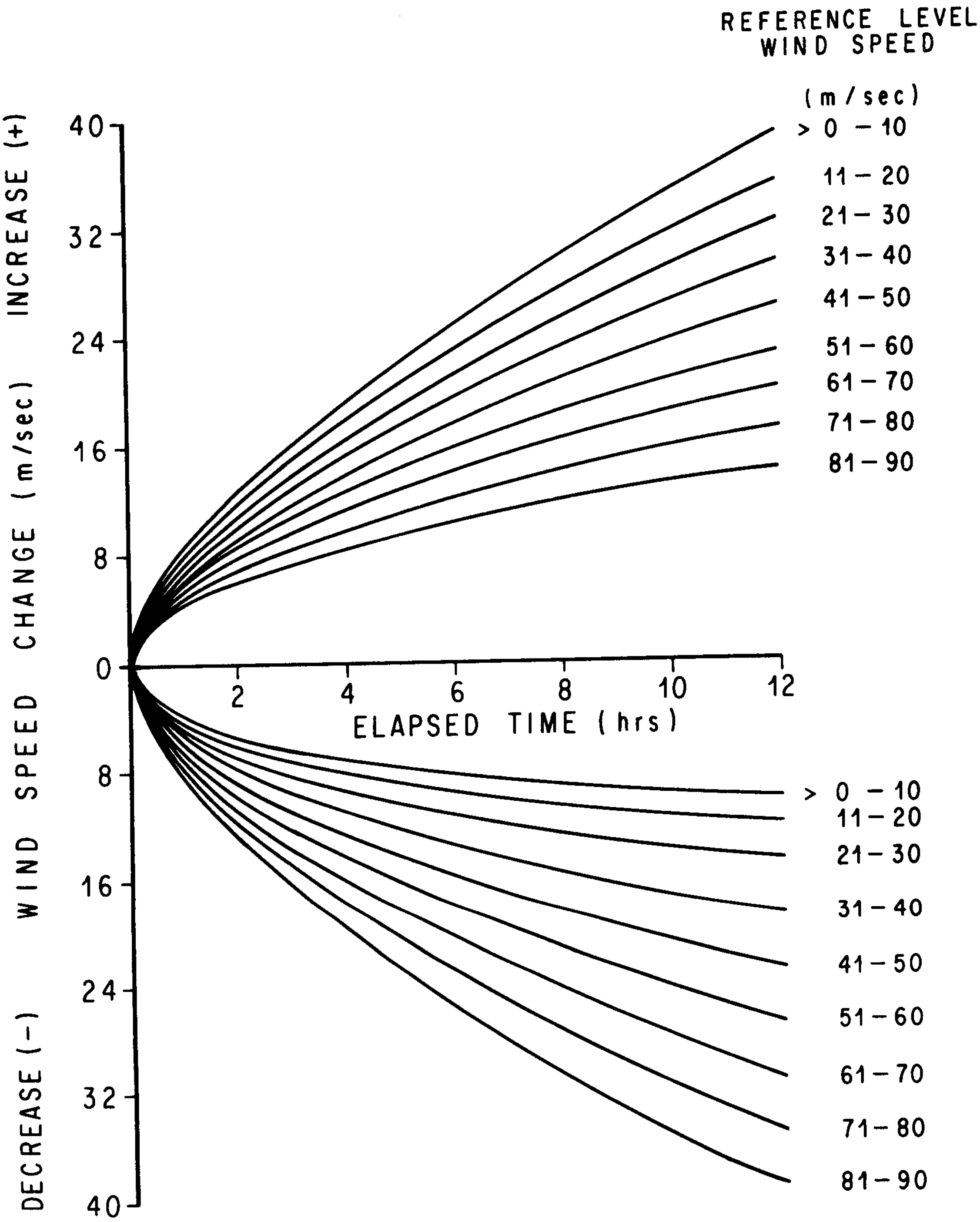

Figure 5.3.7 IDEALIZED 99% WIND SPEED CHANGE AS A FUNCTION OF TIME AND WIND SPEED IN THE 2 - 16 KM REGION OF THE EASTERN TEST RANGE.

Additional information concerning wind speed and direction changes can be found in reports by Camp and Susko (Ref. 5.27), Susko and Kaufman (Ref. 5.58) for Cape Kennedy, and Camp and Fox for Santa Monica (Ref. 5.28). Further details are published in Aerospace Environment Division memorandums and are available on request.

5.3.4 Wind Speed Profiles for Biasing Tilt Program

In attempting to maintain a desired flight path for a space vehicle through a strong wind region, the vehicle control system could introduce excessive bending moments and orbit anomalies. To reduce this problem, it is sometimes desirable to wind bias the pitch program, that is, to tilt the vehicle sufficiently to produce the desired flight path and minimize maximum dynamic pressure level loads with the expected wind profile. Since most inflight strong winds over Cape Kennedy are winter westerlies, it is sometimes expedient to use the monthly or seasonal pitch plane median wind speed profile for bias analyses.

Head and tail wind components and right and left cross wind components from 0- to 60-kilometer altitudes were computed for every 15 degrees of flight azimuth for the Eastern Test Range launch area and were published by NASA (Ref. 5.54 and 5.55). Similar calculations are available upon request for other ranges.

It is not usually necessary to bias the vehicle in the yaw plane because of the flight azimuths normally used at Cape Kennedy. For applications where both pitch and yaw biasing are used at Cape Kennedy, monthly vector mean winds may be more efficient for wind biasing. Such statistics will be made available upon request.

5.3.5 Design Wind Speed Profile Envelopes

The wind data given are not expected to be exceeded by the given percentage of time (time as related to the observational interval of the data sample) based upon the windiest monthly reference period. To obtain the profiles, monthly frequency distributions are combined for each percentile level to give the envelope over all months. The profiles represent horizontal wind flow referenced to the earth's surface. Vertical wind flow is negligible except for that associated with gusts or turbulence. The scalar wind speed envelopes are normally applied without regard to flight directions to establish the initial design requirements. Directional wind cirteria for use with the synthetic wind profile techniques should be applied with care and specific knowledge of the vehicle mission and flight path, since severe wind constraints could result for other flight paths and missions.

5.3.5.1 Scalar Wind Speed Envelopes

Scalar wind speed profile envelopes are presented in Tables 5.3.3 through 5.3.7 and Figures 5.3.8 through 5.3.12. These are idealized steady-state scalar wind speed profile envelopes for five active or potential operational space vehicle launch or landing sites, i.e., Eastern Test Range, Florida; The Space and Missile Test Center (Vandenberg AFB), California; Wallops Island, Virginia; White Sands Missile Range, New Mexico; and Edwards Air Force Base, California. Table 5.3.8 and Figure 5.3.13 envelope the 95 and 99 percentile steady-state scalar wind speed profile envelopes from the same five locations. They are applicable for design criteria when initial design or operational capability has not been restricted to a specific launch site or may involve several geographical locations. However, if the specific geographical location for application has been determined as being near one of the five referenced sites then the relevant data should be applied.

This section provides design nondirectional wind data for various percentiles; therefore, the specific percentile wind speed envelope applicable to design should be specified in the appropriate space vehicle specification documentation. For engineering convenience the design wind speed profile envelopes are given as linear segments between altitude levels; therefore, the tabular values are connected, when graphed, by straight lines between the points.

5.3.5.2 Directional Wind Speed Envelopes

Directional wind speed envelopes, prepared using the windiest monthly reference period concept, may be used to estimate the winds relative to a given percentile level that may be encountered at any flight azimuth. Figure 5.3.14 was constructed by plotting the component wind speed at the appropriate percentile (extracted from empirical cumulative percentage frequencies) and the appropriate flight azimuth. The coordinate system was rotated to obtain all flight azimuths and the plotting convention was chosen to indicate the direction from which the wind was blowing. Directional wind component values for other altitudes are available upon request to the Aerospace Environment Division, MSFC.

To illustrate the use of the envelopes, suppose an estimate of the strongest winds (99 percentile head, tail, and cross) in the 9- to 13-kilometer altitude region for several launch azimuths – perhaps 40, 180, 250, and 330 degrees – is required at Edwards AFB. For the 40-degree launch azimuth, read the headwind component along 40 degrees, the tailwind along 220 degrees, the right crosswind along 130 degrees, and the left crosswind along 310 degrees.

TABLE 5.3.3 SCALAR WIND SPEED V (m/sec) STEADY-STATE ENVELOPES AS FUNCTIONS OF ALTITUDE H (km) FOR VARIOUS PROBABILITIES P (%) FOR THE EASTERN TEST RANGE

P = 50		P = 75		P = 90		P = 95		P = 99	
H	V	H	V	H	V	H	V	H	V
1	8	1	12	1	16	1	19	1	25
4	15	5	27	5	34	6	44	5	48
10	39	11	57	10	62	10	69	11	88
12	45			12	68	12	75	12	92
13	44	13	57	13	67	13	74		
16	32	16	39					15	70
19	13	19	18	18	30	18	34	17	48
20	13	20	15	20	19	20	22	20	31
23	13	23	15	23	19	23	22	23	31
50	85	50	100	50	112	50	120	50	135
60	85	60	100	60	112	60	120	60	135
75	55	75	70	75	83	75	90	75	105
80	55	80	70	80	83	80	90	80	105

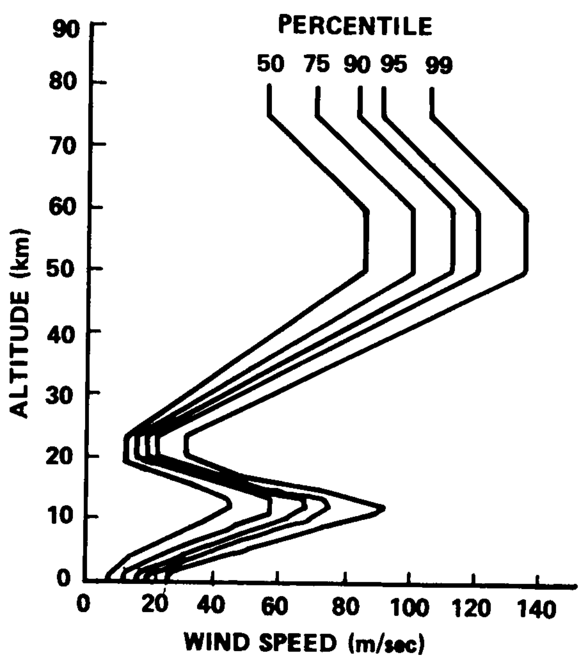

FIGURE 5.3.8 SCALAR WIND SPEED PROFILE ENVELOPES STEADY-STATE, FOR THE EASTERN TEST RANGE

TABLE 5.3.4 SCALAR WIND SPEED V (m/sec) STEADY-STATE ENVELOPES AS FUNCTIONS OF ALTITUDE H (km) FOR VARIOUS PROBABILITIES P (%) FOR THE SPACE AND MISSILE TEST CENTER
Vandenberg AFB, California

P = 50		P = 75		P = 90		P = 95		P = 99	
H	V	H	V	H	V	H	V	H	V
1	6	1	10	1	13	1	15	1	22
						4	31	2	23
7	22	7	32			8	52	7	59
				9	49			9	69
11	31	11	42			11	63	11	78
12	31	12	43	12	55	12	63	12	79
14	27					14	48	14	57
		15	30	16	32	16	36	16	43
								19	29
20	8	20	11	20	15	20	19	20	29
23	8	23	11	23	15	23	19	23	29
50	85	50	104	50	120	50	140	50	155
60	85	60	104	60	120	60	140	60	155
75	60	75	77	75	93	75	102	75	120
80	60	80	77	80	93	80	102	80	120

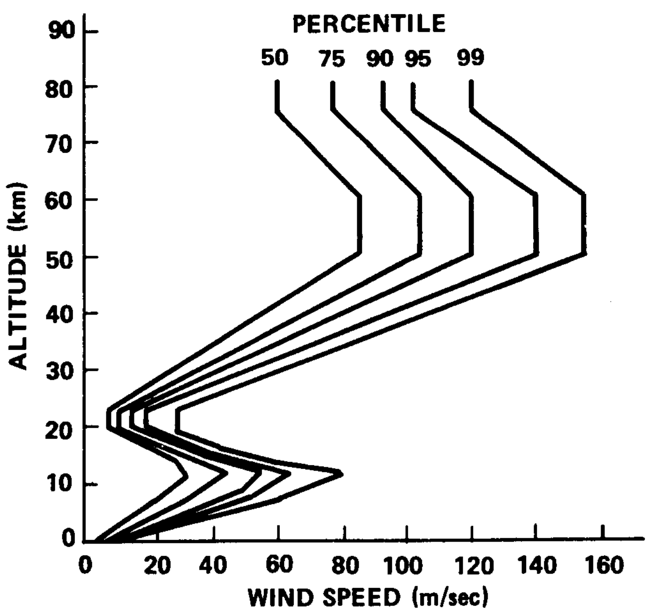

FIGURE 5.3.9 SCALAR WIND SPEED PROFILE ENVELOPES, STEADY-STATE FOR THE SPACE AND MISSILE TEST CENTER, Vandenberg AFB, California

TABLE 5.3.5 SCALAR WIND SPEED V (m/sec) STEADY-STATE ENVELOPES AS FUNCTIONS OF ALTITUDE H (km) FOR VARIOUS PROBABILITIES P (%) FOR WALLOPS TEST RANGE

P = 50		P = 75		P = 90		P = 95		P = 99	
H	V	H	V	H	V	H	V	H	V
1	11	1	15	1	19	1	22	1	28
		3	24	3	28	3	31	3	38
7	36	7	46	7	55	6	54		
9	47	10	60	10	69	10	75	9	82
11	51							11	88
12	50	12	60	12	69	12	75		
17	25	17	33	17	39	15	54		
20	15	20	21	20	26	20	29	20	38
23	15	23	21	23	26	23	29	23	38
50	102	50	120	50	140	50	150	50	170
60	102	60	120	60	140	60	150	60	170
75	85	75	100	75	113	75	120	75	135
80	85	80	100	80	113	80	120	80	135

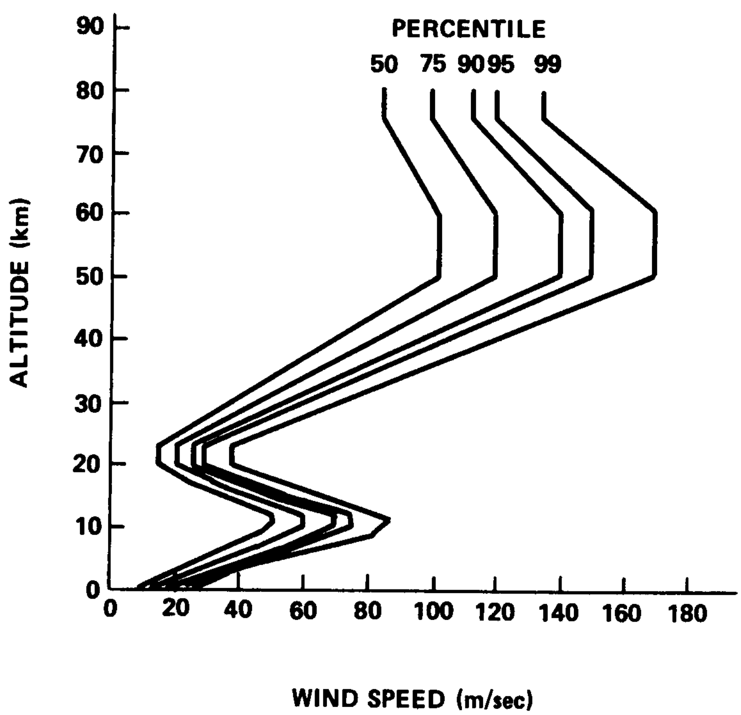

FIGURE 5.3.10 SCALAR WIND SPEED PROFILE ENVELOPES, STEADY-STATE FOR WALLOPS TEST RANGE

TABLE 5.3.6 SCALAR WIND SPEED V (m/sec) STEADY-STATE ENVELOPES AS FUNCTIONS OF ALTITUDE H (km) FOR VARIOUS PROBABILITIES P (%) FOR WHITE SANDS MISSILE RANGE

P = 50		P = 75		P = 90		P = 95		P = 99	
H	V	H	V	H	V	H	V	H	V
1	4	1	7	1	11	1	13	1	22
2	5	2	8	2	12	2	15	2	22
						7	50	7	68
		9	45	8	49	9	67	9	88
11	42	10	53	11	71	11	76		
13	42	12	55	13	63	12	78	14	88
				15	45	15	52	15	69
20	10	20	14	20	20	20	24	20	41
23	10	23	14	23	20	23	24	23	41
50	85	50	104	50	120	50	130	50	150
60	85	60	104	60	120	60	130	60	150
75	60	75	77	75	93	75	102	75	120
80	60	80	77	80	93	80	102	80	120

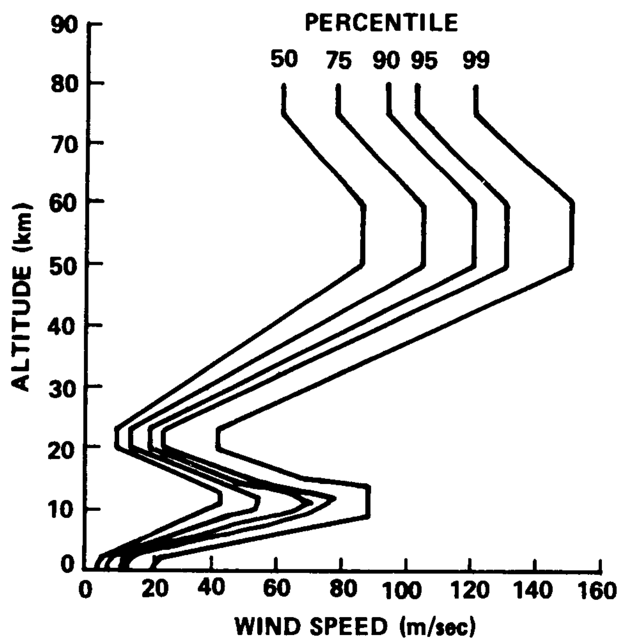

FIGURE 5.3.11 SCALAR WIND SPEED PROFILE ENVELOPES, STEADY-STATE, FOR WHITE SANDS MISSILE RANGE

TABLE 5.3.7 SCALAR WIND SPEED V (m/sec) STEADY-STATE ENVELOPES AS FUNCTIONS OF ALTITUDE H (km) FOR VARIOUS PROBABILITIES P (%) FOR EDWARDS AIR FORCE BASE

P = 50		P = 75		P = 90		P = 95		P = 99	
H	V	H	V	H	V	H	V	H	V
1	8	1	11	1	16	1	17	1	25
2	8	2	12	2	16	2	18	2	28
				5	30	5	36	5	56
10	29			10	51	10	61	10	77
12	32	11	44	11	56			12	77
15	25	13	39	12	56	12	61	14	65
18	13	17	21	17	28	16	38	16	43
20	9	20	13	20	19	20	23	20	30
23	9	23	13	23	19	23	23	23	30
50	85	50	104	50	120	50	130	50	150
60	85	60	104	60	120	60	130	60	150
75	60	75	77	75	93	75	102	75	120
80	60	80	77	80	93	80	102	80	120

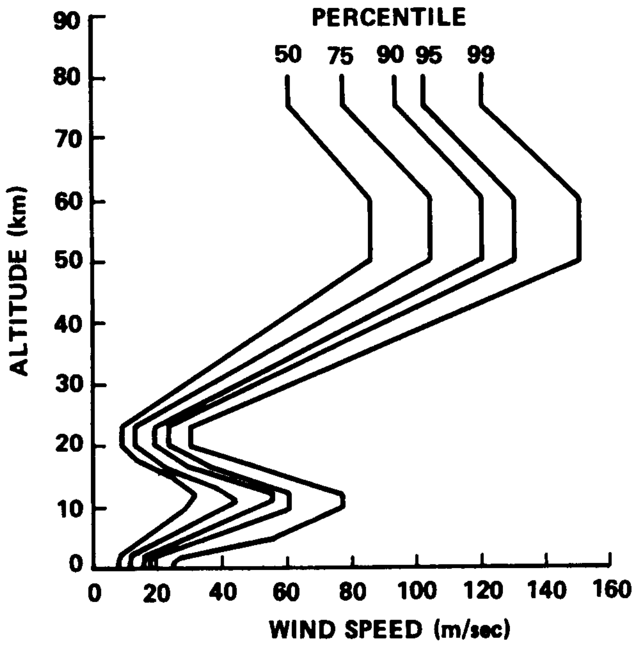

FIGURE 5.3.12 SCALAR WIND SPEED PROFILE ENVLOPES, STEADY - STATE, FOR EDWARDS AIR FORCE BASE

TABLE 5.3.6 SCALAR WIND SPEED V (m/sec) STEADY-STATE ENVELOPES AS FUNCTIONS OF ALTITUDE H (km) FOR VARIOUS PROBABILITIES P (%) ENCOMPASSING ALL FIVE LOCATIONS

P = 95				P = 99			
H	V	H	V	H	V	H	V
1	22	17	44	1	28	15	70
3	31	20	29	3	38	20	41
		23	29	5	56	23	41
6	54	50	150	6	60	50	170
		60	150	7	68	60	170
10	75	75	120	9	88	75	135
11	76	80	120	11	88	80	135
12	78			12	92		
13	74			13	88		
				14	88		

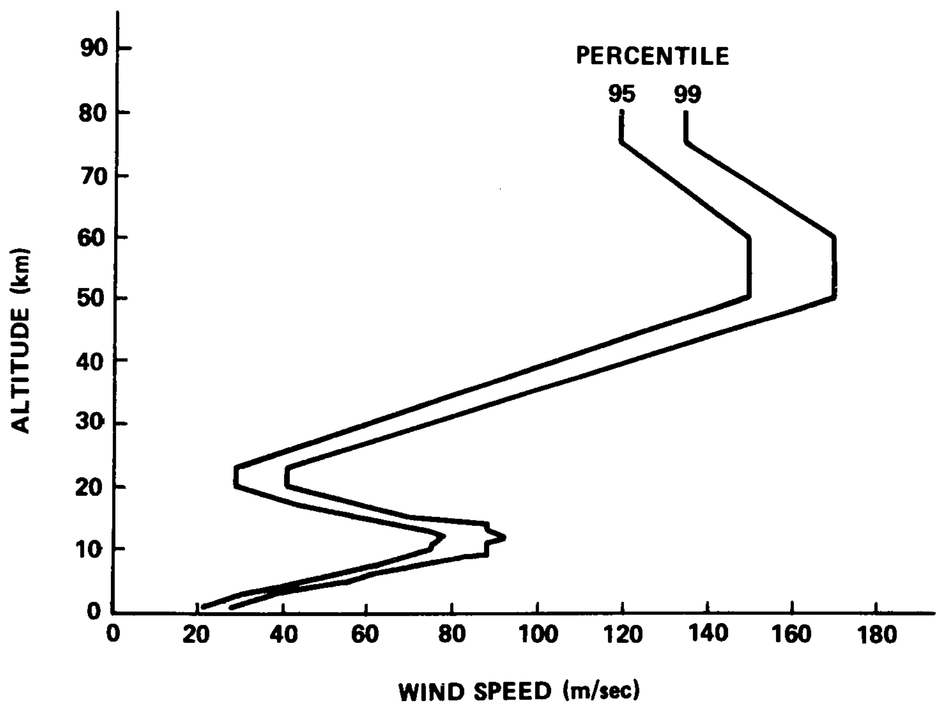

FIGURE 5.3.13 SCALAR WIND SPEED PROFILE ENVELOPES, STEADY-STATE FOR ALL FIVE LOCATIONS

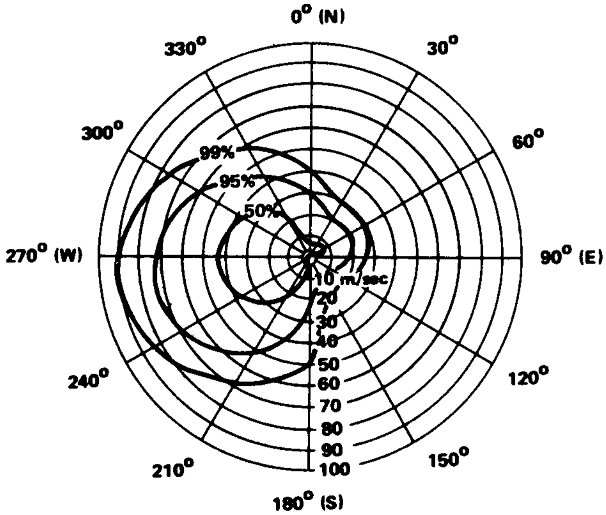

CAPE KENNEDY; 10-14 km ALTITUDE LAYER

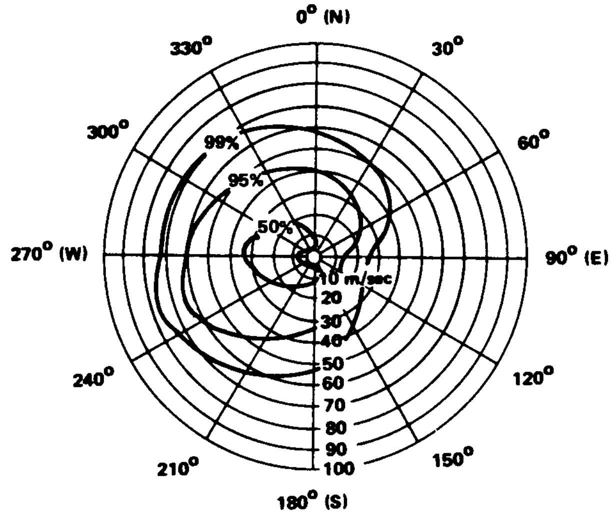

EDWARDS AFB; 9-13 km ALTITUDE LAYER

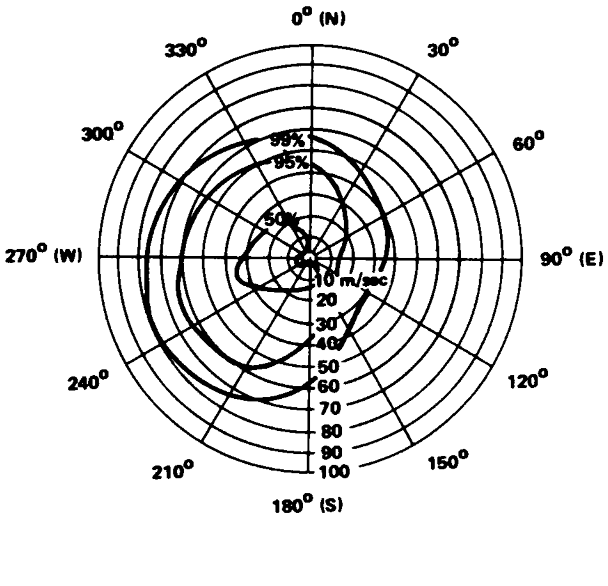

VANDENBERG, AFB; 9-13 km ALTITUDE LAYER

FIGURE 5. 3. 14 DIRECTIONAL WIND COMPONENT ENVELOPES (steady-state) FOR 99, 95, and 50 PERCENTILES

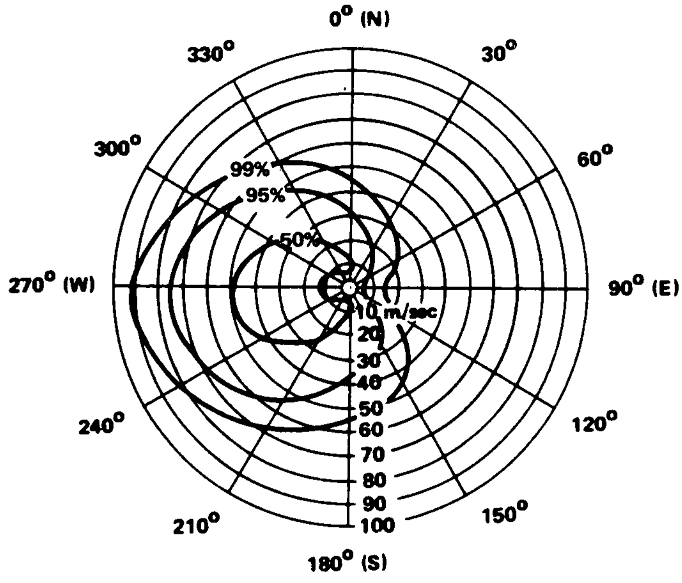

WALLOPS ISLAND; 9-13 km ALTITUDE LAYER

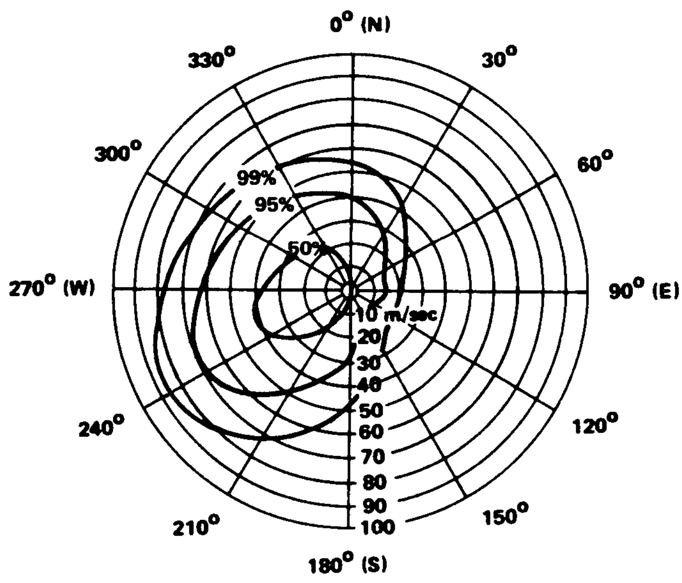

WHITE SANDS; 9-13 km ALTITUDE LAYER

FIGURE 5. 3. 14 DIRECTIONAL WIND COMPONENT ENVELOPES (steady-state) FOR 99, 95, and 50 PERCENTILES (Concluded)

It is emphasized that the procedure followed in the construction of these envelopes permits no connection between the component winds. The data insure that the speed will in no month be exceeded at that probability level for a given azimuth relative to the launch azimuth selected. Design use requires a careful check of vehicle response in pitch and yaw for all planned flight azimuths.

An example of directional wind profile envelopes is given in Table 5. 3. 9 for several flight azimuths for Cape Kennedy (Eastern Test Range), Florida, and Vandenberg AFB (SAMTEC), California. These profiles were prepared from advance data on the upper altitude regions for which the complete results of the analysis are available upon request. If so designated by the development agency, such envelope profiles may be employed for initial design and performance studies as synthetic profiles with the appropriate values of wind shear/gust as noted in the following sections. Due to method used in constructing these directional profile envelopes, they are applied independently as head, tail, right, and left cross wind inputs for the given flight azimuth. The direction producing the largest vehicle response is used in the design analysis. It is again emphasized, however, that directional wind criteria should be applied with care and specific knowledge of the vehicle design mission(s) configurations and flight azimuths, since severe wind constraints could result for other flight azimuths, missions, or launch sites.

5.3.6 Wind Speed Change (Shear) Envelopes

This section provides representative information on wind speed change (shear) for scales of distance $\Delta H \leq 5000$ meters. Vector shears are not included in this document, but may be obtained from the Aerospace Environment Division upon request. Scalar wind speed change is defined as the total magnitude (speed) change between the wind vectors at the top and bottom of a specified layer, regardless of wind direction. Wind shear is the wind speed change divided by the altitude interval. When applied to space vehicle synthetic wind profile criteria, it is frequently referred to as a wind build-up or back-off rate depending upon whether it occurs below (build-up) or above (back-off) the reference height of concern. Thus, a build-up wind value is the change in wind speed which a vehicle may experience while ascending vertically through a specified layer to the known altitude. Back-off magnitudes describe the speed change which may be experienced above the chosen level. Both build-up and back-off wind speed change data are presented in this section as a function of reference level wind vector magnitude and geographic location. Wind build-up or back-off may be determined for a vehicle with other than a vertical flight path by multiplying the wind speed change by the cosine of the angle between the vertical axis and the vehicle trajectory. Wind shears for scales of distance $\Delta H \geq 1000$ meters thickness are computed from rawinsonde and rocketsonde observations, while the small scale shears associated with scales of distance

TABLE 5.3.9 DIRECTIONAL WIND SPEED (m/sec) PROFILE ENVELOPES (95th percentile) FOR SELECTED FLIGHT AZIMUTHS

Altitude	Cape Kennedy Flight Azimuth (α)								Vandenverg AFB Flight Azimuth (α)							
	α = 38 degrees[a]				α = 90 degrees[a]				α = 182 degrees[a]				α = 198 degrees[a]			
	Head Wind	Tail Wind	Right Cross Wind	Left Cross Wind	Head Wind	Tail Wind	Right Cross Wind	Left Cross Wind	Head Wind	Tail Wind	Right Cross Wind	Left Cross Wind	Head Wind	Tail Wind	Right Cross Wind	Left Cross Wind
1	12	15	11	13	12	16	13	10	12	13	10	7	12	12	11	8
2																7
3							14									
4	9		7		9	30										
5		30					18	12	18					23	32	
6							19			33	37		24			12
7																
8				39											46	
9			8		11	60			33	42		15		36		
10	14							22	41		51		40			
11		59		55		70	28			44	58	15	42	36		
12		59		56		72	28	28	36	41	58		40		56	14
13	22	57	13	54	19	70	27								57	
14	21											6		21		
15										23						
16			9								34	5			32	6
17	12		9		12				11				15	12		
18					13					13						
19	12						9	8								
20	14	16	15	15	19	20	8	8	4	10	18	11	8	10	17	10
23	14	16	15	15	19	20	8	8	4	10	18	11	8	10	17	10
50	47	95	65	97	72	120	52	30	60	28	140	88	60	28	140	88
60	47	95	65	97	72	120	52	30	60	28	140	88	60	28	140	88
75	30	70	34	50	50	90	30	20	32	25	98	25	32	25	98	25
80	30	70	34	50	50	90	30	20	32	25	98	25	32	25	98	25

a. Wind speeds given are applicable for α plus or minus 10 degrees.

$\Delta H < 1000$ meters are computed from a relationship developed by Fichtl (Ref. 5.29) based on experimental results from FPS-16 radar/Jimsphere balloon wind sensor measurements of the detail wind profile structure. This relationship states that the back-off or build-up wind shear Δu for $\Delta H < 1000$ meters for a given risk of exceedance is related to the $\Delta H = 1000$ meter shear, $(\Delta u)_{1000}$, at the same risk of exceedance, through the expression

$$\Delta u = (\Delta u)_{1000} \left(\frac{\Delta H}{1000} \right)^{0.7} \tag{5.26}$$

where ΔH has units of meters.

An envelope of the 99 percentile wind speed build-up is used currently in constructing synthetic wind profiles. For most design studies, the use of this 99 percentile scalar build-up wind shear data is warranted. The envelopes for back-off shears have application to certain design studies and should be considered where appropriate. These envelopes are not meant to imply perfect correlation between shears for the various scales of distance; however, certain correlations do exist, depending upon the scale of distance and the wind speed magnitude considered. This method of describing the wind shear for vehicle design has proven to be especially acceptable in preliminary design studies since the dynamic response of the structure or control system of a vehicle is essentially influenced by specific wavelengths as represented by a given wind shear. Construction of synthetic profiles for vehicle design applications is described in subsection 5.3.9.

Wind speed change (shear) statistics for various locations differ primarily because of prevailing meteorological conditions, orographic features, and data sample size. Significant differences, especially from an engineering standpoint, are known to exist in the shear profiles for different locations. Therefore, consistent vehicle design shear data representing five active or potentially operational space vehicle launch or landing sites are presented in Tables 5.3.10 through 5.3.19; i.e., for Eastern Test Range, Space and Missile Test Center, Wallops Island, White Sands Missile Range, and Edwards Air Force Base. Tables 5.3.20 and 5.3.21 envelope the 99 percentile shears from these five locations. They are applicable for design criteria when initial design or operational capability has not been restricted to a specific launch site or may involve several geographical locations. However, if the specific geographic location for application has been determined as being near one of the five referenced sites, then the relevant data should be applied. Reference 5.30 further substantiates that the shear data presented in this document are representative for higher altitudes and applicable for engineering design. Equation (5.26) was used to construct Tables 5.3.10 through 5.3.21 for scales of distance $\Delta H < 1000$ m.

TABLE 5.3.10 BUILD-UP DESIGN ENVELOPES OF 99 PERCENTILE SCALAR WIND SPEED CHANGE, 1- TO 80-km ALTITUDE REGION, EASTERN TEST RANGE

Wind Speed at Top of Altitude Layer (m/sec)	Scales of Distance (m)									
	5000	4000	3000	2000	1000	800	600	400	200	100
$\geq$ 90	65.6	59.5	52.3	43.5	34.0	29.0	23.8	17.9	11.2	6.8
80	60.4	55.5	49.7	42.0	32.7	27.7	22.7	17.0	10.6	6.5
70	56.0	51.7	47.0	40.4	31.2	26.6	21.8	16.4	10.1	6.2
60	51.3	48.5	44.5	38.6	30.0	25.6	21.1	15.8	9.8	6.0
50	46.5	45.0	41.2	36.5	28.5	24.4	20.0	15.0	9.2	5.7
40	38.5	37.7	36.8	34.9	26.5	22.6	18.5	13.8	8.6	5.3
30	28.0	27.5	26.5	24.5	20.8	17.8	14.5	10.8	6.7	4.1
20	17.6	17.3	16.6	15.8	14.6	12.5	10.2	7.2	4.7	2.9

TABLE 5.3.11 BACK-OFF DESIGN ENVELOPES OF 99 PERCENTILE SCALAR WIND SPEED CHANGE, 1- TO 80-km ALTITUDE REGION, EASTERN TEST RANGE

Wind Speed at Top of Altitude Layer (m/sec)	Scales of Distance (m)									
	5000	4000	3000	2000	1000	800	600	400	200	100
$\geq$ 90	77.5	74.4	68.0	59.3	42.6	36.4	29.7	22.4	13.8	8.5
80	71.0	68.0	63.8	56.0	40.5	34.7	28.5	21.4	13.2	8.1
70	63.5	61.0	57.9	52.0	38.8	33.1	27.0	20.3	12.5	7.7
60	56.0	54.7	52.3	47.4	36.0	31.0	25.3	18.9	11.7	7.2
50	47.5	47.0	46.2	43.8	33.0	28.3	23.2	17.5	10.7	6.6
40	39.0	38.0	37.0	35.3	29.5	25.3	20.6	15.5	9.6	5.9
30	30.6	30.0	29.4	26.9	22.6	19.4	15.8	11.9	7.3	4.5
20	18.0	17.5	16.7	15.7	14.2	12.2	9.9	7.5	4.6	2.8

TABLE 5.3.12 BUILD-UP DESIGN ENVELOPES OF 99 PERCENTILE SCALAR WIND SPEED CHANGE, 1- TO 80-km ALTITUDE REGION, SPACE AND MISSILE TEST CENTER (Vandenberg AFB)

	Scales of Distance (m)									
Wind Speed at Top of Altitude Layer (m/sec)	5000	4000	3000	2000	1000	800	600	400	200	100
≥ 90	75.8	73.1	70.5	62.9	43.0	36.8	30.0	22.5	14.0	8.6
80	70.7	69.5	67.0	58.8	40.4	34.9	28.4	21.4	13.2	8.1
70	62.2	61.6	60.4	54.4	38.2	32.6	26.7	20.1	12.3	7.6
60	55.0	54.5	53.5	48.0	35.7	30.5	24.9	18.7	11.5	7.1
50	47.4	46.8	45.9	42.5	33.4	28.5	23.4	17.6	10.8	6.7
40	35.5	35.0	33.5	31.5	27.8	23.8	19.5	14.6	8.9	5.5
30	27.5	26.8	26.0	24.5	20.5	17.5	14.3	10.8	6.6	4.1
20	18.5	17.8	17.5	16.7	15.4	13.1	10.7	8.1	5.0	3.1

TABLE 5.3.13 BACK-OFF DESIGN ENVELOPES OF 99 PERCENTILE SCALAR WIND SPEED CHANGE, 1- TO 80-km ALTITUDE REGION, SPACE AND MISSILE TEST CENTER (Vandenberg AFB)

	Scales of Distance (m)									
Wind Speed at Top of Altitude Layer (m/sec)	5000	4000	3000	2000	1000	800	600	400	200	100
≥ 90	78.2	74.2	67.5	57.3	43.8	37.5	30.5	23.0	14.0	8.7
80	71.2	68.6	63.0	53.5	41.0	35.0	28.5	21.2	13.2	8.2
70	64.0	61.1	56.6	48.1	37.2	32.0	26.1	19.7	12.1	7.4
60	54.4	52.3	49.0	43.0	33.0	28.3	23.2	17.4	10.7	6.6
50	45.0	43.9	40.7	36.2	29.5	25.2	20.7	15.6	9.6	5.9
40	36.3	34.9	32.5	29.6	25.3	21.6	17.7	13.3	8.1	5.0
30	28.0	26.5	24.8	22.8	19.5	16.7	13.7	10.3	6.3	3.9
20	18.0	17.5	16.6	15.5	13.0	11.1	9.0	6.8	4.2	2.6

TABLE 5.3.14 BUILD-UP DESIGN ENVELOPES OF 99 PERCENTILE SCALAR WIND SPEED CHANGE, 1- TO 80-km ALTITUDE REGION, WHITE SANDS MISSILE RANGE

Wind Speed at Top of Altitude Layer (m/sec)	Scales of Distances (m)									
	5000	4000	3000	2000	1000	800	600	400	200	100
≥ 90	70.7	67.0	61.2	52.4	42.0	36.0	29.4	22.1	13.6	8.4
80	66.0	63.0	57.7	50.0	40.2	34.5	28.1	21.2	13.0	8.0
70	60.2	57.0	53.0	46.5	38.0	32.6	26.6	20.0	12.3	7.6
60	52.4	50.0	46.5	42.3	35.5	30.5	24.9	18.7	11.5	7.1
50	44.8	43.0	40.2	36.5	32.0	28.3	23.1	17.4	10.7	6.6
40	36.4	35.3	33.8	31.0	27.5	23.6	19.3	14.5	8.9	5.5
30	27.4	26.5	25.6	24.3	20.6	17.7	14.4	10.8	6.7	4.1
20	18.4	17.7	17.3	16.5	15.0	12.9	10.5	7.9	4.9	3.0

TABLE 5.3.15 BACK-OFF DESIGN ENVELOPES OF 99 PERCENTILE SCALAR WIND SPEED CHANGE, 1- TO 80-km ALTITUDE REGION, WHITE SANDS MISSILE RANGE

Wind Speed at Top of Altitude Layer (m/sec)	Scales of Distance (m)									
	5000	4000	3000	2000	1000	800	600	400	200	100
≥ 90	66.2	62.0	57.0	50.0	37.0	31.7	25.9	19.5	12.0	7.4
80	62.0	58.5	54.0	48.0	35.8	30.7	25.1	18.9	11.6	7.1
70	57.5	54.5	50.7	44.3	34.2	29.3	23.9	18.0	11.1	6.8
60	52.6	49.2	45.5	40.5	32.8	28.1	23.0	17.3	10.6	6.5
50	45.0	42.8	40.1	37.0	31.0	26.6	21.7	16.3	10.0	6.2
40	36.5	35.5	34.8	33.5	29.3	25.1	20.5	15.4	9.5	5.8
30	27.4	27.0	26.4	24.8	22.0	19.3	15.8	11.8	7.3	4.5
20	17.7	17.3	16.7	15.8	14.1	12.1	9.9	7.4	4.6	2.8

TABLE 5.3.16 BUILD-UP DESIGN ENVELOPES OF 99 PERCENTILE SCALAR WIND SPEED CHANGE, 1- TO 80-km ALTITUDE REGION, WALLOPS ISLAND

Wind Speed at Top of Altitude Layer (m/sec)	Scales of Distance (m)									
	5000	4000	3000	2000	1000	800	600	400	200	100
≥ 90	71.0	66.2	60.2	50.5	37.6	32.3	26.3	19.8	12.2	7.5
80	66.5	62.5	57.5	48.8	37.0	31.7	25.9	19.5	12.0	7.4
70	61.2	58.5	53.8	46.5	35.8	30.7	25.1	18.9	11.6	7.1
60	54.4	52.5	50.0	44.2	34.5	29.6	24.2	18.2	11.2	6.9
50	45.2	43.4	42.3	38.8	33.0	28.3	23.2	17.4	10.7	6.6
40	36.1	35.6	34.5	32.3	27.6	23.7	19.3	14.5	8.9	5.5
30	27.0	26.3	25.3	24.2	20.6	17.7	14.4	10.8	6.7	4.1
20	17.7	17.3	16.8	16.4	15.2	13.0	10.6	8.0	4.9	3.0

TABLE 5.3.17 BACK-OFF DESIGN ENVELOPES OF 99 PERCENTILE SCALAR WIND SPEED CHANGE, 1- TO 80-km ALTITUDE REGION, WALLOPS ISLAND

Wind Speed at Top of Altitude Layer (m/sec)	Scales of Distance (m)									
	5000	4000	3000	2000	1000	800	600	400	200	100
≥ 90	72.5	67.0	59.2	49.0	31.5	27.0	22.1	16.6	10.2	6.3
80	66.3	62.0	56.0	46.0	30.0	25.7	21.0	15.8	9.7	6.0
70	60.0	56.5	51.5	43.6	28.5	24.5	20.0	15.0	9.2	5.7
60	53.5	50.7	46.8	40.4	27.0	23.2	18.9	14.2	8.7	5.4
50	46.2	44.2	41.0	35.8	25.2	21.6	17.6	13.3	8.2	5.0
40	36.7	35.2	32.7	28.7	21.5	18.4	15.1	11.3	7.0	4.3
30	27.2	26.1	24.8	22.5	18.2	15.6	12.7	9.6	5.9	3.6
20	17.8	17.3	16.4	15.2	13.0	11.1	9.0	6.8	4.2	2.6

TABLE 5.3.18 BUILD-UP DESIGN ENVELOPES OF 99 PERCENTILE SCALAR WIND SPEED CHANGE, 1- TO 80-km ALTITUDE REGION, EDWARDS AIR FORCE BASE

Wind Speed at Top of Altitude Layer (m/sec)	Scales of Distance (m)									
	5000	4000	3000	2000	1000	800	600	400	200	100
≥ 90	69.0	65.0	59.5	52.0	39.5	33.9	27.7	20.8	12.8	7.9
80	64.9	61.8	56.9	50.0	38.2	32.8	26.7	20.1	12.4	7.6
70	59.0	57.0	53.0	46.8	37.0	31.7	25.9	19.5	12.0	7.4
60	51.8	50.4	47.8	43.6	35.5	30.5	24.9	18.7	11.5	7.1
50	44.8	43.6	41.3	38.2	31.8	27.5	22.4	16.9	10.4	6.4
40	36.5	35.5	34.3	32.0	26.5	23.0	18.8	14.1	8.7	5.3
30	28.0	27.3	26.3	24.5	20.8	17.8	14.6	11.0	6.7	4.2
20	18.0	17.7	17.4	16.7	15.2	13.0	10.6	8.0	4.9	3.0

TABLE 5.3.19 BACK-OFF DESIGN ENVELOPES OF 99 PERCENTILE SCALAR WIND SPEED CHANGE, 1- TO 80-km ALTITUDE REGION, EDWARDS AIR FORCE BASE

Wind Speed at Top of Altitude Layer (m/sec)	Scales of Distance (m)									
	5000	4000	3000	2000	1000	800	600	400	200	100
≥ 90	75.2	72.0	67.3	59.0	42.8	36.7	30.2	22.5	13.9	8.5
80	68.0	66.3	62.5	55.5	40.8	35.0	28.6	21.5	13.2	8.1
70	60.4	59.0	56.8	51.4	38.7	33.2	27.0	20.4	12.5	7.7
60	53.0	51.8	49.3	45.0	36.0	30.9	25.2	19.0	11.7	7.2
50	44.5	43.3	41.5	38.4	32.0	27.5	22.4	16.9	10.4	6.4
40	35.7	35.3	34.5	33.0	27.0	23.2	18.9	14.2	8.8	5.4
30	27.1	27.0	26.9	26.3	21.4	18.4	15.0	11.3	6.9	4.3
20	18.0	17.0	16.6	15.7	14.2	12.2	9.9	7.5	4.6	2.8

TABLE 5.3.20 BUILD-UP DESIGN ENVELOPES OF 99 PERCENTILE SCALAR WIND SPEED CHANGE, 1- TO 80-km ALTITUDE REGION, FOR ALL FIVE LOCATIONS

Wind Speed at Top of Altitude Layer (m/sec)	Scales of Distance (m)									
	5000	4000	3000	2000	1000	800	600	400	200	100
≥ 90	75.8	73.1	70.5	62.9	43.0	36.8	30.0	22.5	14.0	8.6
80	70.7	69.5	67.0	58.8	40.4	34.9	28.4	21.4	13.2	8.1
70	62.2	61.6	60.4	54.4	38.2	32.6	26.7	20.1	12.3	7.6
60	55.0	54.5	53.5	48.0	35.7	30.5	24.9	18.7	11.5	7.1
50	47.4	46.8	45.9	42.5	33.4	28.5	23.4	17.6	10.8	6.7
40	38.5	37.7	36.8	34.9	27.8	23.8	19.5	14.6	8.9	5.5
30	28.0	27.5	26.5	24.5	20.8	17.8	14.5	10.8	6.7	4.1
20	18.5	17.8	17.5	16.7	15.4	13.1	10.7	8.1	5.0	3.1

TABLE 5.3.21 BACK-OFF DESIGN ENVELOPES OF 99 PERCENTILE SCALAR WIND SPEED CHANGE, 1- TO 80-km ALTITUDE REGION, FOR ALL FIVE LOCATIONS

Wind Speed at Top of Altitude Layer (m/sec)	Scales of Distance (m)									
	5000	4000	3000	2000	1000	800	600	400	200	100
≥ 90	78.2	74.4	68.0	59.3	43.8	37.5	30.5	23.0	14.0	8.7
80	71.2	68.6	63.8	56.0	41.0	35.0	28.5	21.2	13.2	8.2
70	64.0	61.1	57.9	52.0	38.9	33.4	27.0	20.3	12.5	7.7
60	56.0	54.7	52.3	47.4	36.0	31.0	25.3	18.9	11.7	7.2
50	47.5	47.0	46.2	43.8	33.0	28.3	23.2	17.5	10.7	6.6
40	39.0	38.0	37.0	35.3	29.5	25.3	20.6	15.5	9.6	5.9
30	30.6	30.0	29.4	26.9	22.6	19.4	15.8	11.9	7.3	4.5
20	18.0	17.5	16.7	15.7	14.2	12.2	9.9	7.5	4.6	2.8

5.3.7 Wind Direction Change Envelopes

This section provides representative information on wind direction change $\Delta\theta$ for scales of distance $\Delta H \leq 4000$ meters. Wind direction change is defined as the total change in direction of wind vectors at the top and bottom of a specified layer. Wind direction changes can occur above or below a reference point in the atmosphere. As in the case of the wind speed changes in Section 5.3.6 we shall call changes below the reference level build-up wind changes and those above the reference level back-off wind direction changes. These changes can be significantly different. For example if the reference point is at the 4 km level, the build-up changes between the 1- and 4-kilometer levels will be distinctly different from the back-off changes between the 5- and 7-kilometer levels. This results from the fact that variations of wind direction tend to be larger in the atmospheric boundary layer (0-2 km) than in the free atmosphere above the atmospheric boundary layer. In this light the following model is recommended as an integrated wind direction change criteria for design studies. The model consists of the 8-16 km 99% direction changes in Figure 5.3.15 and a set of functions $R(\Delta H, H_r, \bar{u}_r)$ to transfer these changes to any reference level H_r above the 1-kilometer level, where $\bar{u}_r$ is the reference level wind speed. The quantity R is defined such that multiplication of the 8-16 km wind direction changes by $R(\Delta H, H_r, \bar{u}_r)$ will yield the changes in wind direction over a layer of thickness ΔH with top or bottom of the reference level located at height H_r above sea level and reference level wind speed equal to $\bar{u}_r$. The functions $R(\Delta H, H_r, \bar{u}_r)$ for back-off and build-up wind direction changes are defined as

Back-off:

$$R = R^*, \qquad 1 \leq H_r \leq 1.5 \text{ km}$$

$$R = 2(1-R^*)(H_r - 1.5) + R^*, \qquad 1.5 \leq H_r \leq 2 \text{ km}$$

$$R = 1 \qquad 2 \text{ km} \leq H_r$$

Build-up:

$$R = R^*, \qquad 0 < H_r \leq 2 \text{ km}$$

$$\left.\begin{aligned} R &= \left[\frac{R^* - 1}{2}\right]\left[1 - \cos\pi(\Delta H - H_r + 3)\right] + 1, \; 1 < \Delta H \leq H_r - 2 \\ R &= R^*, \; H_r - 2 < \Delta H \leq H_r \end{aligned}\right\}, \; 2 < H_r \leq 3 \text{km}$$

$$R = 1, \quad 0 < \Delta H \leq H_r - 3 \text{ km}$$

$$\left.\begin{array}{l} R = \left[\frac{R^* - 1}{2}\right]\left[1 - \cos\pi(\Delta H - H_r + 3)\right] + 1, \quad H_r - 3 < \Delta H \leq H_r - 2 \\ R = R^*, \quad H_r - 2 < \Delta H \leq 4 \text{km} \end{array}\right\}, \quad 3 < H_r \leq 6\text{km}$$

$$R = 1, \qquad 6\text{km} \leq H_r,$$

where ΔH, and H_r have units of kilometers and R is a nondimensional quantity. The quantity R^* is a function ΔH and $\bar{u}_r$ and is given in Figure 5.3.16.

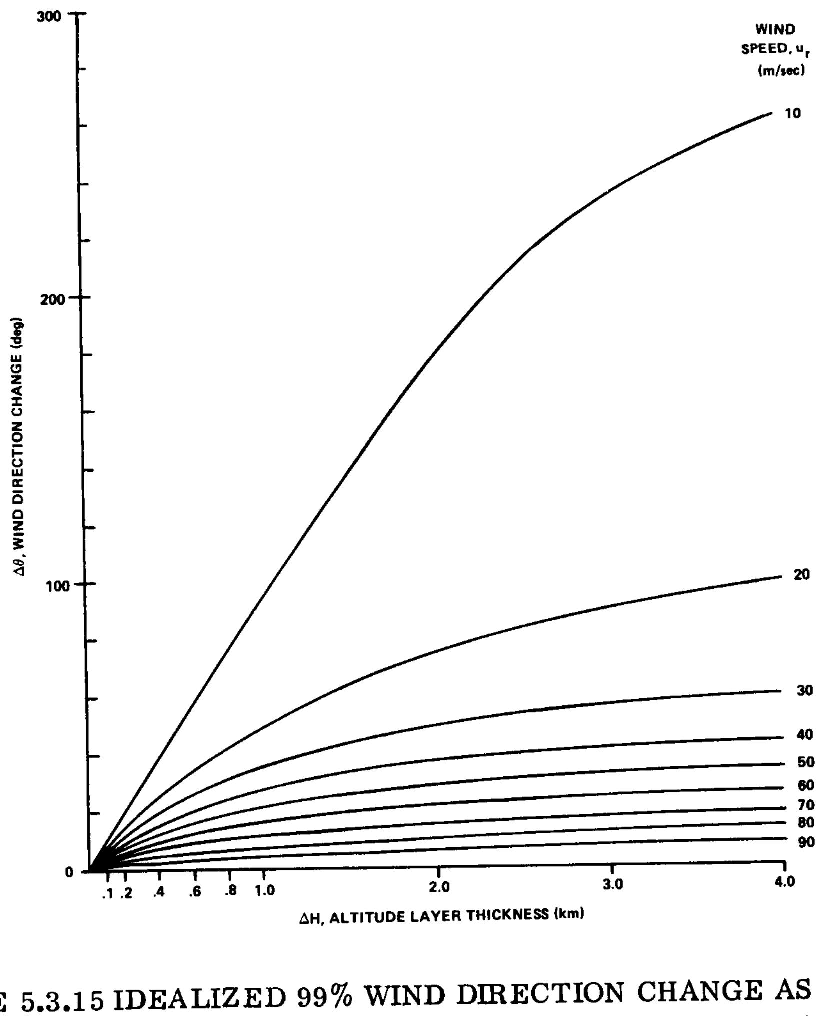

FIGURE 5.3.15 IDEALIZED 99% WIND DIRECTION CHANGE AS A FUNCTION OF WIND SPEED FOR VARYING LAYERS IN THE 8-16 KM ALTITUDE REGION OF THE EASTERN TEST RANGE

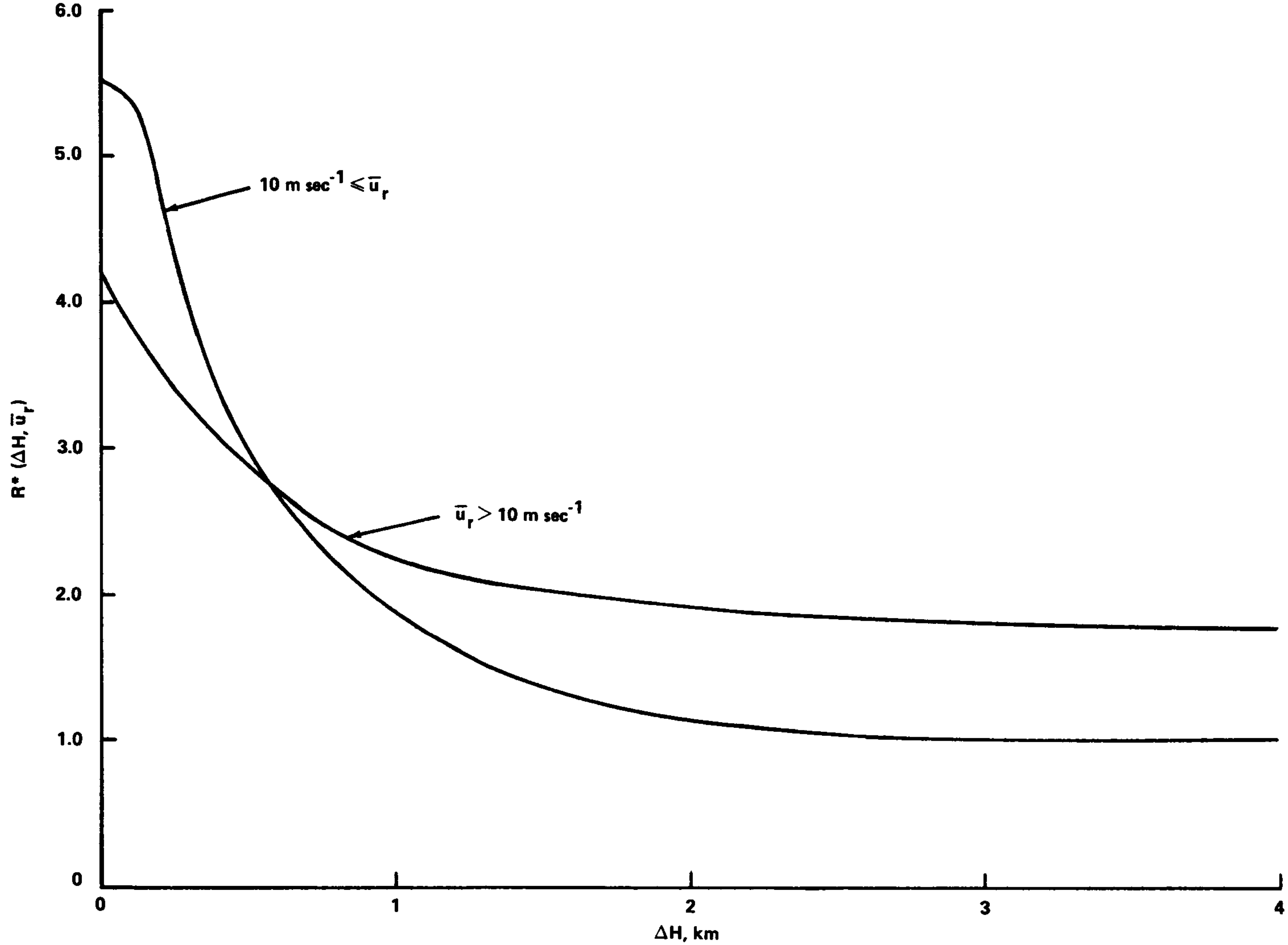

FIGURE 5.3.16 THE FUNCTION R^* VERSUS ΔH FOR VARIOUS CATEGORIES OF WIND SPEED $\overline{u}_r$ AT THE REFERENCE LEVEL.

To apply these wind direction change data, one first constructs a synthetic wind profile (see Section 5.3.9) wind profile envelopes and wind shear envelopes, with or without gust (see Section 5.3.8) as the case may be. A point (reference point) at height H_r above sea level of potential concern on this synthetic wind profile is selected for analysis. One then turns the wind direction above or below this point according to the schedule of wind direction changes given by the above model. Thus, for example, if the 12-kilometer reference point wind speed and direction are 20 m sec^{-1} and 90^o (east wind i.e., a wind blowing from the east) then according to the wind direction change model discussed above the wind directions at 0.2, 0.6, 1.0, 2.0, 3.0, and 4.0 km below or above the 12-kilometer reference point, as the case may be, are 107^o, 123^o, 140^o, 165^o, 180^o, and 190^o for clockwise turning of the wind vector starting with the reference point wind vector at 12 km and looking toward the earth. Counterclockwise turning is also permissible. The direction of rotation of the wind vector should be selected to produce the most adverse wind situation from a vehicle response point of view.

In view of the unavailability of wind direction change statistics above the 16-kilometer level, at this time, it is recommended that the above procedure be used for $H_r > 16$ km.*

5.3.8 Gusts — Vertically Flying Vehicles

The steady-state inflight wind speed envelopes presented in subsection 5.3.5 do not contain the gust (high frequency content) portion of the wind profile. The steady-state wind profile measurements have been defined as those obtained by the rawinsonde system. These measurements represent wind speeds averaged over approximately 1000 meters in the vertical and, therefore, eliminate features with smaller scales. These smaller scale features are contained in the detailed profiles measured by the FPS-16 Radar/Jimsphere system.

A number of attempts have been made to represent the high frequency content of vertical wind profiles in a suitable form for use in vehicle design studies. Most of the attempts resulted in gust information that could be used for specific applications, but, to date, no universal gust representation has been formulated. Information on discrete and continuous gust representations is given below relative to vertically ascending space vehicles.

---

* See Section 5.3.14.2 for wind direction change statistics valid below the 1-kilometer level for take-off and landing design studies.

5.3.8.1 Discrete Gusts

Discrete gusts are specified in an attempt to represent, in a physically reasonable manner, characteristics of small scale motions associated with vertical wind velocity profiles. Gust structure usually is quite complex and it is not always understood. For vehicle design studies, discrete gusts are usually idealized because of their complexity and to enhance their utilization.

Well defined, sharp edged, and repeated sinusoidal gusts are important types in terms of their influence upon space vehicles. Quasi-square-wave gusts with amplitudes of approximately 9 m/sec have been measured. These gusts are frequently referred to as embedded jets or singularities in the vertical wind profile. By definition, a gust is a wind speed in excess of the defined steady-state value; therefore, these gusts are employed on top of the steady-state wind profile values.

If a design wind speed profile envelope without a wind shear envelope is to be used in a design study it is recommended that the associated discrete gust vary in length from 60 to 300 meters. The leading and trailing edge* should conform to a 1-cosine build-up of 30 meters and a corresponding decay also over 30 meters as shown in Figure 5.3.17. The plateau region of the gust can vary in thickness from zero to 240 m. An analytical expression for the value of this gust of height H above natural grade is given by

$$\left.\begin{aligned} u_g &= \frac{A}{2}\left\{1 - \cos\left[\frac{\pi}{30}(H-H_b)\right]\right\}, \quad H_b \le H \le H_b + 30\text{m} \\ u_g &= A, \quad H_b + 30\text{ m} \le H \le H_b + \lambda - 30\text{m} \\ u_g &= \frac{A}{2}\left\{1 - \cos\left[\frac{\pi}{30}(H - H_b - \lambda)\right]\right\}, \quad H_b + \lambda - 30\text{m} \le H \le H_b + \lambda \end{aligned}\right\} \quad (5.27)$$

where H_b is the height of the base of the gust above natural grade, λ is the gust thickness ($60 \le \lambda \le 300$m), A is the gust amplitude, and MKS units are understood.

The gust amplitude is a function of H_b and for design purposes the 1% risk gust amplitude is given by

---

* Leading and trailing edges are used here in the sense that as height H increases one first encounters the gust leading edge and then the trailing edge.

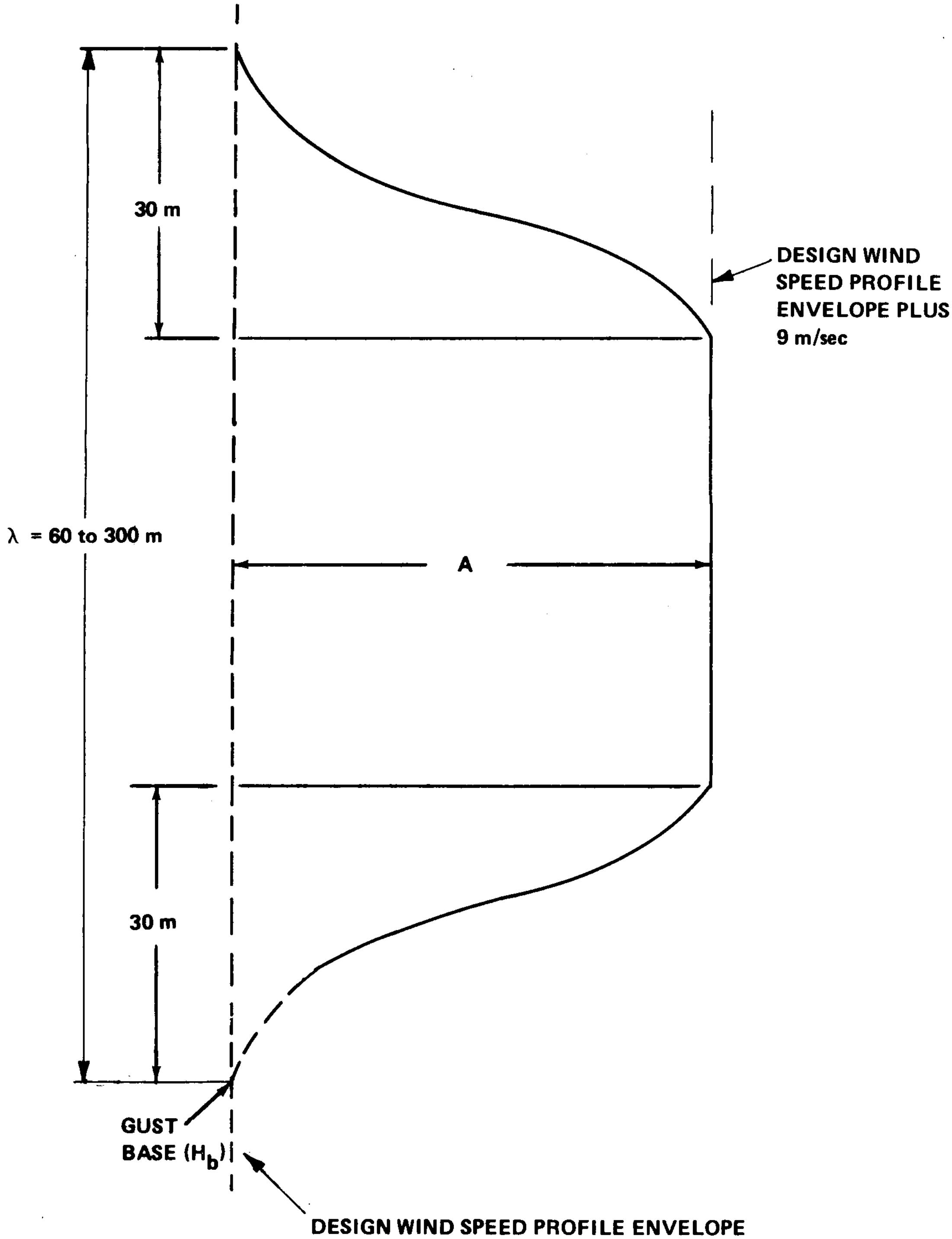

FIGURE 5.3.17 RELATIONSHIP BETWEEN DISCRETE GUST AND/OR EMBEDDED JET CHARACTERISTICS (quasi-square-wave shape) AND THE DESIGN WIND SPEED PROFILE ENVELOPE

$$\left.\begin{aligned} A &= 6\ \text{m/sec},\ H_b < 300\,\text{m} \\ A &= \frac{3}{700}\,(H_b - 300) + 6,\ 300\ \text{m} \le H_b \le 1000\ \text{m} \\ A &= 9\ \text{m/sec}^{-1} \quad 1000\ \text{m} < H_b . \end{aligned}\right\} \qquad (5.28)$$

If a wind speed profile envelope with a build-up wind shear envelope (Section 5.3.6) is to be used in a design study it is recommended that the above mentioned discrete gust be modified by replacing the leading edge 1 - cosine shape with the following formula

$$u_g = 10A\left\{\left(\frac{H-H_b}{30}\right)^{0.9} - 0.9\left(\frac{H-H_b}{30}\right)\right\},\ H_b \le H \le H_b + 30\,\text{m} \qquad (5.29)$$

The height of the gust base H_b corresponds to the point where the design wind speed profile envelope intersects the design build-up shear envelope. If a discrete gust is to be used with a back-off wind shear envelope then the 1-cosine trailing edge shall be given by

$$u_g = 10A\left\{\left(\frac{H_b+\lambda-H}{30}\right)^{0.9} - 0.9\left(\frac{H_b+\lambda-H}{30}\right)\right\},\ H_b + \lambda - 30\text{m} \le H \le H_b + \lambda \qquad (5.30)$$

and the leading edge shall conform to a 1-cosine shape. In this case the height, $H_b + \lambda$, of the end of the gust corresponds to the point where the design wind speed profile envelope intersects the design back-off shear envelope. This modification of the 1-cosine shape at the leading and trailing edges as the case may be results in a continuous merger of the shear envelope and the discrete gust. See Section 5.3.9 for further details. When applying the discrete gust with wind shears the discrete gust and shears should be reduced by a factor of 0.85 to account for the non-perfect correlation between wind shears and gusts (see Section 5.3.9.2 for details).

Another form of discrete gust that has been observed is approximately sinusoidal in nature, where gusts occur in succession. Figure 5.3.18 illustrates the estimated number of consecutive sinusoidal type gusts that may occur and their respective amplitudes for design purposes. It is extremely important when applying these gusts in vehicle studies to realize that these are pure sinusoidal representations that have never been observed in nature. The degree of purity of these sinusoidal features on the vertical wind profiles has not been established. These gusts should be superimposed symmetrically upon the steady-state profile. The data presented here on sinusoidal discrete gusts are at best preliminary and should be treated as such in design studies.

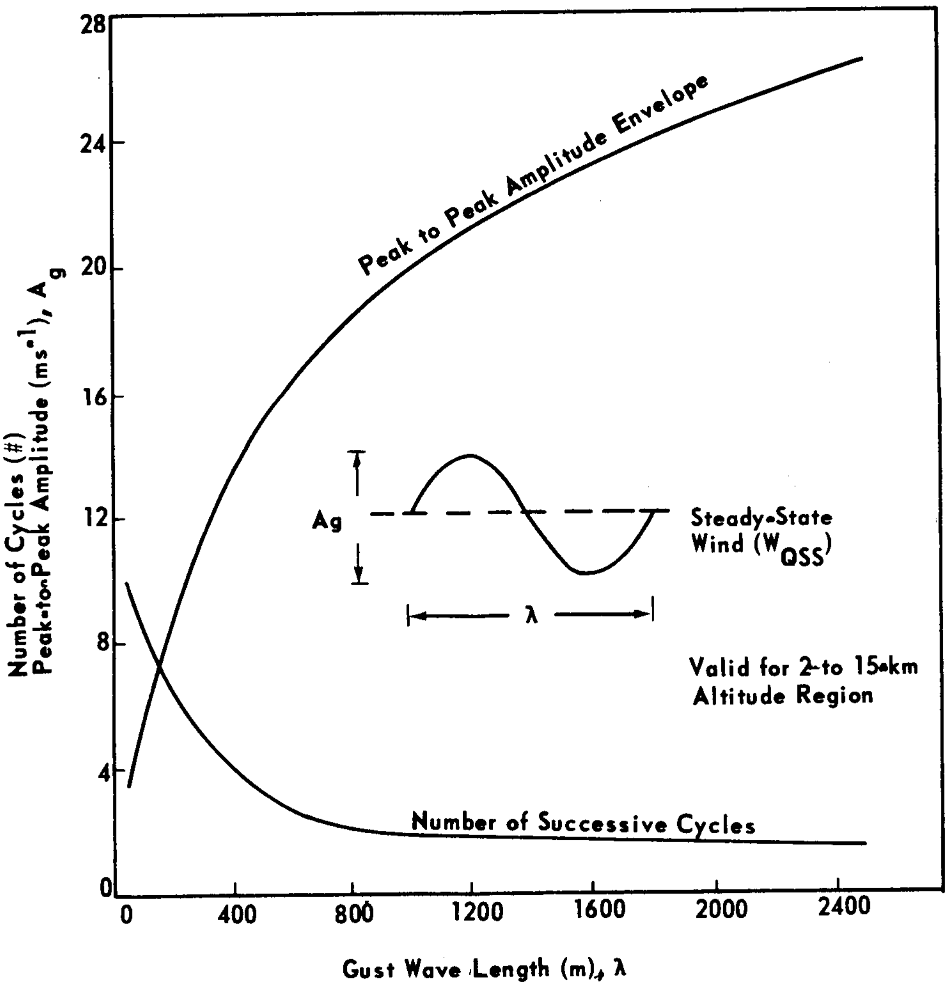

FIGURE 5.3.18 BEST ESTIMATE OF EXPECTED (≧ 99 percentile) GUST AMPLITUDE AND NUMBER OF CYCLES AS A FUNCTION OF GUST WAVELENGTHS

5.3.8.2 Spectra

In general, the small scale motions associated with vertical detailed wind profiles are characterized by a superposition of discrete gusts and many random frequency components. Spectral methods have been employed to specify the characteristics of this superposition of small scale motions.

A digital filter was developed to separate small scale motions from the steady-state wind profile. The steady-state wind profile defined by the separation process approximates those obtained by the rawinsonde system.[13] Thus, a spectrum of small scale motions is representative of the motions included in the FPS-16 radar/Jimsphere measurements, which are not included in the rawinsonde measurements. Therefore, a spectrum of those motions should be considered in addition to the steady-state wind profiles to obtain an equivalent representation of the detailed wind profile. Spectra of the small scale motions for various probability levels have been determined and are presented in Figure 5.3.19. The spectra were computed from approximately 1200 detailed wind profile measurements by computing the spectra associated with each profile, then determining the probabilities of occurrence of spectral density as a function of wave numbers (cycles/4000 m). Thus the spectra represent envelopes of spectral density for the given probability levels. Spectra associated with each profile were computed over the altitude range between approximately 4 and 16 kilometers. It has been shown that energy (variance) of the small scale motions is not vertically homogeneous; that is, it is not constant with altitude. The energy content over limited altitude intervals and for limited frequency bands may be much larger than that represented by the spectra in Figure 5.3.19. This should be kept in mind when interpreting the significance of vehicle responses when employing the spectra of small scale motions. Additional details on this subject are available upon request. Envelopes of spectra for detailed profiles without filtering (solid lines) are also shown in Figure 5.3.19. These spectra are well represented for wave numbers ≥ 5 cycles per 4000 meters by the equation

$$E(k) = E_0 k^{-p}, \qquad (5.31A)$$

where E is the spectral density at any wave number k (cycles/4000 m) between 1 and 20, $E_0 = E(1)$, and p is a constant for any particular percentile level of occurrence of the power spectrum.

13. This definition was selected to enable use of the much larger rawinsonde data sample in association with a continuous type gust representation.

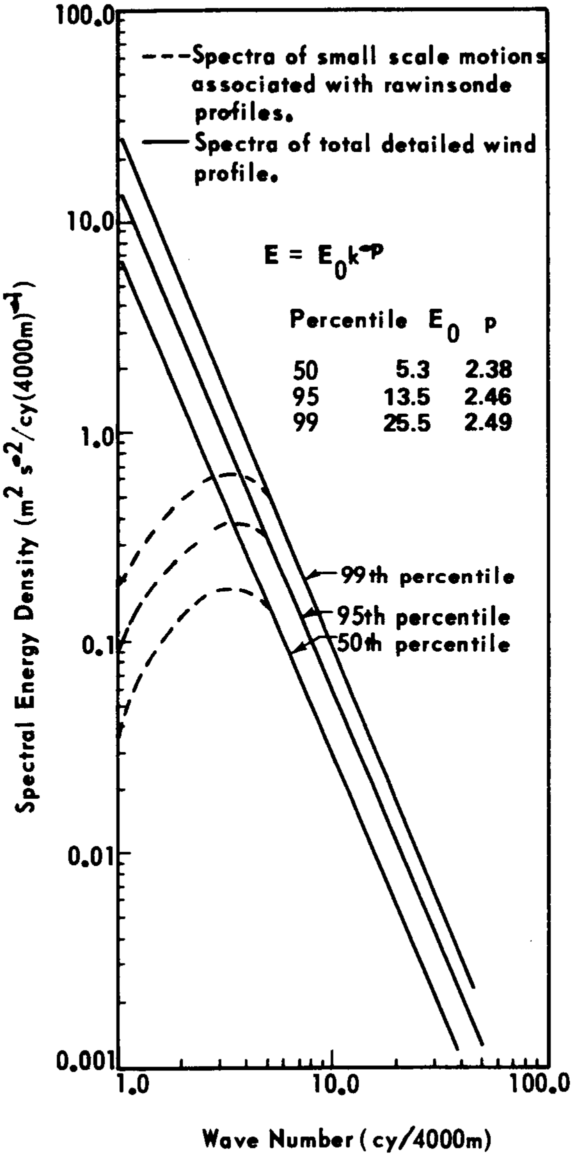

FIGURE 5.3.19 SPECTRA OF DETAILED WIND PROFILES

Spectra of the total wind speed profiles may be useful in control systems and other slow response parametric studies for which the spectra of small scale motions may not be adequate.

The power spectrum recommended for use in elastic body studies is given by the following expression:

$$E(\kappa) = \frac{683.4\ (4000\,\kappa)^{1.62}}{1 + 0.0067\ (4000\,\kappa)^{4.05}}, \tag{5.31B}$$

where the spectrum $E(\kappa)$ is defined so that integration over the domain $0 \leq \kappa \leq \infty$ yields the variance of the turbulence. In this equation $E(\kappa)$ is now the power spectral density [$m^2\ sec^{-2}$/(cycles per meter)] at wave number κ (cycles per meter). This function represents the 99 percentile scalar wind spectra for small-scale motions given by the dashed curve and its solid line extension into the high wave number region in Figure 5.3.19. The associated design turbulence loads are obtained by multiplying the load standard deviations by a factor of three. (Spectra for meridional and zonal components are available upon request).

Vehicle responses obtained from application of this turbulence spectra should be added to rigid vehicle responses resulting from use of the synthetic wind speed and wind shear profile (with the 0.85 factor on shears) but without a discrete gust.

5.3.9 Synthetic Wind Speed Profiles

Methods of constructing synthetic wind speed profiles are described herein. One method uses design wind speed profile envelopes (subsection 5.3.5), and discrete gusts or spectra (subsection 5.3.8) without consideration of any lack of correlation between the shears and gusts. Another method takes into account the relationships between the wind shear and gust characteristics.

5.3.9.1 Synthetic Wind Speed Profiles for Vertical Flight Path Considering Only Speeds and Shears

In the method that follows, correlation between the design wind speed profile envelope and wind shear envelope is considered. The method is illustrated with the 95 percentile design nondirectional (scalar) wind speed profile and the 99 percentile scalar wind speed build-up envelope for the Eastern Test Range (Figure 5.3.20) and is stated as follows:

a. Start with a speed on the design wind speed profile envelope at a selected (reference) altitude.

b. Subtract the amount of the shear (wind speed change) for each required altitude layer from the value of the wind speed profile envelope at the selected altitude. For example, in Figure 5.3.20, by using the selected altitude of 10 kilometers on the 95% wind speed profile envelope for Eastern Test Range (Figure 5.3.3) to determine the point at 10 kilometers on the shear build-up envelope, a value of wind speed change (build-up) of 30.0 m/sec is obtained from Table 5.3.10, Eastern Test Range, for ≥ 69 m/sec wind speed and 1000 meters scale of distance. By subtracting 30.0 m/sec from 69 m/sec, the value of the wind speed profile envleope of 39.0 m/sec is obtained.

c. Plot values obtained for each altitude layer at the corresponding altitudes. (The value of 39.0 m/sec, obtained in the example in b, would be plotted at 9 km.) Continue plotting values until a 5000-meter layer is reached (5000 meters below the selected altitude).

d. Draw a smooth curve through the plotted points starting at the selected altitude on the wind speed profile envelope. The lowest point is extended from the origin with a straight line tangent to the plotted shear build-up curve. This curve then becomes the shear build-up envelope.

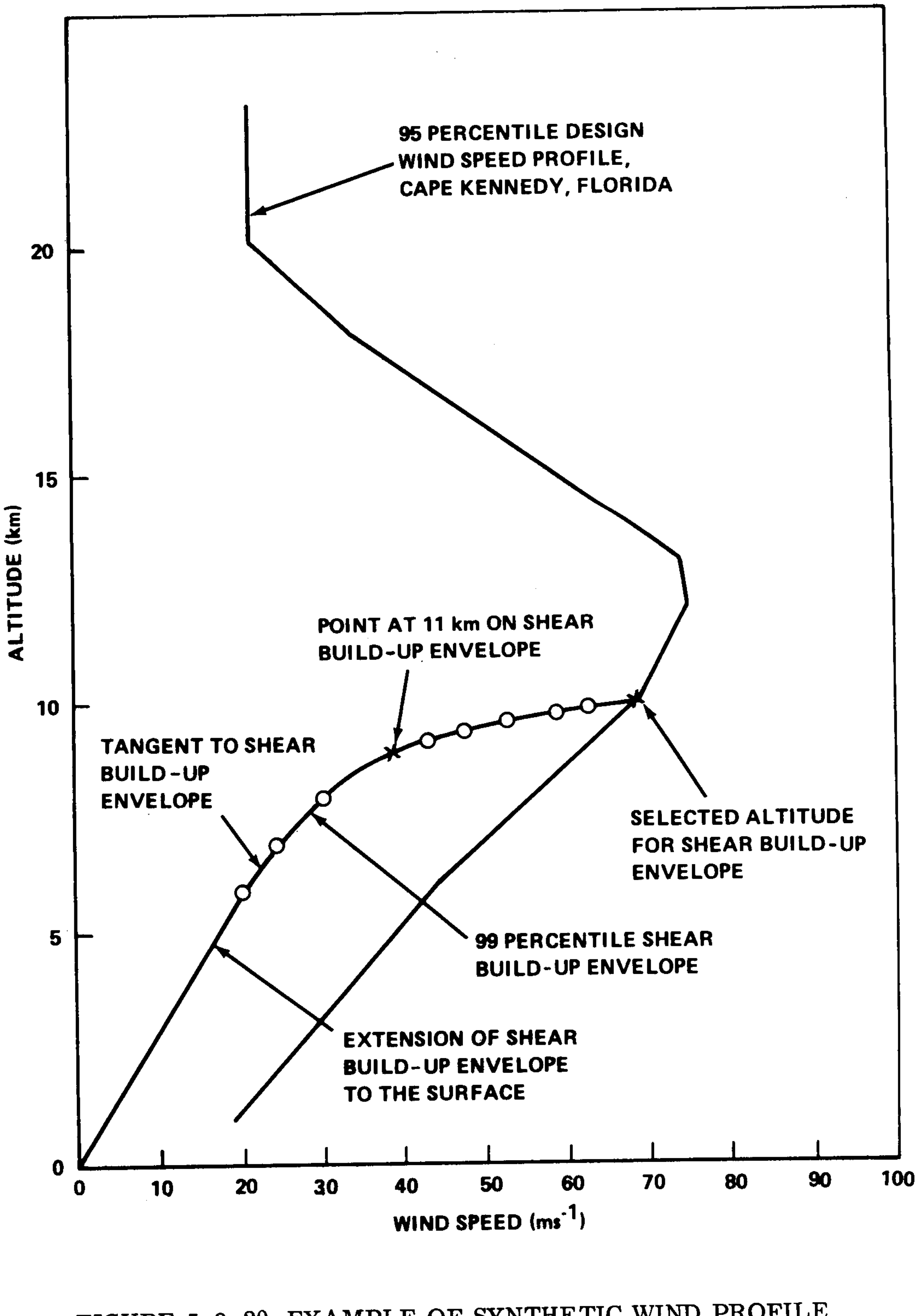

FIGURE 5. 3. 20 EXAMPLE OF SYNTHETIC WIND PROFILE CONSTRUCTION, WITHOUT ADDITION OF GUST

5.3.9.2 Synthetic Wind Speed Profiles For Vertical Flight Path Considering Relationships Between Speeds, Shears, and Gusts.

In the construction of a synthetic wind speed profile, the lack of perfect correlation between the wind shear and gust can be taken into account by multiplying the shears (wind speed changes) (subsection 5.3.6) and the recommended design discrete gusts (subsection 5.3.8) by a factor of 0.85 before constructing the synthetic wind profile. This is equivalent, as an engineering approximation, to taking the combined 99 percentile values for the gusts and shears in a perfectly correlated manner. This approach was used successfully in the Apollo/Saturn vehicle development program.

Thus, to construct the synthetic wind speed profiles (considering relationships between shears, speeds, and gusts, using the design wind speed envelopes given in subsection 5.3.5), the procedure that follows is used. Figures 5.3.21 and 5.3.22 show an example using the 95 percentile design wind speed profile envelope, the 99 percentile wind speed build-up envelope, and the modified one-minus-cosine discrete gust shape.

a. Construct the shear build-up envelope in the way described in subsection 5.3.9.1, except multiply the values of wind speed change used for each scale-of-distance by 0.85. (In the example for the selected altitude of 10 km, the point at 9 km will be found by using the wind speed change of 30.0 x 0.85, or 27.8 m/sec.) This value subtracted from 69 m/sec then gives a value of 43.5 m/sec for the point plotted at 9 kilometers instead of the value of 39.0 m/sec used when shear and gust relationships were not considered.

b. The discrete gust is superimposed on the build-up wind shear envelope/wind speed profile envelope by adding the gust given by equation (5.27) with leading edge in the region $H_b \leq H \leq H_b + 30$ m replaced with equation (5.29). The base of the discrete gust is located at the intersection of the build-up wind shear envelope and the wind speed profile envelope (see Figure 5.3.21). The gust amplitude, A, shall be decreased by a factor of 0.85, in order to account for the nonperfect correlation between shears and gusts. Figure 5.3.22 gives an example of a synthetic profile with shears and gust in combination.

c. When the gust ends at the design wind envelope, the synthetic wind profile may follow the design wind speed envelope or shear back-off profile. If the synthetic wind profile follows the design wind speed envelope then the trailing edge of the discrete gust will be a 1-cosine shape as given by equation (5.27). If the synthetic wind profile follows the shear back-off profile then the trailing edge of the discrete gust will be that given by equation (5.30). This

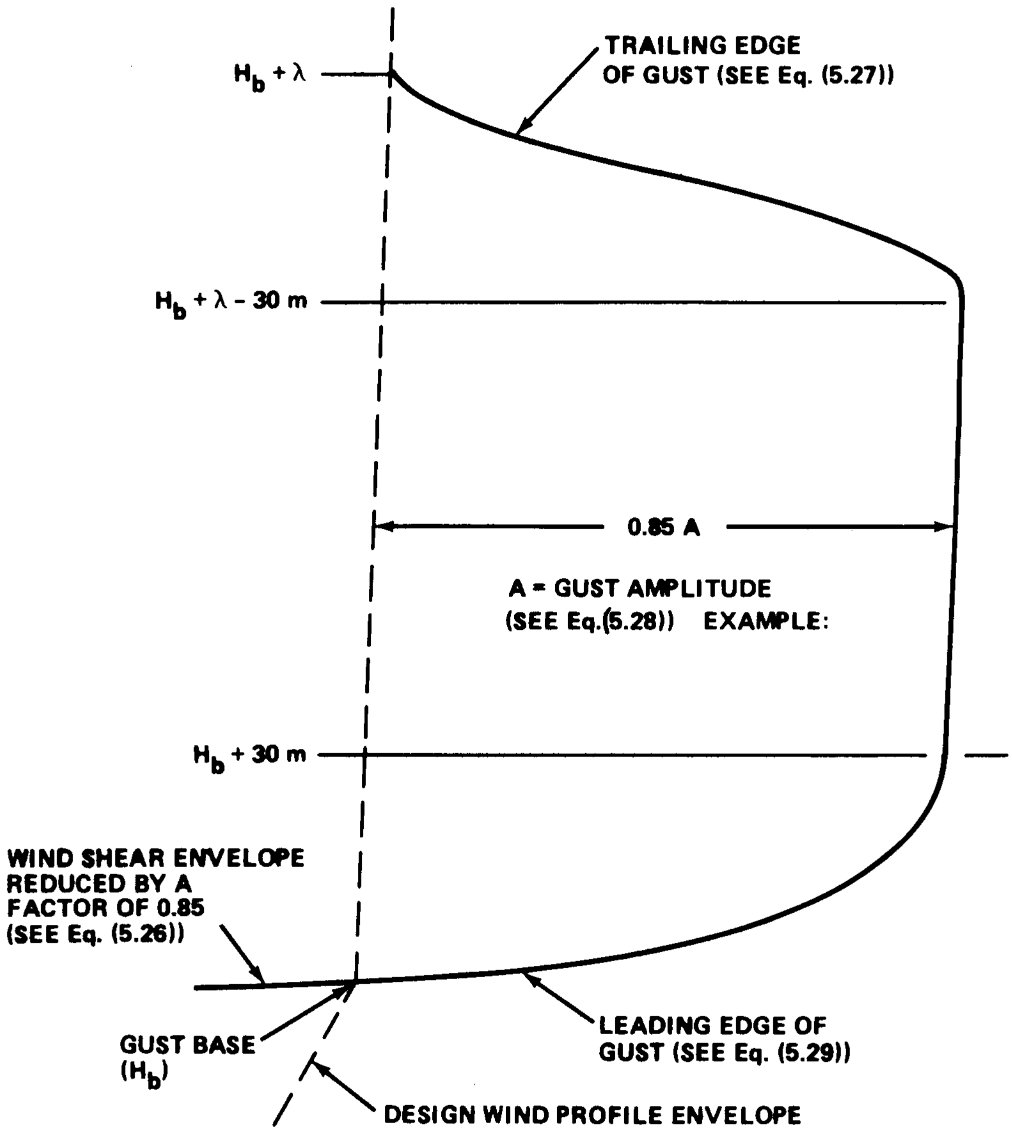

FIGURE 5.3.21 RELATIONSHIP BETWEEN REVISED GUST SHAPE, DESIGN WIND PROFILE ENVELOPE, AND SPEED BUILD-UP (SHEAR) ENVELOPE

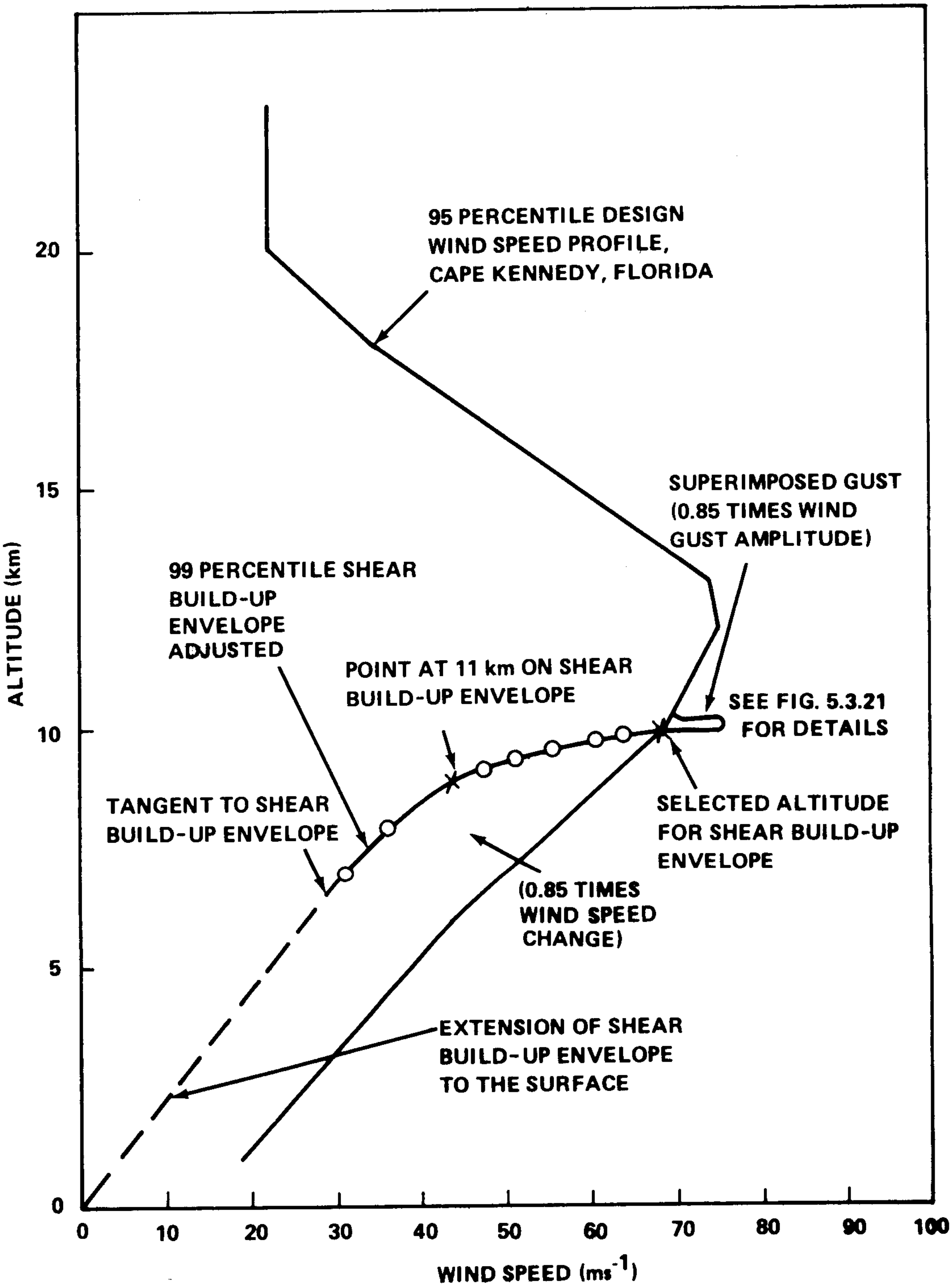

FIGURE 5.3.22 EXAMPLE OF SYNTHETIC WIND PROFILE CONSTRUCTION, WITH RELATIONSHIP OF WIND SHEARS AND GUSTS ASSUMED

modified gust shape will guarantee a continuous transition from the gust to the back-off shear envelope. Vehicle response through both the wind profile envelope with gusts and the synthetic wind profile with shears and gusts in combination should be examined.

d. If a power spectrum representation (see 5.3.8.2) is used then disregard all references to discrete gusts in the above. Use the 0.85 factor on shears and apply the spectrum as given in subsection 5.3.8.2.

5.3.9.3 Synthetic Wind Profile Merged to the Ground Wind Profile

Up to this point we have considered only those wind shear envelopes which are linearly extrapolated to a zero wind condition at the ground. This procedure does not allow for the possibility of the vehicle (Space Shuttle) to enter a wind shear envelope/gust above the H = 1000 m in a perturbed state resulting from excitations of the control system by the ground wind profile and the associated ground wind shears and gusts. To allow for these possibilities, it is recommended that the wind shear envelopes which begin above the 3000-meter level be combined with the wind profile envelope and discrete gust as stated in Section 5.3.9.2; however, a linear extrapolation shall be used to merge the wind defined by the shear envelope at the 3000-meter level with the 1000-meter wind on the wind profile envelope.

The steady-state ground wind profile up to the 150-meter level is defined by the peak wind profile (see Section 5.2.5.2) reduced to a steady-state wind profile by division with a 10-minute average gust factor profile (see Section 5.2.7.1). To merge this steady-state wind profile into the 1000-meter level steady-state wind speed envelope the steady-state wind speed in the layer between 150 to 300 meters shall take on a constant value equal to the steady-state wind at the 150-meter level defined by the peak wind profile and gust factor profile between the surface of the earth and the 150-meter level. The flow between the 300-meter level and the 1000-meter level shall be obtained by linear interpolation. If the discontinuities in slope of the wind profile at the 150-, 300- and 1000-meter levels resulting from this merging procedure introduce significant false vehicle responses it is recommended that this interpolation procedure be replaced with a procedure involving a smooth continuous function which closely approximates the piece-wise linear segment interpolation function between the 150- and 1000-meter levels with continuous values of wind speed and slope at the 150- and 1000-meter levels.

5.3.9.4 Synthetic Wind Speed Profiles For Non Vertical Flight Path

To apply the synthetic wind profile for other than vertical flight, multiply the wind shear build-up and back-off values by the cosine of the angle between the vertical axis (earth fixed coordinate system) and the vehicle's flight path. The gust (or turbulence spectra) is applied directly to the vehicle without respect to the flight path angle. The synthetic wind profile is otherwise developed according to procedures given in Section 5.3.9.2.

5.3.10 Characteristic Wind Profiles to a Height of 18 Kilometers

5.3.10.1 Features of Wind Profiles

A significant problem in space vehicle design is to provide assurance of an adequate design for flight through wind profiles of various configurations. During the major design phase of a space vehicle, the descriptions of various characteristics of the wind profile are employed in determining the applicable vehicle response requirement. Since much of the vehicle is in a preliminary status of design and the desired detail data on structural dynamic modes and other characteristics are not known at this time, the use of statistical and synthetic representations of the wind profile are desirable. However, after the vehicle design has been finalized and tests have been conducted to establish certain dynamic capabilities and parameters, it is desirable to evaluate the total system by simulated dynamic flight through wind profiles containing adequate frequency resolution (Ref 5.31). The profiles shown in Figures 5.3.23 through 5.3.28 are profiles of scalar wind measured by the FPS-16 Radar/Jimsphere wind measuring system, and they illustrate the following: (1) jet stream winds, (2) sinusoidal variation in wind with height, (3) high winds over a broad altitude band, (4) light wind speeds, and (5) discrete gusts.

These profiles show only a few of the possible wind profiles that can occur. Jet stream winds (Figure 5.3.23) are quite common to the various test ranges during the winter months and can reach magnitudes in excess of 100 m/sec. These winds occur over a limited altitude range, making the wind shears very large. Figure 5.3.24 depicts winds having sinusoidal behavior in the 10- to 14-kilometer region. These types of winds can create excessive loads upon a vertically rising vehicle, particularly if the reduced forcing frequencies couple with the vehicle control frequencies and result in additive loads. It is not uncommon to see periodic variations occur in the vertical winds. Some variations are of more concern than others, depending upon wavelength and, of course, amplitude. Figure 5.3.25 is an interesting

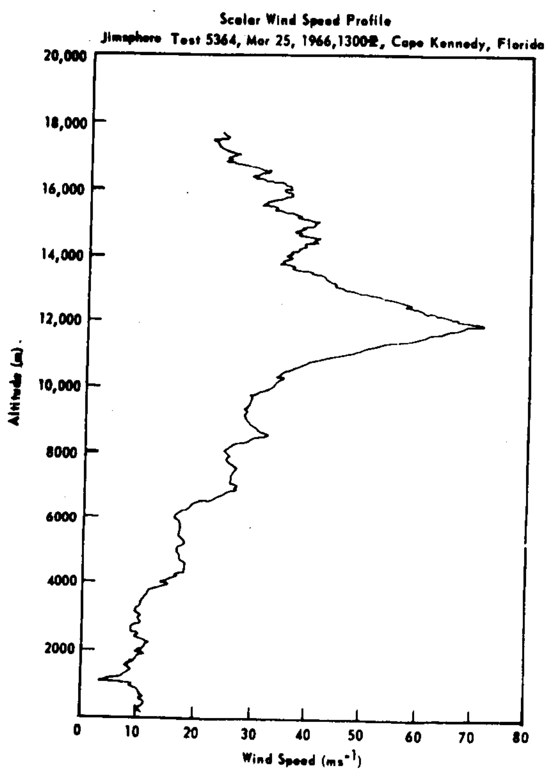

FIGURE 5.3.23 EXAMPLE OF JET STREAM WINDS

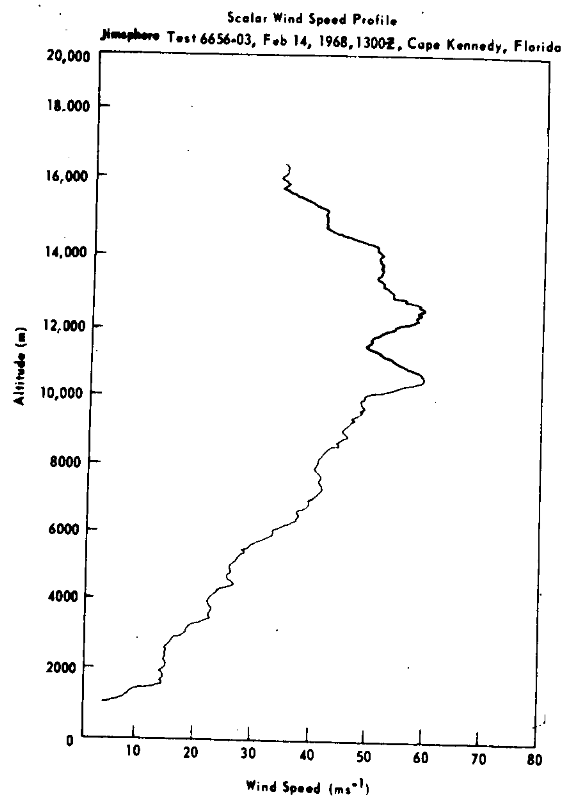

FIGURE 5.3.24 EXAMPLE OF SINE WAVE FLOW IN THE 10- TO 14-km ALTITUDE REGION

example of high wind speeds that occurred over 6 kilometers in depth. Such flow is not uncommon for the winter months. Figure 5.3.26 shows scalar winds of very low values. These winds were generally associated with easterly flow over the entire altitude interval (surface to 16 km) at Kennedy Space Center, Florida. The last examples (Figures 5.3.27 and 5.3.28) illustrate two samples of discrete gusts.

5.3.11 Detail Wind Profile Representative Samples

5.3.11.1 Introduction

FPS-16 Radar/Jimsphere detailed wind profile measurements have been made at Cape Kennedy since December 1964. The reduction technique used to reduce the radar data provides a mean wind velocity (direction and speed) associated with an altitude layer of about 50 meters (Ref. 5.32).

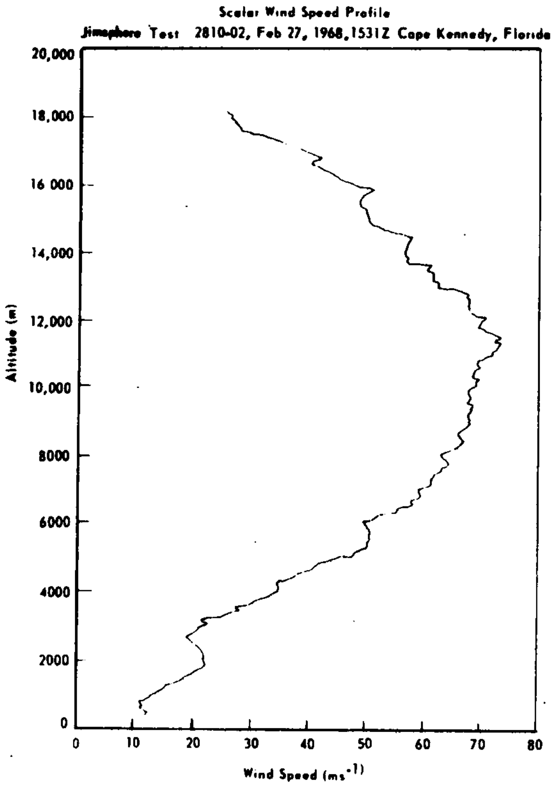

FIGURE 5.3.25 EXAMPLE OF HIGH WIND SPEEDS OVER A DEEP ALTITUDE LAYER

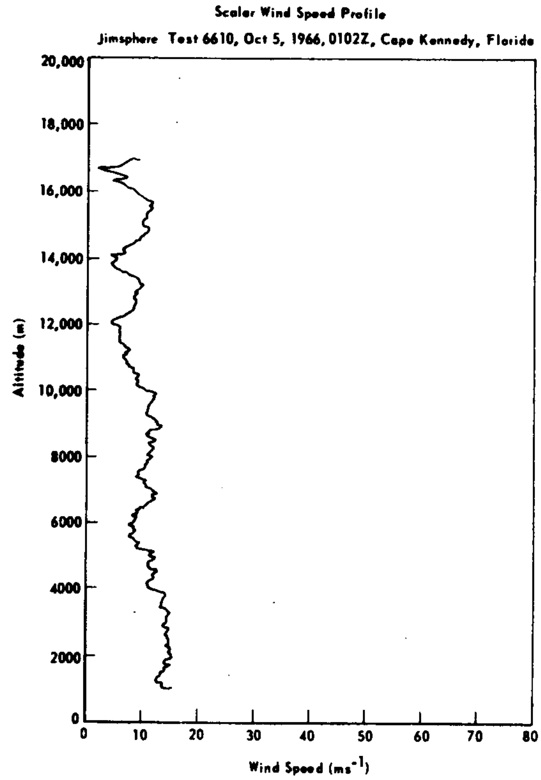

FIGURE 5.3.26 EXAMPLE OF LOW WIND SPEEDS

A discussion on the accuracy of these data is presented in Reference 5.33. A magnetic tape data record containing 1800 wind profiles has been established for engineering use in aerospace vehicle design verification and launch delay risk calculations. These data sets are designated as MSFC/NASA Jimsphere Wind Data Tape for Design Verification and are available upon request to the Aerospace Environment Division, NASA-Marshall Space Flight Center, Huntsville, Alabama 35812 (Ref. 5.34).

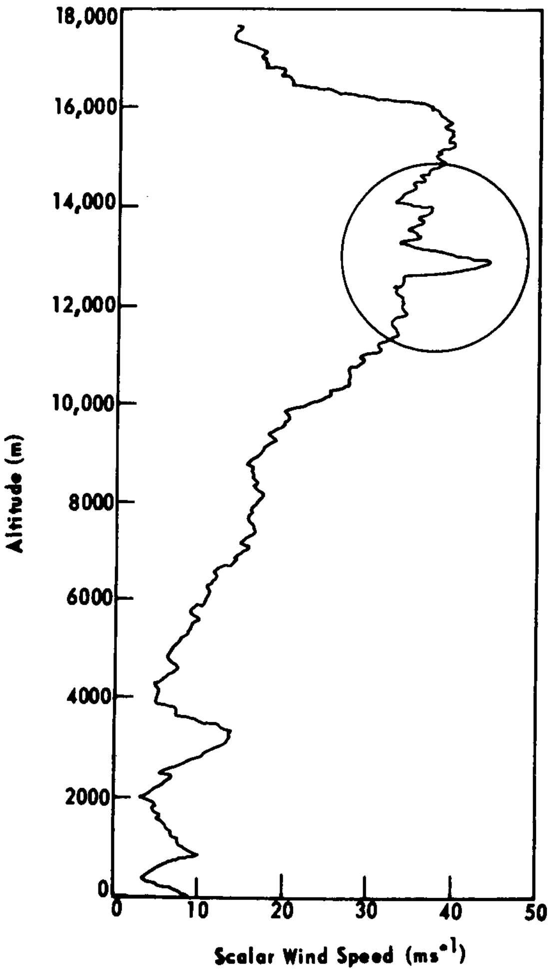

FIGURE 5.3.27 EXAMPLE OF A DISCRETE GUST OBSERVED BY A JIMSPHERE RELEASED AT 2103Z ON NOVEMBER 8, 1967, AT THE EASTERN TEST RANGE

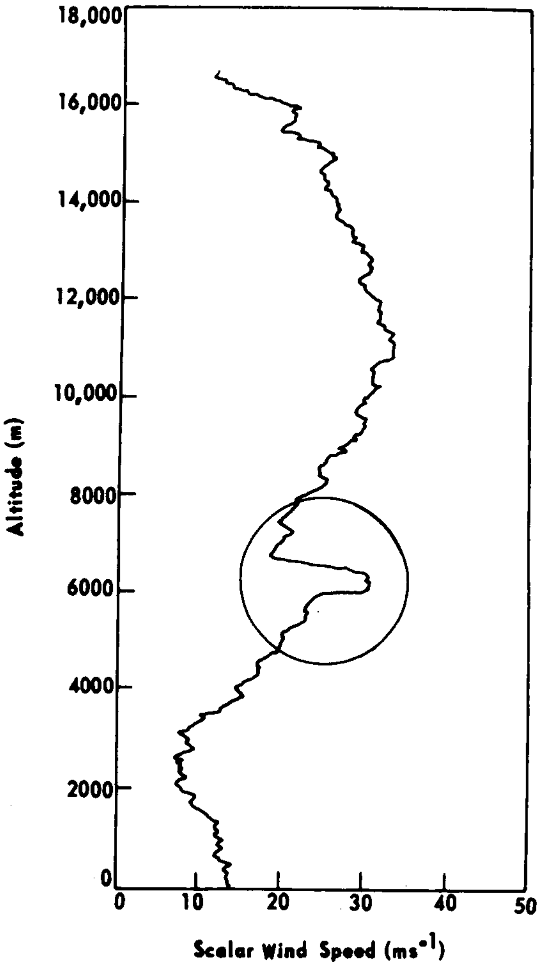

FIGURE 5.3.28 EXAMPLE OF A DISCRETE GUST OBSERVED AT 1300Z ON JANUARY 21, 1968, AT THE EASTERN TEST RANGE

5.3.11.2 Utilization of MSFC Jimsphere Wind Data for Design Verification

These records provide a representative selection of detailed wind velocity profiles for each of the twelve monthly periods for a given launch site. The data encompass a frequency content which exceeds the frequency of the first structural mode of most aerospace vehicles. Therefore, no additional allowance is required for high frequency components as is necessary for conventional rawinsonde profile data records. These data are intended for use in aerospace vehicle final design verification analyses to determine vehicle systems operational capabilities from near the earth's surface to approximately 18 kilometers altitude. Data have been interpolated for the lower few hundred meters and upper few kilometers to provide a complete profile (surface to 20 km) for computer use. Statistical comparisons of aerospace vehicle responses calculated from these wind profile records will be more easily assessed on the month-to-month basis using an equal number of profiles for each month provided by these records.

For vehicle operational capabilities analysis the vehicle simulations should be conducted with adequate representation of the vehicle's aeroelastic and dynamic characteristics to warrant utilization of detailed wind velocity profile data as a forcing function. It is considered that these wind profiles are an adequate selection for use in design verification analyses. Simulations may be conducted and statistically summarized with respect to an annual, seasonal, or monthly reference period. The monthly reference period is recommended.

Vehicle response simulations should be accomplished for the complete range of intended flight azimuths with respect to the total vector wind profile and not the scalar wind speed profiles (i. e., magnitude of the wind vector). Direction variations may be critical to the magnitude of the wind shears. All wind profiles should be utilized for each monthly period since the frequency content of wind profiles with low wind speed magnitudes may be as critical for some vehicle structural and control configurations as those for high wind speed.

The organization that uses these inflight wind data must establish a probability level of launch delay that it is willing to accept in the verification of a vehicle's design relative to the inflight wind influences. The probability level selected is the risk of launch delay and not vehicle loss if an adequate prelaunch monitorship program (Ref. 5.42) is employed.

The following steps outline recommended procedures for using the wind velocity profile data to calculate vehicle operational capability and launch delay risks:

Step 1. Calculate the vehicle response from flight simulation for each profile without wind bias using an appropriate flight simulation model and taking into consideration non-nominal vehicle performance with adequate vehicle aeroelastic and dynamic characteristics. A representative selection should be made of flight azimuths expected for the operational life of the vehicle.

Step 2. If the flight simulations reveal that the vehicle has a capability to fly through all wind profiles for a given month, and the specified flight azimuths, then the probability assigned as the vehicle launch capability relative to inflight winds is N (the number of profiles in the month) divided by N + 1 This probability value for the monthly sample size is 0.9934, based on 150 profiles per month.

Step 3. For other probability levels the maximum response to each wind profile is taken (see Step 1) for the given flight azimuths, grouped for each monthly period, and the associated probability distribution function is determined. From this distribution function the probability that the response will be less than any given value can be determined. Also, the probability that the response is greater than, or equal to, any given value can be determined. This latter probability (expressed in percent) is called the probability of launch delay risk for the given response. If the vehicle launch capability is such that the launch delay risk is less than or equal to a preestablished acceptable level (a suggested level is 5 percent which provides on the average a launch delay risk of 1.5 days during a month) for given flight azimuths in each monthly reference period, then the design shall be considered verified relative to the specified launch site.

Step 4. If the launch delay risk is significantly greater (in a statistical sense) then the preestablished acceptable level, then potential areas of design enhancement to permit the desired launch probability may be considered. Some methods are (a) structural/control systems modification and (b) the wind implementation of a bias trajectory.

Step 5. If conditions are not satisfied by Step 4, then operational constraints may be imposed such as restrictions on flight azimuth or acceptance of a larger launch delay risk for certain months for the specified launch site(s).

Final launch delay probability calculations for an operational vehicle may be computed in the same manner. However, in this case, the specific mission flight azimuth(s) and month of launch should be used in the calculation. Adequate vehicle aeroelastic and dynamic representation and allowance for non-nominal vehicle characteristics should be made. The individual vehicle peak response should be ordered as stated above and the launch probability determined with respect to the desired flight azimuth.

5.3.12 Wind Profile Data Availability

5.3.12.1 Availability of FPS-16 Radar/Jimsphere Wind Veloctiy Profiles

There are currently over 3100 profiles from Cape Kennedy, 375 profiles from Point Mugu, 550 profiles from White Sands Missile Range, 500 profiles from Green River, and 375 profiles from Wallops Island which have been reduced and edited. Vandenberg AFB, California, measurements were initiated in the spring of 1971. Some of these profile data have been published (Ref. 5.35). All the data are available on magnetic tapes. Master tapes have been prepared to make the data readily accessible for use in research studies. These data will be made available to aerospace, scientific, and engineering organizations upon request to the Chief, Aerospace Environment Division, Aero-Astrodynamics Laboratory, NASA-George C. Marshall Space Flight Center, Marshall Space Flight Center, Alabama 35812.

5.3.12.2 Availability of Rawinsonde Wind Velocity Profiles

Serially complete, edited, and corrected rawinsonde wind profile data are abailable for 14 years, two observations per day, for Cape Kennedy (Eastern Test Range), and for 9 years, four observations per day, for Santa Monica (Space and Missile Test Center), and for 5 years, two observations per day, for Vandenberg Air Force Base (SAMTEC). Qualified requestors in aerospace, scientific, and engineering organizations may obtain these data, which are also on magnetic tapes, upon request to the Chief, Aerospace Environment Division, Aero-Astrodynamics Laboratory, NASA-George C. Marshall Space Flight Center, Marshall Space Flight Center, Alabama 35812. They are also available as card deck 600 from the National Climatic Center, NOAA, Asheville, North Carolina 28801.

5.3.12.3 Availability of Rocketsonde Wind Velocity Profiles

Rocketsonde wind profile data have been collected for approximately 10 years from various launch sites around the world. These data can be obtained from the World Data Center A, Asheville, North Carolina 28801. Reference 5.59 gives a discussion of some of the rocketsonde instrumentation at Cape Kennedy, Florida that are used to measure winds in the mesosphere. References 5.60 and 5.61 contain examples of the kinds of analyses that can be accomplished with these data from engineering and scientific points of view, respectively.

5.3.12.4 Availability of Smoke Trail Wind Velocity Profiles

A limited amount of wind velocity data has been obtained by the use of smoke trail techniques to determine the small scale variations of wind velocity with altitude. References 5.36 and 5.37 should be consulted for obtaining such data.

5.3.12.5 Utility of Data

All wind profile data records should be checked carefully by the user before employing them in any vehicle response calculations. Where-ever practical, the user should become familiar with the representativeness of the data and frequency content of the profile used, as well as the measuring system and reduction schemes employed in handling the data. For those organizations that have aerospace meteorology oriented groups or individuals on their staffs, consultations should be held with them. Otherwise, various government groups concerned with aerospace vehicle design and operation can be of assistance. Such action by the user can prevent expensive misuse and error in interpretation of the data relative to the intended application.

5.3.13 Atmospheric Turbulence Criteria for Horizontally Flying Vehicles

In this section is presented the continuous turbulence random model for the design of aerospace vehicles capable of flying horizontally, or nearly so, through the atmosphere. In general both the continuous random model (sections 5.3.13 and 5.3.14) and the discrete model (section 5.3.15) are used to calculate vehicle responses with the procedure producing the larger response being used for design.

To a reasonable degree of approximation, inflight atmospheric turbulence experienced by horizontally flying vehicles can be assumed to be homogeneous, stationary, Gaussian, and isotropic. Under some conditions, these assumptions might appear to be drastic, but for engineering purposes they seem to be appropriate, except for low level flight in approximately the first 300 meters of the atmosphere. It has been found that the spectrum of turbulence first suggested by von Karman appears to be a good analytical representation of atmospheric turbulence. The longitudinal spectrum is given by

$$\Phi_u (\Omega, L) = \sigma^2 \frac{2L}{\pi} \frac{1}{[1 + (1.339 L\Omega)^2]^{5/6}} , \qquad (5.32)$$

[redacted]

where σ^2 is the variance of the turbulence, L is the scale of turbulence, and Ω is the wave number in units of radians per unit length. The spectrum is defined so that

$$\sigma^2 = \int_0^\infty \Phi_u(\Omega, L)\, d\Omega \quad . \tag{5.33}$$

The theory of isotropic turbulence predicts that the spectrum Φ_w of the lateral and vertical components of turbulence are related to the longitudinal spectrum through the differential equation

$$\Phi_w = \frac{1}{2}\left(\Phi_u - \Omega \frac{d\Phi_u}{d\Omega}\right) \quad . \tag{5.34}$$

Substitution of equation (5.32) into equation (5.34) yields

$$\Phi_w = \sigma^2 \frac{L}{\pi} \frac{1 + \frac{8}{3}(1.339\, L\Omega)^2}{[1 + (1.339\, L\Omega)^2]^{11/6}} \quad . \tag{5.35}$$

The nondimentional spectra $2\pi\Phi_u / \sigma^2 L$ and $2\pi\Phi_w / \sigma^2 L$ are depicted in Figure 5.3.29 as function of ΩL. As $L\Omega \rightarrow \infty$, Φ_u and Φ_w asymptotically behave like

$$\Phi_u \sim \sigma^2 \frac{2L}{\pi} \frac{(L\Omega)^{-5/3}}{(1.339)^{5/3}} \quad (L\Omega \rightarrow \infty) \tag{5.36}$$

$$\Phi_w \sim \sigma^2 \frac{2L}{\pi} \frac{(L\Omega)^{-5/3}}{(1.339)^{5/3}} \quad (L\Omega \rightarrow \infty) \quad , \tag{5.37}$$

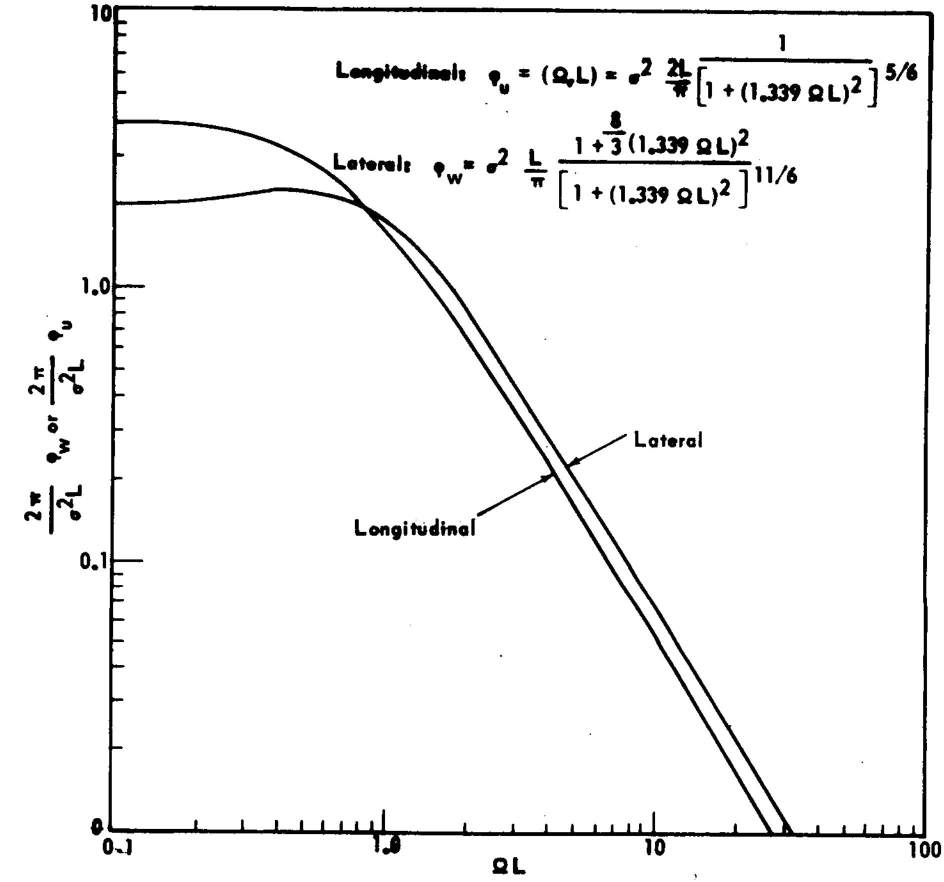

FIGURE 5.3.29 THE DIMENSIONLESS LONGITUDINAL AND LATERAL $\frac{2\pi\Phi_u}{\sigma^2 L}$ AND $\frac{2\pi\Phi_w}{\sigma^2 L}$ SPECTRA AS FUNCTIONS OF THE DIMENSIONLESS FREQUENCY $L\Omega$

consistent with the concept of the Kolmogorov inertial subrange. In addition, $\Phi_w/\Phi_u \rightarrow 4/3$ as $\Omega L \rightarrow \infty$. Design values of the scale of turbulence L are given in Table 5.3.22. Experience indicates that the scale of turbulence increases as height increases in the first 762 meters (2500 ft)[16] of the atmosphere, and typical values of L range from 10 meters (~ 30 ft) near the surface to 610 meters (2000 ft) at approximately a 762-meter (2500-ft) altitude. Above

16. U S. customary units are used in the section in parentheses to maintain continuity with source of data – Air Force Flight Dynamics Laboratory and other documentation.

TABLE 5. 3. 22 PARAMETERS FOR THE TURBULENCE MODEL FOR HORIZONTALLY FLYING VEHICLES

Altitude (m)	Altitude (ft)	Mission Segment[a]	Turbulence Component[b]	P_1 (unitless)	b_1 (m/sec)	b_1 (ft/sec)	P_2 (unitless)	b_2 (m/sec)	b_2 (ft/sec)	L (m)	L (ft)
0 - 304. 8	0 - 1 000	Low Level Contour (rough terrain)	V	1. 00	0. 82	2. 7	10^{-5}	3. 25	10. 65	152. 4	500
0 - 304. 8	0 - 1 000	Low Level Contour (rough terrain)	L, L	1. 00	0. 94	3. 1	10^{-5}	4. 29	14. 06	152. 4	500
0 - 304. 8	0 - 1 000	C, C, D	V, L, L	1. 00	0. 77	2. 51	0. 005	1. 54	5. 04	152. 4	500
304. 8 - 672	1 000 - 2 500	C, C, D	V, L, L	0. 42	0. 92	3. 02	0. 0033	1. 81	5. 94	533. 4	1750
672 - 1 524	2 500 - 5 000	C, C, D	V, L, L	0. 30	1. 04	3. 42	0. 0020	2. 49	8. 17	762	2500
1 524 - 3 048	5 000 - 10 000	C, C, D	V, L, L	0. 15	1. 09	3. 59	0. 00095	2. 81	9. 22	762	2500
3 048 - 6 096	10 000 - 20 000	C, C, D	V, L, L	0. 062	1. 00	3. 27	0. 00028	3. 21	10. 52	762	2500
6 096 - 9 144	20 000 - 30 000	C, C, D	V, L, L	0. 025	0. 96	3. 15	0. 00011	3. 62	11. 88	762	2500
9 144 - 12 192	30 000 - 40 000	C, C, D	V, L, L	0. 011	0. 89	2. 93	0. 000095	3. 00	9. 84	762	2500
12 192 - 15 240	40 000 - 50 000	C, C, D	V, L, L	0. 0046	1. 00	3. 28	0. 000115	2. 69	8. 81	762	2500
15 240 - 18 288	50 000 - 60 000	C, C, D	V, L, L	0. 0020	1. 16	3. 82	0. 000078	2. 15	7. 04	762	2500
18 288 - 21 336	60 000 - 70 000	C, C, D	V, L, L	0. 00088	0. 89	2. 93	0. 000057	1. 32	4. 33	762	2500
21 336 - 24 384	70 000 - 80 000	C, C, D	V, L, L	0. 00038	0. 85	2. 80	0. 000044	0. 55	1. 80	762	2500
above 24 384	above 80 000	C, C, D	V, L, L	0. 00025	0. 76	2. 50	0	0	0	762	2500

a. Climb, cruise, and descent (C, C, D).

b. Vertical, lateral, and longitudinal (V, L, L).

the 762-meter (2500-ft) level, typical values of L are in the order of 762 to 1829 meters (2500 to 6000 ft). The scales of turbulence in Table 5.3.22 above the 300-meter level are probably low, and they would be expected to give a somewhat conservative or high number of load or stress exceedances per unit length of flight. The scale of turbulence indicated for the first 304.8 meters of the atmosphere in Table 5.3.22 is a typical value. The use of this average scale of turbulence may be approximate for load studies; however, it is inappropriate for control system and flight simulation purposes in which event the vertical variation of the scale of turbulence in the first 300 meters of the atmosphere should be taken into account.

The power spectrum analysis approach is applicable only to stationary Gaussian continuous turbulence, but atmospheric turbulence is neither statistically stationary nor Gaussian over long distances. The statistical quantities used to describe turbulence vary with altitude, wind direction, terrain roughness, atmospheric stability, and a host of other variables. Nevertheless, it is valid to a sufficient degree of engineering approximation to recommend that atmospheric turbulence be considered locally Gaussian and stationary and that the total flight history of a horizontally flying vehicle be considered to be composed of an ensemble of exposures to turbulence of various intensities, all using the same power spectrum shape. Furthermore, it is recommended that the following statistical distribution of rms gust intensities be used:

$$p(\sigma) = \frac{P_1}{b_1}\sqrt{\frac{2}{\pi}}\exp\left(-\frac{\sigma^2}{2b_1^2}\right) + \frac{P_2}{b_2}\sqrt{\frac{2}{\pi}}\exp\left(-\frac{\sigma^2}{2b_2^2}\right) , \qquad (5.38)$$

where b_1 and b_2 are the standard deviations of σ in nonstorm and storm turbulence. The quantities P_1 and P_2 denote the fractions of flight time or distance flown in nonstorm and storm turbulence. It should be noted that if P_0 is the fraction of flight time or distance in smooth air, then

$$P_0 + P_1 + P_2 = 1 \qquad . \qquad (5.39)$$

The recommended design values of P_1, P_2, b_1, and b_2 are given in Table 5.3.22. Note that over rough terrain b_2 can be extremely large in the first 304 meters (1000 ft) above the terrain and the b's for the vertical, the lateral, and the longitudinal standard deviations of the turbulence are not equal. Thus in the first 304 meters (1000 ft) of the atmosphere above rough terrain, turbulence is significantly anisotropic and this anisotropy must be taken into account in engineering calculations.

An exceedance model of gust loads and stresses can be developed with the above information. Let y denote any load quantity that is a dependent variable in a linear system of response equations (for example, bending moment at a particular wing station). This system is forced by the longitudinal, lateral, and vertical components of turbulence, and upon producing the Fourier transform of the system, it is possible to obtain the spectrum of y. This spectrum will be proportional to the input turbulence spectra, the function of proportionality being the system transfer function. Upon integrating the spectrum of y over the domain $0 < \Omega < \infty$, we obtain the relationship

$$\sigma_y = A\sigma \quad , \tag{5.40}$$

where A is a positive constant that depends upon the system parameters and the scale of turbulence, and where σ_y is the standard deviation of y.

If the output y is considered to be Gaussian for a particular value of σ, then the expected number of fluctuations of y that exceed y^* with positive slope per unit distance with reference to a zero mean is

$$N(y^*) = N_0 \exp\left(-\frac{y^{*2}}{2\sigma_y^2}\right) \quad , \tag{5.41}$$

where N_0 is the expected number of zero crossings of y unit distance with h positive slope and is given by

$$N_0 = \frac{1}{2\pi\sigma_y}\left[\int_0^\infty \Omega^2 \Phi_y(\Omega)\, d\Omega\right]^{1/2} \quad . \tag{5.42}$$

In this equation, Φ_y is the spectrum of y and

$$\sigma_y = \left[\int_0^\infty \Phi_y(\Omega)\, d\Omega\right]^{1/2} \quad . \tag{5.43}$$

The standard deviation of σ_y is related to standard deviation of turbulence through equation (5.40), and σ is distributed according to equation (5.38). Accordingly, the number of fluctuations of y that exceed y* for standard deviations of turbulence in the interval σ to $\sigma + d\sigma$ is $N(y^*)\ p(\sigma)d\sigma$, so that integration over the domain $0 < \sigma < \infty$ yields

$$\frac{M(y^*)}{N_0} = P_1 \exp\left(-\frac{|y^*|}{b_1 A}\right) + P_2 \exp\left(-\frac{|y^*|}{b_2 A}\right) \quad , \qquad (5.44)$$

where $M(y^*)$ is the overall expected number of fluctuations of y that exceed y* with positive slope. To apply this equation, the engineer needs only to calculate A and N_0 and specify the risk of failure he wishes to accept. The appropriate values of P_1, P_2, b_1, and b_2 are given in Table 5.3.22. Figures 5.3.30 and 5.3.31 give plots of $M(y^*)/N_0$ as a function of $|y^*|/A$ for the various altitudes for the design data given in Table 5.3.22. Table 5.3.23 provides a summary of the units of the various quantities in this model.

5.3.13.1 Application of Power Spectral Model

To apply equation (5.44), the engineer can either calculate A and N_0 and then calculate the load quantity y* for a specified value of $M(y^*)$, or calculate A and calculate the load quantity y* for a specified value of

TABLE 5.3.23 METRIC AND U. S. CUSTOMARY UNITS OF VARIOUS QUANTITIES IN THE TURBULENCE MODEL FOR HORIZONTALLY FLYING VEHICLES

Quantity	Metric Units	U. S. Customary Units
Ω	rad/m	rad/ft
Φ_u, Φ_w	$m^2/sec^2/rad/m$	$ft^2/sec^2/rad/ft$
σ^2	m^2/sec^2	ft^2/sec^2
L	m	ft
b_1, b_2	m/sec	ft/sec
P_1, P_2	dimensionless	dimensionless
σ_y/A	m/sec	ft/sec
$\|y^*\|/A$	m/sec	ft/sec
N_0, N, M	rad/sec	rad/sec

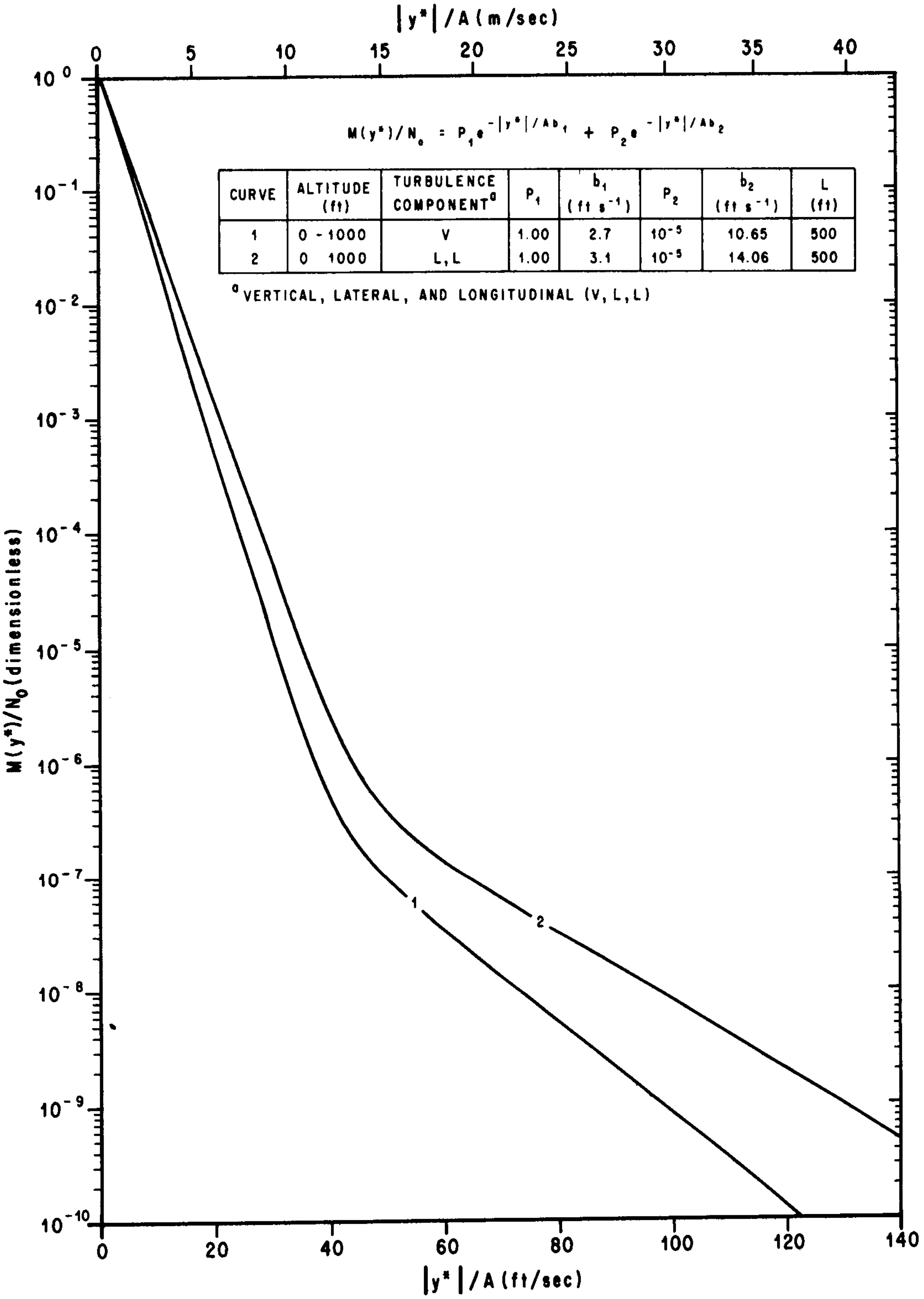

CURVE	ALTITUDE (ft)	TURBULENCE COMPONENT[a]	P_1	b_1 ($ft\ s^{-1}$)	P_2	b_2 ($ft\ s^{-1}$)	L (ft)
1	0 - 1000	V	1.00	2.7	10^{-5}	10.65	500
2	0 1000	L, L	1.00	3.1	10^{-5}	14.06	500

[a] VERTICAL, LATERAL, AND LONGITUDINAL (V, L, L)

FIGURE 5.3.30 EXCEEDANCE CURVES FOR THE VERTICAL, LATERAL, AND LONGITUDINAL COMPONENTS OF TURBULENCE FOR THE 0- TO 1000-ft ALTITUDE RANGE

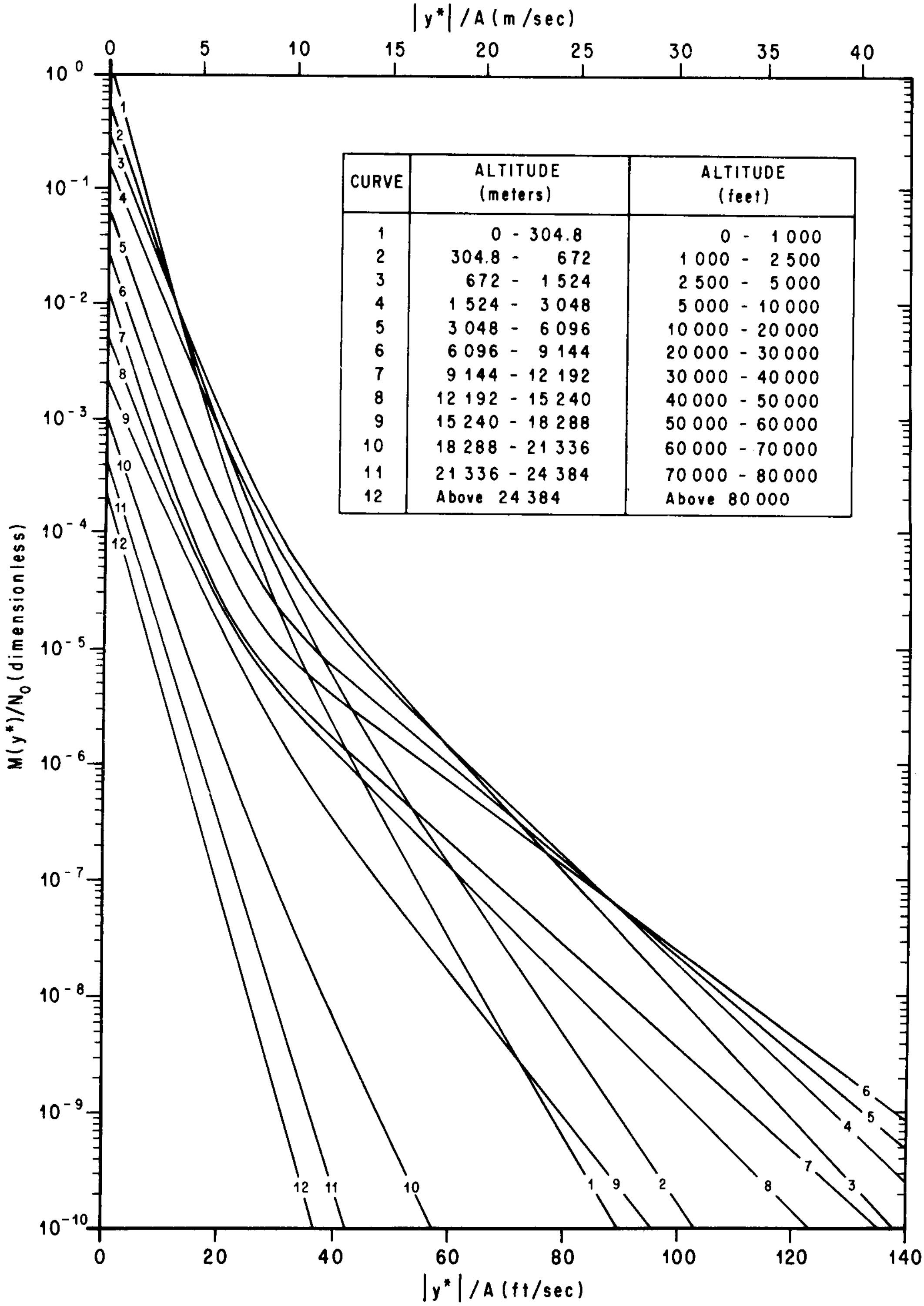

FIGURE 5.3.31 EXCEEDANCE CURVES FOR THE VERTICAL, LATERAL, AND LONGITUDINAL COMPONENTS OF TURBULENCE FOR VARIOUS ALTITUDE RANGES

$M(y^*)/N_0$. In a recent study performed by the Lockheed-California Company for the FAA (Ref. 5.38), design values of $M(y^*)$ and $M(y^*)/N_0$ were calculated. These design criteria were consistent with the limit load capabilities of present day commercial aircraft. The criterion in which $M(y^*)$ is specified is suitable for a mission analysis approach to the design problem. The criterion in which $M(y^*)/N_0$ is specified is suitable for a design envelope approach to aircraft design.

In the design envelope approach, it is assumed that the airplane operates 100 percent of the time at its critical design envelope point. The philosophy is that if the vehicle can operate 100 percent of the time at any point on the envelope it can surely operate adequately in any combination of operating points on the envelope. A new vehicle is designed on a limit load basis for a specified value of M/N_0. According to the authors of Reference 5.38, $M/N_0 = 6 \times 10^{-9}$ is suitable for the design of commercial aircraft. To apply this criterion, all critical altitudes, weights, and weight distributions are specified and associated values of A are calculated. The limit loads are calculated for each of the specified configurations with equation (5.44) for $M/N_0 = 6 \times 10^{-9}$.

In the mission analysis approach, a new aircraft is designed on a limit load basis according to Reference 5. 38 for $M = 2 \times 10^{-5}$ load exceedances per hour. To apply this criterion, the engineer must construct an ensemble of flight profiles which define the expected range of payloads and the variation with time of speed, altitude, gross weight, and center of gravity position. These profiles are divided into mission segments, or blocks, for analysis; and average or effective values of the pertinent parameters are defined for each segment. For each mission segment, values of A and N_0 are determined by dynamic analysis. A sufficient number of load and stress quantities are included in the dynamic analysis to assure that stress distributions throughout the structure are realistically or conservatively defined. Now the contribution to $M(y^*)$ from the ith flight segment is $t_i M_i(y^*)/T$ where t_i is the amount of time spent in the ith flight regime (mission segment), T is the total time flown by the vehicle over all mission segments, and $M_i(y^*)$ is the exceedance rate associated with the ith segment. The total exceedance rate for all mission segments, k say, is

$$M(y^*) = \sum_{i=1}^{k} \frac{t_i}{T} N_{0_i} \left(P_1 e^{-|y^*|/b_1 A} + P_2 e^{-|y^*|/b_2 A} \right) , \quad (5.45)$$

where subscript i denotes the ith mission segment. The limit gust load quantity $|y^*|$ can be calculated with this formula upon setting $M(y^*) = 2 \times 10^{-5}$ exceedances per hour.

The above mentioned limit load design criteria were derived for commercial aircraft which are normally designed for 50,000-hour lifetimes. Therefore, to apply these criteria to horizontally flying aerospace vehicles which will have relatively short lifetimes would be too conservative. However, it is possible to modify these criteria so that they will reflect a shorter vehicle lifetime. The probability F_p that a load will be exceeded in a given number of flight hours T is

$$F_p = 1 - e^{-TM} \quad . \tag{5.46}$$

It it is assumed that the limit load criterion $M = 2 \times 10^{-5}$ exceedances per hour is associated with an aircraft with a lifetime T equal to 50,000 hours, this means that $F_p = 0.63$, i.e., there is a 63 percent chance that an aircraft designed for a 50,000-hour operating lifetime will exceed its limit load capability at least once during its operating lifetime. This high failure probability, based on limit loads, is not excessive in view of the fact that an aircraft will receive many inspections on a routine basis during its operating lifetime. In addition, after safety factors are applied to the design limit loads the ultimate load exceedance rate will be on the order of 10^{-8} exceedances per hour. Substitution of this load exceedance rate into equation (5.46) for $T = 50{,}000$ hours yields a failure probability, on an ultimate load basis, of $F_p = 0.0005$. This means that there will only be a 0.05 percent chance that an aircraft will exceed its ultimate load capability during its operating lifetime of 50,000 hours. Thus, a failure probability of $F_p = 0.63$ on a limit load basis is reasonable for design. Let us now assume that $F_p = 0.63$ is the limit load design failure probability so that equation (5.46) can be used to calculate design values of M associated with a specified vehicle lifetime. Thus, for example, if we expect a vehicle to fly only 100 hours, then according to equation (5.46), we have $M = 10^{-2}$ exceedances per hour. Similarly, if we expect a vehicle to be exposed to the atmosphere for 1000 hours of flight, then $M = 10^{-3}$ exceedances per hour.

The corresponding design envelope criterion can be obtained by dividing the above calculated values of M by an appropriate value of N_0. In the case of the 50,000 hours cirterion, we have $M/N_0 = 6 \times 10^{-9}$ and $M = 2 \times 10^{-5}$ exceedances per hour so that an estimate of N_0 for purposes of obtaining a design criterion is $N_0 = 0.333 \times 10^4\ \text{hr}^{-1}$. Thus, upon solving equation (5.46) for M and dividing by $N_0 = 0.333 \times 10^4\ \text{hr}^{-1}$, the design envelope criterion takes the form

$$\frac{M}{N_0} = \frac{3 \times 10^{-4}}{T} \tag{5.47}$$

where we have used $F_p = 0.63$. Thus, for a 100-hour aircraft, the design envelope criterion is $M/N_0 = 3 \times 10^{-6}$ and for a 1000-hour aircraft $M/N_0 = 3 \times 10^{-7}$.

It is recommended that the power spectral approach be used in place of the standard discrete gust methods. Reasonably discrete gusts undoubtedly occur in the atmosphere; however, there is accumulating evidence that the preponderance of gusts are better described in terms of continuous turbulence models. It has long been accepted that clear air turbulence at moderate intensity levels is generally continuous in nature. Thunderstorm gust velocity profiles are now available in considerable quantity, and they almost invariably display the characteristics of continuous turbulence. Also, low level turbulence is best described with power spectral methods. A power spectral method of load analysis is not necessarily more difficult to apply than a discrete gust method. The present static load plunge-only discrete gust methods can, in fact, be converted to a power spectral basis by making a few simple modifications in the definitions of the gust alleviation factor and the design discrete gust. To be sure, this simple rigid-airplane analysis does not exploit the full potentiality of the power spectral approach, but it does account more realistically for the actual mix of gust gradient distances in the atmosphere and the variation of gust intensity with gradient distance.

5.3.14 Turbulence Model for Flight Simulation

For simulation of turbulence in either an analog or digital fashion, the turbulence realizations are to be generated by passing a white noise process through a passive filter. The model of turbulence as given in subsection 5.3.13 is not particularly suited for the simulation of turbulence with white noise. This results because the von Karman spectra given by equations (5.32) and (5.35) are irrational. Thus, for engineering purposes, the Dryden spectra may be used for simulation of continuous random turbulence. They are given by

$$\text{Longitudinal:} \quad \Phi_u(\Omega) = \sigma^2 \frac{2L}{\pi} \frac{1}{1 + (L\Omega)^2} \tag{5.47}$$

$$\text{Lateral and Vertical:} \quad \Phi_w(\Omega) = \sigma^2 \frac{L}{\pi} \frac{1 + 3(L\Omega)^2}{[1 + (L\Omega)^2]^2} . \tag{5.48}$$

Since these spectra are rational, a passive filter may be generated. It should be noted that the Dryden spectra are somewhat similar to the von Karman spectra. As $\Omega L \to 0$ the Dryden spectra asymptotically approach the von Karman spectra. As $\Omega L \to \infty$ the Dryden spectra behave like $(\Omega L)^{-2}$, while the von Karman spectra behave like $(\Omega L)^{-5/3}$. Thus, the Dryden spectra depart from the von Karman spectra by a factor proportional to $(\Omega L)^{-1/3}$ as $\Omega L \to \infty$, so that at sufficiently large values of ΩL the Dryden spectra will fall below the von Karman spectra. However, this deficiency in spectral energy of the Dryden spectra with respect to the von Karman spectra is not serious from an engineering point of view. If the capability to use the von Karman spectra is already available, the user should use it in flight simulation rather than the Dryden spectra.

The spectra as given by equations (5.47) and (5.48) can be transformed from the wave number (Ω) domain to the frequency domain (ω, rad/sec) with a Jacobian transformation by noting that $\Omega = \omega / V$, so that

$$\Phi_u(\omega) = \frac{L}{V} \frac{2\sigma^2}{\pi} \frac{1}{1 + (L\omega/V)^2} \tag{5.49}$$

$$\Phi_w(\omega) = \frac{L}{V} \frac{\sigma^2}{\pi} \frac{1 + 3(L\omega/V)^2}{[1 + (L\omega/V)^2]^2} . \tag{5.50}$$

The quantity V is the magnitude of the mean wind vector relative to the aerospace vehicle, $\vec{\bar{u}} - \vec{C}$. The quantities $\vec{\bar{u}}$ and $\vec{C}$ denote the velocity vectors of the mean flow of the atmosphere and the aerospace vehicle relative to the earth. In the region above the 300-meter level the longitudinal component of turbulence is defined to be the component of turbulence parallel to the mean wind vector relative to the aerospace vehicle $(\vec{\bar{u}} - \vec{C})$. The lateral and vertical components of turbulence are perpendicular to the relative mean wind vector and act in the lateral and vertical directions relative to the vehicle flight path.

5.3.14.1 Transfer Functions

Atmospheric turbulence can be simulated by passing white noise through filters with the following frequency response functions:

$$\text{Longitudinal:} \quad F_u(j\omega) = \frac{(2k)^{1/2}}{a + j\omega} \tag{5.51}$$

$$\text{Lateral and Vertical:} \quad F_w(j\omega) = \frac{(3k)^{1/2}(3^{-1/2} a + j\omega)}{(a + j\omega)^2} , \tag{5.52}$$

where

$$a = \frac{V}{L} \tag{5.53}$$

$$k = \frac{a\sigma^2}{\pi} \quad . \tag{5.54}$$

To generate the three components of turbulence, three distinct uncorrelated Gaussian white noise sources should be used.

To define the rate of change of gust velocities about the pitch, yaw, and roll axes for simulation purposes, a procedure consistant with the above formulation can be found in Section 3.7.5, "Application of Turbulence Models and Analyses," of reference 5.62. This should be checked for applicability.

5.3.14.2 Boundary Layer Turbulence Simulation

The turbulence in the atmospheric boundary layer, defined here for engineering purposes to be approximately the first 300 meters of the atmosphere, is inherently anisotropic. To simulate this turbulence realistically as possible, the differences between the various scales and intensities of turbulence should be taken into account. There are various problems associated with developing an engineering model of turbulence for simulation purposes. The most outstanding one concerns how one should combine the landing or take-off steady-state wind and turbulence conditions near the ground (18.3-meter level, for example) with the steady-state wind and turbulence conditions at approximately the 300-meter level. The wind conditions near the ground are controlled by local conditions and are usually derived from considerations of the risks associated with exceeding the design take-off or landing wind condition during any particular mission. The turbulence environments at and above the 300-meter level are controlled by relatively large scale conditions rather than local landing or take-off wind conditions, and these turbulence environments are usually derived from considerations of the risks associated with exceeding the design turbulence environment during the total life or total exposure time of the vehicle to the natural environment. The use of the risk associated with exceeding the design wind environment near the ground during a given mission rather than the use of the risk of exceeding the design turbulence environment during the total life of the vehicle is justified on the basis that, if the landing conditions are not acceptable, the pilot has the option to land at an alternate airfield and thus avoid the adverse landing wind conditions at the primary landing site. Similarly, in the take-off problem, the pilot can wait until the adverse low level wind and turbulence conditions have subsided before taking-off. The use of the risk associated with exceeding the design turbulence environment during the total life of the vehicle above the atmospheric boundary layer to develop design turbulence environments for vehicle design studies is justified because the pilot does not have the option of avoiding adverse inflight turbulence conditions directly ahead of the vehicle. In addition, the art of forecasting inflight turbulence has not progressed to the point where a flight plan can be established which avoids inflight turbulence with a reasonably small risk, such that design environments can be established on a per flight basis rather than on a total lifetime basis.

How does one then establish a set of values for L and σ for each component of turbulence which merges together these two distinctly different philosophies? It is recommended that design values for each component of turbulence be established at the 18.3-meter and at the 304.8-meter levels based on the above stated philosophies. Once these values of σ and L are established, the corresponding values between the 18.3- and 304.8-meter levels can be obtained with the following interpolation formulae

$$\sigma(H) = \sigma_{18.3} \left(\frac{H}{18.3}\right)^p \tag{5.55}$$

$$L(H) = L_{18.3} \left(\frac{H}{18.3}\right)^q \tag{5.56}$$

where $\sigma(H)$ and $L(H)$ are the values of σ and L at height H above natural grade, $\sigma_{18.3}$ and $L_{18.3}$ are the values of σ and L at the 18.3-meter level, p and q are constants selected such that the appropriate values of σ and L occur at the 304.8-meter level. Representative values of $L_{18.3}$ for the Dryden spectrum are given by

$$L_{u_{18.3}} = 31.5\text{m}, \; L_{v_{18.3}} = 18.4\text{m}, \; L_{w_{18.3}} = 10.0\text{m} \tag{5.57}$$

where subscript u, v, and w denote the longitudinal, lateral and vertical components of turbulence. The corresponding design values of $\sigma_{18.3}$ are given by

$$\sigma_{u_{18.3}} = 2.5\, u_{*o} \tag{5.58}$$

$$\sigma_{v_{18.3}} = 1.91 u_{*o} \tag{5.59}$$

$$\sigma_{w_{18.3}} = 1.41 u_{*o} \tag{5.60}$$

where u_{*o} is the surface friction velocity which is given by

$$u_{*o} = 0.4 \frac{\bar{u}_{18.3}}{\ln\left(\frac{18.3}{z_o}\right)} \tag{5.61}$$

The quantity $\bar{u}_{18.3}$ is the mean wind or steady-state wind at the 18.3-meter level, z_o is the surface roughness length (see subsection 5.2.6.2) and mks units are understood. The quantity $\bar{u}_{18.3}$ is related to the 18.3-meter level peak wind speed $u_{18.3}$ (see section 5.2.4) through the equation

$$\bar{u}_{18.3} = \frac{u_{18.3}}{G_{18.3}} \tag{5.62}$$

where $G_{18.3}$ is the 18.3-meter level gust factor (see subsection 5.2.7.1) associated with a one-hour average wind. This gust factor is a function of the 18.3-meter level peak wind speed so that upon specifying $u_{18.3}$ and the surface roughness length the quantity u_{*o} is defined by equation (5.61) and the standard deviations of turbulence are in turn defined by equations (5.58) through (5.60).

The values of L and σ must satisfy the Dryden isotropy conditions demanded by the equation of mass continuity for incompressible flow. These isotropy conditions are given by

$$\frac{\sigma_u^2}{L_u} = \frac{\sigma_v^2}{L_v} = \frac{\sigma_w^2}{L_w} \tag{5.63}$$

and must be satisfied at all altitudes. The length scales given by equation (5.57) and the standard deviations of turbulence given by (5.58) through (5.60) were selected such that they satisfy the isotropy condition given by equation (5.63), i.e.,

$$\frac{\sigma^2_{u_{18.3}}}{L_{u_{18.3}}} = \frac{\sigma^2_{u_{18.3}}}{L_{v_{18.3}}} = \frac{\sigma^2_{w_{18.3}}}{L_{w_{18.3}}} \tag{5.64}$$

At the 304.8-meter level, equation (5.63) is automatically satisfied because $\sigma_u = \sigma_v = \sigma_w$ and $L_u = L_v = L_w$ at the 304.8-meter level.

To calculate the value of $\sigma_{304.8}$ appropriate for performing a simulation, the following procedure is used to calculate the design instantaneous gust from which the design value of $\sigma_{304.8}$ shall be obtained. The procedure consists of specifying the vehicle lifetime T; calculating the limit load design value of M/N_o with equation (5.47); and then calculating the limit load instantaneous gust velocity, w*, say, with equation (5.44) for A = 1 with the values of P_1, P_2, b_1, and b_2 associated with the 0-304.8 meter height interval for climb, cruise, wind descent in Table 5.3.22. The instantaneous gust velocity w^* should be associated with the 99.98 percent value of gust velocity for a given realization of turbulence. In addition, the turbulence shall be assumed to be Gaussian, so that the value of $\sigma_{304.8}$ for performing a simulation shall be obtained by dividing w^* by 3.5. This value of $\sigma_{304.8}$ and the values of σ at the 18.3-meter level (see equations (5.58)-(5.60)) shall be used to determine the values of p for each component of turbulence with equation (5.55), i.e.,

$$p = 0.356 \ln \left(\frac{\sigma_{304.8}}{\sigma_{18.3}} \right) \tag{5.65}$$

The integral scale of turbulence at the 304.8-meter level appropriate for simulation of turbulence with the Dryden turbulence model is $L_{304.8}$ - 190 m. This scaling turbulence and the 18.3-meter level scales of turbulence given by equation (5.57) yield the following values of q appropriate for the simulation of turbulence with the Dryden turbulence model in the atmospheric boundary layer:

$$q_u = 0.64, \; q_v = 0.83, \; q_w = 1.05. \tag{5.66}$$

The vertical distributions of σ and L given by equations (5.55) and (5.56) satisfy the isotropy condition given by equation (5.63).

Below the 18.3-meter level σ and L shall take on constant values equal to corresponding 18.3-meter level values.

The steady-state wind profile to be used with this model shall be obtained by the procedure given in section 5.3.9.3 for merging ground winds and inflight wind profile envelopes.

To determine the steady-state wind direction $\Theta(z)$ at any level H between the surface and the 1000-meter level, use the following formula

$$\Theta(z) = \Theta_{1000} + \left[2\left(\frac{H - 1000}{1000}\right) + \left(\frac{H - 1000}{1000}\right)^2 \right] \Delta,$$

where Θ_{1000} is the selected 1000-meter level wind direction and H is altitude above the surface of the earth in meters. The quantity Δ is the angle between the wind vectors at the 10- and 1000-meter levels. This quantity for engineering purposes is distributed according to a Gaussian distribtuion with mean value and standard deviation given by

$$\bar{\Delta} = 31°, \; \bar{u}_{1000} \leq 4 \text{ m sec}^{-1} ,$$

$$\bar{\Delta} = 31 - 2.183 \ln(\bar{u}_{1000}/4), \; \bar{u}_{1000} > 4 \text{ m sec}^{-1} ,$$

$$\sigma\Delta = 64^\circ \quad , \quad \bar{u}_{1000} \leq 4\text{m sec}^{-1} \quad ,$$

$$\sigma\Delta = 64e^{-0.0531(\bar{u}_{1000}^{-4})} \quad , \quad \bar{u}_{1000} > 4\text{m sec}^{-1} \quad ,$$

where $\bar{u}_{1000}$ is the 1000-meter level steady-state wind speed. To avoid unrealistic wind direction changes, Δ, between the surface and the 1000-meter level, only those values of Δ that occur in the interval $-180^\circ \leq 0 \leq 180^\circ$ should be used. It is recommended that ± 1% risk wind direction changes be used for vehicle design studies.

To apply this model, the longitudinal component of turbulence shall be assigned to be that component of turbulence parallel to the horizontal component of the relative wind vector. The lateral component of turbulence perpendicular to the longitudinal component and lies in the horizontal plane. The vertical component of turbulence is orthogonal to the horizontal plane.

The following procedure shall be used to calculate profiles of σ and L in the first 304.8 m of the atmosphere for simulation of turbulence with the Dryden turbulence model:

a. Specify the peak wind speed at the 18.3-meter level consistent with the accepted risks of exceeding the design 18.3-meter level peak wind speed.

b. Calculate the steady-state wind speed at the 18.3-meter level with equation (5.62).

c. Calculate the surface friction velocity with equation (5.61).

d. Calculate the 18.3-meter levels standard deviations of turbulence with equations (5.58) through (5.60).

e. Calculate the 304.8-meter level standard deviation of turbulence consistent with the accept risks of encountering the design instantaneous gust during the total exposure of the vehicle to the natural environments (remember $\sigma_u = \sigma_v = \sigma_w$ at the 304.8-meter level).

f. Calculate p_u, p_v, and p_w with equation (5.65).

g. Calculate the distribution of σ and L with equation (5.55) and (5.56) for the altitudes at and between the 18.3- and 304.8-meter levels.

h. Below the 18.3-meter level σ and L shall take on constant values equal to the 18.3-meter levels values of σ and L.

The reader should consult references 5.63 and 5.64 for a detailed discussion concerning the philosophy and problem associated with the simulation of turbulence for engineering purposes.

5.3.14.3 Turbulence Simulation in the Free Atmosphere (above 304.8 m)

To simulate turbulence in the free atmosphere (above 304.8 m) it is recommended that equations (5.44) and (5.47) and the supporting data in Table 5.3.22 be used to specify the appropriate values of σ.. The turbulence at these altitudes can be considered to be isotropic for engineering purposes so that the integral scales and intensities of turbulence are independent of direction. Past studies have shown that when the Dryden turbulence model is being used the scales of turbulence L = 533.4 m in the 304.8 - 672 m altitude band and L = 762 m above the 672-meter level in Table 5.3.22 should be replaced with the values L = 300 m and L = 533 m respectively (Ref. 5.62). This reduction in scales tends to bring the Dryden spectra in line with the von Karman spectra over the band of wave numbers of the turbulence which are of primary importance in the design of aerospace vehicles. Accordingly, it is recommended that these reduced scales be used in the simulation of turbulence above the 304.8-meter level when the Dryden model is being used.

To calculate the values of σ above the 304.8-meter level appropriate for performing a simulation of turbulence, it is recommended that the procedure used to calculate the 304.8-meter level value of σ be used. The appropriate values of P_1, P_2, b_1, and b_2 for the various altitude bands above the 304.8-meter level are given in Table 5.3.22.

5.3.14.4 Design Flow or Gust Environments

If the design lifetime, T, is sufficiently small it is possible that the turbulence models described herein for horizontally and nearly horizontal flying vehicles will result in a vehicle design gust environment which is characterized by discrete gusts with amplitudes less that 9 m sec^{-1} for $dm/L > 10$ in Figure 5.3.32 above the 1-kilometer level. This is especially true for altitudes above the 18-kilometer level. In view of the wide spread acceptance of the 9 m sec^{-1} gust as a minimum gust amplitude for design studies in the aerospace community and in view of the increased uncertainty in gust data as altitude increases it is recommended that a floor be established on gust environments for altitudes above the 1-kilometer level such that the least permissible value of σ shall be 3.4 m sec^{-1} above the 1-kilometer level.

5.3.15 Discrete Gust Model - Horizontally Flying Vehicles

Often it is useful for the engineer to use discrete gusts in load and flight control system calculations of horizontally flying vehicles. The discrete gust is defined as follows:

$$V_d = 0, \quad x < 0$$

$$V_d = \frac{V_m}{2}\left(1 - \cos\frac{\pi x}{d_m}\right), \quad 0 \le x \le 2d_m$$

$$V_d = 0, \quad x > 2d_m ,$$

where x is distance and V_m is maximum velocity of the gust which occurs at position $x = d_m$ in the gust. To apply the model, the engineer specifies several values of the gust half-width d_m, so as to cover the range of frequencies of the system to be analyzed. To calculate the gust parameter V_m one enters Figure 5.3.32 with d_m/L and reads out V_m/σ. Figure 5.3.32 is based on the Dryden spectrum of turbulence. Accordingly, the procedures outlined in subsections 5.3.14.2 and 5.3.14.3 can be used for the specification of the σ's and L's to determine the gust magnitude V_m from Figure 5.3.32. In the boundary layer, three values of V_m will occur at each altitude, one for each component of turbulence. In the free atmosphere the longitudinal, lateral, and verticle values of V_m are equal at each altitude. In general both the continuous random gust model (sections 5.3.13 and 5.3.14) and the discrete gust model are often used to calculate vehicle responses with the procedure producing the larger response being used for design.

5.3.16 Flight Regimes For Use of Horizontal and Vertical Turbulence Models (Spectra and Discrete Gusts)

Sections 5.3.8, 5.3.13, and 5.3.15 contain turbulence (spectra and discrete gusts) models for response calculations of vertically ascending and horizontally flying aerospace vehciles.

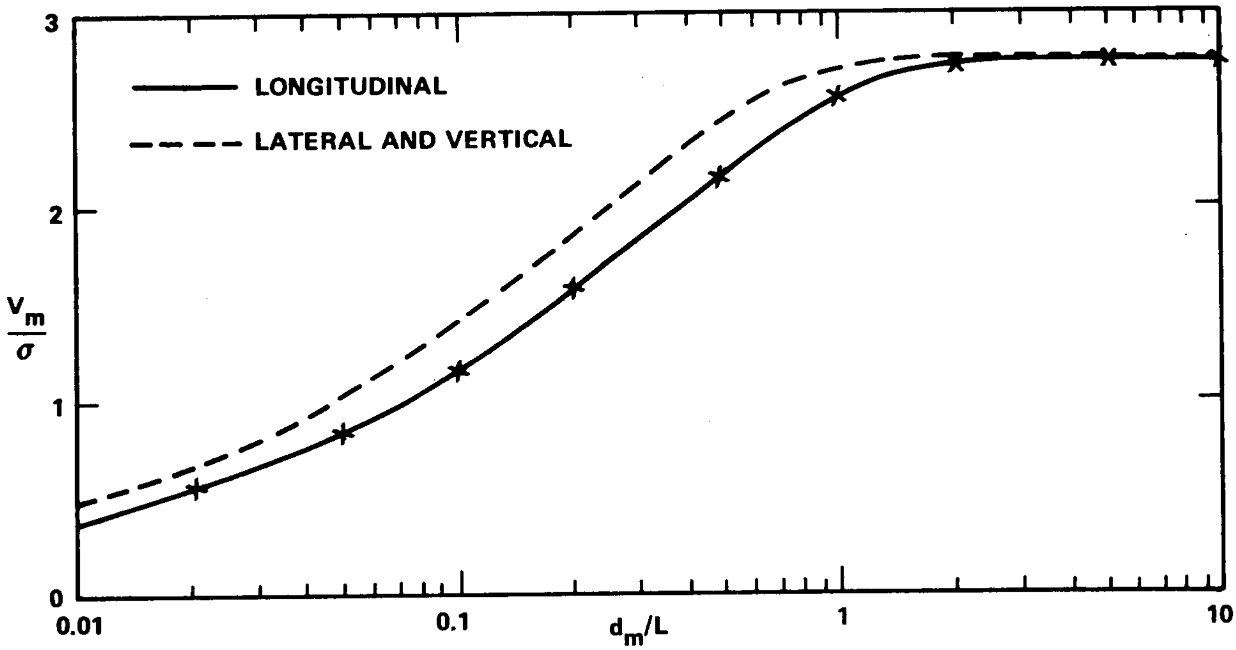

FIGURE 5.3.32. NONDIMENSIONAL DISCRETE GUST MAGNITUDE V_m/σ AS A FUNCTION OF NONDIMENSIONAL GUST HALF-WIDTH

The turbulence model for the horizontally flying vehicles was derived from turbulence data gathered with airplanes. The turbulence model for the vertically ascending or descending vehicles was derived from wind profile measurements made with vertically ascending Jimsphere ballons and smoke trails. In many instances aerospace vehicles neither fly in a pure horizontal flight mode nor ascend or descend in a strictly vertical flight path. At this time there does not appear to be a consistent way of combining the turbulence models for horizontal and vertical flight so as to be applicable to the design of aerospace vehicles with other than near horizontal or vertical flight paths without being unduly complicated or overly conservative. In addition, the unavailability of a sufficient large data sample of turbulence measurements in three dimensions precludes the development of such a combined model.

Accordingly, in lieu of the availability of a combined turbulence model and for the sake of engineering simplicity the turbulence model in section 5.3.8 should be applied to ascending and descending aerospace vehicles when the smallest angle between the flight path and the local vertical is less than or equal to 30 degrees. Similarly, the turbulence model in Sections 5.3.13 and 5.3.15 should be applied to aerospace vehicles when the smallest angle between the flight path and the local horizontal is less than or equal to 30 degrees. In the remaining flight path region between 30 degrees from the local vertical and 30 degrees from the local horizontal, both turbulence models should be independently applied and the most adverse responses used in the design.

5. 4 Mission Analysis, Prelaunch Monitoring, and Flight Evaluation

Wind information is useful in the following three general cases of mission analysis:

a. Mission Planning. Since this activity will normally take place well in advance of the mission, the statistical attributes of the wind are used.

b. Prelaunch Operations. Although wind statistics are useful at the beginning of this period, the emphasis is placed upon forecasting and wind monitoring.

c. Postflight Evaluation. The effect of the observed winds on the flight is analyzed.

5. 4. 1 Mission Planning

From wind climatology, the optimum time (month and time of day) and place to conduct the operation can be identified (Ref. 5. 39). Missions with severe wind constraints may have such a low probability of success that the risk is unacceptable. Feasibility studies based upon wind statistics can identify these problem areas and answer questions such as: "Is the mission feasible as planned?" and "If the probable risk of mission delay or failure is unacceptably high, can it be reduced by rescheduling to a lighter wind period?"

The following examples are given to illustrate the use of some of the many wind statistics available to the mission planner.

If it is necessary to remove the wind loads damper from a large launch vehicle for a number of hours and this operation must be scheduled some days in advance, the well known diurnal ground wind variation should be considered for this problem. If, for example, 10. 3 m/sec (20 knots) were the critical wind speed, there is a 1-percent risk at 0600 EST, but a 13-percent risk at 1500 EST in July. Obviously the midday period in the summer should be avoided for this operation. Since these probability values apply to 1-hour exposure periods, it is important to recognize that the wind risk depends not only upon wind speed, but also upon exposure time. From Figure 5. 4. 1, the risk in percentage associated with 15. 4-m/sec (30-knot) wind at 10 meters in February at Cape Kennedy can be obtained for various exposure times. The upper curve shows the risk increasing from 1 percent for 1-hour exposure

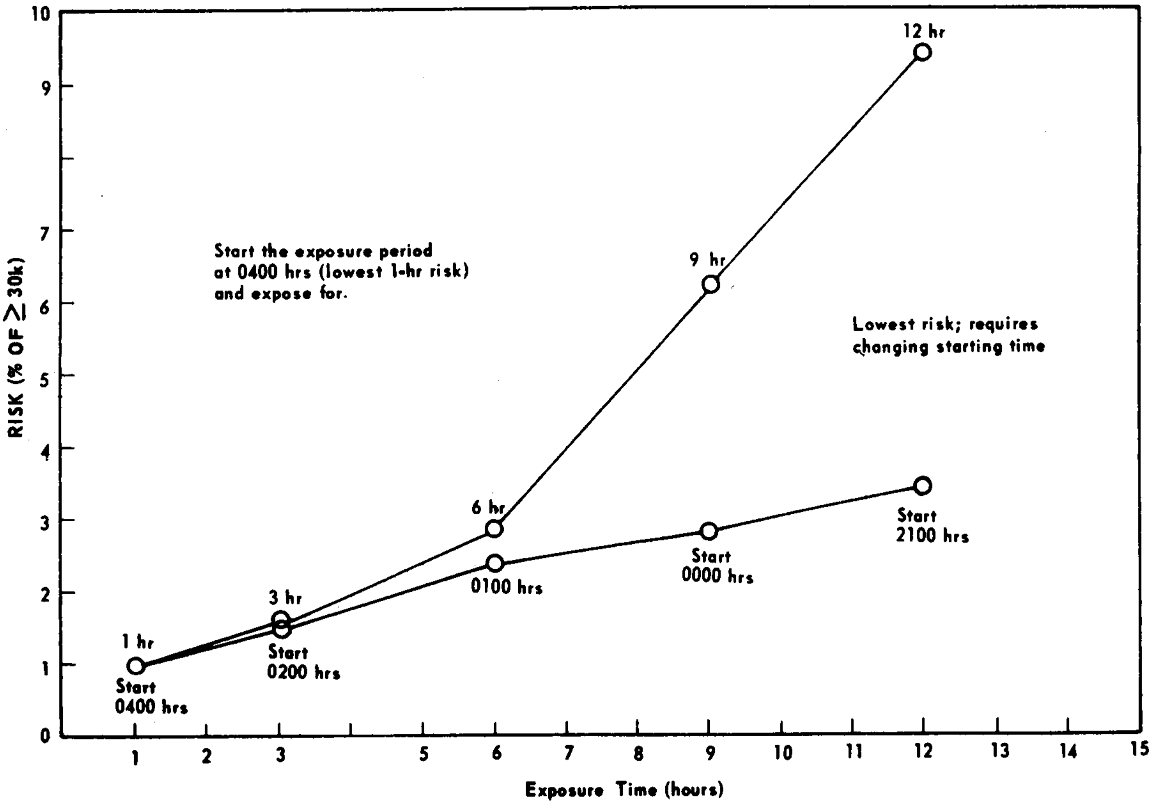

FIGURE 5. 4. 1 EXAMPLE OF WIND RISK FOR VARIOUS EXPOSURE TIMES

starting at 0400 EST to 9. 3 percent for 12-hour exposure starting at 0400 EST. In this case the exposure period extends through the high risk part of the day. The lower curve illustrates the minimum risk associated with each exposure period. The lowest risk, of course, can be realized if the starting times are changed to avoid the windy portion of the day. Although there is no space here for the tabulation, wind risk probabilities by month and starting hour for exposure periods from 1 hour to 365 days are available upon request.

When winds aloft are considered for mission planning purposes, again the first step might be to acquire general climatological information on the area of concern. From Figures 5. 4. 2 and 5. 4. 3 it is readily apparent that for Cape Kennedy most strong winds occur during winter in the 10- to 15-kilometer altitude region (this applies also to nearly all midlatitude locations). It is also true that these strong winds are usually westerly.

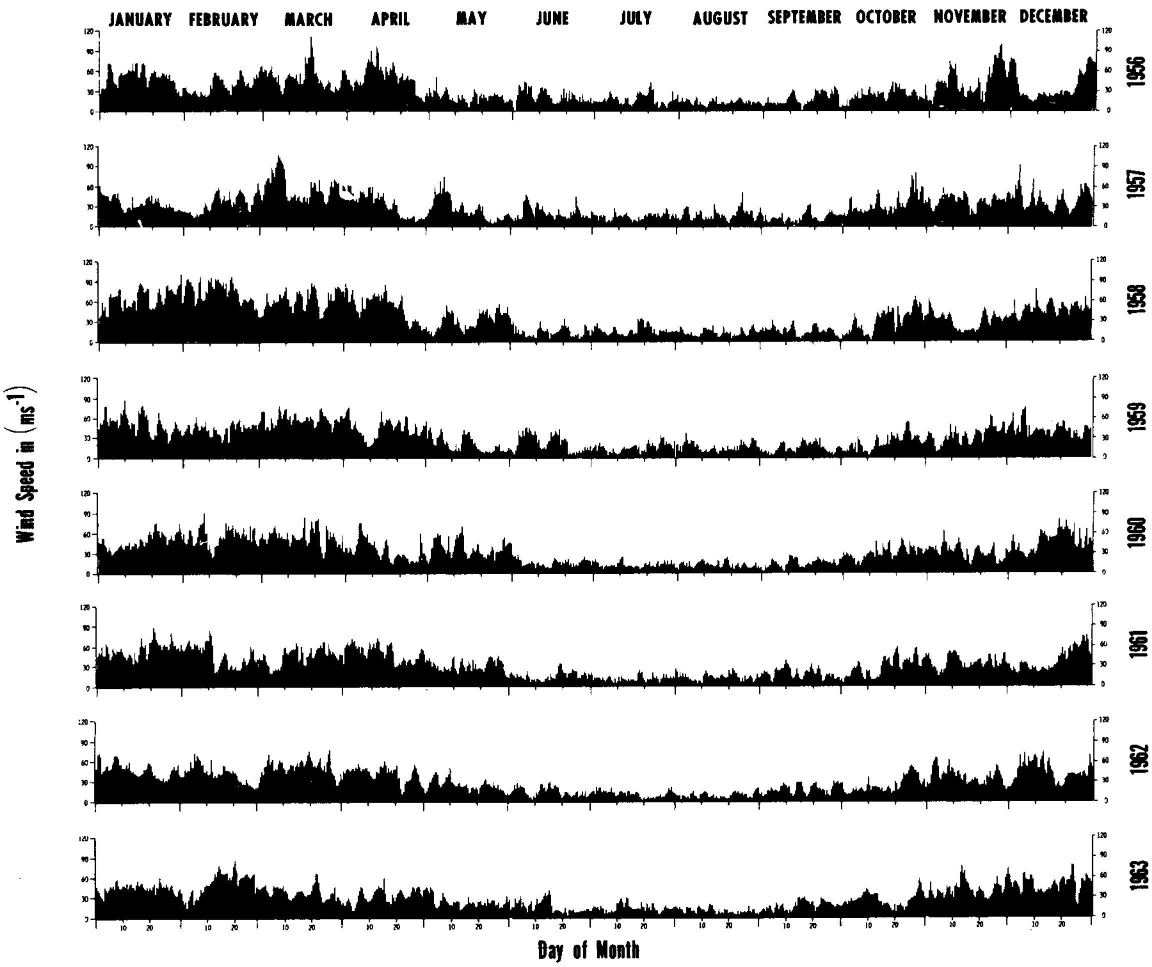

FIGURE 5.4.2 TWICE DAILY MAXIMUM WIND SPEED IN THE 10- TO 15-km LAYER AT CAPE KENNEDY

Next, the mission analyst might ask if a particular mission is feasible. If, for example, the flight is to take place in January and 10- to 15-kilometer altitude winds ≧ 50 m/sec are critical, the probability of favorable winds on any day in January is 0.496. With such a low probability of success, this mission may not be feasible. But, to continue the example, if it is necessary that continuously favorable winds exist for 3 days (perhaps for a dual launch) the probability of success will decrease to 0.256. Obviously an alternate mission schedule must be planned or else the scheduled space vehicle must be provided additional capability through redesign.

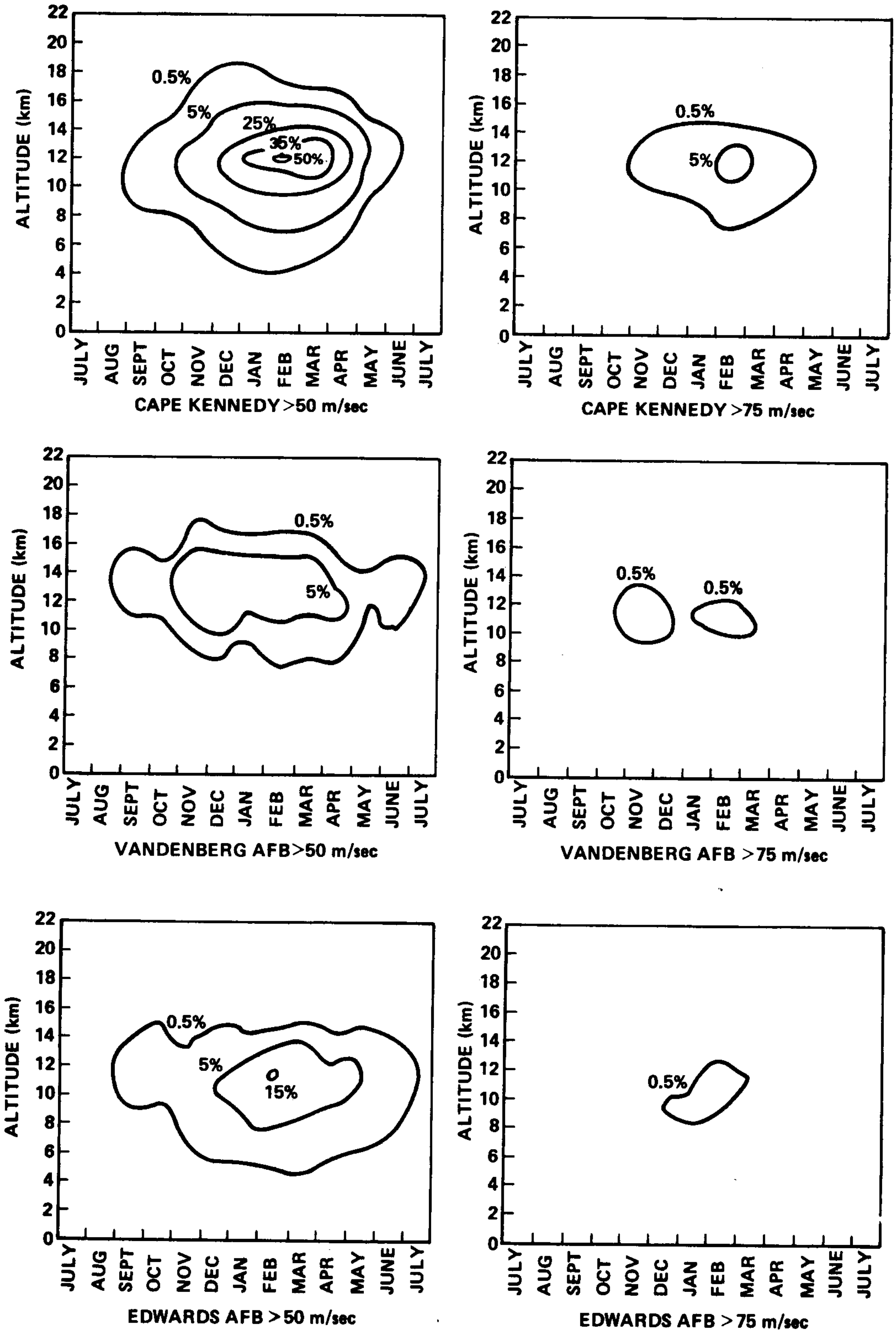

FIGURE 5. 4. 3 FREQUENCY OF SCALAR WIND SPEED EXCEEDING GIVEN WIND SPEED AS A FUNCTION OF ALTITUDE FOR STATIONS INDICATED

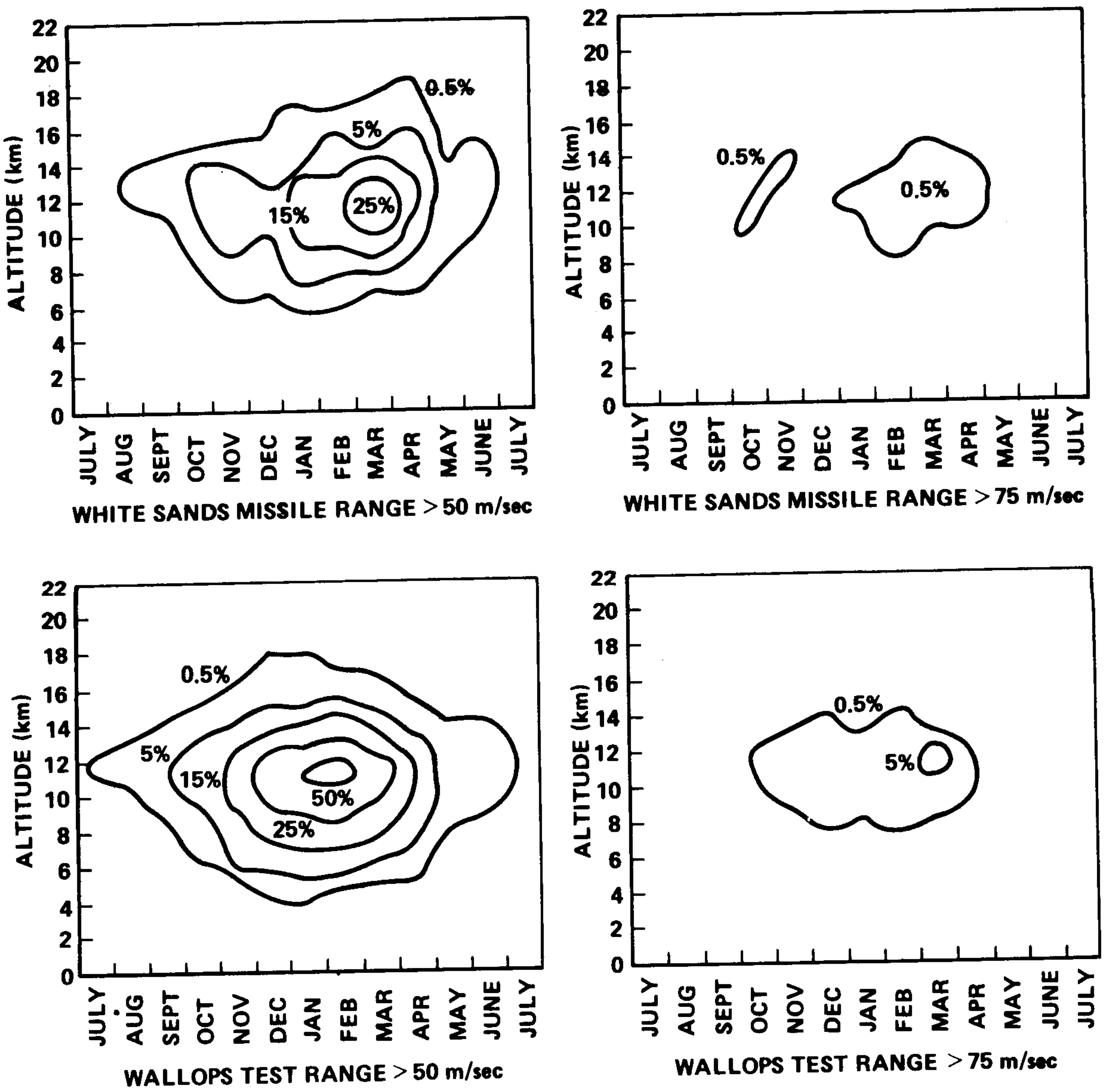

FIGURE 5.4.3 FREQUENCY OF SCALAR WIND SPEED EXCEEDING GIVEN WIND SPEED AS A FUNCTION OF ALTITUDE FOR STATIONS INDICATED (Concluded)

Perhaps the vehicle can remain on the pad in a state of near readiness awaiting launch for several days. In this case it would be desirable to know that the probability of occurrence of at least one favorable wind speed, for example, in a 4-day period is 0.813. If greater flexibility of operation is desired, one might require four favorable opportunities in 4 days. This probability is 0. 550. Now, if consecutive favorable opportunities are required, for example, four consecutive successes in eight periods, the probability of success will somewhat lower (0. 431).

The mission planner might also gain some useful information from the persistence of the winds aloft. The probability of winds < 50 m/sec on any day in January is 0. 496. But if a wind speed < 50 m/sec does occur, then the probability that the next observed wind 12 hours later would be < 50 m/sec is 0. 82, a rather dramatic change. Furthermore, if the wind continues below 50 m/sec for five observations, the probability that it will remain there for one more 12-hour period is 0. 92.

As the time of the operation approaches T-4 to T-1 days, the conditional probability statements assume a more significant role. At this point, as the winds will usually be monitored, the appropriate conditional probability value can be identified and used to greater advantage.

The above is intended to illustrate the type of analysis that can be accomplished to provide objective data for program decisions. This may best be accomplished by a close working relationship between the analyst and those concerned with the decision.

5. 4. 2 Prelaunch Wind Monitoring

Inflight winds constitute the major atmospheric forcing function in space vehicle and missile design and operations (Ref 5. 40). A frequency content of the wind profile near the bending mode frequencies or wind shear with the characteristics of a step input may exceed the vehicle's structural capabilities (especially on forward stations for the small scale variations of the wind profiles). Wind profiles with high speeds and shears exert high structural loads at all stations on a large space vehicle, and when the influences of bending dynamics are high, even a profile with low speeds and high shears can create large loads (Ref. 5. 41).

Because of the possibility of launch into unknown winds, operational missile systems must accept some inflight loss risk in exchange for a rapid-launch capability. But research and development missiles, and space vehicles in particular, cost so much that the overall success of a flight outweighs the consideration of launch delays caused by excessive inflight wind loads. If the exact wind profile could be known in advance, it would be a relatively simple task to decide upon the launch date and time. However, there is little hope of accurately forecasting the detailed wind profile very much into the future.

Over the years, these situations have increasingly put emphasis on prelaunch monitoring of inflight winds. Now, finally, prelaunch and profile determination techniques essentially preclude the risk of launching a space vehicle or research and development missile into an inflight wind condition that would cause it to fail.

Recent development and operational deployment of the FPS-16 Radar/Jimsphere system (Ref. 5.42) significantly minimizes vehicle failure risks when properly integrated into a flight simulation program. The Jimsphere sensor, when tracked with the FPS-16 or other radar with equal tracking capability, provides a very accurate "all weather" detailed wind profile measurement. FPS-16 radars are available at all national test ranges.

In general, the system provides a wind profile measurement from the surface to an altitude of 17 kilometers in slightly less than 1 hour, a vertical spatial frequency resolution of 1 cycle per 100 meters, and an rms error of about 0.5 m/sec or less for wind velocities averaged over 50-meter intervals. The resolution of these data permits calculating the structural loads associated with the first bending mode and generally the second mode of missiles and space vehicles during the critical, high dynamic pressure phase of flight. This provides better than an order-of-magnitude accuracy improvement over the conventional rawinsonde wind profile measuring system (Ref. 5.43).

By employing the appropriate data transmission resources, a detailed wind profile from the FPS-16 radar can be ready for input to the vehicle's flight simulation program within a few minutes after tracking of the Jimsphere. The flight simulation program provides flexibility relative to vehicle dynamics and other parameters in order to make maximum use of the detailed wind profiles.

If very critical wind conditions exist and the mission requirement dictates a maximum effort to launch with provision for last minute termination of the operation, then a contingency plan that will provide essentially real-time wind profile and flight simulation data may be employed. This is done while the Jimsphere balloon is still in flight.

An example of the FPS-16 Radar/Jimsphere system data appears in Figure 5.4.4 — the November 8 and 9, 1967, sequence observed during prelaunch activities for the first Apollo/Saturn-V test flight, AS-501. The persistence over a period of 1 hour of some small scale features in the wind profile structure, as well as the rather distinct changes that developed in the profiles over a period of a few hours, is evident.

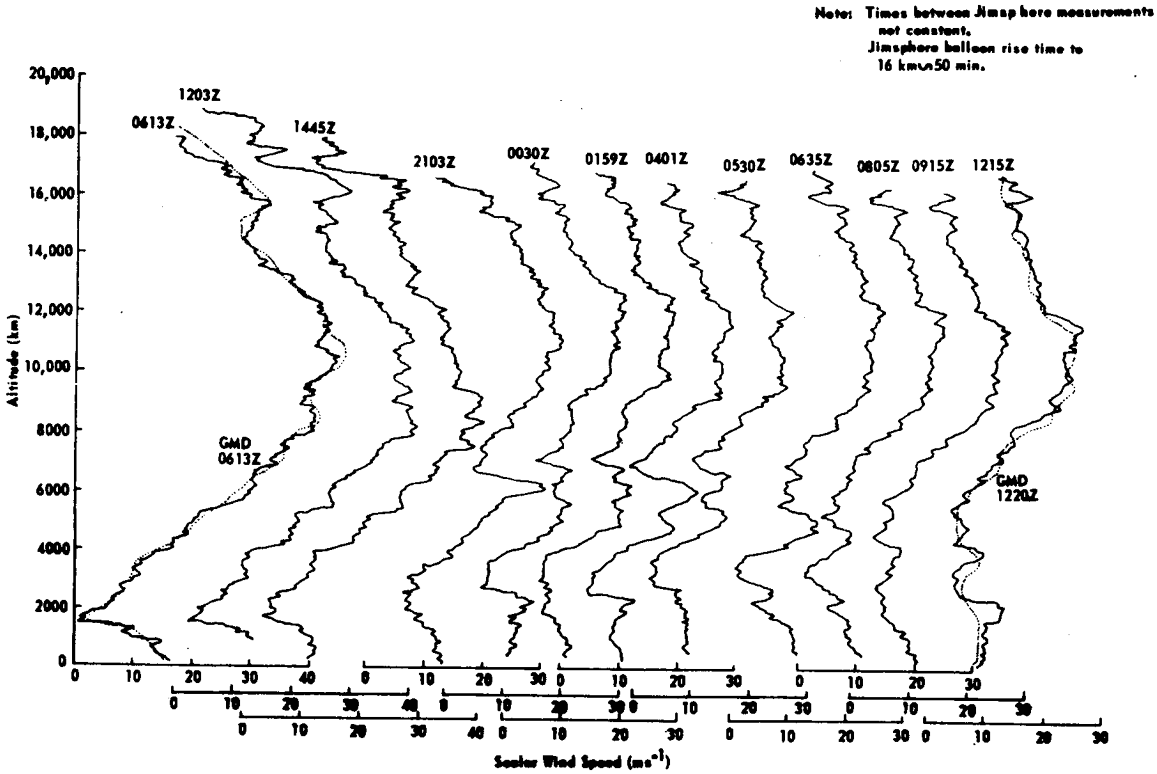

FIGURE 5. 4. 4 EXAMPLE OF THE FPS-16 RADAR/JIMSPHERE SYSTEM DATA, NOVEMBER 8-9, 1967

The FPS-16 Radar/Jimsphere system (Fig. 5. 4. 5) is routinely used in the prelaunch monitoring of NASA's Apollo/Saturn-IB and -V flights. The wind profile data are transmitted to the Johnson Space Center and Marshall Space Flight Center, and the flight simulation results are sent to the launch complex at Kennedy Space Center.

An FPS-16 Radar/Jimsphere operational measurement program capability exists at all the national test ranges to obtain detailed wind profile data for use in space vehicle and missile response studies, airplane turbulence analysis, atmospheric turbulence investigations, and mesometeorological studies. Sequential measurements similar to the Saturn-V data shown here — of eight to ten Jimsphere wind profiles approximately 1 hour apart — are currently being made on at least 1 day per month for each location. Single profile measurements are also made daily at Cape Kennedy.

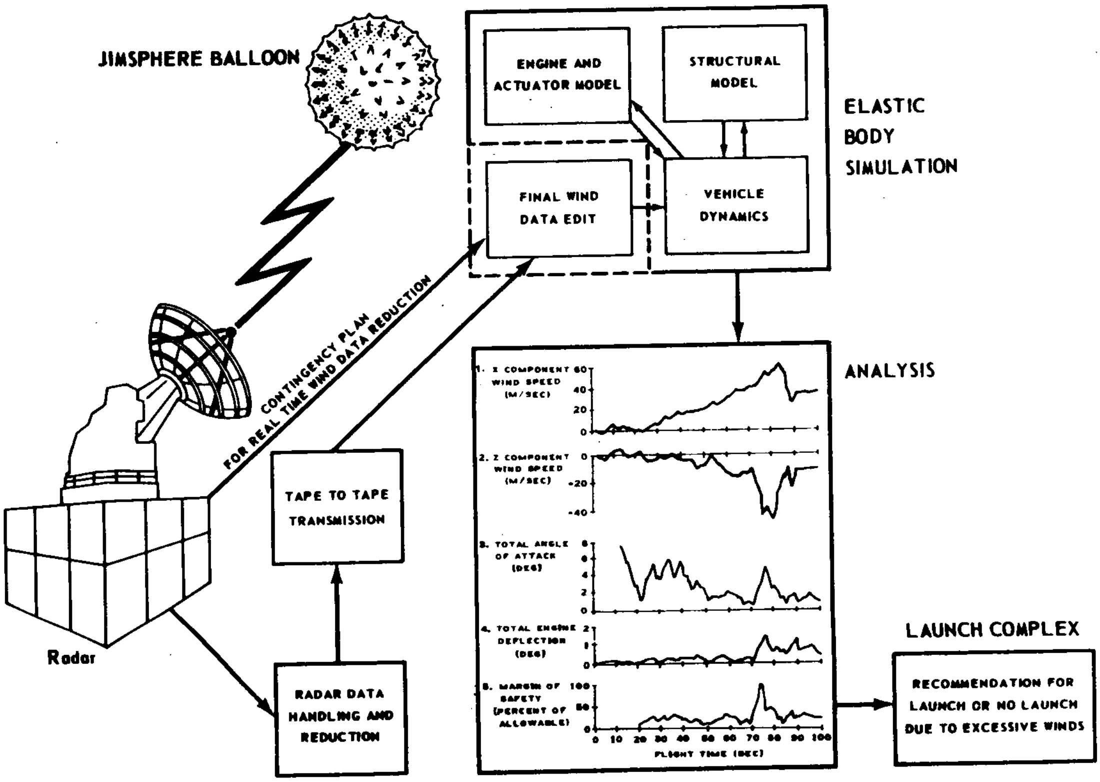

FIGURE 5.4.5 OPERATION OF THE FPS-16 RADAR/JIMSPHERE SYSTEM

5.4.3 Post-Flight Evaluation

5.4.3.1 Introduction

Because of the variable effects of the atmosphere upon a large space vehicle at launch and during flight, various meteorological parameters are measured at the time of each space vehicle launch, including wind and thermodynamic data at the earth's surface and up to an altitude of at least 50 kilometers. To make the data available, meteorological tapes are prepared, presentations are made at flight evaluation meetings, memoranda of data tabulations are prepared and distributed, and a summary is written for the final vehicle flight evaluation report. Reference 5.44 for Apollo/Saturn-503 is an example of one of the reports with an atmospheric section.

5.4.3.2 Meteorological Tapes

Shortly after the launch of each space vehicle, under the cognizance of the Marshall Space Flight Center, preliminary meteorological tape is prepared by combining the FPS-16 Radar/Jimsphere wind profile data and the rawinsonde wind profile and thermodynamic data (temperature, pressure, and humidity) observed as near the vehicle launch time as feasible. This is done under the supervision of the Marshall Space Flight Center's Aerospace Environment Division. The preliminary meteorological tape is normally available within 12 hours after launch time and provides data to about 35 kilometers. The final meteorological tape is prepared with the addition of rocketsonde wind and thermodynamic data extending the data to at least 50 kilometers and is available for use about 3 days after launch.

In the two meteorological data tapes (preliminary and final), thermodynamic data above the measured data are given by Patrick Reference Atmosphere values (Ref 5. 45). To prevent unnatural jumps in the data when the two types are merged, the data are carefully examined to pick the best altitude for the merging.

The meteorological data tapes are made available to all government and contractor groups for their use in the space vehicle launch and flight evaluation. This provides a consistent set of data for all evaluation studies and ensures the best available information of the state of the atmosphere.

Twenty-one parameters of data are included in the meteorological data tape at 25-meter increments of altitude[17] in Table 5. 4. 1.

5. 4. 3. 3 Presentations at Flight Evaluation Working Group Meetings

Unless the space vehicle performance was bad or the magnitude of some atmospheric parameters was near extremes at launch or during flight, only two presentations are made at the flight evaluation meetings on the atmospheric launch environment.

The first presentation is given at the "quick look" meeting normally held on the day following launch. At this meeting, preliminary values of the surface weather conditions (temperature, pressure, dew point or relative humidity, visibility, cloudiness, and launch pad wind speed and direction) are given, and plots of the upper wind speeds, direction, and components are shown up to the highest altitude of the available data. Any unusual features of the data are discussed in detail.

At the "first general" flight evaluation meeting, the final upper wind speeds and component graphs are shown for all the data used in the meteorological data tape.

17. Altitude increments of 25 meters were chosen to provide for maximum engineering value and for use of the available atmospheric data and do not necessarily represent the attainable frequency response of the measurements.

TABLE 5.4.1 FORMAT OF METEOROLOGICAL TAPE

First Record: Identification			
Word	Symbol	Parameter	Units
1	Y_S	Altitude (geometric) ($0=Y_S=700,000$) H=25	m
2	T	Temperature	°K
3	P	Pressure	mb
4	W	Wind Speed	m/sec
5	W_D	Wind Direction	deg
6	U/100	Relative Humidity (U is percent)	(10^{-2}) %
7	E	Water Vapor Pressure	mb
8	ρ	Density	kg/m^3
9	P'	Pressure	$newton/cm^2$
10	$V_S=C_S$	Velocity of Sound	m/sec
11	N_o	Optical Index of Refraction	unitless
12	N_e	Electomagnetic Index of Refraction	unitless
13	W_x	Pitch Component of Wind Velocity	m/sec
14	W_z	Yaw Component of Wind Velocity	m/sec
15	W_{w-e}	Zonal Component of Wind Velocity	m/sec
16	W_{s-n}	Meridional Component of Wind Velocity	m/sec
17	ρ	Density times Gravity	$newton/m^3$
18	μ	Coefficient of Viscosity	$newton\ sec/m^2$
19	T	Temperature	°C
20	S_{x250}	Pitch Component Wind Shear	sec^{-1}
21	S_{z250}	Yaw Component Wind Shear	sec^{-1}

Surface wind speeds and directions are measured and recorded at several locations and heights above the launch pad, starting several hours before launch time. Detailed tabulations are made from the various measuring locations and are distributed by memoranda for flight evaluation purposes.

5.4.3.4 Atmospheric Data Section for Final Vehicle Launch Report

The results of the flight evaluation are presented in a final vehicle launch report. A section in this report gives the information on the atmospheric environment at launch time. Records are maintained on the atmospheric parameters for MSFC sponsored vehicle test flights conducted at Kennedy Space Center, Florida. Requests for summaries of these atmospheric data, or related questions on specific topics, should be directed to the Aerospace Environment Division, NASA-Marshall Space Flight Center, Alabama 35812.

REFERENCES

5.1 Scoggins, J. R.; Vaughan, W. W.; and Smith, O. E., "Role of Applied Meteorology in the Development of Large Space Vehicles." Bulletin of the American Meteorological Society, vol. 44, no. 3, Mar. 1963, pp. 123-127.

5.2 Scoggins, J. R.; and Vaughan, W. W., "Problems of Atmospheric Wind Inputs for Missile and Space Vehicle Design," Journal of Spacecraft and Rockets, vol. 1, no. 2, Mar. 1964, pp. 181-184.

5.3 Vaughan, W. W.; Smith, O. E.; and Canfield, Norman L., "Progress in Circumventing Limitations of Upper Wind Records." Journal of Applied Meteorology, vol. 5, no. 3, June 1966, pp. 301-303.

5.4 Fletcher, Robert D., "Wind Information for Design of Aerospace Vehicles," Astronautics and Aeronautics, vol. 3, no. 5, May 1965, pp. 54-56.

5.5 "Meeting on Ground Wind Load Problems in Relation to Launch Vehicles (a compilation of papers presented at the NASA Langley Research Center, June 7-8, 1966)." NASA TM X-57779, NASA-Langley Research Center, Virginia, June 1966.

5.6 Frost, W., Mans, J. R., and Simpson, W. R., "A Boundary Layer Approach to the Analysis of Atmospheric Motion Over a Surface Obstruction," NASA CR-2182, NASA-George C. Marshall Space Flight Center, Marshall Space Flight Center, Ala., January 1973.

5.7 Smith, O. E.; Falls, L. W.; and Brown, S. C., "Research Achievements Review," Vol. II, Report No. 10, "Terrestrial and Space Environment Research at MSFC," NASA TM X-53706, NASA-George C. Marshall Space Flight Center, Marshall Space Flight Center, Alabama, 1967.

5.8 Fichtl, G. H., McVehil, G. E., "Longitudinal and Lateral Spectra of Turbulence in the Atmospheric Boundary Layer at the Kennedy Space Center," Journal of Applied Meteorology, vol. 9, no. 1, Feb. 1970, pp. 51-63.

5.9 Blackadar, Alfred K.; et al., "Investigation of the Turbulent Wind Field Below 150M Altitude at the Eastern Test Range," NASA CR-1410, NASA-George C. Marshall Space Flight Center, Marshall Space Flight Center, Alabama, Aug. 1969.

REFERENCES (Continued)

5.10 McVehil, G. E.; and Camnitz, H. G., "Ground Wind Characteristics at Kennedy Space Center," NASA CR-1418, NASA-George C. Marshall Space Flight Center, Marshall Space Flight Center, Alabama, Sept. 1969.

5.11 Hathorn, J. W., "Wind Tower Influence Study (for NASA's 150-meter Meteorological Tower at Kennedy Space Center, Florida)." NASA CR-61242, NASA-George C. Marshall Space Flight Center, Marshall Space Flight Center, Alabama, Sept. 23, 1968.

5.12 Slade, David H., (ed), "Meteorology and Atomic Energy – 1968," TID-24190, U. S. Atomic Energy Commission Division of Technical Information.

5.13 Thom, H. C. S., "Distribution of Extreme Winds in the United States," Journal of the Structural Division Proceedings of the American Society of Civil Engineers, vol. 86, Apr. 1960, pp. 11-24.

5.14 Scoggins, James R.; and Vaughan, William W., "Problems of Atmospheric Wind Inputs from Missile and Space Vehicle Design," Journal of Spacecraft and Rockets, vol. 1, no. 2, Mar. 1964, pp.181-184.

5.15 Smith, J. W.; and Vaughan, W. W., "Monthly and Annual Wind Distribution as a Function of Altitude for Patrick Air Force Base, Canaveral, Florida," NASA TN D-610, July 1961.

5.16 Smith, J. W., "Monthly and Annual Wind Distributions as a Function of Altitude for Santa Monica, California (Pacific Missile Range)," NASA TN D-1569, Jan. 1963.

5.17 Weaver, William L.; Swanson, Andrew G.; and Spurling, John F., "Statistical Wind Distribution Data for Use at NASA-Wallops Station," NASA TN D-1249, July 1962.

5.18 IRIG Document No. 104-63, Range Reference Atmosphere Documents published by Secretariat, Range Commander's Council, White Sands Missile Range, New Mexico.

a. The following reference atmospheres have been published:

(1) Atlantic Missile Range Reference Atmosphere for Cape Kennedy, Florida (Part I), 1963.

REFERENCES (Continued)

(2) White Sands Missile Range Reference Atmosphere (Part I), 1964.

(3) Fort Churchill Missile Range Reference Atmosphere for Fort Churchill, Canada (Part I), 1964.

(4) Pacific Missile Range Reference Atmosphere for Eniwetok, Marshall Islands (Part I), 1964.

(5) Fort Greely Missile Range Reference Atmosphere (Part I), 1964.

(6) Eglin Gulf Test Range Reference Atmosphere for Eglin AFB, Florida (Part I), 1965.

(7) Pacific Missile Range Reference Atmosphere for Point Arguello, California (Part I), 1965.

(8) Wallops Island Test Range Reference Atmosphere (Part I), 1965.

(9) Eastern Test Range Reference Atmosphere for Ascension Island, South Atlantic (Part I), 1966.

(10) Lihue, Kauai, Hawaii Reference Atmosphere (Part I), 1970.

(11) Johnson Island Test Site Reference Atmosphere (Part I), 1970.

(12) Edwards Air Force Base Reference Atmosphere (Part I), 1972.

(13) Cape Kennedy, Florida Reference Atmosphere (Part II), 1971.

(14) White Sands Missile Range Reference Atmosphere (Part II), 1971.

(15) Wallops Island Test Range Reference Atmosphere (Part II), 1971.

(16) Fort Greely Missile Range Reference Atmosphere (Part II), 1971.

REFERENCES (Continued)

5.19 Daniels, Glenn E.; and Smith, O. E., "Directional Wind Component Frequency Envelopes, Santa Monica, California (Pacific Missile Range)," NASA TM X-53021, NASA-George C. Marshall Space Flight Center, Marshall Space Flight Center, Alabama, Mar. 9, 1964.

5.20 Daniels, Glenn E.; and Smith, O. E., "Directional Wind Component Frequency Envelopes, Cape Kennedy, Florida, Atlantic Missile Range." NASA TM X-53009, NASA-George C. Marshall Space Flight Center, Marshall Space Flight Center, Alabama, Feb. 21, 1964.

5.21 Henry, Robert M., "A Statistical Model for Synthetic Wind Profiles for Aerospace Vehicle Design and Launching Criteria." NASA TN D-1813, 1963.

5.22 Bieber, Richard E., "Missile Structural Loads by Non-Stationary Statistical Methods." Technical Report No. LMSD 49703, Lockheed Missile and Space Division, S

5.23 Vaughan, William W., "Interlevel and Intralevel Correlations of Wind Components for Six Georgraphical Locations." NASA TN D-561, Dec. 1960.

5.24 Daniels, Glenn E.; and Smith, Orvel E., "Scalar and Component Wind Correlations Between Altitude Levels for Cape Kennedy, Florida, and Santa Monica, California," NASA TN D-3815, Apr. 1968.

5.25 Cochrane, James A.; Henry, Robert M.; and Weaver, William L., "Revised Upper Air Wind Data for Wallops Island Based on Serially Completed Data for the Years 1956 to 1964." NASA TN D-4570, NASA – Langley Research Center, Langley Station, Hampton, Virginia, May 1968.

5.26 Truppi, Lawrence E., "Probabilities of Zero Wind Shear Phenomena Based on Rawinsonde Data Records." NASA TM X-53452, NASA-George C. Marshall Space Flight Center, Marshall Space Flight Center, Alabama, Apr. 26, 1966.

5.27 Camp, Dennis W.; and Susko, Michael, "Percentage Levels of Wind Speed Differences Computed by Using Rawinsonde Wind Profile Data from Cape Kennedy, Florida," NASA TM X-53461, NASA-George C. Marshall Space Flight Center, Marshall Space Flight Center, Alabama, May 12, 1966.

REFERENCES (Continued)

5.28 Camp, Dennis W.; and Fox, Patricia A., "Percentage Levels of Wind Speed Differences Computed by Using Rawinsonde Wind Profile Data from Santa Monica, California." NASA TM X-53428, NASA-George C. Marshall Space Flight Center, Marshall Space Flight Center, Alabama, Oct. 21, 1966.

5.29 Fichtl, G. H., "Small-Scale Wind Shear Definition for Aerospace Vehicle Design." Journal of Spacecraft and Rockets, vol. 9, no. 2, Feb. 1972, pp. 79-83.

5.30 Salmela, Henry A.; and Sissenvine, Norman, "Distribution of ROBIN Sensed Wind Shears at 30 to 70 Kilometers." AFCRL-69-0053, Air Force Cambridge Research Laboratories, L. G. Hanscom Field, Bedford, Massachusetts, Feb. 1969.

5.31 Fichtl, G. H.; Camp, D. W.; and Vaughan, W. W., "Detailed Wind and Temperature Profiles." Clear Air Turbulence and Its Detection, Edited by Yih-Hc Pao and Arnold Goldburg, Plenum Press, New York, 1969, pp. 308-333.

5.32 Scoggins, James R., "An Evaluation of Detail Wind Data as Measured by the FPS-16 Radar/Jimsphere Ballon Technique." NASA TN D-1572, NASA-George C. Marshall Space Flight Center, Marshall Space Flight Center, Alabama, May 1963.

5.33 Susko, Michael; and Vaughan, William W., "Accuracy of Wind Data Obtained by Tracking a Jimsphere Wind Sensor Simultaneously with Two FPS-16 Radars." NASA TM X-53752, NASA-George C. Marshall Space Flight Center, Marshall Space Flight Center, Alabama, July 1968.

5.34 "MSFC Jimsphere Wind Data Tape for Design Verification." Office Memorandum S&E-AERO-YA-98-71, NASA-George C. Marshall Space Flight Center, Marshall Space Flight Center, Alabama, April 16, 1971.

5.35 Scoggins, James R.; and Susko, Michael, "FPS-16 Radar/Jimsphere Wind Data Measured at the Eastern Test Range." NASA TM X-53290, NASA-George C. Marshall Space Flight Center, Marshall Space Flight Center, Alabama, July 1965.

REFERENCES (Continued)

5.36 Manning, James C.; Henry, Robert M.; and Miller, Robert W., "Wind Velocity Profiles Measured by the Smoke-Trail Method at the Eastern Test Range, 1962." NASA TN D-3289, NASA – Langley Research Center, Langley Station, Hampton, Virginia, Mar. 1966.

5.37 Miller, Robert W.; Manning, James C.; and Henry, Robert M., "Wind Velocity Profiles by the Smoke-Trail Method at the Eastern Test Range, 1963." NASA TN D-4880, NASA – Langley Research Center, Langley Station, Hampton, Virginia, Dec. 1968.

5.38 Hoblit, F. M.; Neil, Paul; Shelton, Jerry D.; and Ashford, Francis E., "Development of a Power Spectral Gust Design Procedure." FAA-ADA-53, Federal Aviation Agency, Washington, D. C., AD 651152, Jan. 1966.

5.39 Henry, Robert M.; and Cochrane, James A., "Wind Loads on Vertically Launched Vehicles at Various Georgraphic Locations and Launch Altitudes." NASA TN D-3271, NASA, Washington, D. C., Feb. 1966.

5.40 Fletcher, Robert D., "Wind Information for Design of Aerospace Vehicles." Astronautics and Aeronautics, May 1965, pp. 54-56.

5.41 Ryan, Robert S.; Scoggins, James R.; and King, Alberta W., "Use of Wind Shears in the Design of Aerospace Vehicles." Journal of Spacecraft and Rockets, vol. 4, no. 11, Nov. 1967, pp. 1526-1532.

5.42 Vaughan, William W., "New Wind Monitoring System Protects R and D Launches." Journal of Astronautics and Aeronautics, Dec. 1968, pp. 41-43.

5.43 Scoggins, J. E., "Sphere Behavior and the Measurement of Wind Profiles." NASA TN D-3994, NASA, Washington, D. C., June 1967.

5.44 "Saturn V Launch Vehicle Flight Evaluation Report – AS-503, Apollo 8 Mission." MPR-SAT-FE-69-1, Saturn V Flight Evaluation Working Group, NASA-George C. Marshall Space Flight Center, Marshall Space Flight Center, Alabama, Feb. 20, 1969.

5.45 Smith, Orvel E.; and Weidner, Don K., "A Reference Atmosphere for Patrick AFB, Florida, Annual (1963 Revision). NASA TM X-53139, NASA-George C. Marshall Space Flight Center, Marshall Space Flight Center, Alabama, Sept. 23, 1964.

REFERENCES (Continued)

5.46 Lee, Russel F.; Goodge, Grant W.; and Crutcher, H. L., "Surface Climatological Information for Twelve Selected Stations for Reentry Vehicles," NASA CR-61319, Marshall Space Flight Center, Alabama, 1970.

5.47 Goodge, G. W., Bilton, T. H.; and Quinlin, F. T., "Surface Climatological Information for Twenty Selected Stations for Reentry Vehicles," NASA CR-61342, Marshall Space Flight Center, Alabama, 1971.

5.48 Fichtl, G. H., Kaufman, J. W., and Vaughan W. W., "Characteristics of Atmospheric Turbulence as Related to Wind Loads on Tall Structures." Journal of Spacecraft and Rockets, vol. 6, no. 12, Dec. 1969, pp. 1396-1403.

5.49 Carter, E. A.; and Schuknecht, L. A., "Peak Wind Statistics Associated with Thunderstorms at Cape Kennedy, Florida." NASA CR-61304, NASA-George C. Marshall Space Flight Center, Marshall Space Flight Center, Alabama, August 1969.

5.50 Van der Hoven, Isaac, "Power Spectrum of Horizontal Wind Speed in the Frequency Range from 0.0007 to 900 Cycles Per Hour." Journal of Meteorology, vol. 14, no. 2, Apr. 1957, pp. 160-164.

5.51 Falls, L. W., and Brown, S. C., "Optimum Runway Orientation Relative to Crosswinds." NASA TN D-6930, September 1972.

5.52 Falls, L. W., and Crutcher, H. L., "Determination of Statistics for any Rotation of Axes of a Bivariate Normal Elliptical Distribution." NASA TM X-64595, May 1971.

5.53 Hold, A., "Statistical Theory with Engineering Applications." John Wileyand Sons, Inc., New York, 1962.

5.54 Brown, S. C., "Cape Kennedy Wind Component Statistics Monthly and Annual Reference Periods for all Flight Azimuths from 0 to 70 km Altitude." NASA TM X-53956, NASA-George C. Marshall Space Flight Center, Marshall Space Flight Center, Alabama, Oct. 9, 1969.

5.55 Falls, L. W., "Normal Probabilities for Cape Kennedy Wind Components — Monthly Reference Periods for all Flight Azimuths — Altitudes 0 to 70 km." NASA-George C. Marshall Space Flight Center, Marshall Space Flight Center, Ala., April 16, 1973.

REFERENCES (Continued)

5.56 Buell, C. E., "Correlation Functions for Wind and Geopotential on Isobaric Surfaces." Journal of Applied Meteorology, vol. II, no. 1, Feb. 1972, pp. 5159.

5.57 Buell, C. E., "Variability of Wind with Distance and Time on an Isobaric Surface." Journal of Applied Meteorology, vol. II, no. 7, Oct. 1972, pp. 1085-1091.

5.58 Susko, Michael, and Kaufman, John W., "Monthly and Annual Percentage Levels of Wind Speed Differences Computed by Using FPS-16 Radar/Jimsphere Wind Profile Data from Cape Kennedy, Florida," NASA TM X-64712, NASA-George C. Marshall Space Flight Center, Marshall Space Flight Center, Ala. 35812, Jan. 4, 1973.

5.59 Turner, R. E., Johnson, D. C., and Gilchrist, L. P., "High Altitude Meteorological Rocket Wind Measuring Systems and Results Taken at Cape Kennedy, Florida." NASA TM X-64578, NASA-George C. Marshall Space Flight Center, Marshall Space Flight Center, Ala. 35812, March 30, 1971.

5.60 Brown, S. C., "Cape Kennedy Wind Component Statistics Monthly and Annual Reference Periods for all Flight Azimuths from 0 to 70 km Altitude," NASA TM X-53956, NASA-George C. Marshall Space Flight Center, Marshall Space Flight Center, Ala.35812, October 9, 1969.

5.61 Smith, J. W., "The Genesis of Sudden Stratospheric Warmings and Quasi-Biennial Cycles." NASA TN D-6522, NASA-George C. Marshall Space Flight Center, Marshall Space Flight Center, Ala. 35812, July 1972.

5.62 Chalk, C. R., et al., "Background Information and User Guide for MIL-F-8785B (ASG), 'Military Specification – Flying Qualities of Piloted Airplanes,'" AFFDL-TR-69-72, Air Force Flight Dynamics Laboratory, Air Force Systems Command, Wright-Patterson Air Force Base, Ohio, August 1969.

5.63 Fichtl, G. H., "Problems in the Simulation of Atmospheric Boundary Layer Flows." Presented at the AGARD Flight Mechanics Panel Symposium, "Flight in Turbulence,: at Woburn Abbey, New Bedford, Bedfordshire, United Kingdom, 14-17 May 1973. To be published as an AGARD report.

REFERENCES (Concluded)

5.64 Dutton, J. A., "Broadening Horizons in Prediction of the Effects of Atmospheric Turbulence on Aeronautical Systems." AIAA Selected Reprints Series/Vol. XIII, The Earth's Atmosphere, W. W. Vaughan and L. L. DeVries, Editors. Published by the American Institute of Aeronautics and Astronautics, New York.

5.65 Fichtl, G. H., "Wind Shear Near the Ground and Aircraft Operations." Journal of Spacecraft and Rockets, vol. 9, no. 11, Nov. 1972, pp. 765-770.

5.66 Fichtl, G. H., "Probability Distribution of Vertical Longitudinal Shear Fluctuations." Journal of Applied Meteorology, vol. 11, no. 6, Sept. 1972, pp. 918-925.

5.67 Fichtl, G. H., "Standard Deviation of Vertical Two-Point Longitudinal Velocity Differences in the Atmospheric Boundary Layer." Boundary-Layer Meteorology, vol. 2, 1971, pp. 137-151.

N74-16298

SECTION VI. ABRASION

By

Glenn E. Daniels

6.1 Introduction.

Particles carried by wind will remove paint from exposed surfaces or scratch, abrade, or erode them, and pit transparent surfaces. When the wind velocities are low or moderate, damage can occur whenever the particle hardness is equal to or greater than the exposed surface. When the speed of an object with relation to atmospheric particles is high, erosion will occur even when the particles have a hardness less than the exposed surface. A space vehicle and its associated facilities should be designed to either withstand or be protected from the conditions described for the geographic area of application.

The penetration of sand and dust into moving parts (bearings, gears, etc.) can result in abnormal wear and failure. Large sand and dust particles may be suspended in the atmosphere during periods of high winds and low humidities (under 50 percent). Particles of dust less than 0.002 mm (0.000078 in.) in diameter are common at any time near or over land surfaces except shortly after precipitation. Particles larger than 0.002 mm (0.000078 in.) will settle out rapidly unless wind or other forces are present to keep the particles suspended. Small particles in the atmosphere over the sea will consist almost entirely of salt.

Particle hardness in this section is expressed according to Mohs' hardness scale, which is based on the relative hardness of representative minerals as listed in Table 6.1 (Ref. 6.2).

TABLE 6.1 MOHS' SCALE-OF-HARDNESS FOR MINERALS

Mohs' Relative Hardness	Mineral	Mohs' Relative Hardness	Mineral
1	Talc	6	Orthoclase
2	Gypsum	7	Quartz
3	Calcite	8	Topaz
4	Fluorite	9	Corundum
5	Apatite	10	Diamond

6.2 Sand and Dust at Surface.

The presence of sand and dust can be expected in all geographical areas of interest, but will occur more frequently in the areas with lower water vapor concentration. The extreme values expected are as follows:

6.2.1 Size of Particles.

a. Sand particles will be between 0.080 mm (0.0031 in.) and 1.0 mm (0.039 in.) in diameter. At least 90 percent of the particles will be between 0.080 mm (0.0031 in.) and 0.30 mm (0.012 in.) in diameter.

b. Dust particles will be between 0.0001 mm (0.0000039 in.) and 0.080 mm (0.0031 in.) in diameter. At least 90 percent of these particles will be between 0.0001 mm (0.0000039 in.) and 0.002 mm (0.000079 in.) in diameter.

6.2.2 Hardness and Shape.

More than 50 percent of the sand and dust particles will be composed of angular quartz or harder material, with a hardness of 7 to 8.

6.2.3 Number and Distribution of Particles.

a. Sand. For a wind speed of 10 m sec^{-1} (19.4 knots) at 3 m (9.9 ft) above surface and relative humidity of 30 percent or less, there will be 0.02 g cm^{-3} (1.2 lb ft^{-3}) of sand suspended in the atmosphere during a sand storm. Under these conditions, 10 percent of the sand grains will be between 0.02 m (0.079 ft) and 1.0 m (3.3 ft) above the ground surface, with the remaining 90 percent below 0.02 m (0.079 ft), unless disturbed by a vehicle moving through the storm.

When the wind speed decreases below 10 m sec^{-1} (19.4 knots), the sand grains will be distributed over a smaller distance above the ground surface; while a steady-state wind speed below 5 m sec^{-1} (9.7 knots) will not be sufficient to set the grains of sand in motion.

As the wind speed increases above 10 m sec^{-1} (19.4 knots), the sand grains will be distributed over higher and higher distances above the ground surface.

b. Dust. For a wind speed of 10 m sec^{-1} (19.4 knots) at 3 m (9.9 ft) above surface, and relative humidity of 30 percent or less, there will be 6×10^{-9} g cm^{-3} (3.7×10^{-7} lb ft^{-3}) of dust suspended in the atmosphere. Distribution will be uniform to about 200 m (656 ft) above the ground.

6.3 Sand and Dust at Altitude.

Only small particles (less than 0.002 mm [0.000079 in.]) will be in the atmosphere above 400 m (1312 ft) in the areas of interest. During actual flight, the vehicle should pass through the region of maximum dust in such a short time that little or no abrasion can be expected.

6.4 Snow and Hail at Surface.

Snow and hail can cause abrasion at Huntsville, River Transportation, New Orleans, Wallops Test Range, and White Sands Missile Range areas. Extreme values expected with reference to abrasion are as follows:

6.4.1 Snow Particles.

Snow particles will have a hardness of 2 to 4 (Ref. 6.3) and a diameter of 1.0 mm (0.039 in.) to 5.0 mm (0.20 in.). A wind speed of 10 m sec^{-1} (19 knots) at a minimum air temperature of -17.8°C (0°F) should be considered for design calculations. At New Orleans a minimum air temperature of -9.4°C (15°F) should be used.

6.4.2 Hail Particles.

Hail particles will have a hardness of 2 to 4 and a diameter of 5.0 mm (0.20 in.) or greater. A wind speed of 10 m sec^{-1} (19 knots) at an air temperature of 10.0°C (50°F) should be considered for design calculations.

6.5 Snow and Hail at Altitude.

Snow and hail particles will have higher hardness values at higher altitudes. The approximate hardness of snow and hail particles in reference to temperature is given in Table 6.2 (See paragraph 4.4.2 remarks).

TABLE 6.2 HARDNESS OF HAIL AND SNOW FOR ALL LOCATIONS

Temperature		Relative Hardness (Mohs' Scale)
(°C)	(°F)	
0	32.0	2
-20	- 4.0	3
-40	-40.0	4
-60	-76.0	5
-80	-112.0	6

Although the flight time of a vehicle through a cloud layer will be extremely short, if the cloud layer contains a large concentration of moderate sized hailstones (25 mm [1 in.] or larger) at temperatures below - 20.0°C (-4°F), considerable damage may be expected (especially to antennas and other protrusions) because of the kinetic energy of the hailstone at impact. Tests have shown a definite relationship between the damage to aluminum aircraft wing sections and the velocity of various sized hailstones. Equal dents (sufficient to require repair) of 1 mm (0.039 in.) in 75 S-T aluminum resulted from the following impacts (Ref. 6.4):

a. A 19-mm (0.75 in.) ice sphere at 190 m sec^{-1} (369 knots).

b. A 32-mm (1.25 in.) ice sphere at 130 m sec^{-1} (253 knots).

c. A 48-mm (1.88 in.) ice sphere at 90 m sec^{-1} (175 knots).

6.6 Raindrops.

With the advent of high-speed aircraft a new phenomenon has been encountered in the erosion of paint coatings, of structural plastic components, and even of metallic parts by the impingement of raindrops on surfaces. The damage may be severe enough to affect the performance of a space vehicle. Tests conducted by the British Ministry of Aviation (Ref. 6.1) have resulted in a table of rates of erosion for various materials and coatings. These materials and coatings were tested at speeds of 220 m sec^{-1} (428 knots). Sufficient data are not available to present any specific extreme values for use in design, but results of the tests indicate that materials used should be carefully considered and weather conditions evaluated prior to launch.

REFERENCES

6.1 Fyall, A. A.; King, R. B.; and Strain,R. N. C.: "Rain Erosion Aspects of Aircraft and Guided Missiles." Journal of the Royal Aeronautical Society, vol. 66, July 1962, pp. 447-453.

6.2 Hurlbut, C. S., Jr.: "Dana's Manual of Mineralogy." Sixteenth Edition. John Wiley and Sons, Inc., New York, 1953.

6.3 Blackwelder, Eliot: "The Hardness of Ice." American Journal of Science, vol. 238, pp. 61-63, 1940.

6.4 Sonter, Robert K; and Emerson, Joseph B.: "Summary of Available Hail Literature and the Effect of Hail on Aircraft in Flight." NASA TN D-2734, Langley Aeronautical Laboratory, Langley Field, Virginia, 1952.

N74-16299

SECTION VII. ATMOSPHERIC PRESSURE (SURFACE)

By

Glenn E. Daniels

7.1 Definition

Atmospheric pressure (also called barometric pressure) is the force exerted as a consequence of gravitational attraction, by the mass of the column of air of unit cross section lying directly above the area in question. It is expressed as a force per unit area.

7.2 Pressure

The total variation of pressure from day to day is relatively small. Rapid but slightly greater variations occur as the result of the passage of frontal systems, while the passage of a hurricane can cause somewhat larger, but still not significant changes for pressure environment design of space vehicles. Surface pressure extremes for various locations and their extreme ranges are given in Table 7.1. These data use the results of a study of pressure extremes (Ref. 7.1 and Section XV).

7.3 Pressure Change

a. A gradual rise or fall in pressure of 3 mb (0.04 lb in.$^{-2}$) and then a return to original pressure can be expected over a 24-hour period.

b. A maximum pressure change (frontal passage change) of 6 mb (0.09 lb in.$^{-2}$) (rise or fall) can be expected within a 1-hour period at all localities.

7.4 Data on pressure distribution with altitude are given in Section XIV.

REFERENCES

7.1 Daniels, Glenn E.: "Values of Extreme Surface Pressure for Design Criteria." Institute of Environmental Sciences, 1965 Proceedings, pp. 283-288.

TABLE 7.1 SURFACE PRESSURE EXTREMES (Values apply to station altitude)

Area	Pressure				Station Elevation	
	Units	Maximum	Mean	Minimum	Units	Value
Huntsville	N m^{-2}	102 080	99 543	97 210	m	196
	mb	1020.8	995.4	972.1		
	lb in.$^{-2}$	14.8	14.4	14.1	ft	644
New Orleans	N m^{-2}	104 000	101 600	99 700	m	9
	mb	1040.0	1016.0	997.0		
	lb in.$^{-2}$	15.1	14.7	14.5	ft	30
Wallops Test Range	N m^{-2}	105 000	101 325	90 000	m	88
	mb	1050	1013.25	900		
	lb in.$^{-2}$	15.2	14.7	13.1	ft	289
Cape Kennedy	N m^{-2}	103 690	101 701	10 000	m	5
	mb	1036.9	1017.0	1000.0		
	lb in.$^{-2}$	15.0	14.8	14.5	ft	16
SAMTEC, VAFB	N m^{-2}	102 000	100 250	99 010	m	115
	mb	1020.0	1002.5	990.1		
	lb in.$^{-2}$	14.8	14.5	14.4	ft	378
White Sands Missile Range	N m^{-2}	89 010	87 130	85 200	m	1292
	mb	890.1	871.3	852.0		
	lb in.$^{-2}$	12.9	12.6	12.4	ft	4239
Edwards Air Force Base	N m^{-2}	95 560	93 430	92 030	m	706
	mb	955.6	934.3	920.3		
	lb in.$^{-2}$	13.9	13.6	13.3	ft	2316

N70-16300

SECTION VIII. ATMOSPHERIC DENSITY (SURFACE)

By

Glenn E. Daniels and S. Clark Brown

8.1 Definition.

Density is the ratio of the mass of a substance to its volume. (It also is defined as the reciprocal of specific volume.) Density is usually expressed in grams or kilograms per cubic centimeter or cubic meter.

8.2 Atmospheric Density.

The variation of the density of the atmosphere at the surface from the average for any one station, and between the areas of interest, is small and should have no important effect on preflight operations. Table 8.1 gives the median density at the surface for the five test ranges.

TABLE 8.1 MEDIAN SURFACE* DENSITIES

Area	Surface Altitude	Source of Data	Density	
	m		$kg\ m^{-3}$	$lb\ ft^{-3}$
Eastern Test Range	5	(Ref. 8.1)	1.1835	7.388×10^{-2}
Vandenberg AFB	61	(Ref. 8.2)	1.2267	7.658×10^{-2}
White Sands Missile Range	1219	(Ref. 8.3)	1.049	6.549×10^{-2}
Wallops Test Range	2	(Ref. 8.4)	1.2320	7.691×10^{-2}
Edwards AFB	706	(Ref. 8.5)	1.1244	7.020×10^{-2}

* At station elevation above mean sea level.

8.2

However, atmospheric density, especially low density, is important to aircraft takeoff and landing operations and should therefore be considered when planning Space Shuttle orbiter ferry flights. Table 8.2 gives low density values that are equaled or exceeded approximately 5% of the time during the hottest part of the day in summer. Typical associated temperatures needed for engine power calculations are also listed. Since low density is found at high elevation and high temperatures only the highest enroute airfield and the ferry flight terminals were considered. Since Cape Kennedy and Vandenberg AFB extremes are given in Section 14 only Edwards AFB and Biggs AFB are listed here.

TABLE 8.2 LOW DENSITY (5 PERCENTILE WORST) AND ACCOMPANYING TEMPERATURES FOR ORBITER FERRY OPERATIONS

Location	Low Density		Temperature	
	kgm^{-3}	% Departure from US 62	°C	°F
Edwards AFB California	1.0246	-10.5	39.4	103
Biggs AFB Texas	0.97555	-10.5	38	100

8.3 Data on density distribution with altitude are given in Section XIV.

REFERENCES

8.1 Smith, O. E.; and Weidner, Don K.: "A Reference Atmosphere for Patrick AFB, Florida, Annual (1963 Revision)". NASA TM X-53139, 1964. NASA-Marshall Space Flight Center, Huntsville, Alabama.

8.2 Carter, E. A.; and Brown, S. C. "A Reference Atmosphere for Vandenberg AFB, California, Annual (1971 Version)." NASA TM X-64590, NASA-Marshall Space Flight Center, Alabama, 1971.

8.3 "White Sands Missile Range Reference Atmosphere (Part I)," 1964. IRIG Document No. 104-63, Secretariat, Range Commander's Council, White Sands Missile Range, New Mexico.

8.4 "Wallops Island Test Range Reference Atmosphere (Part I)", 1965. IRIG Document No. 104-63, Secretariat, Range Commander's Council, White Sands Missile Range, New Mexico.

8.5 "Edwards Air Force Base, California (Part I)," IRIG Document No. 104-63, Secretariat, Range Commander's Council White Sands Missile Range, New Mexico (to be published).

N74-16301

SECTION IX. ATMOSPHERIC ELECTRICITY

By

Glenn E. Daniels

9.1 Introduction

Atmospheric electricity must be considered in the design, transportation, and operation of aerospace vehicles. The effect of the atmosphere as an insulator and conductor of high-voltage electricity, at various atmospheric pressures, must also be considered. Aerospace vehicles that are not adequately protected can be damaged by the following:

1. A direct lightning stroke to the vehicle or the launch support equipment while on the ground or after launch.

2. Current induced in the vehicle from the transport of a charge from nearby lightning.

3. A large buildup of the atmospheric potential gradient near the ground as a result of charged clouds nearby.

Also, high-voltage systems aboard the vehicle which are not properly designed can arc or break down at low-atmospheric pressures.

The vehicle can be protected as follows:

1. By insuring that all metallic sections are connected by electrical bonding so that the current flow from a lightning stroke is conducted over the skin without any gaps where sparking would occur or current would be carried inside. Reference 9.1 gives the requirements for electrical bonding.

2. By protecting buildings and other structures on the ground with a system of lightning rods and wires over the outside to carry the lightning stroke into the ground.

3. By providing a zone of protection (as shown in Reference 9.2 for the lightning protection plan for Saturn Launch Complex 39).

4. By providing protection devices in critical circuits Ref. 9.3.

5. By using systems which have no single failure mode. {The Saturn V launch vehicle uses triple redundant circuitry on the auto-abort system, which requires two out of the three signals to be correct before abort is initiated Ref. 9.4}.

6. By appropriate shielding of units sensitive to electromagnetic radiation.

7. For horizontally flying vehicles, by avoiding potentially hazardous thunderstorm areas by proper flight planning and flight operations. Reference 5 has an excellent discussion on geographic areas where thunderstorms and thus potentially dangerous lightning discharges occur frequently.

If lightning should strike a vehicle or the test stand or launch umbilical tower (LUT), sufficient system checks should be made to insure that all electrical components and subsystems of the vehicle are functional.

9.2 Thunderstorm Electricity

On a cloudless day, the potential electrical gradient in the atmosphere near the surface of the earth is relatively low (<300 V/m); but when clouds develop, the potential gradient near the surface of the earth will increase. If the clouds become large enough to have water droplets of sufficient size to produce rain, the atmospheric potential gradient may be sufficient to result in a lightning discharge which would require measured gradients greater than 10 000 volts per meter at the surface. Gradients may be considerably higher at altitude above the surface.

9.2.1 Potential Gradient

The earth-ionospheric system can be considered a large capacitor: the earth's surface as one plate, the ionosphere the other plate, and the atmosphere the dielectric. The earth is negatively charged.

9.2.2 Fair-Weather[1] Potential Gradients

The fair-weather electrical field intensity (the negative of the electrical gradient) measured near the ground is approximately 100 to 300 volts per meter and negative; i.e., the earth is negatively charged and the atmosphere above the earth is positively charged. The fair-weather value of 100 to 300 volts per meter will vary with time at any specific location and will also be different at various locations. These variations in fair weather are caused by the amount of particulate matter in the atmosphere (dust, salt particles, etc.), atmospheric humidity, and location and exposure of the measuring devices Ref. 9.6. The fair-weather potential gradient decreases with altitude and has a value near zero at 10 kilometers. Fair-weather potential gradient over a 100-meter-high vehicle could result in a 10 000-volt, or greater, potential difference between the air near the ground and the air around the vehicle top, causing the vehicle to assume the charge if not grounded.

9.2.3 Potential Gradients with Clouds

When clouds develop, the potential gradient at the ground increases. Because of the increased potential gradient on days when scattered cumulus clouds occur, severe shock may result from charges carried down metal cables connected to captive balloons. Similarly induced charges on home television antennas have been great enough to explode fine wire coils in antenna circuits in television sets. Damage to equipment connected to wires and antennas can be reduced or prevented by the use of lightning arresters with air gaps close enough to discharge the current before the voltage reaches values high enough to damage the equipment.

9.2.4 Potential Gradients During Thunderstorms

When the cloud develops into the cumulo-nimbus state, lightning discharges result. For a discharge to occur, the potential gradient at a location reaches a value equal to the critical breakdown value of air at that location. Laboratory data indicate this value to be as much as 10^6 volts per meter at standard sea-level atmospheric pressure. Electrical fields measured at the

---

1. The term fair weather is used to mean without clouds. Also, the term fine weather is sometimes used.

surface of the earth are much less tha 10^6 volts per meter during lightning discharges for several reasons:

1. Most clouds have centers of both polarities which tend to neutralize values measured at the surface.

2. Each charge in the atmosphere and its image within the earth resembles an electrical dipole, and the intensity of the electrical field decreases with the cube of the distance to the dipole.

3. The atmospheric electric field measured over land at the surface is limited by discharge currents arising from grounded points, such as grass, trees, and other structures, which ionize the air around the points, thus producing screen space charges.

For these reasons, the measured electrical field at the surface is never more than about 15×10^3 volts per meter. The potential gradient values indicated by measuring equipment at the surface will show high values when the charged cloud is directly overhead. As the horizontal distance between the projection of the charged center of the cloud to the ground and the measuring equipment becomes greater, the readings become lower, reaching zero at some distance, and then change to the opposite sign at greater distances(References 9.1 and 9.6).

9.2.5 Corona Discharge

As the atmospheric potential gradient increases, the air surrounding exposed sharp points becomes ionized by corona discharge. The charge induced by a nearby lightning stroke may aid such a discharge. The corona discharge may be quite severe when lightning storms or large cumulus clouds are within about 16 kilometers (10 mi) of the launch pad.

9.3 Characteristics of Lightning Discharges

The following definitions define a lightning discharge and its parts:

Lightning flash or discharge, the total series of electrical and luminous effects comprising a single lightning phenomena with a typical duration of several tenths of a second.

Lightning stroke, any one of the major electrical and luminous effects, the entire series which combined, make up the lightning flash. Many authors restrict the term "stroke" to the "return stroke" of the cloud ground flash.

Continuing currents, the current which flows at the end of a high current stroke for hundreds of milliseconds.

The characteristics of various types of lightning discharges are summarized in Table 9.1 and References 9.7 and 9.8.

9.3.1 Lightning Currents*

The current flow** in a lightning flash (cloud to ground) are conviently separated into categories as follows:

a. Return stroke surges

Peak current from under 20,000 amperes to over 200,000 amperes, with durations of tens of microseconds.

b. Intermediate currents

Peak current from under 2,000 amperes to over 20,000 amperes, with duration of milliseconds.

c. Continuing currents

Peak current from under 200 amperes to over 2,000 amperes with durations of hundreds of milliseconds.

Currents of category (a) mainly produce explosive effects and undesirable coupling transients, while categories (b) and (c) mainly cause hole burning type damage.

The time structure of the ligntning currents is usually less variable between individual flashes, than the amplitudes. Furthermore, there is little connection within an individual discharge between the severity of the three categories, i.e., an initial severe return stroke has minimal influence on the severity of a following continuing current.

*The information in this section was prepared in cooperation with Dr. E. T. Pierce of Stanford Research Institute, Menlo Park, California. See Appendix A, Reference 9.9.

**Note that a broad range of current values are given for each category.

TABLE 9.1 CHARACTERISTICS OF LIGHTING DISCHARGES

Type of Lightning	Average Peak Current per Stroke (A)	Maximum Rate of Rise of Current (A/μsec)	Average Amount of Charge Transferred		Average Total Duration of Stroke (msec)	Average Number of Strokes (unitless)	Average Time Between Strokes (msec)	Remarks
			Per Stroke (C)	Total (C)				
Intercloud lightning	100-2000	100-500	1-5	1-5	300	1		
Discrete lightning strokes to ground								
Leader	100		1-5	5	20	1		
Return stroke	20 000	200 000	5	4-20	0.3	3 to 4	40	Peak current exceeding 100 000 A have been measured about 2 percent of the time.
Long continuing current lightning strokes to ground								
Leader	100		1-5	5	20	1		
Return stroke	20 000	10 000	12-40	12-40	200	1		Average current value of 185 A for long periods (175 msec).

9.3.2 Lightning Characteristics for Design on the Launch Pad or During Ground Transportation

Three models of lightning flashes are presented in this section for use in design studies as follows:

Model 1. A very severe discharge model.

This model involves two high current peak strokes (return strokes), the model is as follows:

a. The first return stroke surge with a current peak of 200,000 amperes and a maximum current rise at a rate of 100,000 amperes per microsecond (100 kA/10^{-6}s) then falling off at a rate of about 2,000 amperes per microsecond for 98 microseconds to 7,000 amperes.

b. An intermediate current, following the first return stroke surge, of an average of 4,000 amperes (7 kA to 1 kA) for 5 milliseconds (5,000 μs).

c. A first continuing current, following the intermediate current, of an average of 700 amperes (1,000 A to 400 A) for 50 milliseconds.

d. A second continuing current, following the first intermediate of an average of 400 amperes, for 300 milliseconds at constant current.

e. A second return stroke surge, following the second continuing current, with a peak current of 100,000 amperes and a maximum current rise at a rate of 50,000 amperes per microsecond then falling off at a rate of about 1,000 amperes per microsecond for 98 microseconds to 3,500 amperes.

f. An intermediate current, following the second return stroke surge, of an average of 2,000 amperes (3.5 kA to 500 A) for 5 milliseconds.

The current time history for this model is shown in Figure 9.1 and Table 9.2. This model is the basis of the Space Shuttle Lightning Protection Design and was developed from measurements of Florida lightning by Dr. Uman (Ref. 9.10)., and work by Dr. Pierce and Dr. Cianos (Ref. 9.20).

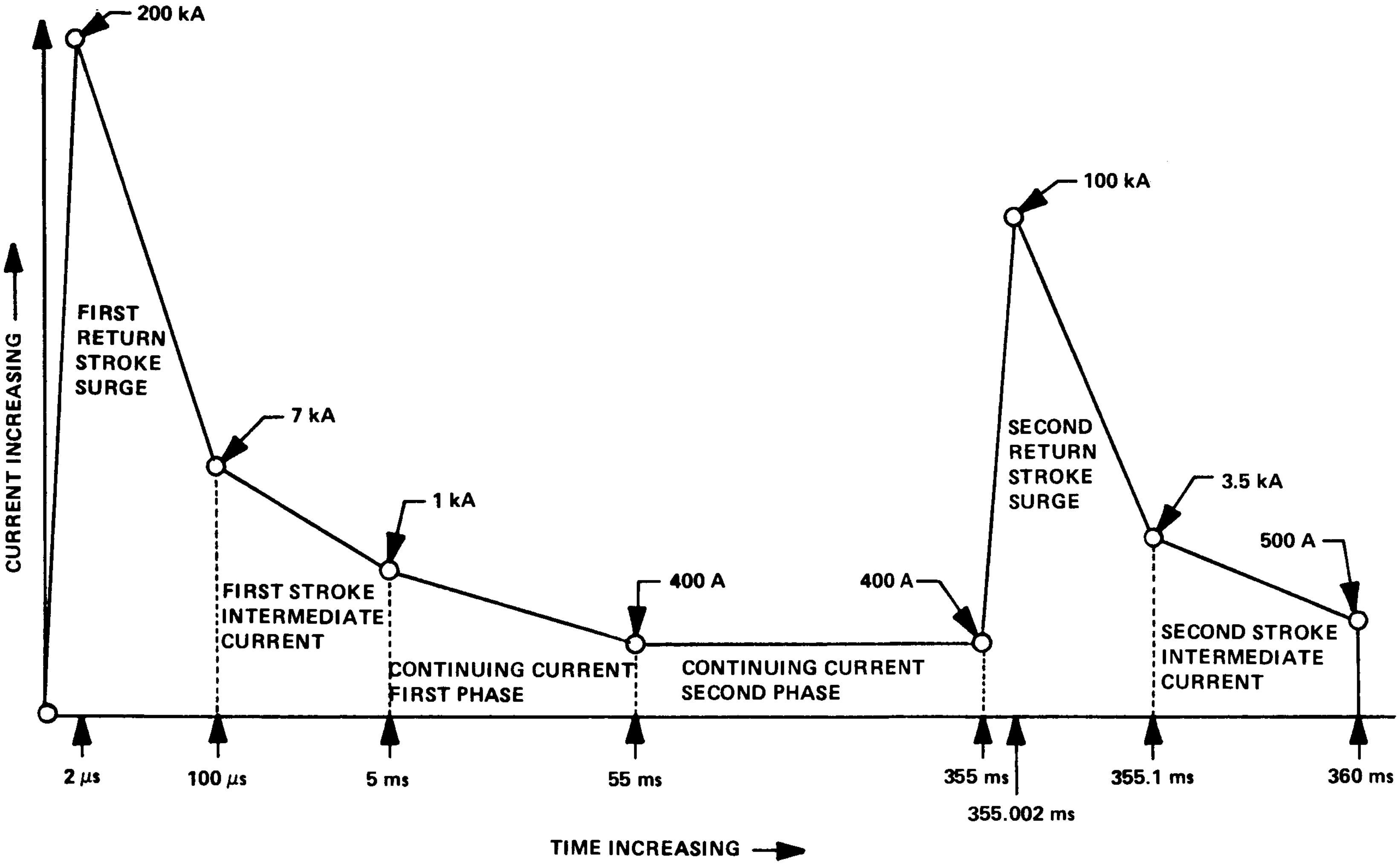

Figure 9.1. - Diagrammatic representation of a very severe lightning model. (MODEL 1)
(Note that the diagram is not to scale.)

TABLE 9.2 DETAILS OF A VERY SEVERE LIGHTNING MODEL (MODEL 1)

Stage	Key Points		Rate of Current Change	Charge Passing
1. First Return Stroke Surge	t = 0	i = 0	Linear Rise - 100 kA/μs	0.2 C
	t = 2 μs	i = 200 kA	Linear Fall - 193 kA in 98 μs	~ 10.2 C
	t = 100 μs	i = 7 kA		
2. First Stroke Intermediate Current	t = 100 μs	i = 7 kA	Linear Fall - 6 kA in 4.9 ms	19.6 C
	t = 5 ms	i = 1 kA		
3. Continuing Current--First Phase	t = 5 ms	i = 1 kA	Linear Fall - 600 A in 50 ms	35.0 C
	t = 55 ms	i = 400 A		
4. Continuing Current--Second Phase	t = 55 ms	i = 400 A	Steady Current	120.0 C
	t = 355 ms	i = 400 A		
5. Second Return Stroke Surge	t = 355 ms	i = 400 A	Linear Rise ~ 50 kA/μs	~ 0.1 C
	t = 355.002 ms	i = 100 kA	Linear Fall - 96.5 kA in 98 μs	~ 5.1 C
	t = 355.1 ms	i = 3.5 kA		
6. Second Stroke Intermediate Current	t = 355.1 ms	i = 3.5 kA	Linear Fall - 3 kA in 4.9 ms	9.8 C
	t = 360 ms	i = 500 A		

Model 2. A 98 percentile peak current model.*

This model involves one high current peak stroke (return stroke). The model is as follows:

a. The first return stroke surge with a current peak of 100,000 amperes and a maximum current rise at a rate of 20,000 amperes per microsecond (20 kA/10^{-6}s) then falling off at a rate of about 1,000 amperes per microsecond for 95 microseconds to 3,500 amperes.

b. An intermediate current, following the first return stroke surge, of an average of 2,000 amperes (3,500 A to 500 A) for 5 milliseconds (5,000 μs).

c. A first continuing current, following the intermediate current, of an average of 350 amperes (500 A to 200 A) for 50 milliseconds.

d. A second continuing current, following the first intermediate current, of an average of 200 amperes, for 300 milliseconds at constant current.

This model current time history is shown in Figure 9.2 and Table 9.3.

Model 3. An average peak current model.

This model involves one high current peak stroke (return stroke). The model is as follows:

a. The first return stroke surge with a current peak of 20,000 amperes and a maximum current rise at a rate of 4,000 amperes per microsecond (4 kA/10^{-6}s) then falling off at a rate of about 190 amperes per microsecond for 95 microseconds to 2,000 amperes.

b. An intermediate current, following the first return stroke surge, of an average of 1,150 amperes (1,700 A to 850 A) for 5 milliseconds (5,000 μs).

---

*The intermediate and continuing currents are not necessarily the 98 percentile values, but are added to represent a more severe burning phase.

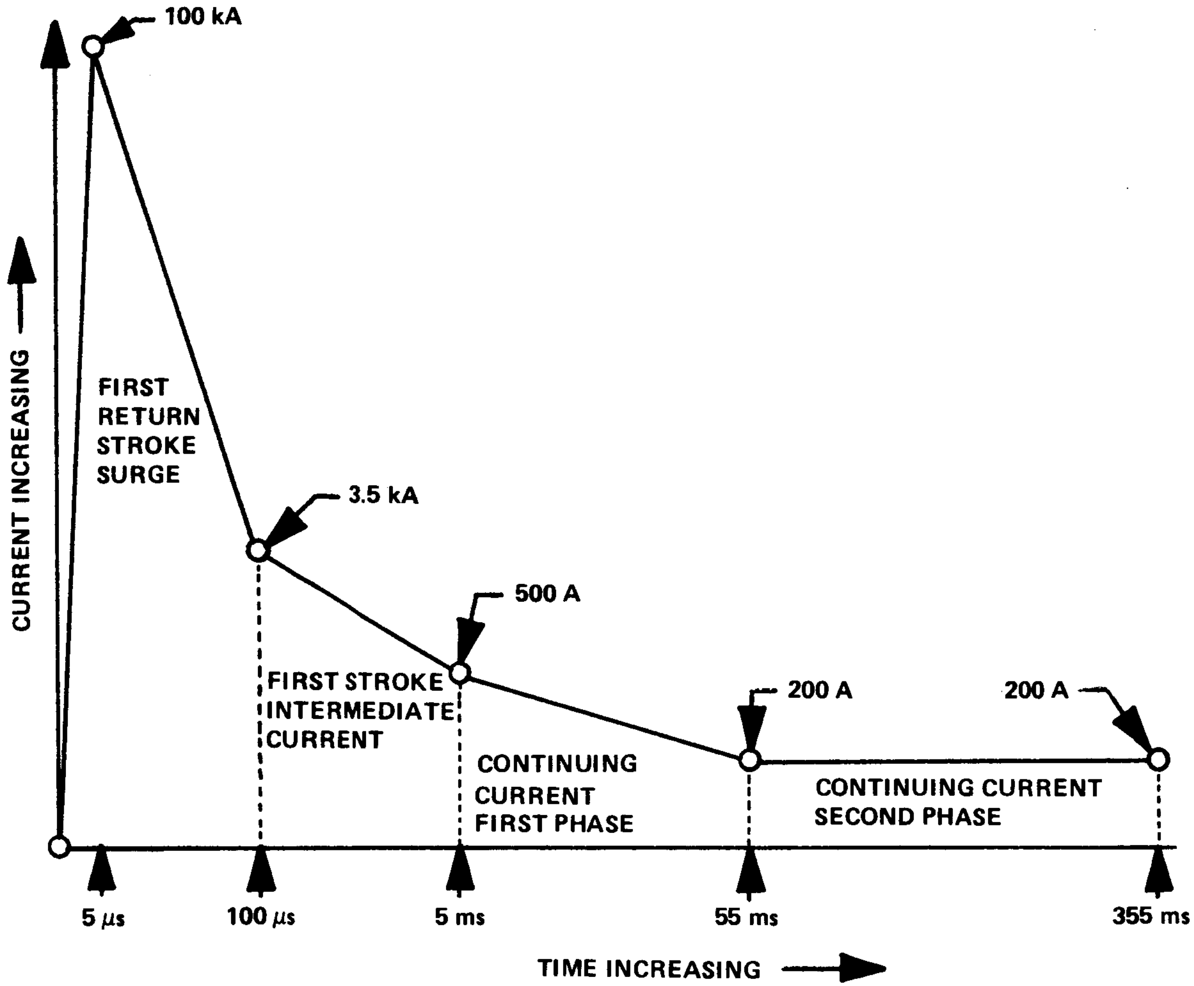

Figure 9.2. - Diagrammatic representation of a 98 percentile peak current lightning model. (MODEL 2)
(Note that the diagram is not to scale.)

TABLE 9.3 DETAILS OF A 98 PERCENTILE PEAK CURRENT LIGHTNING MODEL (MODEL 2)

Stage	Key Points		Rate of Current Change	Charge Passing
1. First Return Stroke Surge	t = 0 t = 5 μs t = 100 μs	i = 0 i 100 kA i 3.5 kA	Linear Rise - 20 kA/μs Linear Fall - 96.5 kA in 95 μs	0.3 C ~ 4.9 C
2. First Stroke Intermediate Current	t = 100 μs t = 5 ms	i 3.5 kA i 500 A	Linear Fall - 3 kA in 4.9 ms	9.8 C
3. Continuing Current-- First Phase	t = 5 ms t = 55 ms	i 500 A i 200 A	Linear Fall - 300 A in 50 ms	17.5 C
4. Continuing Current-- Second Phase	t = 55 ms t = 355 ms	i 200 A i 200 A	Steady Current	60 C

c. <u>A first continuing current</u>, following the intermediate current, of an average of 100 amperes, for 300 milliseconds at constant current.

d. <u>A second continuing current</u>, following the first intermediate current, of an average of 100 amperes, for 300 milliseconds at constant current.

The current-time history for this model is shown in Figure 9.3 and Table 9.4.

9.3.3 Lightning Characteristics for Design During Flight (Triggered Lightning).

The space vehicle while in flight should be capable of withstanding an electrical discharge from triggered lightning equal to Model 3, given in Section 9.3.2 for an average cloud to ground discharge. Designs of most solid and liquid rocket engines are such that more extreme lightning currents may result in serious damage when the engines are burning. Therefore, launch mission rules are needed to prevent a launch when any severe lightning discharges are possible.

9.3.4 Current Flow Distribution from a Lightning Discharge

When lightning strikes an object, the current will flow through a path to the true earth ground. The voltage drop along this path may be great enough over short distances to be dangerous to personnel and equipment Ref 9.2. Cattle and humans have been electrocuted from the current flow through the ground and the voltage potential between their feet while standing under a tree struck by lightning.

The flow of dc and low frequency current in objects struck by lightning will divide into each possible path of resistance, with the lowest resistance paths carrying the greater current inversely proportional to the resistance if we assume no inductance coupling. Figure 9.4 illustrates this principle for the Saturn V vehicle on the launch pad.

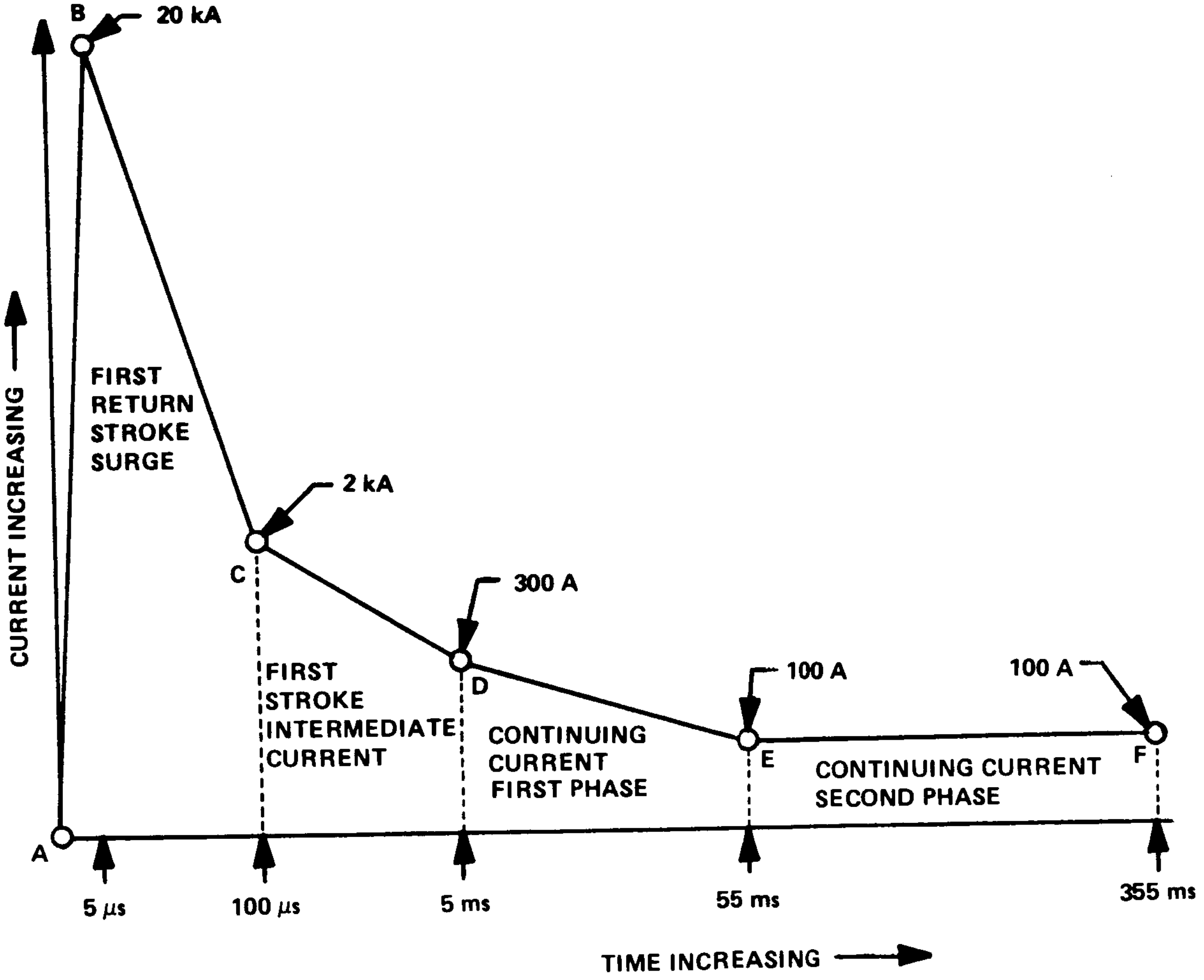

Figure 9.3. - Diagrammatic representation of an average lightning model. (MODEL 3)
(Note that the diagram is not to scale.)

TABLE 9.4 DETAILS OF AN AVERAGE LIGHTNING MODEL (MODEL 3)

Stage	Key Points	Rate of Current Change	Charge Passing
1. First Return Stroke Surge	t = 0 i = 0 t = 5 μs i = 20 kA t = 100 μs i = 2 kA	Linear Rise - 4 kA/μs Linear Fall - 18 kA in 95 μs	0.1 C ~ 1.0 C
2. First Stroke Intermediate Current	t = 100 μs i = 2 kA t = 5 ms i = 300 A	Linear Fall - 1.7 kA in 4.9 ms	5.6 C
3. Continuing Current -- First Phase	t = 5 ms i = 300 A t = 55 ms i = 100 A	Linear Fall - 200 A in 50 ms	10.0 C
4. Continuing Current -- Second Phase	t = 55 ms i = 100 A t = 355 ms i = 100 A	Steady Current	30.0 C

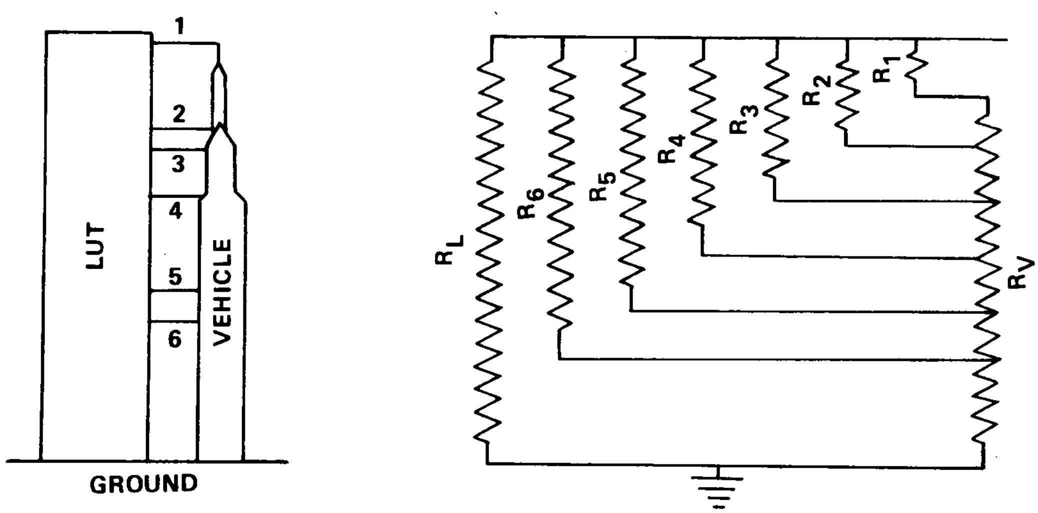

Figure 9.4. Example of dc and low frequency current flow in aerospace vehicle on launch pad and comparable resistance analogy, assuming no inductance coupling.

Therefore,

$$I_L = \frac{R_L}{R_T} I_T \quad ,$$

where

I_L = current through LUT,

I_T = total current of lightning stroke,

R_L = resistance of LUT,

R_T = total resistance of system,

R_1, R_2, etc = resistance of each connecting arm to vehicle,

R_V = resistance of vehicle.

In the case of the Saturn V vehicle, a sizable percentage ~ 30 percent flows through the Saturn V vehicle.

Since lightning usually strikes the highest exposed point, the only ways to be certain that damaging currents will not flow through a space vehicle on the launch pad is to either: (1) prevent the lightning discharge to the launch complex (2) to conduct the lightning discharge around the launch complex using sufficient mass to carry the current through conductors well insulated (high-resistance supports) from the launch complex equipment, or (3) to design the space vehicle to carry the currents without damage.

9.3.5 Radio Interference

When an electrical charge produces a spark between two points, electromagnetic radiation is emitted. This discharge is not limited to a narrow band of frequencies but covers most of the electromagnetic radiation spectrum with various intensities. Most static heard in radio reception is related to electrical discharges, with lightning strokes contributing much of the interference. This interference from lightning strokes is propagated through the atmosphere in accordance with laws valid for ordinary radio transmission and may travel great distances. With the transmission of interference from lightning strokes over great distances, certain frequencies remain prominent, with those near 30 kilohertz being the major frequencies. Interference with telemetering and guidance needs to be considered only when thunderstorms are occurring within 100 kilometers (60 mi) of the space vehicle launch site.

9.4 Frequency of Occurrence of Thunderstorms

According to standard United States weather observing and recording practice, a thunderstorm is reported whenever thunder is heard at the station. It is recorded along with other atmospheric phenomena on the standard weather observer's form, indicating when the thunder is heard. The report ends 15 minutes after thunder is last heard. This type of reporting of thunderstorms may contain a report as one, or one or more thunderstorms during a period. For this reason, these types of observations will be referred to as thunderstorm events, i.e., a period during which one or more thunderstorms are reported. Because of the method of reporting thunderstorms, most analyses of thunderstorm data are based on the number of days per year in which thunder is heard one or more times on a day i.e., thunderstorm days. Reference 9.12 is a detailed study on frequencies of thunderstorms occurring in the Cape Kennedy area.

9.4.1 Thunderstorm Days per Year (Isoceraunic[3] Level)

The frequency of occurrence of thunderstorm days is an approximate guide to the probability of lightning strokes to earth in a given area. The number of thunderstorm days per year is called the isoceraunic level. A direct lightning stroke is possible at all locations of interest, but the frequency of such an occurrence varies among the locations (Table 9.5) References 9.2, 9.3, and 9.13.

9.4.2 Thunderstorm Occurrence per Day

In a study using weather observation data, which reports a thunderstorm when thunder is heard (Reference 9.12), the frequencies were computed on the number of days which had 0, 1, 2, ..., thunderstorms reported, i.e., none or more thunderstorm events. Tables 9.6 and 9.7 and Reference 9.12 give this information.

9.4.3 Thunderstorm Hits

There were sufficient data for the summer months (June-August) at Cape Kennedy to make an analysis of the frequency of occurrence of thunderstorm hits as:

1. A thunderstorm actually reported overhead.

2. A thunderstorm first reported in a sector and last reported in the opposite sector, if it is assumed that thunderstorms move in straight lines over small areas. This information is listed in Tables 9.8 and 9.9 Reference 9.12.

9.4.4 Hourly Distribution of Thunderstorms

Figure 9.5 presents the empirical probability that a thunderstorm will occur in the Cape Kennedy area at each hour of the day during each month. The highest frequency of thunderstorms (24 percent) is around 1600 EST in July. A thunderstorm is reported by standard observational practice if thunder is heard, which can be over a radius of approximately 25 kilometers. Thus, the statistics presented in Figure 9.5 are not necessarily the probability that a thunderstorm will "hit," for example, a vehicle on the launch pad, or occur at a given location on Cape Kennedy.

---

3. This word is also spelled isokeraunic.

TABLE 9.5 FREQUENCY-OF-OCCURRENCE OF "THUNDERSTORM DAYS" (ISOCERAUNIC LEVEL)

Location	Mean Number of Days Per Year of Thunderstorms	Monthly Distribution (% of Annual No. Days)											
		Jan.	Feb.	Mar.	Apr.	May	Jun.	Jul.	Aug.	Sep.	Oct.	Nov.	Dec.
Huntsville	70	1 0.70	3 2.10	6 4.20	8 5.60	11 7.70	19 13.30	22 15.40	18 12.60	9 6.30	1 0.70	1 0.70	1 0.70
River Transportation and New Orleans	75	3 2.25	3 2.25	5 3.75	5 3.75	8 6.0	16 12.0	21 15.75	20 15.0	10 7.5	3 2.25	3 2.25	3 2.25
Gulf Transportation	90	1 0.90	1 0.90	4 3.60	2 1.80	9 8.10	18 16.20	24 21.60	23 20.70	12 10.80	4 3.60	1 0.90	1 0.90
Eastern Test Range	70.09	0.77 0.54	1.94 1.36	4.28 3.00	4.02 2.82	9.73 6.82	18.55 13.00	21.27 14.91	20.23 14.18	13.22 9.27	3.89 2.73	1.18 0.82	0.92 0.64
Panama Canal Transportation	100	1 1.0	1 1.0	4 4.0	2 2.0	9 9.0	18 18.0	24 24.0	23 23.0	12 12.0	4 4.0	1 1.0	1 1.0
West Coast Transportation	6	9 0.54	11 0.66	19 1.14	13 0.78	7 0.42	4 0.24	3 0.18	7 0.42	8 0.48	8 0.48	3 0.24	8 0.48
Vandenberg AFB, California	2	5 0.1	15 0.3	15 0.3	5 0.1	2 0.04	1.5 0.03	10 0.2	10 0.2	25 0.5	1.5 0.03	5 0.1	5 0.1
Sacramento	4	6 0.24	16 0.64	12 0.48	15 0.60	9 0.54	6 0.24	3 0.12	3 0.12	10 0.40	12 0.48	5 0.20	3 0.12
Wallops Test Range[a]	40.6	0.5 0.2	1.2 0.5	5.2 2.1	8.4 3.4	12.6 5.1	17.2 7.0	21.7 8.8	20.4 8.3	7.9 3.2	3.2 1.3	1.0 0.4	0.7 0.3
White Sands Missile Range[b]	38.1	0.8 0.3	0.1 0.05	1.8 0.7	4.7 1.8	7.6 2.9	15.2 5.8	30.5 11.6	23.9 9.1	8.7 3.3	5.2 2.0	0.5 0.2	1.0 0.4
Edwards AFB, California	4.3	2.3 0.1	2.3 0.1	2.3 0.1	7.0 0.3	4.7 0.2	2.3 0.1	23.3 1.0	25.6 1.1	20.9 0.9	7.0 0.3	2.3 0.1	0 0

a. Data from Norfolk, Virginia

b. Data from Holloman AFB, New Mexico

TABLE 9.6 FREQUENCIES OF THE OBSERVED NUMBER OF DAYS THAT EXPERIENCED x THUNDERSTORM EVENTS AT CAPE KENNEDY FOR THE 11-YEAR PERIOD OF RECORD JANUARY 1957 THROUGH DECEMBER 1967

x	Jan	Feb	Mar	Apr	May	Jun	Jul	Aug	Sep	Oct	Nov	Dec	Spring	Summer	Fall
0	335	295	308	299	266	187	177	185	228	311	321	334	873	549	860
1	4	9	20	18	43	77	80	89	54	17	6	3	81	246	77
2	2	4	9	10	25	40	47	30	33	9	3	2	44	117	45
3		2	3	3	3	17	26	24	12	4		2	9	67	16
4			1		3	6	9	10	3				4	25	3
5					0	2	2	3					0	7	
6					1	1							1	1	
n	341	310	341	330	341	330	341	341	330	341	330	341	1012	1012	1001

TABLE 9.7 RELATIVE FREQUENCY OF DAYS THAT EXPERIENCED AT LEAST ONE THUNDERSTORM EVENT AT CAPE KENNEDY

Jan	Feb	Mar	Apr	May	Jun	Jul	Aug	Sep	Oct	Nov	Dec	Spring	Summer	Fall
0.018	0.048	0.097	0.094	0.220	0.433	0.481	0.457	0.309	0.088	0.027	0.021	0.137	0.458	0.141

TABLE 9.8. FREQUENCIES OF THE OBSERVED NUMBER OF DAYS THAT EXPERIENCED x THUNDERSTORM HITS AT CAPE KENNEDY FOR THE 11-YEAR PERIOD OF RECORD JANUARY 1957 THROUGH DECEMBER 1967

x	Jun	Jul	Aug	Summer
0	293	305	300	898
1	27	24	30	81
2	5	6	7	18
3	3	3	2	8
4 or more	2	3	2	7
Total	330	341	341	1012

TABLE 9.9. RELATIVE FREQUENCY OF DAYS THAT EXPERIENCED AT LEAST ONE THUNDERSTORM HIT AT CAPE KENNEDY

Jun	Jul	Aug	Summer
0.112	0.106	0.121	0.113

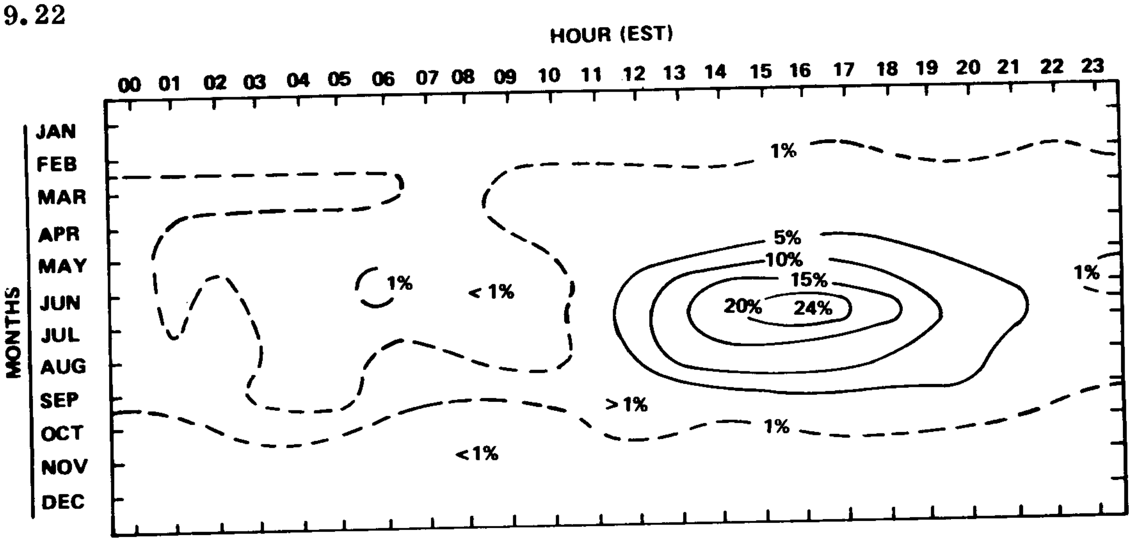

Figure 9.5. Probability (%) of occurrence of thunderstorms by months versus time of day in the Cape Kennedy area.

9.5 FREQUENCY OF LIGHTNING STROKES TO EARTH

Only limited data have been obtained on the number of lightning strokes to ground. These data are difficult ot obtain because lightning stroke measuring equipment does not usually differentiate between cloud-to-ground and cloud-to-cloud strokes. In addition, the equipment may record a strong stroke at a great distance and not record a weak stroke much closer. Therefore, the most reliable data of cloud-to-ground lightning strokes have been obtained visually. Such observations are limited in both number and length of time of observations.

Comparison of data published on cloud-to-ground lightning strokes from measuring equipment, visual observations, actual strikes to objects from insurance claims and magnetic links, and electrical outages confirms that the average number of lightning strokes per year to objects of different heights given in Table 9.10 is realistic of the Cape Kennedy area [Ref 9.14 to 9.16].

Table 9.10 should not be interpreted to mean that 4.4 lightning strokes will be observed on a 152-meter (500-ft) object at Cape Kennedy each year. There may be no strokes or very few during a year, then in another year, a considerable number of strokes. Also one can assume that all strokes that occur will not be observed or known to have occurred within the launch area. Although numerous aerospace vehicles have been launched from Cape Kennedy during the last 10 years, only a few lightning strokes are known to have struck the launch complexes until Apollo 15, when 11 separate strokes were known to have struck the launch complex during 5 different days between June 14 and July 21, 1971 (a period of 37 days) [9.17]

TABLE 9.10 ESTIMATE OF THE AVERAGE NUMBER OF LIGHTNING STROKES PER YEAR FOR VARIOUS HEIGHTS FOR CAPE KENNEDY

Height		Average Number of Lightning Strokes per Year
(m)	(ft)	
30.5	100	0.4
61.0	200	1.1
91.4	300	2.3
121.9	400	3.5
152.4	500	4.4
182.9	600	5.3
213.4	700	5.8

Work is underway to develop a statistical model of probability of lightning strokes to the ground for each month at Cape Kennedy.

9.6 STATIC ELECTRICITY

A static electrical charge may accumulate on an object from its motion through an atmosphere containing raindrops, ice particles, or dust. A stationary object, if not grounded, can also accumulate a charge from windborne particles (often as nuclei too small to be visible) or rain or snow particles striking the object. This charge can build up until the local electric field at the point of sharpest curvature exceeds the breakdown field. The quantity of maximum charge will depend on the size and shape of the object (especially if sharp points are on the object). Methods of calculating this charge are given in Reference 9.7.

If a charge builds up on a vehicle on the launch pad which is not grounded, any discharges which occur could ignite explosive gases or fuels, interfere with radio communications or telemetry data, or cause severe shocks to personnel. Static electrical charges occur more frequently during periods of low humidity and can be expected at all geographical areas.

9.7 ELECTRICAL BREAKDOWN OF THE ATMOSPHERE

The atmosphere of the earth at normal sea-level pressure (101 325 N/m^2) is an excellent insulator, having a resistance greater than 10^{16} ohms for a column 1 square centimeter in cross section and 1 meter long. When there is a charge in the atmosphere, ionization takes place, thus increasing the conductivity of the air. This charge can be from either cloud buildups or electrical equipment. If the voltage is increased sufficiently, the ionization will be high enough for a spark to discharge.

The breakdown voltage (voltage required for a spark to jump a gap) for direct current is a function of atmospheric pressure. The breakdown voltage decreases with altitude until a minimum is reached of 327 volts per millimeter at an atmosphere pressure of 760 newtons per square meter (7.6 mb), representing an altitude of 33.3 kilometers. Above and below this altitude, the breakdown voltage increases rapidly [9.18] being several thousand volts per millimeter at normal atmospheric pressure (Fig. 9.6).

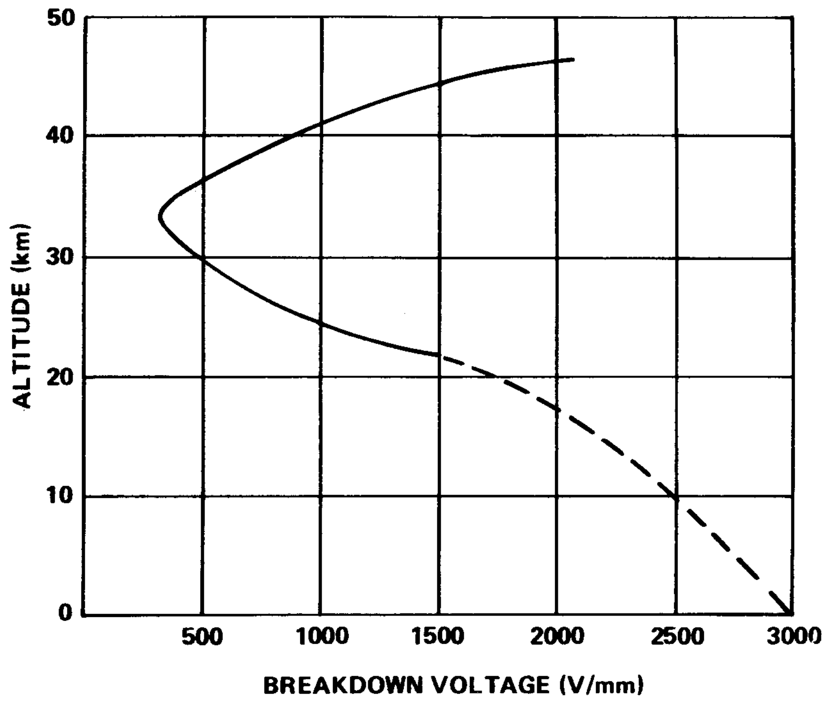

Figure 9.6. Breakdown voltage versus altitude.

The breakdown voltage is also a function of frequency of an alternating current. With an increase of frequency the breakdown voltage decreases decreases. A more complete discussion can be found in Reference 9.19.

The following safety measures can be taken to prevent arcing of high voltage in equipment:

1. Have equipment voltages off at the time the space vehicle is going through the critical atmospheric pressures. Any high-voltage capacitors should have bleeding resistors to prevent high-voltage charges remaining in the capacitors.

2. Eliminate all sharp points and allow sufficient space between high-voltage circuits.

3. Seal high-voltage circuits in containers at normal sea-level pressures.

4. Have materials available to protect, with proper use, against high-voltage arcing by potting circuits.

REFERENCES

9.1 Military Specification, Bonding, Electrical (for Aircraft). MIL-B-5087B(ASG), 1964, and Amendment 1, February 6, 1968.

9.2. Brewster, H. D.; and Hughes, W. G.: Lightning Protection for Saturn Launch Complex 39. Report No. TR-4-28-2-D, Launch Support Equipment Engineering Division, NASA-Launch Operations Center, Cape Kennedy, Florida, 1963.

9.3 Lightning Protection Guidelines for STADAN Ground Equipment. NASA CR-94682, N68-24516, High Voltage Laboratory, General Electric Company, Pittsfield, Massachusetts, Goddard Space Flight Center, Greenbelt, Maryland, November 1967.

9.4 Analysis of Apollo 12 Lightning Incident. Document No. MSC-01540, prepared jointly by Marshall Space Flight Center, Kennedy Space Center, and Manned Spacecraft Center, National Aeronautics and Space Administration, February 1970.

9.5 Appleman, Herbert S: Lightning Hazard to Aircraft. Technical Report 179 (Rev), Headquarters Air Weather Service (MAC), United States Air Force, Scott AFB, Illinois, April 1971.

9.6 Chalmers, J. Alan: Atmospheric Electricity. Pergamon Press, New York, 1957.

9.7 Brook, M.; Holmes, C. R.; and Moore, C. B.: Lightning and Rockets — Some Implications of the Apollo 12 Lightning Event. Naval Research Reviews, Vol. 23, No. 4, April 1970, pp. 1-17.

9.8 Electromagnetic Interference Characteristic Requirements for Equipment. MIL-STD-461A, August 1, 1968.

9.9 Space Shuttle Lightning Protection Criteria Document, Document No. MSC-07636, prepared jointly by Johnson Space Center, Kennedy Space center, and Marshall Space Flight Center, National Aeronaurics and Space Administration, September 1973.

REFERENCES (Continued)

9.10 Uman, Martin A. and McLain, D. Kenneth: Lightning Currents Relative to Space Shuttles: Currents and Electric Field Intensity in Florida Lightning. NASA CR-2161, Marshall Space Flight Center, Alabama.

9.11 Electromagnetic Interference Characteristics, Measurement of. MIL-STD-462, July 31, 1967.

9.12 Falls, Lee W.; Williford, W. O.; and Carter, M. C.: Probability Distributions for Thunderstorm Activity at Cape Kennedy, Florida. NASA TM X-53867, NASA-Marshall Space Flight Center, Alabama. 1970.

9.13 Thunderstorm Rainfall. Hydrometeorological Report No. 5, Hydrometeorological Section, 2 parts, United States Weather Bureau and Corps of Engineers, Waterways Experiment Station, Vicksburg, Mississippi, 1947.

9.14 Prentice, S. A.; and Mackerras, D.: Recording Range of Lightning-Flash Counter. Proc. IEE, Vol. 116, No. 2, February 1969, pp. 294-302.

9.15 Chandrashekhar Arrja, S. V.; and Sonde, B. S.: Number of Cells Developed During the Life-Time of a Thunderstorm. Nature, Vol. 200, November 9, 1963, pp. 562-563.

9.16 Beck, Edward: Lightning Strokes Prefer Tall Structures. Weshtinghouse Engineer, Vol. 9, July 1949, pp. 124-128.

9.17 Apollo 15 Mission Report. MSC 05161, NASA, Manned Spacecraft Center, Houston, Texas, December 9, 1971.

9.18 Spink, Bradley R.: A Practical Solution to the Arcing Problem at High Altitudes. Planetary and Space Science, Vol. 7, July 1961, pp. 11-18.

9.19 Paul, Fred W.; and Burrowbridge, Donald: The Prevention of Electrical Breakdown in Spacecraft, NASA SP-208, NASA, Washington, D. C., 1969.

REFERENCES (Concluded)

9.20 Cianos, N., and Pierce, E.T.; A Ground-Lightning Environment for Engineering Usage, Stanford Research Institute, 1972.

N74-16302

SECTION X. ATMOSPHERIC CORROSION

By

Glenn E. Daniels

10.1 Introduction.

The atmosphere near the ocean will cause corrosion of exposed metals. Wind moving over breaking sea waves will pick up small droplets of salt water. These droplets are small enough to remain suspended in the air. Some will evaporate and leave tiny particles of salt in the air. When these droplets and particles accumulate on surfaces and dry, a film of salt remains on the surface. The efficiency of an optical surface coated with this salt film will be considerably reduced over periods of time. When the relative humidity is near saturation, or when light rain or drizzle occurs, the salt on the surface will absorb water and form a highly conductive solution. Corrosion by electrolytic action can result when two dissimilar metals are involved, and corrosion of a single metal can occur when the solution can react chemically. This solution can provide a conductive electrical path and short electrical equipment.

10.2 Corrosion.

The amount of corrosion is a function of several factors. Among the most important factors are (Ref. 10.1):

a. The distance of the exposed site from the ocean.

b. The length of time the humidity is high — the longer a material is wet, the more the corrosion.

c. Air temperature.

d. The corrosion rate varies with elevation above sea level.

e. Corrosion is dependent on exposure direction, shelter around or near the material, and the direction and magnitude of the prevailing winds.

10.2.1 Laboratory Salt Spray Tests.

Methods have been devised to simulate the effects of salt spray in the laboratory. The following procedures have been taken from MIL-STD-810, Method 509 (Ref. 10.2), (Federal Test Method Standard No. 151; Method 811 has slight differences):

a. A salt solution is formed under the following conditions:

(1) Five percent sodium chloride in distilled water.

(2) pH between 6.5 and 7.2 and specific gravity from 1.027 to 1.041 when measured at a temperature between 33.3° and 36.1° C (92° and 97° F).

b. An air temperature of 35.0° C (95° F) is maintained in the test chamber.

c. The salt solution is atomized and applied so that 0.5 to 3.0 milliliters (0.015 to 0.10 fluid ounces) of solution will collect over an 80-square-centimeter (12.4 square in.) horizontal area in 1 hour.

d. The time of exposure of the test will vary with the material being evaluated.

Increasing the salt concentration will not accelerate the test.

Acceptance of the laboratory tests as an exact representation of the corrosion which will occur at a specific site may result in erroneous conclusions.

In any area where corrosion by the atmosphere can be an important factor, on-the-spot tests are needed. A test such as "Sample's wire-on-bolt test " (Ref. 10.3) should be conducted on the site, with tests made at various heights above the ground.

Protection from salt spray corrosion will be required in the following areas:

(1) New Orleans

(2) Gulf Transportation

(3) Eastern Test Range

(4) Panama Canal Transportation

(5) Space and Missile Test Center

(6) West Coast Transportation

(7) Sacramento

(8) Wallops Test Range

10.3 Obscuration of Optical Surfaces.

The accumulation of salt on exposed surfaces is greatest during onshore winds when many waves are breaking and forming white caps. Extremes expected are as follows (Ref. 10.4):

a. Particle size: Range from 0.1 to 20 microns, with 98 percent of the total mass greater than 0.8 microns.

b. Distribution is uniform above 3048 meters (10 000 ft), but below cloud levels.

c. Fallout of salt particles at Eastern Test Range:

(1) Maximum: 5.0×10^{-7} g cm^{-2} day^{-1}, to produce a coating on an exposed surface of 100 microns day^{-1}. This extreme occurs during precipitation.

(2) Minimum: 2.5×10^{-8} g cm^{-2} day^{-1}, to produce a coating on an exposed surface averaging 5 microns day^{-1}. This fallout occurs continuously during periods of no precipitation, and is independent of wind direction. This coating will not usually be of uniform thickness, but be spots of salt particles unevenly distributed over the optical surface.

REFERENCES

10.1 May, T. P.; and Taylor, V. G.: "Corrosion Testing in Marine Atmospheres." The Journal of Environmental Sciences, vol. 7, no. 7, December 1964, pp 23-27.

10.2 MIL-STD-810 (USAF): "Military Standard Environmental Test Method for Aerospace and Ground Equipment." 1962.

10.3 Doyle, D. P.; and Godard, Hugh P.: "A Rapid Method for Determining the Corrosivity of the Atmosphere at any Location.: Nature, vol. 200, no. 4912, December 21, 1963, pp. 1167-1168.

10.4 Brierly, William B.: "Atmosphere Sea-Salts Design Criteria Areas." The Journal of Environmental Sciences, vol. 8, No. 5, pp. 15-23, October 1965

SECTION XI. FUNGI AND BACTERIA

By

Glenn E. Daniels

Fungi (including mold) and bacteria have the highest rate of growth at temperatures between 20.0°C (68°F) and 37.7°C (100°F) and relative humidities between 75 and 95 percent (Refs. 11.1 and 11.2). Fungi and bacteria secrete enzymes and acids during their growth. These secretions can destroy most organic substances and many of their derivatives. Typical materials which will support growth of fungi and bacteria and are damaged by them if not properly protected are cotton, wood, linen, leather, paper, cork, hair, felt, lens-coating material, paints, and metals. The four groups of fungi used in the fungus-resistance tests for equipment are as follows:

Group	Organism	American Type Culture Collection Number
I	Chaetomuim globosum	6205
	Myrothecium verrucaria	9095
II	Memenialla echinata	9597
	Aspergillus niger	6275
III	Aspergillus flavus	10836
	Aspergillus terreus	10690
IV	Penicillium citrinum	9849
	Penicillium ochrochloron	9112

A suspension of mixed spores made from one species of fungus from each group is sprayed on the equipment being tested in a test chamber. The equipment is then left for 28 days in the test chamber at a temperature of 30° ± 2°C (86° ± 3.6°F) and relative humidity of 95 ± 5 percent.

Equipment is usually protected from fungi and bacteria by incorporating a fungicide-bactericide in the material, by a fungicide-bactericide spray, or by reducing the relative humidity to a degree where growth will not take place. A unique method used in the Canal Zone to protect delicate, expensive bearings in equipment was to maintain a pressure (with dry air or nitrogen) slightly above the outside atmosphere (few millibars) within the working parts of the equipment, thus preventing fungi from entering equipment.

Proper fungus- and bacteria-proofing measures are required at the following areas:

(1) River Transportation

(2) New Orleans

(3) Gulf Transportation

(4) Panama Canal Transportation

(5) Eastern Test Range

REFERENCES

11.1 "Climatic and Environmental Criteria for Aircraft Design." ANC-22, Munitions Board Aircraft Committee, 1952. (Available from U. S. Government Printing Office, Washington, D. C.)

11.2 Schulze, W. M., "Influence of Climate on Material Stressing Under Tropical Conditions," B/Min of Aircraft RTP Trans 2539, (ATI 19792) Jan. 1943.

N74-16304

SECTION XII. ATMOSPHERIC OXIDANTS

By

Glenn E. Daniels

12.1 Introduction.

Air pollution at the earth's surface has received considerable publicity in recent years because the pollutants reduce visibility, cause damage to crops, irritate the eyes, and have an objectional odor. The ingredients which cause the air pollution are a mixture of oxides of organic matter (mostly nitrogen oxides and hydrocarbons) and ozone. In the Los Angeles area, the mixing of the organic oxides, ozone, and water droplets forms the well known smog. Ozone, although considered one of the rare atmospheric gases, needs consideration in design because of its chemical reaction (oxidation) with organic materials, especially rubber, which becomes hard and brittle under tension in a few minutes time. The presence in smog of strong oxidizing agents closely resembling ozone in their action on organic compounds leads one to believe that ozone exists in smog in greater quantities than in the normal atmosphere.

12.2 Ozone.

Ozone, in high concentrations, is explosive and poisonous. One hundred (100) parts per hundred million (phm) of ozone is toxic to man sufficient to cause death. The use of the atmosphere at high altitudes for breathing by pressurizing, requires removal of the ozone. Ozone may be formed in high concentrations by short wavelength ultraviolet light (below 2537Å), or by the arcing or discharge of electrical currents. A motor or generator with arcing brushes is an excellent source of ozone. The natural ozone concentration at the earth's surface is normally less than 3 parts per hundred million (phm), except during periods of intense smog, where it may exceed 5 phm. Ozone concentration increases with altitude, with the maximum concentration of 1100 parts per hundred million being at about 30 km (98,000 ft).

Maximum expected values of natural atmospheric ozone, for purposes of design studies, are as follows: (a) surface, at all areas, a maximum concentration of 3 phm except during smog, when the maximum will be 6 phm, and (b) maximum concentration, with altitude, is given in Table 12.1 (Ref. 12.1).

TABLE 12.1 DISTRIBUTION OF MAXIMUM DESIGN VALUES OF OZONE CONCENTRATION WITH ALTITUDE FOR ALL LOCATIONS

Geometric Altitude (km)	Geometric Altitude (ft)	Ozone (parts per hundred million)	Ozone Concentration (cm/km)
SRF*	SRF*	6	0.006
9.1	30,000	30	0.010
15.2	50,000	200	0.030
21.3	70,000	700	0.040
27.4	90,000	1100	0.024
33.5	110,000	1100	0.009
39.6	130,000	600	0.002
45.7	150,000	400	0.0005

*SRF - Surface

12.3 Atmospheric Oxidants.

At the surface, a maximum of 60 parts per hundred million of oxidants composed of nitrogen oxides, hydrocarbons, sulphur dioxide, sulphur trioxides, peroxides, and ozone can be expected for 72 hours when smog occurs. The effect of these oxidants on rubber cracking and in some chemical reactions will be equivalent to 22 parts per hundred million of ozone, but not necessarily equivalent to this concentration of ozone in other reactions (Ref. 12.2).

REFERENCES

12.1 Ditaranto, R. A.; and Lamb, J. J.: "Preliminary Investigation of Hyper-Environments and Methods of Simulation, Part I, Natural and Induced Environments Above 75,000 ft." WADC Technical Report 57-456, Part I, ASTIA Doc. No. AD-142002, 1957.

12.2 Haagen-Smit, A. J.: "Chemistry and Physiology of Los Angeles Smog." Industrial and Engineering Chemistry, vol. 44, no. 6, June 1952, pp. 1342-1346.

SECTION XIII. ATMOSPHERIC COMPOSITION

By

Glenn E. Daniels

13.1 Composition.

The earth's atmosphere is made up of a number of gases in different relative amounts. Near sea level and up to about 90 km, the amount of these atmospheric gases in clean, relatively dry air is practically constant. Four of these gases, nitrogen, oxygen, argon, and carbon dioxide, make up 99.99 percent by volume of the atmosphere. Two gases, ozone and water vapor, change in relative amounts, but the total amount of these two is very small compared to the amount of the other gases.

The atmospheric composition shown in Table 13.1 can be considered valid up to 90 km geometric altitude. Above 90 km, mainly because of molecular dissociation and diffusive separation, the composition changes from that shown in Table 13.1. Reference is made to the Space Environment Criteria Guidelines document (Ref. 13.2) for additional information on composition above 90 km.

13.2 Molecular Weight.

The atmospheric composition shown in Table 13.1 gives a molecular weight of 28.9644 for dry air (Ref. 13.1). This value of molecular weight can be used as constant up to 90 km, and is equivalent to the value 28.966 on the basis of a molecular weight of 16 for oxygen.

The molecular weight of the atmosphere with relation to height is shown in Table 13.2.

TABLE 13.1 NORMAL ATMOSPHERIC COMPOSITION FOR CLEAN, DRY AIR AT ALL LOCATIONS (VALID TO 90 KILOMETERS GEOMETRIC ALTITUDE)

Gas	Percent by Volume	Percent by Weight*
Nitrogen (N_2)	78.084	75.520
Oxygen (O_2)	20.9476	23.142
Argon (Ar)	0.934	1.288
Carbon dioxide (CO_2)	0.0314	0.048
Neon (Ne)	1.818×10^{-3}	1.27×10^{-3}
Helium (He)	5.24×10^{-4}	7.24×10^{-5}
Krypton (Kr)	1.14×10^{-4}	3.30×10^{-4}
Xenon (Xe)	8.7×10^{-6}	3.9×10^{-5}
Hydrogen (H_2)	5×10^{-5}	3×10^{-6}
Methane (CH_4)	2×10^{-4}	1×10^{-4}
Nitrous Oxide (N_2O)	5×10^{-5}	8×10^{-5}
Ozone (O_3) summer	0 to 7×10^{-6}	0 to 1.1×10^{-5}
winter	0 to 2×10^{-6}	0 to 3×10^{-6}
Sulfur dioxide (SO_2)	0 to 1×10^{-4}	0 to 2×10^{-4}
Nitrogen dioxide (NO_2)	0 to 2×10^{-6}	0 to 3×10^{-6}
Ammonia (NH_3)	0 to trace	0 to trace
Carbon monoxide (CO)	0 to trace	0 to trace
Iodine (I_2)	0 to 1×10^{-6}	0 to 9×10^{-6}

*On basis of Carbon 12 isotope scale for which $C^{12} = 12.000$, as adopted by the International Union of Pure and Applied Chemistry meeting, Montreal, in 1961.

TABLE 13.2 MOLECULAR WEIGHT OF THE ATMOSPHERE FOR ALL LOCATIONS

Geometric Altitude (km)	(ft)	Molecular Weight
SRF* to 90	SRF* to 295,000	28.9644 28.9644

*SRF - Surface

REFERENCES

13.1 "U. S. Standard Atmosphere, 1962." United States Government Printing Office, Washington 25, D.C., 1962.

13.2 "Space and Planetary Environment Criteria Guidelines for Use in Space Vehicle Development (1971 Revision)." TM X-64627, November 15, 1971. NASA-Marshall Space Flight Center, Huntsville, Alabama.

N74-16306

SECTION XIV. INFLIGHT THERMODYNAMIC PROPERTIES

By

S. Clark Brown, Glenn E. Daniels, Dale L. Johnson and Orvel E. Smith

14.1 Introduction

This section presents the inflight thermodynamic parameters (temperature, pressure, and density) of the atmosphere. Mean and extreme values of the thermodynamic parameters given here can be used in application of many aerospace problems, such as (1) research planning and engineering design of remote earth sensing systems; (2) vehicle design and development; and (3) vehicle trajectory analysis, dealing with vehicle thrust, dynamic pressure, aerodynamic drag, aerodynamic heating, vibration, structural and guidance limitations, and reentry analysis. Atmospheric density plays a very important role in most of the above problems. The first part of this section gives median and extreme values of these thermodynamic variables with respect to altitude. An approach is presented for temperature, pressure, and density as independent variables, with a method to obtain simultaneous values of these variables at discrete altitude levels. A subsection on reentry is presented, giving atmospheric models to be used for reentry heating, trajectory, etc., analysis. Various parts of Section XIV have been updated since the last revision of this document (Ref. 14.1).

Standard Sea Level Values used are:

	Metric Units	U. S. Customary Units
Temperature	15.0° C or 288.15° K	59° F or 518.67° R
Pressure	1.013250×10^5 newton m^{-2}	2116.22 lb ft^{-3} or 14.696 lb in^{-2}
Density	1.2250 kg m^{-3}	0.076474 lb ft^{-3}

14.2 Atmospheric Temperature

14.2.1 Air Temperature at Altitude

Median and extreme air temperatures for the following test ranges were compiled from radiosonde frequency distributions of temperature from 0 through 30 kilometers altitude. Meteorological rocketsonde mean and extreme temperatures for the different ranges were used above 30 kilometers altitude.

a. Eastern Test Range air temperature values with altitude are given in Table 14.1 (Ref. 14.3).

b. Space and Missile Test Center air temperature values with altitude are given in Table 14.2.

c. Wallops Test Range air temperature values with altitude are given in Table 14.3.

d. White Sands Missile Range air temperature values with altitude are given in Table 14.4.

e. Edwards Air Force Base air temperature values with altitude are given in Table 14.5.

A comprehensive listing of the extremes of surface temperature for different locations can be obtained from Table 2.6 on page 2.25.

14.2.2 Compartment Extreme Cold Temperature

Extreme cold temperatures during aircraft flight, when compartments are not heated, are given in Table 14.6.

14.3 Atmospheric Pressure

14.3.1 Definition

Atmospheric pressure (also called barometric pressure) is the force exerted, as a consequence of gravitational attraction, by the mass of the column of air of unit cross section lying directly above the area in question. It is expressed as force per unit area (newtons per square meter or newtons per square centimeter).

14.3.2 Pressure at Altitude

Atmospheric pressure extremes for all locations are given in Table 14.7. These data were taken from the radiosonde pressure frequency distributions for the four test ranges. Rocketsonde pressure means and extremes were used above 25 kilometers altitude.

Mean and extreme values of station pressure for different locations are given in Table 7.1, whereas nominal values aloft are given in Tables 14.12 and 14.13 and in Ref. 14.6.

TABLE 14.1 EASTERN TEST RANGE AIR TEMPERATURES AT VARIOUS ALTITUDES

Geometric Altitude (km)	Minimum		Median		Maximum	
	(°C)	(°F)	(°C)	(°F)	(°C)	(°F)
SRF (0.005 MSL)	-3.9	25	23.5	74	37.2	99
1	-8.9	16	17.4	63	27.8	82
2	-10.0	14	12.2	54	21.1	70
3	-11.1	12	7.1	45	16.1	61
4	-13.9	7	1.8	35	11.1	52
5	-20.0	-4	-4.1	25	5.0	41
6	-26.1	-15	-10.5	13	-1.1	30
7	-33.9	-29	-17.4	1	-7.2	19
8	-41.1	-42	-24.8	-13	-13.9	7
9	-50.0	-58	-32.4	-26	-21.1	-6
10	-56.1	-69	-40.0	-40	-30.0	-22
16.2	-80.0	-112	-70.3	-95	-57.8	-72
20	-76.1	-105	-62.8	-81	-47.8	-54
30	-58.9	-74	-42.4	-44	-30.0	-22
35	-47.4	-53	-30.6	-23	-14.6	6
40	-36.7	-34	-17.8	0	1.9	35
45	-23.0	-9	-6.3	21	12.8	55
50	-18.2	-1	-2.5	27	22.0	72
55	-34.4	-30	-12.4	10	18.9	66
60 a	-28.5	-19	-26.1	-15	17.0	63

a. For higher altitudes see References 14.3, 14.4, 14.5, and 14.6 (13).

14.4 Atmospheric Density

14.4.1 Definition

Density (ρ) is the ratio of the mass of a substance to its volume. (It is also defined as the reciprocal of specific volume.) Density is usually expressed in grams or kilograms per cubic centimeter or cubic meter.

TABLE 14.2 SPACE AND MISSILE TEST CENTER
(Vandenberg AFB, California)
AIR TEMPERATURES AT VARIOUS ALTITUDES

Geometric Altitude (km)	Minimum		Median		Maximum	
	(°C)	(°F)	(°C)	(°F)	(°C)	(°F)
SRF (0.1 MSL)	-1.1	30	12.7	55	37.2	99
1	-3.6	26	13.3	56	33.4	92
2	-7.0	19	10.1	50	28.0	82
3	-15.2	5	5.1	41	17.6	64
4	-22.6	-9	-1.0	30	12.1	54
5	-29.7	-22	-7.5	18	3.3	38
6	-35.6	-32	-14.4	6	-2.7	27
7	-43.3	-46	-21.8	-7	-9.9	14
8	-47.4	-53	-29.5	-21	-15.9	3
9	-51.3	-60	-37.3	-35	-26.8	-16
10	-57.0	-71	-44.6	-48	-31.2	-24
16.3	-76.0	-105	-64.0	-83	-51.0	-60
20	-74.9	-103	-59.8	-76	-49.0	-56
30	-63.7	-83	-42.7	-45	-29.4	-21
40	-42.2	-44	-19.3	-3	17.8	64
45	-30.5	-23	-5.8	21	27.6	82
50	-18.2	-1	-2.0	28	28.0	82
55	-21.8	-7	-6.8	20	31.6	89
60	-25.1	-13	-20.5	-5	35.7	96
a						

a. For higher altitudes see References 14.2, 14.4, and 14.5.

TABLE 14.3 WALLOPS TEST RANGE AIR TEMPERATURES AT VARIOUS ALTITUDES

Geometric Altitude (km)	Minimum		Median		Maximum	
	(°C)	(°F)	(°C)	(°F)	(°C)	(°F)
SRF (0.09 MSL)	-15.0	5	13.9	57	39.4	103
1	-21.1	-6	10.0	50	31.1	88
2	-26.1	-15	6.1	43	22.8	73
3	-30.0	-22	1.0	33	15.0	59
4	-33.9	-29	-4.1	25	7.8	46
5	-40.0	-40	-10.0	14	2.8	37
6	-43.9	-47	-16.8	2	-1.1	30
7	-47.8	-54	-24.0	-11	-7.8	18
8	-50.6	-59	-31.5	-25	-15.0	5
9	-56.1	-69	-38.7	-38	-21.1	-6
10	-61.1	-78	-45.9	-51	-27.2	-17
16.5	-77.8	-108	-62.2	-80	-47.2	-53
20	-71.1	-96	-58.3	-73	-46.1	-51
30	-65.0	-85	-43.9	-47	-27.2	-17
40	-35.7	-32	-19.3	-3	5.8	42
45	-27.7	-18	-5.7	22	14.8	59
50	-24.9	-13	-3.2	26	21.8	71
55	-22.6	-9	-5.6	22	35.0	95
a						

a. For higher altitudes see References 14.2, 14.4, 14.5, and 14.6 (15).

TABLE 14.4 WHITE SANDS MISSILE RANGE AIR TEMPERATURES AT VARIOUS ALTITUDES

Geometric Altitude (km)	Minimum		Median		Maximum	
	(°C)	(°F)	(°C)	(°F)	(°C)	(°F)
SRF (1.3 MSL)	-21.1	-6	17.8	64	41.1	106
2	-11.7	11	13.1	56	31.1	88
3	-18.9	-2	6.2	43	22.2	72
4	-23.9	-11	-0.2	32	12.8	55
5	-31.1	-24	-6.7	20	6.1	43
6	-36.1	-33	-13.6	7	0.0	32
7	-42.2	-44	-20.5	-5	-7.2	19
8	-48.9	-56	-29.8	-22	-13.9	7
9	-55.0	-67	-36.7	-34	-21.1	-6
10	-60.0	-76	-43.3	-46	-27.2	-17
16.5	-80.0	-112	-67.1	-89	-47.8	-54
20	-77.8	-108	-60.0	-76	-52.2	-62
30	-58.9	-74	-43.2	-46	-26.1	-15
35	-52.2	-62	-32.2	-26	-7.8	18
40	-41.8	-43	-18.7	-2	5.0	41
45	-30.5	-23	-4.7	24	19.6	67
50	-29.1	-20	-1.6	29	25.9	79
55	-28.7	-20	-4.6	24	30.2	86
60	-35.8	-32	-20.4	-5	28.0	82
65	-36.5	-34	-38.1	-37	31.3	88
a						

a. For higher altitudes see References 14.2, 14.4, 14.5, and 14.6 (14).

TABLE 14.5 EDWARDS AFB TEMPERATURES AT VARIOUS ALTITUDES

Geometric Altitude (km)	Minimum		Median		Maximum	
	(°C)	(°F)	(°C)	(°F)	(°C)	(°F)
SRF (0.7 MSL)	-15.0	5	16.7	62	43.3	110
1	-6.0	21	16.2	61	35.3	96
2	-12.9	9	11.4	53	26.2	79
3	-16.9	2	5.3	42	19.0	66
4	-23.4	-10	-1.3	30	10.7	51
5	-29.7	-21	-8.2	17	5.2	41
6	-35.2	-31	-15.3	4	-2.9	27
7	-42.0	-44	-22.8	-9	-12.1	10
8	-48.9	-56	-30.5	-23	-17.4	1
9	-55.0	-67	-38.3	-37	-24.2	-12
10	-58.8	-74	-45.7	-50	-30.8	-23
17.8	-78.0	-108	-63.3	-82	-53.0	-63
20	-73.5	-100	-60.2	-76	-49.6	-57
25	-73.2	-100	-52.3	-62	-40.4	-41
30	-66.1	-87	-45.1	-49	-29.1	-20
40	-42.2	-44	-19.3	-3	17.8	64
45	-30.5	-23	-5.8	21	27.6	82
50	-18.2	-1	-2.0	28	28.0	82
55	-21.8	-7	-6.8	20	31.6	89
60	-25.1	-13	-20.5	-5	35.7	96
a						

a. For higher altitudes see References 14.2, 14.4, and 14.5.

TABLE 14.6 COMPARTMENT DESIGN COLD TEMPERATURE EXTREMES FOR ALL LOCATIONS

Maximum Flight Altitude (Geometric) of Aircraft Used for Transport		Compartment Cold Temperature Extreme	
(m)	(ft)	(°C)	(°F)
4 550	15 000	-35.0	-31
6 100	20 000	-45.0	-49
7 600	25 000	-50.0	-58
9 150	30 000	-57.0	-71
15 200	50 000	-75.0	-103

TABLE 14.7 ATMOSPHERIC PRESSURE-HEIGHT EXTREMES FOR ALL LOCATIONS

Geometric Altitude (above mean sea level)		Pressure			
		Maximum		Minimum	
(km)	(ft)	(mb)	(lb in.$^{-2}$)	(mb)	(lb in.$^{-2}$)
0	0	(Use values in Table 7.1 for surface pressure for each station)			
3	9 800	730	10.6	680	9.86
6	19 700	510	7.40	457	6.63
10	32 800	295	4.28	251	3.64
15	49 200	135	1.96	116	1.68
20	65 600	60	8.7×10^{-1}	51	7.4×10^{-1}
25	82 000	30	4.4×10^{-1}	22	3.2×10^{-1}
30	98 400	14.5	2.1×10^{-1}	10.4	1.5×10^{-1}
35	114 800	7.4	1.1×10^{-1}	4.9	7.1×10^{-2}
40	131 200	3.8	5.5×10^{-2}	2.4	3.5×10^{-2}
45	147 600	2.0	2.9×10^{-2}	1.2	1.7×10^{-2}
50	164 000	1.2	1.7×10^{-2}	6.1×10^{-1}	8.8×10^{-3}
55	180 400	6.0×10^{-1}	8.7×10^{-3}	3.1×10^{-1}	4.5×10^{-3}
60	196 800	3.2×10^{-1}	4.6×10^{-3}	1.6×10^{-1}	2.3×10^{-3}
65	213 300	1.7×10^{-1}	2.5×10^{-3}	8.3×10^{-2}	1.2×10^{-3}
70	229 700	8.5×10^{-2}	1.2×10^{-3}	4.1×10^{-2}	5.9×10^{-4}
75	246 100	3.1×10^{-2}	4.5×10^{-4}	2.1×10^{-2}	3.0×10^{-4}
80	262 500	1.4×10^{-2}	2.0×10^{-4}	8.9×10^{-3}	1.3×10^{-4}
85	278 900	5.9×10^{-3}	8.6×10^{-5}	3.7×10^{-3}	5.4×10^{-5}
90	295 300	2.6×10^{-3}	3.8×10^{-5}	1.4×10^{-3}	2.0×10^{-5}

14.4.2 Atmospheric Density at Altitude

The density of the atmosphere decreases rapidly with height, decreasing to one-half of the surface at 7 kilometers altitude. Density is also variable at a fixed altitude, with the greatest relative variability occurring at about 70 kilometers altitude in the high northern latitudes (60° N) for altitude ranges up to 90 kilometers. Other altitudes of maximum density variability occur around 16 kilometers and 0 kilometers. Altitudes of minimum variability (isopycnic levels) occur around 8, 24, and 90 kilometers altitude.

Density varies with latitude in the northern hemisphere, with the mean annual density near the surface increasing to the north. In the region around 8 kilometers, the density variation with latitude and season is small (isopycnic level). Above 8 kilometers to about 28 kilometers, the mean annual density decreases toward the north. Mean-monthly densities between 30 and 90 kilometers increase toward the north in July and toward the south in January.

Considerable data are now available on the mean density and its variability below 30 kilometers at the various test ranges from the data collected for preparation of the IRIG Range Reference Atmospheres (Ref. 14.6). Additional information on the seasonal variability of density below 30 kilometers is presented in an article by J. W. Smith (Ref. 14.7). Above 30 kilometers, the data are less plentiful and the accuracy of the temperature measurements (used to compute densities) becomes poorer with altitude.

Extreme minimum and maximum values of density for the Eastern Test Range and Vandenberg AFB are given in Table 14.8. These extreme density values approach the $\pm 3\sigma$ (corresponding to the normal distribution) density values.

The relative density deviations for Cape Kennedy and Vandenberg, as given in Table 14.8, are respectively defined as percentage departures from the Patrick Reference Atmosphere (Ref. 14.3) and the Vandenberg Reference Atmosphere (Ref. 14.10).

Median values of surface density for different ranges are given in Table 8.1 with nominal values with altitude being given in Tables 14.12 and 14.13 and in Reference 14.6.

TABLE 14.8 DENSITY HEIGHT MAXIMUM (≈ +3 SIGMA), AND MINIMUM (≈ -3 SIGMA) FOR CAPE KENNEDY, FLORIDA (ETR) AND VANDENBERG AFB, CALIFORNIA (SAMTEC)

Altitude[a]		Cape Kennedy Density				Vandenberg Density			
		Maximum		Minimum		Maximum		Minimum	
(km)	(ft)	(kg m^{-3})	% Deviation from PRA-63	(kg m^{-3})	% Deviation from PRA-63	(kg m^{-3})	% Deviation from VRA-71	(kg m^{-3})	% Deviation from VRA-71
0	0	1.326	12.0	1.141	-3.6	1.302	5.3	1.140	-7.8
2	6 600	1.047	6.1	9.497×10^{-1}	-3.0	1.046	6.1	9.518×10^{-1}	-3.5
4	13 100	8.287×10^{-1}	3.7	7.824×10^{-1}	-2.1	8.484×10^{-1}	5.7	7.766×10^{-1}	-3.3
6	19 700	6.706×10^{-1}	3.2	6.355×10^{-1}	-2.2	6.906×10^{-1}	5.7	6.299×10^{-1}	-3.6
8	26 200	5.428×10^{-1}	3.1	5.055×10^{-1}	-4.0	5.601×10^{-1}	6.0	4.971×10^{-1}	-6.0
10	32 800	4.352×10^{-1}	3.0	3.938×10^{-1}	-6.8	4.624×10^{-1}	9.5	3.835×10^{-1}	-9.2
15	49 200	2.345×10^{-1}	7.0	1.979×10^{-1}	-9.7	2.337×10^{-1}	12.0	1.851×10^{-1}	-11.3
20	65 600	1.002×10^{-1}	7.5	8.751×10^{-2}	-6.1	1.001×10^{-1}	8.8	8.420×10^{-2}	-8.5
25	82 000	4.274×10^{-2}	5.9	3.790×10^{-2}	-6.1	4.460×10^{-2}	10.0	3.634×10^{-2}	-10.4
30	98 400	1.976×10^{-2}	7.8	1.700×10^{-2}	-7.3	2.085×10^{-2}	13.0	1.634×10^{-2}	-11.5
35	114 800	9.427×10^{-3}	10.3	7.640×10^{-3}	-10.6	9.786×10^{-3}	13.8	7.505×10^{-3}	-12.8
40	131 200	4.637×10^{-3}	12.5	3.512×10^{-3}	-14.8	4.747×10^{-3}	15.0	3.424×10^{-3}	-17.0
50	164 000	1.275×10^{-3}	16.3	8.630×10^{-4}	-21.3	1.325×10^{-3}	22.0	8.473×10^{-4}	-22.0
60	196 800	3.946×10^{-4}	19.4	2.465×10^{-4}	-25.4	4.422×10^{-4}	35.0	2.359×10^{-4}	-28.0
70	229 700	1.100×10^{-4}	23.6	6.666×10^{-5}	-25.1	1.203×10^{-4}	32.0	6.197×10^{-5}	-32.0
80	262 500	2.342×10^{-5}	19.0	1.596×10^{-5}	-18.9	2.617×10^{-5}	26.0	1.433×10^{-5}	-31.0
90	295 300	3.684×10^{-6}	10.9	2.930×10^{-6}	-11.8	4.177×10^{-6}	20.0	2.785×10^{-6}	-20.0

a. Geometric altitude above mean sea level.

14.5 Simultaneous Values of Temperature, Pressure, and Density at Discrete Altitude Levels

14.5.1 Introduction

This subsection presents simultaneous values for temperature, pressure, and density as guidelines for aerospace vehicle design considerations. The necessary assumptions and the lack of sufficient statistical data sample restrict the precision by which these data can presently be presented; therefore, the analysis is limited to Cape Kennedy.

14.5.2 Method of Determining Simultaneous Value

An aerospace vehicle design problem that often arises in considering natural environmental data is stated by way of the following question: "How should the extremes (maxima and minima) of temperature, pressure, and density be combined (a) at discrete altitude levels? (b) versus altitude?" As an example, suppose one desires to know what temperature and pressure should be used simultaneously with a maximum density at a discrete altitude. From statistical principles set forth by Dr. C. E. Buell in Reference 14.8, the solution results by allowing mean density plus three standard deviations to represent maximum density and using the coefficents of variation, correlations, and mean values as expressed in Equation (14.1).

$$\text{maximum } \rho = (\bar{\rho} + 3\sigma_{\rho}) = \bar{\rho}\left(1 + 3\,\frac{\sigma_{\rho}}{\bar{\rho}}\right)$$

$$= \bar{\rho}\left\{1 + 3\left[\underbrace{\left(\frac{\sigma_P}{\bar{P}}\right) r(P\rho)}_{(A)} - \underbrace{\left(\frac{\sigma_T}{\bar{T}}\right) r(\rho T)}_{(B)}\right]\right\} \qquad (14.1)$$

TABLE 14. 9 COEFFICIENTS OF VARIATION AND DISCRETE ALTITUDE LEVEL CORRELATION COEFFICIENTS BETWEEN PRESSURE - DENSITY r(Pρ); PRESSURE - TEMPERATURE r(PT); AND DENSITY - TEMPERATURE r(ρT), CAPE KENNEDY, ANNUAL

ALTITUDE	COEFFICIENTS OF VARIATION (CV)			CORRELATION COEFFICIENTS (r)		
(km)	$\sigma(\rho)/\bar{\rho}$ (percent)	$\sigma(P)/\bar{P}$ (percent)	$\sigma(T)/\bar{T}$ (percent)	r(Pρ) (unitless)	r(PT) (unitless)	r(ρT) (unitless)
0	1.8000	.6000	1.5000	.6250	-0.3500	-0.9500
1	1.7000	.5500	1.6000	.3382	-0.0156	-0.9462
2	1.5000	.8000	1.5900	.1508	.3609	-0.8675
3	1.1800	.9800	1.5700	-0.0485	.6606	-0.7818
4	.9700	.8500	1.4000	-0.1799	.7318	-0.8021
5	.8000	.8700	1.3400	-0.2864	.8203	-0.7830
6	.7400	.8400	1.2600	-0.2690	.8246	-0.7666
7	.8800	.9800	1.4200	-0.1633	.7913	-0.7324
8	.9000	1.1300	1.4700	-0.0364	.7910	-0.6402
9	1.1800	1.4700	1.6200	.2678	.7124	-0.4854
10	1.6300	1.7500	1.7200	.4840	.5588	-0.4553
11	1.8800	1.8000	1.7800	.5328	.4485	-0.5174
12	2.1500	1.8700	1.8500	.5841	.3320	-0.5717
13	2.3800	1.9000	1.8500	.6470	.1946	-0.6220
14	2.6200	1.9200	1.7700	.7373	-0.0066	-0.6804
15	2.7800	1.8800	1.6700	.8107	-0.2238	-0.7520
16	2.8800	1.8400	1.7100	.8262	-0.3154	-0.7953
17	2.8800	1.8000	1.7000	.8338	-0.3537	-0.8113
18	2.7500	1.7500	1.7000	.8036	-0.2706	-0.7904
19	2.5000	1.7800	1.6700	.7449	-0.0492	-0.7031
20	2.2700	1.8500	1.6500	.6969	.1625	-0.5944
21	2.0800	1.9500	1.6200	.6786	.3325	-0.4672
22	1.9800	2.1200	1.5700	.7087	.4565	-0.3041
23	1.9200	2.3200	1.4800	.7721	.5659	-0.0870
24	1.9500	2.4000	1.4300	.8032	.5831	-0.0157
25	2.000	2.4300	1.4200	.8116	.5682	-0.0196
26	2.0800	2.5000	1.5000	.8006	.5565	-0.0523
27	2.1500	2.6000	1.5800	.7948	.5640	-0.0528
28	2.2300	2 6700	1.7500	.7591	.5584	-0.1161
29	2.3700	2.6300	1.8700	.7249	.4877	-0.2479
30	2.5200	2.6300	1.9200	.7228	.4211	-0.3224
31	2.7000	2.7000	2.000	.7257	.3704	-0.3704
32	2.8800	2.7500	2.0800	.7279	.3142	-0.4222
33	3.0700	2.7300	2.1700	.7260	.2310	-0.5014
34	3.2700	2.6800	2.2300	.7361	.1223	-0.5817
35	3.4800	2.6000	2.3200	.7454	.0027	-0.6647
36	3.7000	2.5000	2.4300	.7587	-0.1263	-0.7421
37	3.9200	2.3700	2.5500	.7793	-0.2686	-0.8129
38	4.1200	2.4600	2.6300	.7947	-0.3096	-0.8232
39	4.3300	2.6400	2.6900	.8084	-0.3199	-0.8163
40	4.5500	2.7900	2.7680	.8220	-0.3442	-0.8176
41	4.7500	2.8600	3.0200	.7958	-0.3046	-0.8192
42	4.9300	2.9200	3.2600	.7712	-0.2706	-0.8215
43	5.1300	3.0000	3.3400	.7850	-0.3075	-0.8309
44	5.3200	3.1800	3.3500	.8037	-0.3270	-0.8252
45	5.5000	3.2400	3.6000	.7797	-0.2912	-0.8261
46	5.6700	3.3200	3.8300	.7571	-0.2539	-0.8242
47	5.8300	3.4100	3.9800	.7489	-0.2402	-0.8232
48	5.9800	3.4800	4.1900	.7284	-0.2090	-0.8223
49	6.1300	3.5900	4.1400	.7572	-0.2540	-0.8241
50	6.2700	3.6900	4.1900	.7644	-0.2633	-0.8232
51	6.4200	3.8200	4.0800	.7984	-0.3201	-0.8260
52	6.5500	3.9100	4.1800	.7950	-0.3103	-0.8234
53	6.7000	4.0100	4.2700	.7953	-0.3089	-0.8222
54	6.8000	4.0700	4.3100	.7990	-0.3164	-0.8232
55	6.9200	4.1400	4.3700	.8016	-0.3220	-0.8241
56	7.0300	4.2100	4.4200	.8043	-0.3267	-0.8244
57	7.1500	4.2800	4.4700	.8081	-0.3351	-0.8258
58	7.2700	4.3600	4.5100	.8127	-0.3434	-0.8263
59	7.3700	4.4200	4.5400	.8172	-0.3530	-0.8277
60	7.4700	4.4800	4.5900	.8188	-0.3565	-0.8283

TABLE 14.9 COEFFICIENTS OF VARIATION AND DISCRETE ALTITUDE LEVEL CORRELATION COEFFICIENTS BETWEEN PRESSURE - DENSITY r(Pρ); PRESSURE - TEMPERATURE r(PT); AND DENSITY - TEMPERATURE r(ρT), CAPE KENNEDY, ANNUAL (Concluded)

ALTITUDE	COEFFICIENTS OF VARIATION (CV)			CORRELATION COEFFICIENTS (r)		
(km)	$\sigma(\rho)/\rho$ (percent)	$\sigma(P)/P$ (percent)	$\sigma(T)/T$ (percent)	r(Pρ) (unitless)	r(PT) (unitless)	r(ρT) (unitless)
61	7.5700	4.5400	4.6300	.8217	0.3629	-0.8293
62	7.6500	4.7000	4.8600	.7926	0.2805	-0.8076
63	7.7500	4.9000	5.0000	.7778	-0.2256	-0.7878
64	7.8300	5.1500	5.1500	.7602	-0.1558	-0.7602
65	7.9000	5.3800	5.3800	.7342	-0.0781	-0.7342
66	7.9800	5.5700	5.4400	.7324	-0.0505	-0.7170
67	8.0300	5.6600	5.4700	.7326	-0.0408	-0.7099
68	8.0700	5.7700	5.4000	.7437	-0.0429	-0.6998
69	8.1000	5.8200	5.5100	.7331,	-0.0215	-0.6957
70	8.1200	5.8700	5.4900	.7369	-0.0208	-0.6911
71	8.1200	5.8900	5.4700	.7392	-0.0205	-0.6885
72	8.0700	5.7900	5.3800	.7459	-0.0426	-0.6973
73	8.1200	5.6500	5.2900	.7615	-0.1008	-0.7216
74	8.0700	5.5000	5.1700	.7733	-0.1432	-0.7383
75	7.9000	5.2900	5.4100	.7313	-0.0901	-0.7452
76	7.6800	4.9900	5.6500	.6779	-0.0383	-0.7606
77	7.3800	5.0100	6.1600	.5628	.1390	-0.7403
78	7.0500	5.0400	6.5200	.4587	.2771	-0.7267
79	6.6800	5.1100	6.8400	.3508	.4045	-0.7145
80	6.3200	5.2700	6.7800	.3265	.4730	-0.6784
81	5.9500	5.3600	6.7200	.2975	.5342	-0.6482
82	5.5800	5.5200	6.6600	.2800	.5942	-0.6057
83	5.2500	5.1300	6.6100	.1891	.6259	-0.6475
84	4.9200	4.7800	6.5600	.0855	.6645	-0.6877
85	4.6300	4.4700	6.5100	-0.0232	.7032	-0.7272
86	4.4000	4.1900	6.4500	-0.1271	.7363	-0.7647
87	4.2000	3.9600	6.4000	-0.2296	.7694	-0.7983
88	4.0200	4.0500	6.3400	-0.2344	.7874	-0.7838
89	3.8800	4.1400	6.2800	-0.2255	.7986	-0.7665
90	3.7800	4.0400	5.9600	-0.1608	.7798	-0.7432

The associated values for pressure and temperature are the last two terms of Equation (14.1), (A) and (B), multiplied by $\overline{P}$ and $\overline{T}$, respectively, and then this result is added to $\overline{P}$ and $\overline{T}$ respectively. Appropriate values of r and CV are obtained from Table 14.9.

In general, the three extreme ρ, P, and T equations of interest are

$$\text{extreme } \rho = \left(\bar{\rho} \pm M\sigma_{\rho}\right) = \bar{\rho}\left[1 \pm M\left(\frac{\sigma_{\rho}}{\bar{\rho}}\right)\right]$$

$$= \bar{\rho}\left\{1 \pm M\left[\left(\frac{\sigma_P}{\overline{P}}\right) r(P\rho) - \left(\frac{\sigma_T}{\overline{T}}\right) r(\rho T)\right]\right\} \qquad (14.7a)$$

$$\text{extreme } P = \left(\bar{P} \pm M\sigma_P\right) = \bar{P}\left[1 \pm M\left(\frac{\sigma_P}{\bar{P}}\right)\right]$$

$$= \bar{P}\left\{1 \pm M\left[\left(\frac{\sigma_\rho}{\bar{\rho}}\right) r(P\rho) + \left(\frac{\sigma_T}{\bar{T}}\right) r(PT)\right]\right\} \qquad (14.3)$$

$$\text{extreme } T = \left(\bar{T} \pm M\sigma_T\right) = \bar{T}\left[1 \pm M\left(\frac{\sigma_T}{\bar{T}}\right)\right]$$

$$= \bar{T}\left\{1 \pm M\left[\left(\frac{\sigma_P}{\bar{P}}\right) r(PT) - \left(\frac{\sigma_\rho}{\bar{\rho}}\right) r(\rho T)\right]\right\}, \qquad (14.4)$$

where M denotes the multiplication factor to give the desired deviation. The values of M for the normal distribution and the associated percentile levels are as follows:

	M		Percentile
mean	-3	standard deviations	0.135
mean	-2	standard deviations	2.275
mean	-1	standard deviations	15.866
mean	±0	standard deviations = median	50.000
mean	+1	standard deviations	84.134
mean	+2	standard deviations	97.725
mean	+3	standard deviations	99.865

The two associated atmospheric parameters that deal with a third extreme parameter are listed, in more detail, in the following chart.

	For Extreme Density	For Extreme Temperature	For Extreme Pressure
$P_{assoc.}$ =	$\bar{P}\left[1 \pm \left\{M\left(\frac{\sigma_P}{\bar{P}}\right) r(P\rho)\right\}\right]$	$\bar{P}\left[1 \pm \left\{M\left(\frac{\sigma_P}{\bar{P}}\right) r(PT)\right\}\right]$	
$T_{assoc.}$ =	$\bar{T}\left[1 \pm \left\{M\left(\frac{\sigma_T}{\bar{T}}\right) r(\rho T)\right\}\right]$		$\bar{T}\left[1 \pm \left\{M\left(\frac{\sigma_T}{\bar{T}}\right) r(PT)\right\}\right]$
$\rho_{assoc.}$ =		$\bar{\rho}\left[1 \pm \left\{M\left(\frac{\sigma_\rho}{\bar{\rho}}\right) r(\rho T)\right\}\right]$	$\bar{\rho}\left[1 \pm \left\{M\left(\frac{\sigma_\rho}{\bar{\rho}}\right) r(P\rho)\right\}\right]$

Use + sign when extreme parameter is maximum.
Use - sign when extreme parameter is minimum.

It must be emphasized that this procedure is to be used at discrete altitudes only. Whenever extreme profiles of pressure, temperature, and density are required for engineering application, the use of these correlated variables at discrete altitudes is not satisfactory. Subsection 14.6 deals directly with this problem, since a profile of extreme pressure, temperature, or density from 0 to 90 kilometers altitude is unrealistic in the real atmosphere.

14.6 Extreme Atmospheric Profiles for Cape Kennedy, Florida and Vandenberg AFB, California

Given in this section are the two extreme density profiles that correspond to the summer (hot) and winter (cold) extreme atmospheres for Cape Kennedy, Florida (Tables 14.10A and 14.10B) and Vandenberg Air Force Base California Tables(14.11A and 14.11B).[2] Associated values of extreme temperature and pressure vs. altitude are also tabulated. These extreme atmospheric profiles should be used in the design (aerodynamic heating during ascent, engine performance, trajectory studies, etc.) of vehicles to be launched from Cape Kennedy, Florida or Vandenberg AFB, California. For those aerospace vehicles with ferrying capability, design calculations should use these extreme profiles in conjunction with the hot or cold day design ambient air temperatures over runways from paragraph 15.4.1 of Section XV. The extreme atmosphere producing the maximum vehicle design requirement should be utilized to determine the design.

The envelopes of deviations of density in Table 14.8 imply that a typical individual extreme density profile may be represented by a similarly shaped profile, that is, deviations of density either all negative or all positive from sea level to 90 kilometers altitude. However, examination of many individual density profiles shows that when large positive deviations of density occur at the surface, correspondingly large negative deviations will occur near 15 kilometers altitude and above. Such a situation occurs during the winter season (cold atmosphere). The reverse is also true — density profiles with large negative deviations at lower levels will have correspondingly large positive deviations at higher levels. This situation occurs in the summer season (hot atmosphere). (Figures 14.1 and 14.3).

The two extreme Cape Kennedy density profiles of Figure 14.1 are shown as percent deviations from the Patrick Reference Atmosphere, 1963 density profile. The two profiles obey the hydrostatic equation and the ideal gas law. The extreme density profiles shown here to 30 kilometers altitude

---

2. See Ref. 14.14 for detailed information pertaining to the Vandenberg extreme atmospheres.

were observed in the atmosphere. The results shown above 30 kilometers are somewhat speculative because of the limited data from this region of the atmosphere. Isopycnic levels (levels of minimum density variation) are noted at approximately 8 and 86 kilometers. Another level of minimum density variability is seen at 24 kilometers, and levels of maximum variability occur at 0, 15, and 68 kilometers altitude. The associated extreme temperature[3] profiles for Cape Kennedy are given in Figure 14.2.

The two Vandenberg extreme density profiles are shown in Figure 14.3 as percent deviations from the Vandenberg Reference Atmosphere, 1971. Levels of minimum density variation are located at ~ 8, 30 and 90 km altitude. Levels of maximum variability occur at 0, 15 and 73 km. The Hot and Cold Vandenberg temperature[3] profiles are shown in Figure 14.4. Tables 14.10A and B and 14.11A and B give the numerical data used to prepare Figures 14.1 through 14.4.

These two sets of extreme atmospheres are available as computerized subroutines upon request from the NASA-MSFC Aerospace Environment Division.

14.7 Reference Atmospheres

In design and preflight analysis of space vehicles, special nominal atmospheres are used to represent the mean or median thermodynamic conditions with respect to altitude. For general worldwide design, the U. S. Standard Atmosphere, 1962 (US 62) (Ref. 14.2) is used, but more specific atmospheres are needed at each launch area. A group of Range Reference Atmospheres (Ref. 14.6) have been prepared to represent the thermodynamic medians in the first 30 kilometers at various launch areas.

---

3. Temperatures below 10 kilometers altitude are virtual temperatures. Virtual temperature includes moisture to avoid computation of specific gas constant for moist air.

$$T_V = T(1 + 0.61\ w),$$

where

T_V = virtual temperature (°K)

T = kinetic temperature (°K)

w = mixing ratio (g/kg).

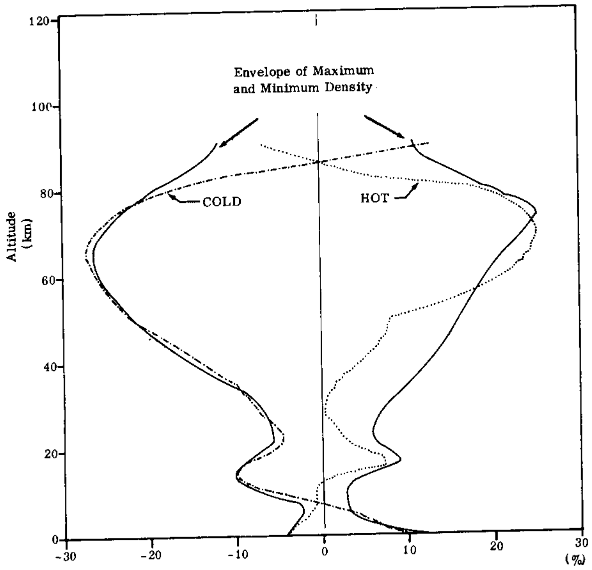

FIGURE 14.1 RELATIVE DEVIATIONS (%) OF EXTREME CAPE KENNEDY DENSITY PROFILES WITH RESPECT TO PRA-63

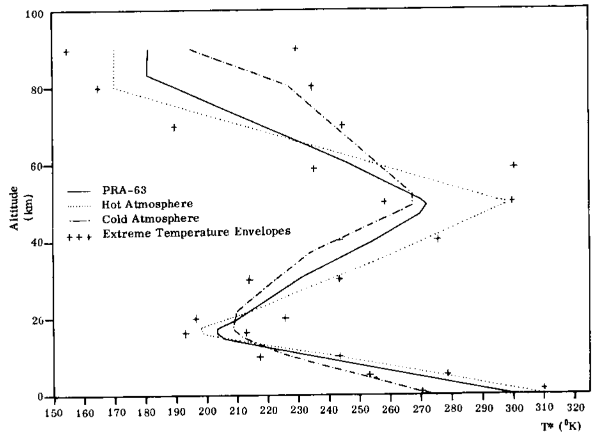

FIGURE 14.2 VIRTUAL TEMPERATURE PROFILES OF THE CAPE KENNEDY HOT, COLD, AND PRA-63

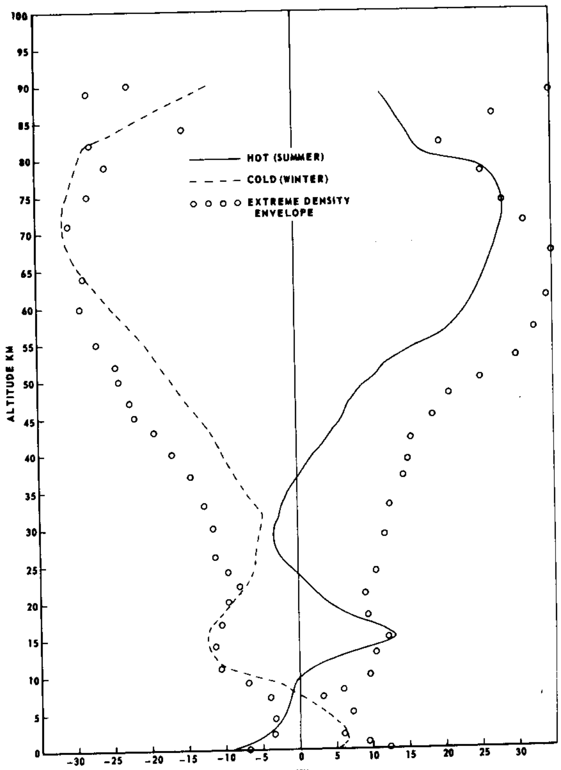

FIGURE 14.3 RELATIVE DEVIATIONS (%) OF EXTREME VANDENBERG DENSITY PROFILES WITH RESPECT TO VRA-71

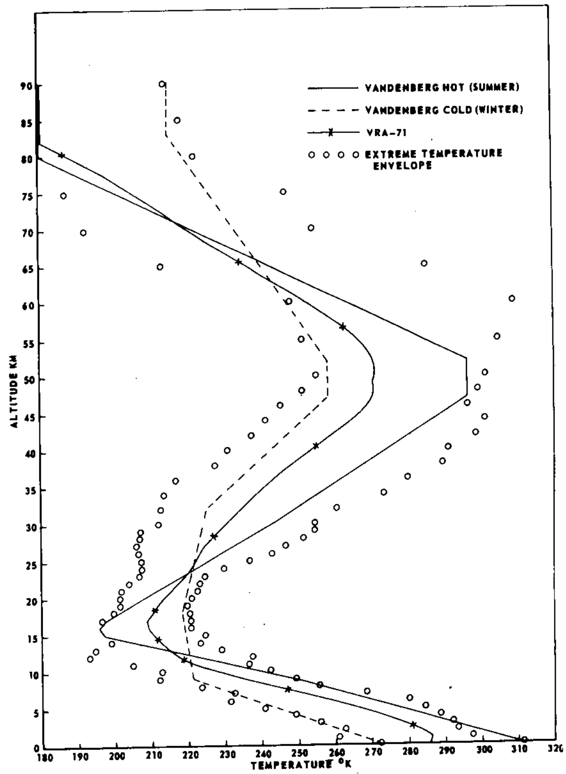

FIGURE 14.4 VIRTUAL TEMPERATURE PROFILES OF THE VANDENBERG HOT, COLD, AND VRA-71

TABLE 14.10A CAPE KENNEDY SUMMER (HOT) ATMOSPHERE (KHA-71)

Geometric Altitude Z(m)	Geopotential Altitude H(m)	Virtual Temperature T* (°K)	Kinetic Temperature T (°K)	Pressure P(N/cm²)	Density D(kg/m³)	Rel. Dev. (T*) with respect to PRA-63 RD(T*)%	Rel. Dev. (P) with respect to PRA-63 RD(P)%	Rel. Dev. (D) with respect to PRA-63 RD(D)%
0.	.0	3.0990000+02	3.0740000+02	1.0100000+01	1.1353705+00	3.52	-.69	-4.07
1000.	998.5	3.0313637+02	3.0105000+02	9.0346817+00	1.0382755+00	3.66	-.29	-3.81
2000.	1996.6	2.9637273+02	2.9470000+02	8.0614293+00	9.4757068-01	3.43	.17	-3.21
3000.	2994.5	2.8960909+02	2.8835000+02	7.1741153+00	8.6296655-01	3.07	.49	-2.52
4000.	3992.0	2.8284546+02	2.8200000+02	6.3668963+00	7.8418111-01	2.74	.82	-1.87
5000.	4989.2	2.7608182+02	2.7565001+02	5.6342022+00	7.1093916-01	2.53	1.13	-1.37
6000.	5986.1	2.6931818+02	2.6931818+02	4.9707288+00	6.4297218-01	2.50	1.43	-1.06
7000.	6982.7	2.6255455+02	2.6255455+02	4.3714321+00	5.8001870-01	2.67	1.74	-.91
8000.	7979.0	2.5579091+02	2.5579091+02	3.8315199+00	5.2182367-01	3.00	2.09	-.89
9000.	8975.0	2.4902728+02	2.4902728+02	3.3464479+00	4.6813915-01	3.44	2.49	-.92
10000.	9970.6	2.4226364+02	2.4226364+02	2.9119117+00	4.1872392-01	3.91	2.98	-.91
11000.	10965.9	2.3550000+02	2.3550000+02	2.5238402+00	3.7334363-01	4.35	3.55	-.81
12000.	11961.0	2.2820000+02	2.2820000+02	2.1780131+00	3.3249312-01	4.29	4.16	-.16
13000.	12955.7	2.2090000+02	2.2090000+02	1.8705877+00	2.9499874-01	3.76	4.73	.92
14000.	13950.1	2.1360000+02	2.1360000+02	1.5983606+00	2.6068215-01	2.61	5.16	2.50
15000.	14944.2	2.0630000+02	2.0630000+02	1.3583010+00	2.2936894-01	.72	5.35	4.64
16000.	15937.9	1.9900000+02	1.9900000+02	1.1475476+00	2.0088866-01	-1.99	5.17	7.33
17000.	16931.4	1.9816257+02	1.9816257+02	9.6617676-01	1.6985547-01	-2.39	4.72	7.27
18000.	17924.5	2.0000000+02	2.0000000+02	8.1369526-01	1.4173245-01	-2.58	4.19	7.05
19000.	18917.4	2.0416667+02	2.0416667+02	6.8712577-01	1.1724374-01	-1.74	3.70	5.66
20000.	19909.9	2.0833333+02	2.0833333+02	5.8222915-01	9.7358475-02	-.96	3.39	4.47
21000.	20902.1	2.1250000+02	2.1250000+02	4.9493667-01	8.1136631-02	-.19	3.23	3.44
22000.	21894.0	2.1566667+02	2.1566667+02	4.2201626-01	6.8172810-02	.14	3.17	2.97
23000.	22885.6	2.1883333+02	2.1883333+02	3.6056887-01	5.7401234-02	.53	3.16	2.51
24000.	23876.9	2.2200000+02	2.2200000+02	3.0875086-01	4.8447590-02	1.00	3.21	2.06
25000.	24867.8	2.2516667+02	2.2516667+02	2.6498604-01	4.0994491-02	1.55	3.30	1.60
26000.	25858.5	2.2833333+02	2.2833333+02	2.2793980-01	3.4775536-02	2.19	3.44	1.15
27000.	26848.8	2.3150000+02	2.3150000+02	1.9649475-01	2.9570541-02	2.89	3.64	.73
28000.	27838.9	2.3466667+02	2.3466667+02	1.6972565-01	2.5199219-02	3.63	3.93	.29
29000.	28828.6	2.3783333+02	2.3783333+02	1.4687393-01	2.1516243-02	4.04	4.35	.30
30000.	29818.0	2.4100000+02	2.4100000+02	1.2732124-01	1.8405121-02	4.42	4.82	.38
31000.	30807.1	2.4416667+02	2.4416667+02	1.1056625-01	1.5773346-02	4.78	5.32	.52
32000.	31795.9	2.4733333+02	2.4733333+02	9.6198730-02	1.3546524-02	5.11	5.86	.72
33000.	32784.4	2.5050000+02	2.5050000+02	8.3870697-02	1.1662445-02	5.40	6.44	.99
34000.	33772.6	2.5366667+02	2.5366667+02	7.3279037-02	1.0065735-02	5.67	7.06	1.32
35000.	34760.4	2.5683333+02	2.5683333+02	6.4129028-02	8.7031249-03	5.90	7.70	1.70
36000.	35748.0	2.6000000+02	2.6000000+02	5.6145477-02	7.5227375-03	6.11	8.37	2.14
37000.	36735.2	2.6288461+02	2.6288461+02	4.9269104-02	6.5290813-03	6.18	9.06	2.71
38000.	37722.1	2.6576923+02	2.6576923+02	4.3294535-02	5.6749344-03	6.24	9.75	3.31
39000.	38708.8	2.6865385+02	2.6865385+02	3.8097067-02	4.9400673-03	6.30	10.44	3.90
40000.	39695.1	2.7153846+02	2.7153846+02	3.3570537-02	4.3068771-03	6.36	11.13	4.49
41000.	40681.1	2.7442308+02	2.7442308+02	2.9622116-02	3.7603684-03	6.43	11.82	5.06
42000.	41666.8	2.7730769+02	2.7730769+02	2.6172104-02	3.2879410-03	6.54	12.51	5.60
43000.	42652.2	2.8019231+02	2.8019231+02	2.3153610-02	2.8787613-03	6.69	13.20	6.10
44000.	43637.3	2.8307692+02	2.8307692+02	2.0507717-02	2.5237846-03	6.89	13.90	6.56
45000.	44622.0	2.8596154+02	2.8596154+02	1.8186378-02	2.2154732-03	7.17	14.63	6.96
46000.	45606.5	2.8884615+02	2.8884615+02	1.6148109-02	1.9474564-03	7.54	15.39	7.30
47000.	46590.7	2.9173077+02	2.9173077+02	1.4355888-02	1.7142868-03	8.02	16.21	7.58
48000.	47574.5	2.9461538+02	2.9461538+02	1.2777672-02	1.5109100-03	8.64	17.10	7.79
49000.	48558.0	2.9750000+02	2.9750000+02	1.1384044-02	1.3330526-03	9.42	18.13	7.96
50000.	49541.3	2.9750000+02	2.9750000+02	1.0148231-02	1.1883979-03	9.94	19.15	9.38
51000.	50524.2	2.9325000+02	2.9325000+02	9.0407466-03	1.0739715-03	8.38	20.16	10.26
52000.	51506.8	2.8900000+02	2.8900000+02	8.0399930-03	9.6910328-04	8.12	21.09	12.00
53000.	52489.1	2.8475000+02	2.8475000+02	7.1372587-03	8.7313598-04	7.32	21.92	13.60
54000.	53471.1	2.8050000+02	2.8050000+02	6.3243675-03	7.8543025-04	6.60	22.67	15.07
55000.	54452.9	2.7625000+02	2.7625000+02	5.5935943-03	7.0539075-04	5.94	23.33	16.42
56000.	55434.2	2.7200000+02	2.7200000+02	4.9378836-03	6.3245458-04	5.32	23.91	17.65
57000.	56415.3	2.6775000+02	2.6775000+02	4.3505454-03	5.6608540-04	4.75	24.41	18.77
58000.	57396.1	2.6350000+02	2.6350000+02	3.8253748-03	5.0578808-04	4.21	24.82	19.78
59000.	58376.6	2.5925000+02	2.5925000+02	3.3566785-03	4.5108956-04	3.69	25.15	20.69
60000.	59356.7	2.5500000+02	2.5500000+02	2.9390943-03	4.0154946-04	3.20	25.39	21.50
61000.	60336.6	2.5075000+02	2.5075000+02	2.5678229-03	3.5675335-04	2.71	25.54	22.23
62000.	61316.1	2.4650000+02	2.4650000+02	2.2383559-03	3.1631672-04	2.24	25.61	22.86
63000.	62295.4	2.4225000+02	2.4225000+02	1.9464898-03	2.7987802-04	1.76	25.59	23.42
64000.	63274.3	2.3800000+02	2.3800000+02	1.6884637-03	2.4709821-04	1.28	25.47	23.89
65000.	64253.0	2.3375000+02	2.3375000+02	1.4609194-03	2.1766889-04	.78	25.25	24.28
66000.	65231.3	2.2950000+02	2.2950000+02	1.2605929-03	1.9129384-04	.27	24.93	24.59
67000.	66209.3	2.2525000+02	2.2525000+02	1.0846496-03	1.6770816-04	-.27	24.50	24.83
68000.	67187.0	2.2100000+02	2.2100000+02	9.3052387-04	1.4666247-04	-.82	23.95	24.98
69000.	68164.5	2.1675000+02	2.1675000+02	7.9586029-04	1.2791753-04	-1.41	23.29	25.05
70000.	69141.6	2.1250000+02	2.1250000+02	6.7856073-04	1.1126780-04	-2.03	22.49	25.04
71000.	70118.4	2.0825000+02	2.0825000+02	5.7664156-04	9.6510648-05	-2.63	21.56	24.92
72000.	71094.9	2.0400000+02	2.0400000+02	4.8844814-04	8.3469629-05	-3.38	20.49	24.70
73000.	72071.1	1.9975000+02	1.9975000+02	4.1236877-04	7.1975231-05	-4.11	19.26	24.37
74000.	73047.0	1.9550000+02	1.9550000+02	3.4700393-04	6.1864137-05	-4.87	17.87	23.91
75000.	74022.6	1.9125000+02	1.9125000+02	2.9097080-04	5.3004503-05	-5.67	16.32	23.31
76000.	74997.9	1.8700000+02	1.8700000+02	2.4319172-04	4.5259875-05	-6.51	14.58	22.56
77000.	75972.8	1.8275000+02	1.8275000+02	2.0245552-04	3.8509607-05	-7.38	12.65	21.63
78000.	76947.5	1.7850000+02	1.7850000+02	1.6777992-04	3.2638311-05	-8.27	10.53	20.50
79000.	77921.9	1.7425000+02	1.7425000+02	1.3800621-04	2.7534485-05	-9.19	8.21	19.16
80000.	78896.0	1.7000000+02	1.7000000+02	1.1290073-04	2.3151398-05	-10.13	5.67	17.58
81000.	79869.7	1.7000000+02	1.7000000+02	9.2306137-05	1.8935204-05	-8.79	3.19	13.13
82000.	80843.2	1.7000000+02	1.7000000+02	7.5511932-05	1.5504837-05	-7.39	.99	9.05
83000.	81816.4	1.7000000+02	1.7000000+02	6.1855316-05	1.2674332-05	-5.90	-.92	5.30
84000.	82789.2	1.7000000+02	1.7000000+02	5.0659180-05	1.0385513-05	-5.90	-2.59	3.51
85000.	83761.8	1.7000000+02	1.7000000+02	4.1408538-05	8.5029602-06	-5.90	-4.24	1.76
86000.	84734.0	1.7000000+02	1.7000000+02	3.3922195-05	6.9713593-06	-5.90	-5.87	.03
87000.	85706.0	1.7000000+02	1.7000000+02	2.7647018-05	5.7010650-06	-5.90	-7.47	-1.67
88000.	86677.6	1.7000000+02	1.7000000+02	2.2735596-05	4.6710968-06	-5.90	-9.05	-3.35
89000.	87649.0	1.7000000+02	1.7000000+02	1.8634796-05	3.8394928-06	-5.90	-10.61	-5.01
90000.	88620.0	1.7000000+02	1.7000000+02	1.5134811-05	3.1070709-06	-5.90	-12.15	-6.64

TABLE 14.10B CAPE KENNEDY WINTER (COLD) ATMOSPHERE (KCA-71)

Geometric Altitude	Geopotential Altitude	Virtual Temperature	Kinetic Temperature	Pressure	Density	Rel. Dev. (T*) with respect to PRA-63	Rel. Dev. (P) with respect to PRA-63	Rel. Dev. (D) with respect to PRA-63
Z(m)	H(m)	T* (°K)	T (°K)	P (N/cm²)	D(kg/m³)	RD(T*)%	RD(P)%	RD(D)%
0.	.0	2.7500000+02	2.7450000+02	1.0270000+01	1.3009948+00	-8.14	.98	9.32
1000.	998.5	2.7000000+02	2.6960000+02	9.0598171+00	1.1689434+00	-7.67	-.01	8.30
2000.	1996.6	2.6500000+02	2.6470000+02	7.9735277+00	1.0481959+00	-7.51	-.99	7.06
3000.	2994.5	2.6000000+02	2.5980000+02	7.0004350+00	9.3797119-01	-7.46	-1.95	5.95
4000.	3992.0	2.5500000+02	2.5490000+02	6.1305847+00	8.3752835-01	-7.38	-2.92	4.80
5000.	4989.2	2.5000000+02	2.5000000+02	5.3547301+00	7.4616589-01	-7.16	-3.89	3.51
6000.	5986.1	2.4523591+02	2.4523591+02	4.6646548+00	6.6278387-01	-6.66	-4.82	1.96
7000.	6982.7	2.4044706+02	2.4044706+02	4.0522889+00	5.8710627-01	-6.03	-5.69	.36
8000.	7979.0	2.3586761+02	2.3586761+02	3.5107186+00	5.1842328-01	-4.97	-6.46	-1.27
9000.	8975.0	2.3160561+02	2.3160561+02	3.0333381+00	4.5620410-01	-3.77	-7.09	-3.49
10000.	9970.6	2.2767153+02	2.2767153+02	2.6141402+00	4.0002236-01	-2.42	-7.55	-5.27
11000.	10965.9	2.2401892+02	2.2401892+02	2.2471262+00	3.4951847-01	-.74	-7.81	-7.15
12000.	11961.0	2.2058508+02	2.2058508+02	1.9269158+00	3.0436223-01	.77	-7.85	-8.59
13000.	12955.7	2.1733175+02	2.1733175+02	1.6484578+00	2.6421523-01	2.16	-7.70	-9.68
14000.	13950.1	2.1428577+02	2.1428577+02	1.4071002+00	2.2869338-01	2.95	-7.41	-10.05
15000.	14944.2	2.1157970+02	2.1157970+02	1.1985998+00	1.9732939-01	3.26	-7.03	-9.94
16000.	15937.9	2.0949258+02	2.0948258+02	1.0191326+00	1.6953508-01	3.19	-6.61	-9.47
17000.	16931.4	2.0849504+02	2.0849504+02	8.6531102-01	1.4460154-01	2.78	-6.20	-8.75
18000.	17924.5	2.0828323+02	2.0828323+02	7.3453635-01	1.2283195-01	1.44	-5.95	-7.19
19000.	18917.4	2.0846620+02	2.0846620+02	6.2346069-01	1.0417007-01	.34	-5.91	-6.13
20000.	19909.9	2.0899749+02	2.0899749+02	5.2929926-01	8.8729208-02	-.64	-6.01	-5.33
21000.	20902.1	2.0982848+02	2.0982848+02	4.4953301-01	7.4658779-02	-1.41	-6.23	-4.87
22000.	21894.0	2.1090961+02	2.1090961+02	3.8218424-01	6.3147604-02	-2.12	-6.54	-4.57
23000.	22885.6	2.1219170+02	2.1219170+02	3.2513529-01	5.3396919-02	-2.52	-6.95	-4.65
24000.	23876.9	2.1362711+02	2.1362711+02	2.7700539-01	4.5168960-02	-2.83	-7.42	-4.85
25000.	24867.8	2.1517109+02	2.1517109+02	2.3622634-01	3.8234467-02	-2.94	-7.94	-5.26
26000.	25858.5	2.1678299+02	2.1678299+02	2.0168165-01	3.2396351-02	-2.97	-8.50	-5.76
27000.	26848.8	2.1842757+02	2.1842757+02	1.7237698-01	2.7482916-02	-2.88	-9.09	-6.38
28000.	27839.9	2.2007615+02	2.2007615+02	1.4748703-01	2.3345394-02	-2.94	-9.67	-7.03
29000.	28828.6	2.2170800+02	2.2170800+02	1.2632431-01	1.9857147-02	-3.04	-10.22	-7.40
30000.	29819.0	2.2331153+02	2.2331153+02	1.0832073-01	1.6910702-02	-3.16	-10.79	-7.97
31000.	30807.1	2.2488554+02	2.2488554+02	9.2998836-02	1.4416779-02	-3.55	-11.39	-8.13
32000.	31795.3	2.2644049+02	2.2644049+02	7.9957733-02	1.2301918-02	-3.79	-12.03	-8.57
33000.	32784.4	2.2799975+02	2.2799975+02	6.8840331-02	1.0507172-02	-4.07	-12.71	-9.01
34000.	33772.6	2.2960097+02	2.2960097+02	5.9314604-02	8.9853973-03	-4.32	-13.40	-9.49
35000.	34760.4	2.3125000+02	2.3125000+02	5.1093979-02	7.6969605-03	-4.65	-14.12	-9.94
36000.	35748.0	2.3383928+02	2.3383928+02	4.4116459-02	6.5724525-03	-4.57	-14.85	-10.77
37000.	36735.2	2.3642857+02	2.3642857+02	3.8148088-02	5.6209221-03	-4.51	-15.56	-11.57
38000.	37722.1	2.3901786+02	2.3901786+02	3.3039589-02	4.8153172-03	-4.45	-16.24	-12.34
39000.	38708.8	2.4160714+02	2.4160714+02	2.8661022-02	4.1323890-03	-4.41	-16.91	-13.08
40000.	39695.1	2.4419643+02	2.4419643+02	2.4901237-02	3.5523605-03	-4.35	-17.57	-13.92
41000.	40681.1	2.4678571+02	2.4678571+02	2.1667652-02	3.0585937-03	-4.28	-18.21	-14.55
42000.	41666.8	2.4937500+02	2.4937500+02	1.8880863-02	2.6376419-03	-4.19	-18.84	-15.29
43000.	42652.2	2.5196428+02	2.5196428+02	1.6474552-02	2.2778053-03	-4.06	-19.46	-16.05
44000.	43637.7	2.5455357+02	2.5455357+02	1.4394226-02	1.9698486-03	-3.88	-20.05	-16.83
45000.	44622.0	2.5714286+02	2.5714286+02	1.2593651-02	1.7059479-03	-3.63	-20.62	-17.63
46000.	45606.5	2.5973214+02	2.5973214+02	1.1034660-02	1.4797821-03	-3.30	-21.15	-18.46
47000.	46590.7	2.6232143+02	2.6232143+02	9.6825027-03	1.2858047-03	-2.87	-21.63	-19.32
48000.	47574.5	2.6491071+02	2.6491071+02	8.5065841-03	1.1187134-03	-2.31	-22.05	-20.20
49000.	48558.0	2.6750000+02	2.6750000+02	7.4803328-03	9.7417116-04	-1.61	-22.37	-21.10
50000.	49541.3	2.6750000+02	2.6750000+02	6.5834379-03	8.5736990-04	-1.15	-22.71	-21.81
51000.	50524.2	2.6750000+02	2.6750000+02	5.7941055-03	7.5457335-04	-.59	-22.99	-22.53
52000.	51506.3	2.6750000+02	2.6750000+02	5.0981116-03	6.6395879-04	.07	-23.19	-23.25
53000.	52489.1	2.6607143+02	2.6607143+02	4.4871795-03	5.8748722-04	.28	-23.35	-23.57
54000.	53471.1	2.6464286+02	2.6464286+02	3.9456653-03	5.1935887-04	.58	-23.49	-23.92
55000.	54452.8	2.6321429+02	2.6321429+02	3.4663939-03	4.5875263-04	.94	-23.59	-24.30
56000.	55434.2	2.6178572+02	2.6178572+02	3.0428338-03	4.0491104-04	1.37	-23.65	-24.68
57000.	56415.3	2.6035714+02	2.6035714+02	2.6690495-03	3.5713458-04	1.85	-23.67	-25.06
58000.	57395.1	2.5892857+02	2.5892857+02	2.3394966-03	3.1478500-04	2.40	-23.65	-25.44
59000.	58376.6	2.5750000+02	2.5750000+02	2.0493507-03	2.7727747-04	2.99	-23.57	-25.79
60000.	59355.7	2.5607143+02	2.5607143+02	1.7940330-03	2.4408293-04	3.63	-23.44	-26.12
61000.	60336.6	2.5464286+02	2.5464286+02	1.5695310-03	2.1473479-04	4.31	-23.24	-26.41
62000.	61316.1	2.5321429+02	2.5321429+02	1.3722539-03	1.8879223-04	5.02	-22.98	-26.66
63000.	62295.4	2.5178572+02	2.5178572+02	1.1990118-03	1.6587544-04	5.76	-22.65	-26.86
64000.	63274.3	2.5035714+02	2.5035714+02	1.0467529-03	1.4563131-04	6.53	-22.24	-27.01
65000.	64253.0	2.4892857+02	2.4892857+02	9.1317415-04	1.2776279-04	7.32	-21.75	-27.09
66000.	65231.7	2.4750000+02	2.4750000+02	7.9591989-04	1.1199284-04	8.13	-21.19	-27.11
67000.	66209.3	2.4607143+02	2.4607143+02	6.9297552-04	9.8073482-05	8.95	-20.51	-27.05
68000.	67187.0	2.4464286+02	2.4464286+02	6.0273170-04	8.5805893-05	9.79	-19.76	-26.91
69000.	68164.5	2.4321429+02	2.4321429+02	5.2362918-04	7.4997425-05	10.62	-18.90	-26.69
70000.	69141.6	2.4178572+02	2.4178572+02	4.5454579-04	6.5495014-05	11.47	-17.93	-26.37
71000.	70118.4	2.4035714+02	2.4035714+02	3.9408684-04	5.7145119-05	12.31	-16.85	-25.97
72000.	71094.9	2.3892857+02	2.3892857+02	3.4146309-04	4.9815655-05	13.16	-15.65	-25.46
73000.	72071.1	2.3750000+02	2.3750000+02	2.9575348-04	4.3401718-05	14.01	-14.33	-24.86
74000.	73047.0	2.3607143+02	2.3607143+02	2.5612631-04	3.7804127-05	14.87	-12.87	-24.15
75000.	74022.6	2.3464286+02	2.3464286+02	2.2185802-04	3.2925129-05	15.77	-11.27	-23.33
76000.	74997.9	2.3321429+02	2.3321429+02	1.9212246-04	2.8688431-05	16.59	-9.51	-22.39
77000.	75972.8	2.3178572+02	2.3178572+02	1.6645908-04	2.4969101-05	17.48	-7.60	-21.35
78000.	76947.5	2.3035714+02	2.3035714+02	1.4385223-04	2.1701813-05	18.38	-5.52	-20.19
79000.	77921.9	2.2892857+02	2.2892857+02	1.2365341-04	1.8788338-05	19.30	-3.26	-18.91
80000.	78896.0	2.2750000+02	2.2750000+02	1.0599136-04	1.6231239-05	20.27	-.80	-17.52
81000.	79869.7	2.2425000+02	2.2425000+02	9.1113408-05	1.4154732-05	20.31	1.80	-15.39
82000.	80843.2	2.2100000+02	2.2100000+02	7.8145265-05	1.2319863-05	20.39	4.49	-13.21
83000.	81816.4	2.1775000+02	2.1775000+02	6.6890716-05	1.0700285-05	20.53	7.25	-11.01
84000.	82789.2	2.1450000+02	2.1450000+02	5.7106018-05	9.2763901-06	18.74	10.06	-7.30
85000.	83761.8	2.1125000+02	2.1125000+02	4.8654079-05	8.0223083-06	16.94	12.67	-3.65
86000.	84734.0	2.0800000+02	2.0800000+02	4.1339397-05	6.9222450-06	15.14	15.05	-.08
87000.	85706.0	2.0475000+02	2.0475000+02	3.5033226-05	5.9589148-06	13.34	17.16	3.37
88000.	86677.6	2.0150000+02	2.0150000+02	2.9604435-05	5.1189661-06	11.54	19.00	6.69
89000.	87649.0	1.9825000+02	1.9825000+02	2.4955273-05	4.3857098-06	9.74	20.52	9.83
90000.	88620.0	1.9500000+02	1.9500000+02	2.0947456-05	3.7453175-06	7.94	21.72	12.76

TABLE 14.11A VANDENBERG SUMMER (HOT) ATMOSPHERE (VHA-73)

Geometric Altitude Z(m)	Geopotential Altitude H(m)	Virtual Temperature T* (K)	Kinetic Temperature T (K)	Pressure P (N/cm²)	Density D(kg/m³)	Rel. Dev. (T*) with respect to VRA-71 RD(T*)%	Rel. Dev. (P) with respect to VRA-71 RD(P)%	Rel. Dev. (D) with respect to VRA-71 RD(D)%
0.	.0	.31270000+03	.31040000+03	.10100000+02	.11252041+01	8.90	-.88	-8.98
1000.	999.5	.30564445+03	.30360000+03	.90433739+01	.10307463+01	6.50	-.05	-6.15
2000.	1998.8	.29858889+03	.29680000+03	.80764172+01	.94228637+00	5.29	.65	-4.41
3000.	2997.7	.29153334+03	.29000000+03	.71933710+01	.85957157+00	4.71	1.25	-3.30
4000.	3996.3	.28447778+03	.28320000+03	.63887240+01	.78235450+00	4.45	1.79	-2.54
5000.	4994.6	.27742223+03	.27640000+03	.56572056+01	.71039274+00	4.39	2.32	-1.97
6000.	5992.5	.27036667+03	.26960000+03	.49937765+01	.64344846+00	4.47	2.88	-1.53
7000.	6990.2	.26331112+03	.26280000+03	.43936324+01	.58128929+00	4.73	3.49	-1.19
8000.	7987.5	.25625556+03	.25600000+03	.38521925+01	.52368784+00	5.15	4.18	-.93
9000.	8984.5	.24920000+03	.24920000+03	.33650957+01	.47042152+00	5.64	4.92	-.67
10000.	9981.3	.24053333+03	.24053333+03	.29268444+01	.42389878+00	5.27	5.64	.35
11000.	10977.7	.23186667+03	.23186667+03	.25326658+01	.38051989+00	4.47	6.43	1.87
12000.	11973.7	.22320000+03	.22320000+03	.21795295+01	.34017810+00	2.48	6.95	4.37
13000.	12969.5	.21453333+03	.21453333+03	.18645095+01	.30276636+00	-.23	7.11	7.36
14000.	13965.0	.20586667+03	.20586667+03	.15847846+01	.26817730+00	-3.30	6.80	10.43
15000.	14960.1	.19720000+03	.19720000+03	.13376399+01	.23630347+00	-6.55	5.90	13.31
16000.	15954.9	.19570000+03	.19570000+03	.11241236+01	.20010642+00	-6.57	4.66	12.02
17000.	16949.5	.19720000+03	.19720000+03	.94468907+00	.16689595+00	-5.57	3.48	9.61
18000.	17943.7	.20073846+03	.20073846+03	.79564330+00	.13807836+00	-4.59	2.53	7.44
19000.	18937.6	.20427692+03	.20427692+03	.67212650+00	.11462241+00	-3.49	1.60	5.33
20000.	19931.2	.20781538+03	.20781538+03	.56943204+00	.95455732-01	-2.61	.97	3.73
21000.	20924.4	.21135385+03	.21135385+03	.48378066+00	.79739984-01	-1.86	.61	2.53
22000.	21917.4	.21489231+03	.21489231+03	.41212652+00	.66810926-01	-1.13	.41	1.52
23000.	22910.0	.21843077+03	.21843077+03	.35200562+00	.56140153-01	-.32	.29	.56
24000.	23902.4	.22196923+03	.22196923+03	.30141799+00	.47305779-01	.58	.21	-.41
25000.	24894.4	.22550769+03	.22550769+03	.25873452+00	.39969694-01	1.60	.19	-1.39
26000.	25886.1	.22904615+03	.22904615+03	.22262406+00	.33859996-01	2.66	.25	-2.30
27000.	26877.5	.23258462+03	.23258462+03	.19199534+00	.28757261-01	3.66	.52	-2.98
28000.	27868.6	.23612308+03	.23612308+03	.16595099+00	.24483823-01	4.44	1.15	-3.18
29000.	28859.4	.23966154+03	.23966154+03	.14375097+00	.20895378-01	5.05	1.64	-3.24
30000.	29849.9	.24320000+03	.24320000+03	.12478311+00	.17874341-01	5.54	2.23	-3.14
31000.	30840.0	.24631765+03	.24631765+03	.10852673+00	.15348961-01	5.90	2.90	-2.84
32000.	31829.9	.24943529+03	.24943529+03	.94554038-01	.13205656-01	6.30	3.64	-2.50
33000.	32819.4	.25255294+03	.25255294+03	.82521473-01	.11382885-01	6.68	4.43	-2.11
34000.	33808.7	.25567059+03	.25567059+03	.72140493-01	.98296066-02	7.05	5.26	-1.66
35000.	34797.6	.25878823+03	.25878823+03	.63168256-01	.85033913-02	7.36	6.13	-1.15
36000.	35786.2	.26190588+03	.26190588+03	.55399955-01	.73688882-02	7.62	7.01	-.57
37000.	36774.5	.26502353+03	.26502353+03	.48662488-01	.63965778-02	7.82	7.91	.08
38000.	37762.5	.26814117+03	.26814117+03	.42809272-01	.55617586-02	7.96	8.81	.79
39000.	38750.2	.27125882+03	.27125882+03	.37715923-01	.48437159-02	8.04	9.71	1.55
40000.	39737.5	.27437647+03	.27437647+03	.33276706-01	.42250443-02	8.07	10.62	2.36
41000.	40724.6	.27749412+03	.27749412+03	.29401561-01	.36910881-02	8.08	11.52	3.18
42000.	41711.4	.28061176+03	.28061176+03	.26013643-01	.32294838-02	8.09	12.42	4.01
43000.	42697.8	.28372941+03	.28372941+03	.23047266-01	.28297812-02	8.13	13.33	4.81
44000.	43683.9	.28684706+03	.28684706+03	.20446185-01	.24831313-02	8.24	14.25	5.55
45000.	44669.8	.28996471+03	.28996471+03	.18162154-01	.21820265-02	8.47	15.20	6.20
46000.	45655.3	.29308235+03	.29308235+03	.16153722-01	.19200863-02	8.88	16.18	6.71
47000.	46640.5	.29620000+03	.29620000+03	.14385216-01	.16918783-02	9.51	17.22	7.04
48000.	47625.4	.29620000+03	.29620000+03	.12818158-01	.15075731-02	9.31	18.27	8.19
49000.	48610.0	.29620000+03	.29620000+03	.11421809-01	.13433452-02	9.51	19.27	8.92
50000.	49594.3	.29620000+03	.29620000+03	.10177570-01	.11970075-02	9.24	20.37	10.20
51000.	50578.3	.29620000+03	.29620000+03	.90688736-02	.10666111-02	9.19	21.31	11.10
52000.	51561.9	.29620000+03	.29620000+03	.80809533-02	.95041952-03	9.39	22.32	11.82
53000.	52545.3	.29205714+03	.29205714+03	.71947919-02	.85819941-03	8.27	23.32	13.91
54000.	53528.4	.28791429+03	.28791429+03	.63951862-02	.77379833-03	7.33	24.23	15.75
55000.	54511.1	.28377143+03	.28377143+03	.56747479-02	.69665172-03	6.54	25.04	17.37
56000.	55493.6	.27962857+03	.27962857+03	.50266259-02	.62622849-03	5.88	25.77	18.78
57000.	56475.7	.27548572+03	.27548572+03	.44444739-02	.56202945-03	5.33	26.41	20.01
58000.	57457.5	.27134286+03	.27134286+03	.39224204-02	.50358588-03	4.87	26.97	21.07
59000.	58439.1	.26720000+03	.26720000+03	.34550394-02	.45045806-03	4.48	27.45	21.99
60000.	59420.3	.26305714+03	.26305714+03	.30373220-02	.40223378-03	4.13	27.86	22.79
61000.	60401.2	.25891429+03	.25891429+03	.26646508-02	.35852718-03	3.83	28.21	23.48
62000.	61381.8	.25477143+03	.25477143+03	.23327743-02	.31897732-03	3.54	28.48	24.09
63000.	62362.1	.25062857+03	.25062857+03	.20377835-02	.28324696-03	3.26	28.69	24.63
64000.	63342.1	.24648572+03	.24648572+03	.17760888-02	.25102138-03	2.97	28.83	25.12
65000.	64321.8	.24234286+03	.24234286+03	.15443988-02	.22200718-03	2.66	28.91	25.57
66000.	65301.2	.23820000+03	.23820000+03	.13396997-02	.19593116-03	2.33	28.93	26.00
67000.	66280.3	.23405714+03	.23405714+03	.11592365-02	.17253926-03	1.96	28.87	26.40
68000.	67259.0	.22991429+03	.22991429+03	.10004939-02	.15159549-03	1.55	28.75	26.78
69000.	68237.5	.22577143+03	.22577143+03	.86117982-03	.13208093-03	1.10	28.55	27.15
70000.	69215.7	.22162857+03	.22162857+03	.73920883-03	.11619280-03	.61	28.28	27.50
71000.	70193.5	.21748572+03	.21748572+03	.63268688-03	.10134350-03	.08	27.92	27.82
72000.	71171.1	.21334286+03	.21334286+03	.53989683-03	.88159774-04	-.49	27.47	28.09
73000.	72148.3	.20920000+03	.20920000+03	.45928474-03	.76481807-04	-1.08	26.92	28.30
74000.	73125.3	.20505714+03	.20505714+03	.38944709-03	.66162417-04	-1.69	26.26	28.43
75000.	74101.8	.20091429+03	.20091429+03	.32911889-03	.57066310-04	-2.29	25.48	28.42
76000.	75078.3	.19677143+03	.19677143+03	.27716227-03	.49069300-04	-2.88	24.56	28.26
77000.	76054.3	.19262857+03	.19262857+03	.23255599-03	.42057614-04	-3.42	23.51	27.88
78000.	77030.0	.18848572+03	.18848572+03	.19438558-03	.35927203-04	-3.89	22.29	27.24
79000.	78005.4	.18434286+03	.18434286+03	.16183412-03	.30583105-04	-4.24	20.91	26.26
80000.	78980.6	.18020000+03	.18020000+03	.13417355-03	.25938802-04	-4.45	19.33	24.90
81000.	79955.4	.18020000+03	.18020000+03	.11100215-03	.21459244-04	-2.22	17.82	20.49
82000.	80929.9	.18020000+03	.18020000+03	.91832393-04	.17753293-04	-.25	16.73	17.02
83000.	81904.1	.18020000+03	.18020000+03	.75973197-04	.14687349-04	-.25	16.10	16.39
84000.	82878.0	.18020000+03	.18020000+03	.62852839-04	.12150885-04	-.25	15.48	15.77
85000.	83851.6	.18020000+03	.18020000+03	.51998330-04	.10052462-04	-.25	14.85	15.13
86000.	84824.9	.18020000+03	.18020000+03	.43018365-04	.83164297-05	-.25	14.22	14.50
87000.	85798.0	.18020000+03	.18020000+03	.35589215-04	.68802057-05	-.25	13.58	13.86
88000.	86770.7	.18020000+03	.18020000+03	.29443057-04	.56920135-05	-.25	12.94	13.22
89000.	87743.1	.18020000+03	.18020000+03	.24358324-04	.47090188-05	-.25	12.30	12.58
90000.	88715.1	.18020000+03	.18020000+03	.20151710-04	.38957845-05	-.25	11.65	11.93

TABLE 14.11B VANDENBERG WINTER (COLD) ATMOSPHERE (VCA-73)

Geometric Altitude	Geopotential Altitude	Virtual Temperature	Kinetic Temperature	Pressure	Density	Rel. Dev. (T*) with respect to VRA-71	Rel. Dev. (P) with respect to VRA-71	Rel. Dev. (D) with respect to VRA-71
Z(m)	H(m)	T* (°K)	T (°K)	P(N/cm²)	D(kg/m³)	RD(T*)%	RD(P)%	RD(D)%
0.	.0	.27270000+03	.27210000+03	.10180000+02	.13004703+01	-5.03	-.10	5.20
1000.	999.5	.26696000+03	.26648000+03	.89693280+01	.11704464+01	-6.98	-.87	6.57
2000.	1998.8	.26122000+03	.26086000+03	.78809183+01	.10510133+01	-7.89	-1.79	6.62
3000.	2997.7	.25548000+03	.25524000+03	.69047074+01	.94151267+00	-8.24	-2.81	5.92
4000.	3996.3	.24974000+03	.24962000+03	.60312686+01	.84131448+00	-8.30	-3.90	4.80
5000.	4994.6	.24400000+03	.24400000+03	.52517769+01	.74981521+00	-8.19	-5.01	3.47
6000.	5992.5	.23830000+03	.23830000+03	.45580398+01	.66633385+00	-7.92	-6.09	1.98
7000.	6990.2	.23260000+03	.23260000+03	.39423968+01	.59045721+00	-7.49	-7.14	.37
8000.	7987.5	.22690000+03	.22690000+03	.33976521+01	.52165360+00	-6.90	-8.12	-1.31
9000.	8984.5	.22120000+03	.22120000+03	.29171198+01	.45941687+00	-6.23	-9.04	-2.99
10000.	9981.3	.22086667+03	.22086667+03	.24993634+01	.39421853+00	-3.34	-9.79	-6.68
11000.	10977.7	.22053333+03	.22053333+03	.21409335+01	.33819466+00	-.63	-10.03	-9.46
12000.	11973.7	.22020000+03	.22020000+03	.18334760+01	.29006526+00	1.11	-10.03	-11.01
13000.	12969.5	.21986667+03	.21986667+03	.15698037+01	.24872747+00	2.25	-9.82	-11.80
14000.	13965.0	.21953333+03	.21953333+03	.13437334+01	.21323105+00	3.12	-9.45	-12.19
15000.	14960.1	.21920000+03	.21920000+03	.11499482+01	.18275763+00	3.88	-8.96	-12.37
16000.	15954.9	.21886667+03	.21886667+03	.98387621+00	.15660248+00	4.49	-8.39	-12.33
17000.	16949.5	.21853333+03	.21853333+03	.84158803+00	.13415895+00	4.64	-7.81	-11.89
18000.	17943.7	.21820000+03	.21820000+03	.71970595+00	.11490479+00	3.71	-7.26	-10.59
19000.	18937.6	.21870000+03	.21870000+03	.61551163+00	.98044963-01	3.32	-6.96	-9.91
20000.	19931.2	.21920000+03	.21920000+03	.52659006+00	.83689297-01	2.72	-6.63	-9.05
21000.	20924.4	.21970000+03	.21970000+03	.45067487+00	.71461329-01	2.01	-6.28	-8.11
22000.	21917.4	.22020000+03	.22020000+03	.38584043+00	.61041925-01	1.32	-6.00	-7.25
23000.	22910.0	.22070000+03	.22070000+03	.33044950+00	.52160359-01	.71	-5.85	-6.57
24000.	23902.4	.22120000+03	.22120000+03	.28310973+00	.44586920-01	.24	-5.87	-6.13
25000.	24894.4	.22170000+03	.22170000+03	.24263648+00	.38126611-01	-.12	-6.05	-5.94
26000.	25886.1	.22220000+03	.22220000+03	.20802155+00	.32613851-01	-.41	-6.32	-5.90
27000.	26877.5	.22270000+03	.22270000+03	.17840657+00	.27907982-01	-.74	-6.59	-5.85
28000.	27868.6	.22320000+03	.22320000+03	.15306042+00	.23889470-01	-1.28	-6.70	-5.53
29000.	28859.4	.22370000+03	.22370000+03	.13136023+00	.20456706-01	-1.95	-7.12	-5.28
30000.	29849.9	.22420000+03	.22420000+03	.11277507+00	.17523275-01	-2.71	-7.61	-5.04
31000.	30840.0	.22470000+03	.22470000+03	.96852294-01	.15015667-01	-3.39	-8.17	-4.95
32000.	31829.9	.22520000+03	.22520000+03	.83205808-01	.12871319-01	-4.03	-8.80	-4.97
33000.	32819.4	.22740000+03	.22740000+03	.71546821-01	.10960685-01	-3.94	-9.46	-5.74
34000.	33808.7	.22960000+03	.22960000+03	.61610998-01	.93481175-02	-3.87	-10.10	-6.48
35000.	34797.6	.23180000+03	.23180000+03	.53130679-01	.79849047-02	-3.83	-10.74	-7.18
36000.	35786.2	.23400000+03	.23400000+03	.45881753-01	.68306486-02	-3.84	-11.37	-7.83
37000.	36774.5	.23620000+03	.23620000+03	.39676265-01	.58517896-02	-3.90	-12.02	-8.45
38000.	37762.5	.23840000+03	.23840000+03	.34356322-01	.50203988-02	-4.02	-12.68	-9.02
39000.	38750.2	.24060000+03	.24060000+03	.29789065-01	.43131945-02	-4.17	-13.35	-9.57
40000.	39737.5	.24280000+03	.24280000+03	.25862528-01	.37107363-02	-4.37	-14.03	-10.10
41000.	40724.6	.24500000+03	.24500000+03	.22482197-01	.31967633-02	-4.58	-14.73	-10.64
42000.	41711.4	.24720000+03	.24720000+03	.19568176-01	.27576534-02	-4.78	-15.43	-11.19
43000.	42697.8	.24940000+03	.24940000+03	.17052817-01	.23819766-02	-4.95	-16.15	-11.78
44000.	43683.9	.25160000+03	.25160000+03	.14878758-01	.20601264-02	-5.06	-16.86	-12.43
45000.	44669.8	.25380000+03	.25380000+03	.12997293-01	.17840174-02	-5.06	-17.56	-13.17
46000.	45655.3	.25600000+03	.25600000+03	.11367000-01	.15468340-02	-4.90	-18.25	-14.03
47000.	46640.5	.25820000+03	.25820000+03	.99526080-02	.13428220-02	-4.54	-18.90	-15.05
48000.	47625.4	.25820000+03	.25820000+03	.87191499-02	.11764019-02	-4.71	-19.55	-15.57
49000.	48610.0	.25820000+03	.25820000+03	.76385581-02	.10306067-02	-4.54	-20.23	-16.44
50000.	49594.3	.25820000+03	.25820000+03	.66918877-02	.90288038-03	-4.78	-20.85	-16.88
51000.	50578.3	.25820000+03	.25820000+03	.58625413-02	.79098361-03	-4.82	-21.58	-17.61
52000.	51561.9	.25820000+03	.25820000+03	.51359787-02	.69295459-03	-4.65	-22.26	-18.47
53000.	52545.3	.25681290+03	.25681290+03	.44978562-02	.61013583-03	-4.80	-22.90	-19.02
54000.	53528.4	.25542581+03	.25542581+03	.39361885-02	.53684501-03	-4.78	-23.54	-19.70
55000.	54511.1	.25403871+03	.25403871+03	.34421577-02	.47202899-03	-4.62	-24.15	-20.48
56000.	55493.6	.25265162+03	.25265162+03	.30079233-02	.41474626-03	-4.33	-24.74	-21.33
57000.	56475.7	.25126452+03	.25126452+03	.26265177-02	.36415558-03	-3.93	-25.30	-22.24
58000.	57457.5	.24987742+03	.24987742+03	.22917537-02	.31950579-03	-3.42	-25.82	-23.19
59000.	58439.1	.24849033+03	.24849033+03	.19981401-02	.28012654-03	-2.84	-26.29	-24.14
60000.	59420.3	.24710323+03	.24710323+03	.17408071-02	.24542004-03	-2.18	-26.72	-25.08
61000.	60401.2	.24571613+03	.24571613+03	.15154383-02	.21485349-03	-1.47	-27.09	-26.00
62000.	61381.8	.24432904+03	.24432904+03	.13182113-02	.18795236-03	-.71	-27.40	-26.88
63000.	62362.1	.24294194+03	.24294194+03	.11457428-02	.16429428-03	.09	-27.64	-27.71
64000.	63342.1	.24155484+03	.24155484+03	.99504000-03	.14350354-03	.91	-27.82	-28.47
65000.	64321.8	.24016774+03	.24016774+03	.86345797-03	.12524613-03	1.74	-27.93	-29.16
66000.	65301.2	.23878065+03	.23878065+03	.74866075-03	.10922543-03	2.58	-27.95	-29.76
67000.	66280.3	.23739355+03	.23739355+03	.64858662-03	.95178066-04	3.41	-27.90	-30.27
68000.	67259.0	.23600645+03	.23600645+03	.56141715-03	.82870431-04	4.24	-27.75	-30.69
69000.	68237.5	.23461936+03	.23461936+03	.48554993-03	.72095449-04	5.06	-27.52	-31.01
70000.	69215.7	.23323226+03	.23323226+03	.41957368-03	.62669672-04	5.88	-27.19	-31.23
71000.	70193.5	.23184517+03	.23184517+03	.36224652-03	.54430708-04	6.69	-26.76	-31.35
72000.	71171.1	.23045807+03	.23045807+03	.31247647-03	.47234922-04	7.49	-26.23	-31.37
73000.	72148.3	.22907097+03	.22907097+03	.26930408-03	.40955355-04	8.31	-25.58	-31.29
74000.	73125.3	.22768387+03	.22768387+03	.23188698-03	.35479860-04	9.16	-24.82	-31.13
75000.	74101.9	.22629678+03	.22629678+03	.19948617-03	.30709463-04	10.05	-23.95	-30.89
76000.	75078.3	.22490968+03	.22490968+03	.17145389-03	.26556878-04	11.01	-22.94	-30.59
77000.	76054.3	.22352258+03	.22352258+03	.14722282-03	.22945183-04	12.07	-21.81	-30.23
78000.	77030.0	.22213549+03	.22213549+03	.12629642-03	.19806644-04	13.27	-20.54	-29.85
79000.	78005.4	.22074839+03	.22074839+03	.10824052-03	.17081662-04	14.67	-19.13	-29.48
80000.	78980.6	.21936129+03	.21936129+03	.92675794-04	.14717842-04	16.31	-17.58	-29.13
81000.	79955.4	.21797420+03	.21797420+03	.79271131-04	.12669159-04	18.28	-15.86	-28.87
82000.	80929.9	.21658710+03	.21658710+03	.67737737-04	.10895218-04	19.89	-13.90	-28.19
83000.	81904.1	.21520000+03	.21520000+03	.57823921-04	.93605867-05	19.13	-11.63	-25.82
84000.	82878.0	.21520000+03	.21520000+03	.49335935-04	.79865441-05	19.13	-9.36	-23.91
85000.	83851.6	.21520000+03	.21520000+03	.42093902-04	.68141977-05	19.13	-7.03	-21.95
86000.	84824.9	.21520000+03	.21520000+03	.35914930-04	.58139402-05	19.13	-4.64	-19.95
87000.	85798.0	.21520000+03	.21520000+03	.30642970-04	.49605106-05	19.13	-2.21	-17.91
88000.	86770.7	.21520000+03	.21520000+03	.26144882-04	.42323563-05	19.13	.29	-15.81
89000.	87743.1	.21520000+03	.21520000+03	.22307069-04	.36110878-05	19.13	2.84	-13.67
90000.	88715.1	.21520000+03	.21520000+03	.19032610-04	.30810154-05	19.13	5.45	-11.48

The Patrick Reference Atmosphere (PRA-63) is a more extensive reference atmosphere presenting data to 700 kilometers for the Eastern Test Range. Because of the utility of this atmosphere, a simplified version is given as Table 14.12 from reference 14.3. The computer subroutine used to prepare these values is available in the subroutine files of the MSFC Computation Laboratory as Computer Subroutine PRA-63. Criteria for orbital studies are in reference 14.5.

A reference atmosphere is also available for SAMTEC (Vandenberg AFB) (Ref. 14.10) Table 14.13. This provides a nominal annual atmosphere model to 700 kilometers and has been designated as Computer Subroutine VRA-71.

In Tables 14.12 and 14.13 the values are given in standard computer printout, where the two-digit numbers that are at the end of the tabular value (number preceded by E) indicate the power of 10 by which the respective principal value must be multiplied. For example, a tabular value indicated as 2.9937265E 02 is 299.37265 or .15464054E-04 is 0.000015464054.

14.8 Reentry (90 Kilometers to Surface)

The atmospheric models to be used for all reentry analyses are the US 62 (Ref. 14.2) and the U. S. Standard Atmosphere Supplements, 1966 (Ref. 14.4), as expanded in the following paragraphs. Primary consideration is given to atmospheric density since it is the most significant parameter in reentry analyses.

For all analyses, the supplemental atmospheres (for mean values) and the extreme densities from Table 14.14, should be used according to the latitude ranges shown in Figure 14.5.

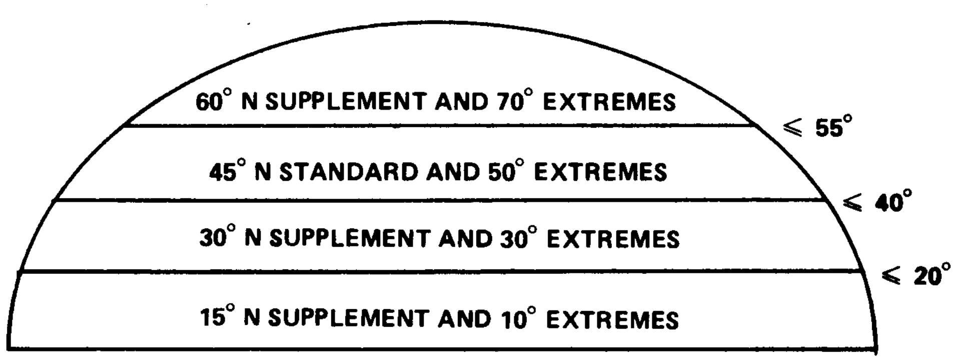

FIGURE 14.5 LATITUDE RANGE OF SUPPLEMENTAL ATMOSPHERES (applicable to both N and S hemispheres)

TABLE 14.12 CAPE KENNEDY (PATRICK) REFERENCE ATMOSPHERE (PRA-63)

GEOMETRIC ALTITUDE	PRESSURE	KINETIC TEMPERATURE	VIRTUAL TEMPERATURE	DENSITY	KINEMATIC VISCOSITY	COEFFICIENT OF VISCOSITY	SPEED OF SOUND
meters	newtons cm^{-2}	degrees K	degrees K	kg m^{-3}	m^2 sec^{-1}	newton-sec m^{-2}	m sec^{-1}
0.	1.0170147+01	2.9567877+02	2.9937265+02	1.1835467+00	1.5454054-05	1.8302431-05	3.4685752+02
1000.	9.0603417+00	2.9059303+02	2.9244317+02	1.0793462+00	1.6687364-05	1.8011442-05	3.4281972+02
2000.	8.0521166+00	2.8533229+02	2.8653089+02	9.7902799-01	1.8137912-05	1.7757524-05	3.3933665+02
3000.	7.1335062+00	2.8025122+02	2.8097135+02	8.8525680-01	1.9779729-05	1.7510140-05	3.3602847+02
4000.	6.3151744+00	2.7491955+02	2.7530996+02	7.9915661-01	2.1583060-05	1.7248245-05	3.3262586+02
5000.	5.5714346+00	2.6909224+02	2.6927405+02	7.2034273-01	2.3526962-05	1.6959240-05	3.2895941+02
6000.	4.9008910+00	2.6267951+02	2.6274498+02	6.4983432-01	2.5603113-05	1.6637782-05	3.2494680+02
7000.	4.2967358+00	2.5571709+02	2.5573003+02	5.8535150-01	2.7820210-05	1.6284602-05	3.2057962+02
8000.	3.7532038+00	2.4833624+02	2.4833460+02	5.2651816-01	3.0208493-05	1.5905320-05	3.1591022+02
9000.	3.2643867+00	2.4073390+02	2.4073421+02	4.7249330-01	3.2824227-05	1.5509244-05	3.1103836+02
10000.	2.8277554+00	2.3314284+02	2.3314653+02	4.2255460-01	3.5754187-05	1.5108096-05	3.0609732+02
11000.	2.4373143+00	2.2567654+02	2.2567654+02	3.7638426-01	3.9076665-05	1.4707842-05	3.0115374+02
12000.	2.0909280+00	2.1882266+02	2.1882266+02	3.3302118-01	4.3046158-05	1.4335282-05	2.9654541+02
13000.	1.7861066+00	2.1289318+02	2.1289318+02	2.9232217-01	4.7922764-05	1.4008836-05	2.9250004+02
14000.	1.5199026+00	2.0815733+02	2.0815733+02	2.5432636-01	5.4046316-05	1.3745403-05	2.8922838+02
15000.	1.2392355+00	2.0482690+02	2.0482690+02	2.1920325-01	5.1853967-05	1.3553591-05	2.8690521+02
16000.	1.0911841+00	2.0304202+02	2.0304202+02	1.8717684-01	7.1899701-05	1.3457959-05	2.8565249+02
17000.	9.2252635-01	2.0285831+02	2.0285831+02	1.5945601-01	8.4866329-05	1.3447580-05	2.8552324+02
18000.	7.8097360-01	2.0530313+02	2.0530313+02	1.3239217-01	1.0261472-04	1.3585386-05	2.8723862+02
19000.	6.6260085-01	2.0778667+02	2.0778667+02	1.1096236-01	1.2368766-04	1.3724675-05	2.8897076+02
20000.	5.6315646-01	2.1035487+02	2.1035487+02	9.3193794-02	1.4880795-04	1.3867977-05	2.9075108+02
21000.	4.7949008-01	2.1291042+02	2.1291042+02	7.8447666-02	1.7858837-04	1.4009341-05	2.9251188+02
22000.	4.0899187-01	2.1537456+02	2.1537456+02	6.6193244-02	2.1370677-04	1.4145944-05	2.9419972+02
23000.	3.4949302-01	2.1768801+02	2.1768801+02	5.5991185-02	2.5491727-04	1.4273120-05	2.9577557+02
24000.	2.9918756-01	2.1981201+02	2.1981201+02	4.7478891-02	3.0306879-04	1.4389370-05	2.9721502+02
25000.	2.5656948-01	2.2172934+02	2.2172934+02	4.0357731-02	3.5913492-04	1.4493892-05	2.9850846+02
26000.	2.2038158-01	2.2344526+02	2.2344526+02	3.4382485-02	4.2425969-04	1.4587102-05	2.9966127+02
27000.	1.8957412-01	2.2498853+02	2.2498853+02	2.9351583-02	4.9982543-04	1.4670658-05	3.0069433+02
28000.	1.6327365-01	2.2643885+02	2.2643885+02	2.5119032-02	5.8716325-04	1.4748972-05	3.0166195+02
29000.	1.4071529-01	2.2860044+02	2.2860044+02	2.1443811-02	6.9321966-04	1.4865272-05	3.0309836+02
30000.	1.2146274-01	2.3079275+02	2.3079275+02	1.8334060-02	8.1720744-04	1.4982731-05	3.0454827+02
31000.	1.0500136-01	2.3302839+02	2.3302839+02	1.5697349-02	9.6207351-04	1.5102004-05	3.0601976+02
32000.	9.0905086-02	2.3531626+02	2.3531626+02	1.3457738-02	1.1312058-03	1.5223539-05	3.0751834+02
33000.	7.8914435-02	2.3766155+02	2.3766155+02	1.1552738-02	1.3284797-03	1.5347578-05	3.0904699+02
34000.	6.8429919-02	2.4006564+02	2.4006564+02	9.9301033-03	1.5583081-03	1.5474160-05	3.1060616+02
35000.	5.9498650-02	2.4252601+02	2.4252601+02	8.5464654-03	1.8256806-03	1.5603116-05	3.1219376+02
36000.	5.1807186-02	2.4507629+02	2.4507629+02	7.3654171-03	2.1362104-03	1.5734081-05	3.1380529+02
37000.	4.5174764-02	2.4759611+02	2.4758611+02	6.3563439-03	2.4961655-03	1.5866486-05	3.1543377+02
38000.	3.9447995-02	2.5016117+02	2.5016117+02	5.4934139-03	2.9124978-03	1.5999574-05	3.1706989+02
39000.	3.4496486-02	2.5274305+02	2.5274305+02	4.7548125-03	3.3928543-03	1.6132386-05	3.1870190+02
40000.	3.0209181-02	2.5530928+02	2.5530928+02	4.1220201-03	3.9455843-03	1.6263778-05	3.2031579+02
41000.	2.6491425-02	2.5783324+02	2.5783324+02	3.5793500-03	4.5797178-03	1.6392413-05	3.2189521+02
42000.	2.3262412-02	2.6028407+02	2.6028407+02	3.1134716-03	5.3049351-03	1.6516765-05	3.2342147+02
43000.	2.0453115-02	2.6262674+02	2.6262674+02	2.7130531-03	6.1315133-03	1.6635121-05	3.2487367+02
44000.	1.8004513-02	2.6482185+02	2.6482185+02	2.3684560-03	7.0702506-03	1.6745577-05	3.2622855+02
45000.	1.5866131-02	2.6682573+02	2.6682573+02	2.0714816-03	8.1323618-03	1.6845038-05	3.2746049+02
46000.	1.3994778-02	2.6859025+02	2.6859025+02	1.8151542-03	9.3293486-03	1.6934206-05	3.2854145+02
47000.	1.2353487-02	2.7006287+02	2.7006287+02	1.5935381-03	1.0672843-02	1.7007582-05	3.2944088+02
48000.	1.0910569-02	2.7118660+02	2.7118660+02	1.4015769-03	1.2174462-02	1.7063446-05	3.3012557+02
49000.	9.6365032-03	2.7187675+02	2.7187675+02	1.2347674-03	1.3846901-02	1.7097702-05	3.3054538+02
50000.	8.5180218-03	2.7061179+02	2.7061179+02	1.0965534-03	1.5534933-02	1.7034884-05	3.2977552+02
51000.	7.5234923-03	2.6909057+02	2.6909057+02	9.7403573-04	1.7410714-02	1.6958658-05	3.2884120+02
52000.	6.6393199-03	2.6770746+02	2.6730746+02	8.5526725-04	1.9497023-02	1.6870136-05	3.2775595+02
53000.	5.8534792-03	2.6531613+02	2.6531613+02	7.6857841-04	2.1920011-02	1.6770390-05	3.2653285+02
54000.	5.1553131-03	2.6312957+02	2.6312957+02	6.8253219-04	2.4409781-02	1.6660461-05	3.2518454+02
55000.	4.5353599-03	2.6077017+02	2.6077017+02	6.0588695-04	2.7301073-02	1.6541354-05	3.2372334+02
56000.	3.9852060-03	2.5825936+02	2.5825936+02	5.3756682-04	3.0534014-02	1.6414073-05	3.2216109+02
57000.	3.4373536-03	2.5561788+02	2.5561788+02	4.7663516-04	3.4155134-02	1.6279538-05	3.2050933+02
58000.	3.0651144-03	2.5286548+02	2.5286548+02	4.2227454-04	3.8218427-02	1.6138669-05	3.1877909+02
59000.	2.6925137-03	2.5002103+02	2.5002103+02	3.7376890-04	4.2786724-02	1.5992347-05	3.1699106+02
60000.	2.3442082-03	2.4710225+02	2.4710225+02	3.3048918-04	4.7933213-02	1.5841408-05	3.1512539+02
61000.	2.0454142-03	2.4412601+02	2.4412601+02	2.9188042-04	5.3743447-02	1.5686660-05	3.1322187+02
62000.	1.7818466-03	2.4110781+02	2.4110781+02	2.5745231-04	6.0317409-02	1.5528856-05	3.1127962+02
63000.	1.5496627-03	2.3806214+02	2.3806214+02	2.2676947-04	6.7772396-02	1.5368710-05	3.0930733+02
64000.	1.3454170-03	2.3500219+02	2.3500219+02	1.9944492-04	7.6246084-02	1.5206886-05	3.0731305+02
65000.	1.1660196-03	2.3193985+02	2.3193985+02	1.7513309-04	8.5900343-02	1.5043993-05	3.0530417+02
66000.	1.0086976-03	2.2888566+02	2.2888566+02	1.5352538-04	9.6925872-02	1.4880581-05	3.0328738+02
67000.	8.7096431-04	2.2584869+02	2.2584869+02	1.3434470-04	1.0954757-01	1.4717135-05	3.0126858+02
68000.	7.5059127-04	2.2283659+02	2.2283659+02	1.1734235-04	1.2403088-01	1.4554074-05	2.9925285+02
69000.	6.4558010-04	2.1985550+02	2.1985550+02	1.0229409-04	1.4068989-01	1.4391745-05	2.9724443+02
70000.	5.5414295-04	2.1690995+02	2.1690995+02	8.8997968-05	1.5989594-01	1.4230414-05	2.9524652+02
71000.	4.7467952-04	2.1400276+02	2.1400276+02	7.7271416-05	1.8208977-01	1.4070257-05	2.9326129+02
72000.	4.0576003-04	2.1113524+02	2.1113524+02	6.6949339-05	2.0778956-01	1.3911374-05	2.9128989+02
73000.	3.4610846-04	2.0830661+02	2.0830661+02	5.7982451-05	2.3761514-01	1.3753747-05	2.8933207+02
74000.	2.9458748-04	2.0551466+02	2.0551466+02	4.9935479-05	2.7229692-01	1.3597277-05	2.8738656+02
75000.	2.5018505-04	2.0275504+02	2.0275504+02	4.2986041-05	3.1270019-01	1.3441743-05	2.8545054+02
76000.	2.1200230-04	2.0002150+02	2.0002150+02	3.6923397-05	3.5984800-01	1.3286811-05	2.8351980+02
77000.	1.7924187-04	1.9730595+02	1.9730595+02	3.1647376-05	4.1494915-01	1.3132031-05	2.8158865+02
78000.	1.5119831-04	1.9459801+02	1.9459801+02	2.7067385-05	4.7942623-01	1.2976814-05	2.7964963+02
79000.	1.2724843-04	1.9188550+02	1.9189550+02	2.3101918-05	5.5495197-01	1.2820455-05	2.7769376+02
80000.	1.0684305-04	1.8915375+02	1.8915375+02	1.9677462-05	6.4348155-01	1.2662084-05	2.7571001+02
81000.	8.9499401-05	1.8638612+02	1.8638612+02	1.6728011-05	7.4729141-01	1.2503639-05	2.7368553+02
82000.	7.4793845-05	1.8356361+02	1.8356361+02	1.4194399-05	8.6901411-01	1.2335133-05	2.7160537+02
83000.	6.2355805-05	1.8066492+02	1.8066492+02	1.2023774-05	1.0116670+00	1.2164056-05	2.6945234+02
84000.	5.1878215-05	1.8065000+02	1.8065000+02	1.0004256-05	1.2157997+00	1.2163173-05	2.6944122+02
85000.	4.3163464-05	1.8065000+02	1.8065000+02	8.3236936-06	1.4612710+00	1.2163173-05	2.6944122+02
86000.	3.5914713-05	1.8065000+02	1.8065000+02	6.9258358-06	1.7562028+00	1.2163173-05	2.6944122+02
87000.	2.9885006-05	1.8065000+02	1.8065000+02	5.7630599-06	2.1105407+00	1.2163173-05	2.6944122+02
88000.	2.4869045-05	1.8065000+02	1.8065000+02	4.7957760-06	2.5362262+00	1.2163173-05	2.6944122+02
89000.	2.0696155-05	1.8065000+02	1.8065000+02	3.9910710-06	3.0475961+00	1.2163173-05	2.6944122+02
90000.	1.7224435-05	1.8065000+02	1.8065000+02	3.3215804-06		1.2163173-05	2.6944122+02

TABLE 14.13 VANDENBURG AFB REFERENCE ATMOSPHERE (VRA-71)

GEOMETRIC ALTITUDE	PRESSURE	KINETIC TEMPERATURE	VIRTUAL TEMPERATURE	DENSITY	KINEMATIC VISCOSITY	COEFFICIENT OF VISCOSITY	SPEED OF SOUND
meters	newtons cm-2	degrees K	degrees K	kg m-3	m2 sec-1	newton-sec m-2	m sec-1
0.	1.0189904+01	2.8588177+02	2.8715277+02	1.2361775+00	1.4386405-05	1.7784150-05	3.3970470+02
1000.	9.0477941+00	2.8642662+02	2.8699761+02	1.0983266+00	1.6216058-05	1.7813528-05	3.3961291+02
2000.	8.0243502+00	2.8329711+02	2.8359425+02	9.8575564-01	1.7913862-05	1.7658691-05	3.3759326+02
3000.	7.1046558+00	2.7821440+02	2.7842384+02	8.8892961-01	1.9595771-05	1.7413372-05	3.3450165+02
4000.	6.2761809+00	2.7217236+02	2.7234509+02	8.0276189-01	2.1316859-05	1.7112362-05	3.3082996+02
5000.	5.5286658+00	2.6563136+02	2.6576157+02	7.2468038-01	2.3163579-05	1.6785203-05	3.2680685+02
6000.	4.8538800+00	2.5871198+02	2.5878904+02	6.5342553-01	2.5155218-05	1.6437062-05	3.2249129+02
7000.	4.2453096+00	2.5139878+02	2.5142269+02	5.8827869-01	2.7304746-05	1.6062801-05	3.1786835+02
8000.	3.6977986+00	2.4368403+02	2.4370449+02	5.2859970-01	2.9632266-05	1.5663607-05	3.1295134+02
9000.	3.2071987+00	2.3586146+02	2.3589045+02	4.7357411-01	3.2207045-05	1.5252423-05	3.0789330+02
10000.	2.7706815+00	2.2850072+02	2.2850072+02	4.2242641-01	3.5177528-05	1.4859917-05	3.0303224+02
11000.	2.3796741+00	2.2193979+02	2.2193979+02	3.7353754-01	3.9832351-05	1.4505341-05	2.9865008+02
12000.	2.0378622+00	2.1778813+02	2.1778813+02	3.2593435-01	4.3808244-05	1.4278611-05	2.9584359+02
13000.	1.7407523+00	2.1502290+02	2.1502290+02	2.8201088-01	5.0092260-05	1.4126562-05	2.9395944+02
14000.	1.4839231+00	2.1289493+02	2.1289493+02	2.4284485-01	5.7666966-05	1.4008983-05	2.9250124+02
15000.	1.2630643+00	2.1101876+02	2.1101876+02	2.0855008-01	6.5674156-05	1.3904901-05	2.9120953+02
16000.	1.0740324+00	2.0946258+02	2.0946258+02	1.7862758-01	7.7358000-05	1.3818273-05	2.9013377+02
17000.	9.1290847-01	2.0883855+02	2.0883855+02	1.5225517-01	9.0528671-05	1.3783459-05	2.8970126+02
18000.	7.7604645-01	2.1039268+02	2.1039268+02	1.2851184-01	1.0792843-04	1.3870081-05	2.9077721+02
19000.	6.6155133-01	2.1166882+02	2.1166882+02	1.0882416-01	1.2810581-04	1.3941003-05	2.9165773+02
20000.	5.6393303-01	2.1339162+02	2.1339162+02	9.2019110-02	1.5253866-04	1.4036472-05	2.9284225+02
21000.	4.8086911-01	2.1536418+02	2.1536418+02	7.7770908-02	1.8188514-04	1.4145373-05	2.9419263+02
22000.	4.1046340-01	2.1733892+02	2.1733892+02	6.5810409-02	2.1659138-04	1.4253967-05	2.9553832+02
23000.	3.5099534-01	2.1914086+02	2.1914086+02	5.5825416-02	2.5709956-04	1.4352690-05	2.9676094+02
24000.	3.0077469-01	2.2068008+02	2.2068008+02	4.7498948-02	3.0393812-04	1.4436741-05	2.9780132+02
25000.	2.5825416-01	2.2196423+02	2.2196423+02	4.0532336-02	3.5730363-04	1.4505670-05	2.9866653+02
26000.	2.2205890-01	2.2311148+02	2.2311148+02	3.4657364-02	4.2077229-04	1.4568995-05	2.9943738+02
27000.	1.9099714-01	2.2436256+02	2.2436256+02	2.9641456-02	4.9379501-04	1.4635803-05	3.0027575+02
28000.	1.6405777-01	2.2609358+02	2.2609358+02	2.5289117-02	5.8247786-04	1.4730351-05	3.0143187+02
29000.	1.4142399-01	2.2814065+02	2.2814065+02	2.1596011-02	6.8719054-04	1.4843574-05	3.0279339+02
30000.	1.2206691-01	2.3043426+02	2.3043426+02	1.8453921-02	8.1086060-04	1.4963557-05	3.0431165+02
31000.	1.0546830-01	2.3258450+02	2.3258450+02	1.5797158-02	9.5449946-04	1.5078363-05	3.0572815+02
32000.	9.1233502-02	2.3466267+02	2.3466267+02	1.3544035-02	1.1214437-03	1.5188873-05	3.0709098+02
33000.	7.9019569-02	2.3673119+02	2.3673119+02	1.1628319-02	1.3156191-03	1.5298438-05	3.0844149+02
34000.	6.6532667-02	2.3884268+02	2.3884268+02	9.9959356-03	1.5416105-03	1.5409839-05	3.0981399+02
35000.	5.9521349-02	2.4103903+02	2.4103903+02	8.6024678-03	1.8047440-03	1.5525252-05	3.1123525+02
36000.	5.1770654-02	2.4335058+02	2.4335058+02	7.4112084-03	2.1111540-03	1.5646202-05	3.1272402+02
37000.	4.5096980-02	2.4579478+02	2.4579478+02	6.3916438-03	2.4578365-03	1.5773532-05	3.1429059+02
38000.	3.9343655-02	2.4837562+02	2.4837562+02	5.5182770-03	2.8826674-03	1.5907357-05	3.1593631+02
39000.	3.4377026-02	2.5109266+02	2.5109266+02	4.7696810-03	3.3643858-03	1.6047047-05	3.1765333+02
40000.	3.0083150-02	2.5388979+02	2.5388979+02	4.1277733-03	3.9224962-03	1.6191175-05	3.1942409+02
41000.	2.6364920-02	2.5675467+02	2.5675467+02	3.5772217-03	4.5670959-03	1.6337515-05	3.2122122+02
42000.	2.3139577-02	2.5961737+02	2.5961737+02	3.1049844-03	5.3085585-03	1.6482991-05	3.2300700+02
43000.	2.0336609-02	2.6239986+02	2.6239986+02	2.6999312-03	6.1570753-03	1.6623690-05	3.2473332+02
44000.	1.7895922-02	2.6500471+02	2.6500471+02	2.3525465-03	7.1219673-03	1.6754759-05	3.2634116+02
45000.	1.5766305-02	2.6731429+02	2.6731429+02	2.0546863-03	8.2107314-03	1.6870477-05	3.2776014+02
46000.	1.3904100-02	2.6918990+02	2.6918990+02	1.7993759-03	9.4277728-03	1.6964107-05	3.2890799+02
47000.	1.2272031-02	2.7047061+02	2.7047061+02	1.5806507-03	1.0772693-02	1.7027864-05	3.2968948+02
48000.	1.0836504-02	2.7097250+02	2.7097250+02	1.3934194-03	1.2278103-02	1.7052811-05	3.2999523+02
49000.	9.5752799-03	2.7049761+02	2.7048761+02	1.2333525-03	1.3806948-02	1.7028710-05	3.2969984+02
50000.	8.4550115-03	2.7115682+02	2.7115662+02	1.0862549-03	1.5707140-02	1.7061957-05	3.3010733+02
51000.	7.4760636-03	2.7127369+02	2.7127369+02	9.6007037-04	1.7777625-02	1.7067771-05	3.3017857+02
52000.	6.6065708-03	2.7078585+02	2.7078585+02	8.4993924-04	2.0052652-02	1.7043536-05	3.2988156+02
53000.	5.8341418-03	2.6976022+02	2.6976022+02	7.5341944-04	2.2553960-02	1.6992517-05	3.2925623+02
54000.	5.1478915-03	2.6826166+02	2.6826166+02	6.6851096-04	2.5306703-02	1.6917808-05	3.2834042+02
55000.	4.5382458-03	2.6535233+02	2.6635233+02	5.9356636-04	2.8341122-02	1.6822337-05	3.2716987+02
56000.	3.9967607-03	2.6409158+02	2.6409158+02	5.2721934-04	3.1692461-02	1.6708879-05	3.2577843+02
57000.	3.5159756-03	2.6153592+02	2.6153592+02	4.6833031-04	3.5402517-02	1.6580072-05	3.2419829+02
58000.	3.0892362-03	2.5873822+02	2.5873822+02	4.1594443-04	3.9520649-02	1.6438394-05	3.2245963+02
59000.	2.7108367-03	2.5574928+02	2.5574928+02	3.6925677-04	4.4105342-02	1.6286194-05	3.2059106+02
60000.	2.3754195-03	2.5261192+02	2.5261192+02	3.2758516-04	4.9225845-02	1.6125656-05	3.1861922+02
61000.	2.0784015-03	2.4937169+02	2.4937169+02	2.9034891-04	5.4964365-02	1.5958838-05	3.1656918+02
62000.	1.8156504-03	2.4606511+02	2.4606511+02	2.5705139-04	6.1417989-02	1.5787579-05	3.1446338+02
63000.	1.5834767-03	2.4272632+02	2.4272632+02	2.2726500-04	6.8702127-02	1.5613589-05	3.1232265+02
64000.	1.3785800-03	2.3938440+02	2.3938440+02	2.0061984-04	7.6953251-02	1.5438349-05	3.1016517+02
65000.	1.1980055-03	2.3606390+02	2.3606390+02	1.7679378-04	8.6333018-02	1.5263141-05	3.0800647+02
66000.	1.0391056-03	2.3278436+02	2.3278436+02	1.5550474-04	9.7032473-02	1.5089010-05	3.0585949+02
67000.	8.9950478-04	2.2956021+02	2.2956021+02	1.3650376-04	1.0927724-01	1.4915755-05	3.0373397+02
68000.	7.7707160-04	2.2640073+02	2.2640073+02	1.1956965-04	1.2333327-01	1.4746916-05	3.0163655+02
69000.	6.6989220-04	2.2330920+02	2.2330920+02	1.0450475-04	1.3951253-01	1.4579723-05	2.9957003+02
70000.	5.7624817-04	2.2028366+02	2.2028366+02	9.1130767-05	1.5818059-01	1.4415118-05	2.9753372+02
71000.	4.9459703-04	2.1731552+02	2.1731552+02	7.9286366-05	1.7976209-01	1.4252583-05	2.9552241+02
72000.	4.2355436-04	2.1439084+02	2.1439084+02	6.8824123-05	2.0474928-01	1.4091690-05	2.9352707+02
73000.	3.6187395-04	2.1148319+02	2.1148319+02	5.9609427-05	2.3370430-01	1.3930980-05	2.9153326+02
74000.	3.0845853-04	2.0858051+02	2.0858051+02	5.1518217-05	2.6726563-01	1.3769049-05	2.8952223+02
75000.	2.6223794-04	2.0563354+02	2.0563354+02	4.4436379-05	3.0614461-01	1.3603953-05	2.8746967+02
76000.	2.2250776-04	2.0260577+02	2.0260577+02	3.8258777-05	3.5111696-01	1.3433306-05	2.8534546+02
77000.	1.8829458-04	1.9944855+02	1.9944855+02	3.2838548-05	4.0300428-01	1.3254226-05	2.8311344+02
78000.	1.5895186-04	1.9610583+02	1.9610587+02	2.8236629-05	4.6263842-01	1.3063349-05	2.8073096+02
79000.	1.3385165-04	1.9251422+02	1.9251422+02	2.4221368-05	5.3080305-01	1.2856776-05	2.7814833+02
80000.	1.1243729-04	1.8860150+02	1.8860150+02	2.0768398-05	6.0813343-01	1.2629957-05	2.7530724+02
81000.	9.4216307-05	1.8428839+02	1.8428839+02	1.7810079-05	6.9438529-01	1.2377743-05	2.7214104+02
82000.	7.8673015-05	1.8065000+02	1.8065000+02	1.5171552-05	8.0170920-01	1.2163173-05	2.6944122+02
83000.	6.5436167-05	1.8065000+02	1.8065000+02	1.2618788-05	9.6399390-01	1.2163173-05	2.6944122+02
84000.	5.4429003-05	1.8065000+02	1.8065000+02	1.0496153-05	1.1588219+00	1.2163173-05	2.6944122+02
85000.	4.5275370-05	1.8065000+02	1.8065000+02	8.7310716-06	1.3930905+00	1.2163173-05	2.6944122+02
86000.	3.7664308-05	1.8065000+02	1.8065000+02	7.2632298-06	1.6746231+00	1.2163173-05	2.6944122+02
87000.	3.1334090-05	1.8065000+02	1.8065000+02	6.0425029-06	2.0129361+00	1.2163173-05	2.6944122+02
88000.	2.6069278-05	1.8065000+02	1.8065000+02	5.0272304-06	2.4194579+00	1.2163173-05	2.6944122+02
89000.	2.1690308-05	1.8065000+02	1.8065000+02	4.1827847-06	2.9079126+00	1.2163173-05	2.6944122+02
90000.	1.8049200-05	1.8065000+02	1.8065000+02	3.4806292-06		1.2163173-05	2.6944122+02

TABLE 14.14 RANGE* OF ATMOSPHERIC DENSITY FOR DESIGN STUDIES

JANUARY								
Altitude	70° latitude		50° latitude		30° latitude		10° latitude	
km	min.	max.	min.	max.	min.	max.	min.	max.
25	-15.4	5.9	-5.0	9.6	-5.7	8.8	-4.9	4.3
30	-22.6	5.0	-9.2	8.8	-11.7	5.8	-7.8	1.9
35	-27.9	5.7	-8.7	9.2	-10.0	7.7	-7.1	3.4
40	-34.3	2.7	-11.6	8.0	-10.8	9.0	-3.6	8.0
45	-40.5	0.1	-14.5	8.3	-8.6	15.7	-0.9	11.9
50	-47.0	-3.8	-18.6	7.5	-9.3	19.8	-0.7	12.9
55	-50.8	-6.0	-24.9	3.0	-10.9	22.1	-0.8	13.6
60	-53.2	-8.1	-31.1	-1.3	-16.2	19.9	1.7	17.4
65	-55.1	-10.6	-36.6	-6.3	-20.8	17.1	2.3	19.0
70	-59.7	-17.3	-41.6	-11.6	-26.0	11.9	0.3	17.5
75	-62.2	-22.7	-42.0	-12.2	-29.2	7.2	-6.1	10.7
80	-63.5	-26.9	-40.5	-9.2	-31.7	4.1	-10.5	6.5
85	-59.1	-18.5	-29.1	5.7	-22.4	15.6	-1.9	17.6
90	-55.1	-9.8	-18.9	17.7	-14.1	24.7	7.5	30.0

APRIL								
Altitude	70° latitude		50° latitude		30° latitude		10° latitude	
km	min.	max.	min	max.	min.	max.	min.	max.
25	-20.2	-1.5	-12.6	4.9	-11.6	6.1	-4.7	4.5
30	-19.3	3.6	-12.6	3.5	-12.0	4.2	-6.5	3.3
35	-19.7	6.3	-13.1	3.5	-10.7	6.4	-6.2	4.4
40	-22.2	6.7	-11.6	7.3	-8.3	11.4	-2.0	9.8
45	-24.6	7.1	-9.5	12.7	-6.7	16.2	1.3	14.5
50	-27.1	6.9	-8.4	17.6	-5.9	20.9	4.6	19.0
55	-28.9	6.6	-11.1	18.5	-8.2	22.4	5.9	21.5
60	-30.9	5.8	-13.0	20.3	-10.8	23.4	9.2	26.1
65	-36.1	1.5	-21.5	12.7	-19.9	15.1	6.1	23.5
70	-41.1	-2.1	-27.0	7.8	-25.4	10.1	2.0	19.4
75	-43.7	-2.7	-28.9	5.1	-28.4	5.9	-5.2	11.7
80	-43.8	-0.4	-23.6	11.7	-24.8	10.0	-10.5	6.5
85	-37.0	12.4	-10.9	28.5	-12.5	26.1	-3.0	16.2
90	-35.2	15.6	-2.7	39.4	0.9	44.6	7.3	29.7

* In percent departure from U. S. Standard Atmosphere, 1962.

TABLE 14.14 (Concluded)

JULY								
Altitude km	70° latitude		50° latitude		30° latitude		10° latitude	
	min.	max.	min.	max.	min.	max.	min.	max.
25	-9.3	8.2	-7.3	8.1	-8.5	6.6	-2.3	10.0
30	-4.3	15.7	-7.5	7.9	-8.3	6.9	-4.9	7.7
35	-0.3	23.2	-4.3	12.4	-7.1	9.1	-3.1	10.5
40	3.9	30.6	-1.4	18.0	-5.2	13.5	0.0	14.9
45	8.2	37.9	2.3	27.4	-4.2	19.2	2.8	19.0
50	10.1	40.6	4.5	33.5	-3.3	23.4	2.6	19.5
55	10.0	40.8	4.7	35.2	-4.0	23.9	2.0	19.7
60	10.6	44.2	3.3	35.3	-5.3	23.9	3.3	22.1
65	7.8	48.8	-2.1	33.6	-11.5	20.7	5.6	25.8
70	6.0	56.0	-8.7	30.6	-20.0	14.5	4.3	25.0
75	5.5	65.4	-12.5	28.9	-27.7	6.5	-1.7	18.6
80	3.4	70.8	-11.3	26.1	-26.4	4.7	-6.6	13.5
85	-0.1	69.3	-7.7	29.4	-16.9	16.4	1.1	23.9
90	-26.0	25.6	-20.5	12.9	-11.9	25.2	10.4	36.3

OCTOBER								
Altitude km	70° latitude		50° latitude		30° latitude		10° latitude	
	min.	max.	min.	max.	min.	max.	min.	max.
25	-19.5	0.2	-7.2	11.3	-8.9	9.3	-4.5	4.8
30	-20.9	4.3	-7.0	10.1	-8.2	8.6	-6.5	3.3
35	-21.1	8.5	-8.4	9.2	-7.6	10.2	-5.1	5.6
40	-22.8	10.9	-9.0	10.6	-5.3	15.0	-2.5	9.3
45	-24.4	12.8	-8.8	13.5	-5.0	18.3	0.6	13.7
50	-27.2	12.3	-10.3	15.2	-5.9	20.9	2.9	17.1
55	-28.5	13.7	-13.3	15.6	-8.0	22.7	4.0	19.2
60	-31.0	13.4	-17.9	13.6	-11.2	22.9	6.5	22.9
65	-35.7	9.3	-25.9	6.4	-20.2	14.6	4.9	22.0
70	-40.0	5.0	-34.9	-3.8	-24.6	11.3	2.2	19.7
75	-44.0	0.5	-39.9	-11.0	-28.0	6.4	-2.4	15.1
80	-46.0	-1.8	-40.7	-13.2	-26.5	7.4	-4.9	13.0
85	-40.2	9.2	-32.8	-3.1	-15.7	21.6	4.1	24.8
90	-36.2	16.4	-27.9	3.3	-5.8	34.9	16.8	41.2

Even though only mean values are tabulated in the U. S. Standard Supplements, 1966, extreme density values suitable for use in vehicle design calculations can be obtained from Table 14.14. For all computations, these tabulated maximum and minimum values may be used with the appropriate mean values of temperature and pressure.

G. V. Groves (Ref. 14.11) has constructed similar nominal latitudinal/seasonal atmospheric models from 25 to 110 kilometers altitude. Results of a study on the distributions of temperature, pressure, and density between 30 and 80 kilometers by Allen E. Cole (Ref. 14.12) gives estimates of probable worldwide extreme values.

14.8.1 Atmospheric Density for Reentry Analyses

Since atmospheric parameters are seldom constant over large areas, it is unrealistic to expect minimum, maximum, or mean values of density to exist over the entire reentry trajectory. However, if one is concerned only with instantaneous vehicle heating computations (not considering accumulated heat), the density value producing the most severe heating may be used at every point of the trajectory (for example, the July maximum values from Table 14.14).

In some design problems, it may be useful to consider density changes along the vehicle trajectory — changes that may occur in the atmosphere. For example, when accumulated heat calculations are made, realistic results can be obtained by allowing the density to change in a somewhat regular manner over the vehicle trajectory. This problem is rather complex because both horizontal and vertical gradients must be considered. Since both high and low density extremes and extreme gradients occur at high latitudes perhaps design studies need consider only those areas. However, if reentry can be limited to low latitudes, say from 30° S to 30° N, less severe density extremes and gradients can be used.

The design procedure outlined here assumes that for heating studies the reentry flight trajectories will be calculated along a reference atmosphere (U. S. Standard Atmosphere, 1962 or U. S. Standard Supplements, 1966) upon which a perturbation (or density gradient) will be imposed. A variety of density changes can be encountered within the bounds indicated in Figure 14.6. By tying all gradients to a common reference — percent departure from US 62 — the density at any point can be evaluated. Also, the horizontal and vertical gradients can be considered separately or additively.

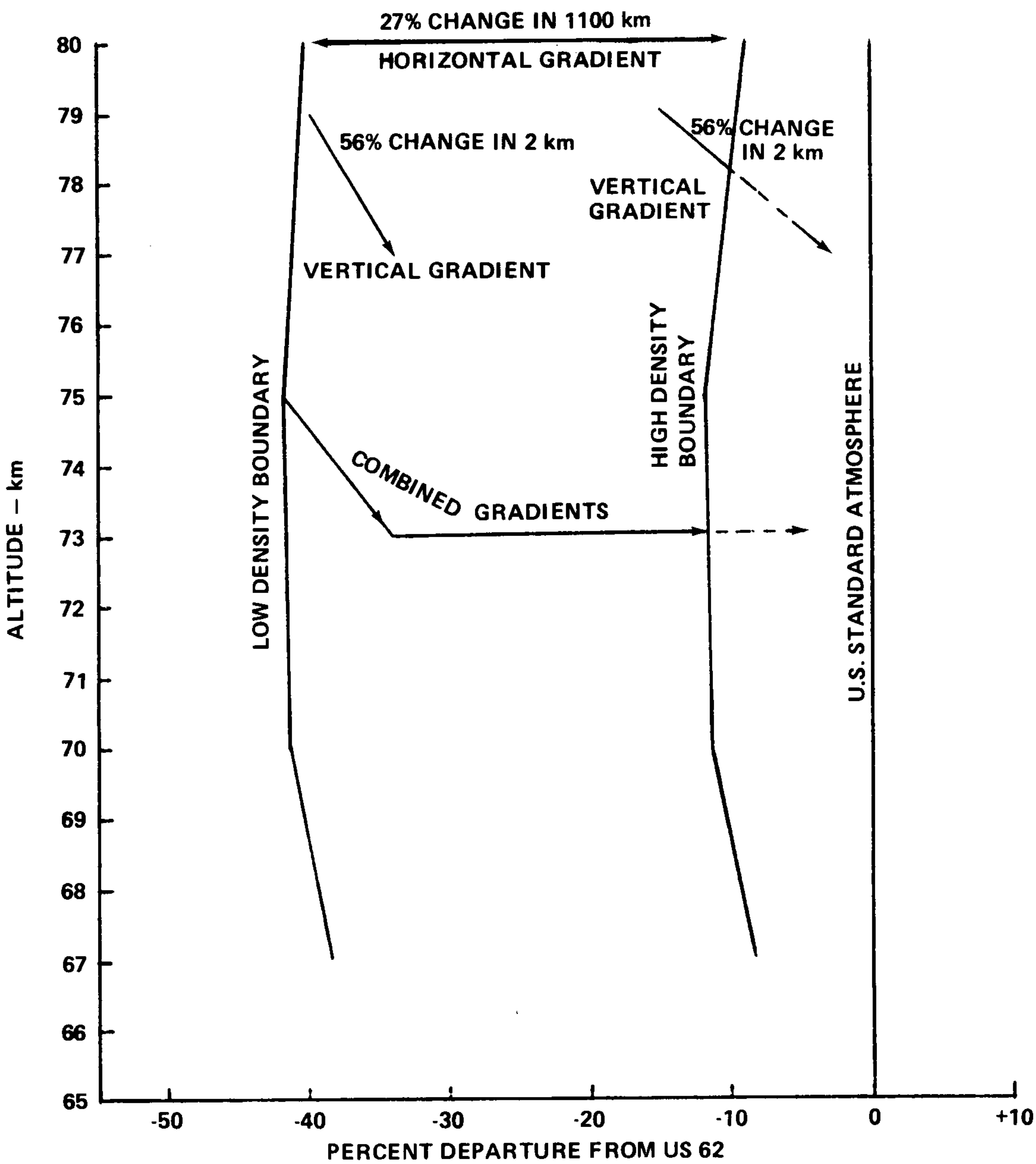

Figure 14.6 Density Gradients, January, 50° N.

A technique (computer subroutine DDP 73') to calculate values of density that might be encountered during flight through the gradients described above is available upon request to S&E-Aero-YT, Marshall Space Flight Center, Ala. 35812.

14.8.1.1 Examples of Density Gradient Calculation

To illustrate the possible density gradients, three cases will be considered.

Case 1. Flight at Constant Altitude. The maximum horizontal density gradients from Table 14.15 may be applied in any direction, i.e., at any time the reentering vehicle may be flying from relatively low to high density or high to low density. This is illustrated in Figure 14.6 at 80 kilometers. In both cases the density change when referenced to percent departure from the US 62 amounts to 27 percent.

Case 2. Vertical Flight. The maximum and minimum density changes from Table 14.16 are relative to the density at the higher level; these values are not percent departures from the US 62. A different reference must be used in this case because the vertical percent change of density is related to the temperature and temperature gradient in a column of air. The horizontal density gradient, on the other hand, was determined from an assumption of the minimum distance between two dissimilar columns of air. Although the vertical and horizontal gradients are referenced to different bases, they can be converted to a common reference while applying the perturbation. In January at 50° latitude temperature and temperature gradients dictate that the density should not increase more than 56 percent while descending from 79 to 77 kilometers. If the density at 79 kilometers is near the minimum, a 56-percent increase amounts to about a 6-percent change in relative departures from the US 62. If the density at 79 kilometers is near the maximum value, a 56-percent increase amounts to about a 12-percent change. Since the 56-percent increase may not be exceeded, the change in percent departure from the US 62 can only be determined after the 56-percent increase is computed. (See Figure 14.6 at 79 km for illustration of vertical gradient.)

Case 3. Flight Along a Trajectory. A combination of horizontal and vertical density gradients may be encountered along the flight path. To simulate this situation (or to apply the maximum perturbation to the reference atmosphere), the vertical gradient should be converted to percent departure from the US 62 so that the difference in the departures may be added to the horizontal gradient. For example, start with minimum density at 75 kilometers (density = 2.5143); apply the vertical gradient for 2 kilometers then increase the resultant density by 2.9 percent per 110 km for 1100 km or until the maximum boundary is reached. The perturbation must be reversed when the density reaches the maximum or minimum boundary. In this example, see Figure 14.6 75-73 km, the maximum density boundary was encountered before the full combined gradient could be exercised.

TABLE 14.15 MAXIMUM HORIZONTAL DENSITY GRADIENTS[4] – CHANGE OF PERCENT DEPARTURE FROM US 62 PER 110 km. (Gradient cannot exist for more than 1100 km)

Altitude (km)	JANUARY Latitude				APRIL Latitude				JULY Latitude				OCTOBER Latitude			
	70°	50°	30°	10°	70°	50°	30°	10°	70°	50°	30°	10°	70°	50°	30°	10°
90	1.7	1.8	1.3	0.8	0.3	1.1	0.8	0.5	0.6	1.0	0.3	0.3	1.0	1.6	0.5	0.5
80	2.2	2.7	1.8	1.1	0.7	1.4	1.1	0.6	1.1	1.4	0.8	0.8	1.5	1.8	0.7	0.7
70	2.3	2.9	1.6	0.9	0.6	1.3	0.8	0.6	1.1	1.2	0.9	0.9	1.4	1.6	0.7	0.7
60	2.2	2.9	1.1	0.8	0.4	0.9	0.4	0.4	0.8	0.9	0.7	0.7	0.9	1.4	0.9	0.7
50	2.6	2.4	0.9	0.4	0.6	0.9	0.6	0.3	0.6	0.5	0.6	0.6	1.0	1.2	0.8	0.5
40	3.0	1.8	0.6	0.4	0.9	0.6	0.5	0.3	0.3	0.4	0.4	0.4	1.0	0.9	0.3	0.3
30	2.6	1.6	0.4	0.4	1.1	0.6	0.3	0.3	0.4	0.4	0.4	0.4	1.1	0.9	0.3	0.3

Note: Use linear interpolation to obtain gradients at altitudes between those listed.

4. Values of change of percent departure from US 62 given in Table 14.15 were computed from

$$\left(\frac{\rho_s - \rho_{a_1}}{\rho_s}\right) 100 - \left(\frac{\rho_s - \rho_{a_2}}{\rho_s}\right) 100 = \text{change of percent departure} \quad (14.8)$$

where

ρ_s = density of US 62

ρ_{a_1} = ambient density at initial point

ρ_{a_2} = ambient density at final point.

TABLE 14.16 VERTICAL DENSITY GRADIENTS[5]
PERCENT INCREASE OF DENSITY IN 2 km LAYERS

JANUARY								
Altitude (km)	70° latitude		50° latitude		30° latitude		10° latitude	
	min.	max.	min.	max.	min.	max.	min.	max.
90	15	64	22	62	26	60	35	55
80	15	60	15	57	30	47	33	47
70	24	53	15	50	29	41	26	45
60	26	38	21	38	23	35	15	33
50	22	40	23	45	23	34	15	33
40	25	40	27	47	28	40	26	43
30	30	48	36	48	31	43	33	43

APRIL								
Altitude (km)	70° latitude		50° latitude		30° latitude		10° latitude	
	min.	max.	min.	max.	min.	max.	min.	max.
90	38	61	38	60	37	50	33	41
80	36	47	35	55	36	47	30	40
70	27	38	25	41	33	41	30	37
60	25	30	25	29	25	33	25	30
50	26	32	26	28	23	31	23	32
40	29	34	32	33	29	37	30	33
30	30	36	33	37	30	39	32	35

5. Values of percent increase in vertical density gradients in Table 14.16 were computed from

$$\left(\frac{\rho_L - \rho_H}{\rho_H}\right) 100 = \text{percent increase of density}$$

where

ρ_L = ambient density at lower altitude

ρ_H = ambient density at higher altitude.

TABLE 14.16 (Concluded)

JULY

Altitude (km)	70° latitude		50° latitude		30° latitude		10° latitude	
	min.	max.	min.	max.	min.	max.	min.	max.
90	40	57	37	58	40	50	35	48
80	37	50	30	55	30	47	35	47
70	26	32	25	45	30	45	30	42
60	24	27	25	29	24	34	22	30
50	25	32	25	30	25	32	23	32
40	30	35	30	35	28	35	27	35
30	34	37	34	37	32	40	27	39

OCTOBER

Altitude (km)	70° latitude		50° latitude		30° latitude		10° latitude	
	min.	max.	min.	max.	min.	max.	min.	max.
90	40	57	40	58	40	50	40	48
80	30	50	35	46	35	39	35	45
70	27	37	27	42	32	36	30	40
60	20	31	23	35	26	31	15	40
50	26	33	25	34	22	32	15	40
40	29	41	26	40	27	39	24	34
30	31	49	35	52	33	42	30	36

REFERENCES

14.1 Daniels, Glenn E., Editor, "Terrestrial Environment Climatic Criteria Guidelines for Use in Space Vehicle Development, 1971 Revision." NASA TM X-64589, NASA-Marshall Space Flight Center, Marshall Space Flight Center, Alabama, May 10, 1971.

14.2 "U. S. Standard Atmosphere, 1962." United States Government Printing Office, Washington, D. C. 20402, Dec. 1962.

14.3 Smith, Orvel E.; and Weidner, Don K., "A Reference Atmosphere for Patrick AFB, Florida, Annual (1963 Revision)." NASA TM X-53139, Sep. 23, 1964.

14.4 "U. S. Standard Atmosphere Supplements, 1966." United States Government Printing Office, Washington, D. C. 20402, 1966.

14.5 "Space and Planetary Environment Criteria Guidelines for Use in Space Vehicle Development, 1971 Revision." TM X-64627, November 15, 1971. NASA-Marshall Space Flight Center, Marshall Space Flight Center, Alabama, November 15, 1971.

14.6 IRIG Document No. 104-63, Range Reference Atmosphere Documents published by Secretariat, Range Commander's Council, White Sands Missile Range, New Mexico. The following reference atmospheres have been published under this title:

(1) Atlantic Missile Range Reference Atmosphere for Cape Kennedy, Florida (Part I), Sep. 1963.

(2) White Sands Missile Range Reference Atmosphere (Part I), Aug. 1964.

(3) Fort Churchill Missile Range Reference Atmosphere for Fort Churchill, Canada (Part I), Dec. 1964.

(4) Pacific Missile Range Reference Atmosphere for Eniwetok, Marshall Islands (Part I), Dec. 1964.

(5) Fort Greely Missile Range Reference Atmosphere (Part I), Nov. 1964.

REFERENCES (Continued)

(6) Pacific Missile Range Reference Atmosphere for Point Arguello, California (Part I), Aug. 1965.

(7) Eglin Gulf Test Range Reference Atmosphere, Eglin AFB, Florida (Part I), Aug. 1965.

(8) Wallops Island Test Range Reference Atmosphere (Part I), Sep. 1965.

(9) Eastern Test Range Reference Atmosphere for Ascension Island, South Atlantic (Part I), Jul. 1966.

(10) Lihue, Kauai, Hawaii Reference Atmosphere (Part I), January 1970.

(11) Johnston Island Test Site Reference Atmosphere (Part I), January 1970.

(12) Edwards Air Force Base Reference Atmosphere (Part I), Sept. 1972.

(13) Cape Kennedy, Florida Reference Atmosphere (Part II), July 1971.

(14) White Sands Missile Range Reference Atmosphere (Part II), July 1971.

(15) Wallops Island Test Range Reference Atmosphere (Part II), July 1971.

(16) Fort Greely Missile Range Reference Atmosphere (Part II), July 1971.

14.7 Smith, J. W., "Density Variations and Isopycnic Layer." Journal of Applied Meteorology, vol. 3, no. 3, Jun. 1964, pp. 290-298.

14.8 Buell, C. E., "Some Relations Among Atmospheric Statistics." Journal of Meteorology, vol. 11, Jun. 1954, pp. 238-244.

REFERENCES (Concluded)

14.9 Smith, Orvel E.; McMurray, William M.; and Crutcher, Harold L., "Cross Sections of Temperature, Pressure, and Density Near the 80th Meridian West." NASA TN D-1641, May 1963.

14.10 Carter, E. A.; and Brown, S. C., "A Reference Atmosphere for Vandenberg AFB, California, Annual (1971 Version). "NASA TM X-64590, NASA-Marshall Space Flight Center, Alabama, May 10, 1971.

14.11 Groves, G. V., "Atmospheric Structure and Its Variations in the Region From 25 to 120 km." Environmental Research Papers, No. 368, AFCRL-71-0410, July 1971.

14.12 Cole, Allen E., "Distribution of Thermodynamic Properties of the Atmosphere between 30 and 80 km.," AFCRL-72-0477, Environmental Research Papers No. 409, Air Force Cambrige Research Laboratories, L. G. Hanscom Field, Bedford, Massachusetts, Aug. 1972.

14.13 Graves, M. E.; et al, "Specification of Mesopheric Density, Pressure, and Temperature by Extrapolation" NASA CR-2223, March 1973.

14.14 Johnson, D. L.; "Hot and Cold Atmospheres for Vandenberg AFB, California (1973 Version)", NASA TM X- 64756, NASA - Marshall Space Flight Center, Alabama, June 26, 1973.

N74-16307

SECTION XV. DISTRIBUTION OF SURFACE EXTREMES IN THE UNITED STATES

By

Glenn E. Daniels and Orvel E. Smith

15. 1 Introduction

For component parts manufactured, transported, or tested in geographical areas not discussed in other sections of this document, this section can be used for environments needed in design and planning. These environments may be applicable to transportation, fabrication, or testing.

15. 2 Environments Included

(a) Air temperature, extreme maximum and minimum,

(b) Snow fall - snow loads, 24-hour maximum and storm maximum,

(c) Hail, maximum size,

(d) Atmosphere pressure, extreme maximum and minimum.

15. 3 Source of Data

The extremes presented have been prepared using data from Weather Bureau stations and published articles. These extremes represent the highest or lowest extreme value measured at each station. The length of record varies from station to station, but most values represent more than 15 years of record. Where the local surroundings have a geographical area with a special influence on an extreme value (such as the minimum temperature on a high mountain peak or other local condition), it will not in general be shown on the maps presented unless a Weather Bureau station is located there. If there is a contractor at such a locality and an item of equipment is especially sensitive to an environment, a study is needed of the local environment where fabrication is to be made.

15. 4 Extreme Design Environments[1]

1. All values of extreme maxima and minima in this section are for design purposes and may or may not exactly reflect extrapolations (theoretical or otherwise) of actual measured values over the available period of record.

15. 4. 1 Air Temperature

The distribution of extreme maximum air temperature in the United States is shown in Figure 15. 1A, while Figure 15. 1B shows the extreme minimum temperature distribution. The maps (Figures 15. 2A and 15. 2B) from Reference 15.1 show the mean temperature and standard deviations of the temperatures from the means for January and July.

To estimate the temperature $\hat{T}$ that is attained or exceeded with a frequency p, from Figures 15. 2A and 15. 2B, find from the appropriate figure, by interpolation as needed, the mean temperature $\bar{T}$ and standard deviation S_T and substitute these in the equation

$$\hat{T} = \bar{T} + S_T \cdot y_s \quad [^\circ F].$$

Values of y_s for various calculated risks are:

Cold Temperatures (Figure 15.2A)		Hot Temperatures (Figure 15.2B)		
p	y_s	p	y_s	
0.20	- 0.84	0.80	+ 0.84	
0.10	- 1.28	0.90	+ 1.28	
0.05	- 1.65	0.95	+ 1.65	(See footnote 2.)
0.025	- 1.96	0.975	+ 1.96	
0.01	- 2.33	0.99	+ 2.33	

15. 4. 2 Snow Fall - Snow Load

The maps in Figures 15. 3 and 15. 4 show the maximum depth of snow and the corresponding snow loads. Figure 15. 3 shows the maximum depth for a 24-hour period; Figure 15. 4 shows the maximum depth and the corresponding snow loads for a storm period. The storm total map shows the same snow depth as in the 24-hour map in the southern low elevation areas of the United States since snow storms seldom exceed 24 hours in these areas.

The terrain combined with the general movement of weather patterns has a great effect on the amount of fall, accumulation, and melting of the snow. Also the length of a single storm varies for various areas. In some

---

2. The 95th percentile value is recommended for hot day design ambient temperatures over runways for landing-takeoff performance calculation using Figure 15.2B, the 5th percentile is for cold day design.

areas in mountain regions much greater amounts of snowfall have been recorded than shown on the maps. Also the snow in these areas may remain for the entire winter. For example, in a small valley near Soda Springs, California, a seasonal snow accumulation of 7.9 meters (26 ft) with a density of about 0.35 was recorded. This gives a snow load of 2772 kg/m^2 (567.7 lb/ft^2). Such a snow pack can do considerable damage to improperly protected equipment buried deep in the snow. This snow pack at Soda Springs is the greatest on record in the United States and was nearly double previous records in the same area. A study of the maximum snow loads in the Wasatch Mountains of Utah (Ref. 15.2) showed that for a 100-year return period at 2740 meters (9000 ft), a snow load of 1220 kg/m^2 (250 lb/ft^2) could be expected.

15.4.3 Hail

The distribution of maximum sized hail stones in the United States is shown in Figure 15.5. The sizes are for single hailstones and not conglomerates of several hail stones frozen together.

15.4.4 Atmospheric Pressure

Atmospheric pressure extremes normally given in the literature are given as the pressure which would have occurred if the station were at sea level. The surface weather map published by the United States Weather Bureau uses sea level pressures for the pressure values to assist in map analysis and forecasting. These sea level pressure values are obtained from the station pressures by use of the hydrostatic equation:

$$dP = \rho g dZ$$

where

dP = pressure difference

ρ = density

g = gravity

dZ = altitude difference.

These sea level data are valid only for design purposes at locations with elevation near sea level. As an example, when the highest officially reported sea level pressure observed in the United States of 106 330 N/m^2 (1063.3 mb) occurred at Helena, Montana (Ref 15.3), the actual station pressure was about 92 100 N/m^2 (921 mb) because the station is 1187 meters (3893 ft) above mean sea level.

Figures 15.6 and 15.7 show the general distribution of extreme maximum and minimum station pressures in the United States. Because of the direct relationship of pressure and station elevation, Figures 15.8 through 15.11 should be used with the station elevation to obtain the extreme maximum and minimum pressure values for any location in the United States. Similar maps and graphs in U. S. Customary Units are given in Reference 15.4. Table 15.1 gives a list of the station elevations for a number of locations in the United States. These are elevations of the barometer at the local Weather Bureau office.

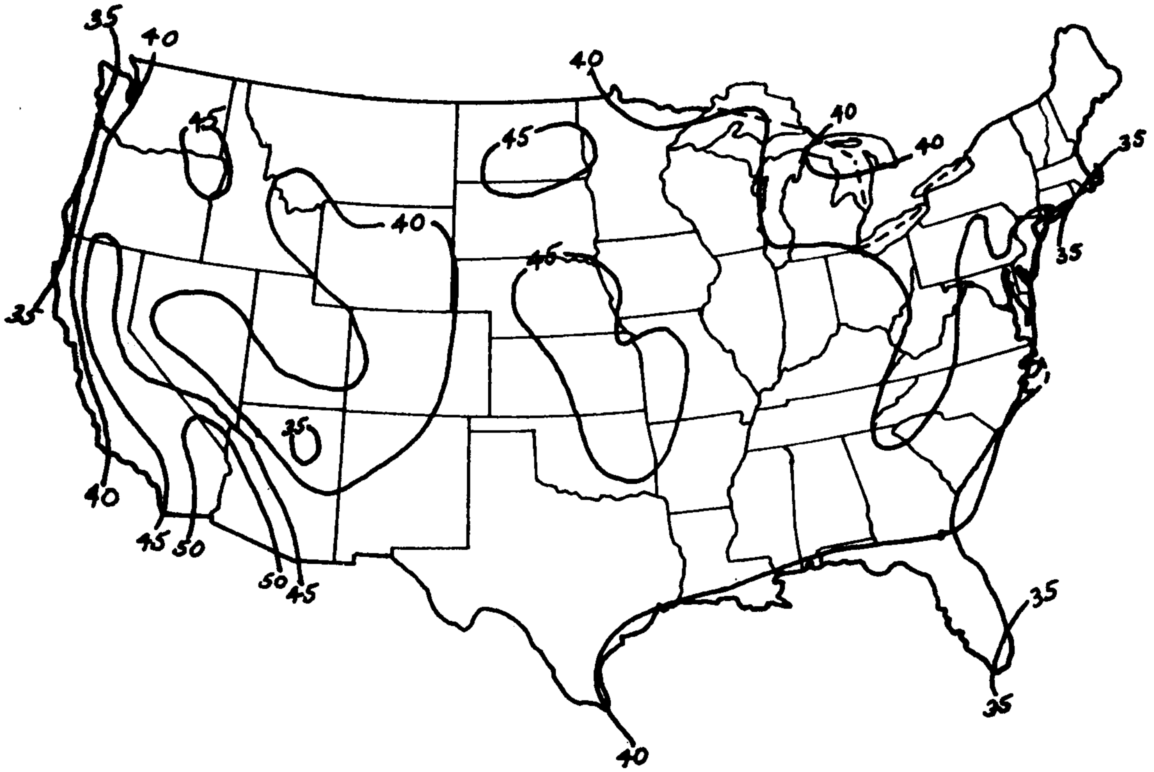

FIGURE 15.1A EXTREME MAXIMUM TEMPERATURE (° C)

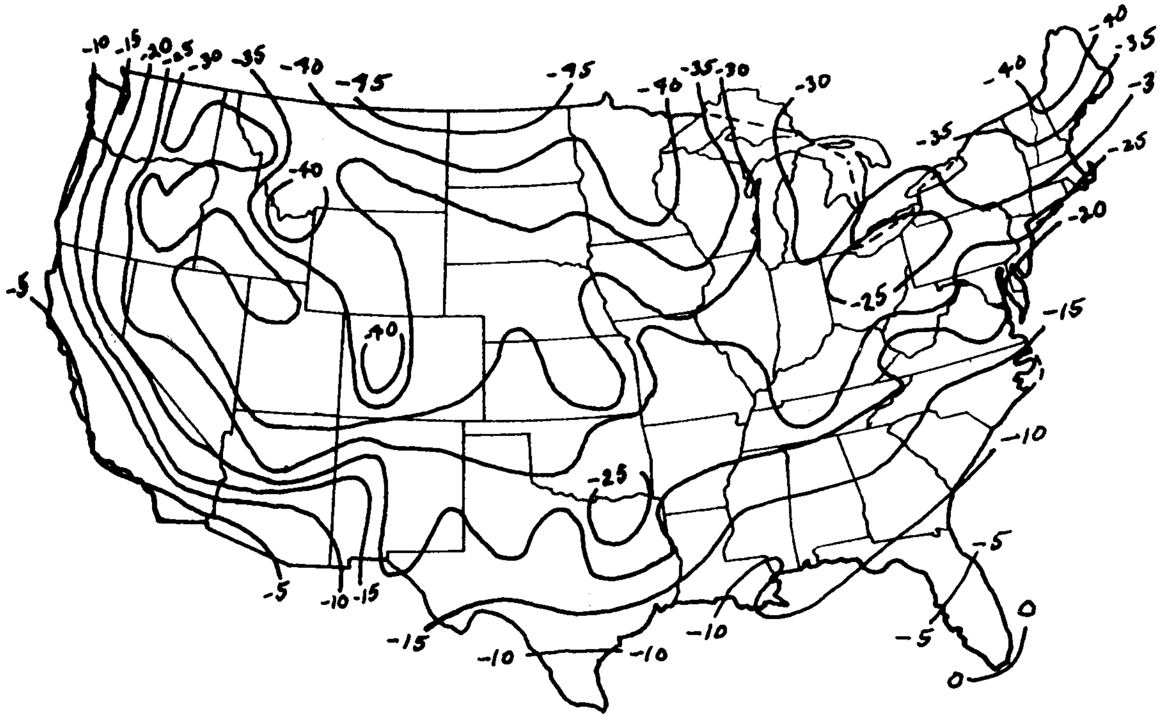

FIGURE 15.1B EXTREME MINIMUM TEMPERATURE (° C)

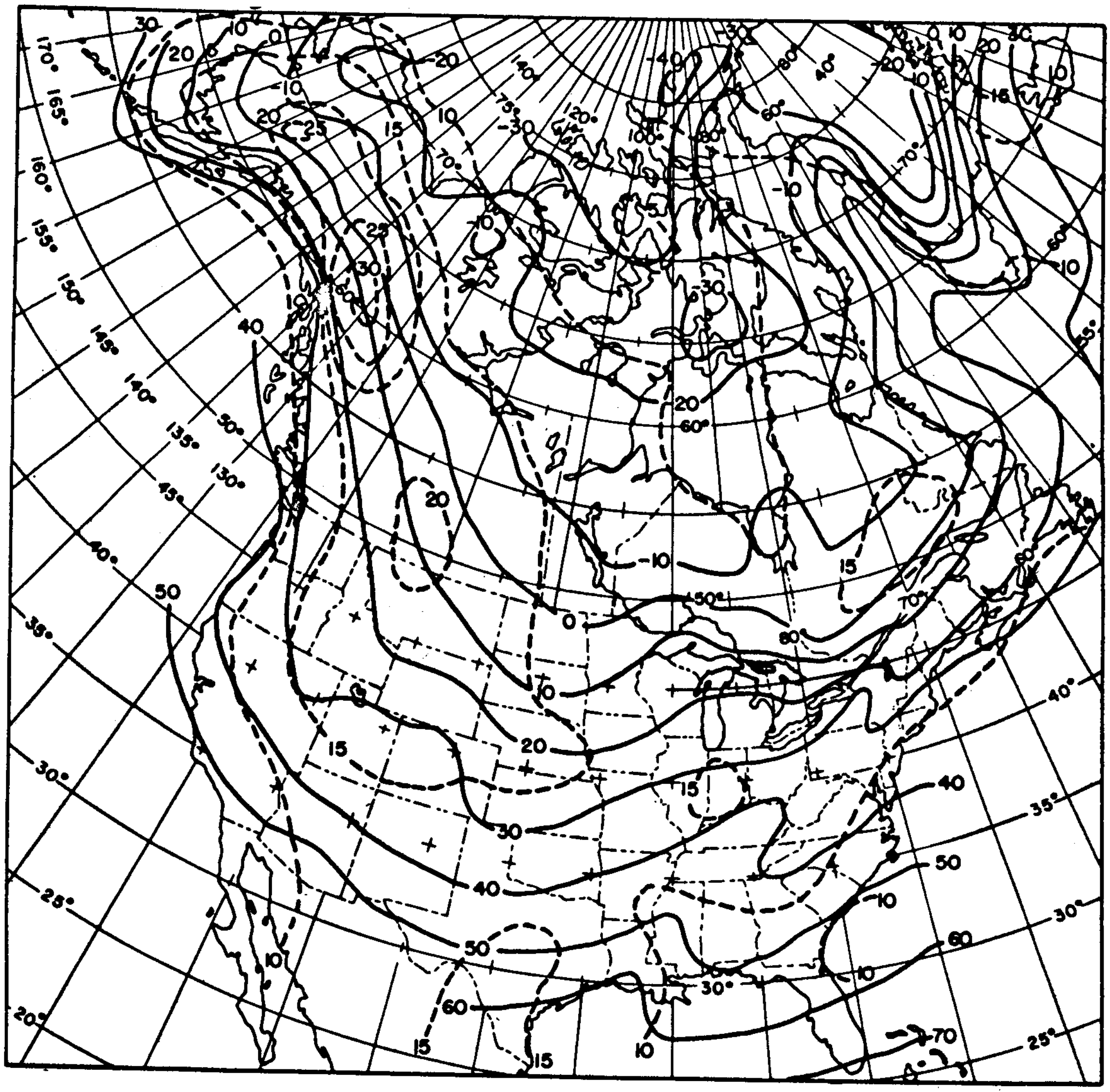

FIGURE 15. 2A ISOTHERMS OF JANUARY HOURLY SURFACE TEMPERATURES (Approximate mean values (° F) are shown by solid lines, standard deviations (° F) by broken lines. The approximations were made to give best estimates of lower 1- to 20-percentile values of temperature by normal distribution.) [3]

3. Valley, Shea L. , "Handbook of Geophysics and Space Environments," McGraw-Hill Book Company, Inc. , New York, 1965.

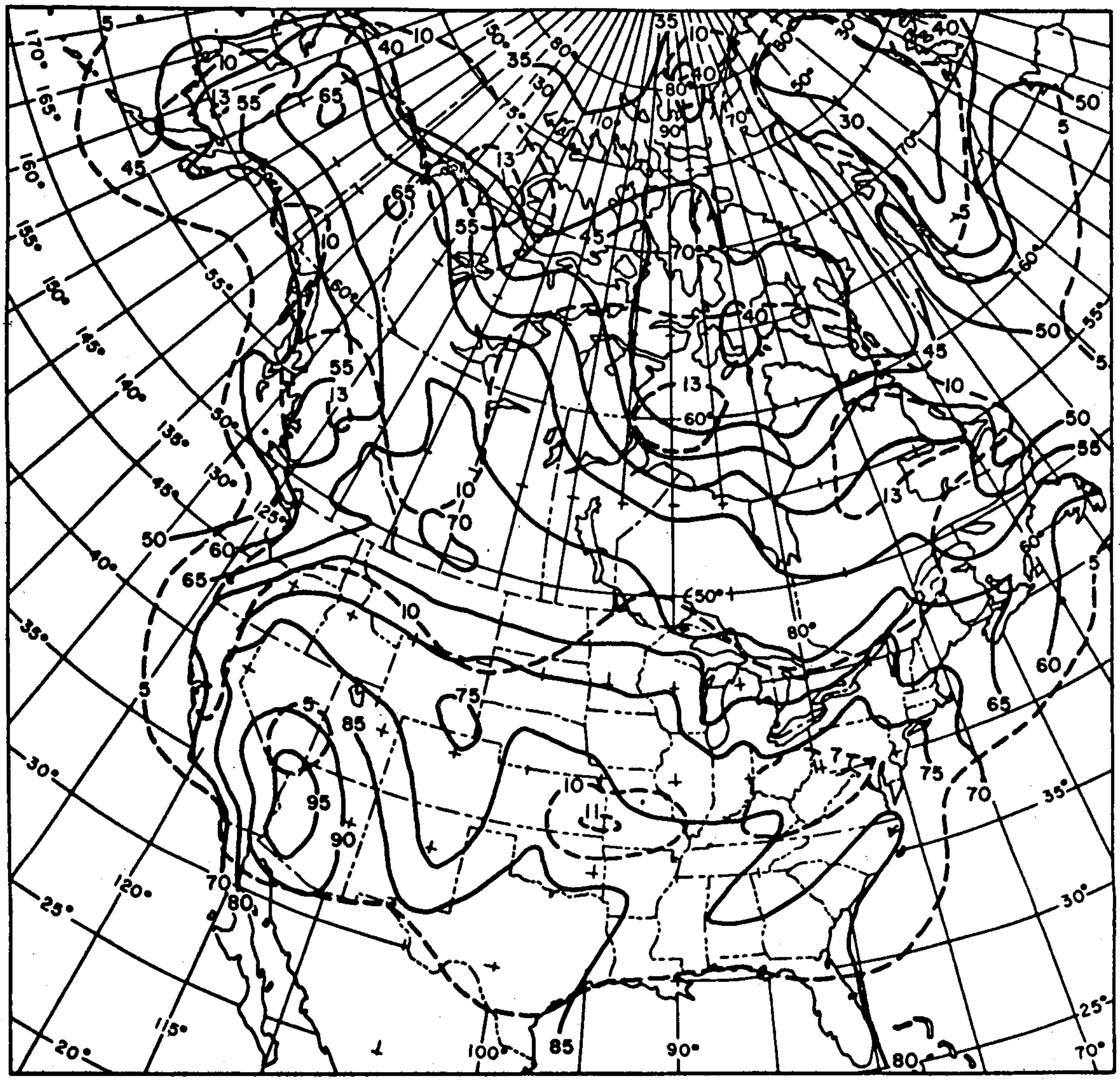

FIGURE 15. 2. B ISOTHERMS OF JULY HOURLY SURFACE TEMPERATURES (Approximate mean values (° F) are shown by solid lines, standard deviations (° F) by broken lines. The approximation were made to yield the best estimates of upper 80- to 99-percentile values by normal distribution)[3]

---

3. Ibid.

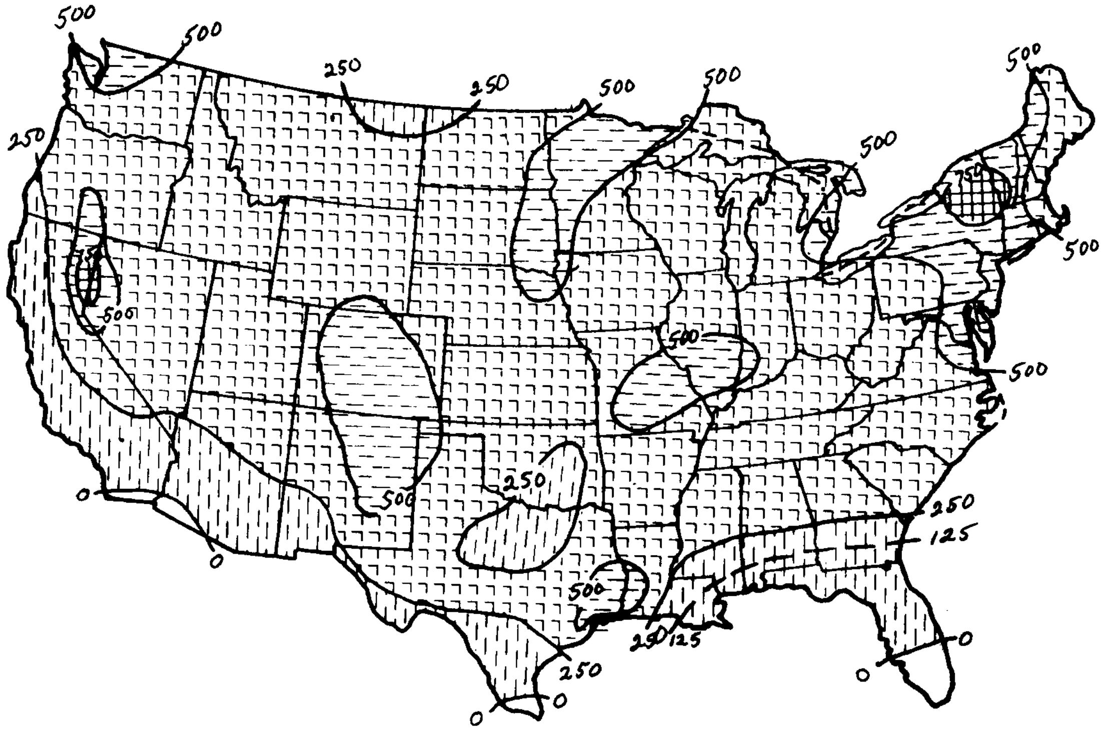

MAXIMUM SNOW LOAD

mm		kg/m^2
0-250		25
250-500		50
500-750		75
over 750		100

FIGURE 15. 3 EXTREME 24-HOUR MAXIMUM SNOW FALL (mm)

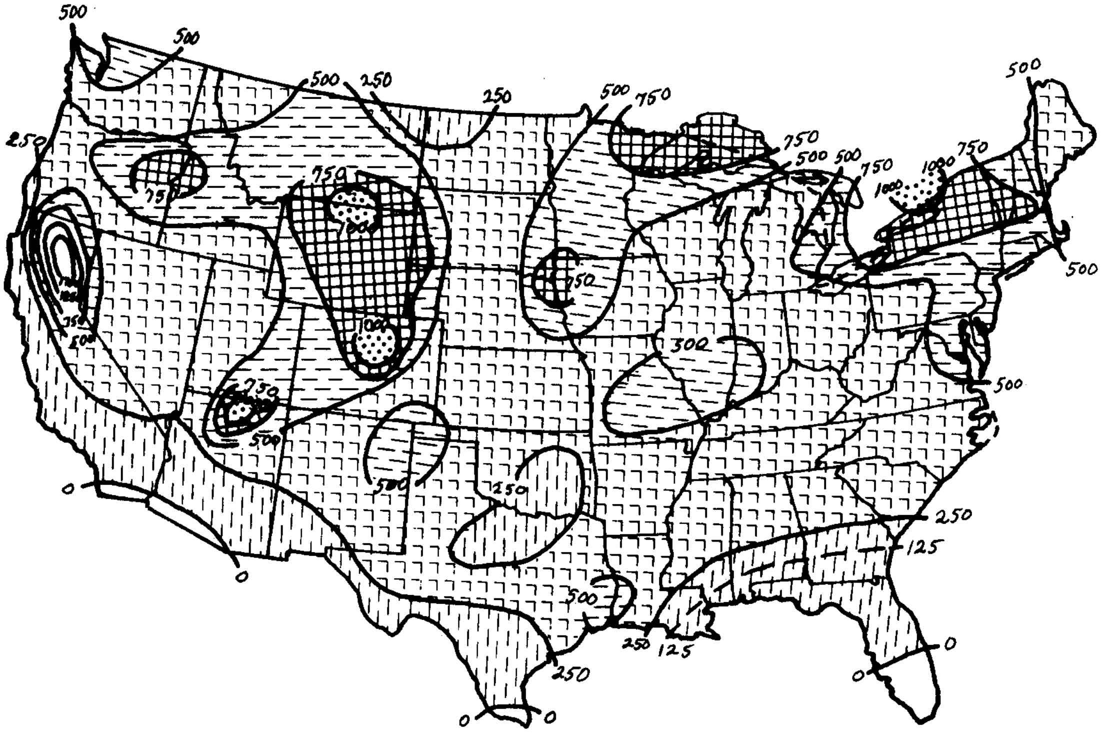

MAXIMUM SNOW LOAD

mm	kg/m²
0-250	25
250-500	50
500-750	75
750-1000	100
1000-1250	125

FIGURE 15. 4 EXTREME STORM MAXIMUM SNOW FALL (mm)

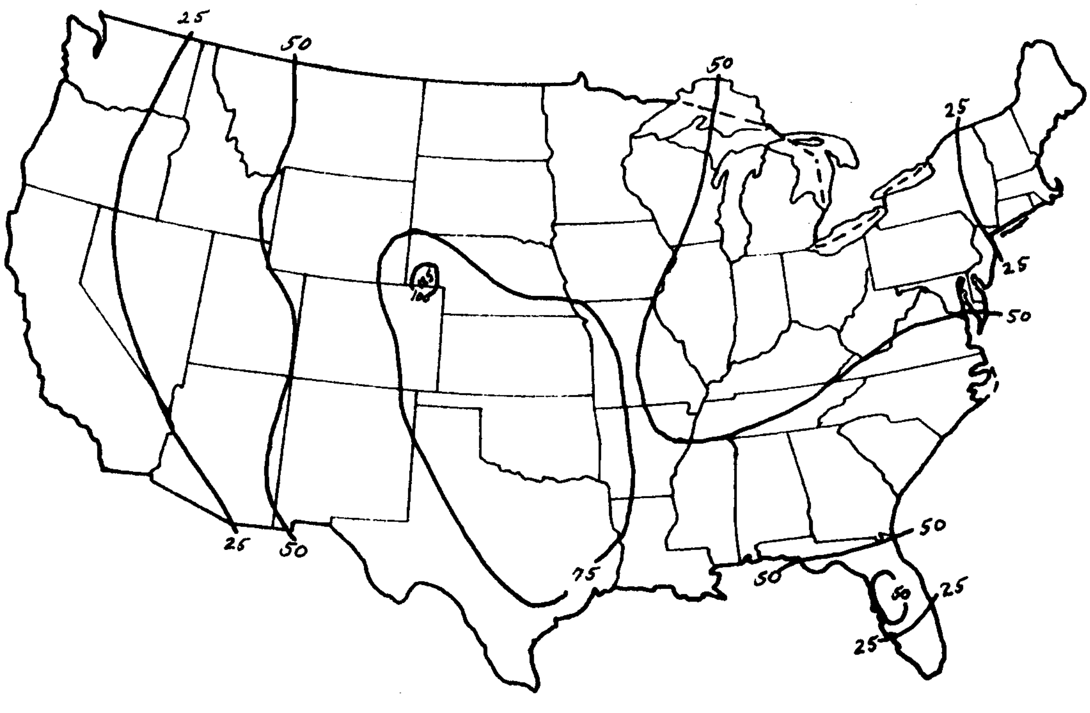

FIGURE 15. 5 EXTREME MAXIMUM HAIL STONE DIAMETERS (mm)

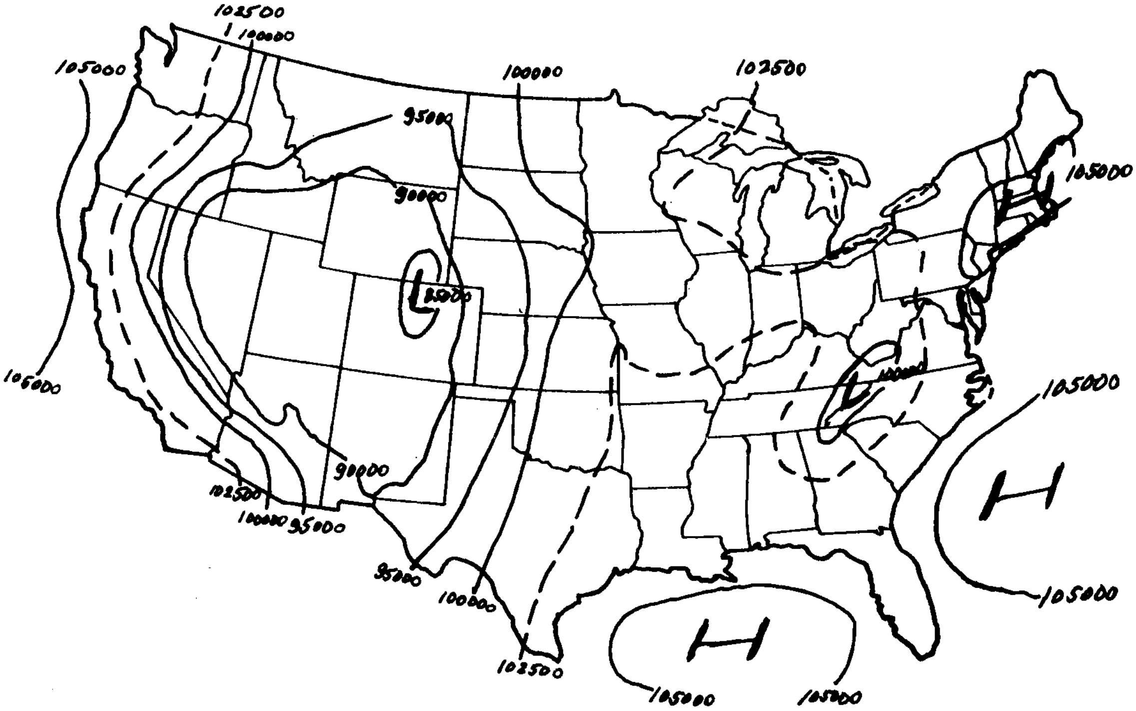

FIGURE 15. 6 MAXIMUM ABSOLUTE STATION PRESSURE (N/m^2)

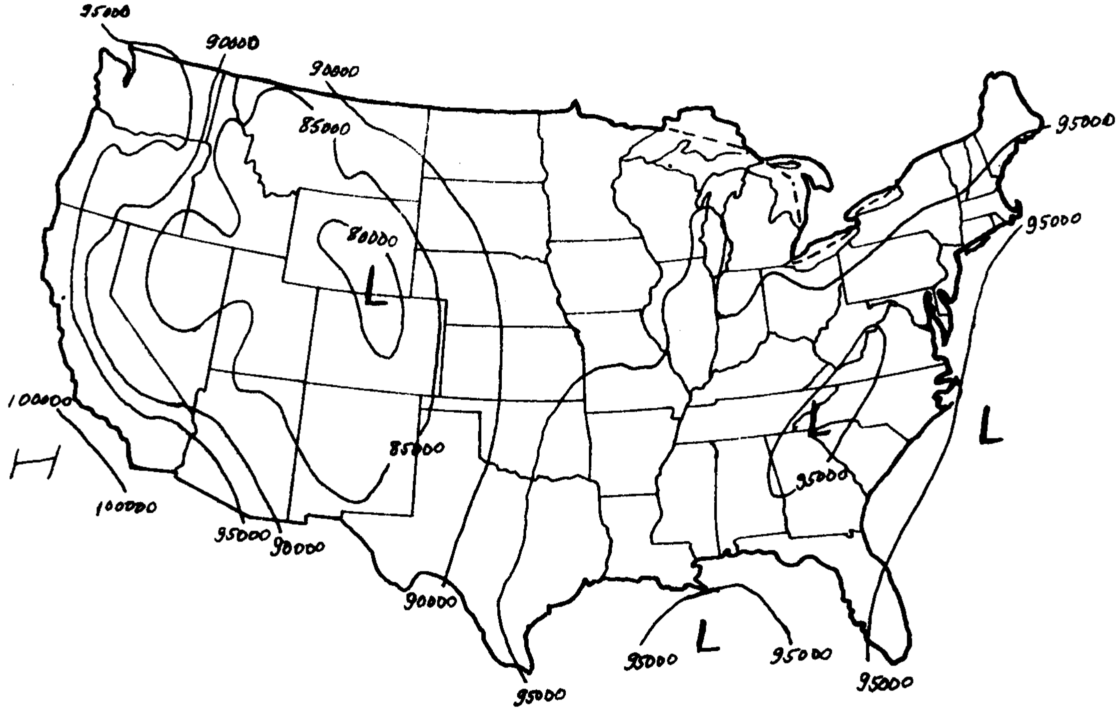

FIGURE 15. 7 MINIMUM ABSOLUTE STATION PRESSURE (N/m^2)

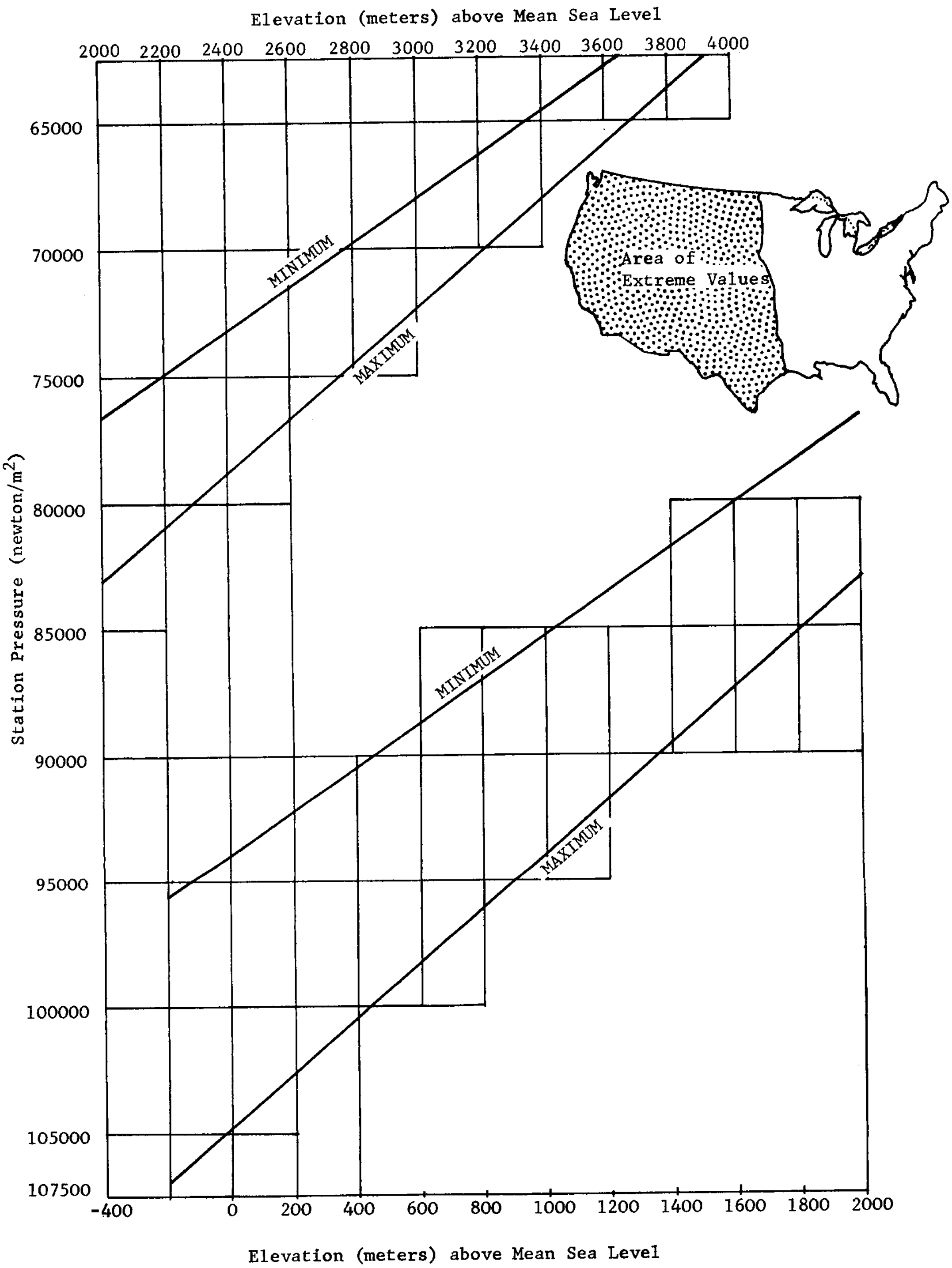

FIGURE 15. 8 EXTREME PRESSURE VALUES VERSUS ELEVATION FOR WESTERN UNITED STATES

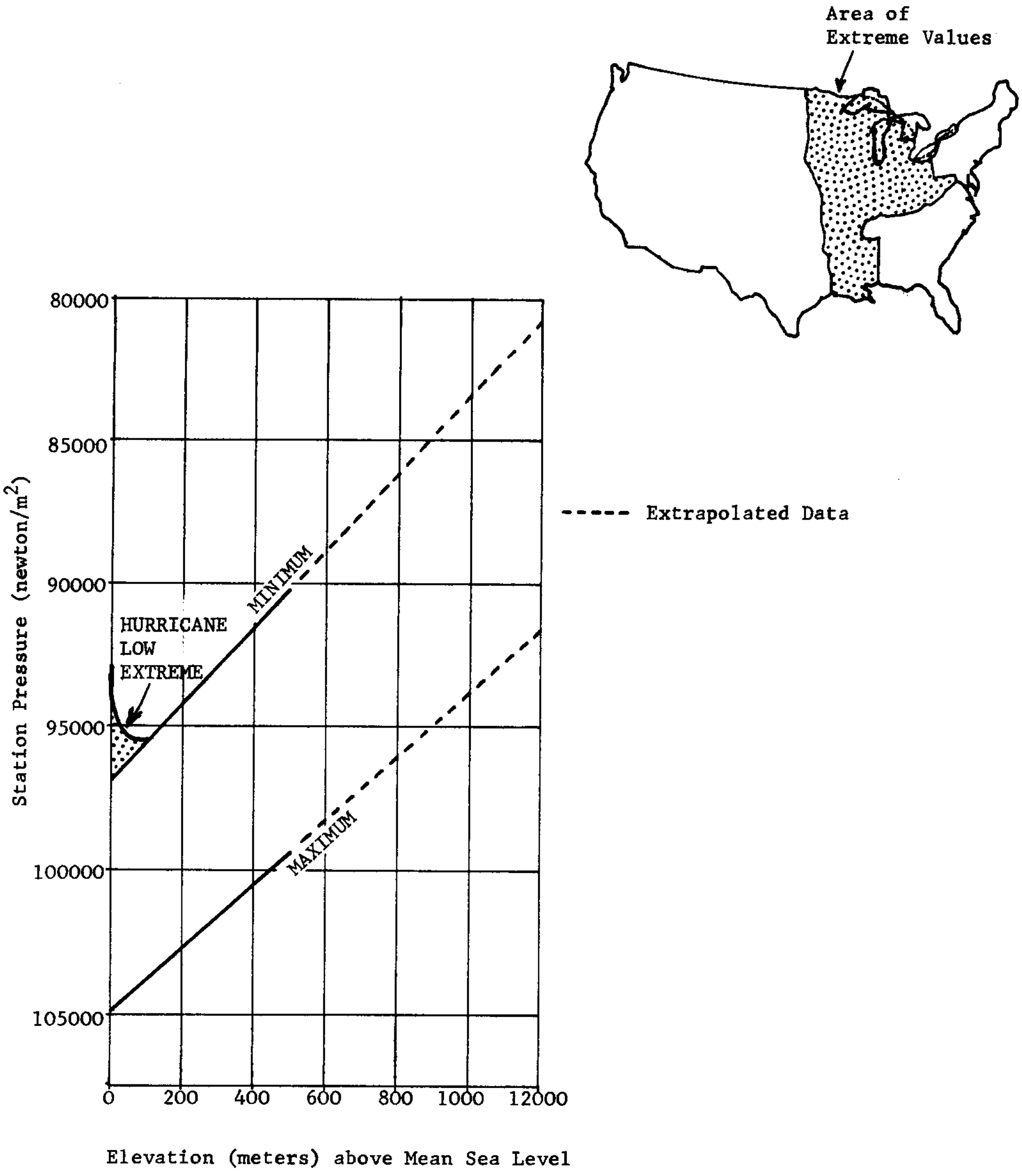

FIGURE 15. 9 EXTREME PRESSURE VALUES VERSUS ELEVATION FOR CENTRAL UNITED STATES

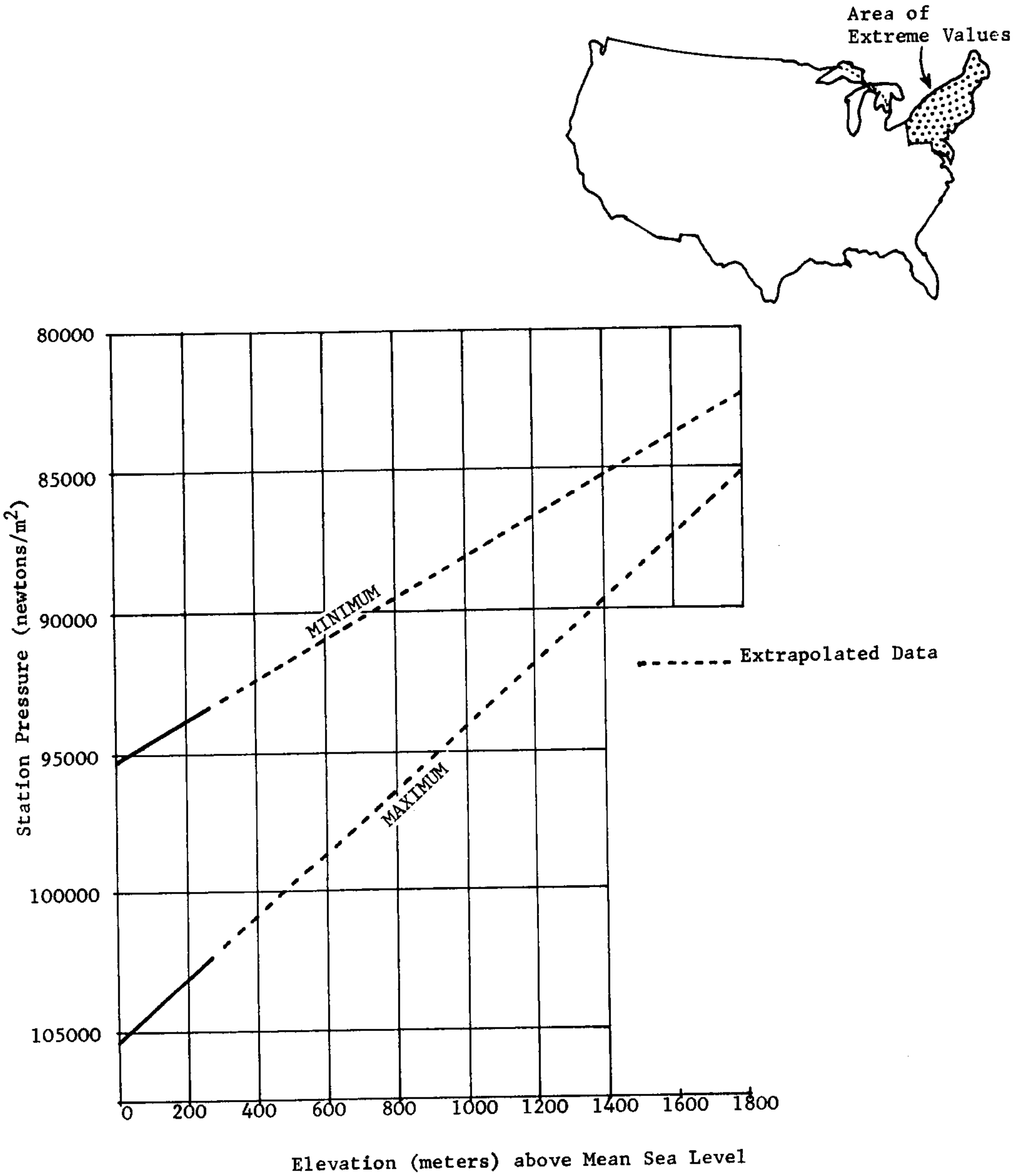

FIGURE 5. 10 EXTREME PRESSURE VALUES VERSUS ELEVATION FOR NORTHEASTERN UNITED STATES

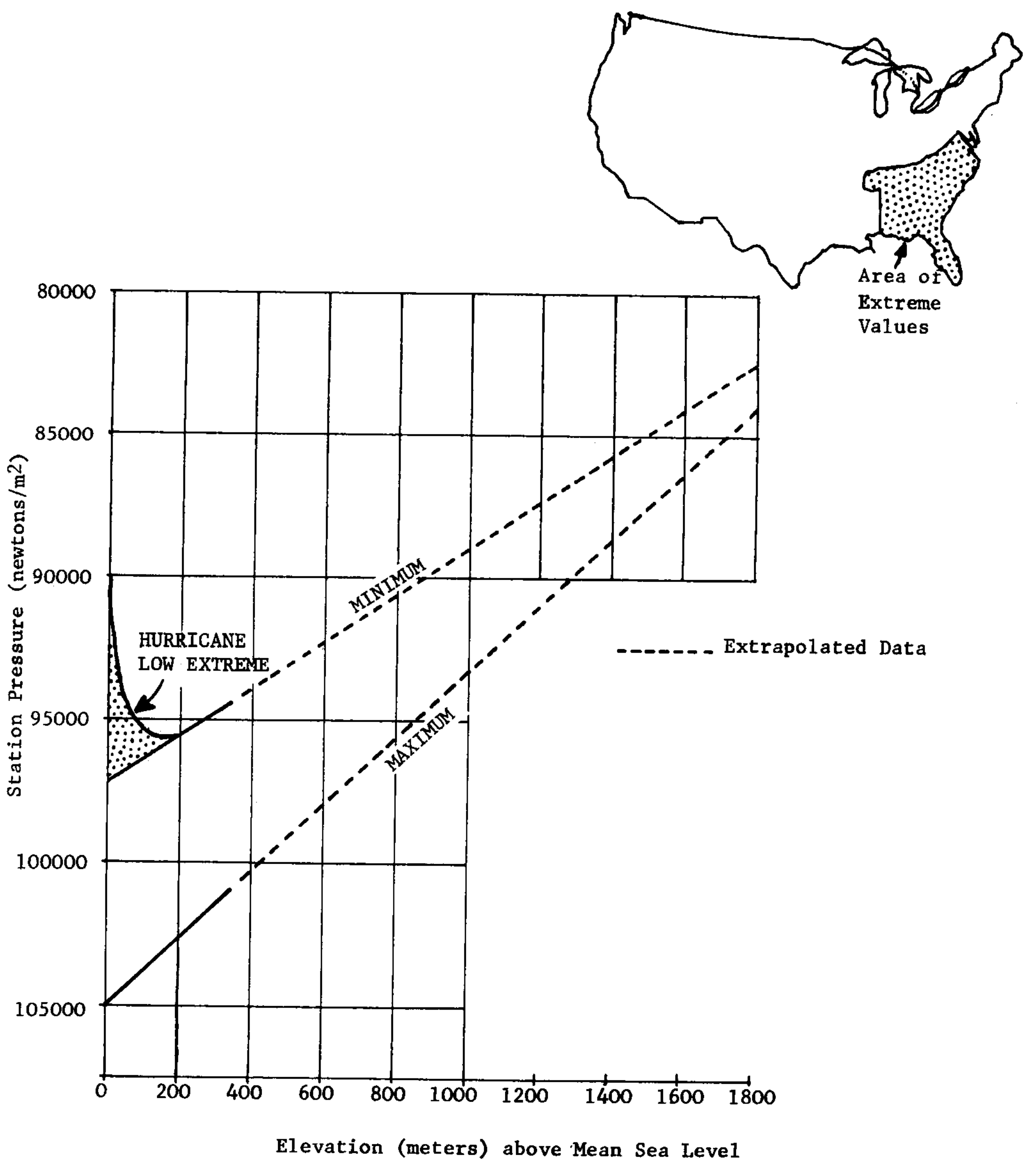

FIGURE 5. 11 EXTREME PRESSURE VALUES VERSUS ELEVATION FOR SOUTHEASTERN UNITED STATES

TABLE 15.1 ELEVATIONS OF CITIES OF THE UNITED STATES (Values are elevation of barometer at U. S. Weather Bureau Station)

Location	Elevation, MSL (feet)	(meters)
ALABAMA		
Birmingham	610	185.9
Mobile	211	64.3
ARIZONA		
Phoenix	1100	335.2
Yuma	199	60.7
ARKANSAS		
Fort Smith	499	152.1
Little Rock	257	78.3
Texarkana	361	110.0
CALIFORNIA		
Eureka	43	13.1
Fresno	331	100.9
Los Angeles	312	95.1
Sacramento	20	6.1
San Diego	19	5.8
San Francisco	52	15.8
COLORADO		
Denver	5292	1613.0
Grand Junction	4849	1478.0
Pueblo	4639	1414.0
CONNECTICUT		
Hartford	15	4.6
New Haven	6	1.8
DISTRICT OF COLUMBIA		
Washington	72	21.9
FLORIDA		
Apalachicola	13	4.0
Fort Myers	15	4.6
Jacksonville	18	5.5
Key West	5	1.5
Miami	7	2.1
Pensacola	13	4.0
GEORGIA		
Atlanta	1054	321.3
Savannah	48	14.6
IDAHO		
Boise	2842	866.2
Pocatello	4444	1354.5
ILLINOIS		
Cairo	314	95.7
Chicago	610	185.9
Springfield	587	178.9
INDIANA		
Evansville	383	116.7
Indianapolis	718	218.8
IOWA		
Des Moines	807	246.0
Sioux City	1094	333.4
KANSAS		
Dodge City	2594	790.7
Goodland	3645	1111.0
Wichita	1321	402.6
KENTUCKY		
Louisville	457	139.3
LOUISIANA		
Lake Charles	12	3.7
New Orleans	3	0.9
Shreveport	174	53.0
MAINE		
Caribou	624	190.2
Portland	61	18.6
MARYLAND		
Baltimore	14	4.3
MASSACHUSETTS		
Boston	15	4.6
Nantucket	43	13.1
MICHIGAN		
Alpena	587	178.9
Detroit	619	188.7
Marquette	677	206.3
Sault Ste. Marie	721	219.8
MINNESOTA		
Duluth	1162	354.2
International Falls	1179	359.4
Minneapolis	830	253.0
MISSISSIPPI		
Jackson	305	93.0
MISSOURI		
Kansas City	741	225.9
St. Louis	809	246.6
MONTANA		
Havre	2488	758.3
Helena	3893	1186.6
NEBRASKA		
Omaha	978	298.1
NEVADA		
Elko	5075	1546.9
Las Vegas	2162	659.0
Winnemucca	4299	1310.3
NEW HAMPSHIRE		
Concord	339	103.3
NEW JERSEY		
Atlantic City	10	3.0
Newark	11	3.4
Trenton	56	17.1
NEW YORK		
Albany	19	5.8
Buffalo	693	211.2
New York City	10	3.0
Rochester	543	165.5
Syracuse	424	129.2
NORTH CAROLINA		
Cape Hatteras	7	2.1
Raleigh	400	121.9
Wilmington	30	9.1
NORTH DAKOTA		
Fargo	900	274.3
Bismarck	1650	502.9
Williston	1877	572.1

TABLE 15.1 (Concluded)

Location	Elevation, MSL (feet)	Elevation, MSL (meters)
OHIO		
Cincinnati	553	168.6
Cleveland	653	199.0
Columbus	724	220.7
Toledo	676	206.0
OKLAHOMA		
Oklahoma City	1254	382.2
Tulsa	672	205.2
OREGON		
Medford	1312	399.9
Pendleton	1492	454.8
Portland	21	6.4
Roseburg	479	146.0
PENNSYLVANIA		
Harrisburg	335	102.1
Philadelphia	7	2.1
Pittsburg	749	228.3
RHODE ISLAND		
Block Island	110	33.5
Providence	12	3.7
SOUTH CAROLINA		
Charleston	9	2.7
Columbia	217	66.1
Greenville	1018	310.3
SOUTH DAKOTA		
Huron	1282	390.8
Rapid City	3165	964.7
Sioux Falls	1420	432.8
TENNESSEE		
Chattanooga	670	204.2
Memphis	263	80.2
Nashville	577	175.9
TEXAS		
Abilene	1759	536.1
Amarillo	3590	1094.2
Brownsville	16	4.9
Corpus Christi	43	13.1
Dallas	476	145.1
El Paso	3920	1194.8
Galveston	5	1.5
San Antonio	792	241.4
Wichita Falls	1002	305.4
UTAH		
Salt Lake City	4220	1286.3
VERMONT		
Burlington	331	100.9
VIRGINIA		
Norfolk	11	3.4
Richmond	162	49.4
WASHINGTON		
Tatoosh Island	101	30.8
Seattle	14	4.3
Spokane	2357	718.4
Walla Walla	949	289.3
WEST VIRGINIA		
Charleston	950	289.6
WISCONSIN		
Green Bay	689	210.0
La Crosse	652	198.7
Madison	857	261.2
Milwaukee	620	189.0
WYOMING		
Casper	5319	1621.2
Cheyenne	6131	1868.7
Lander	5563	1695.6
Sheridan	3942	1201.5

REFERENCES

15.1 Valley, Shea L., "Handbook of Geophysics and Space Environments," McGraw-Hill Book Company, Inc., New York, 1965.

15.2 Brown, Merly J.; and Williams, Philip Jr. : "Maximum Snow Loads along the Western Slopes of the Wasatch Mountains of Utah." Journal of Applied Meteorology, vol. 1, March 1962, pp. 123-126.

15.3 Ludlum, David M.: "Extremes of Atmospheric Pressure in the United States." Weatherwise, vol. 15, no. 3, 1962, pp. 106-115.

15.4 Daniels, Glenn E.: "Values of Extreme Surface Pressure for Design Criteria." Institute of Environmental Sciences, 1965 Proceedings, pp. 283-288; Institute of Environmental Sciences, Mt. Prospect, Illinois.

N74-16308

SECTION XVI. ATMOSPHERIC ATTENUATION RELATIVE TO EARTH-VIEWING ORBITAL SENSORS

By

S. Clark Brown and Robert R. Jayroe, Jr.

16.0 Introduction

Earth-viewing space missions offer exciting new possibilities in several earth resources disciplines – geography, hydrology, agriculture, geology, and oceanography, to name a few. A most useful tool in planning experiments and applying space technology to earth observation is a statistical description of atmospheric parameters. For example, cloud cover statistics might be used to predict mission feasibility or the probability of observing a given target area in a given number of satellite passes.

To meet the need for atmospheric statistics, NASA-MSFC has sponsored the development of the four-dimensional atmospheric models (subsection 16.3) and the world-wide cloud model (subsection 16.2). The goal of this is to produce atmospheric attenuation models to predict degradation effects for all classes of sensors for application to earth-sensing experiments from space-borne platforms. To insure maximum utility and application of these products NASA-MSFC also sponsored the development of an "Interaction Model of Microwave Energy and Atmospheric Variables," a complete description of the effects of atmospheric moisture upon microwaves.

16.1 Interaction Model of Microwave Energy and Atmospheric Variables

While the visible and infrared wavelengths find clouds opaque, the microwave part of the electromagnetic spectrum is unique in that cloud and rain particles vary from very weak absorbers and scatterers to very significant contributors to the electromagnetic environment. This is illustrated in Figures 16.1, 16.2, and 16.3, which are extracted from the final report on the interaction model (Ref. 16.1).

16.1.1 Scattering and Extinction Properties of Water Clouds Over the Range 10 cm to 10μ.

Figures 16.1 and 16.2 show the unit-volume scattering and extinction properties of two modeled cloud drop distributions computed using the Mie theory. Figure 16.1 gives the extinction coefficient as a function

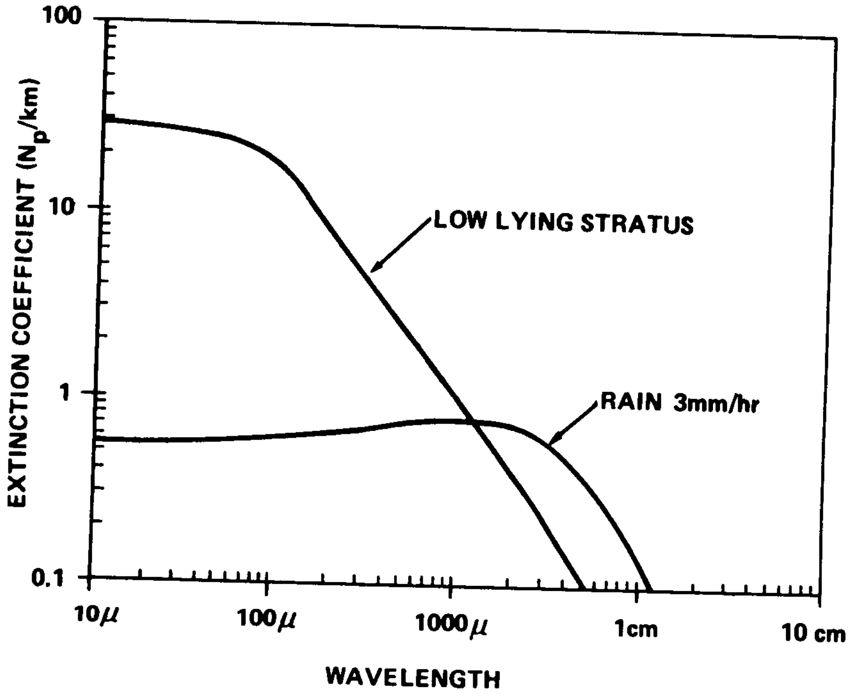

FIGURE 16.1 EXTINCTION COEFFICIENT AS A FUNCTION OF WAVELENGTH

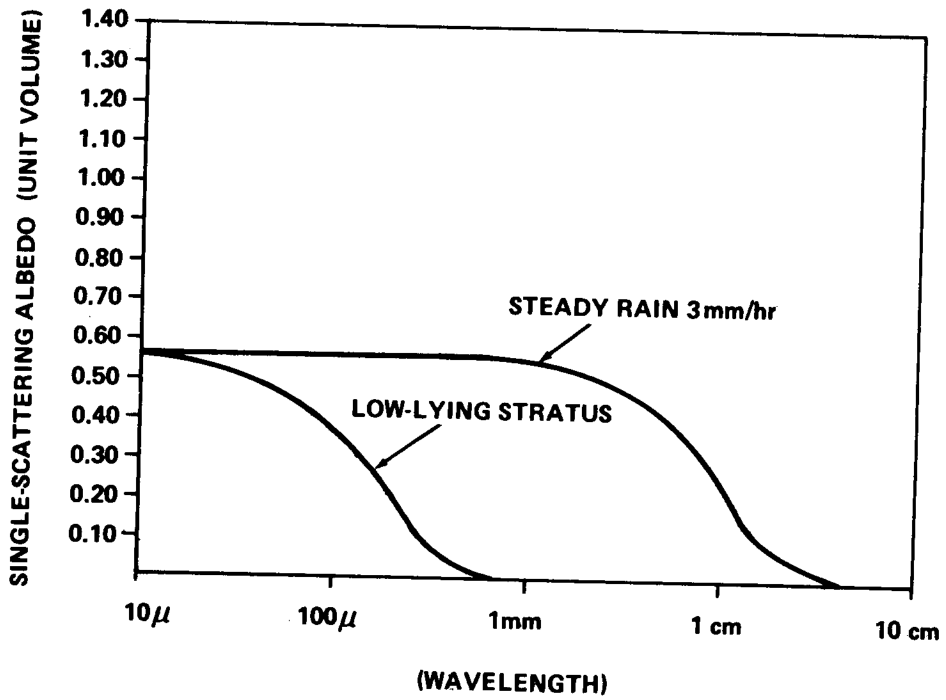

FIGURE 16.2 SINGLE SCATTERING ALBEDO FOR TWO CLOUD MODELS

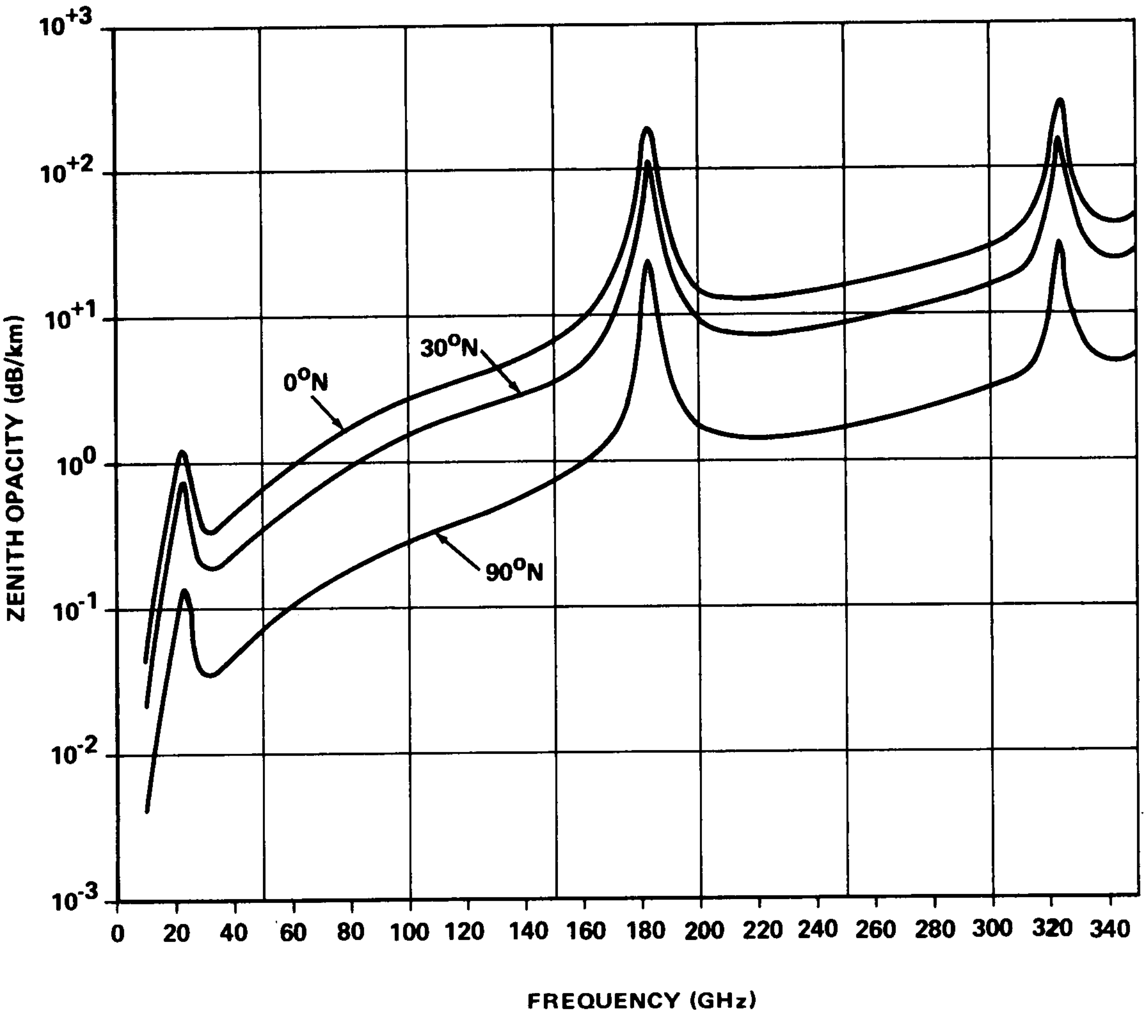

FIGURE 16. 3 ZENITH OPACITY

of wavelength while Figure 16. 2 presents the single scattering albedo for two cloud models representing fair weather and rainy conditions. The curves show the wavelength regimes appropriate to the two cloud types in which scattering effects are relatively unimportant, and in which the extinction coefficient follows the simple Rayleigh ($1/\lambda^2$) dependence.

16. 1. 2 Zenith Opacity due to Atmospheric Water Vapor as a Function of Latitude

In the preparation of Figure 16. 3 five years of climatological data from the MIT Planetary Circulations Project were used to obtain mean water vapor distributions applicable to the latitudes 0° N, 30° N, and 90° N, corresponding to tropical, mid-latitude, and arctic conditions. The total water vapor content for the three cases are 4. 5, 2. 5, and 0. 5 g/cm^2, respectively. The curves demonstrate the effect of climatological extremes in simulating and predicting the influence of atmospheric water vapor upon surface observations from a space observer, over the range from 10 to 350 gigahertz. A detailed report on the interaction model is available upon request.

16. 2 Cloud Cover

16. 2. 1 Introduction

One of the main obstructions to observing the earth's surface from satellite altitudes is cloud cover. Although some sensors show less cloud effect than others, of the three main classes of sensors (cameras, thermal infrared, and radar) cameras are the most advanced, but are also the most sensitive to cloud cover.

The expense and complexity of space missions demand that the consequence of cloud cover be evaluated in advance. First, mission feasibility must be determined. Then, the mission must be planned to provide sufficient time and expendables to insure a high probability of success. Previously, in computer simulations of earth-oriented space missions, clouds were either disregarded completely or were assumed to be present about 50 percent of the time. Now, by using the world-wide cloud cover statistics (Refs. 16. 2 through 16. 7) and the simulation procedure described here, it is possible to provide a realistic evaluation of the consequence of cloud cover on earth-viewing space missions.

Results of the simulations, which can be made for target areas of various size on a global basis, are generally given in two forms. First, the satellite pass number and probability of success are considered as variables with the required percent photographic coverage of the target area fixed. For example, if 95 percent photographic coverage of the target area is required for success, the results would be given as the probability of success versus the pass number. A plot of these results (Figure 16. 4) might show that there is a 60 percent chance of photographing 95 percent of the target area in six satellite passes. Second, the pass number is fixed while the percentage of area photographed and the chance of success are treated as variables. Results in this case are given as the percent chance of achieving some percent of photographic coverage of the target area by some limiting pass number. These results (Figure 16. 5) might show that after eight satellite passes, there is a 60 percent chance of photographing 90 percent of the target area.

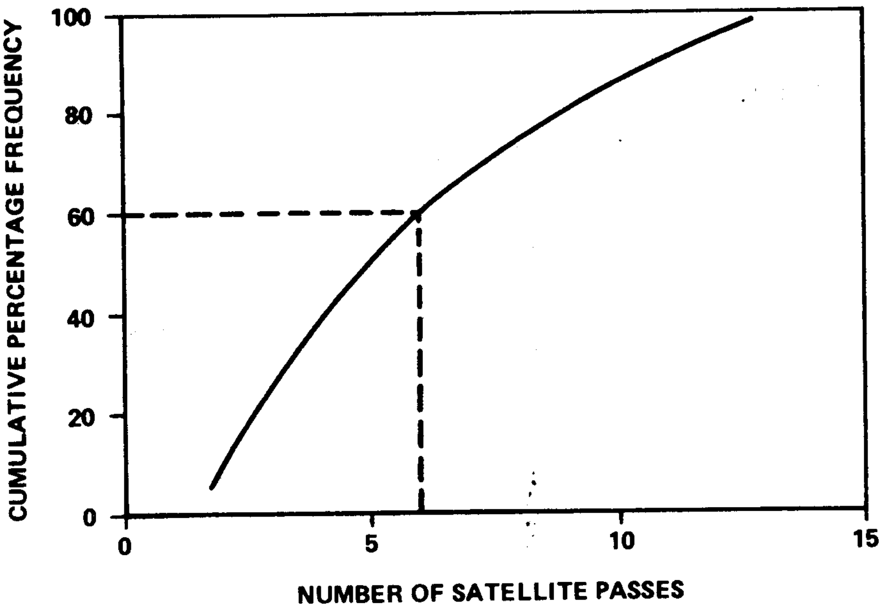

FIGURE 16.4 PROBABILITY OF 95-PERCENT PHOTOGRAPHIC COVERAGE OF TARGET AREA

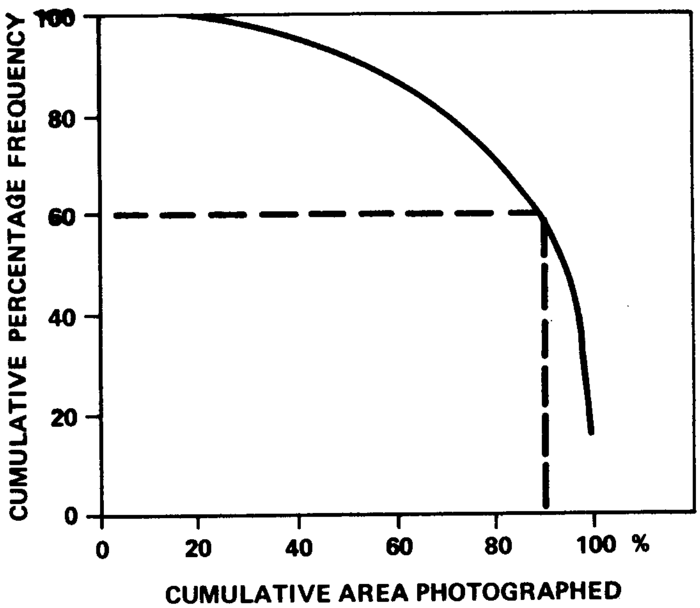

FIGURE 16.5 PHOTOGRAPHIC COVERAGE OF TARGET AREA AFTER EIGHT SATELLITE PASSES

16.2.2 Background

Before the simulation procedure is outlined, it may be helpful to briefly describe the world-wide cloud cover statistics and some simulation applications. These cloud statistics, representing a first effort toward providing cloud data designed expressly for computer simulation exercises, were developed during the period January 1967–January 1968 and March 1970–January 1971 by Allied Research Associates, Inc., under contracts NAS8-21040 and NAS8-25812. After dividing the earth into 29 homogeneous cloud regions, probability distributions for cloud categories by region and monthly reference periods were prepared for each 3-hour interval (Tables 16.1 and 16.2). For application to computer simulation programs, the cloud region boundaries were adjusted to the nearest even numbered lines of latitude and longitude (Figure 16.6).

TABLE 16.1 CLOUD COVER DEFINITION

Category	Tenths	Eighths (Octas)
1	0	0
2	1,2,3	1,2
3	4,5	3,4
4	6,7,8,9	5,6,7
5	10	8

TABLE 16.2 BASIC CLOUD STATISTICS – CLOUD REGION: 19; MONTH: JANUARY

Cloud Category	Time (LST)							
	01	04	07	10	13	16	19	22
1	0.31	0.30	0.18	0.16	0.15	0.16	0.24	0.30
2	0.08	0.06	0.09	0.08	0.12	0.10	0.10	0.08
3	0.04	0.04	0.04	0.04	0.04	0.06	0.05	0.05
4	0.11	0.10	0.15	0.16	0.17	0.21	0.16	0.14
5	0.46	0.50	0.54	0.56	0.52	0.47	0.45	0.43

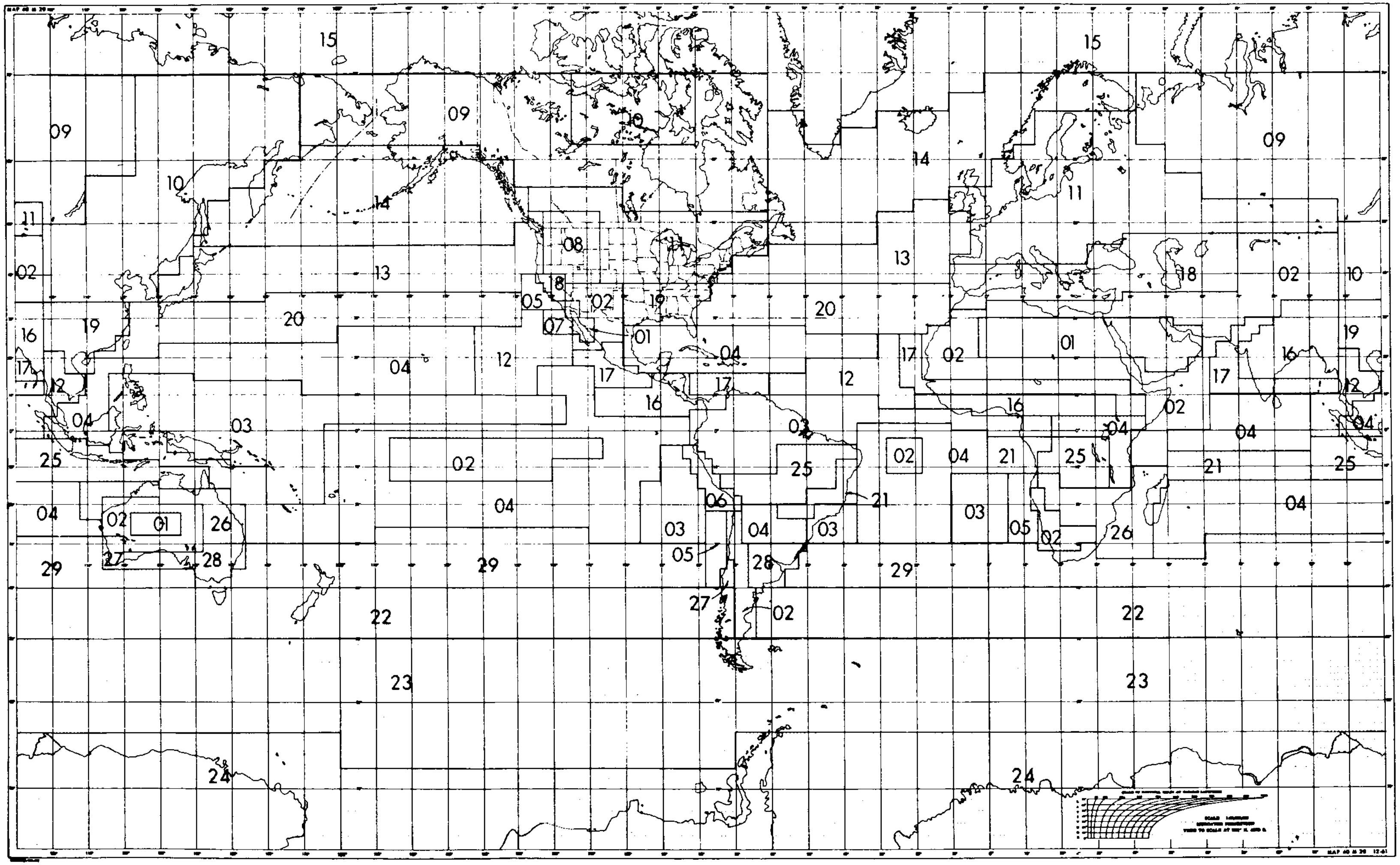

FIGURE 16. 6 CLOUD REGION LOCATION MAP

Since clouds generally display some degree of persistence, time and space conditional statistics were developed for each homogeneous cloud region (Table 16. 3). The basic statistics (Table 16. 2) apply to an area approximately 48. 3 kilometers (30 n. mi.)[1] in diameter, while the conditional data are based on a time separation of 24 hours and space separation of 322 kilometers (200 n. mi). In these same studies, techniques were developed to adjust the conditional statistics for times and distances other than 24 hours and 322 kilometers (200 n. mi.), and to scale both the basic and conditional statistics for application to enlarged target areas.

TABLE 16. 3 CONDITIONAL CLOUD STATISTICS, CLOUD REGION 19, JANUARY

Given Cloud Category	Space Conditionals					Given Cloud Category	Time Conditionals				
	Cloud Category						Cloud Category				
	1	2	3	4	5		1	2	3	4	5
1	0. 68	0. 11	0. 05	0. 09	0. 07	1	0. 41	0. 12	0. 09	0. 25	0. 13
2	0. 13	0. 32	0. 07	0. 13	0. 35	2	0. 23	0. 29	0. 10	0. 23	0. 15
3	0. 09	0. 20	0. 12	0. 42	0. 17	3	0. 14	0. 26	0. 13	0. 35	0. 12
4	0. 09	0. 14	0. 10	0. 58	0. 09	4	0. 16	0. 15	0. 06	0. 43	0. 20
5	0. 11	0. 12	0. 11	0. 27	0. 39	5	0. 18	0. 07	0. 10	0. 28	0. 37

16. 2. 3 The Simulation Procedure

A typical space mission for earth resources might require that an area 161 × 161 kilometers (100 × 100 n. mi.) be photographed in color. Perhaps the orbital parameters are such that the spacecraft will pass over the target area at 24-hour intervals and the photographic requirements will be satisfied with a montage pieced together from increments obtained on each pass. The mission planner might ask, "How many passes will be required to be 95 percent confident of photographing 80 percent of the area?" If the mission were also limited to a specific number of passes by the amount of film or other expendables, the planner would also need an analysis of that limiting pass number. For example, "With what degree of confidence can one expect to photograph 80 percent of the area by pass

---

1. Nautical miles (n. mi.) were used in the contract study by Allied Research Associates.

number 12?" To answer these and other questions, a computer program using a Monte Carlo mission simulation procedure was developed. In this procedure, the target area is divided into 100 equal parts so that each part represents one percent of the area. Before starting the process, the unconditional and conditional statistics, after being scaled for the area size, are arranged in cumulative form by summing across each row. The fraction of target areas that can be photographed under each cloud category is decided upon at some earlier time, primarily on the basis of the sensors being used. In any case, as part of the input, it can be changed as the experimenter desires. Table 16.4 shows a basic set of cloud statistics plus the cumulative arrangement and the maximum part of the area photographable under each cloud category. In this case, it was decided that the photographable part of the area would be 1 minus the mean cloud cover for each category.

To start the procedure, a random number is generated and used to extract from the unconditional summation the cloud category for the first satellite pass. For example, if the first random number gave cloud category 3, to which a 55 percent cloud cover had been assigned, 45 percent of the target area would be photographed on the first pass. Of course, the photographic coverage obtained from each satellite pass over the target could be incremented without specifying which 45 parts were photographed. However, specifying by number those parts of the target area photographed on each pass permits a more realistic accumulation after 80 to 90 percent of the area has been photographed and a finite probability of acquiring 100 percent of the area. The next step then is to determine which 45 parts of the area were photographed on the first pass. This is done according to the season. If frontal clouds predominate, the 45 parts are arranged in an organized contiguous pattern. On the other hand, if air mass cumulus clouds are expected (tropical regions or midlatitude summer months), the 45 parts are scattered randomly throughout the area. For the first pass, then, after the cloud cover was determined by a random number process, the locations of the cloud-free parts of the target area were specified by a prearranged design. Finally, the percentage of the target area photographed was tallied.

The cloud cover encountered on the second pass is selected from the conditional row (summed across) designated by the first pass, or the given category, by means of a new random number. If the random number selects cloud category 4, then 75 percent of the area is cloud covered and 25 percent (or 25 numbered parts) is cloud-free and can be photographed. However, all or part of the 25 percent might have been acquired on the first pass. To account for this possibility, 25 discrete random numbers are drawn to identify the numbered parts of the target area to be photographed on this pass. Of course, only the newly acquired parts of the target area are incremented; those photographed for the second time do not contribute to the total photographic coverage.

TABLE 16.4 ARRANGEMENT OF CLOUD STATISTICS FOR COMPUTER SIMULATION

	Maximum Area Photographable per Pass				
	CC-1	CC-2	CC-3	CC-4	CC-5
	1.000000	0.750000	0.450000	0.250000	0.000000
	Unconditional Probability Statistics				
	CC-1	CC-2	CC-3	CC-4	CC-5
	0.000000	0.030000	0.050000	0.550000	0.370000
Given Cloud Category	Conditional Probability Statistics				
	CC-1	CC-2	CC-3	CC-4	CC-5
1	0.000000	0.110000	0.000000	0.000000	0.890000
2	0.000000	0.130000	0.100000	0.360000	0.410000
3	0.010000	0.100000	0.100000	0.470000	0.320000
4	0.000000	0.070000	0.060000	0.460000	0.410000
5	0.010000	0.090000	0.080000	0.410000	0.410000
	Cumulative Unconditional Probability Statistics				
	CC-1	CC-2	CC-3	CC-4	CC-5
	0.000000	0.030000	0.080000	0.630000	1.000000
Given Cloud Category	Cumulative Conditional Probability Statistics				
	CC-1	CC-2	CC-3	CC-4	CC-5
1	0.000000	0.110000	0.110000	0.110000	1.000000
2	0.000000	0.130000	0.230000	0.590000	1.000000
3	0.010000	0.110000	0.210000	0.680000	1.000000
4	0.000000	0.070000	0.130000	0.590000	1.000000
5	0.010000	0.100000	0.180000	0.590000	1.000000

All subsequent passes are handled in the same way. The cloud cover encountered on the previous pass becomes the given condition and identifies the conditional statistics to be used on the current pass. After selecting the cloud cover, several additional random numbers are generated to identify the parts of the target area that are cloud-free. The parts acquired on each pass are accumulated until the entire area has been photographed or until the maximum number of passes has been made. This procedure is illustrated in Table 16.5. The top sections represent the target area divided into 100 parts; the "1's" depict clouds while the "0's" show the clear parts. The summary at the bottom shows the cumulative percentage of area photographed, the random number used to select each cloud cover, the cloud cover selected for each pass, and the pass number. In this example, the first random number, 0.072, specifies cloud category 3: 55 cloud-covered parts and 45 clear parts. The arrangement of the cloudy area as shown at the top left is an arbitrary design chosen because frontal clouds were considered more likely at this time and location.

To account for cloud persistence, the cloud-cover category selected for pass 2 is taken from row 3 of the cumulative conditional probability statistics (Table 16.4). Entering that row with the new random number, 0.531, give cloud category 4, or 25 clear parts, for pass 2. The locations of the 25 clear parts ("0's") as given by additional random numbers is shown in the top center section of Table 16.5. The top right section showing the cumulative area photographed after pass 2 contains 60 "0's" rather than 70(45 + 25) because 10 of the 25 clear sections of pass 2 were already photographed on pass 1.

A summary of the subsequent passes, comprising one iteration, is shown at the bottom of Table 16.5. Generally, 300 iterations are made to simulate a photographic mission.

This Monte Carlo procedure is most useful when the satellite passes over the target area at intervals of 24 hours or less, where cloud persistence must be considered. If there are long time intervals between satellite passes (perhaps 3 days or more), the cloud events may be considered independent and the probability of success computed from the basic combinatorial equation:

$$P_{100\%} = 1 - [1 - P(1)]^N \qquad (16.1)$$

or

$$N = \frac{\ln\left(1 - P_{100\%}\right)}{\ln\,[1 - P(1)]} \qquad (16.2)$$

TABLE 16.5 PHOTOGRAPHIC PARTS OF THE TARGET AREA

CAP = 45.0 PASS = 1	AP = 25 PASS = 2	CAP = 60.0 PASS = 2
1 1 1 1 1 1 1 1 1 1	1 1 0 1 1 1 1 1 0 1	1 1 0 1 1 1 1 1 0 1
1 1 1 1 1 1 1 1 1 1	0 0 0 1 0 1 0 0 1 1	0 0 0 1 0 1 0 0 1 1
1 1 1 1 1 1 1 1 1 1	1 1 1 1 0 1 1 1 1 1	1 1 1 1 0 1 1 1 1 1
1 1 1 1 1 1 1 1 1 1	1 1 0 0 1 1 0 1 1 1	1 1 0 0 1 1 0 1 1 1
1 1 1 1 1 1 1 1 1 1	1 1 1 1 1 0 1 1 1 1	1 1 1 1 1 0 1 1 1 1
1 1 1 1 1 0 0 0 0 0	0 1 1 0 1 1 0 1 1 1	0 1 1 0 1 0 0 0 0 0
0 0 0 0 0 0 0 0 0 0	1 0 0 1 0 1 0 1 1 1	0 0 0 0 0 0 0 0 0 0
0 0 0 0 0 0 0 0 0 0	1 1 1 1 1 1 1 0 1 1	0 0 0 0 0 0 0 0 0 0
0 0 0 0 0 0 0 0 0 0	0 1 0 1 1 1 1 1 1 1	0 0 0 0 0 0 0 0 0 0
0 0 0 0 0 0 0 0 0 0	0 1 0 1 1 1 1 1 1 1	0 0 0 0 0 0 0 0 0 0

B(N)	RAN	C(N)	N
45.000	0.072	3	1
60.000	0.531	4	2
79.000	0.110	3	3
84.000	0.609	4	4
84.000	0.629	5	5
84.000	0.659	5	6
84.000	0.877	5	7
89.000	0.410	4	8
92.000	0.166	4	9
93.000	0.392	4	10
93.000	0.690	5	11
93.000	0.733	5	12
93.000	0.727	5	13
93.000	0.913	5	14
93.000	0.821	5	15
93.000	0.875	5	16
98.000	0.176	3	17
98.000	0.359	4	18
100.000	0.232	4	19

CAP – Cumulative Area Photographed (%)

AP – Area Photographed (%)

B(N) – Total Area Photographed

RAN – Random Number Used to Select the Cloud Cover

C(N) – Cloud Category Encountered on Each Pass

N – Satellite Pass Number

where

$P_{100\%}$ = required probability level of photographing 100 percent of the area

P(1) = relative frequency of cloud category 1

N = number of independent satellite passes.

16.2.4 Results

16.2.4.1 Individual Target Areas

Statistics from three homogeneous cloud regions (2, 13, and 19, Figure 16.6) were used to illustrate the type of information available from the simulation procedure and to compare the simulation results with those obtained from the combinatorial equation.

One convenient way of comparing the two procedures was to address the question, "How many independent satellite passes are required to be 95 percent confident of encountering at least one pass with 3/10 or less (cloud categories 1 or 2) cloud cover over the target area?" The number of passes obtained from each procedure, as shown in Table 16.6, apply to a target area 161 kilometers (100 n. mi.) in diameter. This mission is flown in January, and the satellite passes over the target area at 1300 hours LST.

TABLE 16.6 COMPARISON OF COMPUTER SIMULATION AND COMBINATORIAL RESULTS

Cloud Region	Combinatorial	Computer Simulation
2	8	8
13	116	119
19	12	12

For this comparison, the computer simulation program was adjusted to consider only the unconditional cloud statistics.

Since the number of passes required to satisfy the conditions stated above may be excessive for some cloudy areas of the earth (for example, region 13), the mission planner may be willing to accept incremental photographic coverage. Also, the satellite may pass over the target area at such frequent intervals that the passes cannot be considered independent. When conditions such as these are imposed, a computer simulation is required to evaluate the consequence of cloud cover on the proposed mission.

Results from the simulation program giving analyses of at least 95 percent coverage of the target area and the photographic coverage after 10 satellite passes are shown in Figures 16.7 and 16.8. In both cases, the

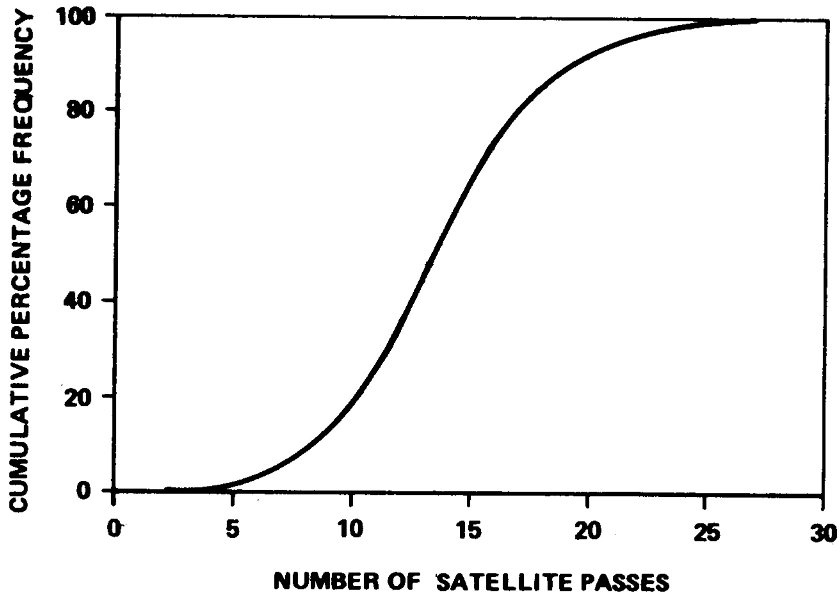

FIGURE 16.7 ANALYSIS OF AT LEAST 95 PERCENT PHOTOGRAPHIC COVERAGE

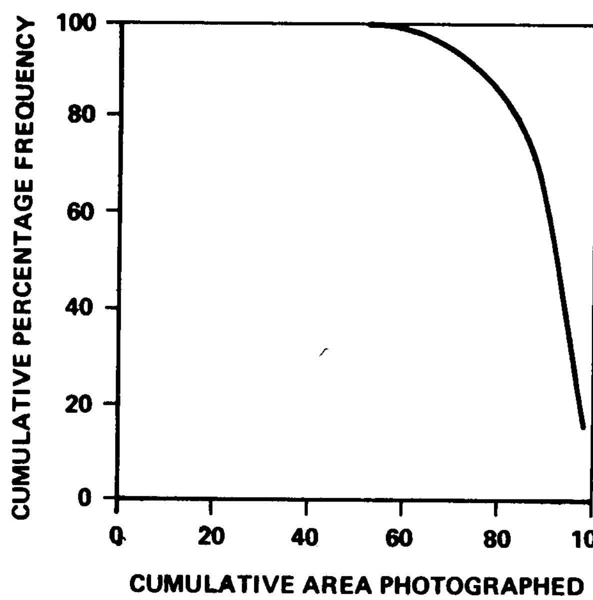

FIGURE 16.8 ANALYSIS OF PHOTOGRAPHIC COVERAGE AFTER TEN PASSES

target is a 161-kilometer (100-n. mi.) diameter area in cloud region 13. The mission is planned for January, and the spacecraft passes over the target area every day at 1300 LST.

Figure 16.7 shows a 50-percent chance of photographing 95 percent of the area in 13 passes, while 19 passes are required to be 90 percent confident.

After 10 passes (Figure 16.8), there is a 50-percent chance of photographing 92 percent of the area and a 90-percent chance of acquiring 76 percent of the target area. These results comprise a summary of 300 iterations of the simulation procedure.

16.2.4.2 Contiguous Target Areas – A Swath

The simulation can also be applied to a series of contiguous target areas, for example, a swath from the Texas Gulf Coast to the Canadian Border (Figure 16.9). To evaluate this type target the swath is divided into several equal-sized areas based upon the width of the swath. If the swath is 161-kilometers (100-n. mi.) wide the dimensions of each target area or "box" become 161 × 161 kilometers (100 × 100 n. mi.). In the case illustrated there are approximately six boxes in cloud region 19 and five boxes in cloud region 11. As before, random numbers dictate the cloud cover applicable to each box. The unconditional cloud distribution is used for pass number 1 over the first box but space conditionals are used for all subsequent boxes. That is, the clouds in box 2 depend upon those in box 1, box 3 depends upon box 2, etc. Box 1 of cloud region 11 depends upon box 6 of cloud region 19, but the cloud draw is made from the statistics applicable to cloud region 11.

Subsequent satellite passes over the swath may use either unconditional or time conditional statistics for box 1 of region 19 depending upon the time interval between passes. All other boxes, however, depend only upon the preceding box and always use the space conditional statistics.

Simulation results evaluating the swath are presented in the same manner as the individual target results.

A question that presents some difficulty is that of identifying and fitting into the mosaic small disjointed fractional parts of the target area. For example, can all of the "0's" of Figure 16.7 acquired on pass 2 really be considered useful? Those isolated parts may be difficult, if not impossible, to identify. Perhaps meaningful photographic results can be obtained only

FIGURE 16.9 EXAMPLE OF 100-n. mi. WIDE SWATH

when small cloud amounts are present. Although this may be a serious problem for the experiment designer, the mission planner, and the atmospheric scientists, it does not affect the simulation program directly. If it is decided that a cloud-cover category will not provide useable photographic results, that category can be assigned 100 percent cloud cover, and nothing will be added to the cumulative coverage when it occurs. It might also be stipulated that isolated parts of the target may not contribute to the total photographic coverage. Many contingencies can be handled as input changes; some may require minor program changes.

16.3 Four-Dimensional Atmospheric Models

In this part of the attenuation model project the emphasis was placed on water vapor rather than clouds. Also, since attenuation calculations are usually made from reference atmosphere inputs the other atmospheric parameters found in reference atmospheres were included in the 4-D work. The basic data are comprised of monthly statistics (mean and standard deviations) of pressure, temperature, density, and moisture content from 0 to 25 kilometers altitude on a global grid network. These data provide information on latitudinal, longitudinal, altitudinal, and temporal variation of the parameters; hence the name "four-dimensional atmospheric models." Of course, a profile of temperature, pressure, density, and moisture content for any global location may be retrieved from these data. Still, to reduce the data to a more manageable amount it was decided to outline homogeneous moisture content regions for which a single set of profile statistics would apply. This procedure would permit the use of one set of profiles for all locations within a homogeneous region. While parts of this procedure are still under development, the basic statistics have been computed and the retrieval plans formulated. For each region analytical functions will be fitted to the statistical data. For moisture, it appears that exponential functions will be most appropriate, while for temperature, a series expansion technique may be used. The result of fitting analytic functions to the statistical climatological profile data will be a library of coefficients for the temperature and moisture profiles. These coefficients will then be used to develop computer subroutines to regenerate the model profiles of temperature and moisture which will also be a function of the homogeneous region and month of the year.

In the compilation of the global statistics, pressure and density were determined from the hypsometric equation and the equation of state, rather than linear or logarithmic interpolation. The purpose of this was to insure hydrostatic consistency, thus, it is likely that the pressure and density profiles can be generated from the temperature profile and the hydrostatic assumption.

The final result of this data analysis will be a series of computer programs that provide mean, maximum, and minimum profiles of moisture, temperature, pressure, and density from the surface to 25 kilometers altitude for any location on the globe and month of the year. The computer programs will contain the equations, data, and library of coefficients necessary to produce the desired results.

The 4-D atmospheric model is described in references 16.6 and 16.7.

16.4 Automatic Data Classification Programs

Computer programs have been developed in conjunction with NASA's Earth Resources Program for the analysis of Earth Resources Technology Satellite imagery and Skylab Earth Resources Experiment Package imagery, References 16.8, 16.9, 16.10 . Because of the large amounts of data involved, these programs were designed to provide a method of analysis that was automatic and free of human supervision as possible.

The input data to these programs consist of digitized multispectral images of the ground scene. The signal in each spectral image or channel of data is proportional to the amount of electromagnetic radiation emitted or reflected from the ground scene, and the computer programs are capable of handling up to 12 channels of multispectral data.

The original earth observation objectives of these programs were to provide the type of information listed below:

a. the homogeneity and patterns of terrain features,

b. the number of spectrally distinct features contained in the ground scene image with their respective mean spectral signatures and variances,

c. the areal extent, location and distribution of the spectral features within the ground scene, and

d. the quantity of ground truth needed and direction for ground truth patrols.

A spectral signature is a vector whose dimension equals the number of channels of data. The components of the signature are the average value of the data in each channel for a particular ground scene feature.

For the above applications, cloud cover is considered a nuisance, However, by redirecting the application of the above objectives, these computer programs possess the potential to contribute in a positive manner to the study of cloud statistics.

Since multispectral data is now available from aircraft or satellite earth observation imagery, that also contains cloud cover, it is possible to obtain a spectral signature and variance for clouds only. This signature could then be used to discriminate cloud cover from sand and possibly snow, since their signatures should be different. In addition, a study of the variation of the components of the cloud signature could possibly provide an input to the categorization of cloud types. For example, the amount of water vapor absorption or infrared opacity of the cloud, as well as opacity in the visible parts of the spectrum, could provide some measure of cloud fleeciness as contrasted to clouds that visually appear to have a distinct shape.

The present capabilities of these programs toward the computation of cloud statistics include:

a. a map showing terrain patterns for ground reference and the location and distribution of cloud cover within the ground scene, and

b. tables indicating percentage of cloud cover and relative sizes of clouds having well defined shapes.

Figure 16.10 is illustrative of the type of computer program output. The left side of figure 16.10 is a boundary map of the ground scene made from multispectral data acquired by the Earth Resources Technology Satellite near Sacramento, Pittsburg, and Stockton, California. The area is mainly an agricultural area with a large man made reservoir at the bottom of the map. The rectangular shaped bright areas are areas that were selected by the computer program for acquiring data to determine the number of different features in the ground scene. A map of the ground scene is then produced showing the location of data that belong to the different features. For example, the map on the right side of figure 16.10 shows unclassified boundary points and data points belonging to the feature water, which are the brightest areas. The large waterway feeding into the reservoir is clearly visible and possibly some pollution, indicated by the dark area of unclassified data points at the junction of the waterway and the reservoir.

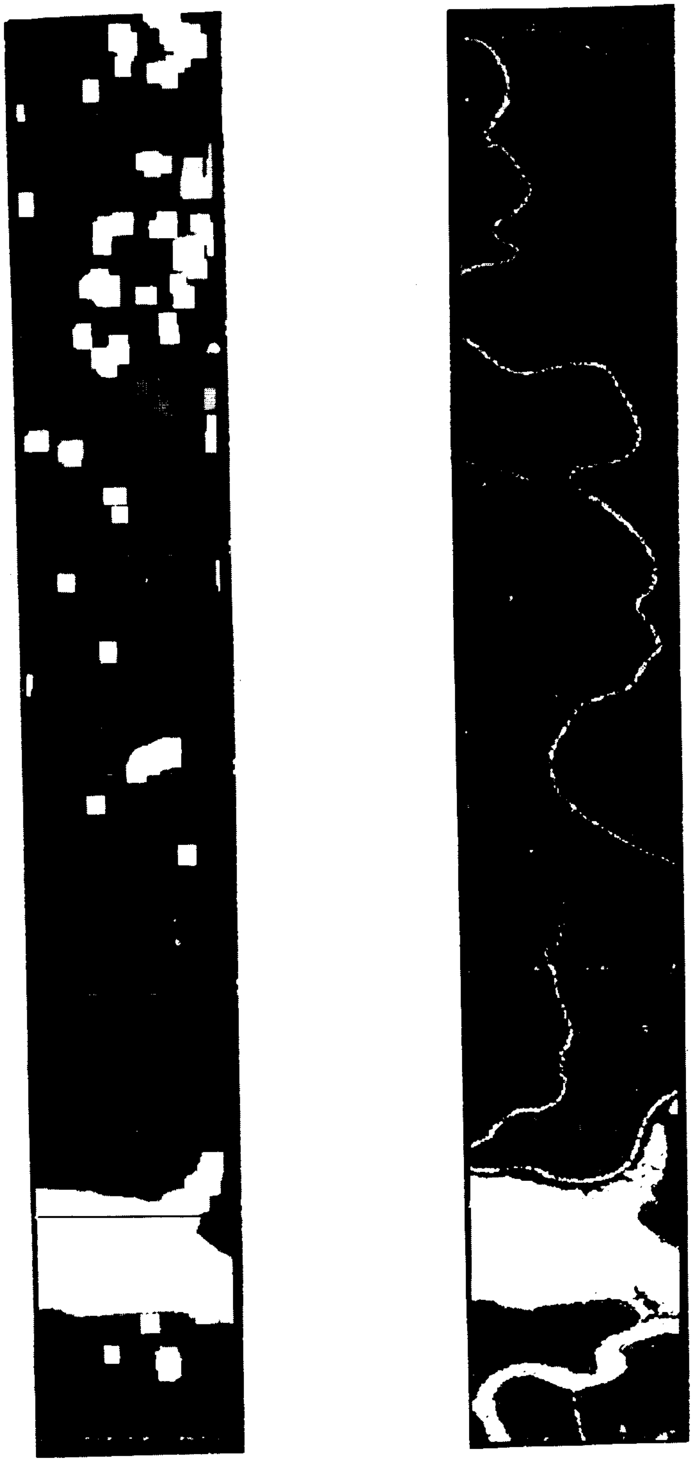

Boundary Map and Homogeneous Feature Location

Extraction of Water Features

Figure 16.10 Feature location and extraction

REFERENCES

16.1 Gaut, N. E., and Reifenstein, E. C. III, "Interaction Model of Microwave Energy and Atmospheric Variables," Environmental Research and Technology, Inc., Final Report of Contract NAS8-26275, Feb. 1971.

16.2 Sherr, P. E., et. al., "World Wide Cloud Cover Distribution for Use in Computer Simulations," Allied Research Associates, NASA CR-61226, Jun. 14, 1968.

16.3 Greaves, J. R., et. al., "Development of a Global Cloud Model for Simulating Earth-Viewing Space Missions," Allied Research Associates, Final Report Contract NAS8-25812, Jan. 1971.

16.4 Brown, S. C., "Simulating the Consequence of Cloud Cover on Earth-Viewing Space Missions," Bulletin of the American Meteorological Society, vol. 51, no. 2, Feb. 1970.

16.5 Chang, D. T., and Willard, J. H., "Further Developments In Cloud Statistics For Computer Simulations," Allied Research Associates, Inc., NASA CR 61389, July, 1972.

16.6 Spiegler, D. B. and Greaves, J. R., "Development of Four-Dimensional Atmospheric Models (Worldwide), Allied Research Associates, Inc., NASA CR-61362, August 1971.

16.7 Spiegler, D. B. and Fowler, M. G., "Four Dimensional World-wide Atmospheric Models (Surface to 25 km Altitudes), Allied Research Associates, Inc., NASA CR-2082.

16.8 Phillips, M. R., "Earth Resources Data Processor," NASA Contractor Report, NASA CR-61399, October 1972.

16.9 Jayroe, R. R. "Unsupervised Spatial Clustering with Spectral Discrimination," NASA Technical Note, in publication.

16.10 Su, M. Y., "The Composite Sequential Clustering Technique for Analysis of Multispectral Scanner Data," NASA Contractor Report, NASA CR-12899, October 1972.

N74-16309

SECTION XVII. WORLDWIDE SURFACE EXTREMES

BY

Glenn E. Daniels

17.1 Introduction

In the original issue of the "Natural Environment Guidelines" document (Ref. 17.1, 1961), information was needed to fabricate, transport, test, and launch Marshall Space Flight Center space vehicles in limited geographical areas only. It became evident with the development of advanced programs such as the Apollo project that statistical meteorological data are needed from other areas as well. Thus, in a later revision, a section called "Distribution of Surface Extremes in the United States" was included. In the present revision, this brief section on worldwide surface extremes has been prepared. This section will also illustrate the much larger extreme values that occur in some areas and will compare them with those currently used in space vehicle design.

17.2 Sources of Data

A great amount of meteorological data have been collected throughout the world. Various agencies have collected such data in a form that can be used for statistical studies. Kendrew's "Climates of the Continents" (Ref. 17.2) is an excellent summary of mean values of the meteorological parameters, temperature, pressure, and precipitation, and it is also the source of many interesting discussions of local meteorological conditions around the world.

"World Weather Records, 1941-50" (Ref. 17.3), compiled by the Weather Bureau (now part of the Environmental Sciences Services Administration), provides another excellent summary of mean values of meteorological data.

Recently, in revising AR 705-15 (now AR 70-38, Ref. 17.4), the Earth Sciences Laboratory NLABS, U. S. Army Natick Laboratories at Natick, Massachusetts, has collected worldwide data on meteorological extremes. For the revised AR 70-38, the Earth Sciences Laboratory NLABS prepared world maps that show worldwide absolute maximum and absolute minimum temperatures.* These maps are reproduced in this section as

* Absolute is defined as the highest and lowest values of data of record.

Figures 17.1 and 17.2, and due credit is given to the Earth Sciences Laboratory NLABS, U. S. Army Natick Laboratories.

The several climatic atlases for various areas of the world provide other sources of data; those of interest will be referred to in the following sections.

17.3 Worldwide Extremes Over Continents

To present all the geographic extremes properly, many large maps similar to Figures 17.1 and 17.2 would be required; therefore, only worldwide extremes of each parameter will be discussed, and available references on each parameter will be given. Individual geographic extremes will be mentioned when pertinent.

17.3.1 Temperature.

Absolute maximum and absolute minimum world temperature extremes are shown in Figures 17.1 and 17.2. Some geographical extreme air temperatures of record are given in Table 17.1

TABLE 17.1 EXTREME AIR TEMPERATURES OF RECORD

Location	Air Temperatures of Record
Salah, Africa	118°F, mean daily max. for 45 days
	127°F, absolute max.
Azizia, Africa*	136°F, absolute max.
Sind, India	123°F, absolute max.
Basra, Iraq	123°F, absolute max.
	78°F, mean daily min. in Aug.
Death Valley, Calif.*	134°F, absolute max.
Stuart, Australia	131°F, absolute max.
Verkhoyansk, U.S.S.R.	-94°F, absolute min.
Rogers Pass, Montana	-70°F, absolute min. for U.S.
Snag, Yukon Territory, Canada	-85°F, absolute min. for North America

Temperatures of the ground are normally hotter than the air temperatures during the daytime. In the Sahara Desert of Africa, temperatures of sand as high as 172°F have been measured. At Stuart, Australia, the sand has reached temperatures so hot that matches dropped into it burst into flame.

*The validity of these temperatures has been questioned, see Ref. 17.8

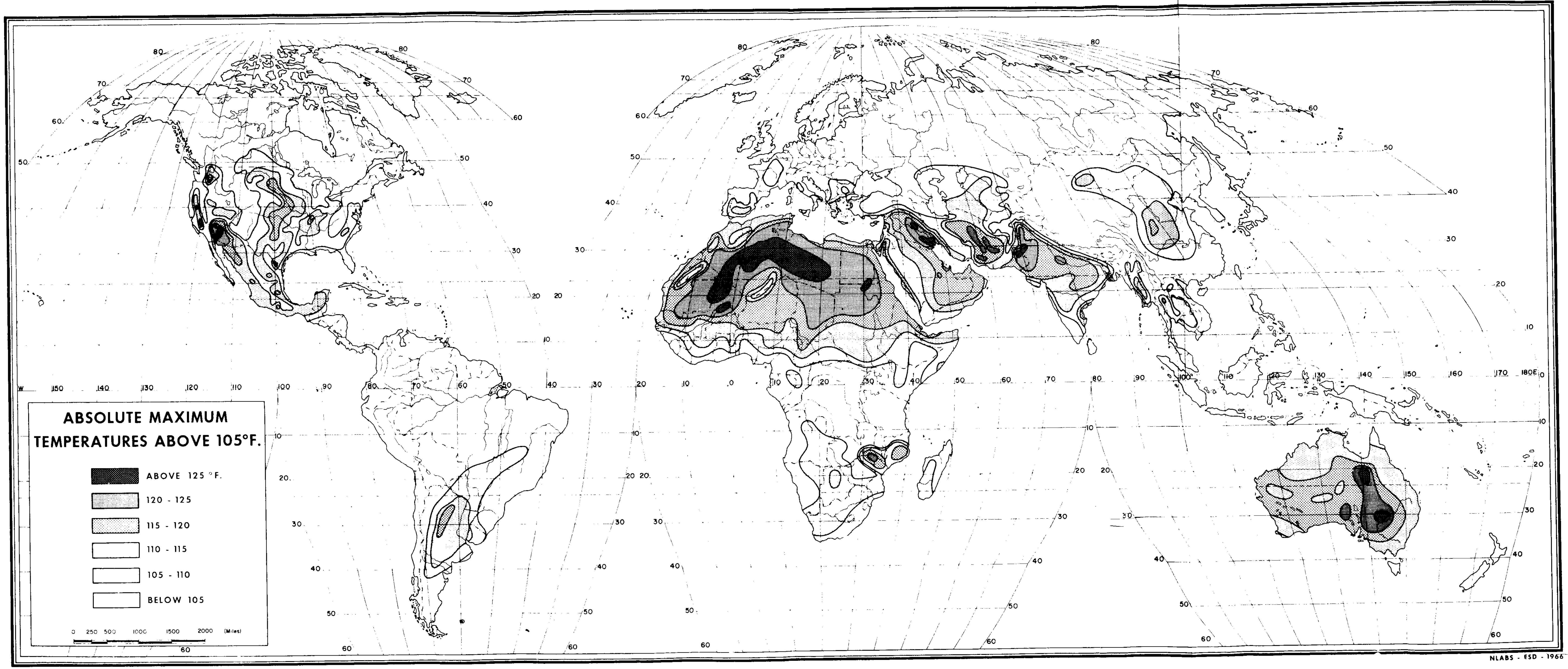

FIGURE 17.1 WORLDWIDE GEOGRAPHIC ABSOLUTE MAXIMUM TEMPERATURES ABOVE 105° F

A B C

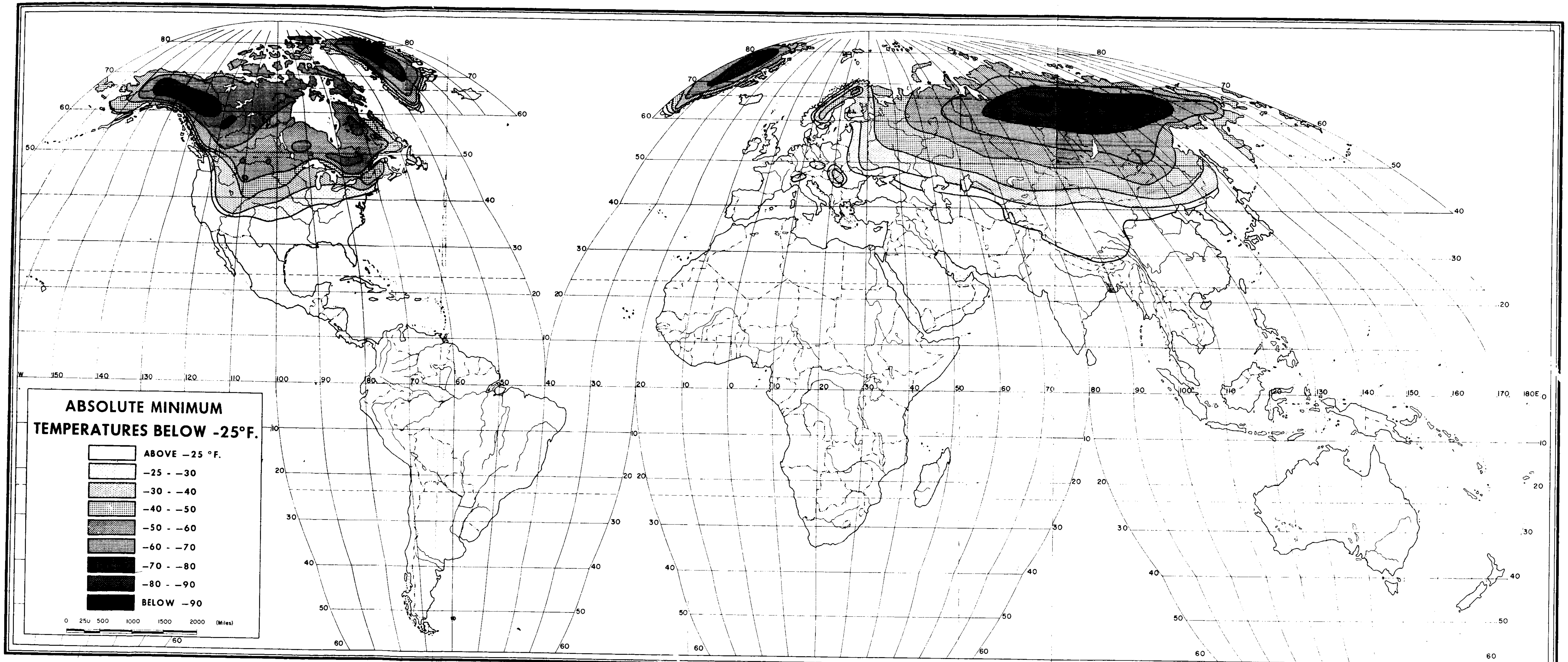

NLABS - ESD - 1966

FOLDOUT FRAME

FOLDOUT FRAME 2

FOLDOUT FRAME 3

In design of equipment for worldwide operations, MIL-STD-210A now uses extreme temperature values of 125°F for a hot temperature and -80°F for a cold temperature. Values outside these limits have been observed. In a study by the Air Force Cambridge Research Laboratories* , June 9, 1969, for Special Assistant for Environmental Service of the Joint Chiefs of Staff, to lower the risk of exposing equipment of MIL-STD-210A, it was recommended that values of 131°F and -87°F would be more realistic for the hot and cold temperatures.

The above recommendation for hot temperature was based upon risk tables, shown in Table 17.2, of extreme high temperatures developed by extreme value theory using 39 extreme annual temperatures at Death Valley, California. Such temperatures persist for one or two hours during a day.

TABLE 17.2 EXTREME HIGH TEMPERATURES WITH RELATION TO RISK AND DESIRED LIFETIME

Risk (%)	Temperatures (°F) Planned Lifetime (years)				
	1	2	5	10	25
1	131	133	134	135	137
10	127	128	130	131	133
25	125	127	128	129	131
50	124	125	127	128	130

The recommendation for cold temperature was based upon risk tables, shown in Table 17.3, of extreme low temperatures, developed by extreme

TABLE 17.3 EXTREME LOW TEMPERATURES WITH RELATION TO RISK AND DESIRED LIFETIME[a]

Risk (%)	Temperature (°F) Planned Lifetime (years)				
	1	2	5	10	25
1	-87	-91	-97	-101	-106
10	-74	-78	-83	- 87	- 92
25	-68	-72	-77	- 81	- 86
50	-63	-67	-73	- 76	- 81

a. Temperatures in Antartica were not considered in the study.

* Norman Sissenwine: "Temperature Extremes Applicable to MIL-STD-210 Area and Risk Considerations." AFCRL, a paper transmitted by a letter dated June 16, 1969, to Chief, Aerospace Environment Division, MSFC.

value theory using 23 annual extreme low temperatures at Snag, Yukon Territory, Canada. The extreme low temperatures will persist for longer periods since they occur during polar darkness.

17.3.2 Dew Point.

High dew points are associated with high temperatures near large bodies of water. Besides being detrimental to equipment, high dew points make living conditions very uncomfortable. Extremely high dew points occur in the following areas, in the vicinity of the water bodies specified:

a. The northern portion of the Arabian Sea in April and May, to 85°F dew point.

b. The Red Sea in July, to 89°F dew point.

c. The Caribbean Sea (includes the western end of Cuba and the Yucatan Penninsula, Mexico) in July, to 81°F dew point.

d. The northern portion of the Gulf of California, to 86°F dew point (data from Puerto Penasco, Mexico, Ref. 17.6).

The Air Force has published the "Atmospheric Humidity Atlas for the Northern Hemisphere" (Ref. 17.5), which shows maps for various percentile levels of dew point for midseason months (January, April, July, and October).

A new report on worldwide humidity is now being published by the U. S. Army Natick Laboratories (Ref. 17.6).

17.3.3 Precipitation.

The worldwide distribution of precipitation is extremely variable; some areas do not receive rain for years, while others receive torrential rain many months of the year. Precipitation is also seasonal; for example, Cherrapunji, India, with its world record total of 905 inches of precipitation in a year, has a mean monthly precipitation of less than one inch in December and January. The heaviest precipitation for long periods (greater than 12 hours) usually occurs in the monsoon type of weather. High rates of rainfall for short periods (less than 12 hours) usually occur in the thunderstorm type of rain and over much smaller areas than the monsoon rain. Some world records for various periods of rainfall are given in Table 17.4 (Ref. 17.2 and 17.7).

TABLE 17.4 WORLD RAINFALL RECORDS

Station	Time Period	Amount (in.)
Unionville, Maryland	1 min	1.23
Plum Point, Jamaica	15 min	8.0
Holt, Missouri	41 min	12.0
D'Hanis, Texas	3 hr	20.0
Baguio, Philippine Islands	1 day	50.0
Cherrapunji, India	30 days	360.0
Cherrapunji, India	1 yr	905.0

Even though the values given in Table 17.4 are considerably higher than the values given in Table 4.2 of Section IV, values in Table 4.2 are considered adequate for most space vehicle design problems within currently expected operational areas.

17.3.4 Pressure.

Surface atmospheric pressure extremes for use in design must be derived from the measured station pressures, not from the computed sea level pressures that are usually published.

Station pressures between stations have great variability because of the difference in altitude of the stations. The lowest station pressures occur at the highest altitudes. The highest station pressures occur at either the lowest elevation stations (below sea level), or in the arctic regions in cold air masses at or near sea level.

Court (Ref. 17.7) has an interesting discussion on worldwide pressure extremes. Some typical high and low pressure values are given in Table 17.5 (Ref. 17.2 and 17.7).

17.3.5 Ground Wind.

Worldwide extreme surface winds have occurred in several types of meteorological conditions: tornadoes, hurricanes or typhoons, mistral winds, and Santa Ana winds. In design, each type of wind needs special consideration. For example, the probability of tornado winds is very low compared with the probability of mistral winds, which may persist for days (see Section 5.2.10).

TABLE 17.5. TYPICAL PRESSURE VALUES OF SELECTED AREAS

Station	Elevation Above Sea Level (ft)	Pressure (mb)	
		Lowest	Highest
Lhasa, Tibet	12 090	645[a]	652[a]
Sedom, Israel	-1 275	—	1081.8
Portland, Maine	61	—	1056
Qutdligssat, Greenland	10	—	1063.4
In a typhoon 400 Miles East of Luzon, Philippine Islands[b]	~0	887	—

a Monthly means.
b Lowest sea level pressure of record.

17.3.5.1 Tornadoes

Tornadoes are rapidly revolving circulations normally associated with a cold front squall line or with warm, humid, unsettled weather; they usually occur in conjunction with a severe thunderstorm. Although a tornado is extremely destructive, the average tornado path is only about a quarter of a mile wide and seldom more than 16 miles long, but there have been a few instances in which tornadoes have caused heavy destruction along paths more than a mile wide and 300 miles long. The probability of any one point being in a tornado path is very small; therefore, design of structures to withstand tornadoes is usually not considered except for special situations where tornado shelters are built underground. Velocities have been estimated to exceed 134 ms^{-1} (260 knots) in tornadoes.

17.3.5.2 Hurricanes (Typhoons).

Hurricanes (also called typhoons, Willy-willies, tropical cyclones, and many other local names) are large tropical storms of considerable intensity. They originate in tropical regions between the equator and 25 degrees latitude. A hurricane may be 1600 kilometers (1000 miles) in diameter with winds in excess of 67 ms^{-1} (130 knots). A tropical storm is defined as a hurricane when winds are equal to or greater than 33 ms^{-1} (64 knots). The winds are frequently associated with heavy rain. Since the hurricanes of the West Indies are as intense as others throughout the world, design winds based upon these hurricanes would be representative for any geographical area. Section 5.2.10 gives hurricane design winds for the area of Cape Kennedy, Florida. Although the highest winds recorded in a hurricane in the area of Cape Kennedy, Florida, were lower than winds from thunderstorms in the same area, the probability still exists that much higher winds could result from hurricanes in the vicinity of Cape Kennedy.

For extremes applicable to equipment, the following Table 17.6 from a study of 39 years of wind data for Taipei, Taiwan (in the Pacific typhoon belt)* , for a height of 10 feet above the natural grade, is representative of all hurricane areas of the world.

TABLE 17.6 EXTREME WINDS IN HURRICANE (typhoon) AREAS WITH RELATION TO RISK AND DESIRED LIFETIME
(3.1-m reference height)

Risk (%)	Extreme Wind Speeds (ms^{-1})				
	Planned Lifetime (years)				
	1	2	5	10	25
1	38	41	46	49	54
5	30	33	38	41	46
10	26	29	34	38	42
25	21	24	29	33	37
50	16	20	25	28	33

17.3.5.3 Mistral Winds (Ref. 17.2).

The mistral wind is a strong polar current between a large anti-cyclone and a low pressure center. These winds frequently have temperatures below freezing. The mistral of the Gulf of Lions and the Rhone Valley, France, is the best known of these winds. Although winds of 37 ms^{-1} (83 mph) have been recorded in the area of Marseilles, France, much higher winds have occurred to the west of Marseilles in the more open terrain, where even railway trains have been blown over. Mistrals blow in the Rhone Valley for about 100 days a year. The force of the mistral wind is intensified by its coldness, and the associated greater air density.

* Norman Sissenwine: "Surface Wind Extremes Applicable to MIL-STD-210 Area and Risk Considerations." AFCRL, a paper transmitted by a letter dated June 16, 1969, to Chief, Aerospace Environment Division, MSFC.

17.3.5.4 Santa Ana Winds.

In contrast to the mistrals, the Santa Ana Winds, which occur in Southern California west of the coast range of mountains, are hot and dry and have speeds up to 41 knots. Similar winds, called Föhn winds, occur in the Swiss Alps and in the Andes, but, because of the local topography, they have lower speeds. The destructiveness of these winds is not from their speeds, but from their high temperatures and dryness, which can do considerable damage to blooming tree and vine crops and exposed equipment and instruments whose seals and paint are critical.

REFERENCES

17.1 Daniels, Glenn E., "Probable Climatic Extremes for Use in MSFC-Space Vehicle Booster and Associated Equipment Development," MTP-AERO-61-93, George C. Marshall Space Flight Center, Marshall Space Flight Center, Ala., Dec. 18, 1961.

17.2 Kendrew, W. G., "The Climates of the Continents," Oxford University Press, Amen House (London), 1961.

17.3 "World Weather Records, 1941-50," U. S. Department of Commerce, Weather Bureau, Superintendent of Documents, U. S. Government Printing Office, Washington, D. C., 1959.

17.4 "Research, Development, Test, and Employment of Material for Extreme Climatic Conditions," AR-70-38 (Supersedes AR-705-15), July 1, 1969.

17.5 Gringorten, I. I., et al., "Atmospheric Humidity Atlas — Northern Hemisphere," AFCRL-66-621, Air Force Cambridge Research Laboratories, L. G. Hanscom Field, Bedford, Mass., Aug. 1966.

17.6 Dodd, Arthur V., "Aerial and Temporal Occurrence of High Dew Points and Associated Temperatures," Technical Report ES- , Department of the Army, U. S. Army Natick Laboratories, Earth Sciences Laboratory, Natick, Mass. (to be published).

17.7 Court, Arnold, "Improbable Pressure Extreme: 1070 mb," Bulletin of the American Meteorological Society, vol. 50, no. 4, Apr. 1969, pp. 248-250.

17.8 Billions, Novella S., "Frequencies and Durations of Surface Temperatures in Hot-Dry Climatic Category Areas. (Cat. 4, AR 70-38)," Technical Report RR-72-13, Dec. 1972, U. S. Army Missile Command, Redstone Arsenal, Alabama.

N74-16310

SECTION XVIII. SEVERE WEATHER, SEA STATE, AND SELECTED CLIMATOLOGIES

By

S. Clark Brown, George H. Fichtl and Orvel E. Smith

18. 1 Introduction

With the development of aerospace launch vehicles which are to be recovered by flying back to the earth's surface, additional climatic data are needed on specific landing sites not covered in other sections of this document. A short discussion is also included on tornadoes, hurricanes, and tropical storms (Ref. 18. 1).

18. 2 Tornadoes

Tornadoes are recognized as the most destructive force winds; because of differential pressures created by tornadoes, buildings have been known to literally explode. Fortunately, the aerial extent of tornadoes is small compared with hurricanes, and the occurrence of tornadoes at the seven stations of interest covered in this document is less frequent than in the Central Plain states of the United States. Tornadoes are observed at times in association with hurricanes in Florida and along the coastal states. Based on Thom's analysis of the number of tornado occurrences (Ref. 18. 2), Table 18. 1 has been prepared giving tornado statistics for stations of interest.

The probability of one or more tornadoes in N years in area (A_1) is given by[1]

$$P(E_1, A_1; N) = 1 - \exp\left(-\bar{x}\,\frac{A_1}{A_2}\,N\right) \qquad (18.1)$$

We choose for the area size for A_1 as 7. 3 km^2 (2. 8 mi^2) because Thom (Ref. 18. 1) reports 7. 2572 km^2 (2. 8209 mi^2) is the average ground area covered by tornadoes in Iowa, and the vital industrial complexes for most locations are of this general size. Thus, taking $A_1 = 7.3$ km^2 (2. 8 mi^2) and $A_1 = 2.59$ km^2 (1 mi^2) and evaluating equation (18. 1) for the values of $\bar{x}$ and A_2 for the stations given in Table 18. 1 yields the data in Table 18. 2.

---

1. Credit is due Prof. J. Goldman, Institute Storm Research, St. Thomas University, Houston, Texas, for this form of the probability expression.

TABLE 18. 1 TORNADO STATISTICS FOR STATIONS SPECIFIED

Station	Number of Tornadoes	Mean Number of Tornadoes Per Year	Area		Mean Number of Tornadoes Per Year at a Point	Mean Recurrence Interval for a Tornado Striking a Point (years)
			(km^2)	(mi^2)		
Cape Kennedy	9	0. 9	10 896	4220	0. 00060	1667
Huntsville	12	1. 2	10 147	3930	0. 00086	1163
New Orleans	9	0. 9	10 689	4140	0. 00061	1639
Mississippi Test Facility	12	1. 2	10 612	4110	0. 00083	1205
Space and Missile Test Center	0	0	9 579	3710	0. 00000	∞
Wallops Island	5	0. 5	9 708	3760	0. 00038	2632
White Sands	2	0. 2	10 405	4030	0. 00015	6667

TABLE 18. 2 PROBABILITY OF ONE OR MORE TORNADO EVENTS IN A 7. 3-km^2 AREA AND A 2. 59-km^2 AREA IN 1, 10, AND 100 YEARS

Station	Mean Number of Tornadoes Per Year in Area, A_2	$P(E_1, A_1; N)$ for A_1 = 7. 3 km^2 (2. 8 mi^2)			$P(E_1, A_1; N)$ for A_1 = 2. 59 km^2 (1. 00 mi^2)		
		N = 1 year	N = 10 years	N = 100 years	N = 1 year	N = 10 years	N = 100 years
Cape Kennedy	0. 9	0. 00060	0. 00596	0. 05797	0. 00021	0. 00213	0. 02110
Huntsville	1. 2	0. 00085	0. 00851	0. 08195	0. 00031	0. 00305	0. 03007
New Orleans	0. 9	0. 00061	0. 00608	0. 05906	0. 00022	0. 00217	0. 02160
Mississippi Test Facility	1. 2	0. 00082	0. 00815	0. 07850	0. 00029	0. 00292	0. 02878
Space and Missile Test Center	0. 0	0. 00000	0. 00000	0. 00000	0. 00000	0. 00000	0. 00000
Wallops Island	0.5	0. 00037	0. 00371	0. 03655	0. 00013	0. 00133	0. 01321
White Sands	0.2	0. 00012	0. 00121	0. 01203	0. 00004	0. 00043	0. 00431

$$P(E_1, A_1; N) = 1 - e^{-\bar{x} \frac{A_1}{A_2} N}$$

Table 18. 2 gives the probability of one or more tornado events in a 7. 3-km^2 (2. 8-mi^2) area and a 2. 59-km^2 (1-mi^2) area in 1 year, 10 years, and 100 years for the indicated seven locations. It is noted that for $A_1 << A_2$ and $N < 100$, equation (18. 1) can be approximated by

$$P(E_1, A_1; N) \doteq \bar{x} \frac{A_1}{A_2} N \quad . \tag{18. 2}$$

An interpretation of the statistics in Table 18. 2 is given using Cape Kennedy as an example. There is a 5. 8-percent chance that at least one tornado will "hit" within a 7. 3-km^2 (2. 8-mi^2) area on Cape Kennedy in 100 years. For a 2. 59-km^2 (1-mi^2) area of Cape Kennedy, the chance of a tornado hit in 100 years is 2. 1 percent. If several structures within a 7. 3-km^2 (2. 8-mi^2) area on Cape Kennedy are vital to a space mission and these structures are not designed to withstand the wind and internal pressure forces of a tornado, then there is a 5. 8-percent chance that one or more of these vital structures will be destroyed by a tornado in 100 years. If the desired lifetime of these structures [or 7. 3-km^2 (2. 8-mi^2) industrial complex] is 100 years and the risk of destruction by tornadoes is accepted in the design, then the design risk or calculated risk of failure of at least one structure due to tornado occurrences is 5. 8 percent. This example serves to point out that the probability of occurrence of an event which is rare in one year becomes rather large when taken over many years and that estimates for the desired lifetime versus design risk for structures discussed in subsection 5. 2. 10 should be made with prudence.

18. 3 Hurricanes and Tropical Storms

The occurrence of hurricanes at Cape Kennedy and other locations for the Eastern Test Range is of concern to the space program because of high winds and because range support for space operations is closed during passage or near approach of a hurricane. This discussion will be restricted to the frequency of tropical storms, hurricanes, and tropical storms and hurricanes combined (tropical cyclones) for annual reference periods and certain monthly groupings, as a function of radial distances from Cape Kennedy only.

By definition, a hurricane is a tropical storm with winds greater than 33 m/sec (64 knots), and a tropical storm is a cyclone whose origin is in the tropics with winds less than 33 m/sec (64 knots). There is no known upper limit for wind speeds in hurricanes, but estimates are as high as 82 m/sec (160 knots). Also, tornadoes have been observed in association with hurricanes.

Tables 18. 3 and 18. 4 give a general indication of the frequency of tropical storms and hurricanes by months within 161- and 644-kilometer (100- and 400-n. mi.) radii of Cape Kennedy. From Table 18. 3 it is noted that hurricanes with 161 and 644 kilometers (100 and 400 n. mi) of Cape Kennedy have been observed as early as May and as late as December, with the highest frequency during September. In the 68-year period (1899 to 1966), there were 117 hurricanes whose path (eye) came within a 644-kilometer (400-n. mi.) radius of Cape Kennedy; there were nineteen hurricanes that came within a 161-kilometer (100-n. mi.) radius of Cape Kennedy during this period. From all available wind records along the coast from Melbourne, Florida, to Titusville, Florida, the highest wind gust during the passage of sixteen of the nineteen hurricanes that came within a 161-kilometer (100-n. mi.) radius of Cape Kennedy were obtained. For the three hurricanes for the years 1899, 1906, and 1925, the peak gusts were not available. Of the sixteen hurricanes that came within a 161-kilometer (100-n. mi.) radius of Cape Kennedy for which the wind records are available, five produced wind gusts greater than 33. 5 m/sec (65 knots),[2] ten produced wind gusts to 26 m/sec (50 knots), and twelve had wind gusts less than 18. 5 m/sec (36 knots). Thus, from these records, even if a defined hurricane path comes within a 161-kilometer (100-n. mi.) radius of Cape Kennedy, hurricane force winds [speeds > 33 m/sec (64 knots)] are not always observed at Cape Kennedy. Hurricanes at greater distances than 161 kilometers (100 n. mi.) could possibly produce hurricane force winds at Cape Kennedy. It is recognized that hurricanes approaching Cape Kennedy from the east (from the sea) will, in general, produce higher winds at Cape Kennedy than those approaching the Cape after crossing the peninsula of Florida (from land).

18. 3. 1 Distribution of Hurricane and Tropical Storm Frequencies

Knowing the mean number of tropical storms or hurricanes (events) per year that come within a given radius of Cape Kennedy, without knowing other information, is of little use. If the distribution of the number of tropical storms or hurricanes is known to be a Poisson distribution, then the mean number of events per year (or any reference period) can be used to completely define the Poisson distribution function.

From Figure 18. 1, the probability of no event, $P(E_0, r)$, for the following can be read: (1) tropical cyclones, tropical storms, and hurricanes for annual reference periods; and (2) tropical storms and hurricanes for

---

2. Highest recorded Cape Kennedy hurricane-associated wind speed was about 39 m/sec (76 knots).

TABLE 18. 3 NUMBER OF HURRICANES IN A 68-yr PERIOD (1899-1966) WITHIN A 161- AND 644-km (100- and 400-n. mi.) RADIUS OF CAPE KENNEDY

Month	Number of Hurricanes Within: 161-km (100-n. mi.) radius	644-km (400-n. mi.) radius
Jan.	0	0
Feb.	0	0
Mar.	0	0
Apr.	0	0
May	1	1
Jun.	2	3
Jul.	2	12
Aug.	3	23
Sep.	5	42
Oct.	5	30
Nov.	0	5
Dec.	1	1
Total	19	117

TABLE 18. 4 NUMBER OF TROPICAL STORMS IN A 96-yr PERIOD (1871-1966) WITHIN A 161- AND 644-km (100- and 400-n. mi.) RADIUS OF CAPE KENNEDY

Month	Number of Tropical Storms Within: 161-km (100-n. mi.) radius	644-km (400-n. mi.) radius
Jan.	0	0
Feb.	1	1
Mar.	0	0
Apr.	0	0
May	2	4
Jun.	6	26
Jul.	6	27
Aug.	22	65
Sep.	22	101
Oct.	32	96
Nov.	1	17
Dec.	1	1
Total	93	338

July-August-September; and (3) tropical storms and hurricanes for July-August-September-October, versus radius, in kilometers, from Cape Kennedy. To obtain the probability for one or more events, $P(E_1, r)$, from Figure 18. 1, the reader is required to subtract the $P(E_0, r)$, read from the abscissa, from unity; that is, $[1 - P(E_0, r)] = P(E_1, r)$. For example, the probability that no hurricane path (eye) will come within 556 kilometers (300 n. mi.) of Cape Kennedy in a year is 0. 31, $[P(E_0, r = 300) = 0.31]$, and the probability that there will be one or more hurricanes within 556 kilometers (300 n. mi.) of Cape Kennedy in a year is 0. 69, $(1 - 0.31 = 0.69)$.

18.4 Climatological Information for Selected Geographic Locations

Climatological information pertinent to the aerospace vehicle landing operation is given in two NASA contractor reports (Refs. 18. 3 and 18. 4). Both documents follow the same format and contain for each site: (1) a short narrative description of the climate, (2) monthly and annual

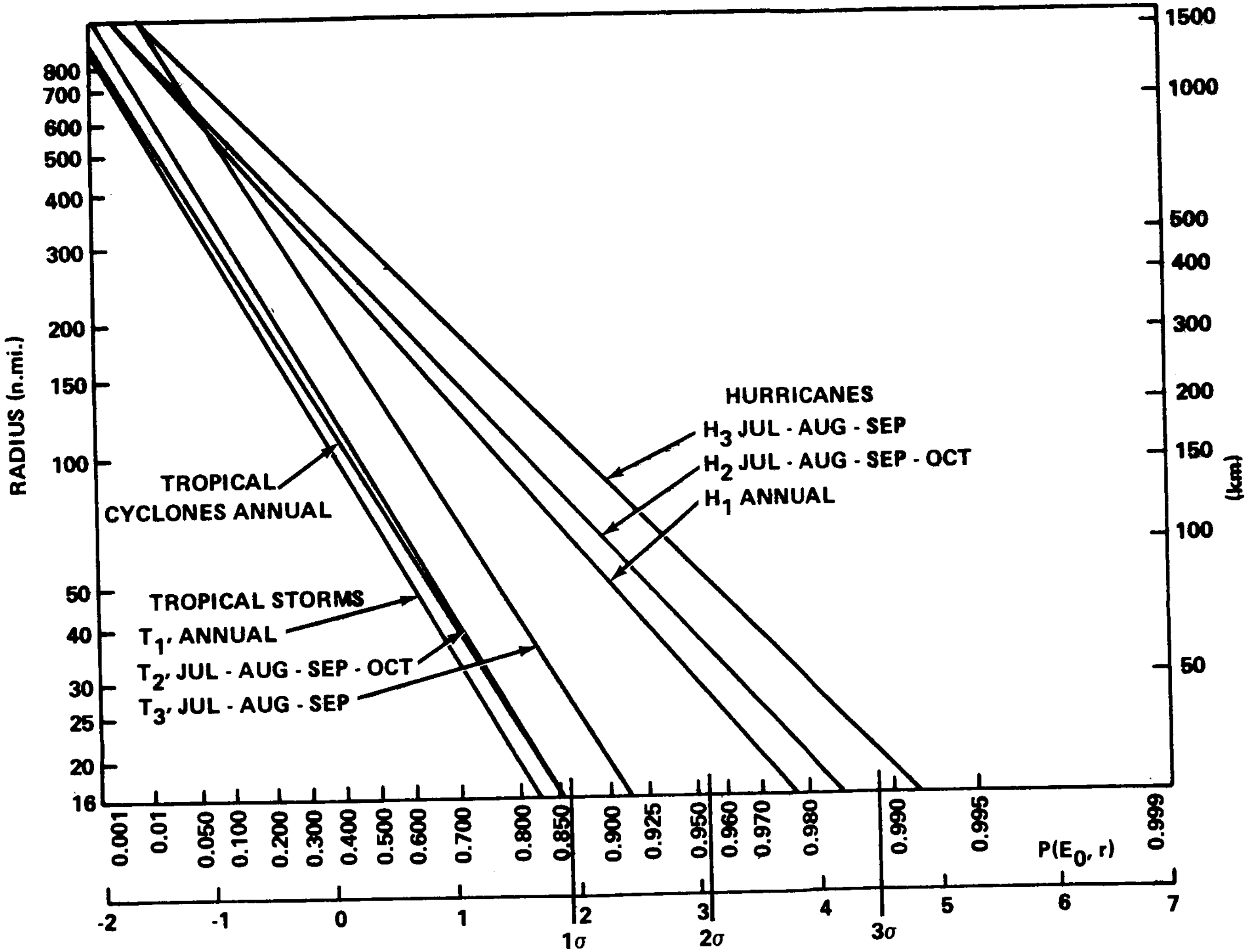

FIGURE 18.1 PROBABILITY OF NO TROPICAL CYCLONES, TROPICAL STORMS, OR HURRICANES FOR VARIOUS REFERENCE PERIODS VERSUS VARIOUS RADII FROM CAPE KENNEDY

temperature and precipitation summaries, (3) percentage frequency of occurrence of specified weather conditions for monthly and annual reference periods (the weather conditions, ceiling and visibility, thunderstorms, precipitation, fog, and other obstructions to vision are given for 3-hour periods to show the diurnal changes and for all hours combined), and (4) ground winds for monthly and annual reference periods. These data give the percentage frequency of occurrence of wind speed versus wind direction.

NASA CR-61319 contains data for nine foreign and three United States sites, while NASA CR-61342 contains twenty United States (two in Alaska) locations, as follows:

NASA CR-61319

Edward AFB, California
Langley AFB, Virginia
Patrick AFB, Florida
Moron, Argentina
Moron De LaFrontera, Spain
Ambala, India
Dhahran, Saudi Arabia
Bloemfontein, South Africa
Reggan, Algeria
Alice Springs, Australia
Honolulu, Hawaii

NASA CR-61342

Eielson AFB, Fairbanks, Alaska
Elmendorf AFB, Anchorage, Alaska
Castle AFB, Merced, California
Vandenberg AFB, Santa Maria, California
McCoy AFB, Orlando, Florida
Columbus AFB, Columbus, Mississippi
Whiteman AFB, Knob Noster, Missouri
Cherry Point MCAS, Havelock, North Carolina
Seymour-Johnson AFB, Goldsboro, North Carolina
Holloman AFB, Alamogordo, New Mexico
McGuire AFB, Wrightstown, New Jersey
Shaw AFB, Sumter, South Carolina
Ellsworth AFB, Rapid City, South Dakota
Bergstrom AFB, Austin, Texas

NASA CR-61342 (Continued)

Biggs AFB, El Paso, Texas
Carswell AFB, Ft. Worth, Texas
Dyess AFB, Abilene, Texas
Ellington AFB, Houston, Texas
Kelly AFB, San Antonio, Texas
Sheppard AFB, Wichita Falls, Texas

18.5 Water Entry and Recovery

Design for water entry, recovery, and transportation of reusable space vehicles, such as the proposed space shuttle booster requires information on the sea state envrionment.

18.5.1 Design Values

Natural environment design information for use in water entry and recovery studies for operation in the Cape Kennedy, Florida Atlantic coastal waters and/or the Vandenberg AFB, California coastal waters — the areas bounded by 27-31° North latitude, 75-80° West longitude and 30°-35° North latitude, 118°-125° West longitude are given in this section.

Along some areas of the Florida coast the water depth increases slowly to ≧ 36m at approximately 90 km offshore. Beyond 120 km the water is deeper than 183m except for the shallow areas near the Bahama Islands. Off California the ocean depth increases quickly to ≧ 183m at about 20 km. The only shallow water is found near islands. Data for other areas are available upon request. Design values are given for

Mean Wind Speed profile 1 km to 10 m.
Wave height
Wave period
Wave slope
Air and water temperatures
Salinity
Current

Air and sea temperatures, water salinity, and current remain constant for all phases of vehicle retrieval activity, but vary according to the location. Values for wave height, wave period, and wave slope vary with the vehicle activity but not with the location. The wind profiles have different values for each location but apply only to the water entry phase.

Design of the vehicle should provide adequate protection for the following environments without detrimental effects on subsequent vehicle operations.

		Cape Kennedy Recovery Area	Vandenberg AFB Recovery Area
Sea Temperatures:	High	= 28°C (83°F)	18°C (65°F)
	Low	= 22°C (72°F)	14°C (57°F)
Air Temperatures:	High	= 36°C (97°F)	29°C (84°F)
	Low	= 5°C (41°F)	4°C (40°F)
Salinity:	Mean annual maximum	= 36%	34%

Vehicle design values should be selected from those tabulated below to conform to the final design philosophy.

18.5.1 Water Entry and Afloat

A. Water Entry — 95 Percentile Values

1.

Criterion	Worst Month	Annual
Sea State Code	5	5
Wave height H 1/3	3.7 m (12.1 ft)	2.9 m (9.4 ft)
Wave height H 1/10	5.1 m (16.7 ft)	3.6 m (12.0 ft)
Wave period	7 sec	6 sec
Wave length	51 m	37 m
Steady state wind 1 km	19 m sec^{-1}	15 m sec^{-1}
150 m	19 m sec^{-1}	15 m sec^{-1}
10 m	11.2 m sec^{-1}	9.5 m sec^{-1}

2.* Conditional Steady-state wind speed profiles at several risk levels - Annual Reference Period.

Altitude	R = 0.5%	R = 1.0%	R = 2.0%	R = 3.0%	R = 4.0%
1 km	18.0	17.3	16.2	15.2	14.6
150 m	18.0	17.3	16.2	15.2	14.6
10 m	10.8	10.5	10.0	9.6	9.3

*Conditionalized against the Cape Kennedy 1 km winds being ≤ the design 95% ascent wind speed of 19 m sec^{-1}.

3. Wave Slope (Θ) — calculated along the wind direction for a fully aroused sea. Applies to both worst month and annual reference period.

Sea State	Risk Level 10%	5%	1%
Code 5 - H 1/3 = 2.5 to 3.7 m	± 11°	± 13°	± 17°
Code 4 - H 1/3 = 1.3 to 2.4 m	± 9°	± 11°	± 15°
Code 3 - H 1/3 = 0.7 to 1.2 m	± 8°	± 9°	± 12°

B. Afloat — wave heights based on 48-hour exposure in a sea state characterized by specified H 1/3

H 1/3	48-Hour Exposure Wave Height 5% Risk	1% Risk
3.7 m (worst month 95%)	9.5 m	10.0 m
2.9 m (annual 95%)	7.4 m	7.9 m
1.6 m (worst month 50%)	4.2 m	4.4 m
1.2 m (annual 50%)	3.2 m	3.4 m
Wave period range	3 - 14 sec	
Wave length range	9 - 204 m	

18.5.2 Secure and Towback Recovery

	72-Hour Exposure Wave Height 5% Risk	1% Risk
H 1/3 = 2.4 m	6.2 m	6.4 m
H 1/3 = 1.8 m	4.7 m	5.1 m

Wave heights are based on 72-hour exposure at mid-point (H 1/3 = 1.8 m) and top (H 1/3 = 2.4 m) of sea state code 4 range.

Wave period range	4 - 12 sec
Wave length range	17 - 150 m

Surface current statistics for recovery areas:

Percentiles in m sec^{-1}	95	99	Direction (from)
Cape Kennedy	2.3	2.8	S
Vandenberg AFB	0.6	1.1	N-NNW

18.5.3 Ocean Wave Spectra

A. Introduction

This ocean wave spectral model is to be used for water entry and retrieval analyses associated with reusable space vehicle design and operations studies. Developed by Pierson and Moskowitz (reference 18.5) is valid for a fully-developed sea and should be considered as preliminary, to be used in lieu of an ocean wave spectral model which possesses the properties of the waves off the Florida coast (27° N-31° N; 75° - 80° W) and the California coast (30° N-35° N; 118° W - 125° W). A fully-developed sea is defined as one in which (1) all the Fourier components of the ocean which can be excited by wind stresses have attained their maximum amplitude, (2) the waves are in equilibrium with the wind turbulence which produces the stresses, and (3) the state of the sea is uniquely specified by the wind at some reference level (the 10-meter level, say). To attain these conditions a wind must blow for a sufficiently long time duration over a sufficiently long fetch.

Wave energy radiates outward from the region of the ocean in which the wind waves are generated and this radiated energy is called swell. Swell transports wave energy from one region of the ocean to other regions, so that it is possible to have locally produced wind waves and swell to coexist. To develop a spectral model of ocean waves for a particular part of the ocean the total ocean must be taken into account. This results because there are contributions to wave energy at a point from swell and local wind wave generation processes. Studies are now being conducted at the MSFC to develop wave spectrum for a fully-developed sea is to be used for vehicle design and operations studies in the areas off the Florida coast 27° -31° N latitude; 75° -80° W longitude° and California coast (30° N latitude; 118° - 125° W longitude).

B. Wind Wave Frequency Spectrum for "Fully-Developed" Sea

According to Pierson and Moskowitz reference 18.5 the frequency power spectrum $\Phi(\omega)$ of wind wave height at a point on the ocean for a "fully-developed" sea is given by

$$\Phi(\omega) = \alpha \frac{g^2}{\omega^5} \exp\left[-\beta\left(\frac{g}{U_o \omega}\right)^4\right], \quad 0<\omega<\infty \qquad (18.5)$$

where ω is radian frequency (radian sec^{-1}), g (=9.8m sec^{-2}) is the acceleration of gravity, U_o is the mean wind at 19.5 meter reference level and α and β are nondimensional universal constants with the following values:

$$\alpha = 8.10 \quad 10^{-3}$$

$$\beta = 0.74 \qquad (18.6)$$

The units of this spectrum are $m^2/(\text{rad sec}^{-1})$ and integration over the interval of $0 < \omega < \infty$ will yield the variance of wave height, namely,

$$\sigma^2 = \alpha \frac{U_o^4}{4\beta g^2} \qquad (18.7)$$

To a sufficient degree of approximation the sea wave height can be assumed to be a Gaussian process. In this case the variance and the significant wave height are connected through the formula

$$\overline{H}^2_{1/3} = 16\,\sigma^2 \qquad (18.8)$$

Thus, combination of equations 18.7 and 18.8 yields

$$\overline{H}_{1/3} = 4\left(\frac{\alpha\, U_o^4}{4\beta g^2}\right)^{1/2} = 0.0214 U_o^2 \qquad (18.9)$$

where U_o and $\overline{H}_{1/3}$ have mks units. Eq (18.7) states that specification of $\overline{H}_{1/3}$ implies a value of a wind speed U_o required to produce a "fully-developed sea which possesses the specified value of $\overline{H}_{1/3}$. The wind speeds that actually occurred with the design of operational values of $\overline{H}_{1/3}$ are not necessarily the wind speeds in the context of equation (18.7). The actual sea state associated with the design value of $\overline{H}_{1/3}$ was probably produced by a mixture of swell and locally generated wind waves. In addition, a variety of combinations of swell and locally produced wind waves could occur to produce the same value of $\overline{H}_{1/3}$. This means that an ensemble of wave height spectra can be associated with a given value of $\overline{H}_{1/3}$. It is for these reasons we shall call U_o the effective wind speed and it is that wind speed required to produce a spectrum for a "fully-developed" sea with a prescribed value of $\overline{H}_{1/3}$. The wave spectrum given by (1) can thus be interpreted as being that associated with an ensemble of sea states in which the wave energy is the result of only local wind generation mechanisms in the absence of wave energy import and export via swell. Nevertheless, this particular spectrum possesses many characteristics of ocean waves and is suitable for design analyses and operations studies.

C. Wind Wave Frequency - Wave Number Spectrum for "Fully-Developed" Sea

Wind waves have horizontal variations in addition to temporal variations. To account for the horizontal variation of wind waves one must introduce the frequency wave number spectrum. To do this we define the frequency-direction of propagation spectrum. This spectrum is given by

$$\Phi(\omega,\theta) = \begin{cases} \Phi(\omega)\,\dfrac{2}{\pi}\cos^2\theta\,; & \begin{cases} 0<\omega<\infty \\ -\dfrac{\pi}{2}<\theta<\dfrac{\pi}{2} \end{cases} \\ 0\,;\ \text{otherwise} & \end{cases} \qquad (18.10)$$

The quantity θ is the angle between the wave number vector and the direction of the wind at the reference level. Thus,

$$\kappa_x = \eta\cos\theta,\ \kappa_y = \eta\sin\theta, \qquad (18.11)$$

where κ_x and κ_y denote the x- and y- directed wave numbers of a Fourier component and

$$\kappa^2 = \kappa_x^2 + \kappa_y^2 \qquad (18.12)$$

The coordinate system is aligned such that the positive x direction is in the direction of the wind. Integration of $\Phi(\omega, \theta)$ over the domain $-\frac{\pi}{2} < \theta < \frac{\pi}{2}$ yields the wave frequency spectrum $\Phi(\omega)$. To a reasonable degree of approximation the frequency ω and the magnitude of the wave number vector are connected through the gravity wave dispersion relation for deep water waves, namely

$$\omega = (g\kappa)^{\frac{1}{2}} \qquad (18.13)$$

Thus, the wave number spectrum $\Psi(\kappa_x, \kappa_y)$ can be obtained from $\Phi(\kappa_x, \kappa_y)$ through the transformation

$$\Psi(\kappa_x \kappa_y) = \frac{\sqrt{g}}{2}(\kappa_x^2 + \kappa_y^2)^{-3/4} \quad \Phi\left[\sqrt{g}(\kappa_x^2 + \kappa_y^2)^{-1/4}, \tan^{-1}\frac{\kappa_y}{\kappa_x}\right] \qquad (18.14)$$

The frequency wave number spectrum $\Psi \; \kappa_x, \kappa_y$ through the equation

$$\Psi(\kappa_x', \kappa_y', \omega) = \Psi(\kappa_x', \kappa_y') \; \delta(\omega' - \omega) \qquad (18.15)$$

where $\delta(\omega' - \omega)$ is the Dirac delta function. This equation states that there are contributions from those Fourier components with wave numbers κ_x' and κ_y' only at frequency $\omega = \omega'$. This is a direct consequence of the fact that the magnitude κ of the wave number vector and the frequency ω are connected through a dispersion relation (see Eq (18.11)).

18.5.4 Application

In view of the fact that the dispersion relation Eq (18.13) exists, the two forms of the wave spectrum Eqs (18.10) and (18.14) are equivalent. The selection of one to use in an engineering problem will depend on the specific application. However, it would appear that three types of problems should be considered for space vehicle operations, namely

1. Vehicle impact loads

2. Response of a freely floating vehicle to ocean waves

3. Response of a vehicle to ocean waves during towing operations.

The criteria for problem one appears to be straight forward. It would seem that all that is needed is the wave slope encountered by a space vehicle on impact with the ocean.

In problems two and three spectral inputs in all likelihood would be required to calculate vehicle responses to ocean waves. In problem two the designer should account for a sufficient number of orientations of a vehicle relative to the wind direction for the prescribed value of significant wave height for the freely floating case. In problem three the designer must transform the spectrum into a spectrum of the ocean waves along a specified straight line in (x, y, t)-space. This would correspond to the given straight line course. Here again the designer should account for a sufficient number of towing directions relative to the wind direction in order to determine the maximum response to ocean waves for the prescribed value of significant wave height for towing operations. Details for this transformation are given in reference 18.6.

18.5.5 Trade-off Studies

One reusable space shuttle vehicle configuration being studied consists of a booster which after lifting the orbiter to approximately 70 km will drop into the sea to be recovered. This entails perhaps three very complex operations - first the impact, then the recovery, and finally the transportation - all of which must be concluded successfully if the booster is to survive. While all operations will undoubtedly be constrained to some degree by the natural environment, it appears that problems associated with the recovery and transportation may be more sensitive to the sea state than will the impact. An acceptable sea state design criteria should take into consideration the recovery and transportation operations as well as the impact conditions. In this situation the recovery/transportation may be the greatest contributor to launch delay if a constraint is placed on launch for acceptable retrieval sea states to exist.

While a decision on the shuttle booster and the engineering details of a proposed water entry and recovery are still undecided it is clear that certain natural environment criteria will be required for design analyses. From present indications it appears that the parameters having the greatest effect upon the entry and recovery operations are wind speed, wave slope, and wave height. In deep water the wave characteristics (sea states) are determined not only by the mean wind speed but also by the fetch (the distance over which it blows) and duration of the wind over the open water. A sea state is generally described by significant wave height which is the average height of the 1/3 highest waves. Of course higher waves exist in any given sea state. For example, from the relationship between wind speed and wave height for a fully arisen sea, as shown in Figure 18.2, it can be seen that in a code 3 sea state with significant wave heights ~1.2 meters, 10% of the waves will average about 1.5m. In other words a wind speed of 8.2 ms^{-1} (fetch and duration unlimited) will produce a sea with the highest 1/3 waves averaging about 1.2m and the highest 1/10 waves averaging about 1.5m.

Figure 18.2 shows the distribution of wave heights versus wind speed at any given instant - information applicable to vehicle water entry. For all other operations (afloat, secure, towback recovery) where some considerable time interval is involved the exposure period concept must be considered. That is, the longer the exposure period the greater the probability of encountering a larger wave. Wave heights at the 1% risk level for exposure periods from 1 to 80 hours in sea state codes 4 and 5 are shown in Figure 18.3. From Figure 18.3, for example, it can be seen that exposure for 1 hour in sea state code 4 entails a 1% risk of encountering at least one wave >4.3m. If the exposure time is increased to 48 hours in the same sea state code 4 condition then the wave height at the 1% risk level becomes 5m.

The foregoing paragraphs dealt with general sea state relationships valid in any deep-water area. This section will present empirical data applicable to the Cape Kennedy, Florida and Vandenberg AFB, California recovery areas. It is emphasized that the following tables (except wind profiles) were generated from observations of significant (average height of the 1/3 highest waves) waves without regard to fetch or duration. In any given sea state there will always be waves higher than the significant heights. Also, exposure time increases the chances of higher waves occurring.

Tables 18.4 through 18.9, developed from reference 18.12, may prove useful in design trade-off studies. From Table 18.4 there is a 3 percent risk of exceeding sea state code 5 and a 68 percent risk of exceeding sea state code 3 in February. Also in February there is a 95 percent chance that the significant wave height will be ≤ 3.7 m and conversely a 5 percent chance that it will exceed 3.7 m. On an annual basis the 95th percentile wave height is 2.9 m in the Cape Kennedy recovery area versus 2.8 m in the Vandenberg AFB recovery area. While the annual $H_{1/3}$ values are very similar some monthly distributions show considerable differences. In general the Cape Kennedy area shows greater seasonal variation and consequently a more severe environment.

The wave slopes shown in Table 18.5, Table 18.7, and those given in Section 18.5.1 were calculated along the wind direction after assuming a gaussian distribution in a fully aroused sea. For the slopes in Section 18.5.1 only the indicated range of $H_{1/3}$ was used while the slopes of Tables 18.5 and 18.7 were calculated from the entire distribution of $H_{1/3}$. The 5% risk slopes from the tables are generally smaller than those of Section 18.5.1 because of the different distributions of $H_{1/3}$ — many more low values being used in the tables calculations.

From Table 18.8 it can be concluded that the heavier sea states are generally of short duration — sea state code 4 lasting on the average only one day.

The steady-state wind speed profiles given in Section 18.5.1.A.2, while based on the annual reference period for Cape Kennedy, are conditionalized against the Space Shuttle ascent wind at 1 km. That is, wind speeds greater than the design ascent wind speed of 19 m s^{-1} were removed from the statistics from which these profiles were developed. The rationale for this procedure is based; first, on a high correlation between winds aloft in the launch and recovery areas and; second, the assumption that the Space Shuttle will not be launched when the winds aloft exceed the design ascent wind speed.

Other steady-state wind speeds and profiles at several risk levels based on the windiest month and annual reference periods are shown in Table 18.10 and Figures 18.4 and 18.5. These "unconditional" winds are somewhat stronger than the conditional values described above because all of the higher speeds are included in the statistics. Since calms or very light winds may also be unfavorable for water entry the 5% lightest winds are shown for both locations under the 5 percentile columns in Table 18.10. These values indicate that 5% of the wind speeds in the lightest wind month and on an annual basis are $\leq 1 ms^{-1}$. At the other end of the table from the 95 percentile columns it can be seen that in the Cape Kennedy recovery area 95% of the wind speeds during the windiest month are $\leq 19\ ms^{-1}$ while during the annual reference period 95% of the wind speeds are $\leq 15\ ms^{-1}$. By turning these values into risk statements; "There is a 5% risk that the speed will > $19\ ms^{-1}$." "There is a 5% risk that the speed will > $15\ ms^{-1}$" the effect of the reference period becomes more apparent.

The steady-state wind speed profiles, Figures 18.4 and 18.5, were constructed as follows:

(1) for altitudes from 1000m to 150m the wind speed remains constant

(2) For altitudes below 150m the wind speed is calculated from

$$\bar{u}_z = \bar{u}_{150m} \left(\frac{z}{150m}\right)^p \qquad (18.16)$$

$$\text{where } p = 0.16\left(\frac{\bar{u}_{150m}}{14ms^{-1}}\right)^{1.9} \quad \text{when } \bar{u}_{150m} \leqq 14ms^{-1} \qquad (18.17)$$

$$p = 0.21\left(\frac{\bar{u}_{150m}}{21ms^{-1}}\right)^{0.67} \quad \text{when } \bar{u}_{150m} > 14ms^{-1} \qquad (18.18)$$

$\bar{u}_z$ — mean wind speed at altitude z

$\bar{u}_{150m}$ — mean wind speed at 150m altitude

z — altitude.

Steady state wind speeds at altitudes above 1 km can be found in section 5.3.5.1 and Tables 5.3.4 and 5.3.5 of this document and in NASA TM 53956, "Cape Kennedy Wind Component Statistics Monthly and Annual Reference Periods for All Flight Azimuths From 0 to 70 km Altitude." dated October 1969.

If additional information on this subject is required refer inquiries to: Chief, Aerospace Environment Division, Marshall Space Flight Center, Alabama.

An excellent text on wave formation is given in reference 18.9. References 18. 8, 18.10, and 18.12 are primarily sources of data on wave height, length, period, etc. These documents also contain graphs showing the relationships among mean wind speed, fetch, duration, wave height, wave period, and wave length. The alternative to providing a vehicle water landing and retrieval capability to meet the above recommended design conditions is either acceptance of an increased launch delay constraint or increased risk of vehicle loss during water entry or retrieval operations. The acceptance of these added constraints (risks) should be thoroughly assessed prior to finalization of a design configuration.

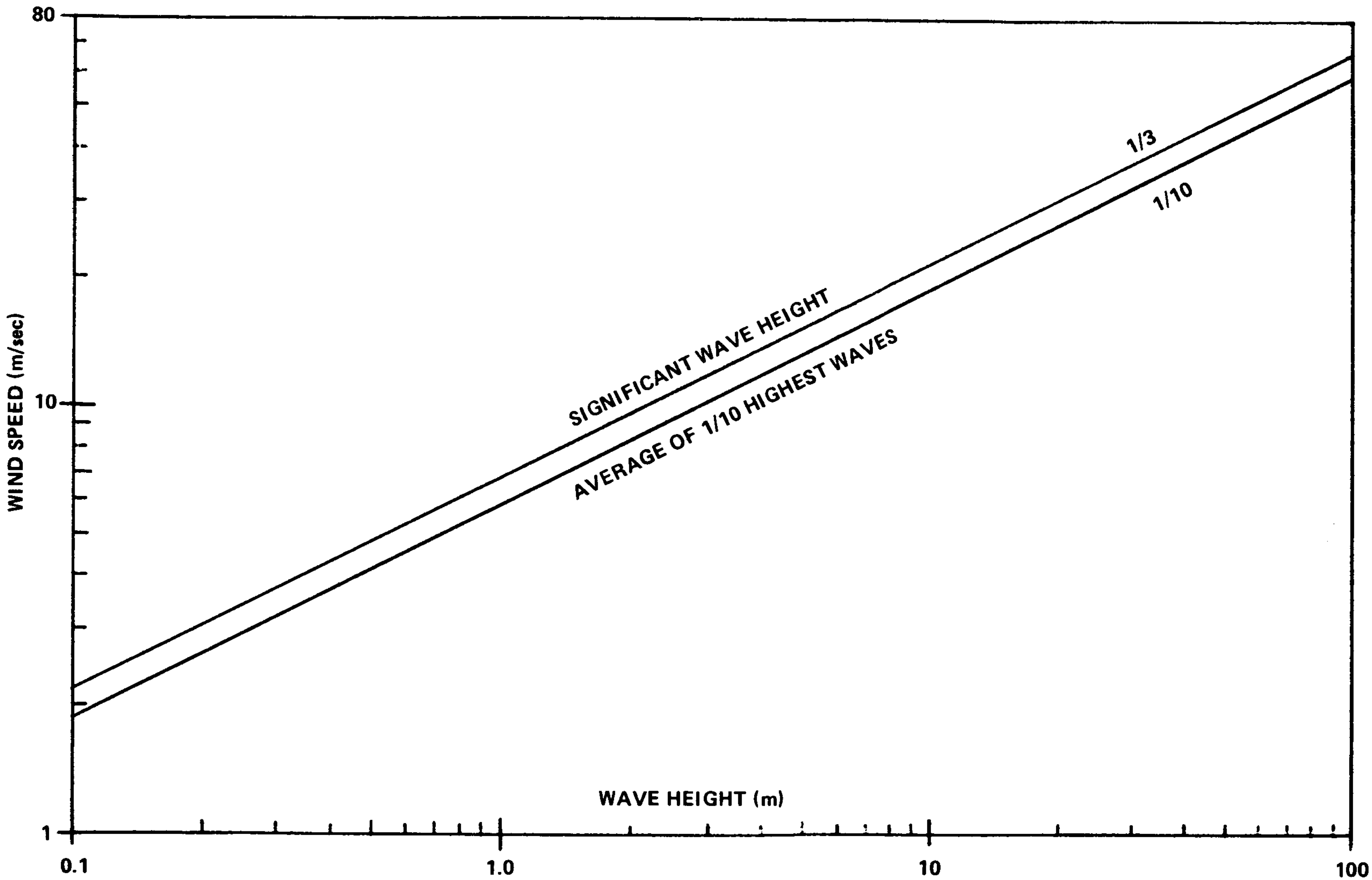

Figure 18.2 Relationship between wave height and wind speed in a fully arisen sea

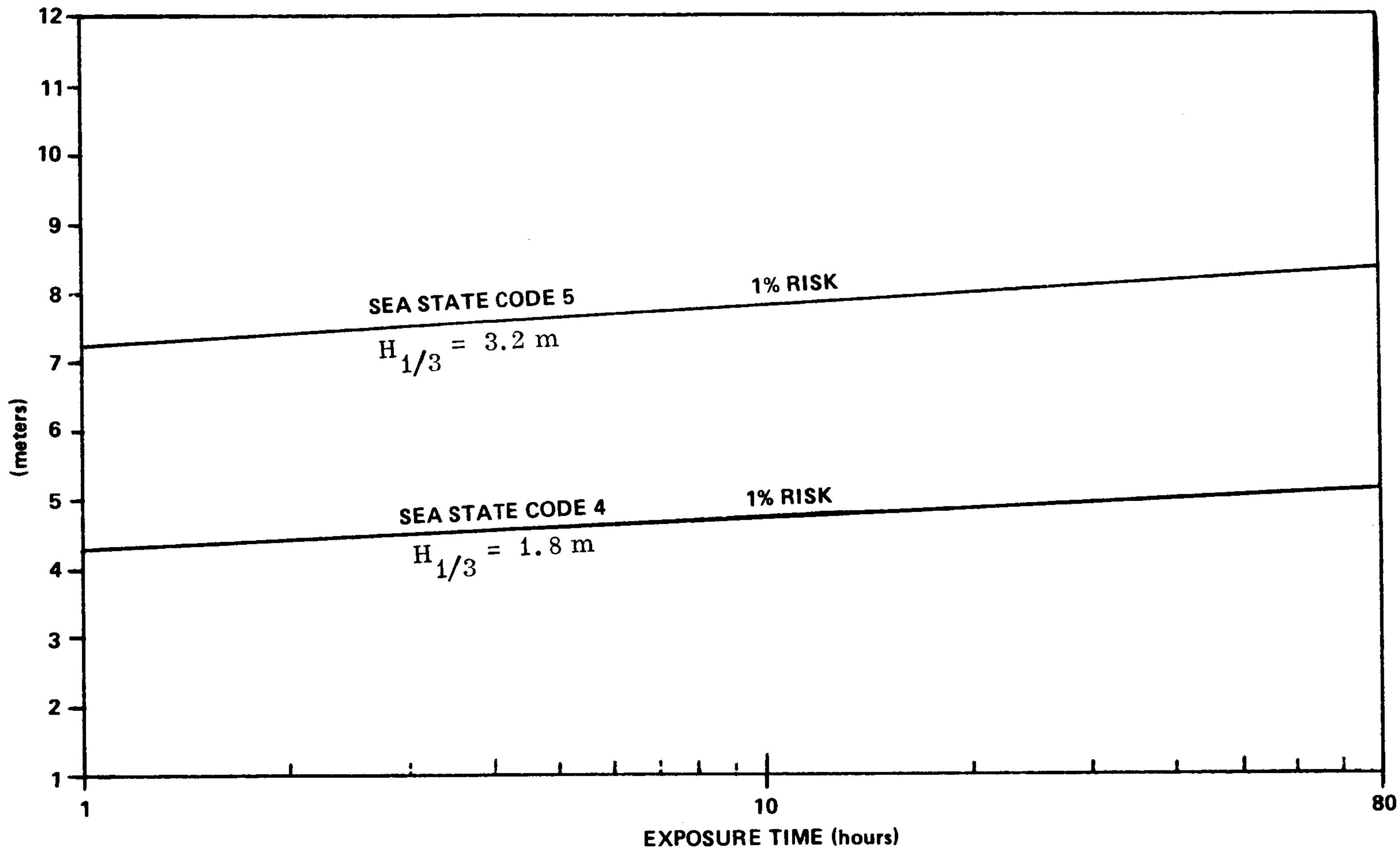

Figure 18.3 One percent risk wave height vs exposure time (assuming sea state category remains unchanged for duration of exposure period)

TABLE 18.4 Cape Kennedy Recovery Area Sea States
(27° N-31° N) (75°-80° W)

Significant Wave Heights Avg. 1/3 Highest (m)	(ft)	Sea State Codes	Percent Probability of Exceeding Indicated Heights J	F	M	A	M	J	J	A	S	O	N	D	A
0.6	2	2	86	90	84	87	68	70	68	58	82	82	84	84	80
1.2	4	3	60	68	54	50	27	35	30	22	55	58	56	56	50
2.4	8	4	14	20	10	8	5	6	3	2	15	12	13	10	9
4.0	13	5	2	3	1	0.5	0.8	0.8	0.2	0.2	2	1.8	1.2	0.8	1
6.1	20	6	0.2	0.3	0.2	<0.1	0.2	0.2	<0.1	<0.1	0.2	0.3	<0.1	<0.1	0.1
PERCENTILES															
50th (meters)			1.4	1.6	1.4	1.2	0.8	0.9	0.8	0.7	1.3	1.4	1.4	1.4	1.2
95th (meters)			3.3	3.7	2.8	2.7	2.4	2.6	2.2	2.1	3.3	3.2	3.0	2.8	2.9

TABLE 18.5 Cape Kennedy Recovery Area Wave Slopes
(Calculated from Significant Wave Heights)

Risk of Exceeding	J	F	M	A	M	J	J	A	S	O	N	D	A
5%	14°	15°	15°	14°	13°	13°	12°	12°	13°	14°	14°	15°	14°

TABLE 18.6 Vandenberg AFB Recovery Area Sea States
(30° N-35° N; 118° W-125° W)

Significant Wave Heights Avg. 1/3 Highest (m)	(ft)	Sea State Codes	Percent Probability of Exceeding Indicated Heights J	F	M	A	M	J	J	A	S	O	N	D	A
0.6	2	2	74	67	76	78	82	82	81	83	77	58	69	74	76
1.2	4	3	42	38	45	49	50	51	47	45	44	37	34	49	44
2.4	8	4	9	9	10	11	10	9	5	6	6	5	4	13	8
4.0	13	5	1.4	1	1.8	1.8	1.2	0.4	0.2	0.1	0.4	0.4	0.5	3	1
6.1	20	6	<0.1	<0.1	<0.1	<0.1	<0.1	<0.1	<0.1	<0.1	<0.1	<0.1	<0.1	<0.5	<0.1
PERCENTILE															
50th (meters)			1.0	0.9	1.1	1.2	1.2	1.2	1.1	1.1	1.1	0.7	0.9	1.2	1.1
90th (meters)			2.9	3.2	3.2	3.0	3.2	2.8	2.4	2.5	2.6	2.4	2.4	3.5	2.8

TABLE 18.7 Vandenberg AFB Recovery Area Wave Slopes (Calculated from Significant Wave Heights)

Risk of Exceeding	J	F	M	A	M	J	J	A	S	O	N	D	A
5%	10°	10°	10°	10°	11°	11°	10°	10°	10°	10°	10°	11°	10°

TABLE 18.8 Cape Kennedy Recovery Area Sea State Duration (Tentative)

Sea State Code	Mean (50%) Time of Duration in Days											
	J	F	M	A	M	J	J	A	S	O	N	D
≧3	3	3	2	2	1	<1	<1	<1	1	1	2	3
≧4	1	1	<1	<1	<1	<1	<1	<1	<1	<1	<1	1
≧5	1	1	<1	<1	<1	<1	<1	<1	<1	<1	<1	1

TABLE 18.9 Vandenberg AFB Recovery Area Sea State Duration (Tentative)

Sea State Code	Mean (50%) Time of Duration in Days											
	J	F	M	A	M	J	J	A	S	O	N	D
	1	1	2	3	3	3	2	2	2	2	1	1
	<1	<1	1	1	1	1	1	1	1	1	<1	<1
	<1	<1	1	1	1	1	1	1	1	1	<1	<1

Table 18.10 Space Shuttle Booster Recovery Area Wind Speeds (ms^{-1}) at 150m Altitude

Cape Kennedy, Florida Recovery Area							
95 Percentile		90 Percentile		50 Percentile		5 Percentile	
W	A	W	A	W	A	L	A
19	15	16	12	8	6	1	1

Vandenberg AFB, California Recovery Area							
95 Percentile		90 Percentile		50 Percentile		5 Percentile	
W	A	W	A	W	A	L	A
15	13	13	11	6	5	1	1

All wind speeds are in meters per second
W - windiest month reference period
A - annual reference period
L - lightest wind month reference period

Profiles below 150m are calculated from

$$\bar{u}_z = \bar{u}_{150m}\left(\frac{z}{150m}\right)^p \qquad p = 0.16\left(\frac{\bar{u}_{150m}}{14ms^{-1}}\right)^{1.9} \text{ when } \bar{u}_{150m} \leq 14ms^{-1}$$

$$p = 0.21\left(\frac{\bar{u}_{150m}}{21ms^{-1}}\right)^{0.67} \text{ when } \bar{u}_{150m} > 14ms^{-1}$$

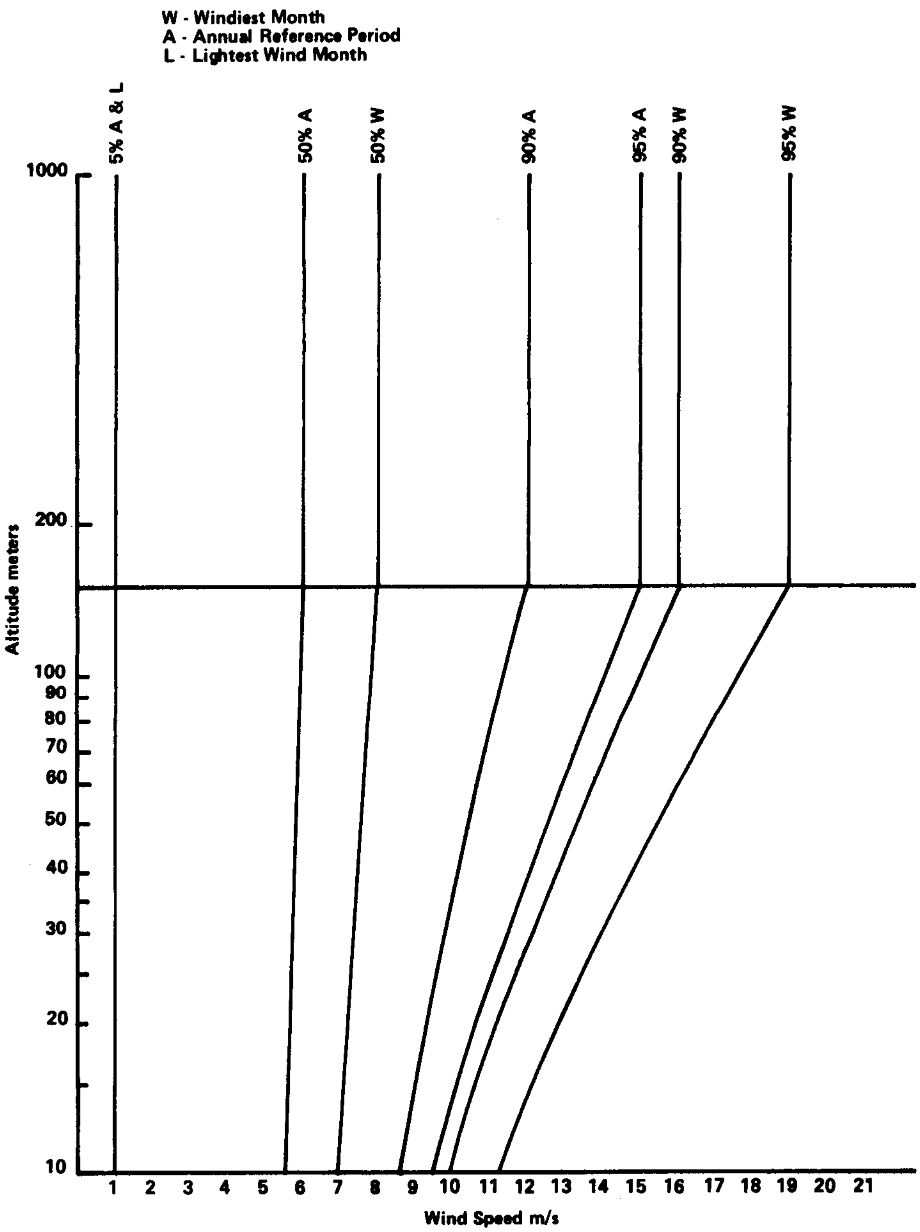

Figure 18.4 Steady state wind speed over water profiles
Cape Kennedy shuttle booster recovery area.

Profiles below 150m are calculated from

$$\bar{u}_z = \bar{u}_{150}\left(\frac{z}{150}\right)^p \qquad p = 0.16\left(\frac{\bar{u}_{150m}}{14ms^{-1}}\right)^{1.9} \text{ when } \bar{u}_{150m} \leqslant 14ms^{-1}$$

$$p = 0.21\left(\frac{\bar{u}_{150m}}{21ms^{-1}}\right)^{0.67} \text{ when } \bar{u}_{150m} > 14ms^{-1}$$

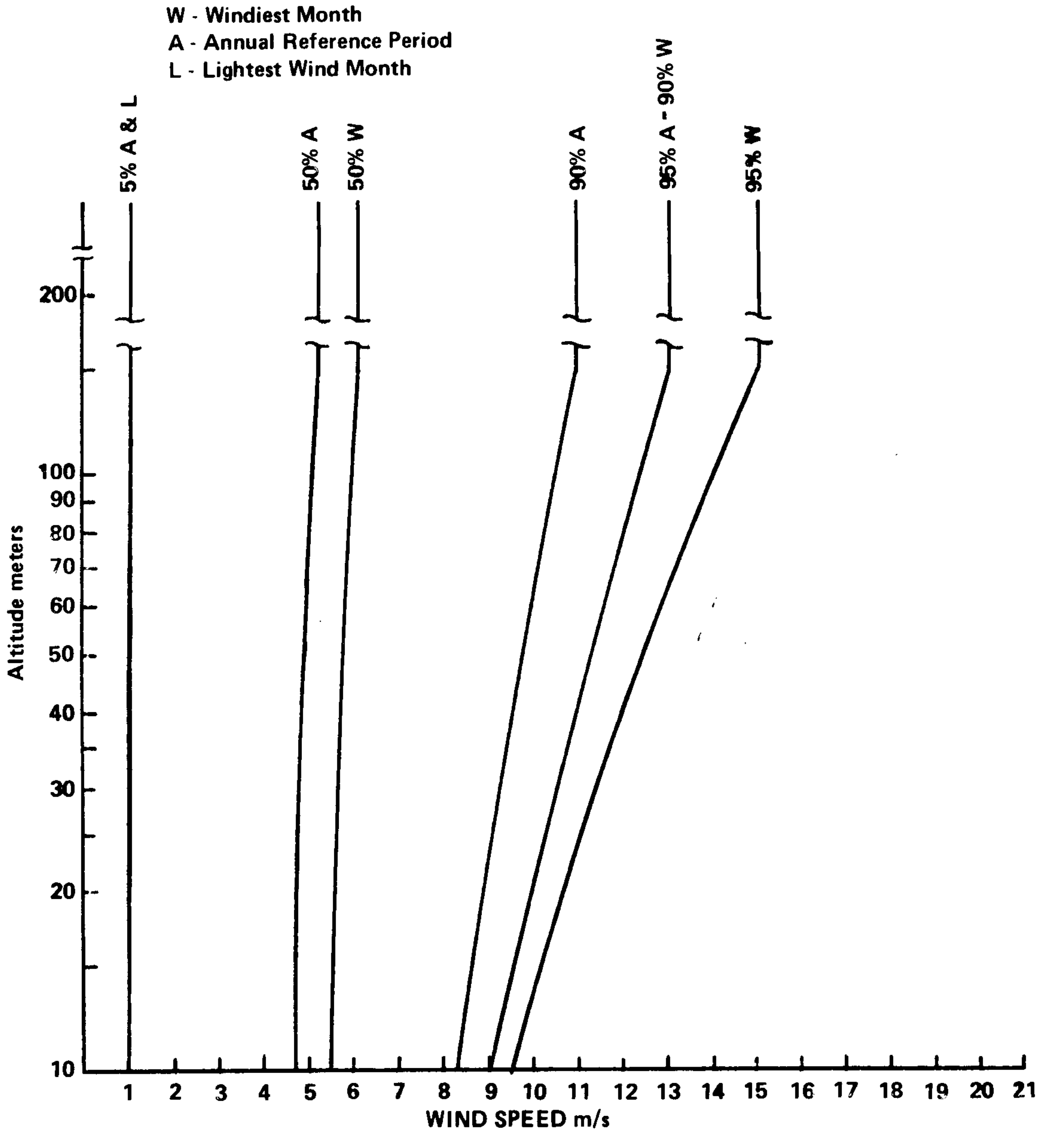

Figure 18.5 Over water steady-state wind speed profiles Vandenberg Air Force Base shuttle booster recovery area.

REFERENCES

18.1 Daniels, Glenn E., "Terrestrial Environment (Climatic) Criteria Guidelines for Use in Space Vehicle Development, 1969 Revision, NASA TM X-53872, NASA-George C. Marshall Space Flight Center, Marshall Space Flight Center, Alabama, 1970, Second Printing, Mar. 15, 1970.

18.2 Thom, H. C. S., "Tornado Probabilities, "Monthly Weather Review, vol. 91, nos. 10-12, Oct.-Dec. 1963, pp 730-736.

18.3 Lee, Russel F.; Goodge, Grant W.; and Crutcher, H. L., "Surface Climatological Information for Twelve Selected Stations for Reentry Vehicles," NASA CR-61319, Marshall Space Flight Center, Alabama, 1970.

18.4 Goodge, G. W.; Bilton, T. H.; and Wuinlin, F. T., "Surface Climatological Information for Twenty Selected Stations for Reentry Vehicles," NASA CR-61342, Marshall Space Flight Center, Alabama, 1971.

18.5 Pierson, W. J. and L. Moskowitz, 1964: A Proposed Spectral Form for Fully Developed Wind Seas Based on the Sinclarity Theory S. A. Kitaigorodshii. Journal of Geophysical Research, 69, 5181-5190.

18.6 St. Dennis, M. and W. J. Pierson, 1953: On the Motions of Ships in Confused Seas. Transactions of the Society of Naval Architects and Marine Engineers, 61, 280-357.

18.7 Smithsonian Meteorological Tables, Smithsonian Institution, Washington, D. C. 1966.

18.8 U. S. Army Coastal Engineering Research Center, "Shore Protection, Planning and Design" Technical Report No. 4, Third Edition, Washington, D. C. 1966.

18.9 Kinsman, Blair, "Wind Waves," Dept. of Oceanography, The John Hopkins University, Prentice-Hall, Inc. Englewood Cliffs, New Jersey 1965.

18.10 U. S. Dept. of Commerce, "Climatological and Oceanographic Atlas for Mariners", Vol. 1, Washington, D. C. 1959.

18.11 Whitnah, Arthur M. and David B. Howes, 1971, "Statistics Concerning the Apollo Command Module Water Landing, Including the Probability of Occurrence of Various Impact Conditions, Successful Impace, and Body X-Axis Loads," NASA TM X-2430, November 71.

18.12 U. S. Naval Weather Service Command, "Summary of Synoptic Meteorological Observations" Vols. 4, 7, and 8, May 1970.

18.13 Pierson, Willard J. Jr., et al, "Observing and Forecasting Ocean Waves," H. O. Pub. No. 603, U. S. Navy Hydrographic Office, Washington, D. C. 1955.

18.14 Beck, Preston E., 1972: "Data on Ocean Conditions For Space Shuttle Booster Recovery Criteria," TR-1180, NASA-John F. Kennedy Space Center, Florida.

18.15 Cummings, Allen D, et al, "Concepts and Procedures Used to determine Certain Sea Wave Characteristics" NASA TN D-6961, September 1972.

18.16 Beck, Preston E., "Qualitative Investigation of Booster Recovery in Open Sea" NASA - John F. Kennedy Space Center, TR-1195, November 1972.

N74-16311

SECTION XIX. ENVIRONMENT HAZARD ESTIMATES

By

John W. Kaufman
J. Briscoe Stephens
C. Kelly Hill
Michael Susko

19.1 INTRODUCTION

With the increasing knowledge of the environmental impact of air pollution, special attention is now being placed on the emission into the atmosphere of aerospace vehicle exhaust effluents and by-products. Limited concern was placed on this problem in the past, especially because vehicles using solid rocket motors were small in size and few were tested and launched. National, state, and local air pollution laws are also becoming more stringent to prevent environmental damage which places additional restrictions on any organization or private citizen in regard to pollution of many types.

In order to determine these environmental hazards the procedure is to apply the proper atmospheric diffusion models to calculate downwind concentrations and dosages from various engine and solid rocket booster (SRB) exhaust by-products. A major effort is being made to gather detailed data on the chemical reactions that take place between the exhaust effluents and the atmosphere. While little is currently known about this problem, research is underway throughout the aerospace research community to determine initial and long term source characteristics.

This section includes statements on the basic diffusion estimation formulas. This is a summary of the salient facets of the hazardous material transport problem which is found in referenced literature. Other than normal exhaust releases and abnormal releases, brief statements will follow on leaks and inadvertent spills. Cloud rise formulas for use in source identification are included and meteorological inputs are covered. The very important issue on toxicity criteria is included in Section 19.5. When referring to the values of various maximum allowable concentration (MAC) of elements and compounds, caution must be strenuously executed in that such values are subject to change and are often different from one research study to another. Subsequently, an example diffusion calculation will follow with basic graphs as required.

19.2 BASIC HAZARD ESTIMATION FORMULAS

19.2.1 Definitions

Concentration is the mass of a pollutant per unit volume at a point in space and is referenced to the ambient atmosphere (units: parts per million, milligrams per cubic meter, etc.).

Dosage is the time-integrated concentration at a point in space and has the units of concentration multiplied by the unit of time.

19.2.2 Generalized Concentration-Dosage Model

The generalized concentration and dosage models describe the behavior of the cloud of toxic material after the cloud establishes equilibrium in the mixing layer. This equilibrium point is known as the cloud source and serves as the origin for the Cartesian coordinate system such that the x-axis is in the mean azimuth wind direction, y is the crosswind or lateral direction, and z is the vertical height above the ground. (The location of the source cloud is addressed in the next section.) It is also assumed that this is an expanding volumetric cloud about a moving reference point in a homogeneous fluid. For diagnostic and interpretation flexibility, these models are formated in a modular form (Ref. 19.1 and 19.2).

The generalized concentration model for a nearly instantaneous source is expressed as the product of five modular terms:

Concentration = {Peak Concentration Term} x {Alongwind Term} x

{Lateral Term} x {Vertical Term} x {Depletion Term};

whereas, the generalized dosage model for a nearly instantaneous source is defined by the product of four modular terms:

Dosage = {Peak Dosage Terms} x {Laterial Term}

x {Vertical Term} x {Depletion Term}

Thus, the mathematical description for the concentration and dosage models permit flexibility in application to various sources and for changing atmospheric parameters while always maintaining a rigorous mass balance.

Two obvious differences exist. First, the peak concentration term refers to the concentration at the point x, y = O, z = H and is defined by the expression

$$\text{point peak concentration} = \frac{Q}{(2\pi)^{3/2}\,\sigma_x\,\sigma_y\,\sigma_z} \tag{19.1}$$

where Q is the source strength and σ_i is the standard deviation of the concentration distribution in the i^{th} direction; whereas, the peak dosage term is given by

$$\text{point peak dosage} = \frac{Q}{2\pi\,\bar{u}\,\sigma_y\,\sigma_z} \tag{19.2}$$

where $\bar{u}$ is the mean wind speed. The second difference between these models is that the concentration contains a modular alongwind term to account for downstream temporal effects not considered in the dosage model. The alongwind term affords an exponential decay in concentration as a function of: cloud transit time, concentration distribution, and the mean wind speed.

The lateral term - which is common to both models - is another exponential decay term, and is a function of the Gaussian spreading rate and the distance laterally from the mean wind azimuth. The vertical term - again common to both models - is a rather complex decay function since it contains a multiple reflection term for the point source which stops the vertical cloud development at the top of mixing layer and eventually changes the form of the vertical concentration distribution from Gaussian to rectangular. The last modular in both models is the depletion term. This term accounts for the loss of material by simple decay processes, precipitation scavenging or gravitational settling.

19.2.3 Maximum Ground-Level Concentration-Dosage Formulas for Normal and Abnormal Launches

19.2.3.1 Definitions

Ground cloud is formed during the first several minutes and contains all of the exhaust by-products formed by the rocket engines from the time of engine ignition until the vehicle passes through the stabilization height, "height of maximum buoyancy rise of the hot exhaust products", of the ground cloud. If the stabilization height is such that some of the ground cloud is contained in a thermally stable layer, only a fraction of the total amount of exhaust products in the ground cloud is available for mixing to the ground surfaces.

Exhaust trail plume - Plume of stabilized exhaust products formed by rocket engine emissions occurring above the stabilization height of the ground cloud.

19.2.3.2 NASA/MSFC Multilayer Diffusion Model (Ref. 19.2)

The normal launch environment will usually involve an atmospheric structure comprised of several horizontal meteorological layers with distinctive wind velocity, temperature, and humidity regimes between the surface and a 5 kilometer altitude. Large horizontal spatial variation in these meteorological parameters may also occur in the surface layer as a consequence of changes in terrain or land-water interfaces, which is accounted for by the diffusion model. The general diffusion model for concentration (Eq. 19-1) and the dosage (Eq. 19-2) assumes an expanding volume about a moving point of reference in a homogeneous environment.

To overcome the obvious shortcomings of the general diffusion model but to stay within the accepted bounds of classical fluid mechanics (Ref. 19.1), a multiple layer concept is introduced to cope with the vertical and horizontal atmospheric gradients. Here, the general diffusion model is applied to individual horizontal layers in which the meteorological structure is reasonably homogeneous and independent of the neighboring layers. These layers have boundaries which are placed at points of major discontinuities in the vertical profiles of wind velocity, temperature, and humidity. Since the Multilayer Diffusion Model has imposed the general restriction of layer independence (no flux of particles or gases entering or leaving an individual layer), special provision must be made for spatial changes in the horizontal meteorology and for gravitational settling or precipitation scavenging. In addition, the type of source within a layer must be considered; that is, whether there is a ground cloud source or a plume cloud source.

The Multilayer Diffusion Model has six submodels (Figure 19-1) to deal with the stages of the development of the exhaust cloud and the complex potentially varying meteorological conditions. These submodels can be used alone to describe all the environmental layers or in combinations where variations in layer meteorology require different modeling. For the introductory overview, however, these combinations will not be considered. The primary output of all submodels is a mapping of the regimes of the concentration and dosage isopleths.

Model 1 is the basic model for the dispersive description of exhaust material from rocket plume. In this model it is assumed that the source extends vertically through the entire layer with a uniform distribution of the concentration of exhaust material, whereas, the horizontal distribution of the material being dispersed along the layer (x & y directions) has a Gaussian distribution. In addition, it is assumed that there is turbulent mixing.

An analogous model would be the wave generated by dropping a rock in a river, where the wave disperses across the surface of the moving river. The significance of the supposition of turbulent mixing is that this mixing action disperses the effluent material across the layer similar to the way the wave is dispersed across the surface of the water. This model is an effective description of the plume cloud where the action of the vehicle passing through a layer leaves a cylindrical cloud of exhaust effluents.

Model 2 is the same as Model 1 except it is assumed that there is no turbulent mixing. This implies that the exhuast material just meanders along the layer without dispersing, very much like a small oil puddle moves on the surface of a river. While the Model 2 is not generally used, movies of rocket firings clearly show that under some special meteorological conditions this model is required. While the multilayer diffusion model is general in applicability, it is specific in meteorological parameters and launch description.

From the standpoint of environmental impact, the description of the fields of the ground deposition of materials from the ground cloud is of primary significance - - this description is afforded by Model 3. Generally, this model is employed in the surface layer, but can be employed in any layer where the source does not extend through the entire layer. In this model a Gaussian distribution is assumed along all three axes, with turbulent mixing occurring.

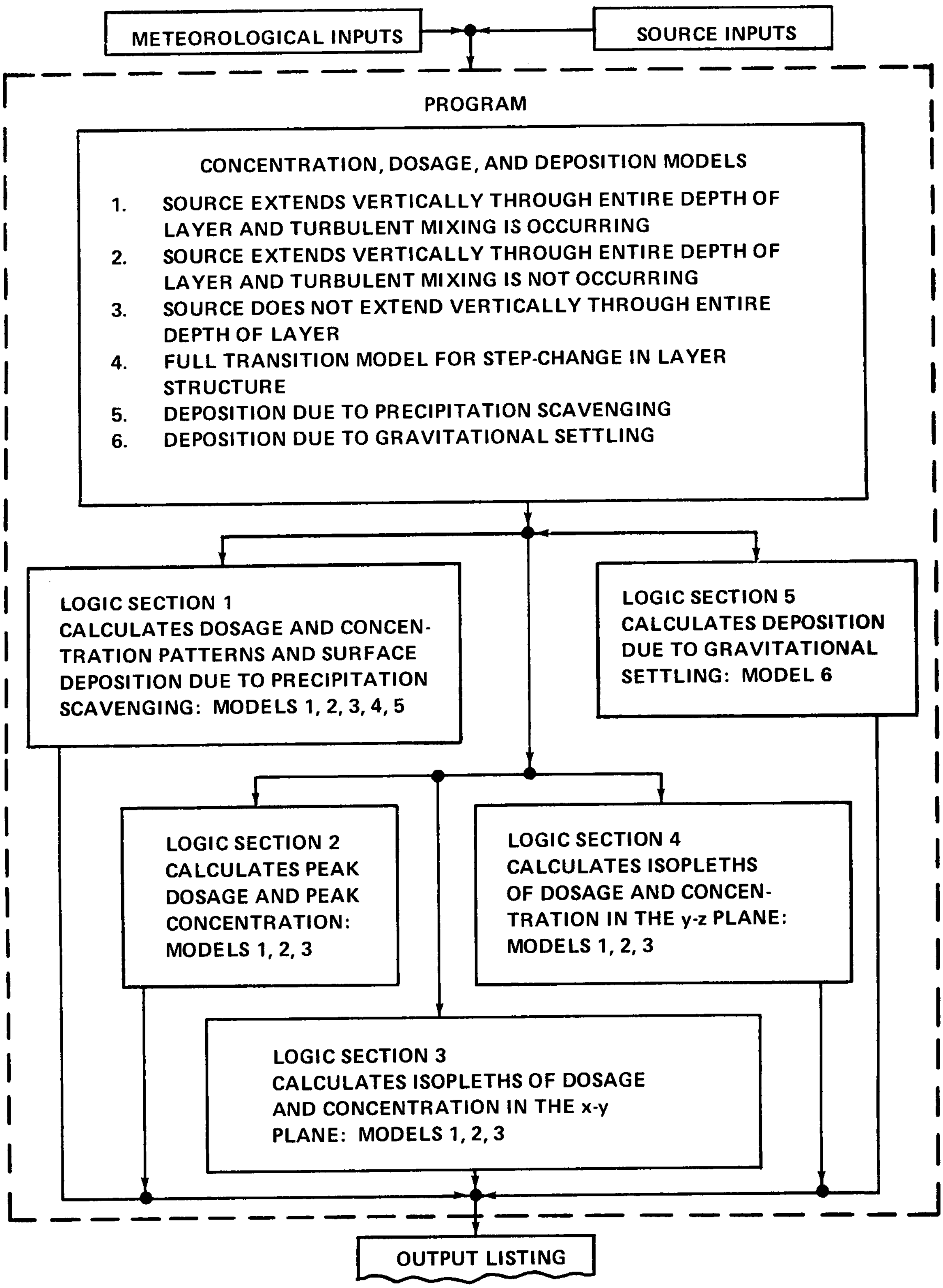

Figure 19.1. Block diagram of the computer program for the Multilayer Diffusion Model.

Model 3 is similar to Model 1 except that, now, rather than the plane two-dimensional dispersion of Model 1, there is a three-dimensional dispersion of the exhaust cloud as the cloud is transported downstream. When the cloud reaches the top of the mixing layer, the distribution of material is reflected back into the expanding vertical distribution. Thus, after a certain time period Model 3 is identical with Model 1. A clear understanding can be obtained if the formulation for this model is examined.

The first three models can be summarized as describing initial transport of the effluents after the cloud reaches equilibrium. While the equations just given for Model 3 are in the general form for any K^{th} layer, it should be noted that $K = 1$ (the surface layer) is used in most applications of this model. If after launch, the rocket explodes in a layer, this can be studied with this model by setting K equal to that layer number.

The remaining models are specialized models which afford a second order description of the transport of the vehicle exhaust materials. These three models incorporate considerations for changes in meteorological conditions and particle effects.

Model 4 updates the diffusion model with changes in meteorological conditions and structure which can occur as the toxic cloud propagates downstream. This model assumes that the vertical concentration of material has become uniform throughout each layer when a step-change in the meteorological conditions is introduced. This step-change results in the destruction of the original layer boundaries and the formation of new layer boundaries. The concentration fields which exist at this time are treated as new sources. In those new layers which now comprise more than one old layer, the old concentration is mapped as two independent concentration sources and then superimposed for the resulting concentration and dosage mappings.

Model 5 accounts for precipitation scavenging. An example of where Model 5 must be used is in solid rocket launches during the occurrence of rain, because the HCl will be scavenged by the rain. Model 6 describes the ground deposition due to gravitational settling of particles of droplets. Wind shears are incorporated in this model to account for the effect of the settling velocity of the particulate matter. There are two forms for the source in this model; namely:

1. The source that extends vertically through the entire layer with

a uniform distribution -- this is the same source model as used with Models 1 and 2, and

2. A volume source in the K^{th} layer — this is the same source — model as used with Model 3.

Model 6 is very important in the analysis of the settling of Al_2O_3 particles released in solid rocket firings.

In summary, the Multilayer Diffusion Model is composed of six submodels. Models 1 and 3 are designed to distinguish between the two sources of toxic cloud formation -- the ground cloud during the initial launch phase (Model 3) and the plume cloud after the initial launch phase (Model 1). Model 2 was injected to account for a lack of turbulent mixing which can occur in the upper atmosphere. Model 4 is employed when a change in meteorological condition occurs during the downstream transport of the cloud. In the event of rain, the precipitation scavenging — both of gases and particles — can be accounted for in Model 5. The fallout of particulate matter on the ground is the domain of Model 6 . These six submodels form the basic algorithms which are available to treat the diffusion problem. To model a specific launch of a vehicle, it is necessary to blend these algorithms together and adjust the model parameters to the specific meteorological conditions of the launch, to the specific terrain around the launch site and to the specific vehicle being launched; thus the degree of complexity in the diffusion model.

19.2.4 Ground-Level Concentration-Dosage Formulas for Cold Spills and Leaks

The treatment of cold spills and fuel leaks that occur near ground level requires a continuous source, but the models that have been considered so far are for discrete sources; therefore, the models must be adapted for the use in predicting concentration-dosage levels downwind from continuous sources.

The layer of the environment influenced by the ground-level spills and leaks can be treated as homogeneous; therefore, the general formula for concentration and dosage (Equations 19.1 and 19.2) presented in the initial discussion would be applicable if we could treat them as continuous sources. To achieve this adaption for these formulas, we must consider the following argument: Assume a source cloud with a concentration distribution that implies a given dosage at a point for this cloud; that is, the dosage per event. If there are a number of similar clouds, discretely spaced, then for each cloud we obtain a dosage for each cloud whose sum corresponds to the total dosage for the entire event.

In the limit as the spacing between clouds approaches zero and the number of clouds becomes large, the discrete source approaches a continuous source whose concentration is the point dosage per unit time. The relation for the continuous concentration, which follows directly from this argument, is

Concentration = (Peak Concentration) x (Lateral Term) x (Vertical Term) x (Depletion Term)

The Peak Concentration Term is given by the expression

$$\text{continuous peak concentration} = \frac{Q}{2\pi \bar{u} \sigma_y \sigma_z t_R}, \qquad (19.3)$$

where

Q = source strength in units of total mass released

$\bar{u}$ = mean wind speed at the effective source height

σ_y = standard deviation of the crosswind concentration distribution

σ_z = standard deviation of the vertical concentration distribution

t_r = release time.

The Lateral Term, Vertical Term, and the subset of equations defining σ_y and σ_z are the same as for the point source dosage (equation 19.2). The continuous dosage is then the continuous concentration times the release time.

19.3 CLOUD RISE FORMULAS

19.3.1 Introduction

The burning of rocket engines results in the formation of a cloud of hot exhaust products which subsequently rises and entrains ambient air until an equilibrium with ambient conditions is reached. Thus far the discussions of the diffusion model have treated this equilibrium point as the source and the model then provides a description of the temporal and spatial transport of the materials in the exhaust cloud. The height of cloud stabilization, which is a parameter in the Multilayer Diffusion Model, is the problem that is addressed in this section.

For normal launches, this cloud is formed principally by the forced ascent of hot turbulent exhaust products that have been deflected laterally and vertically by the launch pad hardware and the ground surface. The height at which this ground cloud stabilizes is determined by the vehicle type and atmospheric stability. The vehicle type determines whether a continuous or instantaneous source model is used. In the instantaneous source model, spherical entrainment is assumed; that is, the entrained ambient air enters the exhaust cloud uniformly from all directions. In the continuous source model, cylindrical entrainment is assumed; that is, the entrained ambient air enters the cloud uniformly only on the sides of the cylinder and not the ends. Thus, this terminology — continuous or instantaneous source — in reference to the cloud rise model does not imply the duration of the exhaust cloud, as it does in the diffusion model, it only implies the form of the entrainment process. The entrainment process is a function of the residence time of the vehicle on the pad. Experience to date indicates that the buoyant rise of exhaust clouds from normal launches of solid-fueled and small liquid-fueled vehicles is best predicted by using a cloud rise model for instantaneous sources; the cloud rise for large liquid-fueled vehicles is best predicted by the use of a cloud rise model for continuous sources. While no cloud rise data are available for on-pad aborts, cloud rise data from static tests of liquid-fueled rockets indicate that the use of a cloud rise model for continuous sources is appropriate in this case.

Each of the models for cloud height is subdivided into two categories to account for the atmospheric temperature lapse rate. The model assumes that the atmosphere is either quasi-adiabatic or stable. Here the quasi-adiabatic is where the adiabatic atmosphere is the limit, which means that the potential temperature difference ($\Delta\theta$) is zero or less, where the potential temperature difference is given by $\Delta\theta = \theta_{\text{max cloud height}} - \theta_{\text{surface}}$. If this potential temperature difference is positive, then the atmosphere is treated as stable. Since in most cases of interest there will be an inversion layer present, the stable cloud rise formula is the normally utilized relation.

19.3.2 Quasi-Continuous Sources

The following formulas for the maximum buoyant rise of clouds from continuous sources are also based on procedures similar to those given by Briggs (1970). The maximum cloud rise z_{mc} downwind from a continuous source in an adiabatic atmosphere is given by

$$z_{mc} = \left[\frac{3F_c x_{sc}^2}{2\gamma_c^2 \bar{u}^3} + \left(\frac{r_R}{\gamma_c} \right)^3 \right]^{1/3} - \frac{r_R}{\gamma_c} \qquad (19.4)$$

The maximum cloud rise z_{mc} downwind from a continuous source in a stable atmosphere is given by

$$z_{mc} = \left[\frac{6F_c}{\bar{u}\gamma_c^2 s} + \left(\frac{r_R}{\gamma_c} \right)^3 \right]^{1/3} - \frac{r_R}{\gamma_c} \qquad (19.5)$$

where F_c is the buoyancy flux parameter and is equal to $\frac{gQ_c}{\pi pC_p T}$, Q_c is the effective rate of heat release, γ_c is the entrainment coefficient, $\bar{u}$ is the mean wind speed, x_{sc} is the downwind distance at which the cloud reaches its stabilization height, s accounts for the vertical gradient of the ambient potential temperature and r_R is the initial cloud radius at the surface. The subscript c implies that the associated parameter is unique to the continuous source. The primary difference in these continuous source relations is that the temperature constraint in the stable atmosphere results in a buoyancy damping.

Equations (19.4) and (19.5) assume that the initial momentum flux imparted to the cloud by dynamic forces is negligible in comparison buoyancy flux. Again, experience in calculating cloud rise for normal launches of large liquid fueled rockets and for static firings has shown that this assumption is reasonable (Ref. 19.2 through 19.12).

19.3.3 Instantaneous Source

The maximum cloud rise z_{mI} downwind from an instantaneous source in an adiabatic atmosphere is given by

$$z_{mI} = \left[\frac{2F_I x_{sI}^2}{\gamma_I^3 \bar{u}^2} + \left(\frac{r_R}{\gamma_I} \right)^4 \right]^{1/4} - \frac{r_R}{\gamma_I} \qquad (19.6)$$

whereas, the maximum cloud rise z_{mI} downwind from an instantaneous source in a stable atmosphere is given by

$$z_{mI} = \left[\frac{8F_I}{\gamma_I^3 s} + \left(\frac{r_R}{\gamma_I}\right)^4\right]^{1/4} - \frac{r_R}{\gamma_I} \qquad (19.7)$$

where

F_I = the buoyancy parameter

$$= \frac{3gQ_I}{4\pi\rho c_p T}$$

g = acceleration due to gravity ($m\ sec^{-2}$)

Q_I = the effective heat released (cal)

c_p = specific height of air at constant pressure ($cal\ gm^{-1}\ {}^\circ K^{-1}$)

T = ambient air temperature (°K)

ρ = density of ambient air ($gm\ m^{-3}$)

γ_I = the entrainment coefficient for an instantaneous source

r_R = the initial cloud radius at the surface (m)

χ_{sI} = the time required for the cloud to reach stabilization (sec)

The subscript I means instantaneous and again is used to flag a difference in the cloud rise models. The buoyancy terms, which is a function of the heat released and the type of entrainment, spherical and cylindrical, reflect the major difference in the two sources.

Equations (19.6) and (19.7) assume that the initial upward momentum imparted to the exhaust gases by reflection from the ground surface and launch pad hardward is insignificant in comparison with the effect of thermal buoyancy. Based on limited experience in predicting cloud rise from launches at Vandenberg Air Force Base, this assumption appears to be justified.

19.4 REPRESENTATIVE SOURCE AND METEOROLOGY INPUTS

19.4.1 Source Inputs

The composition of the rocket exhaust effluents varies between vehicles in accord with vehicle sizes and motor types. The two major rocket classes are the ones that use liquid and solid rocket propellants.

When calculating downwind concentrations from fractional weights of materials in the exhaust definite uncertainties evole. One must determine the actual amounts of elements or compounds available after the exhaust material combines with the ambient atmosphere. Factors that may cause the fractional amounts of effluents to change in the ground cloud are: (1) the exhaust flame evaporates thousands of gallons of deluge water within the flame trench and other water being sprayed on the launcher towers, (2) significant amounts of materials are ablated such as concrete, steel, and paint, (3) other matter such as dust, ocean salt, grease, etc., are vaporized and are contained within the ground cloud. Subsequently, a great deal of research must be accomplished before accurate source inventory data can be made available. This is especially needed for exhaust ground cloud chemistry as such clouds will be composed of both solid and liquid exhaust by-products. Exhaust chemistry, especially after reaction with the air and extraneous material, is essential for identifying initial ground cloud source composition to make atmospheric diffusion computations.

19.4.2 Meteorological Inputs

Reliable atmospheric thermodynamic and kinematic profiles are required to compute diffusion estimates. Consideration must be given to such factors as: (1) local climatology, (2) large scale meteorological conditions, (3) local atmospheric conditions, (4) topographical features, (5) land-water interfaces, (6) exhaust source chemistry with the ambient air, etc. One of the most important factors is having a sound definition of the earth's planetary boundary layer phenomena. This is the main atmospheric layer of concern when determining downwind dispersion of exhaust effluents and potential environmental hazards.

As related in Section 19.2 and 19.3 the meteorological inputs for diffusion modeling are as follows: (1) wind direction, (2) wind speed, (3) standard deviations of vertical and horizontal wind, (4) humidity, (5) atmospheric pressure, (6) temperature profile data, (7) height of stable layers, and (8) air density (Ref. 19.13 through 19.16). Precipitation, cloud heights and types, pressure gradient conditions, and other features of the synoptic state must also be considered. The height of the stable layer is needed because it dictates the height the hot buoyant exhaust clouds will stabilize, especially when dealing with the larger vehicle exhausts.

19.4.3 Variation in Diffusion Climatology for Different Launch Sites

Three sites are being considered for primary utilization during Space Shuttle testing and launch. Mississippi Test Facility (MTF), Kennedy Space Center (KSC), and Vandenberg Air Force Base (VAFB). There are significant climatic differences as well as notable similarities in a comparison of these locations. VAFB is considerably cooler throughout the year than either MTF or KSC, although annually, the number of days recording precipitation is about three times greater at both MTF and KSC (Ref. 19.17). Both KSC and VAFB experience frequent occurrences of the sea breeze but only VAFB records a large number of days with advection fog. Mean relative humidity at VAFB, however, is slightly lower than at the other sites. Thunderstorms are a phenomenon occurring on as many as half the days at KSC and MTF in the summer months, whereas, they are extremely rare at VAFB. Since precipitation is slight and infrequent throughout the year at VAFB and fog is most frequent during the winter months, it is not unexpected to note that mean sky cover amounts are small especially during the summer months. By contrast both KSC and MTF record much greater daytime sky cover amounts than VAFB even though seasonal variations are measured at all sites. Mean wind speeds generally are not significantly different at the three sites and both KSC and VAFB record frequent diurnal periods of on-shore and off-shore winds. MTF, as an inland site, is affected by the prevailing air mass or synoptic weather patterns.

19.5 TOXICITY CRITERIA

Realistic evaluation of the potential hazard arising from high near-field concentrations of toxic effluents from solid rocket exhaust requires both a knowledge of the surface deposition of these effluents — which can be obtained with the MSFC/NASA Multilayer Diffusion Model, and a toxicity criteria to evaluate the hazard from this surface deposition of effluent which is the incumbency for this discussion. The Federal Air Quality Criteria does not presently include any of the solid rocket exhaust effluents, however, the National Academy of Sciences does afford definite guidelines for the exposure to the toxic effluents associated with these exhausts. The Environmental Protection Agency EPA suggests a safety factor of ten (10) be applied to the occupational exposure limits (Ref. 19.20). These guidelines are based on the current limited knowledge of the effects of these effluents, and are the basis of the toxicity criteria given in Table 19.5.1 (Ref. 19.18).

The primary effluents from any solid rocket exhaust are: aluminum oxide, (Al_2O_3), hydrogen chloride (HCl), carbon monoxide (CO), carbon dioxide (CO_2), hydrogen (H_2), nitrogen (N_2) and water vapor (H_2O). While only the first four compounds are toxic in significant concentrations, there is always a potential hazard of suffocation from any gas which results in the reduction of the partial pressure of oxygen to a level below 135 mm Hg (18% by volume at STP). Oxygen level reduction does not appear to be a hazard from solid rocket exhaust due to the large volume of air which is entrained into these exhaust clouds; therefore, this potential hazard can be neglected in this discussion and the attention directed to only the initial four toxic compounds.

The exposure level for toxic effluents are divided into three categories: public exposure level, emergency public exposure level, and occupational exposure level. The public exposure levels are designed to prevent any detrimental health effects both to all classes of human beings (children, men, women, the elderly, those of poor health, etc.) and to all forms of biological life. The emergency level is designed as a limit in which some detrimental effects may occur, especially, to biological life. The occupational level gives the maximum allowable concentration which a man in good health can tolerate — this level could be hazardous to various forms of biological life.

The toxicity criteria for the toxic effluents in solid rocket exhausts are given in Table 19.5.1. Public health levels for aluminum oxide are not given because the experience with these particulates is so limited that, at best, the industrial limits are just good estimates.

Hydrogen chloride is an irritant; therefore, the concentration criterion for an interval should not be exceeded (Ref. 19.19). Since hydrogen chloride is detrimental to biological life, and in view of the fact that most launch sites are encompassed by wild life refuges, the emergency and industrial criteria for hydrogen chloride are not appropriate to the ecological constraints. Because of the large volume of air entrained in the exhaust cloud, the potential hazard from carbon monoxide and carbon dioxide can be neglected.

TABLE 19.5.1 AIR QUALITY TOXICITY STANDARDS*

Toxic Solid Rocket Exhaust Product	Time Interval (Minutes)	Concentration		
		Public **	Emergency	Occupational
Alumina (Al_2O_3) (Aluminum Oxide)	10 30 60 480	5.0 mg/m^3 2.5 mg/m^3 1.5 mg/m^3 1.0 mg/m^3	x x x x	50 mg/m^3 25 mg/m^3 15 mg/m^3 10 mg/m^3
Hydrogen Chloride (HCl)	10 30 60	4 ppm**** 2 ppm 2 ppm	7 ppm 3 ppm 3 ppm	30 ppm 20 ppm 10 ppm
Carbon Monoxide (CO) DOSAGE:	10 30 60	90 ppm 35 ppm 25 ppm 200 ppm/ time interval	275 ppm 100 ppm 66 ppm	1000 (1500***) ppm 500 (800***)ppm 200 (400***)ppm
Carbon Dioxide (CO_2)	480	x x	x x	Average - 5000 ppm Peak - 6250 ppm

*These values were reviewed on the phone by Ralph C. Wands, Director Advisory Center on Toxicology, National Academy of Sciences, 2101 Constitution Avenue, Washington, D. C. 20418, April 1973.

**EPA suggests a safety factor of ten (10) to be applied to occupational exposure limits.

***At these concentrations, headaches will occur along with a loss in work efficiency.

**** Parts of vapor or gas per million parts of contaminated air by volume at 25°C and 760 mm Hg.

Any detrimental health effects due to combined toxicological action of these ingredients has been omitted because of a lack of knowledge in this area. However, investigations are currently underway to study this problem and to learn more about the biological effects of hydrogen chloride.

19.6 EXAMPLE OF GROUND-LEVEL CONCENTRATIONS AND DOSAGES

The highest concentrations and dosages of the exhaust effluents will occur downwind of the launch site at the center of the cloud. In view of the toxicity criteria given in Section 19.5 it is essential that the maximum concentration, the dosage along the centerline, and the average concentration at the centerline must be known. In view of the fact that a launch could occur under marginal atmospheric conditions in which air quality toxicity standards may be exceeded, a detailed knowledge of the downwind concentrations is required. A depiction of centerline concentrations and dosages is given in Figure 19.6.1. Depiction of downwind concentrations and dosages by drawing isopleths which show parts per million, milligrams per cubic meter, etc., in time and space is a unique way to graphically display such data; however, no contours of diffused exhaust clouds are illustrated in this review.

Figure 19.6.1 also shows an example of the maximum centerline concentrations atground-level downwind from the point of cloud stabilization obtained by use of diffusion model 3. Figure 19.6.1 also shows centerline dosages at ground level downwind from the point of cloud stabilization. Dosage can be understood by assuming that continuous sample is taken two meters above the surface at the centerline of the passing cloud. This integrating procedure would then give the dosages at any downwind distance (see Section 19.2). The average alongwind concentrations from the point of cloud stabilization are also given. Section 19.2 should be referenced for the definition, however, the average alongwind dosage is simply the total dosage measured as an entire cloud passes a point divided by the time it took the cloud to pass. Comparison of the concentrations and dosages can be done by considering the limits related in the section on toxicity (Section 19.5).

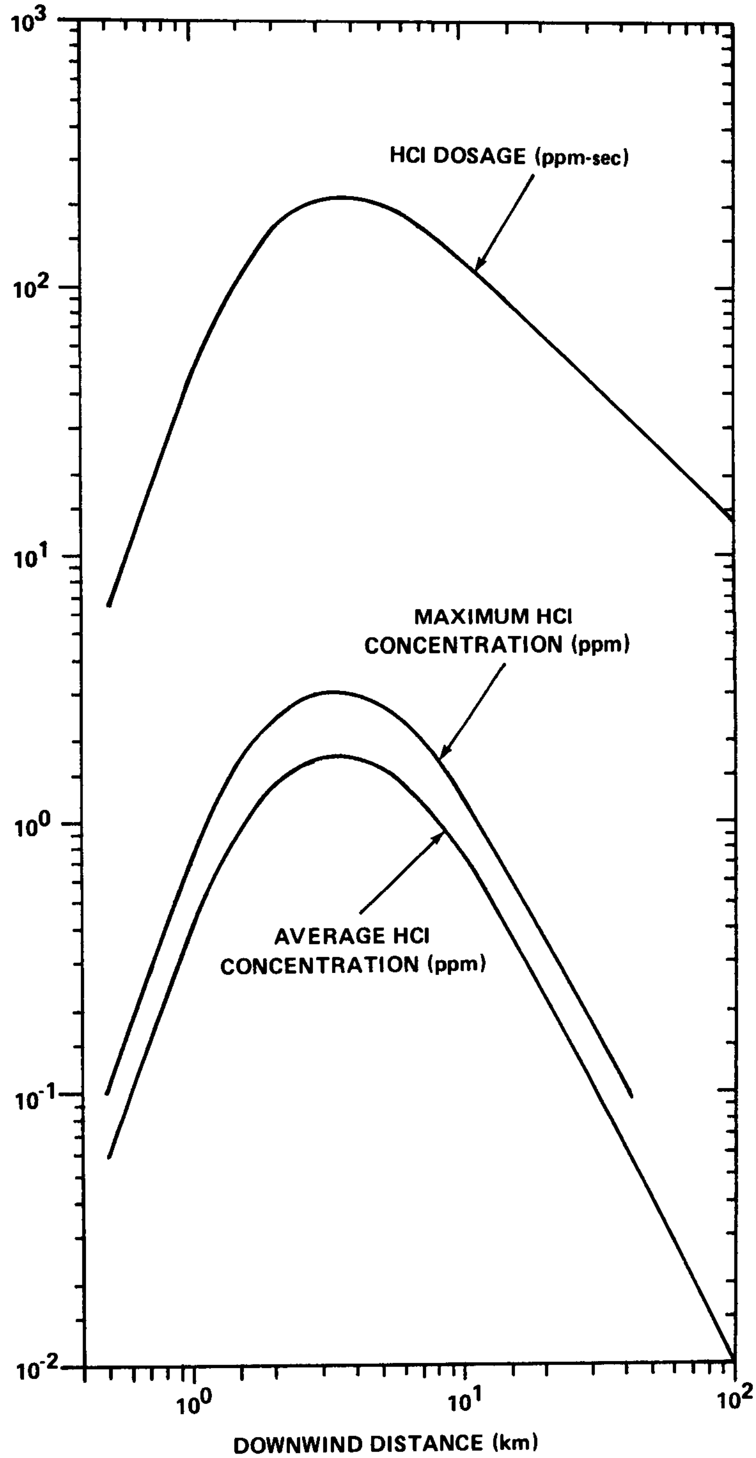

Figure 19.6.1 Maximum centerline concentrations, centerline dosage, and average alongwind concentrations at ground-level downwind from the point of cloud stabilization (Model 3).

REFERENCES

19.1 Landau, L. D. and Lifshitz, E. M.: Fluid Mechanics, Volume 6 of Course of Theoretical Physics, Pergamon Press, 1959.

19.2 Dumbauld, R. K., Bjorklund, J. R., and Bowers, J. F.: NASA/MSFC Multilayer Diffusion Models and Computer Program for Operational Prediction of Toxic Fuel Hazards, H. E. Cramer Company, Inc., TR-73-301-02, March 1973.

19.3 Susko, Michael, Kaufman, John W., and Hill, Kelly, "Rise Rate and Growth of Static Test Vehicle Engine Exhaust Clouds," TM X-53782, Aero-Astrodynamics Research Review No. 7, October 15, 1968, pp 146-166, NASA.

19.4 Briggs, G. A., "Some Recent Analyses of Plume Rise Observations," Paper presented at the 1970 International Union of Air Pollution Prevention Associations, Atmospheric Turbulence and Diffusion Laboratory, National Oceanic and Atmospheric Administration, Oak Ridge, Tennessee, USA, ATDL, No. 38, 1970.

19.5 Hanna, Steven R., "Cooling Tower Plume Rise and Condensation" paper presented at Air Pollution Turbulence and Diffusion Symposium, Las Cruces, New Mexico, December 7 - 10, 1971.

19.6 Smith, Michael R. and Forbes, Richard E., "Mass-Energy Balance for an S-IC Rocket Exhaust Cloud During Static Firing," CR-61357, August 4, 1971, NASA.

19.7 Thayer, Scott D., Chandler, Martin W., and Chu, Ronald T., "Rise and Growth of Space Vehicle Engine Exhaust and Associated Diffusion Models," CR-61331, July 1970, NASA.

19.8 Susko, Michael and Kaufman, John W., "Apollo Saturn Engine Exhaust Cloud Rise and Growth Phenomenon During Initial Launch," paper presented at MSFC's Research Achievement Review, Marshall Space Flight Center, Huntsville, Alabama, December 2, 1971, NASA.

19.9 Church, H. W., "Cloud Rise from High-Explosives Detonations," TID-45000 (53rd Ed) UC-41, Health & Safety, SC-RR-68-903, Sandia Laboratories, Albuquerque, June 1969.

REFERENCES (Continued)

19.10 Hart, W. S., "Dynamics of Large Buoyant Clouds Generated by Rocket Launches," J. Basic Eng., March 1972.

19.11 Susko, Michael and Kaufman, J. W., "Exhaust Cloud Rise and Growth for Apollo Saturn Engines, Journal of Spacecraft and Rockets, May 1973.

19.12 Tucker, G. L. Maj., Malone, H. E., and Smith, R. W. Capt., "Atmospheric Diffusion of Beryllium - Project Adobe" Report No. AFRPL-TR-70-65, Three Volumes, July 1971, Director of Laboratories, Air Force System Command.

19.13 Fichtl, George H., Kaufman, J. W., and Vaughan, W. W., Characteristics of Atmospheric Turbulence as Related to Wind Loads on Tall Structures," Journal of Spacecraft and Rockets, Vol. y, pp. 1396 - 1403, December 1969.

19.14 Kaufman, John W. and Keene, Lester F., "NASA's 150-Meter Meteorological Tower Located at the Kennedy Space Center, Florida," TM X-53699, January 29, 1968, NASA.

19.15 Kaufman, John W. and Susko, Michael, "Review of Special Detailed Wind and Temperature Profile Measurements," Journal of Geophysical Research, Vol. 76, No. 27, September 20, 1971.

19.16 Fichtl, George H. and McVehil, George E., "Longitudinal and Lateral Spectra of Turbulence in the Atmospheric Boundary Layer at the Kennedy Space Center," Journal of Applied Meteorology, Vol. 9, No. 1, February 1970. pp 51-63.

19.17 Climatic Atlas of the United States, U. S. Dept. of Commerce Environmental Science Services Administration, June 1968.

19.18 National Primary and Secondary Ambient Air Quality Standards, Environmental Protection Agency, Part II of Federal Register, Vol. 36, No. 84, April 1971 (Updated November 1971).

REFERENCES (Concluded)

19.19 "Guides for Short-Term Exposures of the Public to Air Pollutants, Vol. II. Guide for Hydrogen Chloride," Committee on Toxicology of the National Academy of Sciences - National Research Council, Washington, D. C., August 1971.

19.20 Letter from Edie Tomkins, Special Technical Assistant, Human Studies Laboratory, United States Environmental Protection Agency, Research Triangle Park, North Carolina, 27711, dated April 13, 1973.

INDEX

A

T

WORLDWIDE EXTREMES

APPROVAL

TM X - 64757

TERRESTRIAL ENVIRONMENT (CLIMATIC) CRITERIA GUIDELINES FOR USE IN AEROSPACE VEHICLE DEVELOPMENT, 1973 REVISION

Glenn E. Daniels, Editor

The information in this report has been reviewed for security classification. Review of any information concerning Department of Defense or Atomic Energy Commission programs has been made by the MSFC Security Classification Officer. This report, in its entirety, has been determined to be unclassified.

This document has also been reviewed and approved for technical accuracy.

WILLIAM W. VAUGHAN
Chief, Aerospace Environment Division

for E. D. GEISSLER
Director, Aero-Astrodynamics Laboratory